Ali, Juma Ahmed Mohmed (2013) *Pyrimidine salvage and metabolism in kinetoplastid parasites.* PhD thesis.

http://theses.gla.ac.uk/4664/

PYRIMIDINE SALVAGE AND METABOLISM IN KINETOPLASTID PARASITES

Juma Ahmed Mohmed Ali

This Thesis is submitted in fulfilment
of the requirements for the degree of
Doctor of Philosophy

Institute of Infection, Immunity & Inflammation
College of Medical, Veterinary & Life Sciences
University of Glasgow

Sep. 2013

Abstract

Pyrimidine uptake has previously been investigated in *Trypanosoma brucei* procyclics and partly investigated in promastigotes of *Leishmania major*; however, no such study has been performed using bloodstream forms of *Trypanosoma* or promastigotes of *Leishmania*. Here we report a comprehensive study of pyrimidine salvage and metabolism in bloodstream forms of *Trypanosoma* and promastigotes of *Leishmania* species.

In *T. b. brucei* bloodstream forms, the uptake of ^{3}H-uracil and ^{3}H-tymidine each appeared to be mediated by a single transporter, designated TbU3 and TbT1, respectively. The procyclic uracil transporter,TbU1, has a high affinity for uracil, with a K_m value of 0.46 ± 0.09 µM and V_{max} of 0.65 ± 0.008 pmol $(10^7 cell)^{-1}$ s^{-1}. These values were similar for TbU3 (K_m = 0.54 ± 0.11 µM; V_{max} = 0.14 ± 0.03), but the main differences between TbU1 and TbU3 are their sensitivity to uridine and 4-thiouracil. Thymidine uptake is detectable at 10 µM over a period from 5 to 30 minutes. This uptake was not inhibited by uracil which indicates that TbT1 is a novel thymidine transporter. The uptake of other pyrimidines, including uridine and 2'-deoxyuridine, by BSF are investigated here but these substrates were also transported by TbU3, and no additional pyrimidine transport activities were found.

In *L. mexicana* and *L. major*, the uptake of ^{3}H-uracil and ^{3}H-uridine was mediated by separate transporters, designated as follows; for uracil uptake LmexU1, LmajU1; and for uridine uptake LmexNT1, LmajNT1 and LmajNT2, respectively. LmexU1 is a uracil transporter with high affinity to uridine and 2'deoxyuridine, and the LmexNT1 is a nucleoside transporter with broad specificity for purine and pyrimidine nucleosides. *L. major* uracil transporter (LmajU1) has already been reported by others; and here we report that there are also two distinct uridine transporters expressed in *L. major*. LmajNT1 is a high affinity uridine transporter which is also inhibited by uracil, inosine and adenine; LmajNT2 is low affinity uridine transporter, with very poor affinity for uracil, inosine and adenine. However, both transporters are inhibited by 2'-deoxyuridine, thymidine and adenosine.

Several fluorinated pyrimidine analogues were assessed against kinetoplastid cells, the most effective compounds, which displayed EC_{50} values at micromolar level, are 5-FU, 5F-2'dUrd, 5-FOA (only against *T. brucei* BSF) and 5F-Urd (only against *L. major*). We induced resistance to 5-FU, 5-F2'dUrd and 5-FOA by *in vitro* exposure of Tbb-BSF and promastigotes of *L. mexicana* and *L. major*. The resistance was performed by stepwise increase concentration of the drugs. For *T. b. brucei* BSF, the resistance factors of clonal lines were 131, 825, and 83-fold, respectively. For *L. mexicana* and *L. major*, the resistance factor for 5-FU were 147 and 17-fold, and for 5F-2'dUrd were >3500 and 381-fold, respectively. We also measured ^{3}H-pyrimidine uptake in these cell lines; the resistant bloodstream form strains showed no changes in pyrimidine uptake, with one exception, which is a 76% reduction in 5-FU uptake. In contrast, each resistant strain of *Leishmania* spp had lost its natural pyrimidine transporter. For example, *Leishmania* cells resistant to 5-FU had lost uracil transport activity, and cells that were resistant to 5F-2'dUrd had lost uridine transport activity. In addition, we identified kinetoplastid genes that appeared to be associated with resistance to fluorinated pyrimidines.

Based on these findings, metabolomic analysis of fluorinated pyrimidines in *T. b. brucei* resistant cell lines was performed in comparison with parental wild-type; for *Leishmania* species we only investigated the metabolism of fluorinated pyrimidine in wild type cells, as the fluorinated analogues were simply not taken up in the resistant clones. The metabolomic analysis data showed that, in *T. b. brucei*, 5-fluorouracil and 5-fluoro orotate are incorporated into a large number of metabolites, but likely act through incorporation into RNA. 5F-2'dUrd and 5F-2'dCtd are not incorporated into nucleic acids but act as prodrugs by inhibiting thymidylate synthase after conversion to 5F-dUMP. Cells treated with 5-fluoro-2'deoxyuridine showed an increase of dUMP, which suggest a block in thymidylate synthase or possibly thymidylate kinase. We also present the most complete model of pyrimidine salvage in *T. brucei* to date, supported by genome-wide profiling of the predicted pyrimidine biosynthesis and conversion enzymes.

The effect of fluorinated pyrimidine analogues in the two *Leishmania* species was almost identical. Each of the tested drugs (5-FU, 5F-2'dUrd and 5F-Urd) produced a limited number of fluorinated metabolites, and their common mode

of action was inhibition in thymidylate synthase by 5F-dUMP and thymidine kinase by 5F-2'dUrd. Interestingly, we found that the cause of *L. mexicana* resistance to 5F-Urd was due to the absence of the 5F-2'dUrd metabolite, as a result of the rapid conversion of 5F-2'dUrd to 5F-dUMP; also we suggest that, in *L. mexicana*, but not in *L. major* the high affinity salvage of thymidine is sufficient to provide the cells with thymidine deoxynucleotides.

It has been found that pyrimidine salvage is not an essential function for *Leishmania* cells *in vitro* conditions. However, it is not known whether either, pyrimidine salvage or biosynthesis, or both of these systems are essential to the trypanosomes *in vitro* and *in vivo* study. As *T. b. brucei* bloodstream forms grew unimpeded *in vitro* in the complete absence of pyrimidines, uptake is clearly not essential. Disruption of the pyrimidine biosynthesis pathway by deletion of the OMPDCase/OPRTase gene resulted in pyrimidine auxotrophic trypanosomes that were unable to grow in the absence of added pyrimidines. The phenotype was rescued by addition of uracil, and to a lesser extent by some pyrimidine nucleosides. Pyrimidine starvation led rapidly to DNA fragmentation. Adaptations to low pyrimidine availability included upregulation of uracil transport capacity and of uridine phosphorylase expression. However, pyrimidine auxotrophic *T. brucei* were able to establish a high parasitemia in mice. We therefore conclude that pyrimidine salvage was not an essential function for bloodstream *T. b. brucei*. However, trypanosomes lacking *de novo* pyrimidine biosynthesis are completely dependent on an extracellular pyrimidine source, strongly preferring uracil, and display reduced infectivity and strongly increased sensitivity to fluorinated pyrimidines. As *T. brucei* are able to salvage sufficient pyrimidines from the host environment, the pyrimidine biosynthesis pathway is not a viable drug target, although any interruption of pyrimidine supply was lethal.

Table of Contents

List of Tables

List of Figures

Acknowledgement

First of all, I acknowledge and thank God for his blessing, insight and support, which insure my success.

I wish to express my gratitude to my supervisor Dr. Harry De Koning, his suggesting the topics, valuable advice and critical corrections during my PhD study.

I would like to thank my assessors, Prof. Mick Turner and Prof. Sylke Muller, for their advice and support. I would also like to thank Prof. Mike Barrett for unlimited scientific sources.

I also would like to thank all our collaborators: Dr. Darren Creek, Dr. Bernardo Foth, Prof. George Cross, Dr. Liam Morrison, Dr. Pascal Maser, Dr. Harriet Allison, Dr. Mark Field, Dr. Karl Burgess, Dr Jane Munday and Anne Donachie.

Very special thanks to my family back in Libya and here in Glasgow for their support and encouragement through my study.

I would also like to thank all my fellow students and the staff of GBRC, Division of Infection, Immunity & Inflammation (University of Glasgow), in particular those in the Harry De Koning group (previous and current members) who contribute in this project for their collaboration and support.

Many thanks to Mike Barrett's group and Jeremy Mottram's group (previous and current members).

Author's declaration

I declare that, except where explicit reference is made to the contribution of others, this dissertation is the result of my own work and has not been submitted for any other degree at The University of Glasgow or any other institution.

List of abbreviations

AAT	Animal African Trypanosomiasis
AAT	Amino acid transporter
ABC	ATP-binding cassette transporters
ADP	Adenosine diphosphate
AIDS	Acquired immunodeficiency syndrome
AmB	Amphotericin B
AMP	Adenosine monophosphate
ANOVA	Analysis of variance
ATP	Adenosine triphosphate
AVG	Average of mean values
AZT	Zidovudine
BBB	Blood brain barrier
bp	Base pair
BSF	Bloodstream form
Ca^{2+}	Calcium ion
cATP	Cyclic adenosine triphosphate
CBSS	Carter's balanced salt solution
CDP	Cytosine diphosphate
CFSPH	The Centre for Food Security and Public Health
cGTP	Cyclic guanosine triphosphate
Ci/mmol	Curies per millimole
CL	Cutaneous leishmaniasis
CMP	Cytosine monophosphate
CNS	Central nervous system
CNT	Concentrative nucleoside transporter
CNV	Copy number variation
CSF	Cerebrospinal fluid
CTP	Cytosine triphosphate
dADP	Deoxy-adenosine diphosphate
dAMP	Deoxy-adenosine monophosphate
dATP	Deoxy-adenosine triphosphate
dCDP	Deoxy-cytosine diphosphate
dCMP	Deoxy-cytosine monophosphate
dCTP	Deoxy-cytosine triphosphate
DDT	Dichlorodiphenyltrichloroethane

DEPC	Diethyl pyrocarbonate
DFMO	□-Difluoromethylomithine
dGDP	Deoxy-guanosine diphosphate
dGMP	Deoxy-guanosine monophosphate
dGTP	Deoxy-guanosine triphosphate
DHFR	Dihydrofolate reductase
DHFR-TS	Dihydrofolate reductase - thymidylate synthase
DHODH	Dihydroorotate dehydrogenase
DMSO	Dimethyl sulfoxide
DNA	Deoxyribonucleic acid
DP	Maximum coverage quality
dTDP	Deoxy-thymidine diphosphate
dTMP	Deoxy-thymidine monophosphate
dTTP	Deoxy-thymidine triphosphate
dUTPase	Deoxyuridine 5'-triphosphate nucleotidohydrolase
EC	Enzyme code number
EC_{50}	Half maximal effective concentration
EDTA	Ethylenediaminetetraacetic acid
ELISA	Enzyme-linked immune-sorbent assay
ENT	Equilibrative nucleoside transporter
F-2'dCyd	Fluoro-2'-deoxycytidine
F2'dURes	Resistant line to 5-fluoro-2'-deoxyuridine
F-2'dUrd	Fluoro-2'-deoxyuridine
FACS	Fluorescence activated cell sorting
FAD	Flavin adenine dinucleotide
FBS	Fetal bovine serum
FCS	Fetal calf serum
Fig.	Figure
FOA	Fluoroorotic acid
FOARes	Resistant line to 5-fluroorotic acid
FU	Fluorouracil
F-Urd	Fluorouridine
FURes	Resistant line to 5-fluorouracil
GDP	Guanosine diphosphate
GlcNAc	N-Acetylglucosamine
GMP	Guanosine monophosphate
GPI	Glycophosphatidylinositol

GTP	Guanosine triphosphate
h	Hour
HAPT	High affinity pentamidine transporter
HAT	Human African Trypanosomiasis
HDL	High Density Lipoprotein
HILIC-LC	Hydrophilic interaction-liquid chromatogram
HIV	Human immunodeficiency virus
HMI-9	Hirumi's medium 9
HMI-9+tmd	Hirumi's medium 9 with thymidine
HMI-9-tmd	Hirumi's medium 9 without thymidine
HMM	Hidden Markov model
HOMEM	Eagle's minimal essential medium
HSVTK	Herpes simplex thymidine kinase
IC$_{50}$	50% inhibitory concentration
IDEOM	Identification and Evaluation of. Metabolomics data
ITS	Internal transcribed spacer
Kg	Kilo gram
Ki	Inhibitor constants
KO	Knockout
L	Litter
LC	Liquid chromatogram
LdNT	*Leishmania donovani* nucleoside transporter
LHPT	Low affinity pentamidine transporter
LmajNT	*Leishmania major* nucleoside transporter
LmajTK	*Leishmania major* thymidine kinase
LmajU	*Leishmania major* uracil transporter
LmexNBT	*Leishmania mexicana* nucleobase transporter
LmexU	*Leishmania mexicana* uracil transporter
M	Molar
MCL	Mucocutaneous leishmaniasis
Mg	Milligram
mHCT	Micro-hematocrit centrifugation
min	Minute
Ml	millilitre
mM	Millimolar
MQ	Minimum mapping quality
mRNA	Messenger ribonucleic acid

NAD	Nicotinamide adenine dinucleotide
Ng	Nanograms
OMP	Orotate monophosphate
OPF	Open reading frame
OPRT	Orotate phosphoribosyl transferase
P2	Amino purine transporter
PBS	Phosphate buffered saline
PCF	Procyclic form
PCR	Polymerase chain reaction
PKDL	Post Kalazar dermal leishmaniasis
PRPP	5-Phosphoribosyl 1-pyrophosphate
PSG	Phosphate-buffered saline plus glucose
PYR6-5$^{-/-}$	Pyrimidine auxotrophic-single knockout
PYR6-5$^{+/-}$	Pyrimidine auxotrophic-double knockout
QUAL	A minimum quality core
RNA	Ribonucleic acid
RNAi	Ribonucleic acid interference
RNR	Ribonucleoside-diphosphate reductase
rpm	Revolutions per minute
RQ	Relative quantification
RT	Reverse transcriptase
s	Second
SB^{III}	Trivalent antimonials
SbV	Pentavalent antimonials
SDM-79	Semi defined medium 79
SDS	Sodium dodecyl sulphate
SE	Standard error of mean
SNP	Single nucleotide polymorphism
STH	Serine transhydroxymethylase
TAE	Tris acetate buffer
TbAT1	*Trypanosoma brucei* adenosine transporter
Tbb	*Trypanosoma brucei brucei*
TbC	*Trypanosoma brucei* cytosine transporter
TbNBT	*Trypanosoma brucei* nucleobase transporter
TbT	*Trypanosoma brucei* thymidine transporter
TbU	*Trypanosoma brucei* uracil transporter
TdlK	Thymidylate kinase

TDP	Thymidine diphosphate
TE	Tri-EDTA
TIC	Total ion chromatogram
TK	Thymidine kinase
TLF	Trypanolytic Factor
Tmd	Thymidine
TMP	Thymidine monophosphate
TS	Thymidylate synthase
TTP	Thymidine triphosphate
UDP	Uridine diphosphate
UMP	Uridine monophosphate
UNAIDS	The United Nations Programme on HIV/AIDS
UP	Uridine phosphorylase
UPRT	Uracil phosphoribosyl transferase
UTP	Uridine triphosphate
UTR	Un-translated region
Vmax	Maximal velocity
VSG	Various Surface Glycoprotein
VSL	Visceral leishmaniasis
WHO	World Health Organization
WT	Wild type
μM	Micromolar

CHAPTER ONE

Introduction

The protozoan order Kinetoplastid contains several parasites and has the following systematic position: Phylum Protozoa, Subphylum Sarcomastigiphora, Superclass Mastigophora, and Class Zoomastigophora. The crucial genera belonging to this group are *Trypanosoma* and *Leishmania*, which cause the most significant human and veterinary diseases, trypanosomiasis and leishmaniasis, respectively.

1 - Trypanosomiasis

1.1 Epidemiology and life cycle

African trypanosomiasis encompasses a number of important animal and human diseases and results from infection with protozoan parasites of the genus *Trypanosoma*. The disease occurs in 37 sub-Saharan countries (Figure 1.1), where there are suitable habitats for its vector, the tsetse fly. Most of these countries are among the least developed in the world (WHO, 2006). African trypanosomes are a monophyletic group of unicellular parasitic flagellate protozoa and belong to the family Trypanosomatidae, genus *Trypanosoma* which has several species, subspecies and strains. Trypanosomiasis affects both animals (animal African trypanosomiasis, AAT) and people (human African trypanosomiasis, HAT).
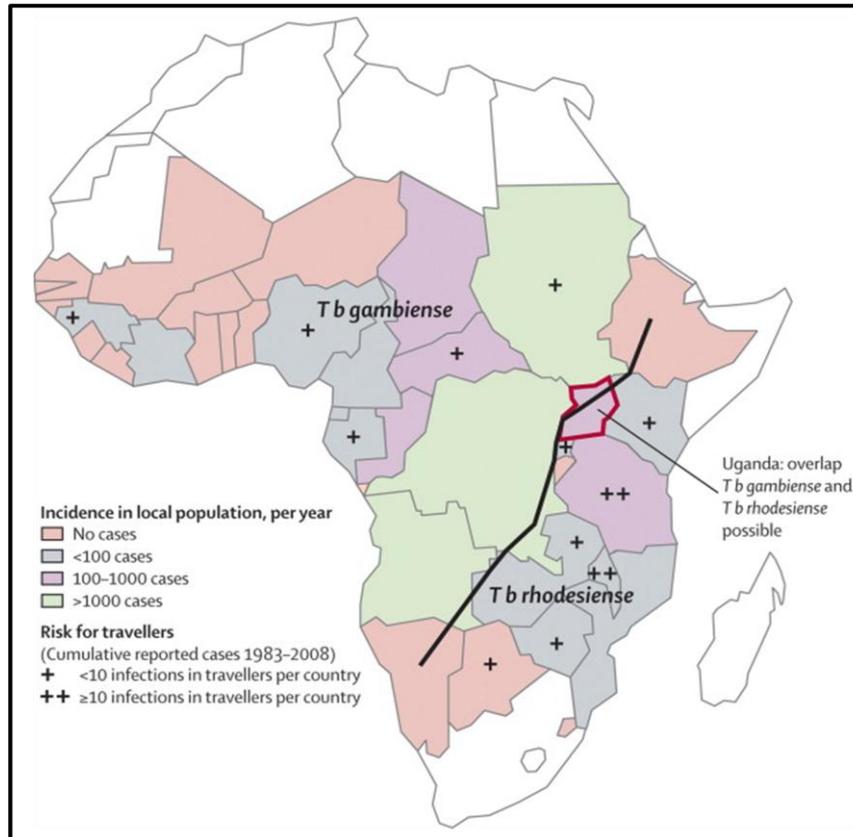
Figure 1.1. Human African trypanosomiasis in affected countries. The black line denotes the boundary between *T. b. gambiense* and *T. b. rhodesiense*. Obtained from (Brun *et al.,* 2010).

AAT is caused by different parasitic species and subspecies of the *Trypanosoma* genus such as *T. brucei, T. congolense, T. vivax, T. simiae* and *T. evansi*.(Grootenhuis *et al.,* 1990). Animals can also be infected by *T. brucei gambiense* (WHO, 2006). The disease affects many wild and domestic animal species. The main effect of AAT on economic development of the rural areas concerns domestic animals, especially cattle (in cattle the disease is called Nangana). The disease leads to direct losses from AAT in livestock, and costs animal producers and consumers an estimated $1340 million per year (Kristjanson *et al.,* 1999). The main losses are connected to cattle mortality and morbidity, diagnosis, treatment costs and the decrease in agricultural production. In Africa, it is estimated that over an area of 8.7 million Km^2 approximately 46 million cattle are exposed to the risk of the disease (Reid *et al.,* 1995). The prevalence of AAT is influenced by the age and breed of the animal (but not sex) and the season of the year (Kalu, 1995).

Although untreated animals infected with *T. brucei* eventually die (CFSPH, 2009), this subspecies is non-infectious to humans because of its

sensitivity to a human serum factor that lyses the parasite (Hager & Hajduk, 1997). The trypanolytic activity is linked to high-density lipoprotein (HDL) particles (Rifkin, 1978; Rifkin, 1991), especially HDL3 (Lorenz *et al.,* 1995). Two proteins in human HDL have been suggested to be the trypanolytic factor (TLF): hepatoglobin-related protein (Drain *et al.,* 2001; Lugli *et al.,* 2004) and apolipoprotein L1 (Perez-Morga *et al.,* 2005; Vanhamme *et al.,* 2003). Trypanosomes transport these particles by receptor-mediated endocytosis and the toxicity is related to this uptake. However, separate reports found that, in rare cases, trypanosomiasis in man might also be caused by normally non-human pathogenic trypanosome species such as *T. congolense* (Truc *et al.,* 1998), *T. evansi* (Joshi *et al.,* 2005) and *T. b. brucei* (Deborggraeve *et al.,* 2008).

HAT, or sleeping sickness, has two classical forms, which mainly differ according to incubation time. The acute form is caused by *Trypanosoma brucei rhodesiense* parasites and occurs in eastern and southern Africa, and the chronic form is connected to *Trypanosoma brucei gambiense* found in western and central Africa (Figure 1.1). However, the separation between *T. b. gambiense* and *T. b. rhodesiense* could soon change because the continued spread of *T. b. rhodesiense* in Uganda towards the northwest might lead to an overlap in the distribution of the two forms of the disease (Kim *et al.,* 2005). Furthermore, it is now recognised that this dichotomy between the two trypanosomes is not fully representative of the disease process (Courtin *et al.,* 2008). HAT is usually fatal in the absence of treatment. The situation in Africa is that approximately 60 million people are at risk of infection with 3-4 million people under surveillance (Cattand *et al.,* 2001). Although (WHO, 2012) reported a decline in the number of new cases in 36 endemic countries by 28% in 2010 compared with 2009 and currently it is estimated that there are 30,000 cases of the disease, the incidence remains high in some countries such as the Congo (500 reported cases in 2010). A recent study has found that around 10000 sleeping sickness cases were reported in 2009 (Simarro *et al.,* 2011). The re-emergence of HAT could be partly attributed to decreased surveillance and control activities, the appearance of parasite and vector chemical resistance, host disease susceptibility, war and migrations of populations (Courtin *et al.,* 2008). In addition, no successful vaccine against HAT is available (Malvy & Chappuis, 2011).

Transmission

Trypanosomes are transmitted by blood-feeding tsetse flies, a grey-brown insect. Both females and males can transmit the disease from one mammalian host to another (Aksoy *et al.,* 2001). Repeated feeding on the same host species by a tsetse fly is likely to increase the disease-transmission risk. About 30 species and subspecies of tsetse flies belong to the genus *Glossina,* the only genus in the family Glossinidae, and they show different abilities to transmit trypanosomiasis (Jordan, 1993). *Glossina* spp infest 10 million Km^2 of the continent of Africa (Rogers & Randolph, 1986) and occupy an area from approximately latitude 14° north to 20° south (Steverding, 2008). *Glossina palpalis* and *G. tachinoides* transmit chronic trypanosomiasis in West Africa, and *G. fuscipes* in central Africa, whereas *G. morstans*, *G. swynnertoni* and *G. pallidipes* are responsible for the acute form of trypanosomiasis (Service, 1996). A control of the trypanosomiasis transmission from their invertebrate host is important in the disease management. Decades ago, several of trypanosomiasis control methods reduced the prevalence of the disease through the use of insecticides (i.e. a DDT spray) and the clearance of vegetation. However, these tools are undesirable because of the environmental pollution, constrain agricultural production and reduce livestock supply. Moreover, the tsetse flies become resistance and tolerant to the used dose of chemical insecticides (Allsopp, 2001). An alternative method used to save the environment and food chain process is trapping insect hosts using fabric traps with attractive shape and colour. Recently, sterile insect techniques have been introduced to interrupt the transmission of parasites. For instance, sterilizing insect males by irradiation and releasing masses of them to target a selected area (where the highest insect population is) led to a significant reduction in the invertebrate host number (Aksoy, 2003; Vreysen *et al.,* 2000).

In addition, transmission of trypanosomiasis can occur by contaminated needles or blood transfusion, or the congenital route (Barrett *et al.,* 2003). Children can be infected via their mothers by the disease crossing the placenta and infecting the foetus causing abortion or perinatal death (De Raadt, 1985; Debroise *et al.,* 1968; Lindner & Priotto, 2010).

Life cycle

African trypanosomes undergo several changes during the transmission process between the blood of the mammalian host and the gut of the tsetse fly (Matthews, 1999;Vickerman, 1985), when the parasite passes from the glucose-rich environment (the bloodstream in the mammalian host) to the insect midgut, its form is changed and the amino acid proline becomes the main source of energy (Ford & Bowman, 1973; Overath *et al.,* 1986). Parasites migrate from gut to salivary glands and emerge as mammal-infective metacyclic trypanosomes. When an infected tsetse fly (genus *Glossina*) takes blood from a mammalian host, it injects metacyclic trypomastigotes into skin tissue. In mammalian cells, the parasite proliferates as long slender forms. The most crucial changes in parasite cells occur in its mitochondrial system as this adapts via changes in their energy metabolism and in the surface membrane to escape the mammalian host's immune defence system (Vickerman, 1971). The attack by parasites triggers the mammalian antibody responses, leading to a sequential expression of variable surface glycoproteins (VSGs) which are connected to the surface membrane by a glycosylphosphatidylinositol anchor (McCulloch, 2004; Pays *et al.,* 2004). The trypanosome genome expresses approximately 1000 gene-encoding sequences for these VSGs (Borst, 2002). Non-proliferative stumpy forms replace the slender trypomastigotes as the parasitemia count decreases (Matthews *et al.,* 2004; Vickerman, 1985). What is more important is that this change arrests stumpy forms in the G1 phase of the cell cycle that serves for the re-entry into the cell cycle after transmission to the tsetse fly (Matthews, 2005). When bloodstream forms are ingested by *Glossina* spp, the short stumpy form rapidly differentiates into procyclic trypomastigote within the posterior part of the tsetse midgut in the endoperitrophic space (Vickerman, 1985), and replaces the VSG coat with a less dense surface coat of glycosylphosphatidylinositol-anchored proteins known as procyclines (Roditi & Liniger, 2002), and the energy supply is also changed from glycolysis to a mitochondrion-based respiratory system, which demands a complicated metabolomic process (Matthews, 2005). After a few days of infection, the procyclic form proliferates, differentiates to the long trypomastigote (proventriculus form) and migrates via the oesophagus, mouthparts and salivary ducts to establish infection in the salivary glands, then transforms to epimastigotes (Van Den Abbeele *et al.,* 1999; Vickerman, 1985).

Epimastigotes transform into uncoated premetacyclics, which become metacyclics - the infective stage. Once the parasite undergoes division arrest during the metacyclic stage, it requires a VSG coat and is released into the salivary glands, where it is ready to infect new mammalian host (Figure 1.2). The cycle in the fly takes about three weeks to progress.
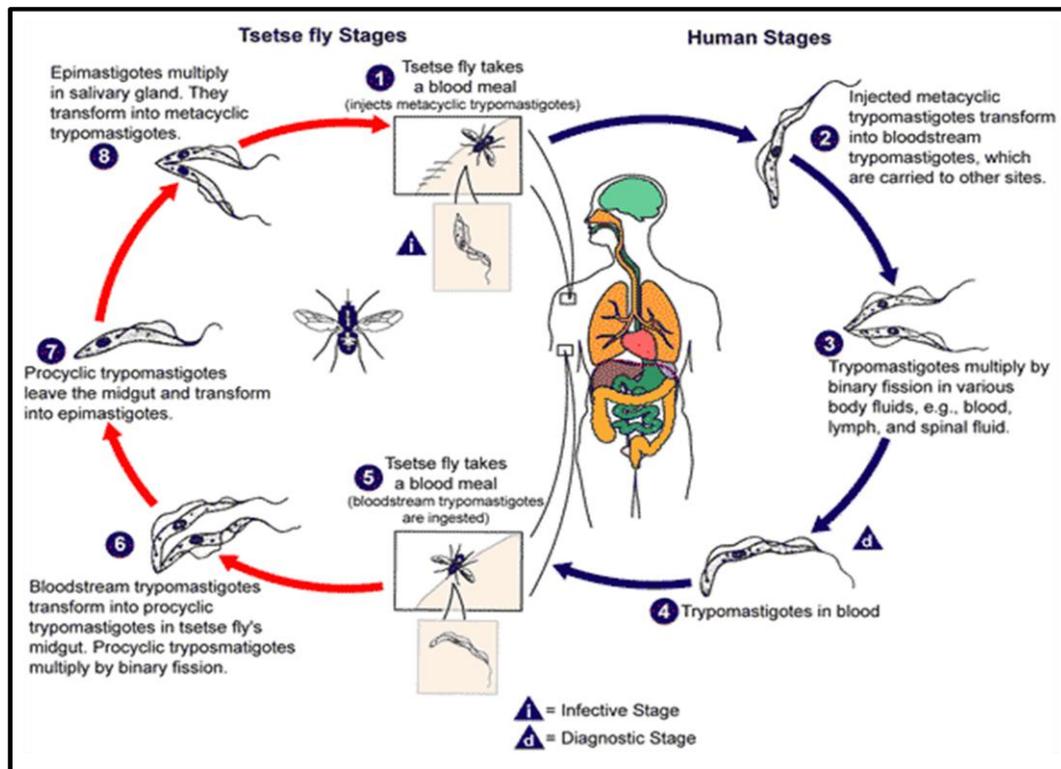
Figure 1.2. life cycle of *Trypanosoma* species. Reproduced from The Centres for Disease Control (http://dpd.cdc.gov/dpdx).

1.2 Pathology

In African animal trypanosomiasis, the incubation time takes between four days to several weeks, and the signs on the localised site of the insect bite are usually unclear (CFSPH, 2009). The parasite rapidly invades the blood in the first days of infection. However, describing clinical symptoms of trypanosomes is difficult because infections with more than one species of trypanosomes frequently occur, as well as infection occurring at the same time with other hemo-parasites being common (Nyeko *et al.,* 1990). The most important clinical symptom is anaemia, which becomes severe two months post-infection, with other clinical signs being intermittent fever, weight loss, oedema, diarrhoea and appetite loss (CFSPH, 2009). In the cases of HAT, trypanosomes are located inside the inoculation lesion of the bite for several days, and then multiply in

blood and lymph tissues. The chancre is usually the first symptom of HAT, primarily for *T. b. rhodesiense*. African trypanosomiasis is classified into two stages: the first stage of the disease is known as the haemolymphatic phase and it occurs during parasite proliferation in the blood and lymph systems. Within stage I, several nonspecific features may occur such as intermittent fever because of the high and low number of parasites, and various parasitemia as a result of various antigenic reactions. Other symptoms may be encountered: lymphadenopathy, pruritus, oedemas, headaches, anorexia, anaemia and hyperesthesia. According to stage I duration, the HAT occur in two forms. In acute infection, stage I may last for only a few weeks, whilst in the chronic form it lasts several years (Barrett *et al.*, 2003).

The following stage is the neurological phase and this begins when the parasite crosses the blood brain barrier (BBB) and invades the central nervous system. A characteristic disturbance of the sleep cycle, which gives the disease its name, is an important feature of the second stage of the disease. Symptoms related to African trypanosomiasis infection vary according to parasite strains and species, host type and environmental factors (Courtin *et al.*, 2008). For example, procyclic forms of *T. b. gambiense* do not cross the *in vitro* model of the human BBB, whereas human-infective bloodstream forms cross it much more efficiently than animal-infective *T. b. brucei* (Nikolskaia *et al.*, 2006). In West African forms of sleeping sickness, the expansion of the neurological stage does not occur for decades. However, invasion of the CNS in East African sleeping sickness occur within weeks. The appearance of neurological problems exists mainly in stage II and includes sleeping disorders, hyperesthesia, neuroendocrine dysfunctions, cachexia and finally coma (Courtin *et al.*, 2008).

Diagnosis

Despite exhibiting various symptoms, AAT is difficult to diagnose unless the parasite is detected via detecting the parasite under microscope examination of the blood or by serological reaction (CFSPH, 2009). There are many parasite detection methods that are currently available for field use. Parasitological diagnosis is based on microscopic examination of the blood. This is simply done by staining the organism in a blood film using Giemsa's stain.

Unfortunately, this parasitological method is limited by the irregular number of trypanosomes, especially in case of *T. b. gambiense* infection where the numbers are typically 10^3 and sometimes fall below 10^2 cells/ml (Chappuis *et al.,* 2005).

The blood concentration technique of microhematocrit centrifugation (mHCT) to investigate HAT has been developed decades ago (Woo, 1971), but it is still in use. In this method, a high speed centrifugation of hematocrit capillary tubes can concentrate the parasites between the plasma and the erythrocytes. However, this simple technique is considered time-consuming and needs skilled workers (Chappuis *et al.,* 2005). The mini-anion-exchange centrifugation technique (mAECT) introduced by (Lumsden *et al.,* 1979) is more sensitive than the thick blood film and mHCT techniques, especially when the method was updated by (Zillmann *et al.,* 1996). The techniques are based on isolating the parasites from blood veins by anion-exchange chromatography, the isolate is slowly centrifuged, then the trypanosomes can be examined using a microscope, but the manipulations in this technique are tedious and time-consuming. In vitro culture and animal inoculation is also used as way of diagnosis (Aerts *et al.,* 1992). However, some obstacles limit this method such as the high cost and the long delay before obtaining results. Furthermore, this method is not recommended in the case of *T. b. gambiense* infection because this species grows poorly in laboratory rodents (Garcia, 2007).

In the second stage of HAT, WHO recommends cerebrospinal fluid (CSF) examination, which can be obtained by lumber puncture. This test relies on the presence of >5 cells per micro litre and/or >370 mg per litre of trypanosomes in cerebrospinal fluid (WHO, 1998). These are counted by the dye-binding protein assay. Immunofluorescence assays have also been successfully used for HAT diagnosis such as enzyme-linked immune-sorbent assay (ELISA) methods, which can detect specific antibodies in the salvia from patients to confirm HAT (Lejon *et al.,* 2003).

1.3 Chemotherapy

Without treatment, sleeping sickness is thought to be almost invariably fatal, especially if it has progressed to the neurological stage. The membrane of trypanosomes in mammals is almost completely covered with VSG, which is the main antigenic determinant for the human immune system (Sternberg, 1998). In addition, the genome of *Trypanosoma* contains about 10^3 genes capable of coding for VSG genes, which are randomly switched on and off at each generation (Donelson *et al.,* 1998). The variant-specific glycoprotein coat enables the parasite to escape destruction by the host immune system (Matthews, 2005) and ultimately cause a fatal invasion of the CNS. Due to the highly variable nature of the glycoprotein coat, all attempts to discover an efficient vaccine have met with little success. This immune mechanism is a major obstacle to developing a successful vaccine. Therefore, the only available option to control HAT is through chemotherapy or vector control. Although chemotherapy for trypanosomiasis has been available since the early 20th century, no ideal drugs have been discovered. There are four trypanosomal drugs currently licensed for the treatment of HAT.

1.3.1 Pentamidine
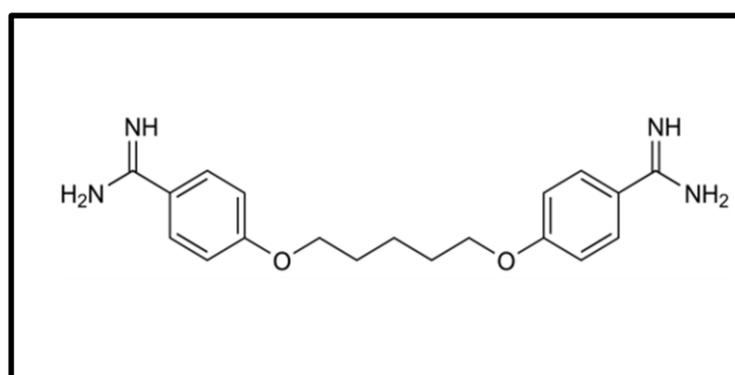
Figure 1.3. Chemical structure of pentamidine.

Pentamidine (Figure 1.3), which is a water-soluble aromatic diamidine drug, was introduced in 1941 to treat early stage trypanosomiasis. The drug is given by intramuscular injections of 4 mg/kg (Jannin & Cattand, 2004). It has been reported that the drug can be taken up by three different transporters: the P2 aminopurine transporter (Carter *et al.,* 1995), the high affinity pentamidine transporter (HAPT1) and the low affinity pentamidine transporter (LAPT1) (De

Koning, 2001). Many studies have focused on the mode of action of pentamidine and the consensus is now that it has a multifactorial impact; as such, its target has not conclusively been defined. Pentamidine is known to bind to mitochondrial DNA and eventually leads to the development of dyskinetoplastic forms (Barrett *et al.,* 2007), but the drug has no effect on nuclear DNA. Recently, (Moreno *et al.,* 2010) found that pentamidine targets the minor groove of DNA where the level of purine nucleobase adenine and its counterpart pyrimidine nucleobase thymine are highly concentrated. Other targets previously studied in trypanosomes were the inhibition of the polyamine biosynthetic pathway, glycolysis and lipid metabolism, as well as effects on amino acid transport and ion exchange. However, it has been reported that pentamidine is effective against early stage *T. b. gambiense* infection, but it is less effective against *T. b. rhodesiense* infection, and is ineffective against the late stage disease (Barrett *et al.,* 2007; Wang, 1995). In addition, the drug has some side effects such as vomiting, abdominal pain and hypoglycaemia (Legros *et al.,* 2002).

Another aromatic diamidine drug is diminazene aceturate (berenil), which has been developed and licensed for veterinary use. It has also been found that the drug is effective against the early stage of *T. b. gambiense* and *T. b. rhodesiense* infections. Moreover, it has been used in combination with melarsoprol for the late stage of the disease. Diminazene uptake via the P2 transporter has been confirmed by using ^{3}H-diminazene (De Koning *et al.,* 2004) or TbAT1 knockout cells (Matovu *et al.,* 2003), indicating that the P2 transporter is the main route of the drug uptake. Like pentamidine, berenil mode of action is linked to kinetoplast DNA binding (Wang, 1995). However, it is proposed that the drug can inhibit topoisomerase II and is believed to interfere in the trypanothione metabolism by inhibiting the decarboxylation of S-adenosylmethionine (Gomes-Cardoso *et al.,* 1999). Although diminazene uptake occurs via the P2 transporter, the other pentamidine transporters, LAPT1 and HAPT1, seem to play a minor role in its transportation (De Koning,2001). However, there is little published on the toxicity of diminazene (Delespaux & De Koning,2007).

1.3.2 Suramin
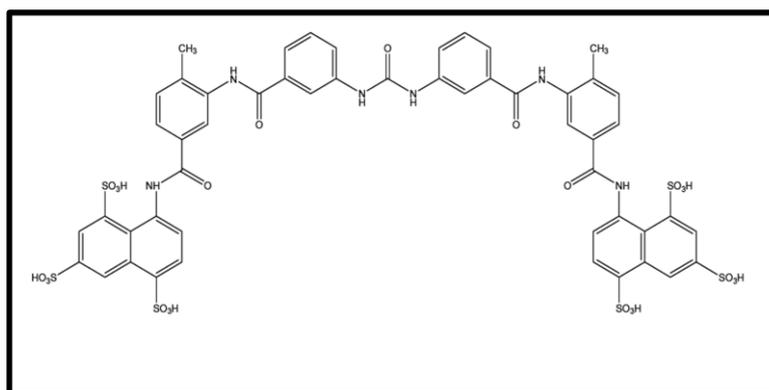
Figure 1.4. chemical structure of suramin

Suramin (Figure 1.4) is a sulfonated naphthylamine polyanionic compound. It has been used to treat the early stage of HAT, particularly of disease caused by *T. b. rhodesiense*, for almost a century, but not the neurologic stage, because the drug does not cross the BBB in concentrations that are able to kill the parasites in the cerebrospinal fluid at doses given to treat the early stage disease. The used dose of suramin is 20 mg/kg/day for five days (Jannin & Cattand, 2004). The main route of suramin entry is through endocytosis (Fairlamb & Bowman, 1980). The drug is negatively charged at physiological pH and is intensively bound to a number of serum proteins, including low-density lipoprotein LDL (Vansterkenburg *et al.,* 1993). Although some suggest that suramin enters during binding to LDL (Bastin *et al.,* 1996; Coppens & Courtoy, 2000), one study suggests that suramin action is not dependent on the LDL receptor (Pal *et al.,* 2002). A recent study reported that suramin action might be mediated via the ISG75 protein family in bloodstream forms (Alsford *et al.,* 2012). It has been found that suramin is a potent inhibitor for 6-phosphogluconate dehydrogenase, which catalyses the oxidative decarboxylation of 6-phosphogluconate to ribulose 5-phosphate in the pentose phosphate pathway (Hanau *et al.,* 1996). Common side effects of the drug are neuropathy, rash, fatigue, anaemia, hyperglycaemia, hypocalcaemia, coagulopathies, neutropenia, renal failure (Barrett *et al.,* 2007) and hypoesthesia, which involved a reduced sense of touch, or a partial loss of sensitivity to sensory stimuli (Legros *et al.,* 2002).

1.3.3 Melarsoprol
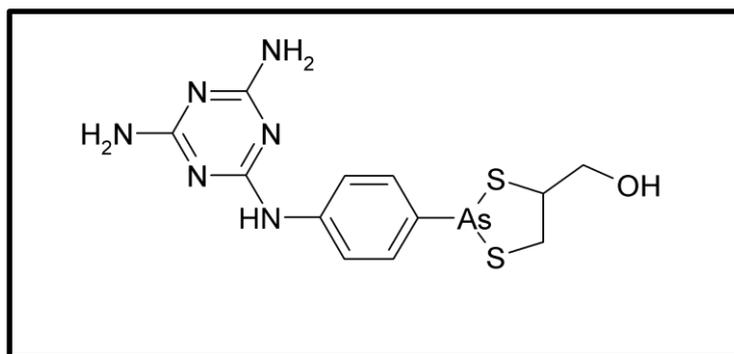
Figure 1.5. Chemical structure of melarsoprol.

Melarsoprol (Figure 1.5), a melaminophenyl-based organic arsenical, was discovered at around the middle of the 20th century (Friedheim, 1949) to treat the late stage of HAT because of its ability to cross the BBB and accumulate in the CNS (Burri *et al.,* 1993). Therefore, it remains the most widely used drug to treat late stages of HAT. It is administered as a 3.6% solution in propylene glycol and the used regimen dose is 2.2 mg/kg for ten consecutive daily intravenous injections (Burri *et al.,* 2000). The drug is amphipathic so that it can diffuse across cellular membranes and rapidly convert to hydrophilic melarsen oxide in plasma (Burri *et al.,* 1993), both melarsoprol and its metabolites cross the BBB. However, the levels of the drug in cerebrospinal fluid might be insufficient to kill all parasites, at least in all patients (Hunter *et al.,* 1992; Jennings, 1995). Several studies proposed that melarsen oxide enters *T. brucei* via the P2 transporter (Carter & Fairlamb, 1993; Maser *et al.,* 1999) or that other transporters are able to carry the drug (Matovu *et al.,* 2003). Melarsoprol, being lipophylic can diffuse across the parasite plasma membrane, but its metabolite melarsen oxide does not do so (Scott *et al.,* 1997). Although exposing trypanosomes to melarsoprol leads to immediate cell lysis (Carter *et al.,* 1995), the mode of action of the drug is still unclear. However, some suggest that melarsen oxide interferes with the glycolytic pathway (Flynn & Bowman, 1974) and inhibits enzymes that produce ATP (Denise & Barrett, 2001). Among the enzymes affected by melarsen oxide is pyruvate kinase. *In vitro* and *in vivo* study found that dihydrotrypanothione combined with melarsen oxide to form a competitive inhibitor of trypanothione reductase (Fairlamb *et al.,* 1989). Melarsoprol has many severe side effects such as a reactive encephalopathy and heart failure (Blum *et al.,* 2001). Other reported common features include fever, headache, pruritus and thrombocytopenia.

1.3.4 Eflornithine
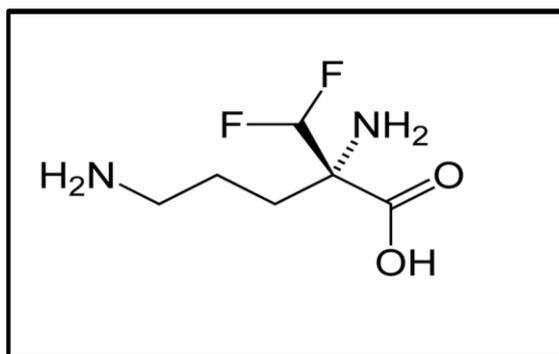
Figure 1.6. Chemical structure of eflornithine

Eflornithine or α-difluoromethylomithine (DFMO; Figure 1.6) is an analogue of the amino acid ornithine. The drug is currently considered as the first-line treatment for late stage *T. b. gambiense* sleeping sickness (Balasegaram *et al.*, 2006). DFMO inhibits the polyamine biosynthetic enzyme ornithine decarboxylase (Bacchi *et al.*, 1980). The recommended dose is 400 mg/kg/day intravenously at 6 hour intervals for 14 days (Barrett *et al.*, 2007). Eflornithine is taken up in mammalian cells by passive diffusion (Erwin & Pegg, 1982) and was believed to cross the plasma membrane of bloodstream trypanosomes via passive diffusion (Bitonti *et al.*, 1986). However, recent separate studies have found that the *T. b. brucei* AAT6 amino acid transporter is involved in DFMO uptake (Baker *et al.*, 2011; Schumann Burkard *et al.*, 2011;Vincent *et al.*, 2010), the same manuscripts attributed DFMO drug resistance to loss of AAT6 transporter. DFMO action on polyamine biosynthesis causes an increase of S-adenosyl methionine at the cellular level (Yarlett & Bacchi, 1988), which leads to unsuitable methylation of cell elements such as nucleic acids, lipids and proteins. (Fairlamb *et al.*, 1987) reported a decrease of trypanothione levels after treatment with DFMO. One drawback of eflornithine could be its similar efficacy on both the parasite and mammalian host ornithine decarboxylase (ODC) (Garofalo *et al.*, 1982; Phillips *et al.*, 1988), and it binds either enzyme irreversibly. The selective action against *T. brucei* is the result of the trypanosomal enzyme being very stable, whereas mammalian ODC is very rapidly replaced (Delespaux & De Koning, 2007). The side effects of eflornithine are diarrhoea, hallucinations, pancytopenia and convulsions (Legros *et al.*, 2002).

1.3.5 Nifurtimox
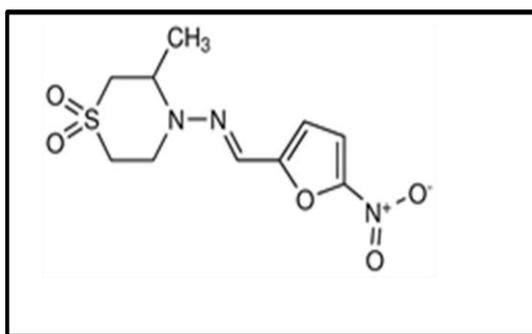
Figure 1.7. Chemical structure of nifurtimox

Nifurtimox (Figure 1.7) was discovered empirically decades ago (Cerecetto & Gonzalez, 2002) and it is a 5-nitrofuran derivative used as a front line drug to treat Chagas' disease caused by *Trypanosoma cruzi* in South America (Docampo, 1990; Gutteridge, 1985). However, as a mono-therapy against *T. b. gambiense* in West Africa, the drug has limited efficacy (Pepin *et al.,* 1989). Against *T. cruzi* infections, 15 mg/kg/day in three divided doses for two months was the recommended dose (Burri *et al.,* 2004; Ministério & Saúde, 2005; Rassi, *et al.,* 2010). The drug can accumulate across the BBB (Jeganathan *et al.,* 2011). African trypanosomes were not highly vulnerable to nifurtimox in a typical *in vitro* study, with IC_{50} values at around 5 μM (Enanga *et al.,* 2003). Nifurtimox uptake in *T. cruzi* has been found to proceed via passive diffusion across the cell membrane (Tsuhako *et al.,* 1991), but transport of the drug in *T. brucei* has not yet been investigated (Barrett & Gilbert, 2006).

On the other hand, a promising use of nifurtimox in combinations to cure trypanosomiasis has been reported to have succeeded (Bisser *et al.,* 2007; Jennings, 1991; Priotto *et al.,* 2006). For example, (Priotto *et al.,* 2006) combined nifurtimox and eflornithine to treat trypanosomiasis in clinical trials and reported cure rates of more than 94%, but combining melarsoprol with nifurtimox is considered to be toxic and the cure rates were less than half (44.4%). The combination of nifurtimox and eflornithine to treat the late stage of sleeping sickness has also been confirmed by (Checchi *et al.,* 2007) in a clinical study in Uganda and is considered to be the most promising new development for years. It has been published that the nifurtimox mechanism of action is due to free-radical generation through its metabolism; this mechanism starts with a reduction of the NO_2-group to a nitro-anion radical (Maya *et al.,*

2007) and finally produces oxidative stress in the organism itself. Recently, it has been found that 2-electron reduction of nifurtimox is catalysed by type I nitroreductase and produced toxic metabolites (Wilkinson *et al.,* 2011). Although this nitroreductase is a trypanosomal enzyme with no close human homologue, toxic side effects of nifurtimox on the nervous system have been reported (Castro *et al.,* 2006). In addition, the typical dose of the drug used to treat Chagas' disease caused some problems such as nausea and vomiting (Barrett *et al.,* 2007).

1.4 Drug resistance

The resistance to current anti-trypanocidal drugs has become a big public health problem, which may prevent the successful treatment of the disease. In addition, the mechanism of resistance to most chemical trypanocides is still unclear. An increasing incidence of resistance to current drugs has been reported in some parts of sub-Saharan Africa (Afewerk *et al.,* 2000). In some cases, the proposed mechanism of the parasite's resistance to drugs is due to the loss of one or more transport functions in the parasite's cell membrane (De Koning, 2001). Other parasite resistance mechanisms (Figure 1.8) include inactivation, excretion or modification of the drug in the cytoplasm of the parasite (Borst & Ouellette, 1995).
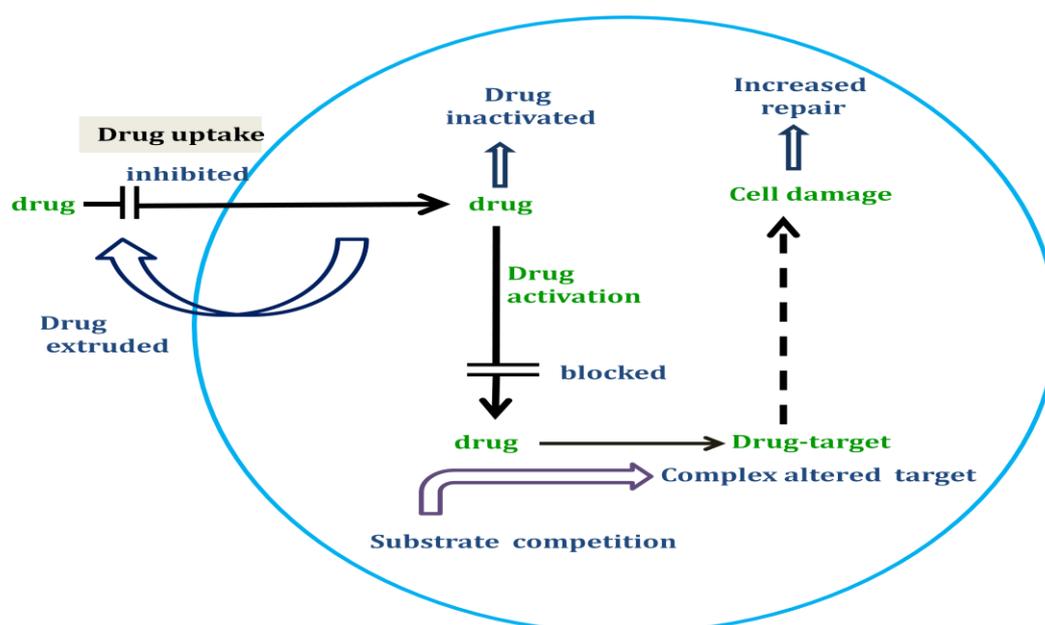
Figure 1.8: The main biochemical mechanisms responsible for drug resistance in protozoal diseases. (Borst & Ouellette, 1995)**.**

It has been demonstrated that the loss of the P2 adenosine transporter function, which mediates the uptake of melarsoprol and diamidines, leads to *T. brucei* resistance to these drugs (Barrett *et al.,* 1995; De Koning & Jarvis, 1999), but pentamidine can enter via other transporters once P2 is lost (De Koning, 2001), which makes the search for the method of resistance developed against this drug difficult. Recently, (Baker *et al.,* 2012) reported that the melarsoprol-resistance trypanosomes with cross resistance to pentamidine is associated with the loss of function of aquaglyceroporins, specifically AQP2; very recently, the same authors have published that this mechanism of resistance may be applicable in clinical conditions (Baker *et al.,* 2013), but in veterinary use the resistance to the drug has been reported in *Trypanosoma* species, such as *T. evansi* (El Rayah *et al.,* 1999; Mutugi *et al.,* 1994). In addition, the selection of cell lines resistant to suramin in the laboratory can readily be achieved (Scott *et al.,* 1997), and the resistance to melarsoprol has been reported in bloodstream forms of *T. brucei rhodesiense* (Bernhard *et al.,* 2007). The resistance mechanism to melarsoprol is related to the selective uptake of organo-arsenicals and to the purine salvage pathway. In strains resistant to melarsen oxide, the loss of P2 transport activity has been reported (Carter & Fairlamb, 1993; Delespaux & De Koning, 2007). The (WHO, 1998) reported an increasing resistance to melarsoprol, reaching 30% in central Africa. In addition, relapse after melarsoprol treatment has been reported in the field (Brun *et al.,* 2001; Legros *et al.,* 1999; Moore & Richer, 2001; Stanghellini & Josenando, 2001). Most parasites selected for resistance to melarsoprol in the laboratory have lost the drug carrier, the P2 transporter (Barrett & Fairlamb, 1999; Carter & Fairlamb, 1993; Maser *et al.,* 1999; Stewart *et al.,* 2005), and isolated parasites from relapse patients have defective aminopurine P2 transporter (Maser *et al.,* 1999; Matovu *et al.,* 2001; Stewart *et al.,* 2005).

Decreased eflornithine uptake has been reported in procyclic forms of *Trypanosoma* (Bellofatto *et al.,* 1987) and they attributed this to the intracellular concentration of N^1, N^8-bis-(glutathionyl)-spermidine. Recently, it was shown that eflornithine resistance in trypanosomes is linked to the loss of Tb927.8.5450: an amino acid transporter gene (Baker *et al.,* 2011; Schumann *et al.,* 2011; Vincent *et al.,* 2010). No drug resistance has been observed in the field (Simarro *et al.,* 2012). *T. cruzi* resistance to nifurtimox has been well

confirmed (Murta *et al.,* 1998); treatment of *T. brucei* has only just recently been introduced, but (Sokolova *et al.,* 2010) reported that the bloodstream forms' resistance to nifurtimox can easily be achieved by in vitro induction. In the absence of alternative drugs and successful vaccine programs, the delay in resistance to available trypanocides should be taken seriously.

2- Leishmaniasis

2.1 Epidemiology and life cycle

Leishmaniasis is a group of parasitic diseases caused by members of the genus *Leishmania*; the parasites were first seen by Cunningham in 1885, and described by Leishman and Donovan in 1903, working separately (Herwaldt, 1999). However, the connection of *Leishmania* to the disease kala-azar was discovered by Bautley in 1904 (Bhamrah & Juneja, 2001). The parasites cause a range of diseases, encompassing cutaneous, mucocutaneous and visceral leishmaniasis. Human and animal leishmaniasis show a wide geographic distribution (Figure 1.9). Leishmaniasis is endemic in 22 countries in the Americas and 88 countries in the rest of the world, most of them in the tropics and subtropical areas (Desjeux, 1996), but it is not endemic in Southeast Asia and Australia (Herwaldt, 1999). With the estimated yearly incidence, there are between 1.5-2 million cases of cutaneous leishmaniasis and half a million cases of visceral leishmaniasis. (Desjeux, 1996) estimated that 350 million people are at risk of leishmaniasis in the world population. More than 90% of the world's cases of visceral leishmaniasis (VL) occur in five countries: India, Bangladesh, Nepal, Sudan and Brazil, whereas 90% of disease caused by cutaneous leishmaniasis (CL) appears in nine countries: Afghanistan, Pakistan, Syria, Saudi Arabia, Algeria, Brazil, Iran and Peru (Desjeux, 2004). The incidence of leishmaniasis has significantly increased over the last few decades (Arias *et al.,* 1996). The prevalence of the disease is more common in men than in women, but this may reflect increased exposure to sand flies. Untreated VL causes a mortality rate of 75–95%, whereas CL may affect the mucosa resulting in death from secondary infection (CFSPH, 2009).
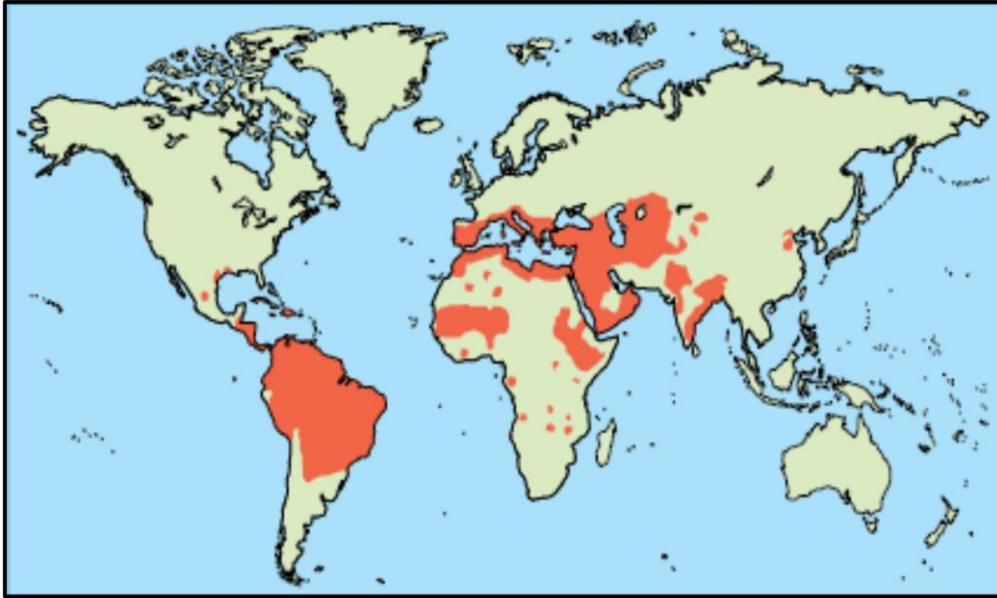
Figure 1.9. Geographical distribution of leishmaniasis. Obtained from (Davies *et al.,* 2003).

Leishmaniasis is considered to be an opportunistic infection that affects HIV-infected people; the majority of co-infection entails the VL form (Desjeux & UNAIDS, 1998). To date, co-infection with leishmaniasis and HIV has been reported in 34 countries in Africa, Asia, Europe and South America (Figure 1.10). In the case of HIV infection, the leishmaniasis cause the symptoms of HIV to occur earlier than expected by increasing immunosuppression and by stimulating multiplication of the virus (Harms & Feldmeier, 2005). This co-existence is increasingly severe, for instance, in Mediterranean European countries about 70% of adult cases of VL are co-infected with AIDS (WHO, 2012).
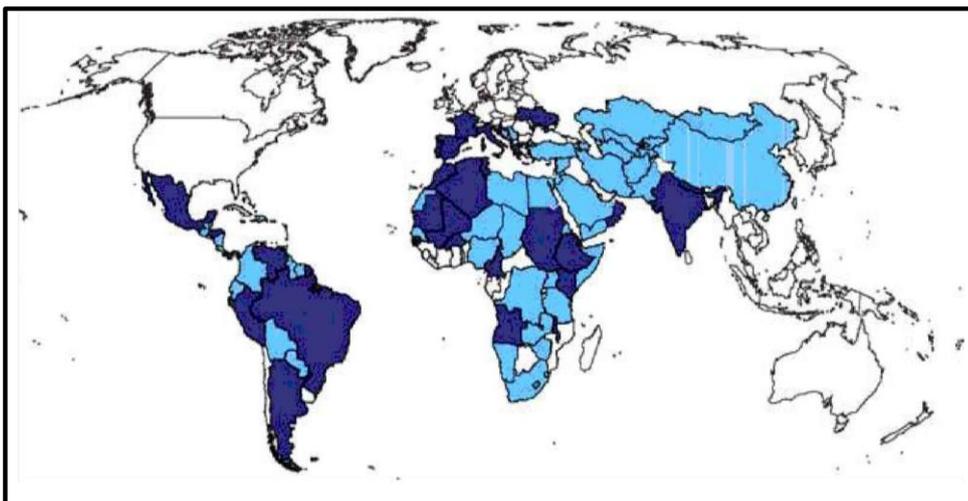
Figure 1.10. World-wide distribution of leishmaniasis ▮ and countries reporting Leishmania/HIV co-infection ▮, obtained from (Desjeux & Alvar, 2003).

Transmission

The distribution of leishmaniasis is connected to the prevalence of the vector. The disease is transmitted from the reservoir host to human beings and animals by the bite of some types of female phlebotomine sand flies – dipteran insects (Bates & Rogers, 2004). 700 species of the insects have been reported, and of these, about 10% have been described as vectors of leishmaniasis (Lane, 1993). The proven vectors of the *Leishmania* parasites are the blood-sucking female of the genus *Lutzomyia* in the Americas and *Phlebotomus* spp in the Old World (Murray *et al.,* 2005). These include *P. argentipes* in India, *P. martini* and *P. orientalis* in Africa and the Mediterranean basin, *P. chinensis* and *P. alexandri* in China and *Lutzomyia longipalpis* in the New World. The host reservoirs of leishmaniasis are animals such as canines and rodents, and humans (Zijlstra & El-Hassan, 2001). Other animals in the surrounding area can become infected and those are referred to as secondary hosts (Arias *et al.,* 1996). Several studies have attempted to reduce leishmaniasis transmissions by targeting the host vector using different methods such as environmental control (i.e. using insecticides such as deltamethrin, malathion and propoxur), prophylactic methods, biological control and remote sensing (WHO, 2010).

Life cycle

The life cycle of *Leishmania* species switches between two shapes (Figure 1.11): flagellated promastigotes in the insect vectors and intracellular amastigotes in the mammalian host (Gossage *et al.,* 2003). Based on *Leishmania* development within the host vector, the genus was subdivided into two subgenera: members of the subgenus *Leishmania* develop exclusively in the midgut and foregut of sand flies, whereas members of the subgenus *Viannia* include a phase of development in the hindgut of their vectors (Lainson & Shaw, 1987). Many species, subspecies and strains infect several mammalian organisms including *Homo sapiens* and are transmitted by the bite of phlebotomine sand flies. The sand-fly vector becomes infected when feeding on the blood of an infected person or an animal reservoir host. *Leishmania* parasites live in the phagolysosomes of macrophages of vertebrate hosts as round-shaped, non-motile amastigotes (3-7 μm in diameter). During the blood meal of the fly, it creates a

wound, which releases skin macrophages and/or freed amastigotes into the pool of blood, and enables their subsequent uptake into the stomach of insects (Lane, 1993). Moving from the bloodstream condition to the transmission vector causes changes in the parasite's life condition such as a decrease in temperature and an increase in the pH, which leads to the development of the parasite in the insect (Bates & Rogers, 2004; Kamhawi, 2006). The first stage in the vector is called procyclic promastigotes. After a few days, the parasite begins to differentiate into elongate forms, non-dividing nectomonad promastigotes, which migrate and accumulate in the alimentary tract of the fly. Some suggest that N-acetylglucosaminidase and chitinase are degraded in the chitin of vertebrate hosts (Schlein *et al.,* 1991). When they move towards the anterior midgut, the nectomonad promastigotes transform into leptomonad promastigotes, which begins the process of parasite multiplication (Gossage *et al.,* 2003). Some of the leptomonads transform to strictly non-dividing metacyclic promastigotes which are the mammal-infective stages (Rogers *et al.,* 2002).
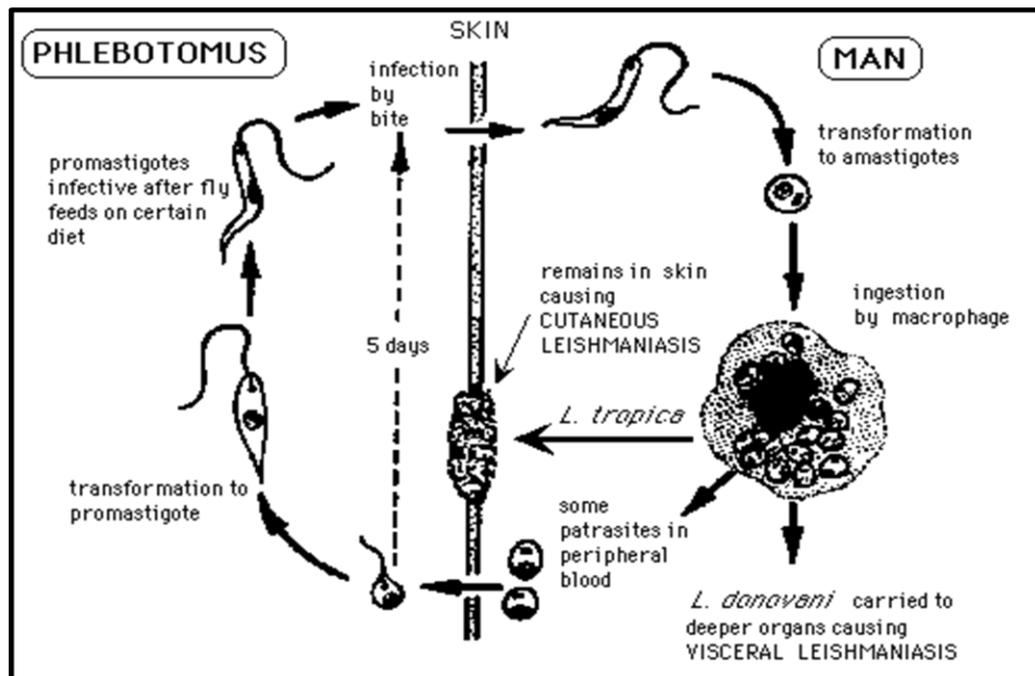
Figure 1.11 *Leishmania* life cycle (Cited from Protozoa as Human Parasites website http://course1.winona.edu/kbates/Parasitology/Images/Leishlifecycle.gif).

The transmission to vertebrate hosts occurs when the infective females feed on the blood of another host leading to the distribution of the disease. In mammalian cells, the macrophage is the main host for the *Leishmania* amastigotes. When the metacyclic promastigotes get into the pool of blood they attach to mononuclear phagocytes by a receptor-mediated mechanism and are

swallowed up via phagocytisis into a phagosome, which combines with lysosomes to form the phagolysosome (Handman & Bullen, 2002). This reaction causes considerable changes to promastigotes and they develop into the intracellular form of the parasite, the amastigote. Once amastigotes are released from the macrophages, they can occupy other macrophages and invade fibroblasts and dendritic cells (Rittig & Bogdan, 2000). Phagocytosis of promastigotes by macrophages, initiated by the attachment of the parasite to receptors on the phagocyte, creates additional receptors on the surrounding membrane (Rittig *et al.,* 1998). However, the mechanism of exit of the amastigotes from the infected macrophages is still poorly described. One accepted idea is that the macrophages burst and release the amastigotes after several hours of infection (Rittig & Bogdan, 2000).

2.2 Pathology

Human leishmaniasis has several clinical aspects. The pattern of the disease is based on the type of *Leishmania* species and on the expressed zymodeme (electrophoretic isoenzyme pattern) in that species. Thus, one isoenzyme may cause CL while another enzyme of the same species may cause VL (Gradoni *et al.,* 1991).

VL is the most severe form of leishmaniases and its incubation period ranges from three to eight months (De Alencar & Neves, 1982). The disease is caused by *L. infantum* in Southern Europe and North Africa and by *L. chagasi* in the New World whereas in India and Kenya it is caused by *L. donovani* (Piscopo & Mallia, 2006). The general symptoms are fever, weight loss, hepatosplenmegaly, lemphadenopathy, pancytopenia and hypergamaglobuliaemia (Zijlstra & El-Hassan, 2001). The disease usually has a chronic pattern and leads to death if left untreated, especially during severe secondary bacterial infections in advanced cases. VL can develop to post-kala-azar dermal leishmaniasis (PKDL) after subsidence of VL. The PKDL is often due to infection by the *L. donovani* sensu stricto (Zijlstra & El-Hassan, 2001), and the skin ulcers usually spread from the perioral area to other areas of the body.

CL is known by different names according to the geographical distribution of the disease. CL is caused by many species of the genus *Leishmania* such as *L. major, L. tropica, L. aethiopica* and rarely *L. infantum*. In the New World, species such as *L. mexicana* complex, *L. braziliensis* complex and *L. guyanensis* complex are responsible for CL infections, especially in the forests from Mexico to northern Argentina.

CL has different clinical features and courses of illness such as chronic skin sores which can be on a single part of the skin or from a large number of lesions (Minodier & Parola, 2007). The disease starts as a pimple at the site of the sandfly bite, the papule increases in size, then crusts and finally ulcerates. The incubation time varies from two weeks to several months. It has been reported in the Old World that CL incubation time can last up to three years (Zijlstra & El-Hassan, 2001). In the Americas, the incubation period is usually from two to eight weeks (Marsden, 1975). However, CL may take from 3 to 18 months to cure in the majority of patients (Mandell *et al.*, 2005).

CL is characterized by a totally curing lesion and intense granuloma occurrence that is called leishmaniasis recidivans; this lesion does not heal, occasionally for several years. In diffuse CL, the amastigote forms of *L. aethiopica* and a few subspecies of *L. mexicana* (*L. m. pifanoi* and maybe *L. m. amazonenzsis*) disseminate through the skin and cause this severe condition.

Another leishmanial manifestation is mucocutaneous leishmaniasis (MCL; espundia), which is distributed across central and South America. The incubation period of MCL is 1–3 months, but it may occur after many years post-healing of the initial cutaneous ulcers. Approximately 5% of patients with CL develop this disease after several months to 30 years from the initial infection (Matlashewski, 2001). This disease is caused by *L. panamensis, L. braziliensis* and *L. guyanensis*. The development of mucosal leishmaniasis depends on the size and the numbers of the primary lesion/s. The disease commonly starts in the nasal septum and mutilates it, and then it may invade other mucous membranes such as the lips, palate, pharynx and tonsils (Grevelink & Lerner, 1996).

Diagnosis

Diagnosis of VL is sometimes confused by the symptoms of other diseases such as malaria, tropical splenomegaly, histoplasmosis and bacterial endocarditis (Singh & Sivakumar, 2003). CL should also be distinguished from some common features such as tropical ulcers, leprosy and impetigo (Herwaldt, 1999; Lainson & Shaw, 1987). There are also some common symptoms that should be recognised from CL infection such as infected insect bites, impetigo and skin cancer due to other causes (Herwaldt, 1999). An early lesion of MCL can also be difficult to differentiate from histoplasmosis, lymphoma, paracoccidioidomycosis and polymorphic reticulosis (Herwaldt, 1999; Zijlstra & El-Hassan, 2001). In addition, the diagnostic methods used for each leishmanial form vary, but the main idea in each case remains to confirm the clinical suspicion. The diagnosis of VL in an endemic area is usually based on microscopic detection of amastigotes in biopsy samples or smears of tissue such as lymph nodes, bone marrow, liver and spleen. Sometimes parasites taken from microscopy-negative tissue samples can be cultured on special medium (Jhingran *et al.*, 2008; Markell *et al.*, 1999) or inoculated into animals such as hamsters. VL can also be detected by serological tests such as the direct agglutination test, which can detect leishmanial antibodies. A variety of nucleic acid detection methods can detect parasite DNA or RNA a few weeks ahead of the occurrence of any clinical symptoms (Singh & Sivakumar, 2003). Some DNA sequences in the *Leishmania* genome can be detected using polymerase chain reaction (PCR) techniques such as for the recombinant *Leishmania* glycoprotein (rgp63) locus (Shreffler *et al.*, 1993), internal transcribed spacer (ITS) region (Schonian *et al.*, 2001; Schonian *et al.*, 2003) and telomeric sequences (Chiurillo *et al.*, 2001).

The diagnosis of CL is usually based on biopsy specimens taken from the edge of lesions or microscopical examination of skin scrapings, but cultures of lesions may be contaminated by bacterial or fungal elements. Furthermore, each species has different growth requirements. The Montenegro skin test, which detects specific cutaneous delayed type hypersensitivity, has been limited because of its inability to distinguish between new and old infections (De Lima Barros *et al.*, 2005). Isoenzyme electrophoresis and monoclonal antibodies can be used to identify *Leishmania* species and strains, but a direct analysis of

clinical specimens using PCR techniques is rapid and achieved with high specificity and better sensitivity (De Oliveira *et al.,* 2003).

The most common, sensitive and specific test is ELISA but the sensitivity and specificity of ELISA is influenced by the antigen used. Many recombinant antigens have been developed over the last few years such as rgp63, rk90 and rk26 from *L. chagasi*, rORFF from *L. infantum* and rGBP from *L. donovani* (Piscopo & Mallia, 2006). ELISA is also used to distinguish between CL and VL due to the absence of the gp63 antigen in the former and its presence in the latter (Shreffler *et al.,* 1993).

2.3 Chemotherapy

Leishmaniasis is assumed to be a treatable disease, and sometimes self-healing in a few months, especially as CL, so that treatment is occasionally not needed. However, some leishmanial lesions diffuse and exist for longer. VL is commonly fatal if not treated. Therefore, several highly effective anti-leishmanial drugs have been introduced, and antimony drugs are considered to be the first line of treatment.

2.3.1 Antimony compounds

Pentavalent antimonials (Sb^Vs) have been used for more than half a century as front line drugs to treat leishmaniasis. Converting SbV to trivalent antimonials (Sb^{III}) is necessary in order to fulfil their anti-leishmanial potential (Shaked-Mishan *et al.,* 2001). There are two different forms of antimonial: glucantime (meglumine antimoniate) and pentostam (sodium stibogluconate), and these compounds are non-covalent chelates of SbV (Castillo *et al.,* 2010). It is suggested that meglumine antimonite consists of antimony and N-methyl-D-glucamine alternatively arranged in chain form, where each N-methyl-D-glucamine moiety is linked on both sides by the antimony molecules (Figure 1.12).
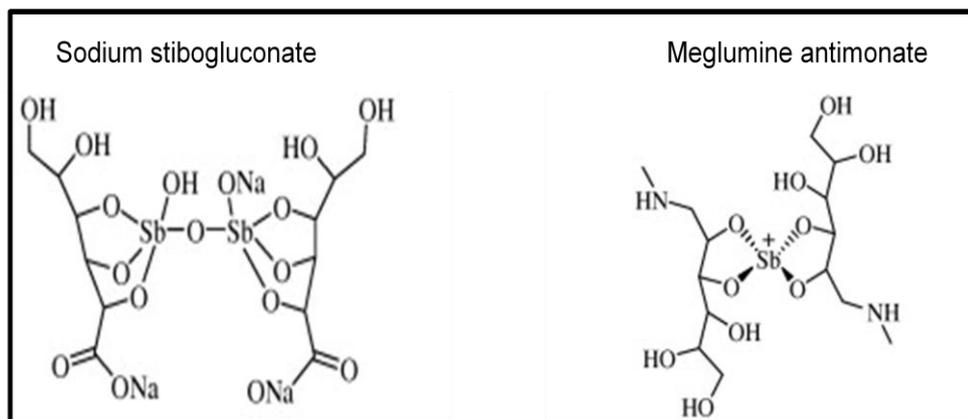
Figure 1.12 The proposed structure of pentavalent antimonial drugs. Obtained from (Frezard *et al.,* 2008).

Initially, antimonials were given at 10 mg/kg for 6–10 days. However, after treatment failures first appeared in India, physicians introduced higher doses and prolonged schemes (up to 20 mg/kg for 30 days) (Sundar *et al.,* 2000). Generally, it has been accepted that SbVs are a prodrug. However, the site and the mechanism of reduction remain unclear (Denton *et al.,* 2004) and the mode of action of these drugs is poorly understood (Castillo *et al.,* 2010). Early studies suggested that pentostam is able to interfere with glycolysis and the ß-oxidation of fatty acids in the amastigote stages of different species of *Leishmania,* causing a depletion of the ATP level in the parasite (Berman *et al.,* 1985; Berman *et al.,* 1987). Sb^{III} and Sb^{V} have been found to induce apoptosis and death by DNA fragmentation and externalization of phosphatidylserine (Sudhandiran & Shaha, 2003). However, specific drug targets have not been identified. (Wyllie *et al.,* 2004) designed a model for the mode of action of antimonial drugs in *Leishmania* (Figure 1.13) and they showed that trivalent antimony intervenes with trypanothione metabolism in the parasite cells via two reactions: Sb^{III} reduced thiol buffering capacity via the equal efflux of intracellular trypanothione and glutathione; Sb^{III} inhibited trypanothione reductase. Furthermore, pentavalent antimony binds to the ribose moiety and forms stable complexes with adenine nucleosides, which act as inhibitors of *Leishmania* purine transporters (Demicheli *et al.,* 2002).
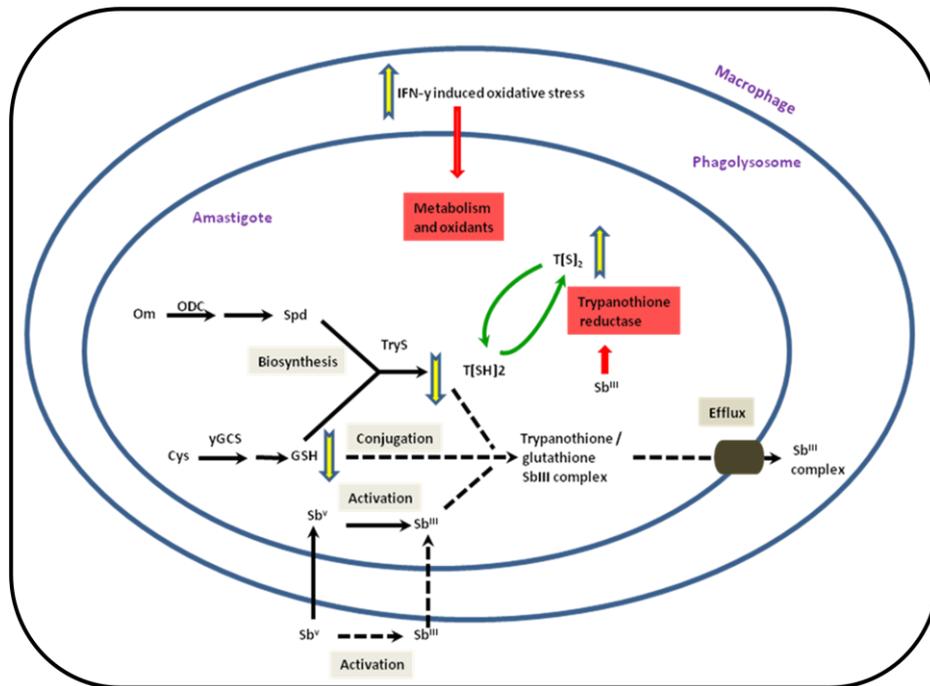
Figure 1.13 A model for the mode of action of antimonial drugs on *Leishmania* amastigotes. Om = ornithine, ODC = ornithine decarboxylase, Spd = spermidine, TryS = trypanothione synthase, Cys = cystine, GSH = Glutathione, γGCS = γ-glutamyl cystine synthase, suggested by (Wyllie *et al.,* 2004).

However, the use of the standard pentavalent antimonial drugs is now threatened because of the emergence of drug resistance (Castillo *et al.,* 2010). In addition, vomiting, malaise and anorexia are the early side effects of pentavalent antimonials. Although the WHO limitation avoids the presence of antimonial side effects, (Balana-Fouce *et al.,* 1998) reported that antimonial drugs were not particularly safe. Furthermore, it has been reported that in patients with increased medication some side effects are common such as headache, anorexia and nausea (Navin *et al.,* 1992). As a result of chemotherapy, the common side effects of antimonials are cardio-toxicity and pancreatitis (Sundar & Chakravarty, 2010).

Combination drugs with different modes of action have also been used. Combinations of sodium stibogluconate with paromomycin (Davidson *et al.,* 2009; Melaku *et al.,* 2007) or allopurinol (Chunge *et al.,* 1985) increased the efficacy against VL. It has also been proven that a combination of glucantime with the specific blocker of the ABC transporter, glibenclamide, decreased the infection rate of *Leishmania major*-infected macrophages (Padron-Nieves *et al.,* 2009).

The preferred second-line drugs (Figure 1.14) include amphotericin B, miltefosine, paromomycin and pentamidine (Croft *et al.*, 2006; WHO, 2000).
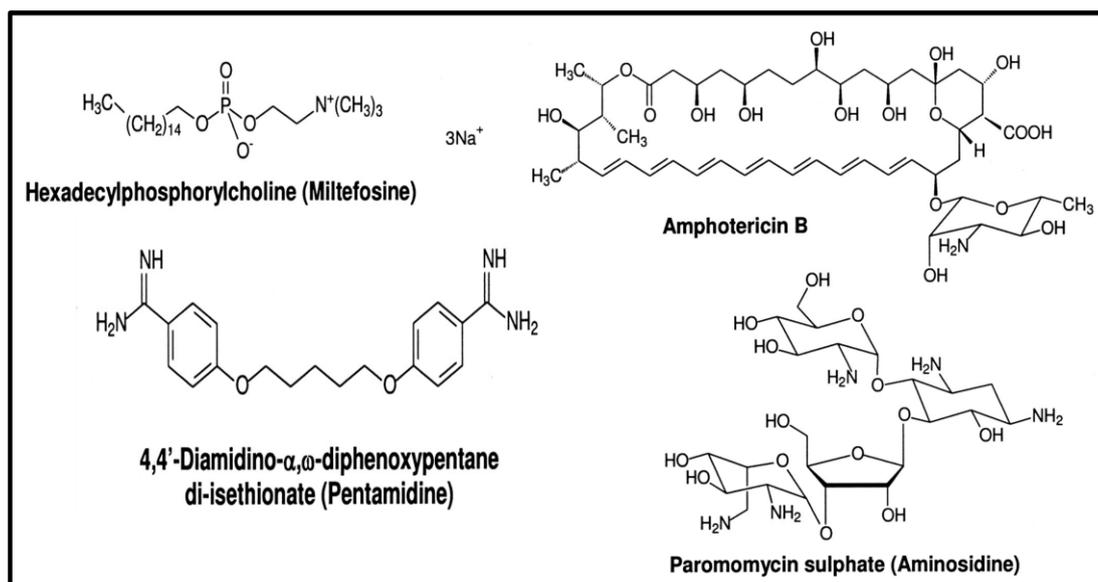
Figure 1.14 Drugs currently used in the treatment of leishmaniasis. Obtained from (Croft *et al.,* 2006).

2.3.2 Amphotericin B

Amphotericin B (AmB) is used for all types of leishmaniases, particularly in HIV-positive patients (Molyneux, 2007). The therapeutic dose of the drug is from 0.5 to 1 mg/kg intravenously on alternate days for a total of 30 days, but a 96% cure rate with a dose of 0.75 mg/kg/day for 15 days has been reported in India (Sundar *et al.,* 2007). Half of the AmB molecule consists of double bonds and is hydrophobic, whereas the other half contains a series of hydroxyl groups and is hydrophilic. Amphotericin molecules can gather in a cluster and interact with the aquaphobic centre of the cell membrane. The cluster is lined with the hydroxyl groups allowing the polar contents of the cell to escape causing cell lysis via the osmotic mechanism. The mode of action of the drug is based on an increase in membrane permeability of leishmanial parasites by affecting sterol metabolism and changing the cell membrane construction (Balana-Fouce *et al.,* 1998; Singh, 2006). Several AmB formulations have been developed to decrease the toxicity, and at the same time increase its effectiveness, for instance, via colloidal depressions and liposomes. Lipid formulations of AmB are specifically taken up by the reticulo-endothelial system and show a highly localised amplified antileishmanial action (Maltezou, 2010). A recent study has assumed that AmB interferes with ergosterol of *Leishmania* and cholesterol of host

macrophages (Paila *et al.,* 2010). The drug is highly toxic and its side effects in mammals are caused by the internalization of AmB-lipoprotein complexes mediated by low-density lipoprotein receptors (Wasan *et al.,* 1994). Prolonged administration and the high cost of the drugs have become the major disadvantage. In addition, it can have some catastrophic effects such as nephrotoxicity, hypokalaemia and infusion-related fevers and chills (Sundar *et al.,* 2007).

2.3.3 Miltefosine

Miltefosine is a phosphorylcholine ester of hexadecanol. The drug, which is used as an anti-cancer agent, was found to be a very effective oral agent for VL (Croft *et al.,* 2005). To date, miltefosine is licensed in India, Germany and Colombia (Maltezou, 2010). The recommended dose of the drug is 2.5 mg/kg/day for 28 days (Sundar *et al.,* 2002). The precise antileishmanial action of the drug remains unknown. (Perez-Victoria *et al.,* 2006) suggested three steps for the intracellular accumulation of miltefosine including engaging with the parasite cell membrane, incorporation of the drug in the cell and intracellular directing and metabolism. Others suggested anti-leishmaniasis action of the drug is due to generating a disturbance in ether-lipid reconstruction (Lux *et al.,* 2000). Although miltefosine is tolerated compared to antimonials and amphotericin, it has a limited use because of its potential teratogenicity (Olliaro *et al.,* 2002) and prolonged half-life. Moreover, diarrhoea and hepatotoxicity are common during the first two weeks of treatment (Sundar *et al.,* 1999).

2.3.4 Paromomycin

Paromomycin is an aminoglycoside antibiotic that has been used for various clinical infections including VL and CL, especially in highly antimony resistant VL (Sundar, 2001). The optimal dose of paromomycin is 14–16 mg/kg/day for three weeks (Thakur *et al.,* 2000). (Maarouf *et al.,* 1997b; Maarouf *et al.,* 1995; Maarouf *et al.,* 1997a) suggested that the mode of action of the drug in *Leishmania* spp is coupled with respiratory dysfunction, mitochondrial membrane potential and ribosomes. (Jhingran *et al.,* 2009) reported that paromomycin could target mitochondrial membrane potential in *L. donovani*. A molecular study proved that paromomycin effects targeted

translation process of *Leishmania* parasites but not their mammalian host (Fernandez *et al.,* 2011). However, it was found that the drug produces nerve toxicity, nephrotoxicity (Sundar, 2001), ototoxicity and pain at the injection site (Sundar *et al.,* 2007). Since the drug has not been used for a long time to treat leishmaniasis, no clinical resistance has been induced.

2.3.5 Pentamidine

Pentamidine is not a widely used antileishmanial drug, but it is used in the case of antimony-failed VL. The used dose of pentamidine is intramuscular injections of 2–4 mg/kg, three times a week for 3–5 weeks (Balana-Fouce *et al.,* 1998). The antileishmanial mechanism of action of pentamidine is still unclear. However, suggested modes of action of the drug include inhibition of polyamine biosynthesis, DNA minor groove binding preferentially binding to AT sequences in kinetoplast DNA (Wilson *et al.,* 2008), inhibition of mitochondrial topoisomerase I (Jean-Moreno *et al.,* 2006), effect on mitochondrial inner membrane potential (Bray *et al.,* 2003; Mukherjee *et al.,* 2006) and may lead to the destruction of the mitochondrion and disintegration of the kinetoplast (Mehta & Shaha, 2004). Several side effects have been reported for this drug such as hyperglycaemia, hypoglycaemia and nephrotoxicity (Balana-Fouce *et al.,* 1998). The pentamidine analogue, diminazene, has also been reported to treat clinical CL (Lynen & Van Damme, 1992). Its mechanism of action is similar to pentamidine.

2.4 Drug resistance

The role of drug resistance in treatment failure is difficult to understand because therapeutic response is multifactorial, and the efficacy of drugs in treatment of leishmaniasis depends on differences in drug sensitivity of *Leishmania* species, the immune status of the patient and the pharmacokinetic properties of the drug (Croft *et al.,* 2006).

In addition to the limited use of antileishmanial agents due to the cost and toxicity, emerging resistance to these drugs has become a serious problem in terms of being able to control different diseases caused by *Leishmania* parasites. Although antimonial compounds have been used for many years, several studies have reported the resistance of *Leishmania* species to these drugs in different

areas. More than half of all patients failed to be treated by antimonials in northern India where VL is highly distributed (Sundar, 2001). In South America (Rojas *et al.,* 2006) and Iran (Hadighi *et al.,* 2006), it has been found that CL patients failed to be treated by antimony. A study in an endemic region of eastern Sudan has reported antimonial resistance (Abdo *et al.,* 2003). Resistance to antimonials is multifactorial; therefore, several mechanisms have been proposed to explain the resistance to antimonial drugs such as drug efflux and metabolism (Croft *et al.,* 2006). (Wyllie *et al.,* 2008) suggested that the main feature of the resistance mechanism to antimonial drugs could be due to an amplified antioxidant defence via overexpression of tryparedoxin peroxidase. Antimonials also have reduced activity in the absence of a T-cell immune response, which has an impact on the treatment of HIV and VL co-infection cases (Cruz *et al.,* 2006; Laguna, 2003). Amphotericin and its formulations have been considered as the second line of treatment since the 1960s, and present excellent activity against VL in India. Resistance to amphotericin in *Leishmania* patients has not yet been recorded, but it has been selected for *in vitro* (Mbongo *et al.,* 1998). Failure of treatment with these drugs is minimal, unless leishmaniasis occurs in HIV-infected patients (Lachaud *et al.,* 2009).

Resistance to miltefosine can be reached easily *in vitro* by single point mutations (Seifert *et al.,* 2007). The common feature of *Leishmania* resistance to miltefosine is due to declining drug uptake, an increase in drug efflux rate, accelerated metabolism or changes in cell membrane permeability (Maltezou, 2010). A study reported that the cure rate for miltefosine in Guatemalan CL-infected patients was about 50% (Soto *et al.,* 2004). A VL case relapsed 10 months after a complete cure with miltefosine in a Nepalese patient (Pandey *et al.,* 2009). These facts imply that drug resistance could develop quickly. An isolated gene from *L. infantum* showed protection against both miltefosine and Sb^{III} (Choudhury *et al.,* 2008). In one laboratory study, exposing *L donovani* to paromomycin *in vitro* showed a decrease in drug uptake compared with the wild-type counterparts (Maarouf *et al.,* 1997b). Pentamidine treatment-resistant cases of kala-azar have been reported in an Indian clinical study (Jha *et al.,* 1991). In one *in vitro* study, pentamidine resistance in promastigote forms have been reported in *L. donovani* and *L. amazonensis* due to decreasing drug uptake by 18- and 75-fold, respectively (Basselin *et al.,* 2002).

3. Pyrimidine biosynthesis in kinetoplastids

3.1. *De novo* biosynthesis of UMP

Purine and pyrimidine nucleotides perform many functions in cells, including being the precursors of nucleic acids (DNA and RNA), modulators of enzyme activities, and as components of several co-enzymes (ATP, GTP, NADH, coenzyme A) and second messenger molecules (cAMP and cGMP) (Hammond & Gutteridge, 1982; Hammond & Gutteridge, 1984). Kinetoplastids differ from their mammalian and insect hosts in terms of purine metabolism, and must rely upon their host to acquire purines. However, no purine-based chemotherapy has emerged for kinetoplastid parasites, in large part because there is so much redundancy in purine transporters and salvage pathways that the inhibition of any one transporter (De Koning *et al.*, 2005) or enzyme (Berg *et al.*, 2010;Luscher *et al.*, 2007) has little or no effect on parasite survival.

In contrast, kinetoplastids can synthesise pyrimidines in pathways similar to their mammalian host, but these parasites can also obtain pyrimidines by uptake from the environment. Although this phenomenon appears to render pyrimidine metabolism less amenable to therapeutic intervention, the selective inhibition of pyrimidine biosynthetic enzymes and/or the blocking of pyrimidine transporter/s may offer new therapeutic agents.

Pyrimidine biosynthesis pathways seem to be common in most parasitic protozoa (Gutteridge & Coombs, 1977) and mammals (Jones, 1980; Levine *et al.*, 1974). In kinetoplastids, the pathway involves the sequential action of six enzymes (Figure 1.15) and begins with the production of carbamoylphosphate from glutamine, ATP and HCO_3 catalysed by carbamoylphosphate synthetase (EC 2.7.2.5). The condensation of aspartate and carbamoylphosphate is then catalyzed by aspartate transcarbamoylase (2.1.3.2). The next reaction is catalysed by dihydroorotase (EC 3.5.2.3), removing a water molecule from carbamoylaspartate to produce dihydroorotate; in this step, the pyrimidine ring is being closed. The next step is the oxidation of dihydroorotate to orotate by dihydroorotate oxidase (1.3.3.1). The 5-phosophoribosyl 1-pyrophosphate (PRPP) is added by orotate phosphoribosyltransferase (EC 2.4.2.10) to form orotidine-5-

monophosphate (OMP), which is decarboxylated by OMP decarboxylase (4.1.1.23) to produce uridine monophosphate (UMP).
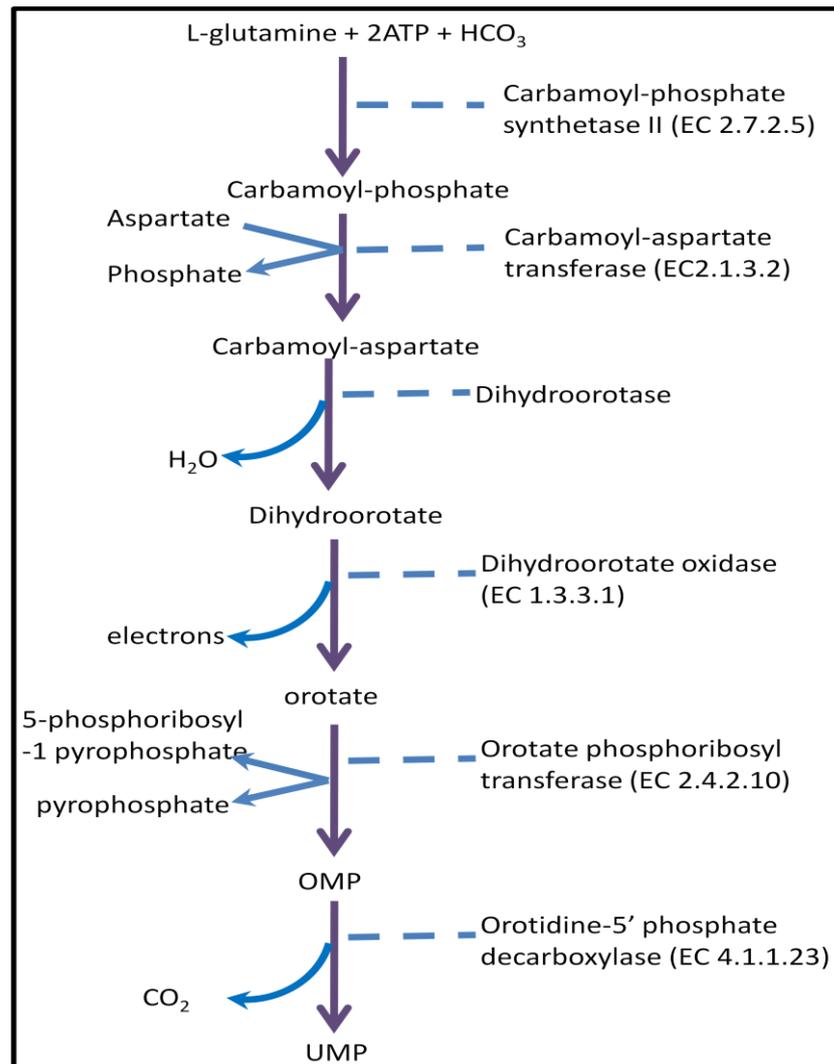
Figure 1.15 Pyrimidine biosynthesis pathways, adapted from (Hammond & Gutteridge, 1984).

Although there are similarities between kinetoplastid parasites and their mammalian hosts in terms of pyrimidine biosynthetic enzyme activity, there are still significant differences related to their organization into polypeptides, allosteric regulation, use of cofactors and cellular localisation (Carter *et al.,* 2008). For instance, the first three pyrimidine biosynthetic enzymes in humans are encoded by a single gene (Carrey, 1995), while the kinetoplastid's enzymes are encoded by isolated genes (Gene DB). Another example is that in humans, the dihydroorotate dehydrogenase is located in mitochondria and needs ubiquinone to be activated (Gero & O'Sullivan, 1985). Paradoxically, in a kinetoplastid it is a cytoplasmic enzyme (Hammond & Gutteridge, 1982) and requires fumarate as a cofactor (Feliciano *et al.,* 2006).

3.2. Interconversion and salvage pathways of pyrimidines

Although all kinetoplastids described to date can synthesise pyrimidines *de novo*, most of the studied species have some salvage pathways, which are used as a source of pyrimidine nucleotides (Hassan & Coombs, 1988). Pyrimidine nucleosides can be converted to their corresponding nucleobases or nucleotides by pyrimidine nucleoside phosphorylase or pyrimidine nucleoside kinase, respectively (Hassan & Coombs, 1988). All pyrimidines entering into the parasites, except thymidine and thymine, are probably converted to uracil, which is phosphoribosylated to UMP by uracil phosphoribosyl transferase (Figure 1.16). Therefore, UMP, the product of both the biosynthetic and salvage pathways, is considered as a precursor for most pyrimidine nucleotides (Carter *et al.*, 2003).
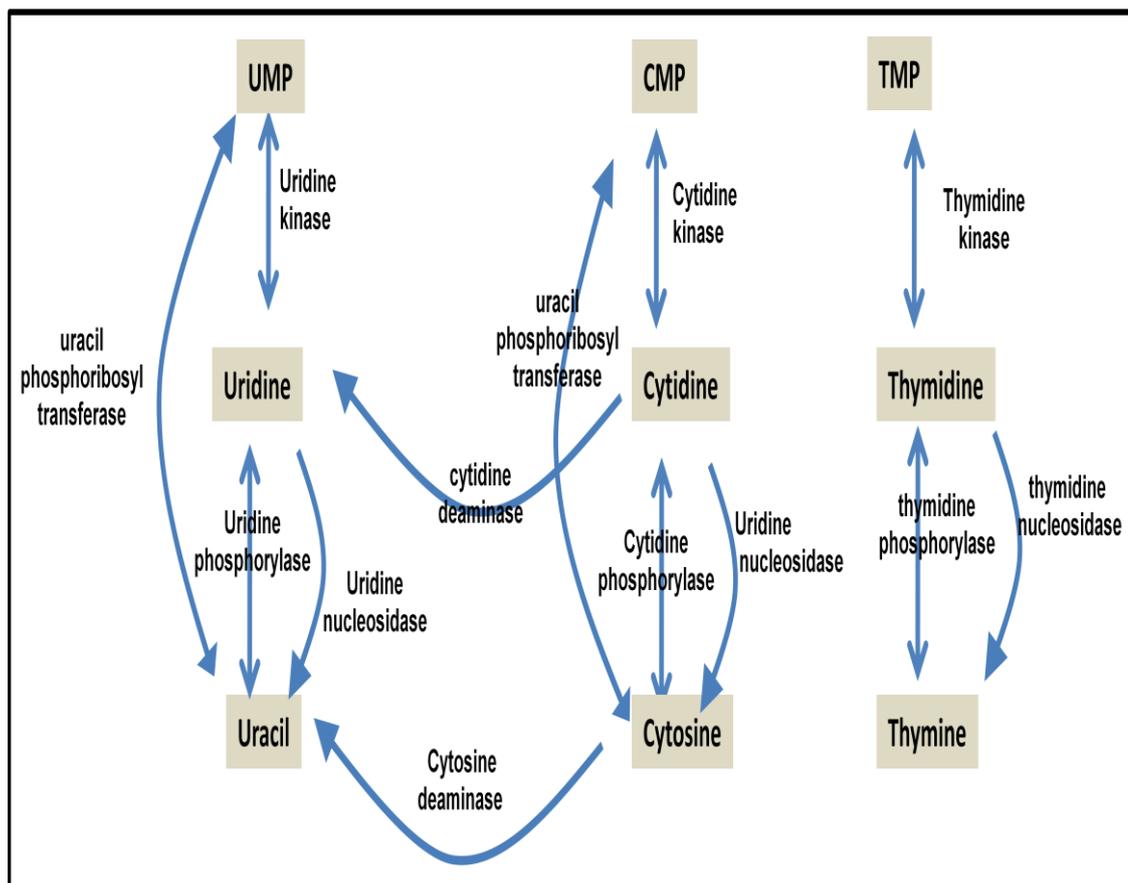
Figure 1.16 Pyrimidine salvage pathways, adapted from (Hammond & Gutteridge, 1984).

UMP can be phosphorylated through uridine diphosphate (UDP) to uridine triphosphate (UTP) by uridine nucleoside kinases in a two-step reaction using ATP as the phosphate donor. UTP is then aminated to CTP by CTP synthetase, which utilises glutamine as the amine donor (Hofer *et al.,* 2001). Kinetoplastids

also possess deaminase activity (Hassan & Coombs, 1986; Kidder, 1984) that can convert cytosine, cytidine and deoxycytidine to uracil, uridine and deoxyuridine, respectively (Hassan & Coombs, 1986). Uridine can then be converted to uracil by uridine phosphorylase (Shi *et al.*, 1999). UMP can be synthesised directly from uridine by uridine kinase, but there is an argument about the presence of this enzyme in kinetoplastid parasites (Carter *et al.*, 2008). Nevertheless, a gene encoding a putative uridine kinase activity is present in the genome database of *Leishmania major* (LmjF.31.2470), *L. infantum* (LinJ.31.2560) and in *L. mexicana* it is encoded by pseudogene (LmxM. 30.2470). Thymidine, which is incorporated into DNA, can be phosphorylated to TMP by thymidine kinase, for which the relevant genes are believed to be present in *Trypanosoma* and *Leishmania*. Thymidine and thymine can be converted reversibly through the action of pyrimidine phosphorylase to produce thymine and thymidine, respectively.

Deoxyribonucleoside triphosphates are needed in DNA synthesis. Deoxyribonucleotides are produced from ribonucleoside diphosphates via ribonucleotide reductase (Figure 1.17).
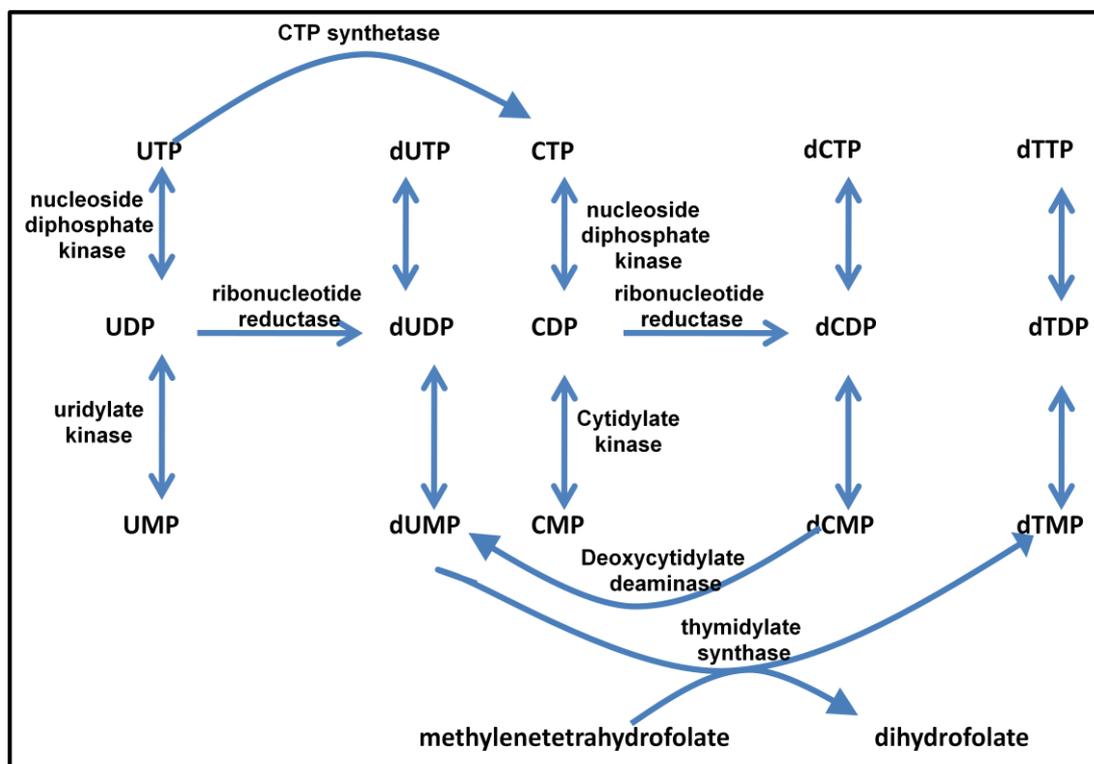
Figure 1.17. Interconversions of pyrimidines, adapted from (Hammond & Gutteridge, 1984).

Consequently, UDP and CDP can be converted to dUDP and dCDP, which are converted reversibly to dUMP and dCMP. In addition, both dUDP and dCDP can be

transformed to dUTP and dCTP respectively, by nucleotide diphosphokinase. Thymidine is crucial for DNA replication. dTMP is produced from thymidine by thymidine kinase (EC 2.7.1.21). However, the other route to supply cells with dTMP is by methylating dUMP with thymidylate synthase utilising methylenetetrahydrofolate as the methyl donor (Figure 1.18). In this reaction, a one-carbon group and two reducing equivalents are transferred from N^5, N^{10}-methylenetetrahydrofolate to dUMP to produce dTMP and dihydrofolate. Regeneration of tetrahydrofolate occurs in a reaction catalysed by dihydrofolate reductase with NADPH as the electron donor (Hassan & Coombs, 1988). In apicoplast parasites, thymidylate synthase and dihydrofolate reductase exist on the same polypeptide as a bifunctional protein (Chalabi & Gutteridge, 1977; Garrett *et al.,* 1984; Ivanetich & Santi, 1990). Trypanosomatids are auxotrophic for folate metabolites (Kaur *et al.,* 1988; Scott *et al.,* 1987), and rely on their transport of this cofactor from their mammalian host. DHFR and thymidylate synthase are validated drug targets for antifolate drugs including methotrexate.
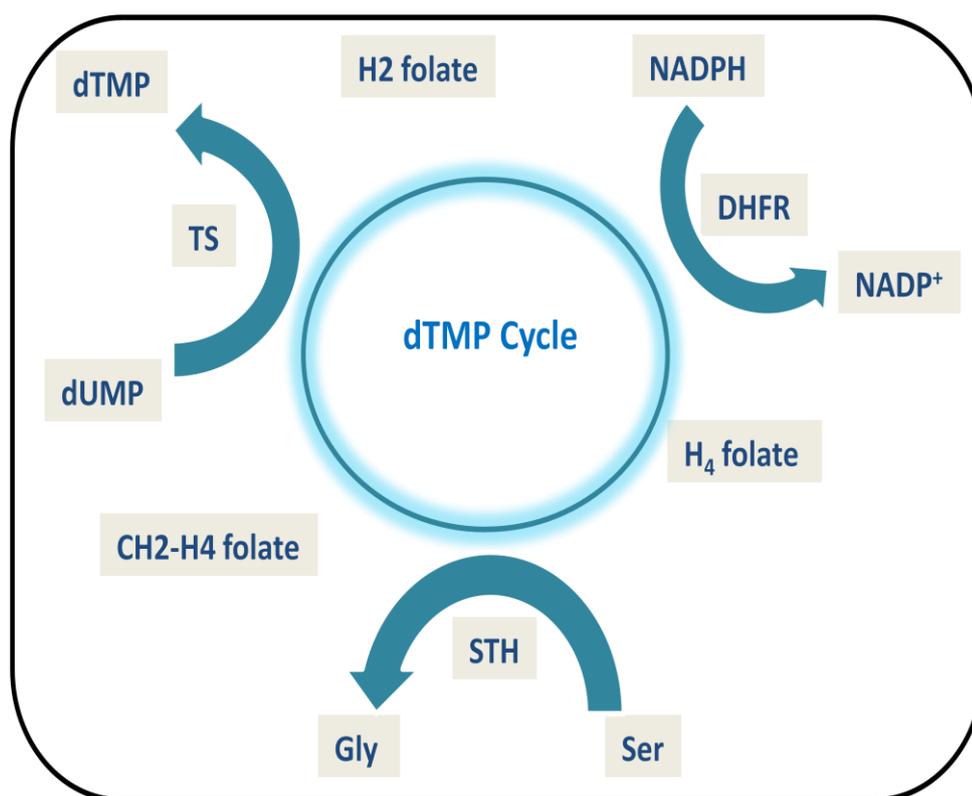
Figure 1.18. dTMP synthesis cycle showing the sequential reactions and metabolic relationships of TS (thymidylate synthase), DHFR (dihydrofolate reductase), and STH (serine transhydroxymethylase). Obtained from (Ivanetich & Santi, 1990).

3.3. Pyrimidine metabolism as a drug target

Rapidly divided cells, such as tumour cells, and plasmodium parasites during the intraerythrocytic stage, increase the requirement of nucleotides to synthesis nucleic acids. Deoxynucleoside triphosphates (dCTP, dTTP, dATP and dGTP) and nucleoside triphosphates (UTP, CTP, ATP and GTP) are the main substrates for the synthesis of nucleic acids DNA and RNA, respectively. Several of these compounds and their derivatives are especially crucial as sources of cellular energy (ATP, GTP), coenzymes (NAD, NADP, FAD), and metabolic regulation (cAMP, cGMP). These participations in cell activity make purine and pyrimidine biosynthesis pathways very good drug targets in different organisms. Specifically, drugs that successfully block pyrimidine biosynthesis have been introduced as antiviral, anticancer and potential anti-protozoal agents.

3.3.1. Antiviral activity

Viruses do not have their own nucleoside metabolism, and rely on a host cell to make their DNA and RNA; therefore, they can only reproduce naturally inside a host cell (Wimmer *et al.,* 2009). Some compounds have antiviral activity that inhibits the viral proteins or host cell proteins that are needed for virus growth.

Both the pyrimidine salvage mechanism and the pyrimidine *de novo* biosynthesis pathway produce the precursor of all pyrimidine nucleotides, uridine monophosphate (UMP), which is needed for RNA (UTP and CTP) and DNA (dTTP and dCTP) synthesis (Li *et al.,* 2007). Some antiviral drugs act by targeting pyrimidine metabolism of host cells and/or depleting pyrimidine pools, which are important for efficient virus replication. For example, dihydroorotate dehydrogenase (DHODH) converts dihydroorotate to orotate in the pyrimidine biosynthesis pathway with the aid of a flavin cofactor and an electron acceptor. This biosynthesis pathway is a target cellular enzyme for brequinar and leflunomide. Both of these antiviral compounds clearly inhibit human DHODH (Greene *et al.,* 1995; Liu *et al.,* 2000; McLean *et al.,* 2001). Recently, a new class of DHODH inhibitors was found by binding the 4-hydrox-1,2,5-oxadiazol-3-yl (hydroxyfurazanyl) scaffold with substituted biphenyl moieties via an amide

bridge (Lolli *et al.,* 2012). Furthermore, a compound called A3 was identified in a high-throughput screen for inhibitors (HTS) of influenza virus replication that act on pyrimidine metabolism. Virus divisions rely on large nucleotide pools, and the antiviral efficacy of compound A3 is due to pyrimidine depletion. It was also shown that the effect of A3 can be reversed, specifically by uracil and orotate (Hoffmann *et al.,* 2011). In addition, the antiviral thymidine analogue, 3'-azido-3'-deoxythymidine (zidovudine or AZT), was found to inhibit thymidine phosphorylation by 50% at a concentration of 5.5 ± 1.7 µM in the brain mitochondria (McCann *et al.,* 2012). Antiviral pyrimidine nucleoside analogues have also been used against viral infections. For example, lamivudine (cytidine analogue; 2',3'-dideoxy-3'-thiacytidine) and stavudine (thymidine analogue; 2'-3'-didehydro-2'-3'-dideoxythymidine) inhibit reverse transcriptase of HIV and lead to termination of DNA synthesis in viruses (Eholie *et al.,* 2012; Srivastav *et al.,* 2010).

3.3.2. Cancer chemotherapy

The topic of pyrimidine analogues that are useful or potentially so in cancer chemotherapy is too enormous to be completely reviewed in this part of the Introduction. However, (Heidelberger, 1967) summarised cancer chemotherapy by purine and pyrimidine analogues from 1965 until 1966. That overview showed that the most-used pyrimidine analogues to treat cancers at the time were 6-azapyrimidines and 5-fluoro-pyrimidines. More recently, several pyrimidine nucleoside analogues have been used to treat cancers. For instance, cytarabine, a deoxycytidine with the presence of a hydroxyl group in the β-configuration at the 2' position of the sugar moiety, was used extensively to treat acute leukaemia (Arlin *et al.,* 1988). Cytarabine triphosphate incorporates into DNA in competition with deoxycytidine triphosphate this incorporation leads to chain termination and results in blocking DNA synthesis and cell cycle arrest at S-phase (Major *et al.,* 1981; Major *et al.,* 1982). Gemcitabine is also a deoxycytidine analogue, but with two fluorine atoms in the 2' position of the sugar moiety, used in the treatment of solid tumours (Burris *et al.,* 1997; Kaye, 1994). Gemcitabine is first phosphorylated to its monophosphate derivative, then subsequently phosphorylated by pyrimidine nucleotide kinases to the active 5'-diphosphate and triphosphate derivatives (Abbruzzese *et al.,* 1991). Gemcitabine is able to incorporate into both nucleic acids, DNA and RNA (Ruiz

van Haperen *et al.,* 1993). The most used fluorinated pyrimidine analogue is 5-FU. As such, its mechanism of action in human cancer cells has been well characterized; several sources described that the main drug toxicity involved the inhibition of thymidylate synthase, by its metabolite 5F-dUMP (Grivicich *et al.,* 2001; Figure 1.19).
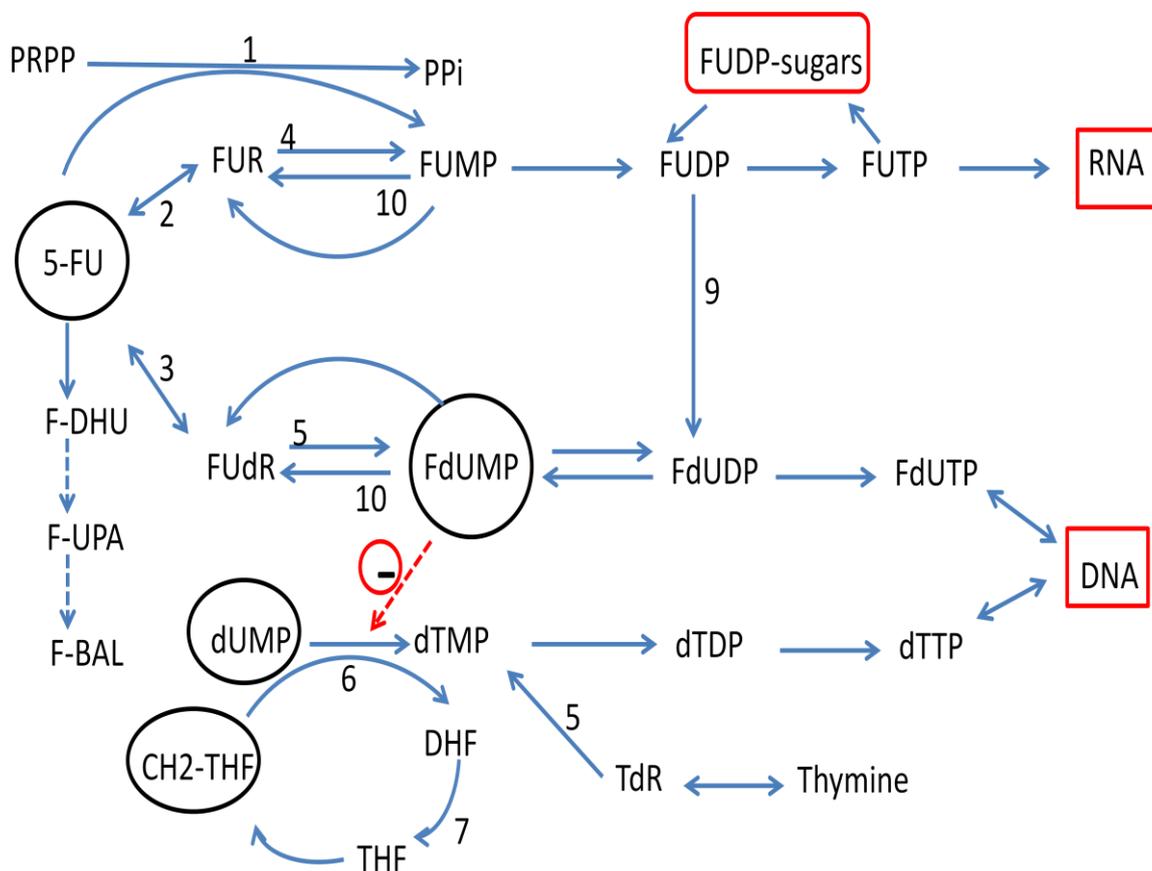
Figure 1.19: Metabolic pathways and mechanism of action of 5-fluorouracil (5-FU) in human cancer cells. Enzymes catalyzing these reactions are 1, orotate phosphoribosyltransferase; 2, uridine phosphorylase; 3, thymidine phosphorylase; 4, uridine kinase; 5, thymidine kinase; 6, thymidylate synthase; 7, dihydrofolate reductase; 8, dihydropyrimidine dehydrogenase; 9, ribonucleotide reductase; 10, 5'-nucleotidases and phosphatases. Abbreviations: FUMP, FUDP, FUTP: fluorouridine -5'-mono-, di-, and triphosphate, respectively; FdUMP, FdUDP, FdUTP: fluorodeoxyuridine-5'-mono-, di-, and triphosphate, respectively; dUMP: deoxyuridine-5'-monophosphate; dTMP, dTDP, dTTP: deoxythymidine-5'-mono-, di-, and triphosphate, respectively; PRPP: 5-phosphoribosyl-1-pyrophosphate; FUR: fluorouridine; FUdR: fluorodeoxyuridine; F-BAL: α-fluoro-ß-alanine; F-UPA: fluoroureidopropionate; F-DHU: 5-fluorodihydrouracil; DHF: dihydrofolate; THF: tetrahydrofolate; TdR: thymidine; PPi: pyrophosphate. Adapted from Grivicich *et al.,* 2001; Peters & Jansen, 1996.

3.3.3. Potential for antiprotozoal agents

Most protozoa parasites are able to synthesis the pyrimidine ring *de novo* (Berens *et al.,* 1995), and yet are also capable of salvaging pyrimidine nucleosides and/or nucleobases (Aronow *et al.,* 1987; De Koning *et al.,* 2003; Gudin *et al.,* 2006; Papageorgiou *et al.,* 2005). Exceptions are *Plasmodium* species, which are unable to use preformed pyrimidines from the host environment, and rely on biosynthesis alone (De Koning *et al.,* 2005; Van Dyke *et al.,* 1970), and the amitochondriate protozoa *Trichomonas vaginalis*, *Tritrichomonas foetus*, and *Giardia spp*, which lack the *de novo* biosynthesis pathway (Hassan & Coombs, 1988; Wang & Cheng, 1984).

Several studies targeted pyrimidine metabolism enzymes to provide new routes for anti-parasitic drugs. (Cassera *et al.,* 2011) reviewed several pyrimidine pathway enzymes that have been targeted in *P. falciparum* using pyrimidine analogues. In an *in vitro* study, *P. falciparum* growth was inhibited to half when exposed to 6 nM of 5-fluoroorotic acid (Rathod *et al.,* 1989); also on the same species, triazolopyrimidine-based dihydroorotate dehydrogenase inhibitors (Figure 1.20A) recorded an EC_{50} at nanomolar levels (Phillips *et al.,* 2008). Another pyrimidine pathway inhibitor is L-6-thiohydroorotate, which moderately inhibited dihydroorotase of malaria (Seymour *et al.,* 1994). (Baldwin *et al.,* 2005) introduced an inhibitor of *P. falciparum* dihydroorotate dehydrogenase with an IC_{50} value of 16 nM. Other inhibitors of dihydroorotate dehydrogenase in *Plasmodium* species have also been identified, for instance, tricyclic aromatic amines (Heikkila *et al.,* 2007).

In addition, the growth of *T. vaginalis* was reported to be inhibited by deoxyuridine analogues, such as 5-methyl-4'-thio-2'-deoxyuridine and 5-iodo-4'-thio-2'-deoxyuridine, with IC_{50} at molecular level concentrations (Strosselli *et al.,* 1998). Benzimidazole derivatives (Figure 1.20B), which modified the second position of the pyrimidine ring, showed anti-parasitic activity against *Trichinella spiralis, Paramecium caudatum* and *Lamblia muris* (Mavrova *et al.,* 2010). Also, hydrophilic derivatives of that pyrimidine analogue, 2,4-diaminothieno[2,3-d]-pyrimidine lipophilic antifolates (Figure 1.20C), inhibited dihydrofolate reductase activity of *Pneumocystis carinii, Toxoplasma gondii* (Rosowsky *et al.,*

1997), and trypomastigotes and amastigotes of *T. cruzi* (Senkovich *et al.,* 2005). The drug was found to be a good substrate of human DHFR enzyme. However, the structures in Figure 1.20 could just as easily be described as purine analogues than as pyrimidine analogues.

Figure 1.20: Structures of pyrimidine analogues. **A.** Triazolo-pyrimidine, **B.** Benzimidazole, **C.** 2,4-diaminothieno [2,3-d]pyrimidine. From: www.ChemSpider.com.
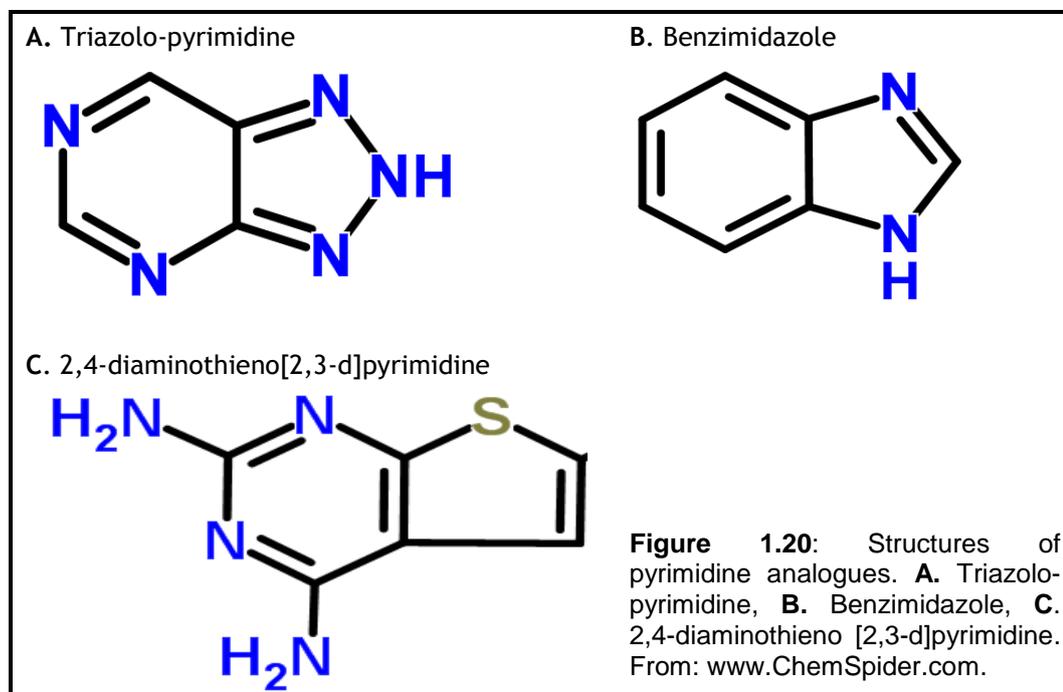
In kinetoplastids parasites, (Nakajima-Shimada *et al.,* 1996) found that *T. cruzi* growth *in vivo* was significantly reduced by 3'-azido-3'-deoxythymidine (Figure 1.21A; AZT) at a concentration around the micromolar level in *in vitro* cultures and also considered that zidovudine may be incorporated into parasite DNA. The growth of *Trypanosoma cruzi*, particularly the amastigote stage, was significantly reduced during genetic interruption of the first pyrimidine pathway enzyme, carbamoyl-phosphate synthetase II (Hashimoto *et al.,* 2012). It was also found that the activity of the fourth enzyme of the pyrimidine pathway (DHOD) was reduced by extracts from two types of brown algae in *T. cruzi* (Nara *et al.,* 2005). Although trypanosomatids are considered folate auxotrophic (Ouellette *et al.,* 2002), enzymes involved in the folate cycle to convert dUMP to dTMP have been of interest as drug targets in these parasites. Several compounds have shown inhibition activities against DHFR of kinetoplastids these include 2,4-diaminopyrimidines (Figure 1.21B) (Pez *et al.,* 2003) and 2,4-diaminoquinazolines (Figure 1.21C) (Khabnadideh *et al.,* 2005). Recently, (Mercer *et al.,* 2011) have reported that 2,4-diaminopyrimidines derivatives can

kill *T. b. brucei* under both *in vitro* and *in vivo* conditions, presumably by targeting mitogen-activated protein kinases and cdc2-related kinases.

Figure 1.21: Structures of pyrimidine analogues. **A**. Zidovudine (AZT), **B**. 2,4-diaminopyrimidines, **C**. 2,4-diaminoquinazolines. From: www.ChemSpider.com.
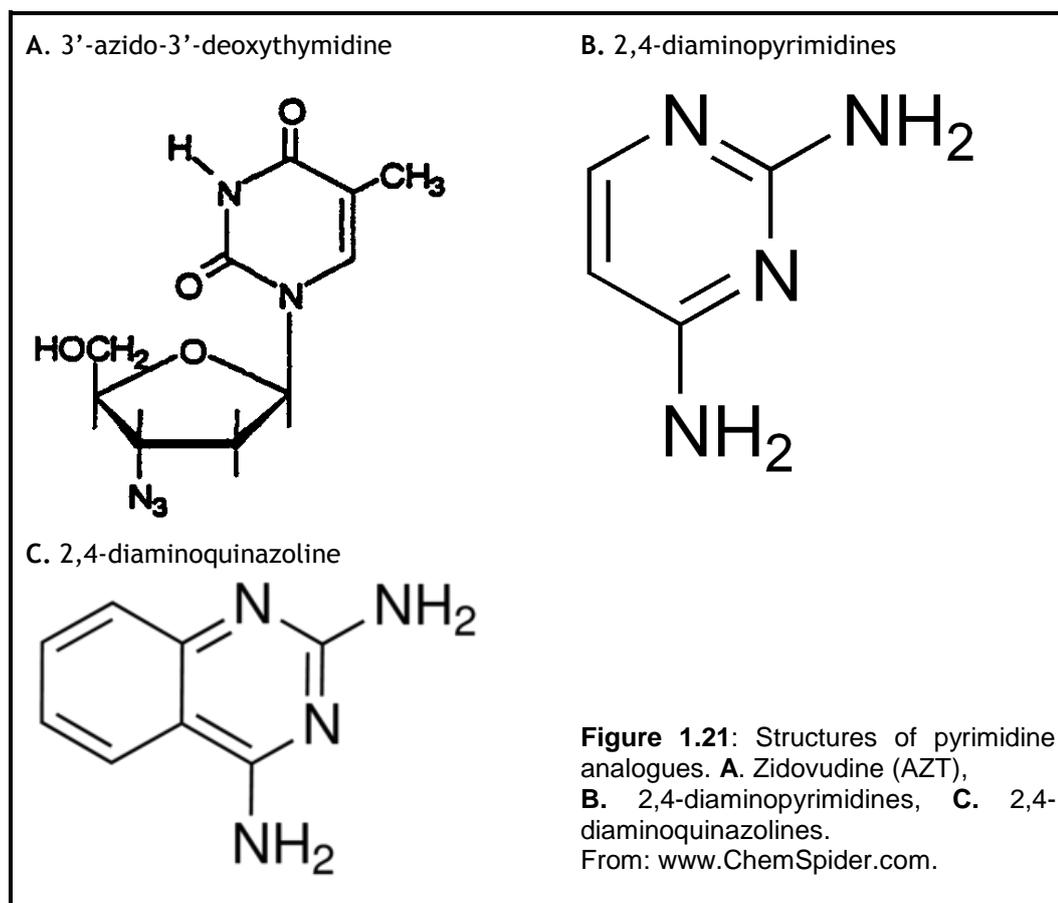
The derived forms from 5-(substituted-benzyl)-2-4-diaminopyrimidine (Figure 1.22A) inhibited leishmanial dihydrofolate reductase with IC_{50} values between 0.2-11 µM (Sirawaraporn *et al.,* 1988). In *L. major*, 5-fluorouracil appeared to be a good substrate for uracil phosphoribosyl transferase, and recorded an IC_{50} value at the micromolar level (Papageorgiou *et al.,* 2005).Acivicin (Figure 1.22B), which inhibits glutamine utilisation, was able to clear *L. donovani* promastigote and amastigote forms (Mukherjee *et al.,* 1990). In the early 1950s, a folic acid analogue, methotrexate (4-amino-N10-methyl-pteroylglutamic acid; Figure 1.22C), was introduced to treat leukaemia (Farber *et al.,* 1948; Meyer *et al.,* 1950), and later found to treat several other mammalian diseases. In mammalian cells (Ingraham *et al.,* 1986), amastigotes of *T. cruzi* (Zuccotto *et al.,* 1999) and promastigotes of *L. major* (Gallego *et al.,* 2005) the drug inhibited dihydrofolate reductase and reduced dTTP synthesis, which led to a rise in dUTP that incorporated into DNA. At 400 nM the drug caused 80% inhibition of the growth of wild type promastigotes of *L. major*.

Figure 1.22: Structures of pyrimidine metabolism inhibitors. **A.** substituted 2,4-diaminopyrimidines, **B.** Acivicin, a glutamine analogue, **C.** Methotrexate (4-amino-N10-methyl-pteroylglutamic acid, a folate analogue. From: www.ChemSpider.com.
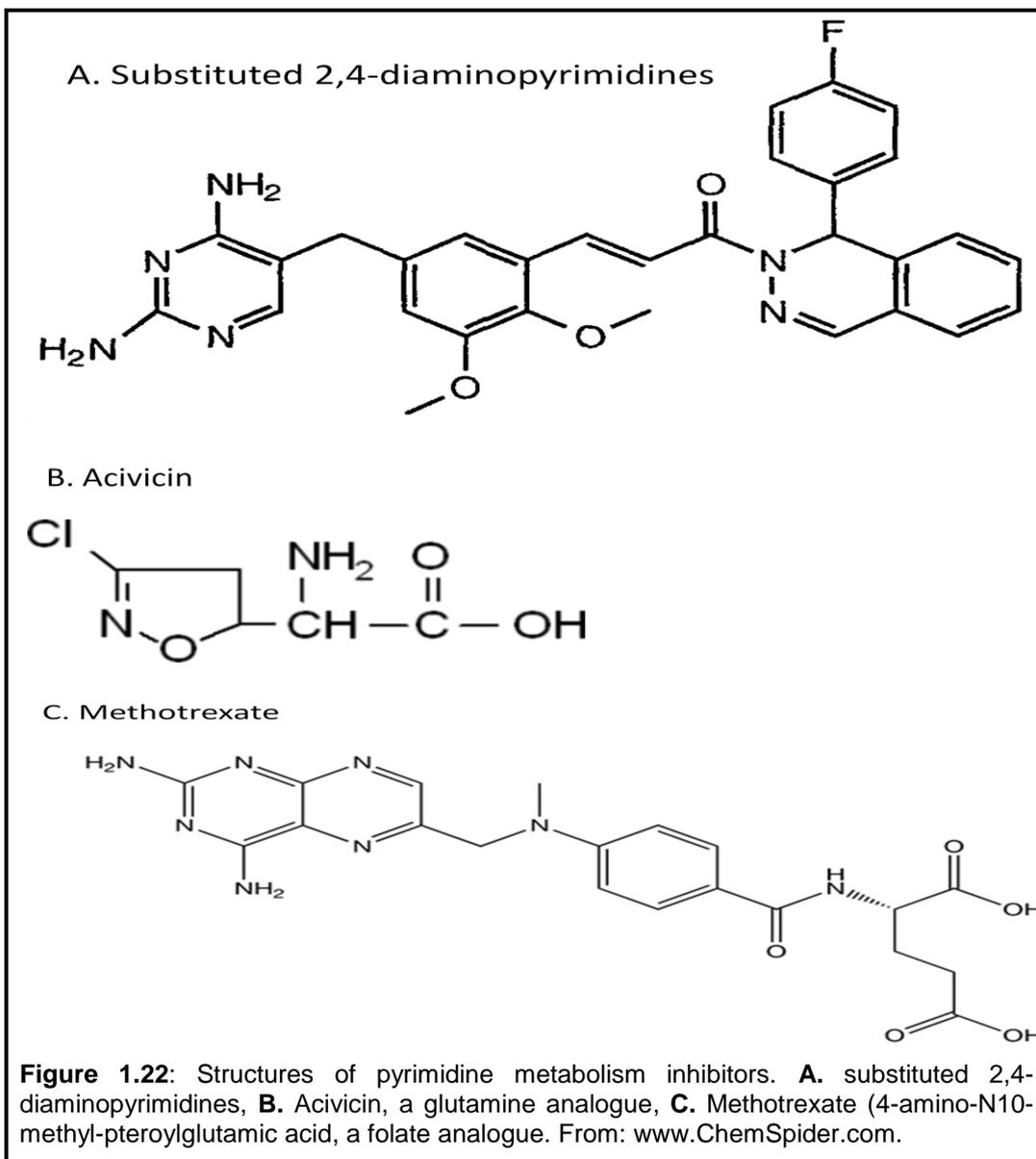
4. Nucleoside and nucleobase transporters of kinetoplastids

4.1. Classification of transporters

Biological organisms consist of cells built of proteins, carbohydrates, lipids and nucleic acids. Chemical analysis of several kinds of membranes reveals that most contain up to 50% protein and 50% lipid. However, organisms might have percentages that different from this 1:1 ratio. About one-third of the proteins of a cell are embedded in biological membranes, and about one-third of these function to catalyze the transport of molecules from one side of the membrane to the other side. The plasma membranes function to isolate the inside of the cell from its environment. The crucial role for transport processes to biological systems was recognized many years ago (Gale & Taylor, 1947; Mitchell, 1949). Membrane proteins serve the cell in several ways: the uptake of essential materials into the cytoplasm then into organelles, the regulation of metabolites and the active release of drug and other toxic substances (Saier, 2000a). Transport proteins are known to uptake solutes by several mechanisms, and a variety of energy combining mechanisms are known to control the active transport and/or extrusion of specific compounds (Fath & Kolter, 1993; Kramer, 1994; Paulsen *et al.*, 1996a; Paulsen *et al.*, 1996b). All uptake across membranes falls into one of two fundamental mechanisms: passive diffusion and active transport. In passive transports, cells do not use any energy to move molecules and substrates diffuse down concentration gradient, while in active transport mechanisms they use energy to pass molecules into or out of the cell against the gradient. Interestingly, membrane transport proteins, which are integral membrane proteins involved in the movement of ions, small or macro molecules across a cell membrane, have the two forms of transport mechanisms, passive and active transport. In transport protein mechanism, the uptake requires the assistance of a transport protein in the membrane to cross the lipid bilayer. Numerous studies have classified membrane transport proteins in several families according to different aspects. (Saier, 2000b) listed all the recognized families of transporters. Of these, there are two main families of transport proteins that mediate the movement of nucleobases and nucleosides across eukaryotic plasma membrane. The two unique families are the concentrative nucleoside transporters (CNT) and the equilibrative nucleoside transporters

(ENT). The CNT, designated SLC29, has three human family members (CNT1, CNT2 and CNT3). They couple nucleoside uptake to the cellular Na^+ or H^+ gradient, and have 13 predicted transmembrane segments. CNTs can be found in many specialized mammalian cell types, such as kidney and intestine, also the first eukaryotic nucleoside transporters whose genes were cloned (Baldwin *et al.,* 1999) belonged to this family. Although CNT family members are widely distributed in both bacteria and eukaryotes, no members of this family have been found to date among the protozoa (De Koning & Diallinas, 2000). The ENT family was designated SLC28. Four human family members of SLC28 have been identified to date (ENT1, ENT2, ENT3 and ENT4); they transport nucleosides across plasma membrane bidirectionally in a Na^+-independent manner. These transporters are distinguished by an overall similarity in predicted topology and characteristically possess 11 transmembrane domains (Figure 1.23). Thus far, all defined protozoan nucleoside and nucleobase transporter genes appertain to the ENT family (Landfear *et al.,* 2004).
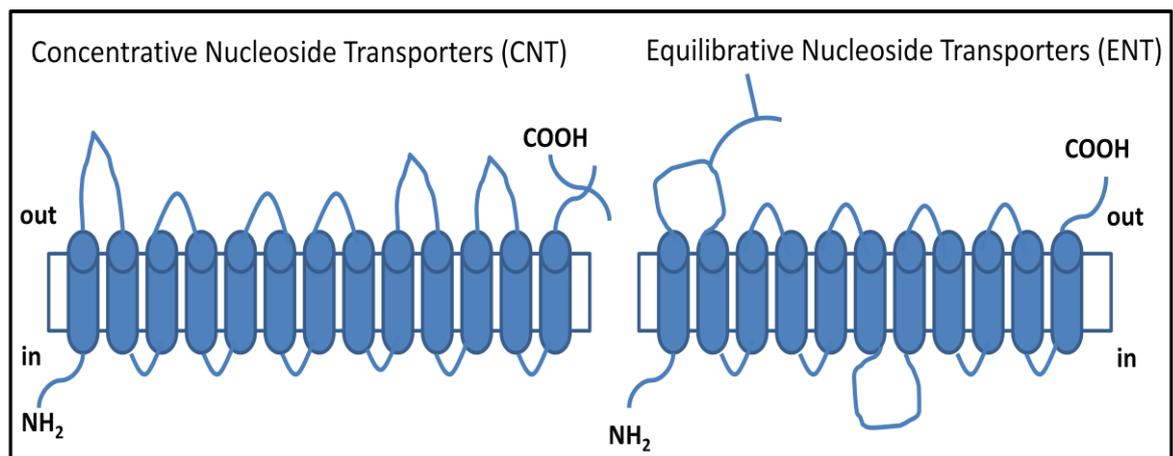
Figure 1.23 Predicted topology of ENT and CNT families. Adapted from (Lee *et al.,* 2001).and (Cass *et al.,* 1998).

The identification and classification of these families are based primarily on sequence homology. Both ENT and CNT families play critical roles in nucleoside salvage pathways. CNT1 prefers pyrimidine nucleosides, CNT2 is purine-nucleoside preferring and CNT3 takes up both pyrimidine and purine nucleosides (Gray *et al.,* 2004). ENTs transport nucleosides and their analogues through facilitated diffusion (Hyde *et al.,* 2001). For instance, in humans, ENTs are likely to mediate the uptake of most of nucleoside analogues (Acimovic & Coe, 2002).

4.2   Characterisation of nucleoside and nucleobase transporters of kinetoplastid parasites

Purine and pyrimidine nucleotides are both considered as nutrients and as modulators of cell homeostasis. These molecules are not only monomeric nucleic acid precursors, but also key determinants of energy metabolism involved in many biosynthetic pathways such as UDP-glucose in glycogen synthesis, CDP-diacylglycerol in phospholipid metabolism and S-adenosylmethionine in essential transmethylation reactions. Also as energy transfer units such as ATP and GTP, as well as adenine nucleotides as component parts of $NAD(P)^+$, FAD and CoA (Aymerich *et al.,* 2005). Furthermore, some nucleosides (adenosine) and nucleotides (ATP) are ligands for purinergic receptors (P1 and P2) (Dal *et al.,* 2011). Moreover, they act as second messenger molecules in cell signals pathways, e.g. cyclic AMP and cyclic GMP (Carter *et al.,* 2003). Since nucleosides and nucleobases are hydrophilic molecules, plasma membrane transporters are required for this process to occur. To clarify, these molecules cannot diffuse across the membrane lipid bilayer, therefore, they use integral membrane proteins (ENTs) to move down their concentration gradients.

4.2.1 Purine transporters

Among the many metabolic differences between protozoan parasites and their mammalian hosts is the fact that they cannot synthesise purine nucleosides. While the unicellular organisms are incapable of purine ring synthesis, their mammalian hosts are capable of *de novo* synthesis from amino acids and other small molecules. Therefore, *Trypanosoma* and *Leishmania* rely solely on the uptake mechanisms of these external nutrients. Consequently, the purine salvage pathways are required for parasite viability in all life cycle stages. The transporters also mediate the uptake of a variety of cytotoxic drugs (Geiser *et al.,* 2005). Over the last decades, this phenomenon has led to intensive studies on purine uptake and metabolism in several protozoa parasites (De Koning *et al.,* 2005). On the other hand, it has been generally demonstrated that kinetoplastid parasites are able to synthesis the pyrimidine ring *de novo* (Gudin *et al.,* 2006). However, it is often difficult to study purine/pyrimidine transporters within the live parasites, as abundant separate transporter genes are expressed simultaneously and specific inhibitors for individual transporters are not available (Gudin *et al.,* 2006). Nucleoside and nucleobase transporters in

kinetoplastid species are still eliciting considerable attention due to their central role in the uptake of antimetabolites.

4.2.1.1 *Trypanosoma spp.*

The first two high-affinity adenosine transport systems in *T. brucei* were identified and designated P1 and P2 (Carter & Fairlamb, 1993), which also accumulate inosine and adenine, respectively. The P1 and P2 transporters have been widely studied since they were first described. P1 is considered to be a conventional purine nucleoside transporter and has a very low affinity for purine nucleobases (De Koning & Jarvis, 1999). In addition, the same authors also found that bloodstream forms of *T. b. brucei* transport hypoxanthine via two distinct transporters differentiated as guanosine-sensitive and insensitive, and defined as purine nucleobase transporter H2 and H3, respectively (De Koning & Jarvis, 1997a). On the other hand, it was demonstrated that the P2 nucleoside transporter mediated the uptake of diamidine drugs, including the widely used trypanocide pentamidine (Carter *et al.,* 1995; De Koning, 2001). The trypanosome expresses two additional transporters: a high affinity pentamidine transporter (HAPT) and a low affinity pentamidine transporter (LAPT), which also contribute as pathways for the uptake of pentamidine (De Koning, 2001). Since P2 is a member of the equilibrative nucleoside transporters (Ortiz *et al.,* 2009a) assumed that it is likely the other ENT family members in *T. brucei* may also mediate the uptake of diamidines.

4.2.1.2 *Leishmania spp.*

An early study, conducted by (Hansen *et al.,* 1982), on the uptake of purine nucleosides and nucleobases in *Leishmania braziliensis* promastigotes, reported on three transport activities, for adenosine, inosine and the last one for the purine bases adenine and hypoxanthine. This model is still being used in purine transport for promastigotes. Another study by (Aronow *et al.,* 1987) investigated the functions of *Leishmania donovani* nucleoside transporters and found that the parasite possesses two independent purine nucleoside transporters that mediate the uptake of adenosine and pyrimidine nucleosides (uridine, cytidine and thymidine) in one case, and of inosine and guanosine in the other case, with K_m values in the micromolar range. Various nucleoside and nucleobase analogues display good activities *in vitro* and/or *in vivo*, but to date

only the purine nucleobase analogue allopurinol has been used in combination therapy against leishmaniasis. It was combined with meglumine antimoniate to treat cutaneous leishmaniasis (Momeni *et al.,* 2002) and with pentamidine to cure visceral leishmaniasis (Das *et al.,* 2001).

In general, *Leishmania* and *Trypanosoma* have shown many similarities in purine nucleobase and nucleoside transporters that mediate the transport purine bases, nucleosides and analogues (Al-Salabi *et al.,* 2003; Burchmore *et al.,* 2003). Moreover, on the level of pyrimidine transporters, both genera express a similar high-affinity uracil transporter, designated LmajU1 (Papageorgiou *et al.,* 2005) and TbU1 (De Koning & Jarvis, 1998), respectively.

4.2.2 Pyrimidine transporters

In contrast to purines, only a few studies have been conducted on pyrimidine uptake in kinetoplastid parasites (Gudin *et al.,* 2006). This might be attributed to the parasites' ability to synthesise the pyrimidine ring, which makes it less attractive to scientists interested in chemotherapy than purine transporter studies. In general, purine transporters can mediate the uptake of purine and/or pyrimidine antimetabolites in kinetoplastid parasites (De Koning & Jarvis, 1998; Papageorgiou *et al.,* 2005; Wallace *et al.,* 2002). (De Koning & Jarvis, 1997a) reported hypoxanthine uptake by the H2 transporter in *T. b. brucei* bloodstream forms was inhibited by uracil and thymine, with K_i values of 60 and 82 μM, respectively. The same authors (De Koning & Jarvis, 1998) described the first high-affinity uracil transporter in kinetoplastid, designated TbU1, with a K_m value of 0.4 μM. The *Leishmania major* transporter, LmajU1, was found to be highly similar to the TbU1 transporter of *T. b. brucei* (Papageorgiou *et al.,* 2005). It has been confirmed that the pyrimidine analogue 5-fluorouracil is an effective agent against both *Leishmania* and *Trypanosoma* parasites (Gudin *et al.,* 2006; Papageorgiou *et al.,* 2005), which suggested a correlation between efficient salvage and therapeutic effect. Also 5-fluorouracil was found as a good inhibitor of both LmajU1 and TbU1 transporters (Gudin *et al.,* 2006). Therefore, it might be possible to develop a new chemotherapy for trypanosomiasis, if this cytotoxic nucleobase has the same effect on uptake systems of the mammalian-infective.

4.3. Cloning of nucleoside and nucleobase transporters

Since nucleoside transporters are responsible for the accumulation of chemotherapeutic agents of many diseases, several permeases have been characterised from a number of species, ranging from prokaryotic to humans. Because of the difficulty to isolate and identify the contribution of a single transporter using radio-labeled permeants and whole organisms, scientists depend on cloning and expressing the gene encoding the putative transporter in a suitable heterologous system (Burchmore *et al.*, 2003). However, the progress on molecular level studies of nucleoside and/or nucleobase transporters from kinetoplastid started only in the late 1990s, and to date all of the protozoan nucleoside and nucleobase transporters identified belong to the ENT family (De Koning *et al.*, 2005). With the completion of the *T. b. brucei* and *L. major* genomes, it is now known how many ENT-family genes each parasite encodes. The genome of *L major* contains a total of 8272 genes (Ivens *et al.*, 2005), whereas the *T. brucei* genome contains 9068 genes (Berriman *et al.*, 2005). Of these, *T. b. brucei* encodes 16 ENT genes (Ortiz *et al.*, 2009a) whereas the *Leishmania* spp genome contains 5 ENT genes (Ortiz *et al.*, 2007).

4.3.1 Mammals

The first identified mammalian nucleoside/nucleobase transporter proteins were hENT1 and its rat ortholog rENT1, they were expressed in *Xenopus laevis* oocytes and efficiently transported hypoxanthine, adenine, guanine, uracil and thymine (Yao *et al.*, 2002). The same authors have demonstrated that hENT1 transports thymine, adenine, uracil and guanine. Recently, it has been shown that uridine nucleoside inhibits hypoxanthine uptake (Yao *et al.*, 2011). A novel human nucleoside transporter 1, designated hNT1, has been described and functionally characterized at the molecular level (Umemoto *et al.*, 2009). The gene, encoding hNT1 transporter was cloned from human breast cancer cells and expressed in *Xenopus* oocytes. The carrier was able to transport the antineoplastic agent, 5-fluorouracil with a very highly affinity (K_m value = 69.2 nM). In addition, hNT1 transporter was strongly inhibited by several nucleosides (uridine, thymidine, cytidine, guanosine, inosine, and adenosine) and the pyrimidine nucleobase, uracil. However, despite the details given in that manuscript it seems doubtful that this gene product of only 82 amino acids

encodes a genuine solute transporter. The TM PRED Server and TMHMM Server did not identify any transmembrane segments in this protein. No homologous genes were present in the *Trypanosoma* or *Leishmania* genomes. (Yamamoto *et al.,* 2010) described the first genuine nucleobase transporter in mammals, defined as *Rattus norvegicus* slc23A4: an mRNA for encoding sodium-dependent nucleobase transporter 1, and designated as rSNBT1. The mRNA of the rSNBT1 contains 1989 base pair and the protein sequence of this transporter consists of 599 amino acids. The transporter was found to be able to take up uracil efficiently, as well as the other nucleobases thymine, guanine, hypoxanthine and xanthine, but adenine, cytosine and nucleosides are not or poorly recognized. Furthermore, inhibitory studies on the rSNBT1 found that the transporter can recognize the nucleobase analog, 5-fluorouracil. However, it was also reported that the gene orthologous to the rSNBT1 gene is genetically not present in human. The rSNBT gene is part of the NAT-families, which has no protozoan equivalents either (De Koning & Diallinas, 2000; Gournas *et al.,* 2008).

4.3.2 *Trypanosoma* spp

The first cloned nucleoside transporter gene from this species was designed Adenosine Transporter 1 (TbAT1) (Maser *et al.,* 1999). The gene was functionally expressed in a purine uptake and biosynthesis deficient yeast mutant; the result showed that TbAT1 possessed high affinity transport activities for adenine and adenosine, TbAT1 was shown to encode the P2 transporter. The second transporter, Nucleoside Transporter 2 (TbNT2) (Sanchez *et al.,* 1999), is a P1-type transporter. The TbNT2 gene was expressed in *Xenopus* oocytes and it can take up adenosine, inosine and guanosine. (Sanchez *et al.,* 2002) identified an array of six genes on chromosome 2 of *T. b. brucei* strain 927, consisting of TbNT2 up to TbNT7. The open reading frames of these genes exhibit high identity to each other. Expressing these six genes in *Xenopus* oocytes showed that NT2/927, NT5, NT6 and NT7 seem to possess high affinity to adenosine, inosine and guanosine with K_m values of (0.3 – 4.3 µM). Unlike NT2/927, those transporters are also able to transport hypoxanthine to a limited extent. On the other hand, no substrates were identified for the TbNT3 and TbNT4 transporters when expressed in *Xenopus* oocytes, and their function, if any, is as yet unknown. It is important to note that these transporters failed to accumulate

pyrimidines, including uracil, thymine, thymidine, and uridine (Sanchez *et al.,* 2002).

A related gene, designated TbNBT1 (Burchmore *et al.,* 2003), from *T. b. brucei* was identified and expressed both in a strain of yeast lacking purine transporters, and in *Xenopus* oocytes, and assayed for transport of nucleosides and nucleobases. TbNBT1 was the first cloned nucleobase transporter gene, with high affinity for adenine, hypoxanthine, guanine and xanthine. TbNBT1 also transported guanosine, albeit with affinity lower than its corresponding base, whereas affinities for inosine and adenosine were very much lower. Generally, rates of uptake for nucleosides were also much lower than for nucleobases. A similar study was conducted by (Henriques *et al.,* 2003), which identified another bona fide nucleobase transporter gene from *T. b. brucei*, designated TbNT8.1. Both genes, TbNBT1 and TbNT8.1, which differ in only 3 amino acids, mediate the uptake of the same four purine substrates. Further investigations of the *T. b. brucei* database have identified another four ENT family members, TbNT9 (Al-Salabi *et al.,* 2007), TbNT10 (Sanchez *et al.,* 2004), and TbNT11/TbNT12 (Ortiz *et al.,* 2009a). TbNT9 and TbNT10 were cloned and shown to transport purine nucleosides, adenosine, inosine and guanosine in a very similar way as TbNT2. The genes encoding TbNT11 and TbNT12 were expressed in a *Leishmania donovani* line deficient in purine nucleoside or nucleobase uptake, and identified as purine nucleobase transporters. Both transporters were also shown to have a high affinity to diamidine drug pentamidine.

4.3.3 *Leishmania* spp

The first protozoan nucleoside transporter genes, LdNT1 (Vasudevan *et al.,* 1998) and LdNT2 (Carter *et al.,* 2000) were cloned from *Leishmania donovani* by functional rescue of a transport-deficient mutant. LdNT1 was expressed in *Xenopus* oocytes and in adenosine transport-deficient *L. donovani*. This approach identified two almost identical genes, designated LdNT1.1 and LdNT1.2, which transport adenosine and the pyrimidine nucleosides with a micromolar range of K_m values. LdNT2 was also expressed in *Xenopus* oocytes and in a mutant cell line of *L. donovani* deficient in inosine and guanosine transport activities, and confirmed that LdNT2 appeared as a single gene

encoding 499 amino acids, which has a highly affinity for its substrates and mediates the uptake of the oxopurine nucleosides, inosine and guanosine, with sub-micromolar of K_m values. The first nucleobase transporter to be cloned and functionally expressed from *L. major* was LmaNT3 (Sanchez *et al.,* 2003), which shared 33% amino acid identity with LdNT1.1. LmaNT3 displays high rates of adenine, guanine, xanthine and hypoxanthine transport, with a range of K_m values ranging from 8.5 to 16.5 μM. The final member of the ENT family identified in the *Leishmania major* genome database is LmaNT4 (Ortiz *et al.,* 2007). When the LmaNT4 gene was expressed in a *nt3*$^{(-/-)}$ null mutant, it was shown that LmaNT4 was able to transport adenine but with low affinity.

5. Research strategy and aims

The current chemotherapies against kinetoplastid parasites have several important disadvantages as mention above. Therefore, searching for new routes to treat these neglected diseases is urgently needed. This study will attempt to study pyrimidine transporters and metabolism. One of the more promising approaches to identify pathways involved in the action of potential pyrimidine antimetabolites is to study resistance mechanisms to this compound. Therefore, we studied the mechanism of resistance and mode of action of pyrimidine analogues in kinetoplastid parasites. The study also focuses on the essentiality of pyrimidine *de novo* biosynthesis or salvage to the survival of the parasite. The specific aims are:

1. To assess the uptake of all natural pyrimidine nucleobases and nucleosides into kinetoplastid parasites and identify the pyrimidine transporters, thereby increasing our understanding of pyrimidine salvages in protozoa parasites.

2. To evaluate pyrimidines as subversive chemotherapeutic agents against kinetoplastid parasites, and establish for each their mode of action and their metabolites, as well as to develop and characterise kinetoplastid strains resistant to fluorinated pyrimidines.

3. To present an improved model of pyrimidine salvage and metabolism in kinetoplastids, supported by genome-wide profiling of the predicted pyrimidine biosynthesis and conversion enzymes.

4. To establish whether pyrimidine *de novo* biosynthesis is or is not essential for infectivity of African trypanosomes.

5. To identify kinetoplastid genes associated with resistance to fluorinated pyrimidines.

CHAPTER TWO
Material and Methods

2.1 Culturing Kinetoplastid cells

Parasite cells were kept in liquid nitrogen stores. Before starting this project, the genotypes of used kinetoplastid cell cultures were confirmed by members of the De Koning Lab. Genotyping of wild type bloodstream forms of *T. b. brucei* was proved using multiplex polymerase chain reaction (PCR), and the genotyping of wild type promastigotes of *Leishmania mexicana* and *Leishmania major* was confirmed by restriction analysis of the amplified ITS1 region.

2.1.1 *Trypanosome brucei brucei* bloodstream forms

T. b. brucei bloodstream forms *in vitro*

The standard culture of *T. b. brucei*, bloodstream forms of strain 427-wild type were incubated in sterile culture flasks at 37 °C and 5% CO_2 in HMI-9 medium (obtained from Invitrogen) supplemented with 10% Heated-Inactivated fetal bovine serum (FBS) as described by (Hirumi & Hirumi, 1989). The medium was made by dissolving a sachet of HMI-9 powder and 500 ml of FBS in 4.5 liter of distilled water using a magnetic stirrer overnight at 4 °C. Next, 71.5 µl of 14.3 M ß-mercaptoethanol was added to the medium and the pH was adjusted to 7.4. The medium was sterilized through a Millipore Stericup filter with pore size 0.22 µm inside a flow cabinet. Mid-logarithmic stage of bloodstream forms were regularly passaged (every second day) in small vented-culture flasks containing 10 ml fresh HMI-9 medium.

T. b. brucei bloodstream forms *in vivo*

A number of 200 g adult female Wistar rats (Harlan, UK) were injected intraperitoneally with 2 ml HMI-9 medium inoculated to a density of 10^5 cells/ml of bloodstream forms of *T. b. brucei* s427-wild type. Parasitemia was checked daily by examination of a tail venipuncture. The raped matching method (Herbert & Lumsden, 1976) was used to estimate the number of parasites in the blood samples. When parasitemia reached around 10^9 cells/ml the animal was anesthetized using CO_2 and the blood from infected animal was collected into 50 ml falcon tube supplemented with 500 units/ml of heparin suspended in Carter's

balanced salt solution (CBSS; D-glucose 11.1 mM, HEPES 25 mM, KCl 5.4 mM, NaCl 120 mM, Na_2HPO_4 5.6 mM, $CaCl_2$ 0.55 mM, $MgSO_4$ 0.4 mM, the pH adjust to 7.4). The blood was centrifuged at 2500 rpm at 4 $^\circ$C for 15 minutes to separate its components. Parasites, which lay between the red blood cells and plasma in a buffy coat layer, were resuspended in phosphate-buffered saline plus glucose (PSG buffer; 13.48g Na_2HPO_4 (anhydrous), 0.78g $NaH_2PO_4.2H_2O$ and 4.25 g NaCl, in distilled water with 1% glucose, adjusted to pH 8.0). The contents were applied to the DEAE cellulose (DE-52) anion-exchanger column (Lanham, 1968) where the red blood cells were negatively charged and stick to the cellulose and the trypanosomes were positively charged and pass through the column. Then parasite cells were washed twice more in uptake assay buffer (section 2.3), and resuspended in the same buffer at 10^8 cells/ml for transport assays.

2.1.2 *L. mexicana* and *L. major* promastigotes *in vitro*

Promastigotes of *L. mexicana* (MNY/BZ/62/M379 strain) and *L. major,* (Friedlin strain) were incubated at 25 $^\circ$C in sterilized small vented flasks. Five ml of HOMEM culture medium (Gibco) pH 7.4 provided with 10% FBS were seeded with 10^5 cells/ml of mid-log phase culture. The cells were allowed to grow up to reach late-log stage and then passaged again in fresh medium.

2.1.3 Pyrimidine auxotrophic *T. b. brucei*

Pyrimidine auxotrophic *T. b. brucei in vitro*

Pyrimidine auxotrophic line of *T. b. brucei* bloodstream forms is a genetic deletion mutant lacking the final step of the pyrimidine biosynthesis pathway, which in trypanosomes is a fusion of the two enzymes orotidine monophosphate decarboxylase (pyr6-OMPDCase) and orotate phosphoribosyl transferase (pyr5-OPRTase). Pyrimidine auxotrophic trypanosomes strain (pyr6-5$^{-/-}$) was routinely grown in HMI-9 medium, exactly as described for wild-type *T. b. brucei* bloodstream forms. Where indicated, Pyr6-5$^{-/-}$ cell cultures grown in a pyrimidine-free medium that was identical to the standard HMI-9 except that it did not contain thymidine; this medium was lab-made and abbreviated HMI-9^{-tmd} (Appendix I). The thymidine-free HMI-9 medium was supplemented by 10%

dialysed serum (first thoroughly dialysed and to become pyrimidine-free serum). Dialysis tubing for serum was obtained from Medicell International Ltd, with molecular weight cut off 12-14 kDa. Before use, the tubing was boiled in 4 liters of dialysis buffer (10 mM $NaHCO_3$ and 1mM EDTA adjust pH 8.0) for 30 minutes, rinsed thoroughly in distilled water, then boiled again for 10 minutes in 1 mM EDTA pH 8.0. Tubing was stored in 20% ethanol at 4 °C with tubing submerged. To dialyse FBS, the dialysis tubing was clipped at one end and 50 ml of the serum solution was pipetted into the tubing then the other end was clipped. The FBS was dialysed against PBS pH 7.4 and stirred with magnetic stirrer at 4 °C. The BPS was replaced every 12 hours and the dialysis process continued for around 60 hours.

Pyrimidine auxotrophic *T. b. brucei in vivo*

Six-weeks-old female ICR (CD1) Swiss outbred mice (Harlan, UK) were fed a standard diet for more than a week to adapt the new environment. These mice were divided into 3 groups of six mice each and injected intraperitoneally with 200 µl of HMI-9 medium seeded with 10^5 cells/ml of bloodstream forms of *T. b. brucei* strains: 427-WT, Pyr6-5$^{+/-}$ (single knockout) and Pyr6-5$^{-/-}$ (double knockout). The HMI-9 medium was supplemented with 10% FBS. To quantify parasitemia, 1 µl of blood was daily harvested from the tail of each infected mouse and appropriately diluted in Red Blood Cell Lysis Buffer (Roche). 10 µl of the diluted cells was examined under a light microscope at 40-fold magnification using a haemocytometer and parasitemia was expressed as a number of parasites per ml of blood.

Growth of pyrimidine auxotrophic trypanosomes on different pyrimidine sources

Growth of pyrimidine auxotrophic (*PYR6-5$^{-/-}$*) and/or bloodstream forms of *T. b. brucei* s427-wild type strains were assessed in standard HMI-9 medium provided with 10% FBS and/or HMI-9^{-tmd} supplemented with 10% dialysed serum (section 2.1.3). Cells were seeded at 1×10^5 and/or 5×10^5 cells/ml and grown in 12-well plates. Incubation was in appropriate media at 37 °C and 5% CO_2. Monitoring of cells growth using cell counts was performed in triplicate every 12 or 24 hours. The experiments were performed independently on three separate occasions.

2.1.4 Adaptation of kinetoplastid parasites to tolerance for pyrimidine analogues

Kinetoplastid resistant cell lines were established in order to study pyrimidine analogues metabolism, understand fluorinated pyrimidine mode of action, investigate the resistance factor/s and identify pyrimidine transporters in kinetoplastid cells.

Resistance induction in *T. b. brucei* bloodstream forms

T. b. brucei BSF wild type s427 cells were grown in HMI-9 medium as described previously. Strains adapted to selected pyrimidine analogues were derived from s427-WT through *in vitro* exposure to increasing levels of the drugs over several months. The pyrimidine analogues used were the three most effective fluorinated pyrimidines (5-fluorouracil, 5-fluoro-2'-deoxyuridine and 5-fluoroorotic acid), which displayed micromolar level EC_{50} values (Effective Concentration which inhibits growth by 50%). The first drug concentrations used, starting the adaptation process, were the half EC_{50} values of each drug. Surviving cells were passaged to three flasks, one flask contained drug free, other flask contained the same sub-lethal concentration and the last flask contained twice the previous concentration. The procedure was repeated until a high level of tolerance to the drug was obtained.

Resistance induction in *Leishmania* promastigotes

Promastigotes of Wild type strains of M379 *L. mexicana* promastigotes and Friedlin *L. major* were grown in HOMEM medium as described above. Separate cultures were exposed to non-lethal concentrations (1/2 EC_{50}) of 5-fluorouracil and 5-fluoro-2'-deoxyuridine. The cells were then visually observed for viability and sub-passaged to tolerated concentration of the drugs as mentioned above.

2.1.5 Cloning of kinetoplastid cells

When the strains became viable in higher concentrations of the drugs, adapted strains were cloned out (derived from a single cell) by limiting doubling dilution. This consists of taking a dilute culture (3×10^5 cells/ml) and serially diluting them two-fold across a 96-well transparent plate. The plates were incubated in appropriate conditions for several days, colonies that were grown in the wells

numbered 15-24 are considered as a single cell when the previous wells (at least two wells) are free of growth. The selected clones were then re-cloned again at least twice in the same way. The successful clones were given the following abbreviations: *Trypanosoma* strains adapted to 5-FU, 5-FOA and 5-F2'dUrd referred to as Tbb-5FURes, Tbb-5FOARes and Tbb-5F2'dURes, respectively. *L. mexicana* strains adapted to 5-FU and F2'dUrd were called Lmex-5FURes and Lmex-5F2'dURes; the *L. major* lines adapted to the same drugs were abbreviated Lmaj-5FURes and Lmaj-5F2'dURes, respectively.

2.1.6 Establishing stabilates

Clonal population of parasites were diluted 1:1 in their relative fresh media (HMI-9 medium for trypanosomes and HOMEM for leishmanias) containing 30% sterilized glycerol. The cells were thus stabilated in 15% glycerol and frozen at -80 °C before being transferred to liquid nitrogen for long term storage. New stabilates were brought from the store, thawed at room temperature and passaged to the appropriate medium. Throughout the study, the cell cultures were renewed by bringing out new stabilates after ≤20 passages.

2.2 Chemicals

2.2.1 Radiolabeled compounds

The following radiolabeled substances were used through the study: [5,6-^{3}H]-Uracil (40.3 Ci/mmol) was purchased from Perkin Elmer. [5,6-^{3}H]-Uridine (30 Ci/mmol), [5-^{3}H]-2'-deoxycytidine (20 Ci/mmol) and [2-^{3}H]-Adenosine (40 Ci/mmol) were from American Radiolabel Chemicals Inc. All other radioactive isotopes including: [methyl-^{3}H]-Thymidine (84 Ci/mmol), [methyl-^{3}H]-Thymine (56.3 Ci/mmol), [5-^{3}H]-Cytidine (25.6 Ci/mmol), [5-^{3}H]-Cytosine (25.6), [6-^{3}H]-2'-deoxyuridine (17.8 Ci/mmol), [6-^{3}H]-5-fluorouracil (20 Ci/mmol), [5-^{3}H]-Orotic Acid (23 Ci/mmol) and [2,8-^{3}H]-Inosine (20 Ci/mmol) were from Moravek Biochemicals.

2.2.2 Purines, pyrimidines and their analogues

Uracil, 5-fluorouracil, 5-fluorouridine, uridine, 2-deoxyuridine, 5-chlorouracil, thymine, thymidine, orotic acid, 5-fluoro orotic acid, cytosine, cytidine, 2'-deoxycytidine, 5-fluoro-2'-deoxycytidine, adenine, adenosine, hypoxanthine, inosine, xanthine, 5-iodouridine, 3-deoxythymidine, uridine-5-triphosphate sodium salt, uridine-5-diphosphate sodium salt, uridine-5-monophosphate sodium salt, 3-deazauridine, 2'-4'- dihydroxy-6-methylpyrimidine, 1-methyluracil, 6-methyluracil, 2-mercaptopyrimidine, 3-deazauracil, 4(3H)-pyrimidone, 4-thiouracil, 5-Iodouracil, 5,6-dihydrouracil and 6-azauracil were from Aldrich Sigma. 5-bromouracil, 5-bromouridine and 5-iodo-2'-deoxyuridine were from Avocado Organic. 3'-deoxyuridine, 2-thiouridine and 4-thiouridine were from TriLink Bio Tech. 5-fluorocytidine, 5-chlorouridine, 5'-deoxyuridine, 5'-deoxy-5'-flurouridine, 2'-3'-dideoxyuridine and 2'-deoxy-5-fluorocytidine were from Carbosynth. 5-fluoro-2'-deoxyuridine and 5-fluorocytosine were from Fluka. 2-thiouracil was from ICN Biomedicals. 3'4'- dihydroxy-6-methylpyrimidine was from Merck.

2.2.3 Media and growth chemicals

Hirumi's modified Iscove's (HMI-9) medium was purchased from Invitrogen. Eagle's minimal essential medium (HOMEM) was from GIBCO. Heat-inactivated fetal bovine serum was from PAA Laboratories. Potassium chloride, sodium dihydrogen phosphate hydrate and (4-(2-hydroxyethyl)-1-piperazineethanesulfonic acid (HEPES) were from BDH Prolabo Chemicals. Di-*n*-butylphalate, mineral oil and scintillation fluid [Optiphase HiSafe III] were from Perkin-Elmer. Sodium chloride, sodium hydrogen carbonate, glucose and glycine were from Fisher. Sodium selenite and serine were from Fluka. Threonine was from Acros Organics. Acetonitrile was from Fisher Scientific. Exonulease III was from Takara Biotechnology, Trizol was from Life Technologies. Restriction enzymes, primers and molecular reagents were purchased from Promega. All other chemicals were available from Sigma.

2.3 Transport assays

2.3.1 Preliminary uptake assay establishing the required range (time course):

Assays for transport of [³H]-pyrimidines and/or purines by kinetoplastid cells were performed exactly as described by (Gudin *et al.*, 2006). Cells in the mid to late logarithmic stage of growth were harvested by centrifugation at 2500 rpm for 10 min and washed twice with transport assay buffer (Glucose 2.53 g, HEPES 8.0 g, MOPS 5.0 g, NaHCO$_3$ 2.0 g, KCl 0.3475 g, MgCl.6H$_2$O 0.0625 g, NaCl 5.7 g, NaH$_2$PO$_4$.2H$_2$O 0.9135 g, CaCl$_2$.2H$_2$O 0.0407 g, and MgSO$_4$.H$_2$O 0.0199 g dissolved in 1 litre distilled water, adjusted to pH 7.3 and stored at 4°C). The cells were resuspended at a density of 10^8 parasite cells/ml in the same buffer prior to use in transport experiments. Suspended parasites were left for 20-30 minutes to recover centrifugation stress. Cells were examined and counted in 16 haemocytometer sections of 0.1 mm^3 using a light microscope at 40-fold magnification. Transport was measured at 22 °C, essentially as described by (De Koning & Jarvis, 1997b). Tritium concentration of tested pyrimidines was prepared at 4× in uptake assay buffer. The same volume of 4× radiolabel and the assay buffer were mixed in a clean 15 ml polystyrene tube. In parallel, another volume of 4× radiolabel was mixed with the same volume of 4× related unlabelled pyrimidine in order to bring concentrations down to half in both cases. A volume of 100 µl of cells at 10^8 cells/ml was added to an eppendorf tube containing 300 µl of mixture oil (1:7 mixture of mineral oil and di-n-butyl phthalate) and 100 µl of the 2× diluted tritium compound. The reaction was incubated at ambient temperature for predetermined times. The uptake was terminated by adding 1 ml of ice cold buffer containing saturating levels of unlabeled permeant. Cells were separated from extracellular label by immediate centrifugation at 13000 rpm for 45 seconds in a bench top centrifuge. The cells were spun through the oil layer to form a pellet in the bottom of the tube, isolated from the radiolabel in the aqueous phase above the oil. The entire reaction tube was then flash frozen in liquid nitrogen. The pellets were cut off and collected in scintillation vials, 250 µl of 2% sodium dodecyl sulphate (SDS; 10g sodium dodecyl sulphate in 500 ml distilled water) was added to each vial, and pellets were left for 20 minutes at room temperature. A volume of 3 ml scintillation fluid (Optiphase HiSafe III) was added to the samples and these left

overnight at room temperature to observe the radio activity from the sample and convert that energy to light which is detected by the counter. Parallel triplicate determinations of 4× tritium permeant and 2% SDS were included to calculate the saturable mediated uptake in pmoles per 10^7 cells per sec. The presence of radioactivity was measured in a Beckman LS6000 TA scintillation counter and corrected for non-specific association of the label with the cell pellet. Cells numbers, viability and motility were checked under a phase contrast microscope after each uptake assay experiment.

2.3.2 Dose response assay

Serial two-fold dilutions were prepared, starting at concentrations up to 4 × 10 mM down to 4 × 10 nM giving up to 13 separate dilutions of unlabeled compound (inhibitor). Next, 100 µl of a 1:1 mixture of 4 × label and 4 × inhibitor dilutions were layered over 300 µl of oil in an eppendorf tube, resulting in a mixture containing both the label and the inhibitor at 2 × concentration. The mixture was centrifuged for 20 seconds to collect it in one layer. As a negative control, 100 µl of 2 x radiolabeled compound without inhibitor was pipetted into an eppendorf tube containing 300 µl oil. The transport assay itself started when 100 µl of 10^8 parasite cells/ml was added to the aqueous phase of 2 × radiolabel. The reaction was incubated for a predetermined time as appropriate for each experiment, but always within the linear phase of transport, which was determined from time course experiments before inhibition experiments were undertaken. The uptake was terminated by the addition of 1 ml ice-cold unlabeled test compound at 1–5 mM in assay buffer. The cells were then isolated from the radiolabel in the assay buffer by full speed (13,000×g) centrifugation through the oil, and collected in the bottom of the tube. The experiment continued just as described above (section 2.3.1). The dose response assays were performed to determine the K_m (Michaelis-Menten constant) and V_{max} (Maximum velocity) values of the test compounds, as well as K_i values (Inhibition constants) for potential inhibitors. Inhibition data and time courses were plotted to equations for hyperbolic, sigmoid lines or linear regression, as appropriate, using Prism 5.0 (GraphPad).

2.4. Drug sensitivity assay

Several methods have been used to test the susceptibility of kinetoplastid parasites to drugs and other test compounds. The Alamar Blue (resazurin sodium salt; Sigma) assay was used in this thesis and is a method that has been used widely to determine the sensitivity of kinetoplastid cells to anti-parasitic compounds. This assay depends on metabolic functions of the cells, where live cells can metabolize the dye resazurin from dark blue and non-fluorescence to fluorescent resorufin with a pink colour. This study used Alamar Blue assay to determine the cytotoxicity of several pyrimidine analogues on kinetoplastid cells. Pyrimidine analogues were dissolved in dimethyl sulfoxide (DMSO) and diluted in the appropriate medium for use, with DMSO ≤1%.

2.4.1 Drug sensitivity assay in bloodstream forms of trypanosomes

Drug sensitivity assay in trypanosomes using Alamar Blue dye was performed as described by (Raz *et al.,* 1997). A volume of 100 µl of HMI-9 medium supplemented with 10% FBS was loaded in a white-bottomed 96-well plate (Greiner) except the first well, which was left empty. Known concentrations of tested drugs were diluted in HMI-9 medium and added in the first well at a volume of 200 µl; up to four drugs could be tested in one plate, each being diluted over two rows. The four drugs were doubly diluted, and gently mixed, over 23 wells per drug leaving the last well of each dilution as a negative control (drug free). Pentamidine or diminazene were used as positive controls throughout the study. 100 µl of bloodstream forms of *T. b. brucei* at a density of 2×10^5 cells/ml were inoculated into each well to reach a final density of 1×10^5 cells/ml. In the case of *T. b. brucei* pyrimidine auxotrophic cells, Alamar Blue experiments were performed in the presence of 2 µg/ml of hygromycin, to keep selective pressure on the knockout construct. After 48 hours of incubation the plates at 37 °C and 5% CO_2, 20 µl of Alamar Blue assay buffer was added to each well (12.5 mg of resazurin sodium salt dissolved in 100 ml of PBS, mixed by stirring for half an hour, filtered with a 0.22 µm filter in an aseptic environment, stored at -20 °C and well-protected from light). Plates were incubated for a further 24 hours in the same conditions. Live cells reduce the dark blue dye to a pink colour. The concomitant change in fluorescence was measured using a

FLUOstar Optima plate reader (BMG Labtech, Durham, NC) at wavelengths of 544 nm for excitation and 620 nm for emission. The EC_{50} values were calculated by analysing the data with the Prism 5.0 software. Each experiment was performed at least on three independent occasions.

2.4.2 Drug sensitivity assay in promastigotes of *Leishmania* spp

Alamar Blue assay in *Leishmania* spp (Mikus & Steverding, 2000) was performed as described for trypanosomes (section 2.4.1) with few changes. HOMEM medium supplemented with 10% FBS was used for culturing *L. major* and *L. mexicana* promastigotes. A preliminary cell culture was diluted to a density of 2×10^6 cells/ml for a final density of 1×10^6 cells/ml. The 96-well plates were incubated at 25 °C for 72 hours before adding the Alamar Blue dye. Since *leishmania* parasites metabolise the Alamar Blue dye slower than trypanosomes (Gould *et al.*, 2008), the cells were incubated with the dye for a further of 48 hours. Fluorescence measurements and EC_{50} calculations were performed as described above (section 2.4.1).

2.5 Trypanosomes cell cycle using flow cytometry analysis

Flow cytometry assay can be used to assess the effects of anti-protozoan compounds on African trypanosomes cell cycle (Hammarton, 2003; Mutomba *et al.*, 1997). However, the method in this study was used to investigate the DNA content of individual, fixed, pyrimidine auxotrophic trypanosomes grown in different natural pyrimidine sources. Pyrimidine auxotrophic trypanosomes (*PYR6-5$^{-/-}$*) were incubated in 25 ml flasks containing 10 ml of HMI-9^{-tmd} supplemented with 10% dialysed serum; each flask was provided with 0.1 mM of only one natural pyrimidine source. The supplemented natural pyrimidine sources included nucleobases (uracil, cytosine, thymine), ribonucleosides (uridine, cytidine, thymidine) or 2'-deoxynucleosides (2'-deoxyuridine, 2'-deoxycytidine). The flasks were incubated for various time points (24, 36 and 48 hours), a sample was taken from each culture in a clean autoclaved tube for assessment of DNA content as described by (Ibrahim *et al.*, 2011). The cells were centrifuged at 1000 rpm for 10 minutes at 4 °C. Next, the pellet was resuspended and fixed in 1 ml of 70% methanol diluted in PBS pH 7.4 and kept

overnight at 4 °C. The fixed cells were spun at 2500 rpm for 10 minutes at 4 °C and washed twice in 1 ml of PBS. Subsequently, the pellet was resuspended in 1 ml of PBS containing 10 µg/ml of propidium iodide and the same concentration of RNase A. Stained samples were kept in the dark for 45 minutes at 37 °C prior the analysis. DNA contents assessed by a Becton Dickinson Fluorescence Activated Cell Sorter Calibur (FACSCalibur) using the FL2-Area detector and CellQuest software. ModFit software was used for cell cycle analysis and quantification (ERITY 1995-1996 Software House Inc).

2.6 Molecular techniques

The nucleotide and amino acid sequences for genes were found by searching in GeneDB or TriTrypDB websites. These websites were used for searching with the Basic Local Alignment Search Tool (BLAST) to compare genes sequences. In addition, the TMHMM server at http://www.cbs.dtu.dk/services/TMHMM/ was used to estimate the number of transmembrane domains in indicated genes. Also the CLC workbench software was used to create sequence alignments.

2.6.1 Generation and confirmation of pyrimidine auxotrophic trypanosomes

The plasmid pLHTL-PYR6-5 (Scahill *et al.,* 2008) was generously donated by Professor George Cross of Rockefeller University, New York, USA. This construct contained a hygromycin resistance cassette (hygromycin phosphotransferase) and a negative selection marker, *Herpes simplex* Thymidine Kinase (*HSVTK*) open reading frame (ORF) between *loxP* domains (Sternberg *et al.,* 1981) and was targeted to the *PYR6-5* locus by flanking sequences of 496 base pair (bp) immediately downstream of the target locus and of 365 bp commencing 134 bp upstream of the ORF. Bloodstream forms of *T. brucei* s427-WT were cultivated to a density of ~1-2 × 10^7 cells/ml and washed into Human T-Cell lysis buffer (Schumann *et al.,* 2011; 90 mM Na_3PO_4, 5 mM KCl, 0.15 mM CaCl, 50 mM HEPES, pH 7.3) for transfection with the *LHTL-PYR6-5* cassette (liberated by digestion with *Pvu*II) using an Amaxa Nucleofector electroporator exactly as described by (Scahill *et al.,* 2008), creating a single knockout (*PYR6-5$^{+/-}$*) strain. Transformants were grown and cloned out in standard HMI-9 medium supplemented with 10% FBS containing 2 µg/ml hygromycin. The loss of the

second *PYR6-5* allele was induced by exposure of the clonal lines to 100 µM of 5-fluoroorotic acid, resulting in a double knockout strain (*PYR6-5$^{-/-}$*) that was cloned by limiting dilution. *PYR6-5* single and double knockout clones were confirmed by PCR and Southern blot technique.

PCR confirmation of double knockout

DNA was extracted from WT-s427, and from single and double knockout auxotrophic strains using a standard Qiagen DNeasy Blood and Tissue Kit, following the manufacturer's instruction. Primers were designed to amplify an 870 bp part of the *PYR6-5* gene. PCR was performed on 200 nanograms (ng) of the isolated DNA using 0.75 µl of forward primer (5´ GTTCTCGAGTGCAAGCGGAT) and 0.75 µl reverse primer (5´CACAATGCGGTCAAACTGCA). Each reaction contained 4.0 µl 5× reaction buffer, 1 µl of 10 mM dNTPs (dATP, dCTP, dGTP and dTTP) and 0.2 µl Go Taq polemerase. The PCR reaction was made up to 20 µl with distilled water. Amplification was performed on PCR System (G-STORM, Thermo Scientific). Primers were annealing at 56 °C for 30 seconds and extension at 72 °C for 60 seconds. Agarose gel was prepared in 100 ml TAE buffer (84.4g Trizma base, 100 mM EDTA in 1 liter distilled water, adjust pH 8.0 with glacial acid) with 1% agarose and 8 µl of SYBR Safe stain (10,000 x Invitrogen). The DNA samples were run on the gel at 80–100 mV alongside 1 kb ladder for about one hour. DNA in the gel was visualised by ultraviolet light on a trans-illuminator (UVP Laboratory Products).

Southern blot confirmation of double knockout

A Southern blot was also performed to confirm knockouts, using restriction digest of 10 µg DNA and blotting performed as described by (Martin & Smith, 2006), using DNA probes specific for the *PYR6-5* and hygromycin B phosphotransferase genes. The *PYR6-5* probe was generated using the primers and conditions given above for the PCR confirmation, whilst the hygromycin probe was generated by a PCR to amplify 1029 bp using forward primer (5'ATGAAAAGCCTGAACTCAC) and reverse primer (5'ACTCTATTCCTTTGCCCTCG). Primers were allowed to anneal at 55 °C for 30 seconds and extension was performed at 72 °C for 60 seconds. Whole PCR products were run on 1% agarose gel alongside 1 kb ladder as an appropriate DNA

marker. DNA fragments that appeared of the right size were cut off using a clean scalpel and transferred to a sterile tube. The DNA was then extracted using a Qiagen gel extraction Kit, following the manufacturer's instruction. DNA concentrations were measured using a NanoDrop device.

Approximately 10 µg of extracted DNA from s427-WT, and single and double knockout were digested at 37 °C for overnight using restriction enzymes *Cla*I and *Spe*I. Digested DNAs were run on 400 ml of 0.7% agarose gel and run at 30 volts cm^{-1} overnight. The gel was then immersed in 500 ml of depurination solution (22.7 ml of 11 M HCl in 1 liter distilled water) for ~10 minutes. Denatured DNA was performed by immersing the gel in 500 ml of a denaturing solution (20 g NaOH and 87.664 g NaCl in 1 L distilled water) for 15 minutes. Next was immersion of the gel in 500 ml of neutralising solution (87.6 g NaCl and 78.8 g Tris base in 1 L distilled water, pH 7.4) for 15 minutes. All these steps were performed at room temperature with gentle shaking. The DNAs were then transferred from the gel to nylon membrane (Hybond^{TM}-N, Amersham Biosciences) at room temperature overnight. Membrane was stained with methylene blue for 10 minutes, rinsed several times for one minute by distilled water until the DNA bands became visible, wrapped in clingfilm and stored at 4 °C. Membrane was then pre-hybridised for 2 hours at 42 °C on the rotational shaker using hybridization solution (15 ml 50% formamide, 7.5 ml 5× SSC (sodium chloride and sodium citrate solution)), 6 ml 50× Denhardt's solution, 0.3 ml 10% SDS, 0.6 ml 1 M NaH$_2$PO$_4$ pH6.5, 0.3 ml 0.5 M EDTA pH 8, 0.6 ml 10 mg/ml Herring Sperm DNA denatured for 5 minutes at 95 °C). Next, a radioactive probe (Prime-it II Random Primer Labelling (Stratagene)) was prepared by mixing 25 ng probe DNA with 10 µl random oligo primers, made up to 37 µl with ddH$_2$O and heated at 95 °C for 5 minutes. After a brief centrifugation the following mixture (10 µl 5× primer buffer, 2 µl γ^{32}P dATP and 1 µl Klenow (5 U/µl)) was added and incubated at 37 – 40 °C for 10 minutes. The probes were purified by resuspending resin in column by vortexing and adding the labeled probe (25 - 50 µl) to top centre of the resin and spinning for 3 minutes. The probe was then denatured for 5 minutes, added to the tube containing the hybridisation solution and membrane and incubated for more than 16 hours. Next, the hybridization mixture was washed into washing buffer (0.1 × SSC and 0.1% SDS) at room temperature. Some of the wash buffer (200 ml) was pre-heated to 55 °C in the

shaking water bath and 20 ml of pre-heated wash buffer was added to the tube and incubated at 55 °C for 20 minutes for the first wash and 45 minutes for the second wash. The filter was monitored with a Geiger counter and the probe should hybridise to the DNA on the filter. A sheet of MXB Film was added in the dark room then exposed to X-ray at -80 °C. Finally, auto-radiographs were developed using the Xomat according to the manufacturer's instructions.

2.6.2 Quantitative PCR of uridine phosphorylase

RNA isolated from *T. b. brucei* s427-WT and PYR6-5$^{-/-}$ cells was quantified using a NanoDrop device; 2 μg of RNA was diluted in RNase-free water to a total volume of 25 μl. Complementary DNA (cDNA) was produced using a Reverse Transcriptase (RT) kit (Primerdesign, UK). cDNA for each sample was diluted 1:10 and then used for Real Time-PCR. Amplification of cDNA was performed in a 7500 Real Time PCR System (G-STORM, Thermo Scientific). The dissociation curve was used to ensure the amplification of only one product; samples without RT or cDNA were used as controls. A constitutively expressed gene, GPI8 (Lillico *et al.,* 2003), was used as internal control, with primer sequences 5´- TCTGAACCCGCGCACTTC and 5´- CCACTCACGGACTGCGTTT. For uridine phosphorylase (UP), the ΔΔCT method was used for relative quantification (RQ) using WT cells in HMI-9 as a calibrator or internal control. Data was analyzed using Applied Biosystems 7500 SDS Real-Time PCR systems software. Primers used for the amplification of UP were 5´-TTTGACCCCTCCACCATGA and 5´- GATTCAGCAGGTGAGCCACAA. The entire experiment was performed on three independent occasions, starting from independent cell cultures and RNA isolation. This experiment was performed in our laboratory in collaboration with Daniel Tagoe.

2.6.3 Extraction of DNA from *T. b. brucei*

Kinetoplastid cells were grown in a large culture flask to mid log phase. The cells were spun down for 5 minutes at 2500 rpm. The pellet was resuspended in 1 ml of PBS and transferred to eppendorf tube and spun again for 5 minutes at 1500 rpm. After removing the supernatant, a volume of 500 μl lysis buffer (100 mM NaCl, 10 mM Tris-HCl pH 8.0 and 5 mM EDTA), 25 μl of 10% SDS and 50 μl of 10 mg/ml RNase A was added to the sample and incubated overnight at 37 °C.

The sample was washed twice in an equal volume of phenol:chloroform:isoamyl-alcohol (25:24:1; saturated with 10 mM Tris, pH 8.0 and 10 mM EDTA). The sample was shaken gently for 5 minutes then spun for 5 minutes at high speed. The aqueous phase was washed again twice more in an equal volume of chloroform, shaken and spun for 5 minutes. Next, the aqueous phase was transferred to a clear 15 ml polystyrene tube contains 1.5 ml absolute ethanol. The cloud of DNA was removed and transferred to 1 ml of 70% ethanol in a centrifuge tube. The DNA was spun down at top speed for 10 minutes, then the supernatant was removed and the precipitated DNA was drained off. Finally, DNA was resuspended in 30-50 µl of 1× Tris-EDTA buffer (10 mM Tris-HCl, pH 7.5 and 1 mM EDTA) and left overnight at 4 °C (without mixing).

2.6.4 Isolation of RNA from *T. b. brucei*

Cell culture at 2×10^6 was collected by centrifugation at 2500 rpm for 10 minutes at 4 °C. Supernatant was removed and cell pellet was resuspended thoroughly in 1 ml of Trizol (Life Technologies; contains guanidine isothiocyanate which is a protein denaturant in which RNases are not active, and phenol where soluble RNA can be separated from the phenol soluble protein), RNases are thus separated from RNA. After 5 minutes of incubation at room temperature, a volume of 200 µl of chloroform was added and mixed by inverting continuously for 1 minute. The homogenised sample was centrifuged at full speed for 20 minutes at 4 °C. After centrifugation, the mixture was separated into lower red, phenol-chloroform phase, an interphase and colourless upper aqueous phase. RNA remained exclusively in the aqueous phase. Since RNases are of biological origin all reagents and plastics should be RNase free to avoid reintroducing RNase by simple precautions. The aqueous phase was transferred to 500 µl of isopropanol, incubated at room temperature for 10 minutes and centrifuged at full speed for 20 minutes at 4 °C. The RNA precipitated in the side of the bottom of the tube. RNA was washed in 1 ml of 75% ethanol and vortexed until the pellet was loosened from the wall of the tube. Next, the sample was centrifuged at full speed for 5 minutes at 4 °C and the supernatant was removed carefully. The pellet was air dried on the bench for 10 minutes. 50-100 µl of autoclaved water treated by diethyl pyrocarbonate (DEPC; 500 µl of DEPC with 500 ml ddH$_2$O was shaken and left overnight at room temperature, then autoclaved and

kept at room temperature) was added to the RNA and heated at 65 °C for 10 minutes. Dissolved RNA was pulse spun and stored at –80 °C until use.

2.6.5 Full genome sequences

DNAs from parasite cells were extracted as described in section (2.6.4). The used DNA was 2-5 µg of double stranded DNA in TE buffer at a concentration greater than 20 ng/µl, in a volume of 20 - 100 µl, and in fragments >500 bp. In collaboration with the Sanger Institute in Hinxton, UK we sequenced the extracted DNA from several cell lines: bloodstream forms of *T. b. brucei* including s427-WT, Tbb-5FURes, Tbb-5FOARes and Tbb-5F2'dURes; promastigotes of *Leishmania* spp including *L. mexicana* sM379-WT, Lmex-5FURes intermediate adapted to 5-FU, Lmex-5FURes (highly adapted), *L. major* sFriedlin-WT, Lmaj-5FURes and Lmaj-5F2'dURes.

Illumina sequencing and SNP analysis: genomic DNA preparations were used to create Illumina paired-end sequencing libraries that were sequenced on Illumina HiSeq machines using standard procedures yielding paired sequence reads of 75 bases length. For each parasite strain, the data yield from the sequencing machines (passing the default purity filter) was between 12.5 million and 36.6 million read pairs (median of 17.3 million) which corresponds to a nominal genome coverage of between 58.5-fold and 171.1-fold (median of 81.6-fold). Mapping of the paired sequencing reads to the genome reference sequences from GeneDB (*Trypanosoma brucei* TREU927, *Leishmania major* Friedlin, and *L. mexicana*-M379) was carried out with SMALT (http://www.sanger.ac.uk/resources/software/smalt/), version 0.5.7 using the following parameters: wordlength -k = 13, skipstep -s = 7, maximum insert size -i = 1000, minimum Smith-Waterman score -m = 65, and with the exhaustive search option (-x) enabled. Of the sequencing reads, the following percentages were thus mapped as "proper pairs" (i.e. with the two mates of a sequence read pair mapped within the expected distance and in the correct orientation) to the genome reference sequences: between 42.3% and 42.8% of reads for *T. brucei*, between 76.6% and 78.8% for *L. major*, and between 61.1% and 72.9% for *L. mexicana*. The median insert size between read pairs was between 467 and 601 nucleotides. Only sequence reads mapped as "proper pairs" were used for subsequent analyses and the first 5 and last 15 nucleotides were clipped from all

reads prior to subsequent analysis. Genotypes for every genomic position were determined with SAMtools version 0.1.17 (Li *et al.,* 2009) by using the "samtools mpileup" command with minimum baseQ/BAQ ratio of 15 (-Q) followed by SAMtools' "bcftools view" command with options -c and -g enabled. For a given parasite strain, single nucleotide polymorphisms (SNPs) were identified by comparison with the parental wild-type parasite strain and by filtering all genotype calls according to the following criteria: a minimum of 8 high-quality base calls (DP4), a maximum coverage depth (DP) of the median plus 3 times the standard deviation, a minimum quality score (QUAL) of 23, a minimum mapping quality (MQ) of 23, a minimum second best genotype likelihood value (PL) of 35, a maximum fraction of conflicting base calls for homozygous genotype calls of 10%, and a minimum percentage of 5% for base calls (as a fraction of all base calls for a given genotype) that map either to the forward or the reverse strand of the reference sequence.

2.7 Metabolomic technologies

Metabolite extraction techniques have been developed by (TKindt *et al.,* 2010) and (Saunders *et al.,* 2010), and very recently, methodological advances in metabolomics have been applied to kinetoplastid parasites (Creek *et al.,* 2011; Creek *et al.,* 2012a).

2.7.1 Metabolomic sample preparation

Kinetoplastid parasites were grown in an appropriate medium to log phase stage, resuspended at 2×10^6 cells/ml in 50 ml relevant medium (HMI-9 for trypanosomes and HOMEM for leishmania) provided with 10% FBS in culture flask and incubated with 100 µM of the test compound for 8 hours in excellent appropriate conditions. Cells were transferred to a 50-ml centrifuge tube and instantly cooled down to 4 °C using a dry ice/ethanol bath. This culture was centrifuged at 2500 rpm for 10 min at 4 °C and the pellet was lysed by addition of 200 µl of chloroform/methanol/water (1:3:1 v/v/v) with internal standards for mass spectrometry (1 µM each of theophylline, Cl-phenyl-cAMP, N-methyl glucamine, canavanine and piperazine), followed by vigorous mixing for one hour at 4 °C. Precipitated proteins and cellular debris were removed from

metabolites by centrifugation at 13000 rpm for 3 minutes. Metabolite extracts were stored in HPLC vials at -80 °C until use. Control samples were also performed in parallel, including untreated cells grown in parallel, unused growth medium, 100 µM of the test compound prepared in relevant medium and extraction solvent blanks. All experiments were established separately in triplicate.

2.7.2 Metabolomics sample analysis

Metabolomic samples were analyzed by hydrophilic interaction liquid chromatography (HILIC-LC) coupled to high resolution mass spectrometry (MS). LC separation utilized a zwitterionic ZIC-pHILIC column (Merck Sequant) with ammonium carbonate alkaline gradient as recently described by (Zhang *et al.,* 2012). The method was performed on a Dionex RSLC3000 (Thermo Fisher) LC system coupled to an Exactive Orbitrap (Thermo Fisher) operating at 50,000 resolution in positive and negative mode ESI (rapid switching) with MS parameters as previously published (Creek *et al.,* 2011). Mass calibration was performed immediately before the batch, followed by analysis of authentic metabolite standards to determine standard retention times (Creek *et al.,* 2011). Samples were analyzed in random order and signal stability assessed by periodic analysis of pooled quality control samples. Data from each sample were manually inspected and irreproducible samples excluded from analysis based on total ion chromatogram (TIC) signals and internal standards.

2.7.3 Metabolomic data analysis

Metabolomics data was analyzed using the IDEOM application (http://mzmatch.sourceforge.net/ideom.php) with default parameters (Creek *et al.,* 2012b) after selecting the pHILIC chromatography method, raw files were converted to mzXML format and peaks were detected using the XCMS Centwave algorithm (Tautenhahn *et al.,* 2008). Peak data for all samples was combined, filtered and saved in peakmL files using mzMatch (Scheltema *et al.,* 2011). Noise filtering and putative metabolite identification was performed in IDEOM based on accurate mass and retention time, parameters are available in the supplementary IDEOM file. In addition to the automated identification of metabolites from the IDEOM database, data were screened for novel fluorinated

metabolites by the addition of 17.9906 to all known metabolite masses, which detected peaks with accurate mass and retention times consistent with 5-fluoro-UDP, 5-fluoro-UTP, fluoro-N-carbamoyl-L-aspartate, 5-fluoro-orotic acid (detected primarily as the CO_2–loss fragment) and fluorinated UDP-hexose and UDP-*N*-acetyl-hexosamine (putatively identified as 5-fluoro-UDP-glucose and 5-fluoro-UDP-*N*-acetylglucosamine). LC-MS peak heights were used for semi-quantitative analysis of metabolite abundances, and statistical analyses comprised pair-wise comparisons of study groups by unpaired rank products analyses with *P*-values for probability of false positives based on 200 permutations.

2.8 DNA degradation

Pyrimidine auxotrophic trypanosomes (*Pyr6-5$^{-/-}$*) were incubated with 100 µM of 5-fluoro-2'-deoxyuridine or 5-fluorouracil for 12 hours in HMI-9^{-tmd} supplemental with 10% dialysis serum (section 2.1.3). In parallel, untreated control cells were cultured in the same medium. Extracted DNA from these cultures was resuspended in 30 µl TE buffer and quantified using a NanoDrop device, typically containing 4–5 µg DNA/ml. 10 µl of 10× exonulease III buffer, 1000 units of Exonulease III enzyme and 85 µl distilled water were added to the resuspended DNA. The reaction was followed by incubation at 37 °C for 48 hours. From the digest 20 µl was mixed vigorously with 60 µl of chloroform/methanol/water (section 2.7.1) and centrifuged at high speed for 5 minutes. The supernatant was stored at -80 °C until use in metabolomic analysis.

2.9 RNA degradation

Pyrimidine auxotrophic *T. b. brucei* (*Pyr6-5$^{-/-}$*) were exposed to 100 µM of 5-fluorouracil for 12 hours using HMI-9 free pyrimidine medium (section 2.1.3). Extracted RNAs from those cells were incubated overnight at 37 °C with 10 µl of 10 mg/ml phosphodiesterase II (3'exonuclease). The RNAs extracted from untreated cells grown in parallel were used as negative control. The digested RNA was mixed with 80 µl chloroform/methanol/water (section 2.8.1) and centrifuged for 5 minutes at high speed. Supernatant was stored at -80 °C until use in metabolomic analysis.

2.10 Construction of a profile library for enzymes of the pyrimidine pathways

Reference sequences for the enzymes of pyrimidine metabolism were downloaded from UniProt (www.uniprot.org), searching by enzyme code number (EC) in the manually annotated SwissProt section. Each of the obtained sets of sequences was redundancy reduced by ≤50% identity, aligned with ClustalW (Thompson *et al.,* 2002), and converted into a HMM-profile with *hmmbuild* of the HMMer 3.0 package (Eddy, 2009). The profiles were concatenated to a library. Predicted proteomes were downloaded from Integr8 (www.ebi.ac.uk/integr8) and searched with *hmmscan* of the HMMer package. Hierarchical clustering of proteomes based on the best scores obtained to each of the profiles was performed with the R package pvclust (Suzuki & Shimodaira, 2006), using Canberra distance and the McQuitty algorithm. This part was performed by our collaborator Pascal Mäser (Swiss Tropical and Public Health Institute, Basel, Switserland.

2.11 Effect of 5-FU on glycosylation in *T. b. brucei*

Bloodstreams of *T. b. brucei* WT-s427 and pyrimidine auxotrophic cultures were adjusted to 1×10^6 cell/ml and incubated for 12 hours in HMI-9 medium supplemented with 10% FBS in the presence or absence of 100 μM 5-FU or 5F-2'dUrd. Cell cultures were spun down at 2500 rpm at 4 °C and washed three times in sterilized PBS. Consequently, the pellets were suspended at a density of 10^7 cells/ml in 100 μl protein gel loading buffer (50 mM Tris-HCl pH 6.8; 2% SDS; 10% glycerol; 1% ß-mercaptoethanol; 12.5 mM EDTA and 0.02% bromophenol blue). The samples were then incubated at 95 °C for 15 minutes and stored at -20 °C until use. Interaction of glycoproteins with lectins was visualized by separating proteins by reducing SDS-PAGE (using 10% gels and 10^7 cell equivalents/lane) and then Western blotting onto Immobilon-P transfer membranes (Millipore). Gels were stained with Brilliant Blue electrophoresis reagent to check for equal cell loading and for visualization of protein bands. Membranes were stained using Erythrina cristigalli lectin (1:1,000) or Ricinus communis lectin (1:1,000) (both obtained from Vector Laboratories) and washed extensively before incubation with streptavidin-HRP (1:7,000) (Thermo Scientific) as recently described by (Mehlert *et al.,* 2012). Further extensive

washing was followed by visualization of bands using ECL reagents (GE Healthcare). This experiment was performed in the laboratory of our collaborator Mark Field at the University of Cambridge, UK.

CHAPTER THREE

Trypanosoma brucei: Pyrimidine transporters and trypanocidal pyrimidine analogues

3.1 Introduction

Membrane transporters have been involved in many drug uptake processes, thus studying this phenomenon requires the identification, detailed characterization and cloning of parasite-specific high-affinity transporters for substrates with a low concentration in the host tissues. The kinetoplastid transporters for purines and pyrimidines seem to meet these criteria. Since trypanosome parasites are unable to synthesize the purine ring *de novo* , these purine transporters have been studied extensively (Gudin *et al.,* 2006). To date, sixteen members of the equilibrative nucleoside transporter (ENT) family, which encodes all the protozoan plasma membrane purine transporters, have been identified and cloned in *Trypanosoma* spp. Although purine transporters can mediate the uptake of purine and/or pyrimidine antimetabolites in kinetoplastid parasites (De Koning & Jarvis, 1998; Papageorgiou *et al.,* 2005; Wallace *et al.,* 2002), pyrimidine nucleosides and nucleobases failed to inhibit with high affinity the uptake of purines in procyclics and bloodstream forms of *Trypanosoma brucei*, suggesting that separate pyrimidine transporters must be present in the plasma membrane.

In contrast to purines, *Trypanosoma* species are known to possess both salvage and biosynthesis routes for pyrimidines (De Koning *et al.,* 2005; Hammond & Gutteridge, 1982; Hassan & Coombs, 1986; Papageorgiou *et al.,* 2005). Only few studies have been conducted on pyrimidine uptake in kinetoplastid parasites, this might be attributed to the parasites' ability to synthesise the pyrimidine ring. The first high affinity transporter for uracil was described in procyclic forms of *T. b. brucei* and designated TbU1 (De Koning & Jarvis, 1998). The uptake of [³H]-uracil by TbU1 was not inhibited by a broad range of purine and pyrimidine nucleosides and nucleobases. (Gudin *et al.,* 2006) found that TbU1 transporter was also able to mediate uridine uptake, in their survey of pyrimidine transport activities, they identified a very high-affinity transporter for cytosine in *T. b. brucei* procyclic forms which was designated TbC1. This transporter was inhibited by cytosine and uracil with high affinity but no cytidine uptake was detectable in procyclics. The other pyrimidine transporter identified by the same workers in *T. b. brucei* procyclics is TbU2; this transporter was a higher-affinity uridine transporter. To date, those three pyrimidine transporters are the only pyrimidine-specific permeases identified

and characterized in *Trypanosoma* spp. The well known anticancer drug 5-fluorouracil, a halogenated pyrimidine nucleobase, was found to be a good inhibitor to [3H]-uracil uptake in *Trypanosoma* spp, and killed trypanosomes efficiently (De Koning & Jarvis, 1998; Gudin *et al.*, 2006; Papageorgiou *et al.*, 2005).

Currently information on pyrimidine transporters in bloodstream trypanosomes is very incomplete, and no study systematically assessed the effect of pyrimidine analogues on bloodstream forms of *T. b. brucei*. The potential for resistance against pyrimidine nucleoside and nucleobase analogues by kinetoplastid species has also not been investigated. The lack of information about pyrimidine transport activities in bloodstream forms of *T. b. brucei* s427 delays efforts to develop a pyrimidine-based chemotherapy. Therefore, this study systematically assessed the uptake of all natural pyrimidine nucleobases and nucleosides into bloodstream trypanosomes. In addition, we screened the potential for the accumulation of some halogenated pyrimidine compounds through pyrimidine transporters and generated cell lines resistance to toxic pyrimidine analogues in BSF of *T. b brucei*.

3.2. Uracil uptake in *T. b. brucei* BSF-WT

In procyclic trypanosomes, pyrimidine uptake is mostly mediated by the TbU1 transporter, the main substrate of which is uracil. Therefore, this study investigated [3H]-uracil transport in bloodstream forms in order to assess whether pyrimidines are salvaged in a similar way in this life-cycle stage, and if so, whether it could be mediated by the same transporter.

Transport of 0.15 µM [3H]-uracil was linear for at least 120 seconds (r^2 = 0.99), and significantly different from zero (F test; $P<0.0001$), with a rate of 0.034 ± 0.002 pmol·10^7 cells^{-1}·s^{-1} and was almost entirely inhibited by 1 mM of unlabelled uracil (Figure 3.1), transport was reduced by >97% but still significantly different from zero (F-test, P = 0.03). This showed that [3H]-uracil uptake is transporter-mediated and that simple diffusion does not play a significant role in this process, at least at low uracil concentrations. Subsequent [3H]-uracil assays used 0.15 µM of label and a 30 seconds incubation time very much within the linear phase of uptake.
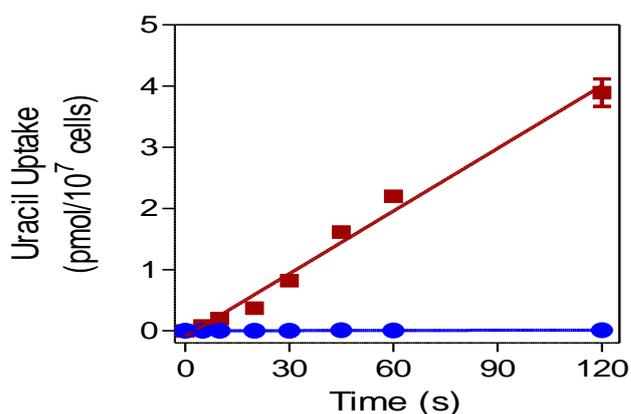
Figure 3.1. Timecourse of [^{3}H]-uracil transport in *T. b. brucei* bloodstream forms over 2 min. The figure shows transport of 0.15 µM [^{3}H]-uracil (■) was linear and totally inhibited in the presence of 1 mM unlabelled uracil (●). Error bars are SE, and when not shown fall inside the symbol. The experiment was performed in triplicate and was one of several independent experiments with highly similar outcomes. The uptake was terminated by the addition of 1 ml ice-cold 1 mM uracil in assay buffer and immediate centrifugation through oil.

Next determinations were the uracil K_m and V_{max} values for BSF of *T. b. brucei*. This was possible as all inhibition data were consistent with monophasic inhibition with Hill slopes near -1, i.e. a single transporter model. The graph in Figure 3.2A shows a representative inhibition profile of [^{3}H]-uracil inhibited by unlabeled uracil and shows the conversion to a Michaelis-Menten saturation plot (Figure 3.2B). The average K_m values over six identical triplicate experiments was 0.54 ± 0.11 µM, with a V_{max} of 0.14 ± 0.03 pmol·10^7 cells^{-1}·s^{-1}. This K_m value was similar to the value previously reported for TbU1 (0.46 ± 0.09 µM) but the V_{max} is almost 5-fold lower than in procyclics.
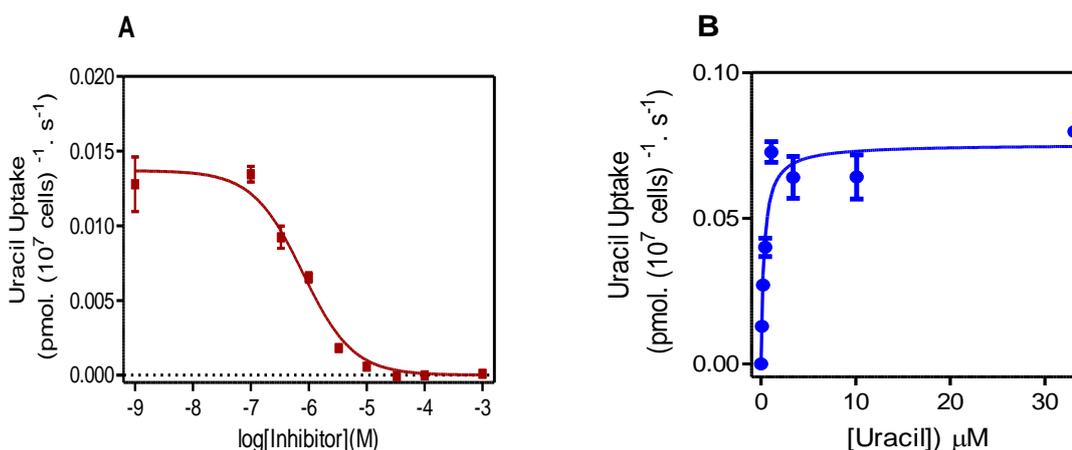
Figure 3.2. Characterization of [^{3}H]-uracil transport in *T. b. brucei* BSF. **A.** Inhibition of 0.15 µM [^{3}H]-uracil uptake over 30 seconds by various concentrations of unlabelled uracil (■). **B.** Conversion the data from frame A to Michaelis-Menten saturation plot (●), for 30 seconds incubations. The uptakes were terminated by the addition of 1 ml ice-cold 1 mM uracil in uptake assay buffer and immediate centrifugation through oil. Error bars were SE of triplicate determinations.

In order to investigate whether the same transport activity was expressed in both life cycle forms of *T. b. brucei,* the affinity of BSF uracil transporter was assessed. Whereas TbU1 displayed moderately high affinity (33 μM) for the nucleoside uridine (De Koning & Jarvis, 1998), uracil uptake in BSF was virtually insensitive to uridine, with 10 mM of the nucleoside uridine inhibiting just approximately 50% of 0.15 μM [^{3}H]-uracil uptake (Figure 3.3). However, TbU1 and TbU3 transporters were similarly sensitive to the fluorinated uracil counterpart, 5-fluorouracil (Figure 3.3). The striking difference in uridine sensitivity between uracil transport activities in procyclics and BSF showed that these were distinct transporters, and we designated the novel BSF uracil transporter TbU3.
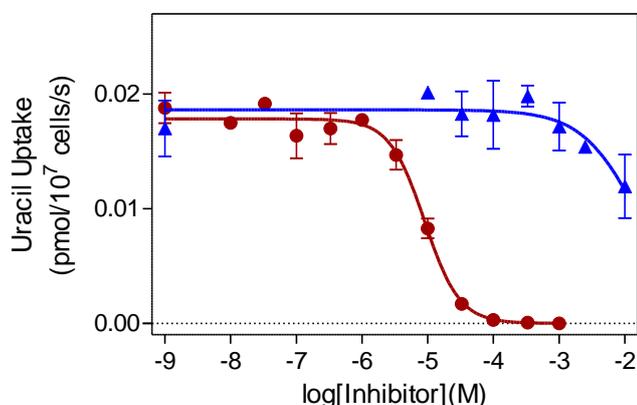
Figure 3.3. Inhibition of 0.15 μM [^{3}H]-uracil transport by unlabelled uridine (▲) and unlabelled 5-fluorouracil (●) for 30 sec incubations. The inhibition processes were terminated by the addition of 1 ml ice-cold 1 mM uracil in assay buffer and immediate centrifugation through oil. Error bars were SE of triplicate determinations.

3.3. Comparing substrate profiles of TbU1 and TbU3

An overview of pyrimidine transporters in *T. b. brucei* procyclics and BSF was summarized in Table 3.1. The data showed that TbU1 and TbU3 have a very similar inhibitor profile, and thus it is highly likely TbU1 and TbU3 bind uracil in a very similar way, with the defining difference being the different affinity for uridine. The only other notable difference was the lower affinity of TbU3 for 4-thiouracil with K_i values of 159 ± 24 μM versus 22 ± 7 μM for TbU1 (7.2-fold). On the other hand, the K_i values for 2-thiouracil by TbU1 and TbU3 were highly similar (640 ± 110 and 700 ± 130 μM, respectively). The lower affinity for 4-thiouracil is likely to reflect a stronger hydrogen bond at the 4-keto group than was the case for TbU1, as a result of a subtle shift in position or a different amino acid facing this group.

Table 3.1. Substrate profiles of the *T. b. brucei* strain 427-wild type pyrimidine transporters of procyclic forms and bloodstream forms: K_m and K_i values in µM. Entries in bold typescript indicate K_m rather than K_i values. NE, no effect on uptake at concentration indicated. Blanks showed where values not determined. Data for procyclic forms were taken from (De Koning & Jarvis, 1998; Gudin *et al.,* 2006; Papageorgiou *et al.,* 2005), and included here for comparison. The chemical structure of used pyrimidines and their analogues are shown in Appendix II; and the actual single values are shown in Appendix III-IV.

	Procyclic forms			Bloodstream forms	
	TbU1	TbU2	TbC1	TbU3	TbT1
Pyrimidine nucleobases					
Uracil	**0.46 ± 0.09**		0.36 ± 0.06	**0.54 ± 0.11**	>2500
Thymine	>1000			>2500	NE, 1000
Cytosine	NE, 1000		**0.048 ± 0.009**	>2500	
Orotic acid				630 ± 48	NE, 1000
Pyrimidine nucleosides					
Uridine	33 ± 5	**4.1 ± 2.1**		**9500 ± 2700**	199 ± 38
2'-Deoxyuridine				**804 ± 132**	320 ± 47
Thymidine	NE, 1000	0.38 ± 0.07		>10000	**1240 ± 310**
Cytidine	NE, 1000	0.057 ± 0.019	0.42 ± 0.16		>10000
2'-Deoxycytidine					
Pyrimidine analogues					
1-Methyluracil	NE, 10000			>5000	
2-Mercaptopyrimidine	NE, 500			1640 ± 510	
2-Thiouracil	640 ± 110			700 ± 130	
3-Deazauracil	>2500			>5000	
4(3H)-Pyrimidinone	1670 ± 180			4410 ± 1090	
4-Thiouracil	22 ± 7			159 ± 24	
5-Bromouracil				180 ± 36	
5-Fluorouracil	3.0 ± 0.8			**2.6 ± 0.01**	>1000
5-Chlorouracil	900 ± 140			560 ± 180	
5-Iodouracil				1300 ± 70	
5,6-Dihydrouracil	830 ± 200			>5000	
6-Azauracil	~1000			663 ± 125	
6-Methyluracil	>2500			>5000	
2',3'-Dideoxyuridine				2260 ± 540	
2',5'-Dideoxyuridine				>2500	
5'-Deoxyuridine				>2500	
5-Fluoroorotic acid				330 ± 47	
Purines					
Adenosine	NE, 1000				2.3 ± 0.3
Hypoxanthine	NE, 1000			NE, 1000	
Inosine	NE, 1000				**0.89 ± 0.15**
Xanthine				NE, 1000	
Adenine	NE, 1000				

The many close similarities between TbU1 and TbU3 inhibitor profiles, including similar affinity for 5-halogenated uracil analogues (Figure 3.4), seem to indicate common transporter structure. However, the specific differences suggest that TbU3 has more steric limitations than TbU1 when it comes to binding nucleosides rather than nucleobases. The lower K_i value for 2'-deoxyuridine in TbU3 (1150 ± 340 µM) compared to uridine (K_i = ~10 mM) suggests that the 2'-hydroxyl group is a significant factor in the non-binding of uridine. In contrast, the further removal of the 3'-hydroxyl group (2', 3'-dideoxyuridine), or of the 5'-hydroxyl (2', 5'-dideoxyuridine and 5'-deoxyuridine), did not lead to higher affinity.
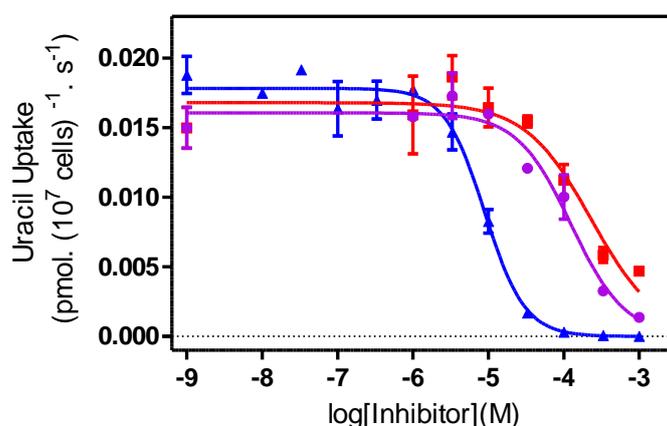
Figure 3.4. Inhibition of 0.15 µM [^{3}H]-uracil transport by 5-fluorouracil (▲), 5-chlorouracil (■) and 5-bromouracil (●) for 30 seconds incubations. The uptake was terminated by the addition of 1 ml ice-cold 1 mM uracil in uptake assay buffer and immediate centrifugation through oil. Error bars were SE of triplicate determinations. Experiments were performed in triplicate and were representative of three identical experiments performed on different dates.

3.4 Uridine and 2'-deoxyuridine uptake in *T. b .brucei* BSF-WT

Procyclic *T. b. brucei* express a separate uridine transporter designated TbU2, in addition to a modest rate of uridine uptake through TbU1, which is primarily a uracil transporter. With TbU3 displaying almost no affinity for uridine, this study investigated whether a separate uridine transporter was expressed in bloodstream forms as well. Saturable transport of [^{3}H]-uridine was hardly detectable in bloodstream forms, and not at all at submicromolar concentrations (Figure 3.5A) or at short time intervals (2 minutes; Figure 3.5B). A measurable rate (pmol·10^7 cells^{-1}·s^{-1}) was obtained at 2.5 µM [^{3}H]-uridine, using a timecourse over 30 minutes (Figure 3.5C).
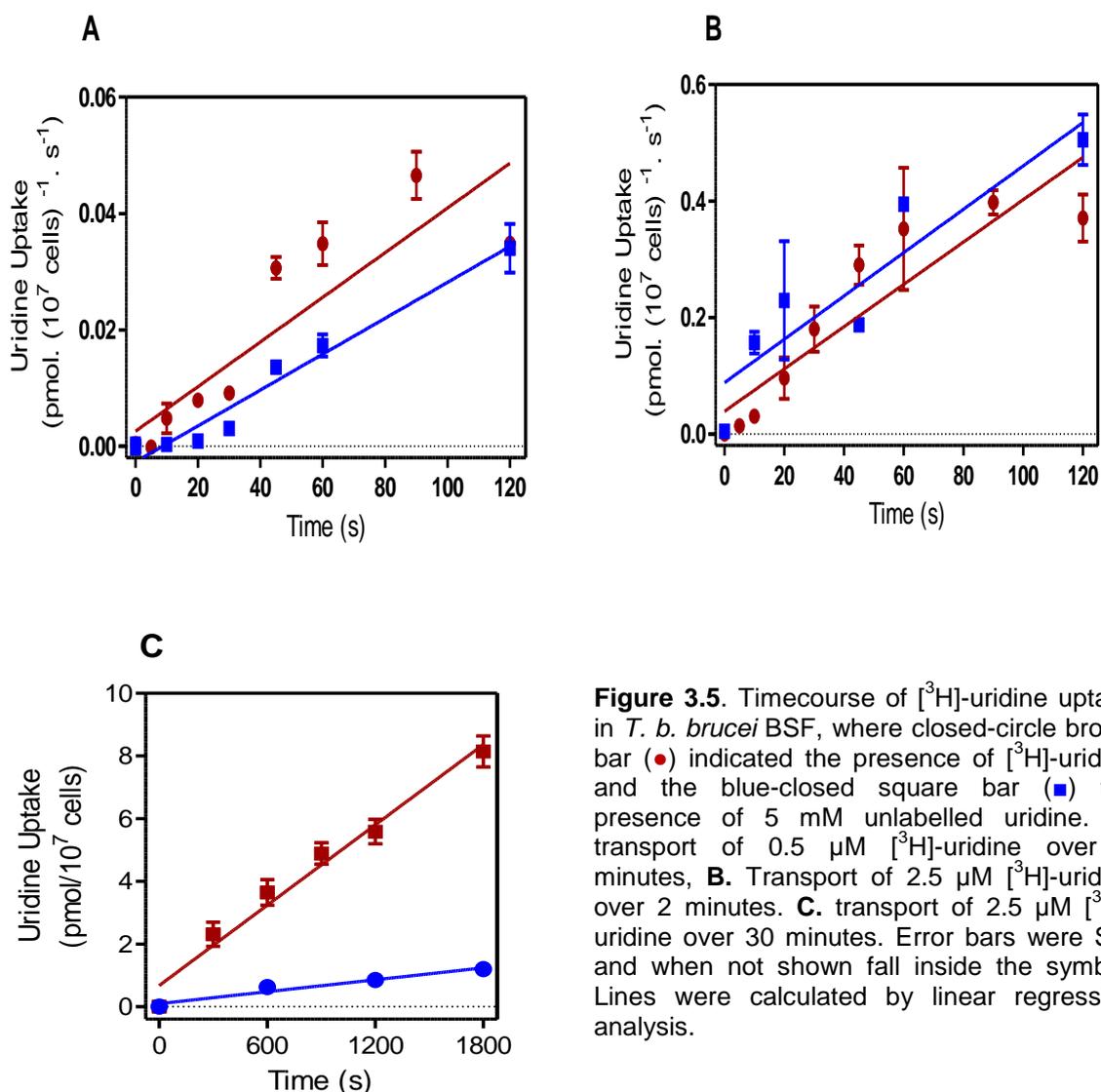
Figure 3.5. Timecourse of [^{3}H]-uridine uptake in *T. b. brucei* BSF, where closed-circle brown bar (●) indicated the presence of [^{3}H]-uridine and the blue-closed square bar (■) the presence of 5 mM unlabelled uridine. **A.** transport of 0.5 µM [^{3}H]-uridine over 2 minutes, **B.** Transport of 2.5 µM [^{3}H]-uridine over 2 minutes. **C.** transport of 2.5 µM [^{3}H]-uridine over 30 minutes. Error bars were SE, and when not shown fall inside the symbol. Lines were calculated by linear regression analysis.

The subsequent experiments were performed using 2.5 µM [^{3}H]-uridine and 15 minutes incubation times - very much within the linear phase of uptake. This allowed the determination of an apparent K_m value of 9500 ± 2700 µM and a V_{max} of 16 ± 4 pmol·10^7 cells^{-1}·s^{-1} (Figure 3.6A). This extremely low affinity was entirely consistent with uridine being transported by TbU3 only at very high concentrations. This was confirmed by inhibition of 2.5 µM [^{3}H]-uridine uptake by uracil, with a K_i value of just 1.6 ± 0.2 µM (Figure 3.6B), highly similar to the TbU3 K_m value for uracil.

A

B
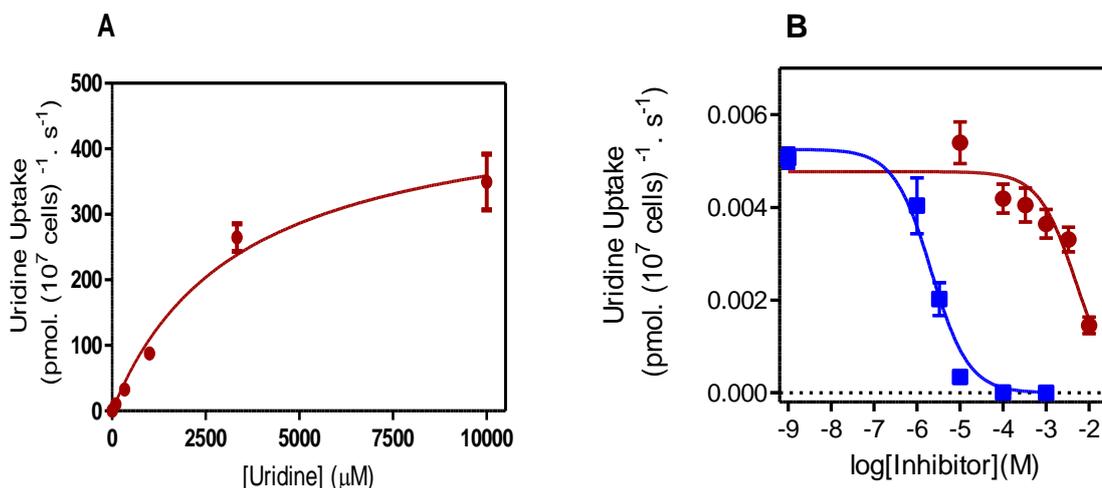
Figure 3.6. Characterization of [3H]-uridine transport in *T. b. brucei* BSF. **A.** The inhibition of 2.5 µM [3H]-uridine uptake for 15 minutes incubation by various concentrations of unlabelled uridine was converted to a Michaelis-Menten saturation plot to determine K_m and V_{max} values. The inhibition data was taken from frame B (the closed-brown circles). **B.** Inhibition of 2.5 µM [3H]-uridine transport for 15 minutes incubation by unlabelled uridine (●) and unlabelled uracil (■). The uptake was terminated by addition of 1 ml ice-cold 10 mM unlabelled uridine. Error bars were SE of triplicate determinations. Lines were calculated using an equation for sigmoid curve; where inhibition was above 50% but not complete at the highest inhibitor concentration, the Hill slope was set at -1 and the bottom level at zero for the purpose of extrapolation.

At the low permeant concentration of 0.5 µM [3H]-2'deoxyuridine the rate of uptake was barely detectable over 2 minutes, with a rate of 0.00045 pmol·10^7 cells^{-1}·s^{-1} (Figure 3.7A), indicating the absence of high affinity transport for uridine nucleosides. Transport of 5 µM [3H]-2'deoxyuridine was linear over 4 minutes with a rate of 0.0051 ± 0.0003 pmol·10^7 cells^{-1}·s^{-1}, which was 76% inhibited by 2.5 mM unlabelled 2'-deoxyuridine (Figure 3.7B).

A

B
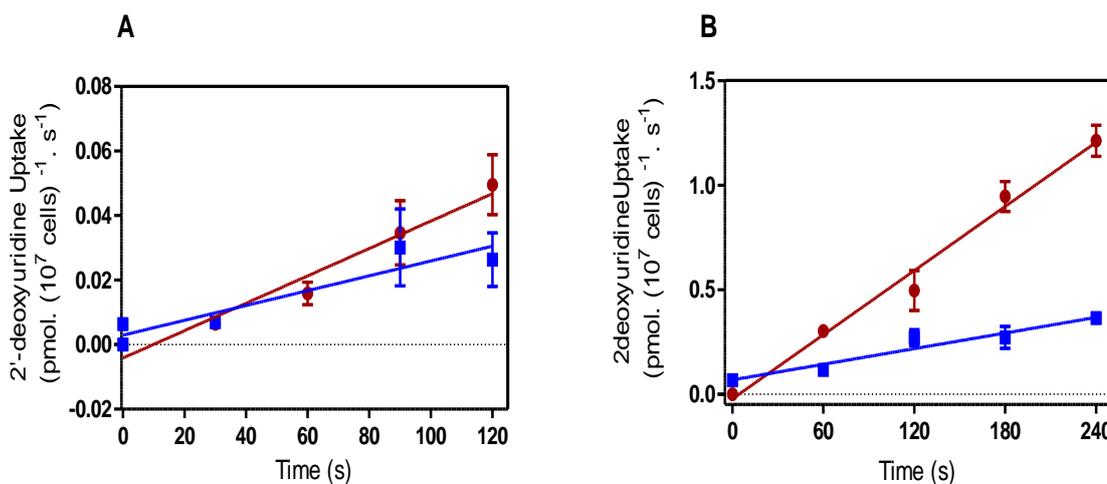
Figure 3.7. Transport of [3H]-2'deoxyuridine (●) in *T. b. brucei* BSF in the presence of 2.5 mM unlabelled 2'-deoxyuridine (■). **A.** Transport of 0.5 µM [3H]-2'deoxyuridine over 2 minutes **B.** transport of 5 µM [3H]- 2'-deoxyuridine over 4 minutes. Error bars were SE, and when not shown fall inside the symbol. Lines were calculated by linear regression analysis.

Characterization of the transport of 2'-deoxyuridine was performed using 5 µM of label and 180 seconds as incubation time. This transport activity displayed a K_m of 804 ± 132 µM, and a V_{max} of 1.3 ± 0.7 pmol·10^7 cells^{-1}·s^{-1} (n=3; Figure 3.8A). The uptake of tritium 2'-deoxynucleoside was inhibited by unlabelled uracil with a K_i value (1.1 ± 0.1 µM) very close to TbU3 Michaelis constant (Figure 3.8B).
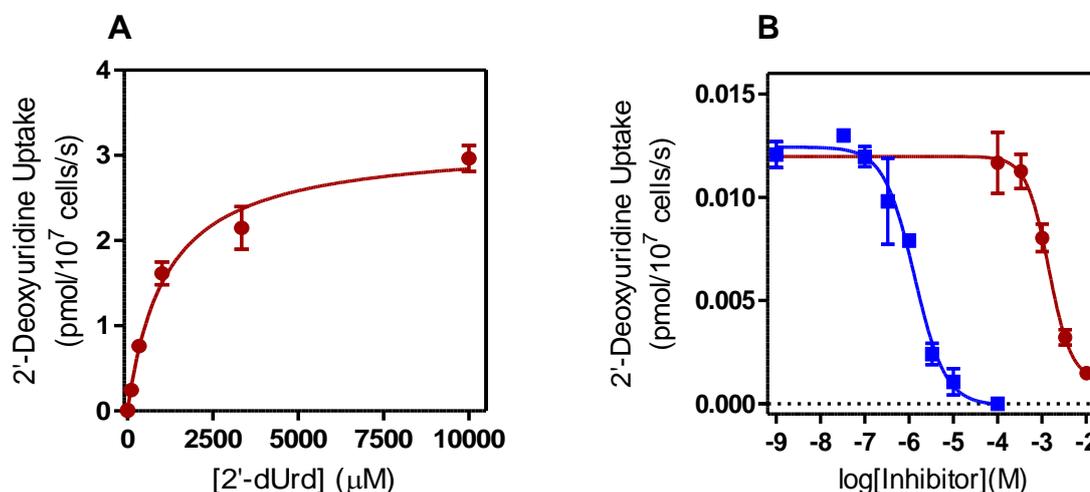
Figure 3.8. Characterization of [^{3}H]-2'deoxyuridine transport in *T. b. brucei* BSF. **A.** The inhibition of 5 µM [^{3}H]-2'deoxyuridine uptake for 3 minutes incubation by various concentrations of unlabelled 2'deoxyuridine was converted to a Michaelis-Menten saturation plot to determine K_m and V_{max} values. The inhibition data was taken from frame B (the closed brown circles). **B.** Inhibition of 5 µM [^{3}H]-2'deoxyuridine transport for 3 minutes incubation by unlabelled 2'-deoxyuridine (●) and unlabelled uracil (■). The uptake was terminated by addition of 1 ml ice-cold 5 mM unlabelled 2'-deoxyuridine. Error bars were SE of triplicate determinations. Lines were calculated using an equation for sigmoid curve with variable Hill slope; extrapolation of incomplete inhibitions was as described in the legend to Figure 3.6.

The K_i and K_m values of uracil, uridine and 2'-deoxyuridine were entirely consistent with all three pyrimidines being taken up by a single transport protein, TbU3. However, the low affinity for the nucleosides showed that TbU3 was a uracil transporter and will not accumulate significant amounts of uridine and 2'-deoxyuridine under physiological conditions.

3.5 Thymidine uptake in *T. b. brucei* BSF-WT

No significant amounts of thymidine transport by BSF of *T. b. brucei* could be detected at submicromolar (Figure 3.9A) or low micromolar concentrations (Figure 3.9B) over 2 minutes. However, we were able to measure transport of 10 µM thymidine over a period from 5 to 30 minutes (Figure 3.9C), with a rate of 0.0015 ± 0.0003 pmol·10^7 cells^{-1}·s^{-1}, which was 80% inhibited by 2.5 mM unlabelled thymidine.
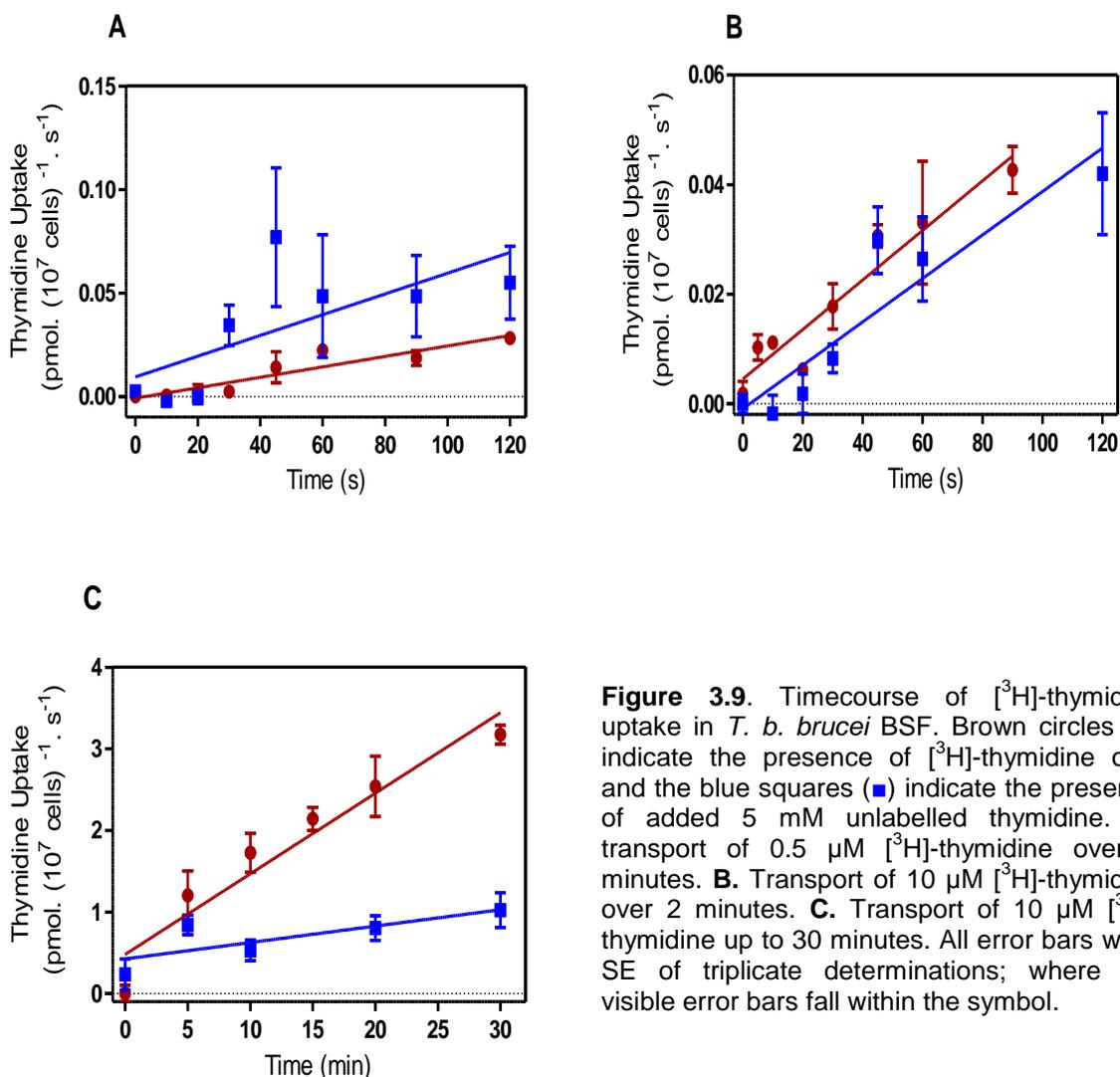
Figure 3.9. Timecourse of [³H]-thymidine uptake in *T. b. brucei* BSF. Brown circles (●) indicate the presence of [³H]-thymidine only and the blue squares (■) indicate the presence of added 5 mM unlabelled thymidine. **A.** transport of 0.5 µM [³H]-thymidine over 2 minutes. **B.** Transport of 10 µM [³H]-thymidine over 2 minutes. **C.** Transport of 10 µM [³H]-thymidine up to 30 minutes. All error bars were SE of triplicate determinations; where not visible error bars fall within the symbol.

Using 10 µM of [³H]-thymidine and an incubation time of 15 minutes led to a possibility to derive reproducible K_m values (Figure 3.10A) and inhibition profile (Table 3.1). The average K_m value was 1240 ± 310 µM and the V_{max} was 0.067 ± 0.008 pmol·10^7 cells^{-1}·s^{-1} (n=3), yielding an efficiency ratio V_{max}/K_m of just 0.0001. Thymidine transport was not sensitive to inhibition by uracil, consistently failing to reach 50% inhibition even at 2.5 mM (Figure 3.10B; n=4), clearly showing that this is a distinct transporter from TbU3. Therefore, we designated bloodstream form thymidine transporter TbT1.
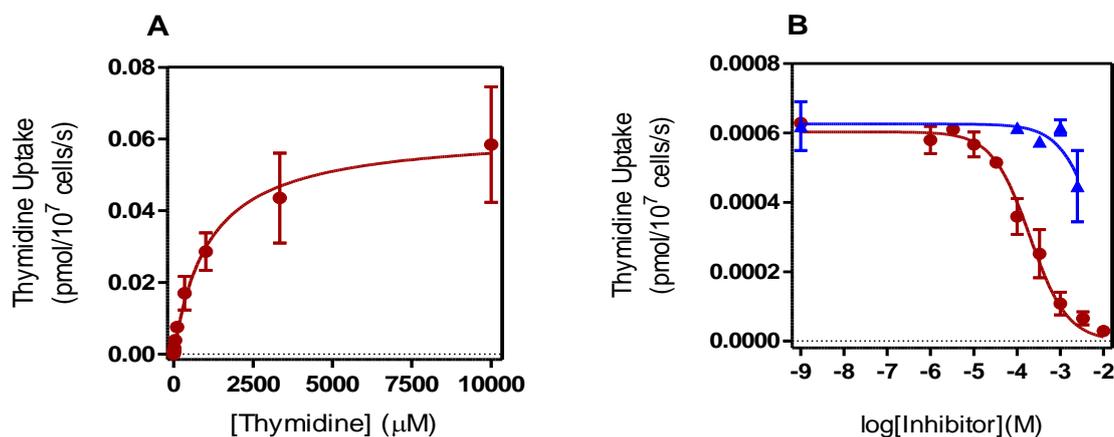
Figure 3.10 Characterization of [^{3}H]-thymidine transport in *T. b. brucei* BSF. **A.** The conversion of thymidine inhibition data to a Michaelis-Menten saturation plot was performed to determine K_m and V_{max}, incubations (15 minutes). The inhibition data was taken from frame B (the closed brown circles). **B.** Inhibition of 5 µM [^{3}H]-thymidine transport by thymidine (●) and uracil (▲), incubations (15 minutes). All data are averages and SEM of triplicate determinations and representative of at least three independent experiments.

Moreover, the transporter was completely inhibited by adenosine with a K_i value of just 2.3 ± 0.3 µM (Figure 3.11A), whereas adenosine has no effect on TbU1 mediated uracil transport. Uridine and 2'-deoxyuridine also inhibited this novel nucleoside transport activity (Figure 3.11B), but several other pyrimidines including orotic acid, thymine, cytidine and 5-fluorouracil had little or no effect on thymidine uptake (Table 3.1).
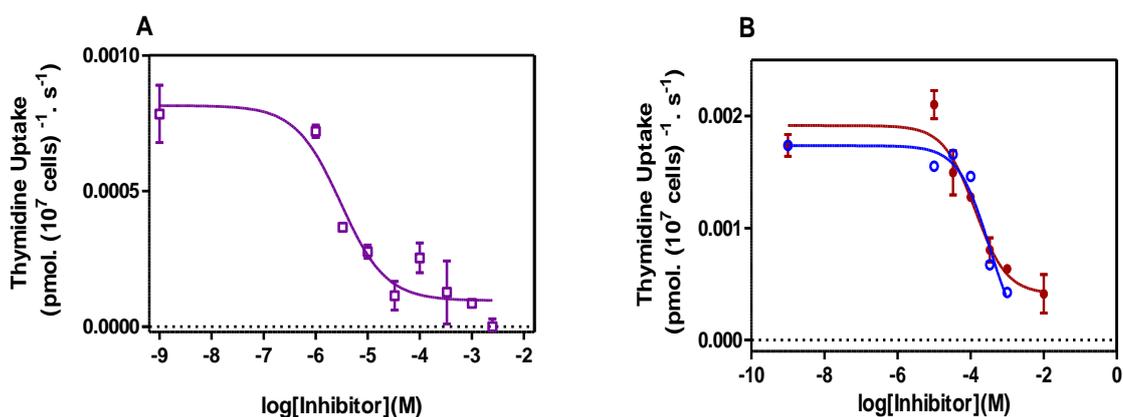
Figure 3.11 Inhibition of 10 µM [^{3}H]-thymidine transport by **A.** adenosine (□) **B.** uridine (●) and 2'deoxyuridine (○), for 15 minutes incubations. Experiments were performed in triplicate and were representative of three identical experiments performed on different dates.

The extremely low thymidine affinity and translocation efficiency of TbT1 led us to speculate that it would not contribute substantially to pyrimidine salvage *in vivo*, unless it was expressed at very much higher levels of activity *in vivo* rather than under the 'rich' *in vitro* growth conditions of standard HMI-9/FBS. This would parallel the situation with the TbAT1/P2 aminopurine transporter, which was highly expressed in rodent-grown trypanosomes but barely detectable in *in vitro* cultured trypanosomes (Ward *et al.*, 2011). However, despite a trend suggesting a minor increase in [^{3}H]-thymidine uptake from cells grown *in vivo* (Figure 3.12; n=3), the study was unable to detect a clear difference in thymidine transport rates in trypanosomes isolated from rat blood or from culture in HMI-9/FCS.
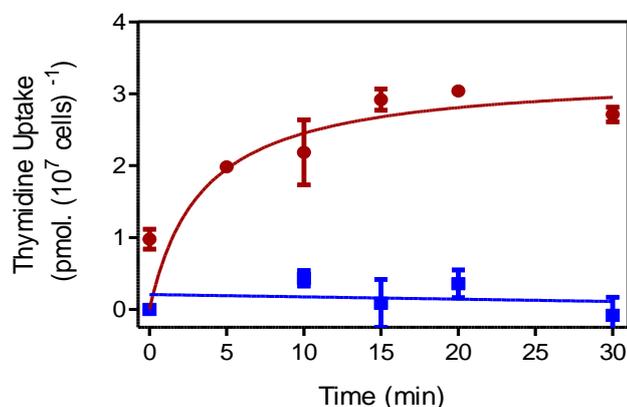
Figure 3.12 Timecourse of [^{3}H]-thymidine uptake by *in vivo* grown *T. b. brucei* BSF, where closed brown circles (●) show uptake of 10 μM [^{3}H]-thymidine and the blue squares (■) show uptake of the label in the presence of 2.5 mM unlabelled thymidine. Incubations were up to 30 minutes and performed in triplicate.

The function of this transporter was not primarily the uptake of thymidine, but of purines. Considering the high affinity for adenosine, the transporter could be the previously described P2 aminopurine transporter (De Koning & Jarvis, 1999) or any of a number of P1-type purine nucleoside transporters (Al-Salabi *et al.*, 2007; De Koning & Jarvis, 1999). It was thus tested whether [^{3}H]-thymidine uptake was sensitive to inosine, and it was found that the purine nucleoside inhibited TbT1-mediated thymidine uptake with a K_i value of 1.6 ± 0.6 μM (n=3; Figure 3.13A). As P2 is insensitive to even very high levels of inosine (De Koning & Jarvis, 1999) this clearly established that the T1 was a P1-type nucleoside transporter, although it is currently unclear which one of the multiple P1-type transporter genes in the *T. b. brucei* genome (De Koning *et al.*, 2005) would encode this activity. To test this hypothesis, the inhibition of [^{3}H]-

inosine by thymidine was assessed in BSF and it was found that inosine uptake was inhibited by thymidine in a monophasic way with a K_i value of 214 ± 51 µM (Figure 3.13B). This activity displayed a K_m for inosine of 0.89 ± 0.15 µM and V_{max} 0.075 ± 0.015 pmol·10^7 cells^{-1}·s^{-1} (Figure 3.13C), all completely consistent with the hypothesis that TbT1 was a P1-type nucleoside transporter (Al-Salabi *et al.*, 2007; De Koning *et al.*, 2005; De Koning & Jarvis, 1999).
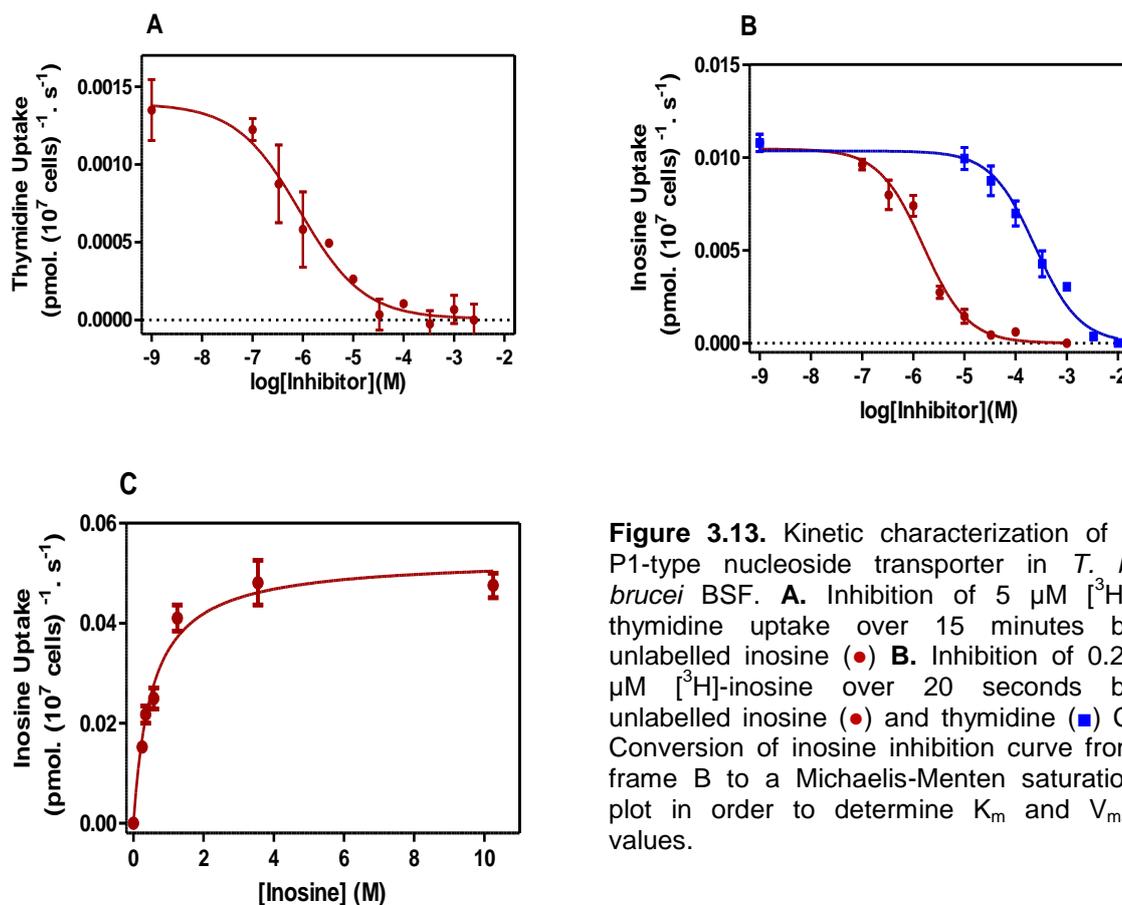
Figure 3.13. Kinetic characterization of a P1-type nucleoside transporter in *T. b. brucei* BSF. **A.** Inhibition of 5 µM [^{3}H]-thymidine uptake over 15 minutes by unlabelled inosine (●) **B.** Inhibition of 0.25 µM [^{3}H]-inosine over 20 seconds by unlabelled inosine (●) and thymidine (■) C. Conversion of inosine inhibition curve from frame B to a Michaelis-Menten saturation plot in order to determine K_m and V_{max} values.

3.6 Uptake of other pyrimidines by *T. b. brucei* BSF-WT

Attempts were made to measure transport of other natural pyrimidine nucleosides and nucleobases. A very slow accumulation of 0.5 µM [^{3}H]-cytidine was measured with incubation times up to 30 minutes. The rate of uptake was just 6.5×10^{-5} ± 4.1×10^{-6} pmol·10^7 cells^{-1}·s^{-1} but [^{3}H]-cytidine transport was only partly inhibited by 2.5 mM unlabelled cytidine (Figure 3. 14A). Consistent with this observation, an effort to determine the K_m value for 0.5 µM [^{3}H]-cytidine, using a 20-minutes incubation time, found only partial saturation at 10 mM cytidine and the study concluded that bloodstream forms of *T. b. brucei* do not

salvage significant amounts of cytidine through uptake from their environment. Similarly, just detectable accumulation of 2.5 μM [³H]-2'deoxycytidine over 15 minutes was not saturated by 10 mM unlabelled 2'-deoxycytidine (Figure 3. 14B). We have also attempted to measure the uptake of 0.25 μM [³H]-cytosine (Figure 3. 14C) and 1 μM [³H]-thymine (Figure 3. 14D), but they did not detectably accumulate in BSF even up to 15 minutes incubation time.
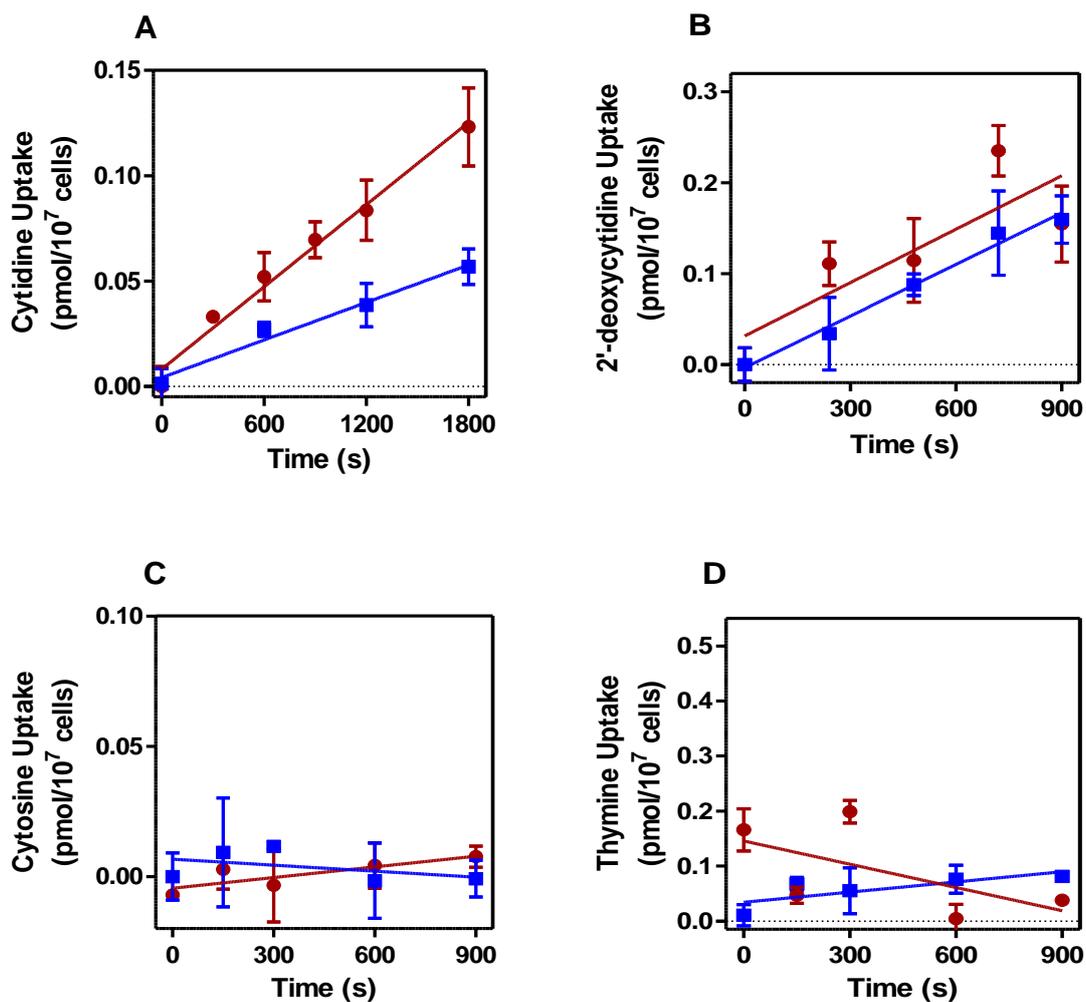
Figure. 3. 14. In *T. b. brucei* BSF the transport of [³H]-pyrimidines (●) was not, or hardly, inhibited by the corresponding unlabelled permeants (■): **A.** Uptake of 0.5 μM [³H]-cytidine inhibited by 2.5 mM unlabelled cytidine over 30 minutes. **B.** Uptake of 2.5 μM [³H]-2'deoxycytidine inhibited by 10 mM of unlabelled 2'-deoxycytidine over 15 minutes. C. Uptake of 0.25 μM [³H]-cytosine inhibited by 2.5 mM unlabelled cytosine over a 15 minute period. D. Uptake of 1 μM [³H]-thymine inhibited by 10 mM unlabelled thymine for 15 minutes.

In summary, under the standard *in vitro* conditions used, *T. b. brucei* BSF express a high affinity uracil transporter, TbU3, and a P1-type nucleoside transporter capable of low affinity uptake of thymidine, TbT1. Uptake of uridine, 2'-deoxyuridine, cytidine and 2'-deoxycytidine can all be measured but displays very low affinity and efficiency compared to [^{3}H]-uracil transport, and is unlikely to play any significant role in pyrimidine metabolism *in vivo*.

3.7 Sensitivity of *T. b. brucei* BSF s427-WT to analogues of pyrimidine nucleosides and nucleobases

The effects of a number of pyrimidine nucleoside and nucleobase analogues were tested on bloodstream trypanosomes in order to be evaluated as potential drugs and as tools to investigate the pyrimidine salvage pathways (Table 3.2). Thiouridines (2-thiouridine, 4-thiouridine), 4-thiouracil, 5-fluorouridine, 3'-deoxypyrimidine nucleosides (3'-deoxyuridine, 2',3'-dideoxyuridine, 3'-deoxythymidine) and 5'-deoxyuridines (5'-deoxyuridine, 5-fluoro-5'deoxyuridine) all had no effect up to one millimolar drug concentration. In addition, uracil and uridine analogues with 5-position halogenations other than fluorine (i.e. chlorine, bromine or iodine) all displayed EC$_{50}$ values ≥2.5 mM or no effect at all, and the other tested pyrimidine analogues including 5-fluorocytosine and 5-fluorocytidine had no effect at tested concentrations.

Table 3.2. The activity of pyrimidine analogues against BSF of *T. b. brucei* s427-WT *in vitro* culture. Indicated values in the table were EC_{50} in μM, SE refer to standard error. The structure of pyrimidines and their analogues are shown in Appendix II; and the actual single values are shown in Appendix V.

Pyrimidine analogues	EC_{50} Value	
	AVG	SE
Nucleobase analogues		
5-Fluorouracil	35.9	1.5
5-Chlorouracil	2500	212
5-Bromouracil	>5000	
5-Iodouracil	>5000	
5-Fluorocytosine	>5000	
5-Fluoroorotic acid	14.1	0.9
6-Azauracil	958	34
4-Thiouracil	>5000	
Nucleoside analogues		
5-Fluorouridine	>5000	
5-Chlorouridine	>5000	
5-Bromouridine	>5000	
5-Iodouridine	>5000	
5-Fluorocytidine	>5000	
2-Thiuridine	>5000	
4-Thiouridine	>5000	
Deoxynucleoside analogues		
5-Fluoro2'-deoxyuridine	5.2	0.2
5-Chloro2'-deoxyuridine	54	1.7
5-Bromo2'-deoxyuridine	>5000	
5-Iodo2'-deoxyuridine	2709	209
5-Fluoro2'deoxycytidine	49.4	3
5-deoxyuridine	1740	71
5'-deoxy-5-fluorouridine	>5000	
2'-3'-dideoxyuridine	>5000	
3'-deoxyuridine	>5000	
3'-deoxythymidine	>5000	

The disappointing activity of some of the ribonucleoside analogues on *T. b. brucei* BSF s427-WT may reflect the poor uptake of uridine and its close analogues. Therefore, we tested 5-fluorouridine against procyclic forms of *T. b. brucei* of s427-WT, which have previously been shown to take up uridine moderately well (Table 3.1). The analogue 5-flurorouridine at 1 mM inhibited procyclic growth by approx 60% over several days (Figure 3.15) but this modest effect still seems to indicate that 5-fluorouridine is also a poor substrate for uridine phosphorylase, which would convert it to 5-fluorouracil in the cell, or that this activity is not (highly) expressed in the life cycle stages investigated here.
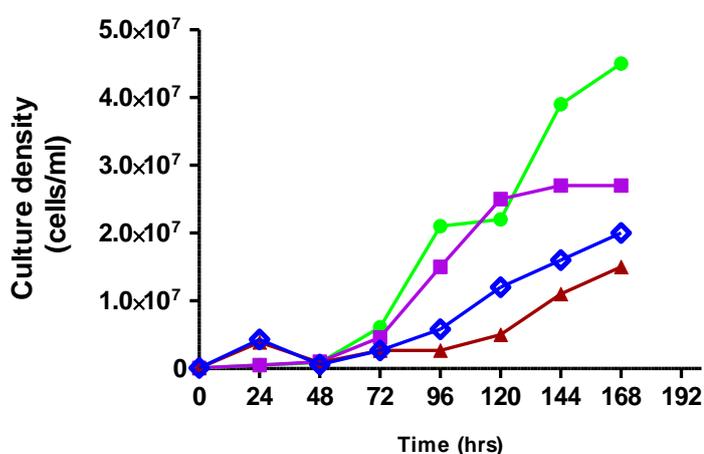
Figure. 3.15. The effect of 5-fluorouridine on the growth of *T. b. brucei* procyclic forms s427-WT in semi defined medium 79 (SDM-79; Biosera) supplemented with 10% FBS cultured at 28 °C. Cultures containing 10^5 trypanosomes/ml were incubated in SDM-79 medium with 0.01 mM (■), 0.1 mM (◊) or 1 mM (▲) of the drug, using drug-free medium (●) as a positive control. Every 24 hours time, samples were taken and counted microscopically using a haemocytometer.

The 2'-deoxynucleoside analogues were much more active against BSF than corresponding ribonucleosides; 5-fluoro-2'deoxyuridine, 5-chloro-2'deoxyuridine and 5-fluoro-2'deoxycytidine, all displayed micromolar activity against trypanosomes (Fig 3.16A). In addition, pyrimidine nucleobase analogues also displayed significant antiprotozoal effects, including 5-fluorouracil and 5-fluoroorotic acid with EC_{50} values at micromolar levels (Figure 3.16B).
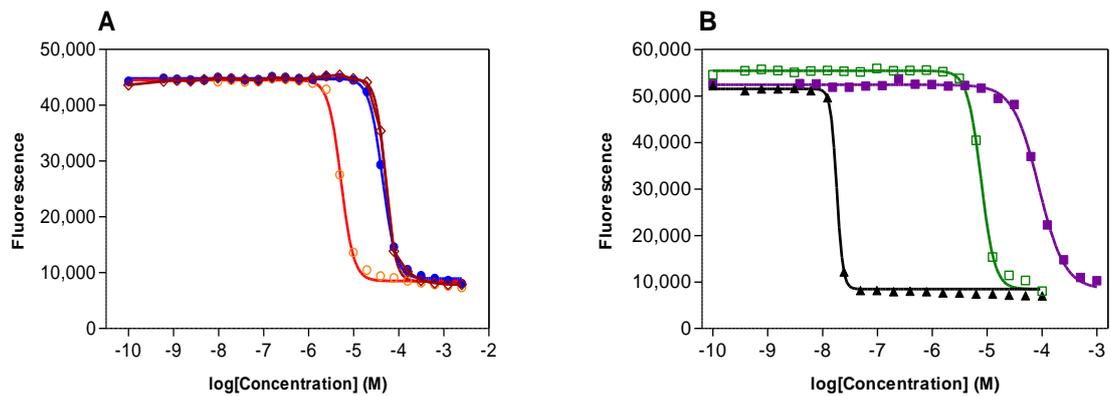
Figure 3.16. Sensitivity of bloodstream forms of *T. b. brucei* s427-WT to pyrimidine analogues. **A.** Fluorinated deoxynucleosides: 5-fluoro-2'-deoxyuridine (○), 5-fluoro-2'-deoxycytidine (●) and 5-chloro-2'-deoxyuridine (◊). **B.** Fluorinated nucleobases: 5-fluorouracil (■), 5-fluoroorotic acid (□) and pentamidine (▲) as a control. Using Alamar Blue assay, cell culture at $1{\times}10^5$ cells/ml was incubated with the indicated concentrations.

Although 6-azauracil is an inhibitor of pyrimidine *de novo* biosynthesis pathway, being an inhibitor of orotidylate decarboxylase in trypanosomes (Jaffe, 1961), its EC_{50} value against BSF of *T. b. brucei* was around one millimolar. Presumably because 6-azauracil was a poor substrate for TbU3 (Table 3.1) and inhibition of *de novo* UMP biosynthesis was non-lethal because of uracil and pyrimidine nucleosides salvage. None of the fluorinated pyrimidines killed trypanosomes very quickly, even at 500 µM, although they appeared to induce almost immediate growth arrest (Figure 3.17).
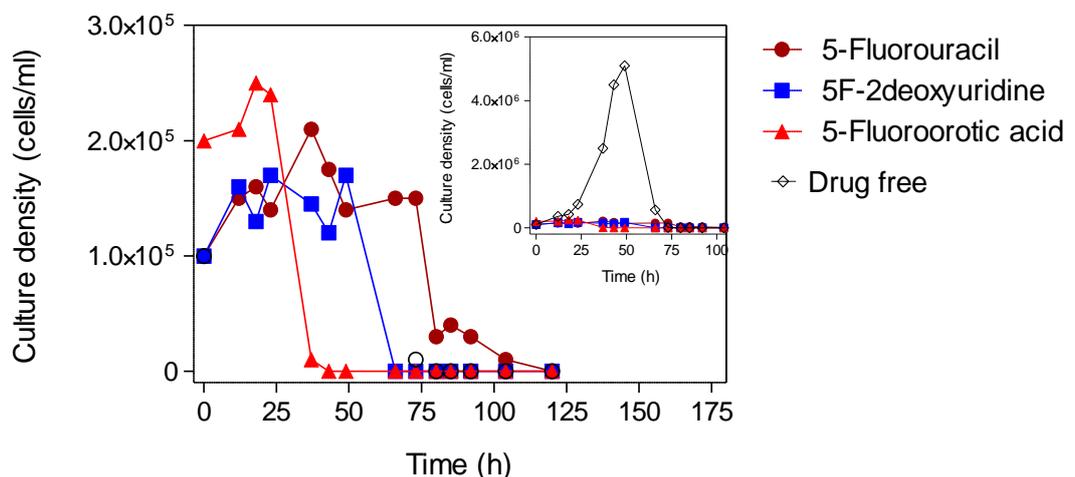
Figure 3.17. Effect of fluorinated pyrimidines on growth of bloodstream forms s427-WT. Cultures containing $1{\times}10^5$ or $2{\times}10^5$ trypanosomes/ml were incubated with 500 µM of 5-FU (●), 5-FOA (▲), 5-fluoro-2'deoxyuridine (■) or control (◊). At various times samples were taken and counted microscopically using a haemocytometer. The inset is the same data as in the main figure but including the control (no added drug) culture and on a different scale.

3.8 Induction of resistance to selected pyrimidine antimetabolites and cross resistance profiles

To further investigate in which way the most active analogues rely on salvage enzymes or transporters, this study induced resistance to 5-fluorouracil (5-FU), 5-fluoroorotic acid (5-FOA) and 5-fluoro-2'deoxyuridine (5F-2'dUrd) by *in vitro* exposure of *T. b. brucei* BSF s427-WT to stepwise increasing concentrations of the compounds (Figure 3.18).
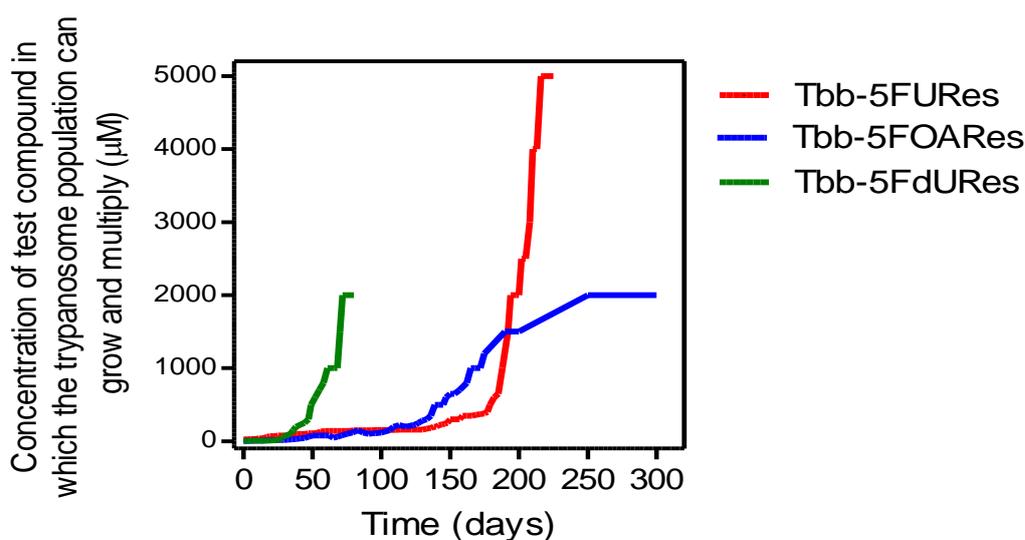
Figure 3.18. Adaptation of s427 BSF of *T. b. brucei* to high concentrations of fluorinated pyrimidines during *in vitro* culturing. Concentrations indicated were the analogue added to the medium, in which the cells managed to survive and multiply.

When the trypanosomes became resistance to high concentrations of the drugs the new strains were cloned out. This resulted in clonal lines Tbb-5FURes (Resistance Factor 131 to 5-FU; Figure 3.19A), Tbb-5FOARes (Resistance Factor 83 to 5-FOA; Figure 3.19B) and Tbb-5F2'dURes (Resistance Factor 825 to 5F-2'dUrd; Figure 3.19C). The trypanocidal drug pentamidine was used as a positive control throughout the assessment.

A. 5-FU

B. 5-FOA

C. 5-F2'dUrd

Figure 3.19 Sensitivity of resistant line of *T. b. brucei* to fluorinated pyrimidines (■) comparing with s427-WT (○) **A.** the sensitivity of Tbb-5FURes and s427-WT to 5-FU **B.** the sensitivity of Tbb-5FOARes and s427-WT to 5-FOA **C.** the sensitivity of Tbb-5F2'dURes and s427-WT to 5F-2'dUrd.
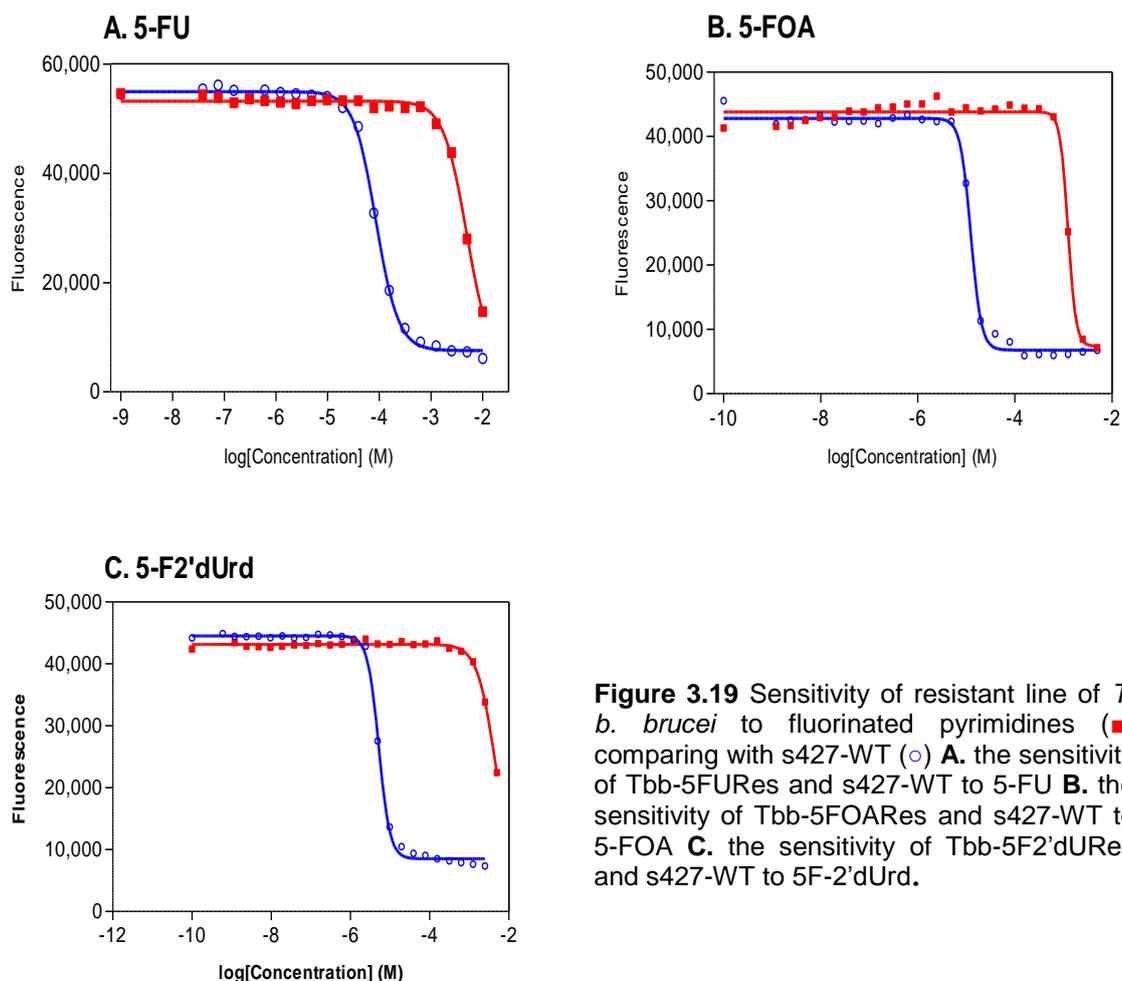
The induced resistant strains were characterized with respect to cross-resistance to other pyrimidine analogues (Table 3.3). Tbb-5FURes was not cross-resistant to pyrimidine nucleoside analogues but displayed 6.9-fold resistance to 5FOA, showing that at least one of multiple changes impacted on a joint pathway. Interestingly, Tbb5-FURes displayed increased sensitivity to 6-azauracil, probably indicating a reduced uracil salvage pathway and increasing reliance on *de novo* synthesis. In addition, Tbb-5FURes was ~15-fold more sensitive to 5-chloro-2'deoxyuridine, possibly an indication that this analog also inhibits *de novo* pyrimidine biosynthesis. Similarly, Tbb-5FOARes showed 13-fold resistance to 5-FU, a fraction of the resistance to 5-FOA itself, and even less resistance to the nucleoside analogues. Tbb-5F2'dURes was not cross-resistant to the nucleobase analogues 5-FU, 5-FOA and 6-azauracil showing that the resistance was not due to loss of TbU3 activity since its natural pyrimidine (2'deoxyuridine) uptake was totally inhibited by the main substrate for TbU3, uracil. However, this strain was resistant to 5-fluoro-2'-deoxycytidine to the limit tested (5 mM), although not to 5-chloro-2'-deoxyuridine, confirming that

the latter has a different mode of action than 5F-2'dUrd. This observation strongly suggests that 5-fluoro2'-deoxycytidine is converted to 5F-2'dUrd in the cell, presumably by cytidine deaminase, and that its mechanism of action is completely dependent on that conversion.

Table 3.3. Resistance and cross-resistance characterization of *T. b. brucei* BSF adapted to high levels of fluorinated pyrimidines, compared to the parental s427-wild type. Indicated values in the table were EC_{50} in µM. SE stand for standard error, RF symbolize resistance factor which means EC_{50} of resistance cells/ EC_{50} of s427-WT cells. The actual single values are shown in Appendix V.

Compounds	s427-WT	Tbb-5FURes		Tbb-5FOARes		Tbb-5F-2'dURes	
	AVG ± SE	AVG ± SE	RF	AVG ± SE	RF	AVG ± SE	RF
5F-uracil	35.9 ± 1.5	4707 ± 307	**131**	448 ± 32	**13**	76.1 ± 2.2	**2.1**
5F-orotic acid	14.1 ± 0.9	98 ± 2	**6.9**	1178 ± 99	**83**	13.3 ± 0.1	**0.94**
5F-2'd-uridine	5.2 ± 0.2	3.2 ± 0.3	**0.61**	31 ± 2	**5.9**	4295 ± 267	**825**
5Chl-2'd-uridine	54 ± 1.7	3.7 ± 0.2	**0.07**	91 ± 6	**1.7**	22.0 ± 1.0	**0.4**
5F2'd-cytidine	49.4 ± 3	55 ± 5	**1.1**	126 ± 10	**2.6**	>5000	**>100**
6-Azauracil	958 ± 34	157 ± 2	**0.16**	1387 ± 78	**1.4**	1103 ± 44	**1.2**

3.9 Assessment of pyrimidine transport in the resistant clones

We investigated whether Tbb-5FURes cells resistance to 5-FU was linked to changes in uracil and/or 5-fluorouracil transport. Whereas transport of 0.5 µM [3H]-uracil was almost identical in s427-WT and Tbb-5FURes cells (Figure 3.20A), the uptake of the same concentration of [3H]-5FU was reduced in Tbb-5FURes cells by 76 ± 6% (n=3; *P*<0.01, paired Student's t-test; Figure 3.20B). The K_m and V_{max} value of [3H]-uracil uptake in Tbb-5FURes cells were unchanged relative to s427-WT, as well as were the sensitivity to uridine and 5-FU (the average of K_i values were ~10 mM and 3.7 ± 0.7 µM, respectively (Figure 3.20C).

A

B

C

Figure 3.20. Transport of 0.5 µM of **A.** [^{3}H]-uracil **B.** [^{3}H]-5fluorouracil in BSF of *T. b. brucei* WT-s427 (•) and Tbb-5FURes cell line (■). **C.** Inhibition of 0.1 µM [^{3}H]-uracil transport by (•) uridine and (■) 5-fluorouracil in Tbb-5FURes cells. Incubations of 30 seconds were terminated by the addition of 1 ml ice-cold 1 mM uracil in assay buffer and immediate centrifugation through oil. Error bars were SE of triplicate determinations. The graph was representative of three similar experiments. Lines were calculated by linear regression.

A subtle change in the TbU3 transporter reduced transport rates for 5-fluorouracil but not for uracil and without changing affinity for 5-fluorouracil (Table 3.4). Consistent with this interpretation, the transport efficiency (V_{max}/K_m) for [^{3}H]-5fluorouracil in Tbb-5FURes was 0.088 compared with 0.25 for [^{3}H]-uracil. In WT cells the difference between the uracil and 5-FU transport efficiencies was much lower compared with the difference in Tbb-5FURes cells. However, based on the considerable insensitivity of Tbb-5FURes cells to 5FU (131-fold), we can assume that the reduction in 5-FU uptake efficiency is small and most likely only one contributing factor to the high level of resistance observed in Tbb-5FURes.

Table 3.4. Kinetic parameters of uracil and 5-fluorouracil transport in *T. b. brucei* BSF of s427-WT and Tbb-5FURes.

Permeant	Strains	K_m (µM)		V_{max} (pmol·10^7 cells^{-1}·s^{-1})		Efficiency (V_{max}/K_m)
		AVG	SE	AVG	SE	
[^{3}H]-Uracil	s427 WT	1.5	0.3	0.27	0.05	0.18
	Tbb-5FURes	0.66	0.15	0.16	0.02	0.25
[^{3}H]-5Fluorouracil	s427 WT	2.5	0.01	0.27	0.02	0.11
	Tbb-5FURes	2.3	0.4	0.2	0.02	0.088

We have also investigated whether reduced uptake of orotic acid might partly explain the phenotype of Tbb-5FOARes cells. Uptake of 2.5 µM [^{3}H]-orotic acid was linear in BSF of *T. b. brucei* s427-WT (r^2 = 0.98) and significantly different from zero (F-test, *P* = 0.002) with a rate of 2.1×10^{-4} ± 2.1×10^{-5} pmol·10^7 cells^{-1}·s^{-1}. However, uptake appeared to be non-saturable in the presence of ≥1 mM of unlabelled orotic acid. [^{3}H]-orotic acid uptake was not significantly inhibited by uracil and thymidine either (Figure 3.21). As such, it was impossible to determine kinetic parameters and characterize orotic acid uptake in bloodstream forms of *T. b. brucei* s427-WT.
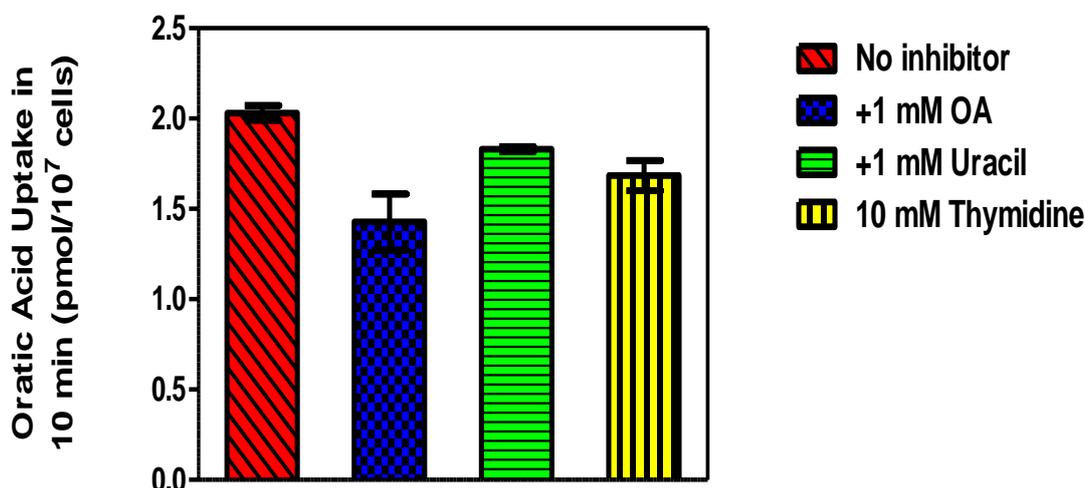
Figure 3.21. *T. b. brucei* BSF, representative inhibition transport of 2.5 µM [^{3}H]-orotic acid by unlabelled orotic acid, uracil and thymidine, using 10 minutes incubations. Error bars were SE of triplicate determinations.

However, it was clear that, when the uptake of 2.5 µM [^{3}H]-orotic acid was measured, accumulation of orotic acid was less in Tbb-5FOARes cells than in s427-WT cells; in two experiments (each performed in triplicate). The uptake of 2.5 µM [^{3}H]-orotic acid over 10 minutes was reduced by 68.1% (*P*<0.01; Figure

3.22A) and 62.8% (*P*<0.001; Figure 3.22B; Student's t-test). However, it was unsafe to attribute this to either reduced transport or a reduced rate of orotic acid metabolism as it was difficult to establish an initial rate of mediated transport for this permeant and metabolic usage of the [^{3}H]-orotic acid could therefore be the rate-determining step.
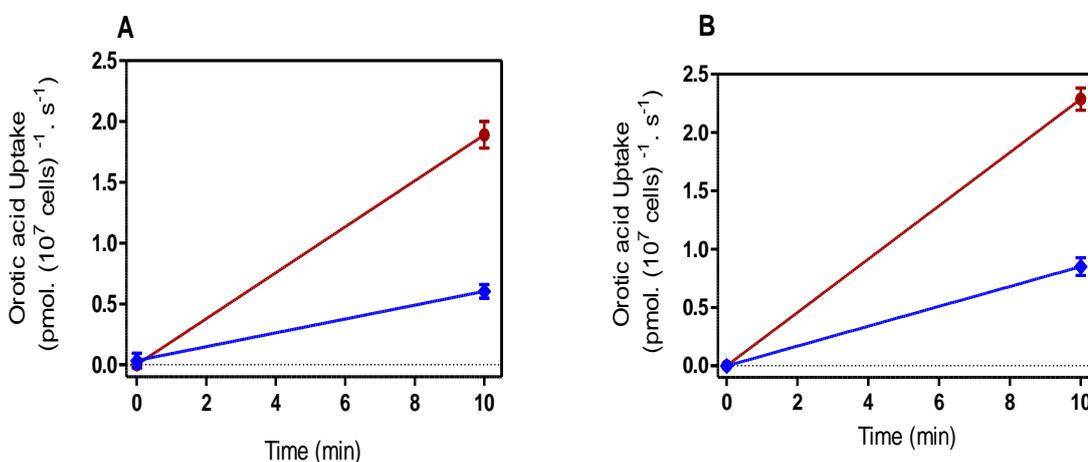
Figure 3.22. **A** and **B** were two identical separate experiments showed transport of 2.5 μM [^{3}H]-orotic acid over 10 minutes incubations by bloodstream forms of *T. b. brucei* s427-WT (■) and Tbb-5FOARes cells (●).

3.10. Discussion

Pyrimidine analogs have been extremely successful in anti-cancer (Galmarini *et al.*, 2003) and anti-viral chemotherapy (Hoffmann *et al.*, 2011). For instance, fluorinated pyrimidines capecitabine and 5-fluoro-2'deoxyuridine (Floxuridine), are both pro-drugs of the well known anticancer drug 5-fluorouracil. As a first step towards a rational evaluation of possible pyrimidine chemotherapy for trypanosomatid infections, it is incumbent to understand which natural pyrimidines would efficiently reach the target cell's interior (Luscher *et al.*, 2007). Natural pyrimidine nucleobases and nucleosides, and many analogues, do not have an appreciable diffusion rate and thus require transport proteins to enter cells. Therefore, this study attempted to investigate the transport of all natural pyrimidines, and of 5-fluorouracil, by bloodstream trypanosomes. Evidence was found for only one such transporter, TbU3, with high affinity for uracil and very low affinity for uridine and 2'-deoxyuridine. The reciprocal K_i and K_m values of uracil with uridine and 2'-deoxyuridine are entirely consistent with all uptakes of these nucleosides proceeding through the TbU3 transporter, but the low affinity for the nucleosides shows that TbU3 is a uracil transporter. This is confirmed by comparing the transport efficiencies, expressed as V_{max}/K_m, this index is identical for uridine and 2'deoxyuridine (0.0017) but two orders of

magnitude higher for uracil (0.18). No separate transport activity, other than TbU3, could be detected for uridine, 2'deoxyuridine, cytidine, 2'-deoxycytidine, cytosine, orotate and thymine. Transport of [^{3}H]-thymidine was evident, and mediated by a transport activity that was distinct from TbU3 and designated TbT1. However, its low affinity for thymidine, its high affinity inhibition by adenosine and reciprocal inhibition by inosine clearly shows this thymidine flux is mediated by one of the P1-type purine nucleoside transporters expressed in *T. b. brucei* bloodstream forms (Al-Salabi *et al.,* 2007; De Koning *et al.,* 2005; De Koning & Jarvis, 1999; Sanchez *et al.,* 2002).

The uracil transporter found in procyclic forms, TbU1, has been well characterized (De Koning & Jarvis, 1998; Papageorgiou *et al.,* 2005) and, like the corresponding transporter of *L. major,* binds its substrate through hydrogen bonds to both keto groups and both ring nitrogens in protonated state (Papageorgiou *et al.,* 2005). The many close similarities between procyclic TbU1 and bloodstream form TbU3 inhibitor profiles seem to indicate a common transporter structure, but the specific differences, particularly the low affinity for uridine by TbU3, suggest that TbU3 has more steric limitations than TbU1 when it comes to binding nucleosides rather than nucleobases – either in the binding site itself or in extracellular access to it. As a K_i value for 2'-deoxyuridine could be established (1150 ± 340 µM) it appears that the 2'-hydroxyl group is a significant factor in the non-binding of uridine. In contrast, the further removal of the 3'-hydroxyl group (2',3'-dideoxyuridine), or of the 5'-hydroxyl (2',5'-dideoxyuridine and 5'-deoxyuridine), did not lead to higher affinity. In addition, the lower affinity for 4-thiouracil in TbU3 is likely to reflect a stronger hydrogen bond at the 4-keto group than was the case for TbU1, as a result of a subtle shift in position or a different amino acid facing this group.

Of all the 5-halogenated pyrimidines, 5-fluorouracil seems to be the only cytotoxic pyrimidine nucleobase taken up efficiently by BSF trypanosomes. The notable affinity of 5-fluorouracil but not (5-chloro and 5-bromo)- uracil for TbU3 suggests size limitations on position 5 of uracil: fluorine has a small size compared to other halogens. Furthermore, the carbon-fluor bond is one of the strongest bonds in organic chemistry which contributes to its stability. When fluorine, the halogen atom of 5-fluorouracil, was substituted by chloro, iodo,

bromo or a methyl group (i.e. thymine) there was no considerable inhibition on [^{3}H]-uracil uptake.

Of particular interest was the observation that 5-FOA displayed >3-fold higher activity than 5-FU although the orotate uptake rate was just a fraction (≤1%) of the transport rate of [^{3}H]-5-fluorouracil. Interestingly, 5-FOA displays even much higher activity against *Plasmodium falciparum*, with reported *in vitro* EC$_{50}$ values in the low nanomolar range (Rathod *et al.*, 1989). It seems highly likely that the 100-fold higher antimalarial activity of 5-FOA can be attributed to the fact that orotic acid is, alone among all pyrimidines, efficiently taken up by *Plasmodium* spp and incorporated into nucleic acids (Gutteridge & Trigg, 1970). The strict selectivity of kinetoplastid uracil transporters was also noted for the procyclic TbU1 and *Leishmania major* LmajU1 carriers (De Koning & Jarvis, 1998; Papageorgiou *et al.*, 2005) and is in contrast to some of the kinetoplastid nucleoside transporters, particularly the aminopurine transporter TbAT1/P2 which is involved in uptake of many of the current first line trypanosomiasis drugs (Al-Salabi *et al.*, 2007; De Koning *et al.*, 2004; De Koning, 2001).

(Hofer *et al.*, 2001) was unable to detect incorporation of radiolabeled cytosine and cytidine into the *T. b. brucei* nucleotide pool using nanomolar concentrations. They concluded that CTP synthase was the only route to obtain cytidine nucleotides and the inhibition of the enzyme reduced proliferation both *in vivo* and *in vitro* (Fijolek *et al.*, 2007; Hofer *et al.*, 2001). The likely explanation is the use of submicromolar concentrations of pyrimidines used by Hofer; at these concentrations uracil is rapidly taken up and incorporated into nucleotide pools, but cytosine and cytidine are taken up very poorly at low concentrations, although their uptake is noted at high substrate levels. In chapter 7 it will be shown that pyrimidine auxotrophic trypanosomes can survive and multiply, albeit poorly, on 1 mM cytidine as sole pyrimidine source.

In summary, this study assessed pyrimidine salvage by bloodstream forms of *T. b. brucei* and reports that only uracil is efficiently taken up through a high affinity transporter, TbU3. The lack of high affinity transporters for most pyrimidine antimetabolites (Table 3.1) may limit the achievable trypanocidal activity with water-soluble pyrimidines.

CHAPTER FOUR
Leishmania spp: characterisation of pyrimidine
transporters and analysis of anti-leishmanial action
of selected pyrimidine analogues

4.1. Introduction

A few microorganisms are incapable of pyrimidine salvage, such as *Plasmodium* (Van Dyke *et al.,* 1970; Gutteridge and Trigg, 1970) or lack *de novo* pyrimidine biosynthesis pathways, such as *Trichomonas vaginalis, Trichomonas foetus* and *Giardia* spp (Wang & Cheng, 1984). However, most organisms are capable of salvage and biosynthesis of pyrimidine molecules, including kinetoplastid cells. In addition, most of the inter-conversion pyrimidine metabolizing enzymes, and the enzymes of the biosynthesis pathways are shared among the various organisms. With respect to salvage, *Leishmania* and *Trypanosoma* parasites have shown similarities in pyrimidine transport activities. For instance, a similar high-affinity uracil transporter was characterized in promastigotes of *L. major* (Papageorgiou *et al.,* 2005), procyclic forms of *T. b. brucei* (De Koning & Jarvis, 1998) and, very recently, bloodstream forms of *T. b. brucei* (Ali *et al.,* 2013a). In addition, all of these uracil transporters showed very high affinity to 5-fluorouracil and the drug was effective against the parasites, with EC_{50} values at micromolar concentrations. It was also shown that 5-FU was incorporated into RNA of bloodstream form of trypanosomes (Ali *et al.,* 2013a). In this project, we characterized pyrimidine uptake and assessed the activity of pyrimidine analogues against *Leishmania* cells. In addition, we created and analysed resistant strains to the most effective pyrimidine analogues.

4.2. Characterization of pyrimidine transporters in *L. mexicana* promastigotes

The first purine nucleobase transporter in *L. mexicana*, LmexNBT1, was identified and characterized in the amastigote stage; this transporter has high affinity to purine nucleobases and low affinity for nucleosides and pyrimidines, and was also involved in the uptake of the anti-leishmanial drug allopurinol (Al-Salabi & De Koning, 2005). At the start of this project, the pyrimidine transport activities of *L. mexicana* promastigotes were unknown, with no information regarding the number of individual pyrimidine transporters, or their characteristics. Therefore, this study investigated pyrimidine transporters expressed in the insect stage of *L. mexicana*.

4.2.1 Uracil uptake in *L. mexicana* promastigotes

When testing [³H]-uracil uptake at 1.0 µM over 2 minutes, the rate of [³H]-uracil uptake was 0.0028 ± 0.0004 pmol·10^7 cells-1·s^{-1} (linear regression, r^2 = 0.96) and was >95% inhibited by 1 mM unlabelled uracil (Figure 4.1A). The first effort to characterise the uracil transporter was performed using 0.5 µM [³H]-uracil over 30 seconds – within the linear phase, but this incubation time was insufficient to present a consistent monophasic graph (Figure 4.1B), due to the low amount of radiolabel accumulated. Therefore, we next performed the uracil timecourse using a maximum 10 minutes incubation time. [³H]-uracil at 0.5 µM was transported by *L. mexicana* promastigotes in linear manner over 10 minutes with a rate of uptake of 0.1073 ± 0.01552 pmol·107 cells-1·s-1, which was 38.3-fold higher than the rate of 1 µM [³H]-uracil for 120 seconds incubation, indicating that the transporter has not yet saturated at 1 µM for 120 seconds. The rate of 0.5 µM [³H]-uracil uptake for 10 minutes incubation was 94% inhibited by 1 mM unlabelled uracil (Figure 4.1C). These findings showed that uracil was mediated by a saturable protein membrane transporter. All subsequent experiments were performed using 0.5 µM [³H]-uracil and 4 minutes incubations – very much within the linear phase of uptake.
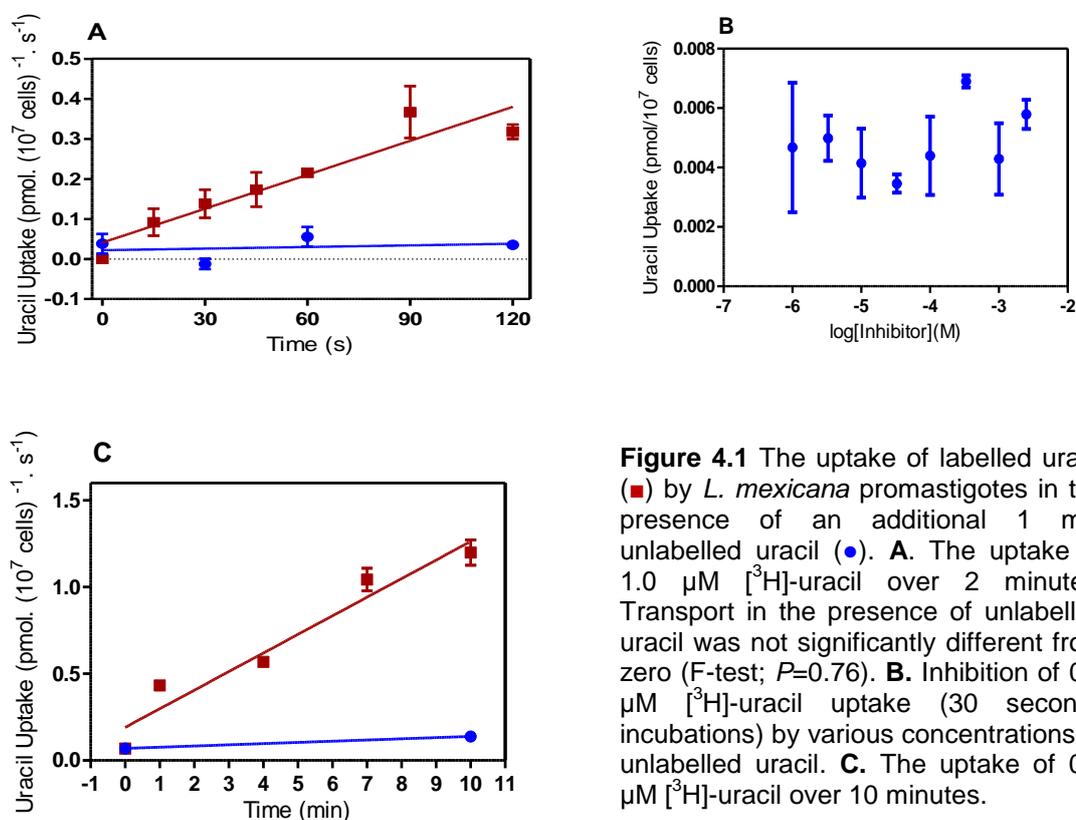
Figure 4.1 The uptake of labelled uracil (■) by *L. mexicana* promastigotes in the presence of an additional 1 mM unlabelled uracil (●). **A**. The uptake of 1.0 µM [³H]-uracil over 2 minutes. Transport in the presence of unlabelled uracil was not significantly different from zero (F-test; *P*=0.76). **B.** Inhibition of 0.5 µM [³H]-uracil uptake (30 seconds incubations) by various concentrations of unlabelled uracil. **C.** The uptake of 0.5 µM [³H]-uracil over 10 minutes.

The transport experiments with 0.5 µM [^{3}H]-uracil in promastigotes of *L. mexicana* over a 4 minute period produced sigmoid curves consistent with monophasic inhibition, with Hill slopes close to -1. The inhibition of [^{3}H]-uracil by increasing concentrations of unlabelled uracil and 5-fluorouracil was consistent between experiments, and showed monophasic inhibition with Hill slopes near -1, i.e. a single transporter model (Figure 4.2A). The uracil inhibition data was converted to Michaelis-Menten plots and displayed an average of K_m value of 29.7 ± 4.4 µM and average V_{max} value of 0.088 ± 0.01 pmol·10^7 cells^{-1}·s^{-1} (n=3; Figure 4.2B). This was the first pyrimidine nucleobase transporter identified in *L. mexicana* and it was tentatively designated *L. mexicana* uracil transporter 1 (LmexU1). Based on apparent K_m and V_{max} values of LmexU1, it appeared that the transport efficiency for uracil, expressed as V_{max}/K_m, was very low compared with the purine nucleobase transporter, LmexNBT1 (0.003 versus 0.057, respectively). This is consistent with the greater need for purine salvage than for pyrimidine uptake in this species.
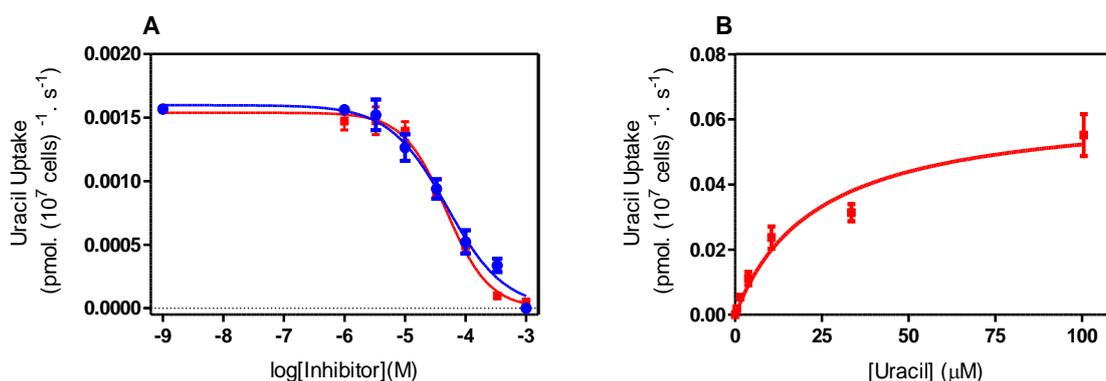
Figure 4.2. Characterization of [^{3}H]-uracil transport in promastigotes of *L. mexicana*. **A.** Inhibition of 0.5 µM [^{3}H]-uracil uptake over 4 minutes by various concentrations of unlabelled uracil (■) and 5-fluorouracil (●). **B.** Conversion uracil inhibition data from frame A to Michaelis-Menten saturation plot to determine the K_m and V_{max} values.

Purines and pyrimidines were assessed for inhibition of the uptake of 0.5 µM [^{3}H]-uracil in order to investigate the specificity of LmexU1 (Table 4.1). The data from LmexU1 inhibition profile showed that the average K_i value for 5-FU inhibition of uracil transport was almost identical to the average of K_m values for uracil uptake. Thus the anticancer drug 5-fluorouracil was almost as good a substrate as uracil for LmexU1 (Figure 4.2A) and displayed anti-leishmanial activity at micromolar level (Table 4.3). When the fluor atom of 5-FU was replaced with a methyl group to form thymine, the binding of the nucleobase with LmexU1 was not observed; this is likely linked to the larger size of the

methyl group as compared to the fluor (Schlosser & Michel, 1996). Although LmexU1 has high affinity for some pyrimidine nucleobases, cytosine up to 5 mM did not show any inhibition of 0.5 μM [³H]-uracil uptake. With respect to purine nucleobases, LmexU1 showed low affinity to adenine, which displayed poor inhibition activity against uracil uptake and an average K_i value of >0.3 mM (Figure 4.3A). The substitute of hydrogen atom on carbon position-5 of uridine with a methyl group, to form thymidine, was once again rejected from binding with LmexU1, consistent with the observations with thymine. Furthermore, neither hypoxanthine nor adenosine was a good substrate for the uracil transporter. LmexU1 was very sensitive to uridine nucleosides, thus the apparent affinities of LmexU1 for uridine and 2'-deoxyuridine against uracil uptake were higher than the affinity of LmexU1for uracil, by 14.8-fold and 3.2-fold, respectively (Figure 4.3B). As the data showed that LmexU1 is a uracil transporter with high affinity to uridine nucleosides, the uptake of [³H]-uridine by *L. mexicana* promastigotes was investigated next.
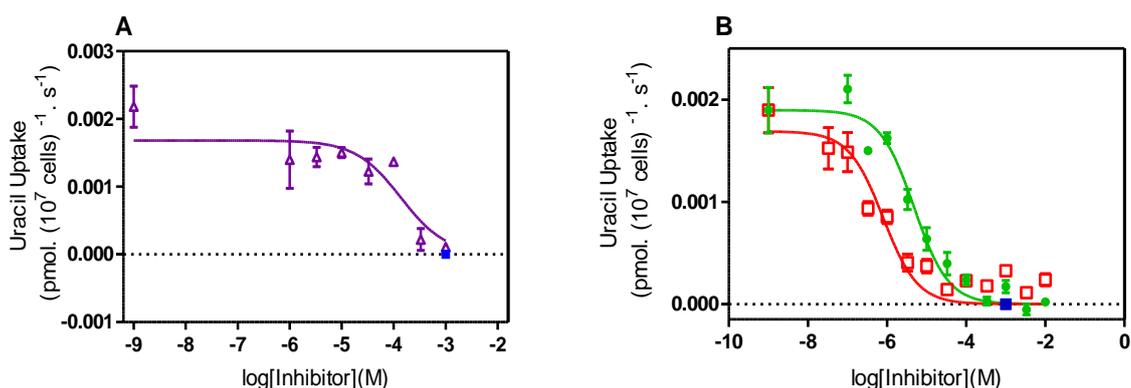
Figure 4.3 Pyrimidine transport in *L. mexicana* promastigotes. Dose-dependent inhibition of 0.5 μM [³H]-uracil uptake by increased concentrations of **A.** unlabelled adenine (△) B. unlabelled uridine (□) and 2'-deoxyuridine (●). The blue closed-square symbol (■) is the zero transport in the presence of 1 mM unlabelled uracil. All incubations were over one minute and performed in triplicate; average and SE are shown.

4.2.2 Uridine uptake in *L. mexicana* promastigotes

This study assessed the uptake of 0.25 μM [³H]-uridine by promastigotes of *L. mexicana* and found that the transport was linear for at least 2 minutes with a rate of 0.004 ± 0.0003 pmol·10^7 cells^{-1}·s^{-1} (r^2= 0.96). The uptake was completely inhibited by 1 mM unlabelled uridine indicating that the uptake was saturable (Figure 4.4A). The following [³H]-uridine experiments used 0.15 μM of label and one minute incubation time – very well inside the linear phase. Uridine transport at room temperature complied with the Michaelis-Menten equation as shown in

the inset of figure 4.4B. Uridine uptake displayed an apparent K_m value of 7.2 ± 0.9 μM and V_{max} value of 0.33 ± 0.11 pmol·10^7 cells^{-1}·s^{-1} (n=5). As all uridine inhibition results were consistent with monophasic inhibition with Hill slope very close to -1, it is possible that uridine is taken up by a single transporter.
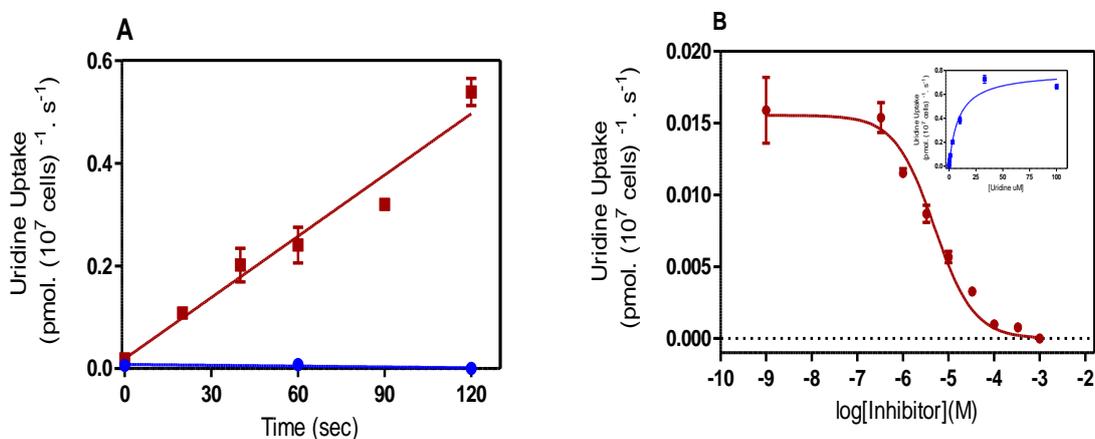
Figure 4.4. Transport of [^{3}H]-uridine by promastigotes of *L. mexicana*. **A.** Transport of 0.25 μM [^{3}H]-uridine (■) was performed over 2 minutes and entirely inhibited by 1 mM unlabelled uridine (●) **B.** Inhibition of 0.15 μM [^{3}H]-uridine uptake over one minute by various concentrations of unlabelled uridine. The inset indicates conversion of the data to a Michaelis-Menten saturation plot.

In order to investigate whether the uridine and uracil shared the same transporter, the inhibition by various concentrations of unlabelled uracil of 0.15 μM [^{3}H]-uridine uptake was assessed. In five independent experiments, the apparent K_i value for uracil inhibition of uridine transport was statistically equal to the uracil K_m value for LmexU1 (Figure 4.5A); however, uracil up to 2.5 mM inhibited only 55.6 ± 3.1% of 0.15 μM [^{3}H]-uridine uptake, taking inhibition by 1 mM unlabelled uridine as 100% (n=5). Furthermore, 5 mM of 5-fluorouracil did not inhibit 0.15 μM [^{3}H]-uridine transport (Figure 4.5B); therefore, the effect of 5-FU on uridine transport is very different from its activity against uracil uptake. As the partial inhibition by uracil shown in figure 4.5A was very consistent, and represented less than 50% inhibition of [^{3}H]-uridine transport, it appears that *L. mexicana* expresses 2 distinct uridine transporters: one being uracil-sensitive and one being uracil insensitive. Therefore, the uptake of [^{3}H]-uridine in the presence of 1 mM unlabelled uracil was investigated, so as to obtain a characterization of the uracil-insensitive uridine transporter in isolation.
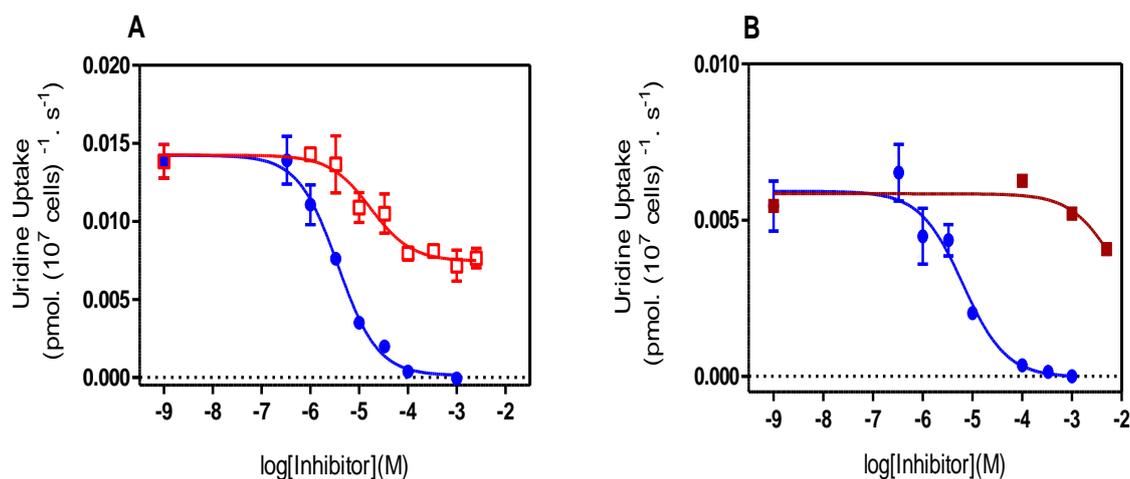
Figure 4.5. Inhibition of 0.15 µM [³H]-uridine uptake over 60 second incubations by various concentrations of unlabelled uridine (●), **A.** unlabelled uracil (□) **B.** unlabelled 5-FU (■).

The uptake of 0.15 µM [³H]-uridine in presence of 1 mM unlabelled uracil over 1 min was inhibited by various concentrations of unlabelled uridine (Figure 4.6A); the inhibition data was consistent with Michaelis-Menten kinetics (Figure 4.6B). The K_m value for uridine uptake in presence of 1 mM uracil (4.1 ± 0.2 µM) was almost identical to the K_m value for uridine uptake in the absence of uracil (7.2 ± 0.9 µM), also the average V_{max} value was equal 0.32 ± 0.07 pmol·10^7 cells^{-1}·s^{-1}. This uracil-insensitive uridine transporter was designated *L. mexicana* Nucleoside Transporter 1 (LmexNT1), whereas the uridine/uracil transporter is referred to as LmexU1. Comparing the transport efficiencies the index (V_{max}/K_m) was for LmexNT1 (using uridine as a substrate) was 26-fold higher than for LmexU1 (using uracil as a substrate). As the blue closed-circle symbol in figure 4.6A indicates the level of uridine uptake without additional uracil, in three independent experiments we once again confirmed that 1 mM of unlabelled uracil inhibited about half of 0.15 µM [³H]-uridine uptake (55 ± 3.5%). Uracil and uridine can be transported by both LmexU1 and LmexNT1, albeit with different efficiencies.
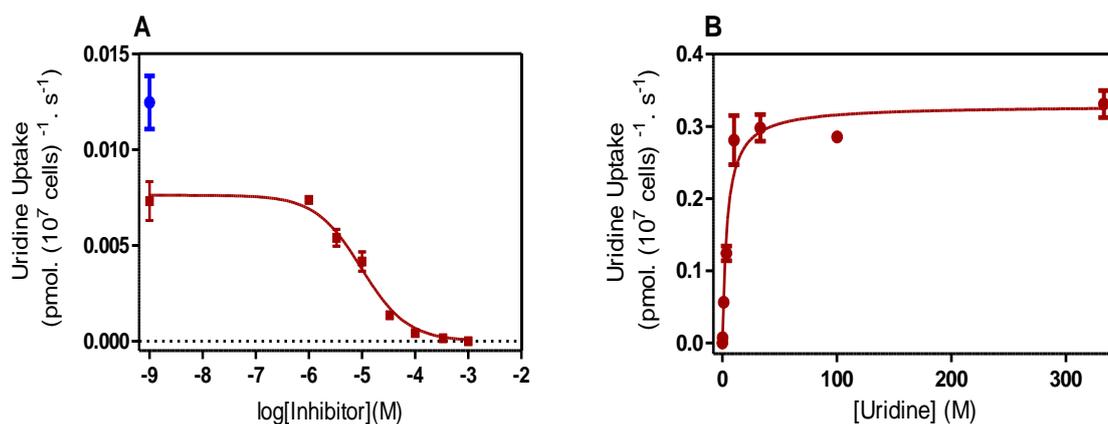
Figure 4.6. *L. mexicana* promastigotes, characterization of [³H]-uridine transport in presence of 1 mM unlabelled uracil. **A.** Inhibition of 0.15 µM [³H]-uridine uptake over one minute by various concentrations of unlabelled uridine (■), the blue closed-circle symbol (●) shows the uptake of 0.15 µM [³H]-uridine without uracil. **B.** The data derived from frame A was converted to a Michaelis-Menten saturation plot. Error bars were SE of triplicate determinations.

In order to investigate the specificity of LmexNT1, the effects of several purines and pyrimidines were assessed for inhibition of the uptake of 0.15 µM [³H]-uridine in the presence of 1 mM unlabelled uracil (Table 4.1). The inhibition profiles demonstrated Hill coefficients near -1 and maximum inhibition was consistently identical to the level of inhibition of the control (i.e. 1 mM unlabelled uridine) – all consistent with the LmexNT1 transport activity representing a single gene product. Interestingly, the apparent average K_i value for 2'-deoxyuridine was identical to its 5-fluorinated counterpart, and it was concluded that the presence or absence of fluor on carbon position 5 of the nucleoside has no effect on substrate binding with LmexNT1. The data in figure 4.7 shows that uptake of [³H]-uridine in the presence of 1 mM unlabelled uracil is also sensitive to thymidine (K_i = 10 ± 2.6) and very sensitive to adenosine (K_i = 0.39 ± 0.09), and the uptake of adenosine was therefore further investigated.
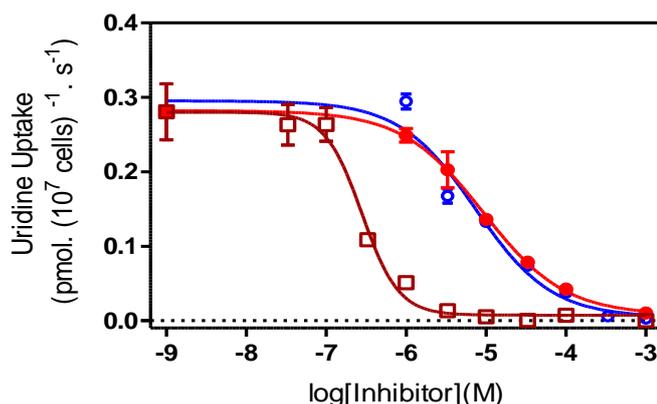
Figure 4.7 Dose-dependent inhibition of 0.15 µM [³H]-uridine transport in the presence of 1 mM unlabelled uracil by unlabelled uridine (●), adenosine (□) and thymidine (○). Incubation time was 60 seconds.

Initial experiments tested the uptake of 0.1 µM [³H]-adenosine over 2 minutes, in the presence or absence of 1 mM unlabelled adenosine. However under these conditions, the [³H]-adenosine in the media was quickly depleted, resulting in a non-linear rate of uptake (Figure 4.8A). Subsequent uptake assay with [³H]-adenosine was performed using shorter incubations , which presented a linear uptake with a rate of 0.20 ± 0.01 pmol·10^7 cells^{-1}·s^{-1} (r^2=0.98) over 25 seconds; transport was completely inhibited by 1 mM unlabelled adenosine (Figure 4.8B), showing that adenosine uptake is mediated by a saturable transporter rather than by simple diffusion.
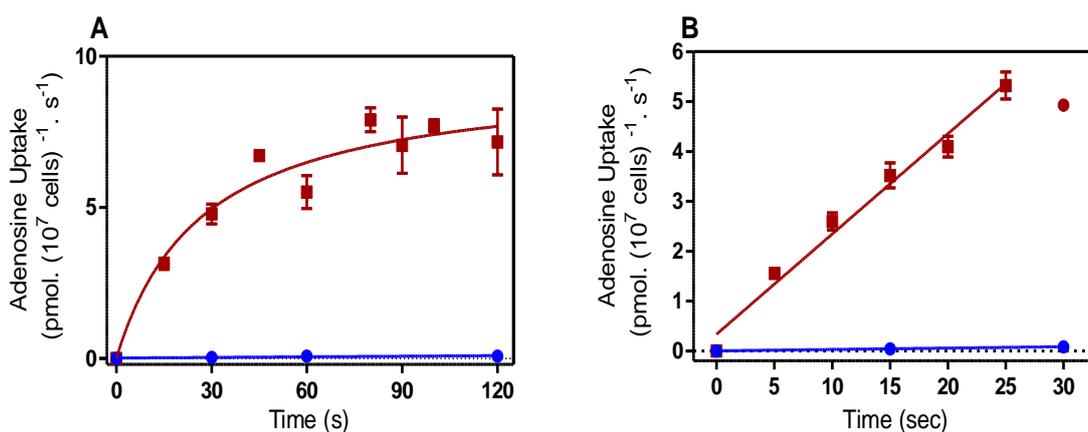
Figure 4.8. *L. mexicana* promastigotes, timecourse of 0.1 µM [³H]-adenosine transport over incubation time up to **A.** 120 seconds **B.** 30 seconds.

The use of 0.05 µM [³H]-adenosine and an incubation time of 15 seconds – within the linear phase – allowed us to characterize adenosine uptake. The inhibition data of adenosine (Figure 4.9A) was converted to a Michaelis-Menten saturation plot to determine the average of K_m and V_{max} values. Based on adenosine K_m of 0.83 ± 0.16 µM and V_{max} of 1.13 ± 0.21 pmol·10^7 cells^{-1}·s^{-1} (Figure 4.9B), the difference between the adenosine and uridine transport efficiencies was very substantial, being 1.36 versus 0.08, respectively. We conclude that *L. mexicana* promastigotes express a high affinity nucleoside transporter that preferentially transports adenosine over uridine.
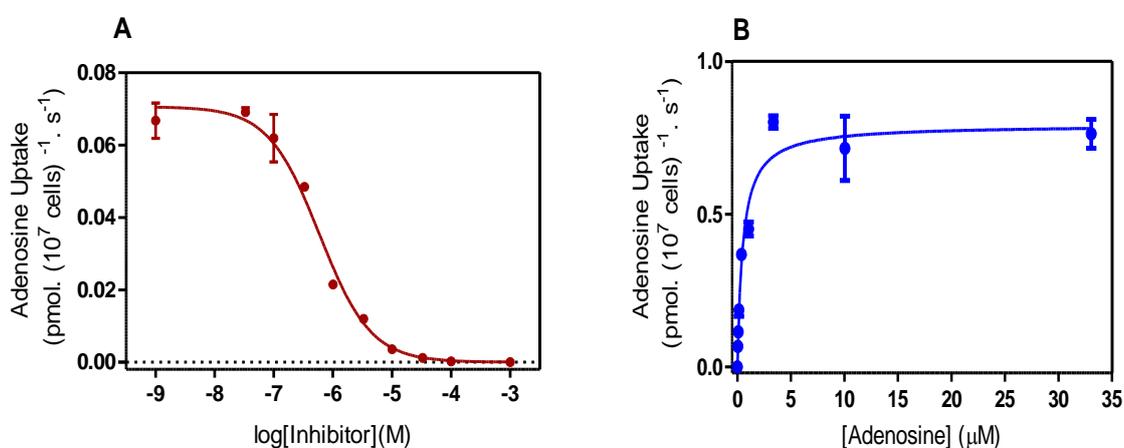
Figure 4.9. Characterization of [³H]-adenosine transport in *L. mexicana* promastigotes. **A.** Inhibitions of 0.05 µM [³H]-adenosine uptake over 15 second, by various concentrations of unlabelled adenosine. **B.** Conversion of the inhibition data from frame A to a Michaelis-Menten saturation plot.

The inhibition profiles of labeled adenosine uptake showed Hill coefficients close to -1 and the maximum inhibition was equal to the level of inhibition of 1 mM unlabelled adenosine. In three independent experiments, uridine and thymidine inhibited the uptake of [³H]-adenosine with almost identical K_i values, 24.2 ± 2.2 µM and 18.5 ± 0.64 µM, respectively (Figure 4.10A). As the adenosine K_m value is 5-fold lower than the uridine K_m ($P<0.0001$, Student's t-test) and was almost identical to the K_i value for adenosine inhibition of [³H]-uridine transport, we conclude that adenosine is taken up by LmexNT1, which is a nucleoside transporter with high affinity to adenosine. To prove that LmexNT1 is specifically a nucleoside transporter and not a nucleobase transporter, the inhibition of [³H]-adenosine by various concentrations of unlabelled uracil and adenine were performed in three separate experiments.

The results demonstrate that neither uracil nor adenine at 1 mM inhibited the uptake of 0.05 µM [³H]-adenosine (Figure 4.10B), confirming LmexNT1 as a straightforward nucleoside transporter. Another notable observation was that thymidine similarly inhibited the uptake of both labeled uridine and adenosine with identical level (9.8 ± 2.6 µM and 18.5 ± 0.64 µM, respectively), showing that thymidine is most likely also a LmexNT1 substrate, even though thymidine was not a substrate for LmexU1 (see above). To confirm these findings we also assessed the uptake of thymidine in promastigotes of *L. mexicana*.
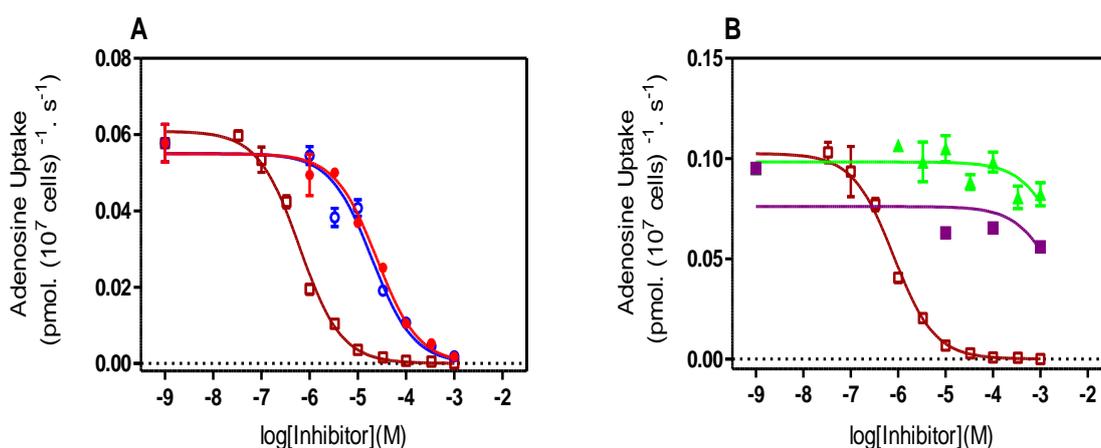
Figure 4.10. Dose-dependent inhibition of 0.05 µM [³H]-adenosine uptake by unlabelled adenosine (□), **A.** unlabelled nucleosides, uridine (●) and thymidine (○) **B.** unlabelled nucleobases uracil (■) and adenine (▲). Incubations were for 15 seconds.

The transport of [³H]-thymidine at 1 µM was determined over 30 seconds and showed a linear uptake with a rate of 0.08 ± 0.004 pmol·10^7 cells^{-1}·s^{-1} (r^2=0.98); it was entirely inhibited by 1 mM unlabelled thymidine (Figure 4.11A). These data showed that thymidine enters *L. mexicana* promastigotes via membrane protein(s) and that simple diffusion does not play a significant role in this process. All subsequent [³H]-thymidine experiments were performed using 1 µM label and 20 s incubations – well within the linear phase. In triplicate dose-response experiments, the results showed that the inhibition activity of [³H]-thymidine transport displayed Hill coefficients close to -1 and the maximum inhibition was identical to the level of inhibition of 1 mM unlabelled thymidine. Conversion of the inhibition data to Michaelis-Menten plot displayed an apparent K_m value of 4.2 ± 0.4 µM and V_{max} value of 0.85 ± 0.12 pmol·10^7 cells^{-1}·s^{-1} (Figure 4.11B).
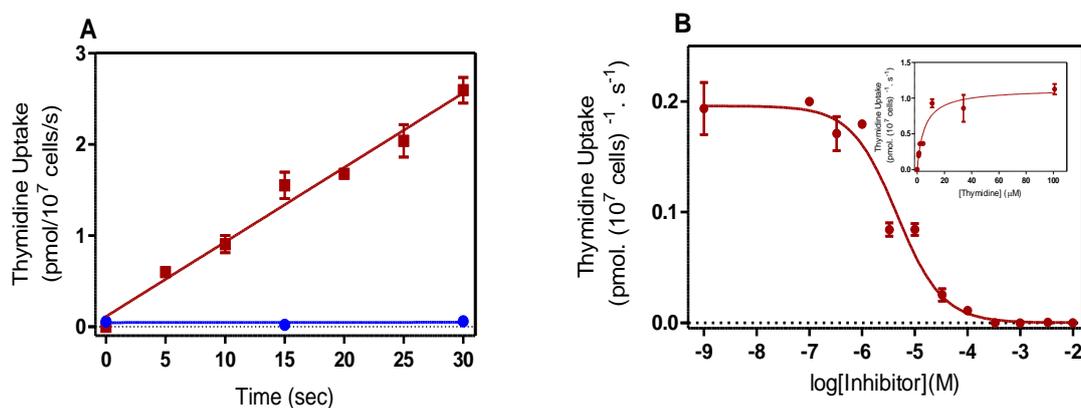
Figure 4.11. Characterization of [³H]-thymidine transport in *L. mexicana* promastigotes. **A.** Timecourse of 1 µM [³H]-thymidine transport (■) in the presence of 1 mM unlabelled thymidine (●); incubation was up to 30 seconds. **B.** Inhibition of 1 µM [³H]-thymidine uptake over 20 s by various concentrations of unlabelled thymidine (●). The inset indicated conversion the data to Michaelis-Menten saturation plot.

Inhibition activity for uridine and adenosine against thymidine uptake was very consistent and presented K_i values of 6.0 ± 0.6 µM and 0.25 ± 0.04 µM, respectively (Figure 4.12A) also against thymidine uptake cytidine showed K_i value of 82 ± 5.3 µM, but uracil did not show any activity against 1 µM [³H]-thymidine uptake even at 2.5 mM unlabelled uracil (Fig 4.12B).
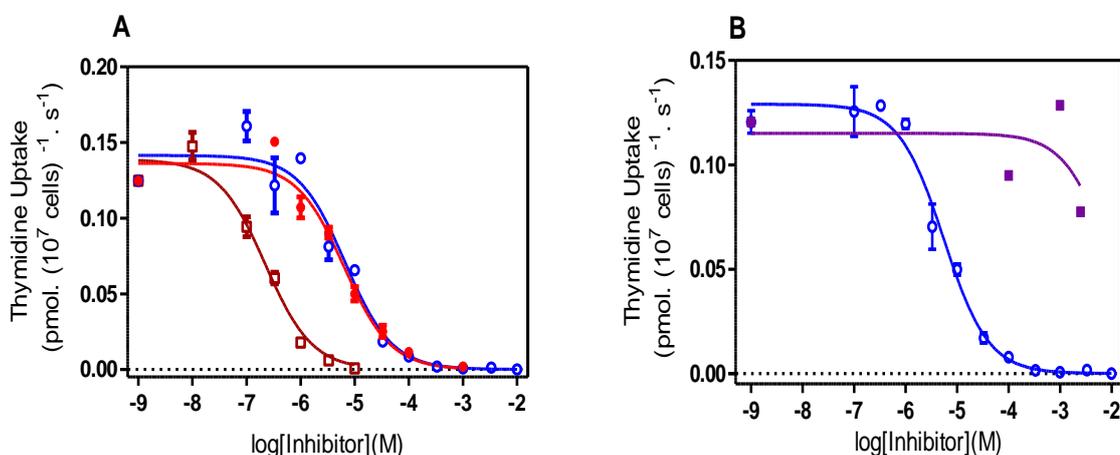
Figure 4.12. Dose-dependent inhibition of 1.0 µM [³H]-thymidine transport for 20 second incubations by unlabelled thymidine (○), **A.** uridine (●) and adenosine (□) **B.** uracil (■).

The most consistent findings were that the affinity of LmexNT1 for thymidine was very similar to uridine. In addition, the K_i values for adenosine inhibition of uridine and thymidine were identical. The thymidine uptake data also confirmed that neither uracil nor adenine was a good substrate for

LmexNT1. Therefore, we can conclude that LmexNT1 is specifically a nucleoside transporter and substrate binding depends very much on the presence of the ribose ring. However, the data from inhibition experiments showed that 2'-deoxyuridine inhibited [^{3}H]-uridine uptake with almost the same affinity as uridine itself, showing that the absence of the hydroxyl group from ribose ring on carbon position-2' does not play a major role in LmexNT1 substrate binding. In conclusion, under the standard *in vitro* conditions used, *L mexicana* promastigotes express at least two pyrimidine transporters, a nucleoside transporter with broad specificity for purine and pyrimidine nucleosides (LmexNT1), and a uracil/uridine transporter (LmexU1).

Table 4.1 Substrate profile of LmexU1 and LmexNT1, the values were expressed in µM. Entries in bold typescript indicate K_m rather than K_i values. NE, no effect on uptake at concentration indicated; blanks were values not determined. The structure of pyrimidines and their analogues are shown in Appendix II; and the actual single values are shown in Appendix III-IV.

Substrates	LmexU1	LmexNT1
Nucleobases		
Uracil	**29.7 ± 4.4**	25.7 ± 6.6
Cytosine	NE, >5000	
Thymine	563 ± 193	
Hypoxanthine	NE, >500	
Adenine	288 ± 67	NE, >1000
Nucleosides		
Uridine	2 ± 0.5	**4.1 ± 0.2**
2'-deoxyuridine	9.3 ± 2.6	7.2 ± 0.78
Thymidine	NE, >10000	**4.2 ± 0.4**
Cytidine		78 ± 15.1
Adenosine	NE, >3500	**0.83 ± 0.16**
Inosine		1010 ± 193
Pyrimidine analogs		
5-fluorouracil	56.3 ± 6.4	>5000
5-fluoro-2'deoxyuridine		7 ± 0.11

4.3. Characterization of pyrimidine transporters in *L. major* promastigotes

4.3.1 Uracil uptake in *L. major* promastigotes

The first pyrimidine nucleobase transporter in *Leishmania* cells was previously identified in promastigotes of *L. major* and designated LmajU1 with K_m value of 0.32 ± 0.07 µM and V_{max} value of 0.68 ± 0.15 pmol·10^7 cells^{-1}·s^{-1} (Papageorgiou *et al.*, 2005). The transporter was highly sensitive to uracil and 5-fluorouracil, but moderately inhibited by uridine; however, the authors of that study did not investigate the uptake of [^{3}H]-uridine by those cells. Yet, uridine transport in promastigotes of *Leishmania donovani* has been well described and proceeds efficiently via the LdNT1 adenosine/ pyrimidine nucleoside transporter (Aronow *et al.*, 1987;Vasudevan *et al.*, 1998), although for this species pyrimidine nucleobase transport was not investigated. Amastigotes of the same species also express a high affinity adenosine/pyrimidine nucleoside transporter, designated T1 (Ghosh & Mukherjee, 2000). Therefore, we assess here uridine transport by *L. major* promastigotes in order to understand whether uridine is taken up by the same or different transporter(s) and obtain the complete model of pyrimidine transport for *Leishmania major*. The combined data of pyrimidine uptake in multiple *Leishmania* spp will establish how well conserved nucleoside/nucleobase transport is across the *Leishmania* species. This is essential information if a pyrimidine-based anti-leishmanial therapy is to be developed, which must be similarly active against most, if not all, subspecies.

4.3.2 Uridine uptake in *L. major* promastigotes

The uptake of 0.25 µM [^{3}H]-uridine by *L. major* promastigotes was linear over 15 minutes with a rate of uptake of 0.14 ± 0.01 pmol·10^7 cells^{-1}·s^{-1} (r^2= 0.96); transport was completely inhibited by 1 mM unlabelled uridine (Figure 4.13A). Subsequent experiments were performed using 0.25 µM [^{3}H]-uridine and incubations for 7 min - very much within the linear phase of uptake. Inhibition of 0.25 µM [^{3}H]-uridine uptake by various concentrations of unlabelled uridine was monophasic with average Hill-coefficients near -1 (Figure 4.13B). The inhibition data was converted to a Michaelis-Menten saturation plot and showed an average of K_m value of 3.1 ± 0.6 µM and V_{max} value of 0.036 ± 0.004 pmol·10^7 cells^{-1}·s^{-1}. Figure 4.13B also shows that 1 mM of unlabelled uracil inhibited 77.3 ± 2.7% of

0.25 µM [³H]-uridine uptake with a K_i value similar to the K_m value for uridine. While this confirms that the majority of uridine uptake is through a uracil-sensitive nucleoside transporter, designated LmajNT1, the uracil-insensitive part (22.7%) of uridine influx is possibly mediated by another transporter, designated LmajNT2.
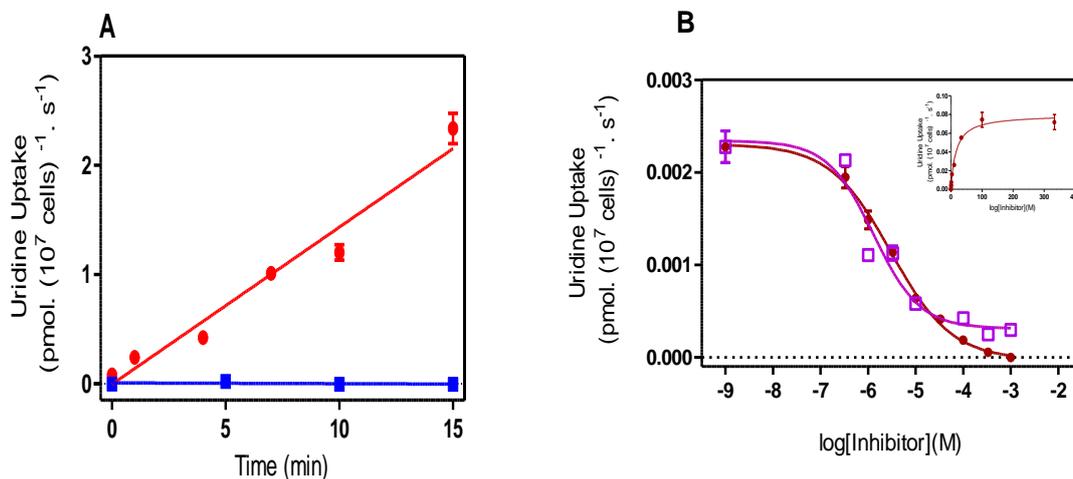
Figure 4.13. [³H]-uridine uptake by *L. major* promastigotes **A.** Timecourse of 0.25 µM [³H]-uridine transport (●) in the presence of 1 mM unlabelled uridine (■) over 15 minutes. **B.** Dose-dependent inhibition of 0.25 µM [³H]-uridine uptake by unlabelled uridine (●) and uracil (□) for 7 minute incubations. Inset: conversion the uridine inhibition data in frame B to Michaelis-Menten saturation plot to calculate the K_m and V_{max} values.

In order to determine the specificity of LmajNT1, the study assessed the effect of several pyrimidines and purines against labelled 0.25 µM [³H]-uridine uptake (Table 4.2). The inhibition profile for LmajNT1 showed that nucleosides (thymidine, 2'deoxyuridine and adenosine) completely inhibited the uptake of labelled uridine in a monophasic manner (Figure 4.14A), with the level of inhibition by 1 mM of these nucleosides similar to the effect of 1 mM unlabelled uridine (closed-green square symbol in figure 4.14). Interestingly, adenine and inosine (up to 1 mM) only partially inhibited (60 ± 4.1% and 50 ± 7%, respectively) [³H]-uridine uptake compared to 1 mM of unlabelled uridine (Figure 4.14B). Consistently, a mixture of 1 mM adenine and 1 mM inosine, represented by the upside-down closed black triangle symbol in figure 4.14B, inhibited uridine uptakes exactly as 1 mM unlabelled adenine activity, showing that adenine and inosine both inhibit the same part of the uridine flux, and dividing this into an adenine/inosine-sensitive uptake activity and an adenine/inosine-insensitive activity - both of which are equally sensitive to adenosine, thymidine and 2'deoxyuridine.
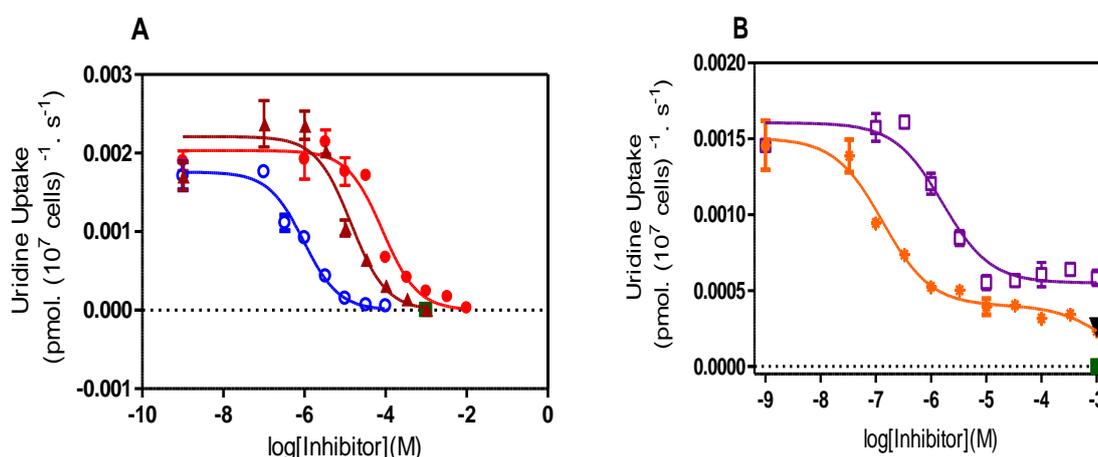
Figure 4.14. Dose-dependent inhibition of 0.25 μM [^{3}H]-uridine in *L. major* promastigotes by a concentration of 1 mM unlabelled uridine (■) in presence of various concentrations of unlabelled substrates. **A.** thymidine (●), 2'deoxyuridine (▲), adenosine (○), **B.** adenine (□), inosine (*). The black closed upside-down triangle is adenine and inosine together, each at 1mM.

Thus, the part of [^{3}H]-uridine uptake that is not inhibited by uracil, adenine and inosine shows that *L. major* expressed at least two pyrimidine nucleoside transporters: a high affinity uridine transporter (LmajNT1), which has high affinity for uracil, adenine and inosine; and a lower affinity uridine transporter(LmajNT2), which is insensitive to uracil, adenine and inosine. Both transporters are sensitive to 2'-deoxyuridine, thymidine and adenosine. In order to differentiate the two uridine activities, the uridine inhibition data from figure 4.13B was converted to a Lineweaver-Burk plot (Lineweaver & Burk, 1934); this conversion identified high and low uridine affinity transport activities. The data showed that the K_m value of the high affinity uridine transporter was 10-fold lower than the value for the low affinity transporter (3.1 ± 0.6 μM against 33.5 ± 7 μM, respectively). The average V_{max} was higher in the latter than in the former (0.036 ± 0.004 versus 0.152 ± 0.038 pmol·10^7 cells^{-1}·s^{-1}; Figure 4.15), and the transport efficiency index (V_{max}/ K_m for the former was 2.5-fold higher than for the latter.
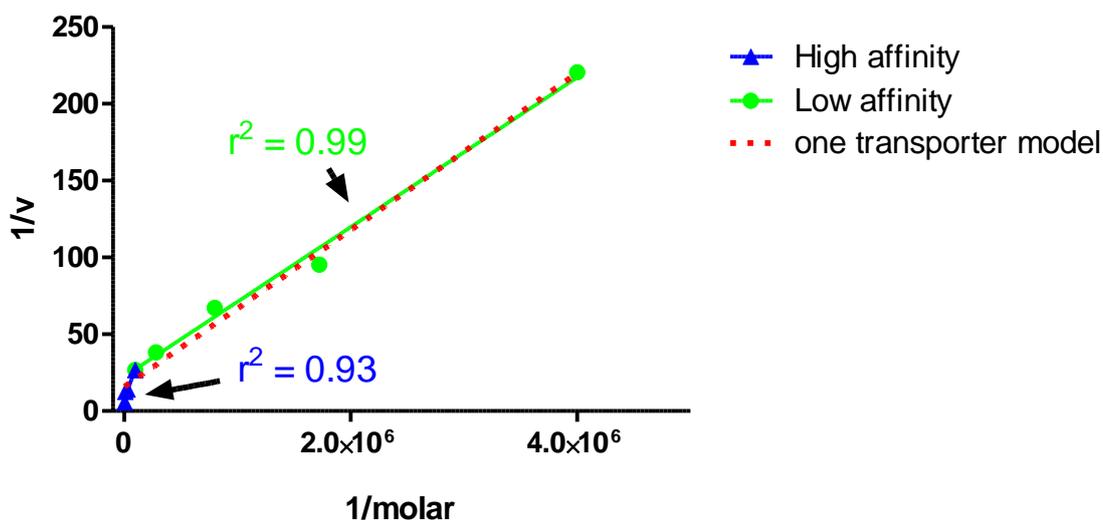
Figure 4.15. Conversion of unlabelled uridine inhibition data against [³H]-uridine uptake from figure 4.11B to Lineweaver-Burk plot. The data best fitted a two-transporter model (LmajNT1 and LmajNT2), with linear regression through 4 and through 5 points, respectively. The experiment was performed in triplicate and representative of three identical repeats. The red dashed line represents linear regression of all data points for comparison.

In conclusion, *L. major* expresses at least two nucleoside transporters with different affinities to uridine; a high affinity uridine transporter LmajNT1, which was sensitive to inhibition by uridine, uracil, inosine and adenine; and a low affinity uridine transporter, designated LmajNT2, which has lower affinity to uridine and is insensitive to uracil, inosine and adenine. Both transporters are inhibited by 2'-deoxyuridine, thymidine and adenosine. Table 4.2 gives the K_i values for these inhibitors in the LmajNT1 column as the large majority of [³H]-uridine uptake was through this transporter, but LmajNT2 must have similar values. These could be separately determined in the presence of 1 mM inosine, for example.

Table 4.2 Substrate profile of LmajU1, LmajNT1 and LmajNT2 the value was expressed in μM. Entries in bold typescript indicate K_m rather than K_i values. NE, no effect on uptake at concentration indicated in μM; where left blank, the values were not determined. Data for LmajU1 were taken from (Papageorgiou *et al.,* 2005) and included for comparison. The structure of pyrimidines and their analogues are shown in Appendix II; and the actual single values are shown in Appendix III-IV.

Substrates	LmajU1	LmajNT1	LmajNT2
Nucleobases			
Uracil	**0.32 ± 0.07**	2.5 ± 0.6	
Adenine	NE, 200	5.1 ± 2.1	
Nucleosides			
Uridine	10.9 ±3.2	**3.1 ± 0.6**	**33.5 ± 7**
2'-deoxyuridine		12.4 ± 4.5	
Thymidine	NE, 200	110 ± 20	
Adenosine		1.9 ± 0.5	
Inosine		0.14 ± 0.004	
Pyrimidine analogs			
5-fluorouracil	0.66 ± 0.14		

4.4 Anti-leishmanial activity of pyrimidine analogues

4.4.1 The activity of pyrimidine analogues against *L. mexicana* promastigotes

The EC_{50} values of several pyrimidine analogues on *Leishmania* cells were determined using the Alamar Blue fluorescence assay. Pentamidine and diminazene were used as positive controls throughout the assessment. The nucleobase analogues 5-chlorouracil, 5-bromouracil, 5-iodouracil, 5-fluorocytosine, 5-fluoroorotic acid, 6-azauracil and 4-thiouracil, and the nucleoside analogues 5-fluorouridine, 5-chlorouridine, 5-bromouridine, 5-iodouridine, 5-fluorocytidine, 2-thiuridine and 4-thiouridine, as well as the deoxynucleoside analogues 5-chloro-2'-deoxyuridine, 5-bromo-2'-deoxyuridine, 5-iodo-2'-deoxyuridine, 5'-deoxy-5-fluorouridine, 2'-3'-dideoxyuridine, 3'-deoxyuridine and 3'-deoxythymidine, all had no effect on *L. mexicana* promastigotes up to at least 1 mM of compound. The only tested pyrimidine analogues to show activity against *L. mexicana* promastigotes were 5-fluorouracil, 5-fluoro-2'deoxyuridine and 5-fluoro-2'deoxycytidine; these analogues displayed EC_{50} value at micromolar level (Table 4.3). In addition, 5'-deoxyuridine showed an average EC_{50} value 461 ± 80 μM. Interestingly, despite

the fact that *L. mexicana* pyrimidine transporters were much more sensitive to nucleosides than nucleobases, ribonucleoside analogues did not show anti-leishmanial activity against these cells even at millimolar concentrations. Pentamidine and diminazene as positive controls against promastigotes of *L. mexicana* cells demonstrated EC_{50} values of 1.0 ± 0.1 µM and 7.4 ± 0.3 µM, respectively.

Table 4.3. The EC_{50} values per µM of effective 5-fluoro-pyrimidines on *L. mexicana* and *L. major* promastigotes using Alamar Blue fluorescent assays. The structure of pyrimidines and their analogues are shown in Appendix II; and the actual single values are shown in Appendix V.

	L. mexicana	*L. major*
5-Fluorouracil	9.3 ± 0.6	8.5 ± 0.6
5-Fluorouridine	>5000	18 ± 1.6
5-Fluoro-2'deoxyuridine	1.4 ± 0.06	1.7 ± 0.1
5-Fluoro-2'deoxycytidine	17.3 ± 1.8	38 ± 1.7
5'-Deoxyuridine	461 ± 80	525 ± 46
Pentamidine	1.0 ± 0.1	3.3 ± 0.2
Diminazene	7.4 ± 0.3	9.8 ± 0.3

4.4.2 The activity of pyrimidine analogues against *L. major* promastigotes

The activity of the above listed pyrimidine analogues against promastigotes of *L. major* was also determined. The sensitivity of *L. major* to these compounds was very similar to *L. mexicana*. The effect of pyrimidine analogues on *L. major* showed that only four compounds displayed an average of EC_{50} values at micromolar level, whereas 21 of 25 compounds were nontoxic up to 1 mM of the reagent (Table 4.3). The main difference was 5-fluorouridine, which displayed no activity against *L. mexicana* at concentrations up to 5 mM (Figure 4.16A), but killed promastigotes of *L. major* at concentrations below 20 µM (Figure 4.16B). In contrast, the average of EC_{50} values of 5'-deoxyuridine was very similar (525 ± 46 µM for *L. major*). The effects of pentamidine (3.3 ± 0.2 µM) and diminazene (9.8 ± 0.3 µM) on promastigotes of *L. major* were also identical to *L. mexicana* cells. However, the sensitivity of *L. major* promastigotes to 5-fluoro-2'deoxycytidine was >2-fold lower than for *L. mexicana*.
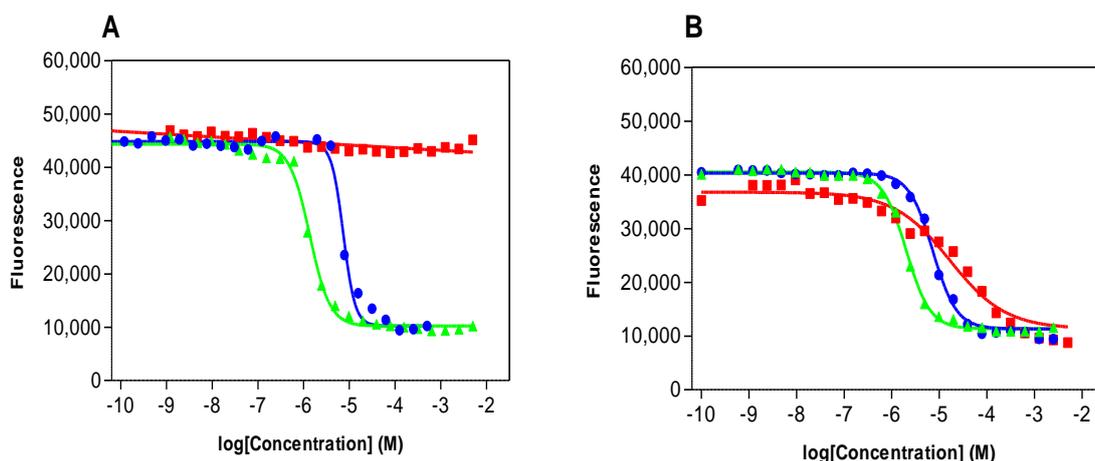
Figure 4.16. The sensitivity of **A.** *L. mexicana* promastigotes and **B.** *L. major* promastigotes to 5-FU (●), 5F-2'dUrd (▲) and 5F-Urd (■), using Alamar Blue assays.

4.4.3 The effect of fluorinated pyrimidines on growth of *Leishmania* spp

The effective fluorinated pyrimidines identified above were tested for effect on the growth of promastigotes during *in vitro* culture of *L. mexicana* and *L. major* by exposing the cells to 0.5 mM of each drug separately. The density of *Leishmania* promastigotes cultures at mid-log phase were adjusted to 10^6 cells/ml in 10 ml culture flasks, and 500 μM of one of the effective drugs (5-FU, 5F-2'dUrd and 5F-Urd) was added. The cell count was monitored until the death of the parasite populations. For *L. mexicana*, the nucleobase and deoxynucleoside analogues killed the cells after a few days of exposure to the indicated drugs. However, these cells were insensitive to 5F-Urd (Figure 4.17A), although the drug arrested the growth for few days, after which the cells started multiplying. This observation was entirely consistent with the Alamar Blue data. *L. major* promastigotes were sensitive to all fluorinated pyrimidines tested (Figure 4.17B), and the drugs arrested the growth of the cells before killing them off. None of the pyrimidine analogues killed *Leishmania* cells very quickly, which is the same observation made in trypanosomes.
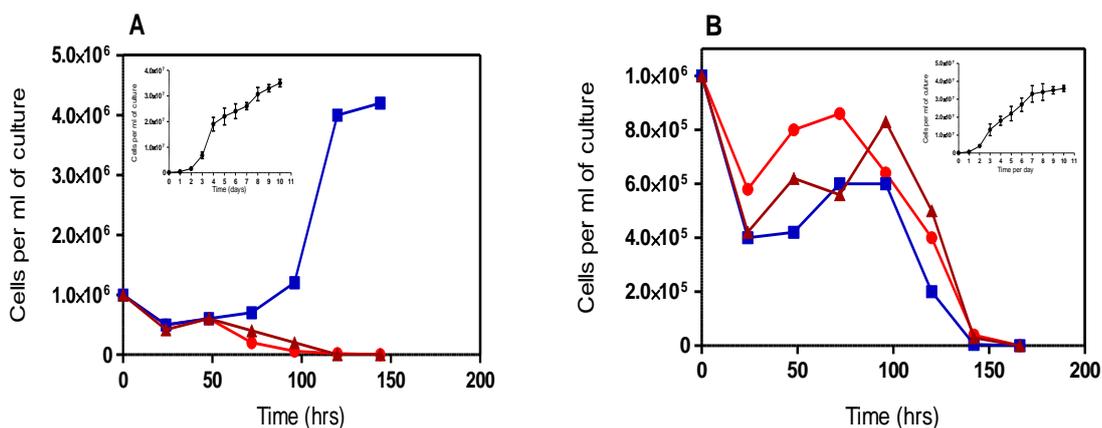
Figure 4.17. The effect of fluorinated pyrimidines on the growth of **A.** *L. mexicana* sM379-WT **B.** *L. major* Friedlin-WT. Cultures containing 10^6 promastigotes/ml were incubated in HOMEM medium with 0.5 mM of 5-FU (●), 5F-Urd (■) or 5F-2'dUrd (▲). The inset for each figure shows the growth of *Leishmania* in drug free standard HOMEM medium.

4.5. Induction of resistance to selected pyrimidine analogues and cross-resistance profiles

To assess the extent to which anti-leishmanial pyrimidine analogues depend on salvage enzymes and/or transporters, resistance to 5-fluorouracil and 5-fluoro-2'deoxyuridine was induced by *in vitro* exposure of wild type *L. mexicana* sM379 and *L. major* sFriedlin promastigotes to stepwise increasing concentrations of the drugs (Figure 4.18). It was noted that *Leishmania* cells adapted to 5F-2'dUrd more quickly than to 5-FU; while *Leishmania* cells became insensitive to high concentrations of 5F-2'dUrd in a few months, the resistance induction to 5-FU required around a year. Clonal lines were generated from each strain that displayed resistance to high concentrations of 5-FU or 5F2'dUrd. 5-FU-adapted clones from *L. mexicana* and *L. major* were abbreviated Lmex-5FURes and Lmaj-5FURes, whereas cells adapted to 5F-2'dUrd were called Lmex-5F2'dURes and Lmaj-5F2'dURes, respectively. Regarding the Lmex-5FURes strain, an intermediate strain, which was able to survive and proliferate in 500 µM of 5-FU, was also cloned out in order to be able to investigate intervening changes.
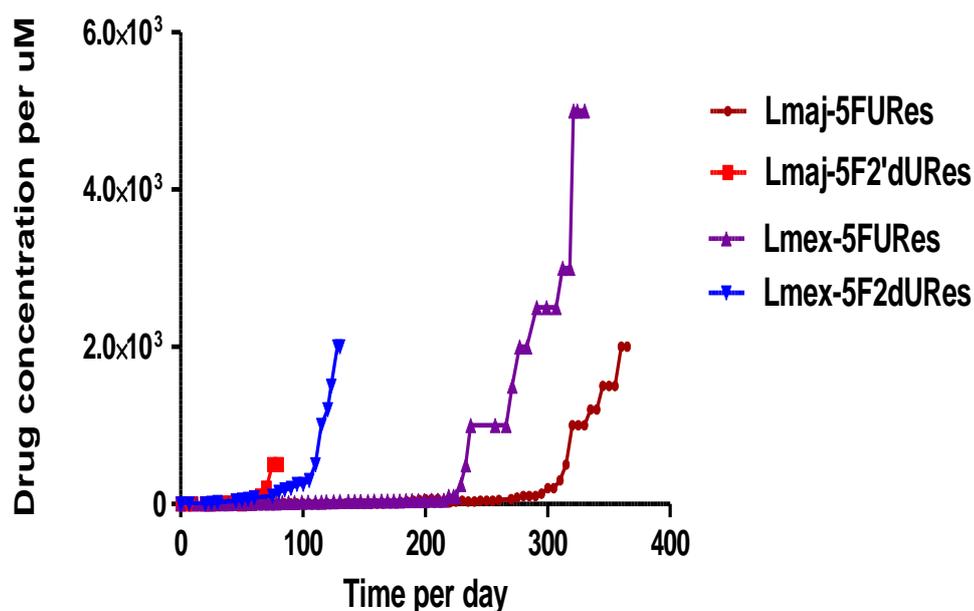
Figure 4.18. Adaptation of promastigotes of *Leishmania spp* to high concentrations of fluorinated pyrimidine analogues during *in vitro* culturing. Concentrations indicated are the concentrations of analog added to the medium, in which the cells managed to survive and multiply., i.e. 5-fluorouracil to generate the adapted cell line 5FURes, and 5F-2'dUrd to generate the cell line 5F-dURes; After adaptation of the cultures the promastigotes were cloned out by limiting dilution so that the eventual cell lines that were characterized were all grown from a single cell.

The anti-leishmanial activity and the cross-resistance patterns of cytotoxic pyrimidine analogues were investigated for each adapted cell line; the assessment was performed in parallel with the parental wild-type strains. Using Alamar Blue assays average EC_{50} values were generated for several pyrimidine analogues against resistant strains (Table 4.4). These determinations allowed us to identify possible cross-resistance, which in turn is indicative of common mechanisms of action. In general, resistant clones exhibited a high level of resistance to each individual drug as well as some cross-resistance to other fluorinated pyrimidines, but resistant clones were not cross-resistant to pentamidine and diminazene.

Table 4.4. Phenotype of *Leishmania* promastigotes strains adapted to high level resistance to fluorinated pyrimidines. All EC_{50} values were obtained using the Alamar blue assay and are given in μM. WT = wild-type sensitive control strain. Resistance Factor = EC_{50} (resistant clone)/ EC_{50} (WT). The actual single values are shown in Appendix V

Strains/drugs	5-FU	5F2'dUrd	5F2'dCyd	5FUrd
L. mexicana-WT	9.3 ± 0.6	1.4 ± 0.06	17.3 ± 1.8	>5000
Lmex5FURes	1374 ± 123	1.5 ± 0.2	24 ± 0.9	>5000
RF	147	1	1.38	1
Lmex5F2'dURes	1773 ± 301	>5000	>5000	>5000
RF	190	>3500	>289	1
L. major-WT	8.5 ± 0.6	1.7 ± 0.1	38 ± 1.7	18 ± 1.6
Lmaj5FURes	150 ± 5.2	6.1 ± 0.5	17 ± 1.8	110 ± 17
RF	17	3.6	0.4	6
Lmaj5F2'dURes	12 ± 1.0	381 ± 83	3870 ± 621	1232 ± 341
RF	1.3	224	101	68

Lmex-5FURes cells displayed high levels of resistance to 5-FU, but retained the same sensitivity to 5-fluoro-2'deoxy-pyrimidines. On the other hand, Lmex-5F2'dURes were completely adapted to tested concentration of 5-fluoro-2'deoxy-pyrimidines, and were slightly more resistant to 5-FU than Lmex-5FURes (RF 190 versus 147). *L. major* promastigotes adapted to 5-fluoro-pyrimidines were different from *L. mexicana* in terms of resistance factors and cross-resistance pattern and particularly with respect to the sensitivity to 5-fluorouridine. However, both Lmex-5FURes and Lmaj-5FURes cells displayed almost the same sensitivity to fluorinated nucleosides as their respective parental cell lines. The main difference is that whereas *L. mexicana* cells adapted to high levels of fluorinated pyrimidine nucleosides such as 5F-2'dUrd were also highly resistant to 5-FU, Lmaj-5F2'dURes cells were not at all cross resistance to 5-FU. To understand in which way the resistance response of *Leishmania* species to pyrimidine analogous rely on salvage enzymes or transporters, the study attempted to compare the transport of [³H]-pyrimidines in the adapted lines with the wild type promastigotes of each species.

4.6. Assessment of pyrimidine uptakes in *Leishmania* resistant strains

4.6.1. *Leishmania* strains adapted to 5-fluorouracil

The uptake of 0.5 µM of [3H]-uracil (Figure 4.19A) or [3H]-5-fluorouracil (Figure 4.19B) over 10 minutes in the presence or absence of 1 mM unlabelled uracil or 5-FU was assessed in Lmex-5FURes promastigotes in parallel with their WT counterparts. [3H]-uracil and 5-FU uptakes were linear for 10 minutes in *L. mexicana* M379-WT cells with a rate of 0.11 ± 0.01, and 0.30 ± 0.03 pmol·10^7 cells^{-1}·s^{-1}, respectively. However, the uptake of both labeled uracil and 5-fluorouracil in Lmex-5FURes was profoundly reduced and became identical to the [3H]-uptakes in the presence of 1 mM unlabeled nucleobases, meaning that there was no evidence for transporter-mediated uracil or 5-FU uptake in Lmex-5FURes. This observation very much confirmed that uracil and 5-FU share the same transporter, LmexU1, and that this transport activity is lost through adaptation to 5-FU without an obvious *in vitro* growth phenotype.
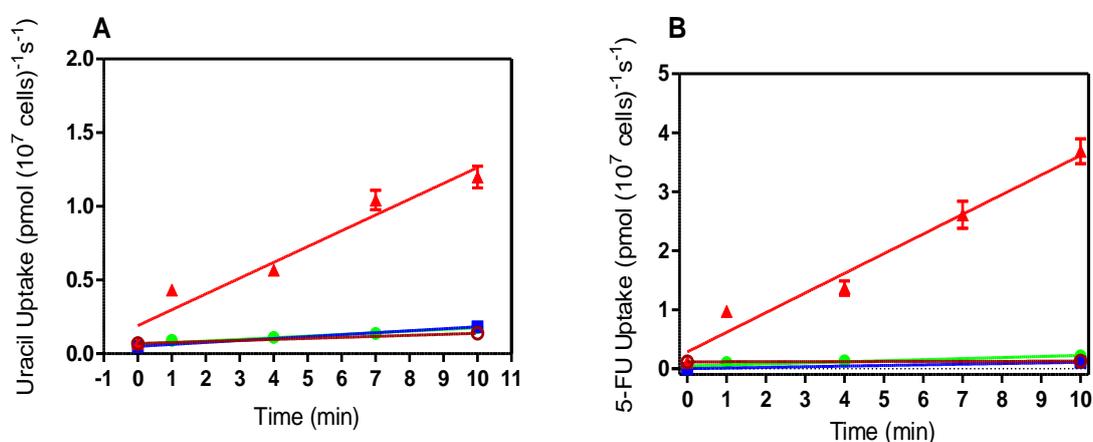
Figure 4.19. [3H]-pyrimidine transport by promastigotes of *L. mexicana* strains. **A.** Transport of 0.5 µM [3H]-uracil by Lmex-5FURes (●) and sM379-WT (▲) in the presence or absent of 1 mM unlabelled uracil, (○) and (■), respectively. **B.** Transport of 0.5 µM [3H]-5fluorouracil by Lmex-5FURes (●) and sM379-WT (▲) in the presence of 1 mM unlabelled 5-FU (■) and (○), respectively. Incubations were for up to 10 minutes.

Transport of 0.5 μM [^{3}H]-uridine was also investigated in Lmex-5FURes and compared with M379-WT (Figure 4.20). The results showed that the rate of 0.5 μM [^{3}H]-uridine uptake in Lmex-5FURes and M379-WT was almost identical (0.65 ± 0.05 pmol·10^7 cells^{-1}·s^{-1} versus 0.68 ± 0.1 pmol·10^7 cells^{-1}·s^{-1}, respectively); in both strains [^{3}H]-uridine transport was completely inhibited in the presence of 1 mM unlabelled uridine. These findings show very clearly that uracil and uridine are taken up by separate transporters in *L. mexicana* promastigotes, and that meant that Lmex-5FURes had lost the nucleobase transporter (LmexU1), but not the nucleoside transporter (LmexNT1). This suggestion is also confirmed by the lack of resistance of Lmex-5FURes to fluorinated nucleosides.
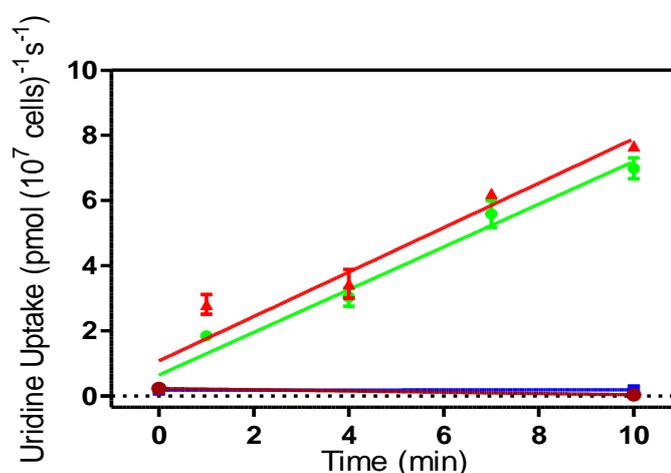
Figure 4.20. [^{3}H]-uridine transport in promastigotes of *L. mexicana* strains. Transport of 0.5 μM [^{3}H]-uridine by Lmex-5FURes (●) and sM379-WT (▲) was measured over 10 minutes in the presence or absence of 1 mM unlabelled uridine, (■) and (○), respectively.

For *L. major* promastigotes, the uptake of 0.5 μM [^{3}H]-uracil and [^{3}H]-uridine in Lmaj-5FURes cells, in comparison with sFriedlin-WT, was also investigated. The uptake of labeled uracil was performed in the presence and absence of 1 mM unlabeled uracil over 10 minutes. Figure 4.21A showed that [^{3}H]-uracil transport in sFriedlin-WT was linear with a rate of uptake 0.3 ± 0.009 pmol·10^7 cells^{-1}·s^{-1} (r^2=0.99). However, [^{3}H]-uracil uptake was 96% reduced in the resistant clone and was almost equal to [^{3}H]-uracil uptake in the presence of 1 mM unlabelled uracil, uracil uptake was still significantly non-zero (P<0.027; F-test). We can assume that the strain Lmaj-5FURes cells have totally lost uracil activity (LmajU1) and have become unable to salvage this nucleobase, with the minor uracil flux being attributable to LmajNT1, which has a relatively low

affinity for uracil (Table 4.2). However, as [^{3}H]-uridine transport was compared in Lmaj-5FURes and sFriedlin-WT, it was found that in two separate experiments transport of 0.5 µM [^{3}H]-uridine in these strains was clearly different. While the uptake was linear in sFriedlin-WT cells with a rate of 0.08 ± 0.007 pmol·10^7 cells$^-$^{1}·s^{-1}, in Lmaj-5FURes the uptake was nonlinear and saturable over the indicated time with an apparent rate of 0.29 ± 0.07 pmol·10^7 cells^{-1}·s^{-1} over the first five minutes, becoming subsequently saturable with a rate of just 0.058 ± 0.003 pmol·10^7 cells^{-1}·s^{-1} for the rest of the 10 minute incubations (Figure 4.21B). These findings agree with the Alamar Blue data (Table 4.4, above) which showed that Lmaj-5FURes cells were still sensitive to cytotoxic pyrimidine nucleosides. As Lmaj-5FURes has lost the high affinity uracil transporter (LmajU1), the Lmaj-5FURes strain relies on the nucleoside transporter(s) to provide the cells with pyrimidine sources; the apparent increase in the rate of uridine uptake during the initial incubations could be due to up-regulation of LmajNT1/LmajNT2; the non-linearity suggests that, under the assay conditions, the rate of uridine uptake in Lmaj-5FURes exceeded its metabolic usage, resulting in a high initial rate of transport, and a lower secondary rate representing uridine metabolism, which became rate limiting for overall uptake after a few minutes.
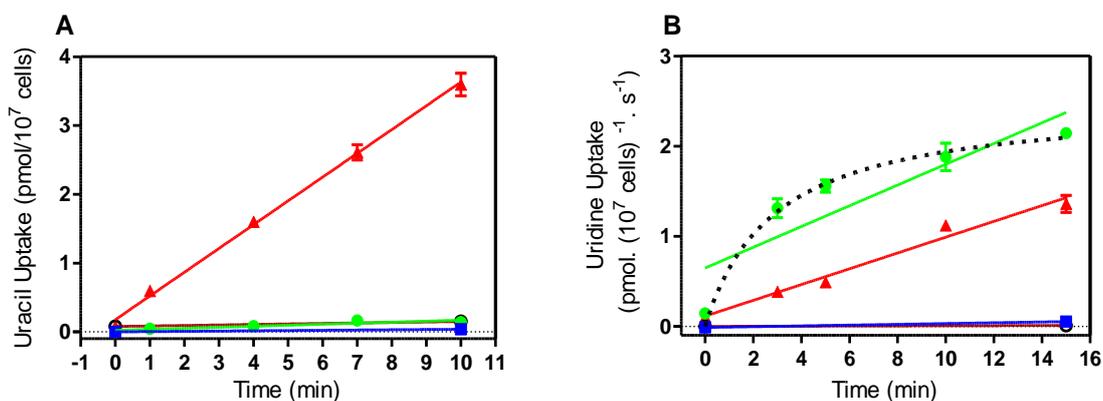
Figure 4.21. [^{3}H]-pyrimidine uptake in *L. major* strains. **A.** Transport of 0.5 µM [^{3}H]-uracil by Lmaj-5FURes (●) and sFriedlin-WT (▲) in the presence of 1 mM unlabelled uracil (■) and (○), respectively. **B.** Uptake of 0.5 µM [^{3}H]-uridine by Lmaj-5FURes (●) and sFriedlin-WT (▲) over 15 minutes in the presence of 1 mM unlabelled uridine (■) and (○), respectively. The dashed line is showing the rate of uptake without linear regression calculation.

4.6.2 *Leishmania* strains adapted to 5-fluoro-2'-deoxyuridine

In section 4.2.2 it was shown that *L. mexicana* promastigotes take up uridine and adenosine through the nucleoside transporter LmexNT1, and that the uptake can be inhibited by 2'-deoxyuridine, which is the natural deoxynucleoside equivalent of 5F-2'dUrd. Specifically, the K_m values for uridine (7.15 ± 0.9 µM) and the K_i values for 2'deoxyuridine (7.2 ± 0.78 µM) were shown to be identical. In this section the uptake of 0.5 µM [³H]-uridine and of 0.1 µM [³H]-adenosine was investigated in Lmex-F2'dURes, and compared with the parental strain M379-WT. The uptake of [³H]-uridine (Figure 4.22A) and [³H]-adenosine (Figure 4.22B) was linear over the 600 s (uridine) and the 25 s (adenosine) duration of the experiment in *L. mexicana* M379-WT with a rate of 0.68 ± 0.1 pmol·10^7 cells^{-1}·s^{-1} and 0.037 ± 0.002 pmol·10^7 cells^{-1}·s^{-1}, respectively. In contrast, the transport of [³H]-uridine by Lmex-F2'dURes was completely reduced and became identical to the uptake in the presence of 1 mM unlabeled uridine, so that it is believed that the Lmex-5F2'dURes cells have lost the uridine transport activity (LmexNT1). Furthermore, the uptake of [³H]-adenosine by Lmex-5F2'dURes was reduced by 81% compared with M379-WT cells; thus very low level (19%) of adenosine uptake could be maintained by an unknown low affinity adenosine transporter. As Lmex-5F2'dURes cells showed cross-resistance with 5-FU we decided to assess uracil uptake in those cells as well.
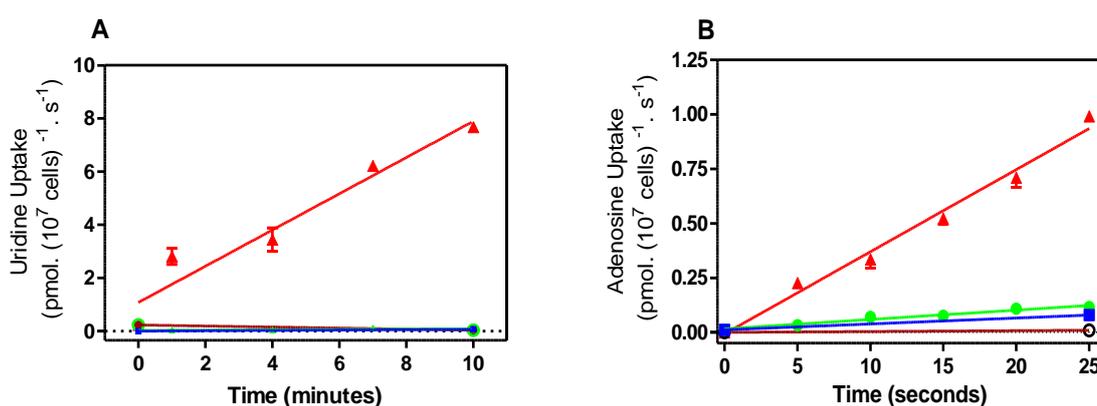
Figure 4.22. [³H]-pyrimidine uptake by promastigotes of *L. mexicana* strains. **A.** Transport of 0.5 µM [³H]-uridine by Lmex-5F2'dURes (●) and sM379-WT (▲) in the presence of 1 mM unlabelled uridine (○) and (■), respectively. **B.** Transport of 0.1 µM [³H]-adenosine by Lmex-5F2'dURes (●) and sM379-WT (▲) in the presence of 1 mM unlabelled adenosine (■) and (○), respectively.

In order to test the rate of 0.5 µM [3H]-uracil transport in Lmex-F2'dURes against wild type promastigotes of *L. mexicana*, uracil uptake was determined at various intervals over 10 minutes. The results show that the rate of 0.5 µM [3H]-uracil uptake in Lmex-5F2'dURes was completely identical to the rate in M379-WT, with an average of 0.096 ± 0.01 pmol·10^7 cells^{-1}·s^{-1} and 0.097 ± 0.01 pmol·10^7 cells^{-1}·s^{-1}, respectively (Figure 4.23); uptake of 0.5 µM labeled uracil in both strains was equally sensitive to 1 mM of unlabeled uracil. It is clear that Lmex-5F2'dURes are still maintaining the uracil transport activity Lmex-U1, but lost uridine transporters. Notwithstanding the observation that uridine and uracil transporters had overlapping inhibition profiles (section 4.2), these data clarify that uracil and uridine are taken up by different transport proteins (LmexU1 and LmexNT1, respectively).
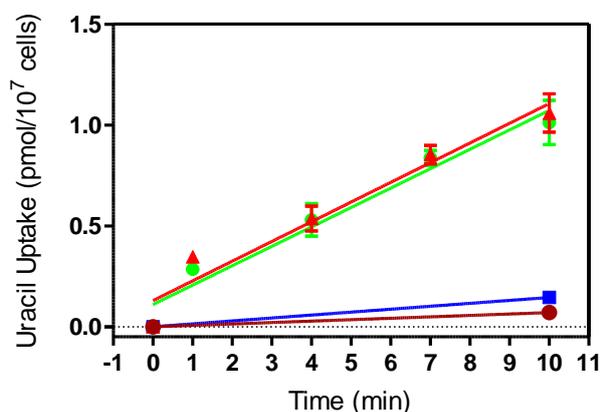
Figure 4.23 [3H]-pyrimidine uptake by promastigotes of *L. mexicana* strains. Uptake of 0.5 µM [3H]-uracil by Lmex-F2'dURes (●) and M379-WT (▲) over 10 minutes in the presence of 1 mM unlabelled uracil, (■) and (●), respectively; n=3.

Uridine uptake in Lmaj-5F2'dURes in parallel with sFriedlin-WT was investigated in two separate experiments. The study found that the uptake of 0.5 µM [3H]-uridine was linear over 10 minutes in sFriedlin-WT cells with a rate of uptake of 0.11 ± 0.01 pmol·10^7 cells^{-1}·s^{-1}, which was totally inhibited by 1 mM unlabeled uridine (Figure 4.24A). However, the transport of [3H]-uridine was reduced by 83% in Lmaj-F2'dURes cells. It can be argued that Lmaj-5F2'dURes strain had lost the most part of uridine activity. As described previously (section 4.3.2), *L. major* promastigotes expressed two uridine activities (high and low affinity uridine transporters); therefore it is suggested that Lmaj-5F2'dURes cells have lost one of the uridine transporters (LmajNT1 or LmajNT2), but retain a

reduced capacity for uridine uptake through the other uridine transporter, and possibly through LmajU1. These findings prompted us to assess uracil uptake in Lmaj-5F2'dURes.

The transport of 0.5 µM [³H]-uracil in Lmaj-5F2'dURes were performed in parallel with sFriedlin-WT over 10 minutes. The uptake of [³H]-uracil by sFriedlin-WT cells was linear for 10 minutes with a rate of 0.54 ± 0.02 pmol·10⁷ cells⁻¹·s⁻¹, and the transport was totally inhibited by 1 mM unlabelled uracil. However, the uptake of [³H]-uracil was reduced by 82% in Lmaj-5F2'dURes cells compared with sFriedlin-WT, with a rate of uptake 0.10 ± 0.02 pmol·10⁷ cells⁻¹·s⁻¹ (Figure 4.24B). The most interesting observation was that uracil and uridine transport were equally reduced in Lmaj-5F2'dURes cells (17% and 18%, respectively), compared with sFriedlin-WT. This suggests that the low affinity uridine transporter (LmajNT2) is potentially the only active pyrimidine transporter in Lmaj-5F2'dURes.
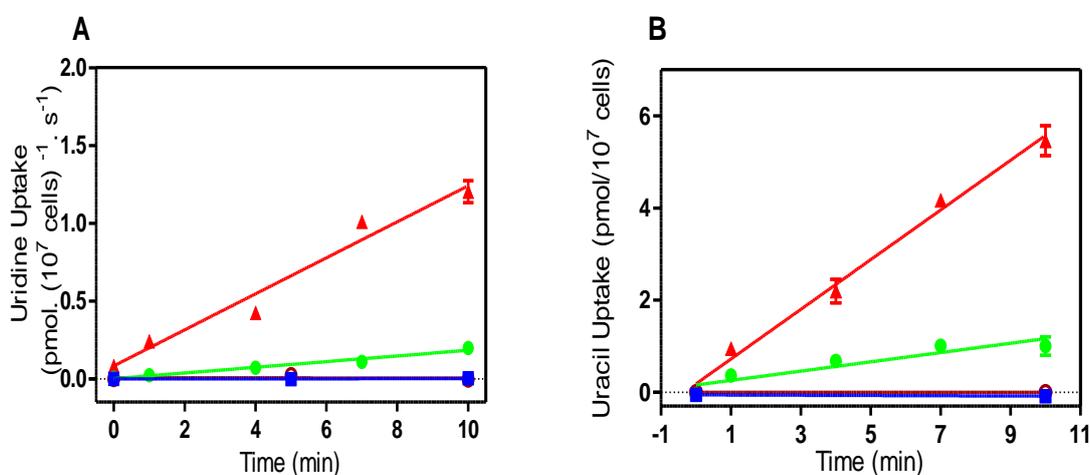
Figure 4.24 [³H]-pyrimidine uptake in *L. major* strains. **A.** Transport of 0.5 µM [³H]-uridine by Lmaj-5F2'dURes (●) and sFriedlin-WT (▲) over 10 minutes in the presence of 1 mM unlabelled uracil (■) and (○), respectively. **B.** Transport of 0.5 µM [³H]-uracil by Lmaj-5F2'dURes (●) and sFriedlin-WT (▲) over 10 minutes in the presence of 1 mM unlabelled uridine (■) and (○), respectively.

4.7. Discussion

As membrane transporters are involved in drug uptake, the study of this phenomenon thus requires the identification, detailed characterization and cloning of parasite-specific high-affinity transporters for substrates with a low concentration in the host tissues. The kinetoplastid transporters for purines and pyrimidines appear to meet this description. Because kinetoplastid parasites are unable to synthesise the purine ring *de novo*, purine metabolism and transport were studied extensively (Boitz *et al.,* 2012a; Boitz *et al.,* 2012b; Carter *et al.,* 2010; Carter *et al.,* 2008; De Koning *et al.,* 2005; Looker *et al.,* 1983; Ortiz *et al.,* 2007). On the other hand, the majority of protozoan parasites synthesise pyrimidines in pathways similar to their mammalian host (Berens *et al.,* 1995), and can also obtain pyrimidines by uptake from their environment (Aronow *et al.,* 1987; De Koning *et al.,* 2005; De Koning *et al.,* 2003; Gudin *et al.,* 2006; Papageorgiou *et al.,* 2005). Although this phenomenon appears to render pyrimidine metabolism less amenable to therapeutic intervention than purine salvage, the selective inhibition of pyrimidine biosynthetic enzymes and/or the blocking of pyrimidine transporters may offer new therapeutic avenues.

The bond lengths of fluorine and of hydrogen with carbon are very similar; the fluorine (1.35Å) - carbon bond has a length of 1.26-1.41Å, and the hydrogen (1.1Å) – carbon bond requires 1.08-1.1Å (Heidelberger *et al.,* 1957), so that substituting hydrogen with fluorine may lead to a very small change in the substrate size, and intruding on the steric limitations of the transporter's binding pocket. About half a century ago, Heidelberger designed the widely used anticancer drugs 5-FU and 5F-2'dUrd (Heidelberger *et al.,* 1958), these drugs were found to be metabolized in a similar way to their natural counterparts. This study has proved that in *Leishmania* promastigotes 5-FU shares a transporter with uracil, and the fluorinated ribo- and 2'-deoxy-nucleosides prefer nucleoside transporter(s). Fluorinated pyrimidines need transport and metabolic activation to their active forms before they can exert their cytotoxicity. Pyrimidine nucleosides and nucleobases do not show appreciable diffusion rates; therefore, they need carrier proteins to move into the cells. In order to identify which cytotoxic pyrimidine analogues would efficiently target the interior of *Leishmania* cells, we attempted to investigate the efficient transport of natural pyrimidines by promastigotes of *Leishmania*. We also

induced resistance clones to anti-leishmanial pyrimidine analogues to understand how the resistance to these analogues depends on salvage enzymes or transporters.

Several previous studies have been performed on purine transport in *Leishmania* parasites, the first purine nucleobase transporters identified in *Leishmania* species were LmajNBT1 in promastigotes of *L. major* (Al-Salabi *et al.,* 2003) and LmexNBT1 in amastigotes of *L. mexicana* (Al-Salabi & De Koning, 2005). However, the only pyrimidine specific transporter in *Leishmania* promastigotes was LmajU1 (Papageorgiou *et al.,* 2005). To date, no study has been performed to evaluate the uptake of pyrimidines by *L. mexicana* promastigotes. As a first effort to evaluate potential pyrimidine chemotherapy against *Leishmania* cells, it is necessary to be aware of which natural pyrimidines and cytotoxic analogues would efficiently cross the cell membrane and reach the parasite's interior. Therefore, we studied the uptake of natural pyrimidines, particularly uracil and uridine, by promastigotes of *Leishmania*. We found evidence that *L. mexicana* and *L. major* promastigotes are taking up natural nucleosides and nucleobases with various efficiencies, and we demonstrated that *Leishmania* cells transport pyrimidine nucleobases and nucleosides via distinct transporters, but these pyrimidine transporters have some overlapping inhibitor profiles, which may indicate a common transporter structure. For nucleobase uptake, LmajU1 has higher affinity for uracil and 5-FU than LmexU1; both transporters also displayed different K_i values for uridine (Figure 4.25A&B).

Nucleoside uptake was also diverse among *Leishmania* spp; LmexNT1 has the same affinity for uridine and thymidine, and was very sensitive to adenosine; *L. major* expressed both high and a low affinity uridine transporters. *L. major*'s high and low affinity transporters were sensitive to nucleosides but they differ in their affinity for uridine; additionally, whereas the high affinity uridine transporter was sensitive to nucleobases (uracil, adenine) and strongly inhibited by inosine, the low affinity uridine transporter was insensitive to these compounds.

In general, while the *L. mexicana* NT1 transporter has higher affinity for pyrimidine nucleosides and their fluorinated analogous than the corresponding *L. major* NT1 nucleoside transporter, the latter was much more sensitive to uracil

and 5-FU than the former (Figure 4.25A&B). As pyrimidine transporters have not yet been identified at the genetic level, it is not possible to attribute distinct characteristics of pyrimidine transporters to differences in sequence. It is unlikely that the nucleoside and nucleobase transporters are encoded by members of the same gene family, because the nucleoside transport activities are encoded by the Equilibrative Nucleoside Transporter (ENT) family, and all the kinetoplastid ENT family members have been cloned and characterised to different degrees; none were shown to be pyrimidine-specific transporters (De Koning, 2008). However, the different substrate and inhibitor profiles among the transporters could be a result of a shift in amino acid position, or (a) different amino acid(s) facing the active site of the substrates or translocation. The correlation of different substrate affinities to primary sequence will have to wait until the gene for each transporter is identified.

Fluorinated pyrimidines have been introduced as pyrimidine salvage inhibitors against *T. gondii* (Youn *et al.,* 1990) and *L. amazonensis* (Katakura *et al.,* 2004). As the toxicity of fluorinated pyrimidines depends on the concentration and duration of exposure, these factors were standardised to compare the effect of active drugs against kinetoplastid cells. Fluorinated pyrimidines were not systematically proposed as clinical anti-leishmanials; however, this study is the first effort to evaluate the toxicity of pyrimidine anti-metabolites on *Leishmania* parasites. In terms of the sensitivity to pyrimidine analogues, it seems that promastigotes of *Leishmania* are similar to bloodstream form trypanosomes. For example, 5-FU, 5F-2'dUrd and 5F-2'dCyd were much more active against these strains than any of the other halogenated pyrimidines tested. In contrast, 5-fluoroorotic acid, which its EC_{50} at micromolar level on trypanosomes, showed no activity at all against *Leishmania* species. These findings agree with French *et al.,* 2011 who found that pyrimidine auxotrophic *of L. donovani* are unable to grow in 100 µM orotate as sole pyrimidine source. Notwithstanding the observation that most fluorinated pyrimidines have identical cytotoxicity against multiple *Leishmania* species, the effect of 5-fluorouridine was an exception. The drug was active against *L. major* promastigotes, and killed them at concentrations below 20 µM; however, *L. mexicana* cells were very insensitive to 5F-Urd. It is reported above (chapter 3) that bloodstream form trypanosomes are also naturally resistant to 5F-Urd.

Leishmania cells become resistant to high concentrations of fluorinated deoxynucleosides faster than to fluorinated nucleobases. In addition, all cells that are resistant to 5F-2'dUrd became also highly resistant to 5-fluoro-2'deoxycytidine; this observation is very similar to the case of trypanosomes and shows that these deoxynucleoside pyrimidine analogues have the same mode of action, with 5F-2'dCtd converted to 5F-2'dUrd by cytidine deaminase. Lmex-5FURes were unable to take up uracil, but the rate of uridine uptake was identical to *L. mexicana* M379-WT cells. As *L. mexicana* promastigotes metabolize 5-FU and 5F-2'dUrd through almost the same pathway and end up with the same fluorinated pyrimidine metabolites (chapter 6) we could not attribute the mechanism of resistance in Lmex-5FURes to changes in pyrimidine metabolism. This clearly shows that Lmex-5FURes cells have lost their uracil transport activity completely, and that this is the cause of their resistance, while retaining wild-type sensitivity to fluorinated pyrimidine nucleosides, which are taken up by a different transporter.

Although Lmex-5FURes cells were not cross-resistant to deoxynucleoside analogues, Lmex-5F2'dURes cells were very cross-resistant to 5-FU; but the uracil rate of uptake by Lmex-5F2'dURes was equal to promastigotes of *L. mexicana* M379-WT. Here we can assume that the high level of resistance (190-fold) of Lmex-5F2'dURes to 5-FU is not due to the lack of uracil transport activity, but rather to changes in 5-FU metabolism, which might be mutations in thymidylate synthase and/or thymidine kinase. It must be noted that we assessed uracil not 5-FU uptake by Lmex-5F2'dURes, so changes in affinity of LmexU1 specifically to 5-FU could reduce uptake rates for 5-FU but not for uracil. However, we present no evidence for this possibility and since the adaptation was to 5F-2'dUrd rather than to 5-FU we believe it is much more likely that the resistance mechanism to 5-FU by Lmex-5F2'dURes cells is related to adaption in pyrimidine-metabolising enzymes rather than to changes in transport activity, particularly the part of the pyrimidine metabolomic pathway shared by 5-FU and 5F-2'dUrd, i.e. thymidine kinase and thymidylate synthase.

The Alamar blue experiments showed that 5-FU and 5F-2'dUrd have almost the same activity against *L. major* promastigotes as against *L. mexicana*. However, the *L. major* strains adapted to these compounds resistant barely showed cross-resistance between fluorinated nucleobases and nucleosides. Lmaj-5FURes cells

were 17-fold resistant to 5-FU compared with the wild-type control, but the rate of uracil uptake by Lmaj-5FURes cells was almost completely flat for 10 minutes, clearly showing that Lmaj-5FURes cells have lost uracil activity (LmajU1), just like LmexU1 was lost through adaptation to 5-FU. Yet, a small but significant uptake rate of uracil could still be detected in these cells, and was attributed to LmajNT1; this explains the relatively low level of 5-FU resistance in Lmaj-5FURes, and the lack of strong cross-resistance with the fluoro-nucleosides.

Lmaj-5F2'dURes cells are resistant to all fluorinated pyrimidine nucleosides, but are not at all resistant to 5-FU. Uptake of low concentrations of uridine and uracil was equally reduced, by just over 80%, compatible with loss of both the LmajU1 and one of the uridine transport activities (LmajNT1 or LmajNT2), yet the remaining capacity of 5-FU uptake was clearly sufficient for its anti-leishmanial activity, indicating uptake through a lower-affinity, high capacity transporter that is therefore more active at the ~10 μM concentration of the 5-FU EC$_{50}$. We suggest that these cells may have lost LmajNT2, which is the uracil-insensitive nucleoside transporter, but more experiments would clearly be required for a definitive answer to this puzzle. Nor can we currently do more than speculate as to the selective mechanism of resistance to the fluoro-nucleosides by Lmaj-5F2'dURes, as a significant nucleoside transport capacity is retained and the mechanism of action is shared with 5-FU. The only explanation for the resistance pattern that presents itself to us is that LmajNT2 has very low tolerance for the 5-fluoro substitution, compared to LmajNT1. Experiments to verify this hypothesis are being scheduled.

Notwithstanding that sensitivity and cross-resistance to fluorinated pyrimidines was similar among kinetoplastid cells, the mechanism of resistance to these analogues is totally different within trypanosomes and *Leishmania* cells. Bloodstream form trypanosomes adapted to high concentrations of pyrimidine analogues through changes in the level of some pyrimidine pathway enzymes, as well as a limited reduction in the uptake of 5-FU, which was observed only in Tbb-5FURes cells. In contrast, all resistant *Leishmania* promastigotes responded to increased concentrations of pyrimidine analogues by a significant or complete reduction in the transport capacity for natural pyrimidines. The apparent ease by which *Leishmania* promastigotes 'loose' a pyrimidine transport activity is

possibly related to the fact that they have several, whereas bloodstream trypanosomes express only TbU3 (Ali *et al.*, 2013a; and this thesis).

Although *Leishmania* promastigotes showed different mechanisms of resistance to fluorinated pyrimidine analogues, through loss of different transporters, mostly, there were many close similarities between the cellular effects of fluorinated pyrimidine analogues (5-FU, 5F-2'dUrd and 5F-Urd), indicating a common mode of action on *L. mexicana* and *L. major*. The specific difference was the effect of 5F-Urd, particularly in that *L. mexicana* was extremely resistant to the compound, whereas the other species was very sensitive. This cannot be attributed to differences in uridine transport between the species, which, if anything, seems to be higher affinity and more efficient in *L. mexicana* (Tables 4.1 and 4.2). Nor can it be argued that LmexNT1 does not transport substrates with the 5-fluoro substitution, as 5F-2'dUrd displayed the exact same affinity as 2'dUrd for this carrier (Table 4.1), and 5F-2'dUrd was highly active against *L. mexicana* promastigotes (Table 4.4). This phenomenon will be interpreted in Chapter six.

Figure 4.25. The model of pyrimidine uptake in **A.** *L. mexicana* and **B.** *L. major.*
Entries in bold typescript indicate K_m or $K_i \leq 10$ μM, rather K_m or $K_i \geq 10$ μM.
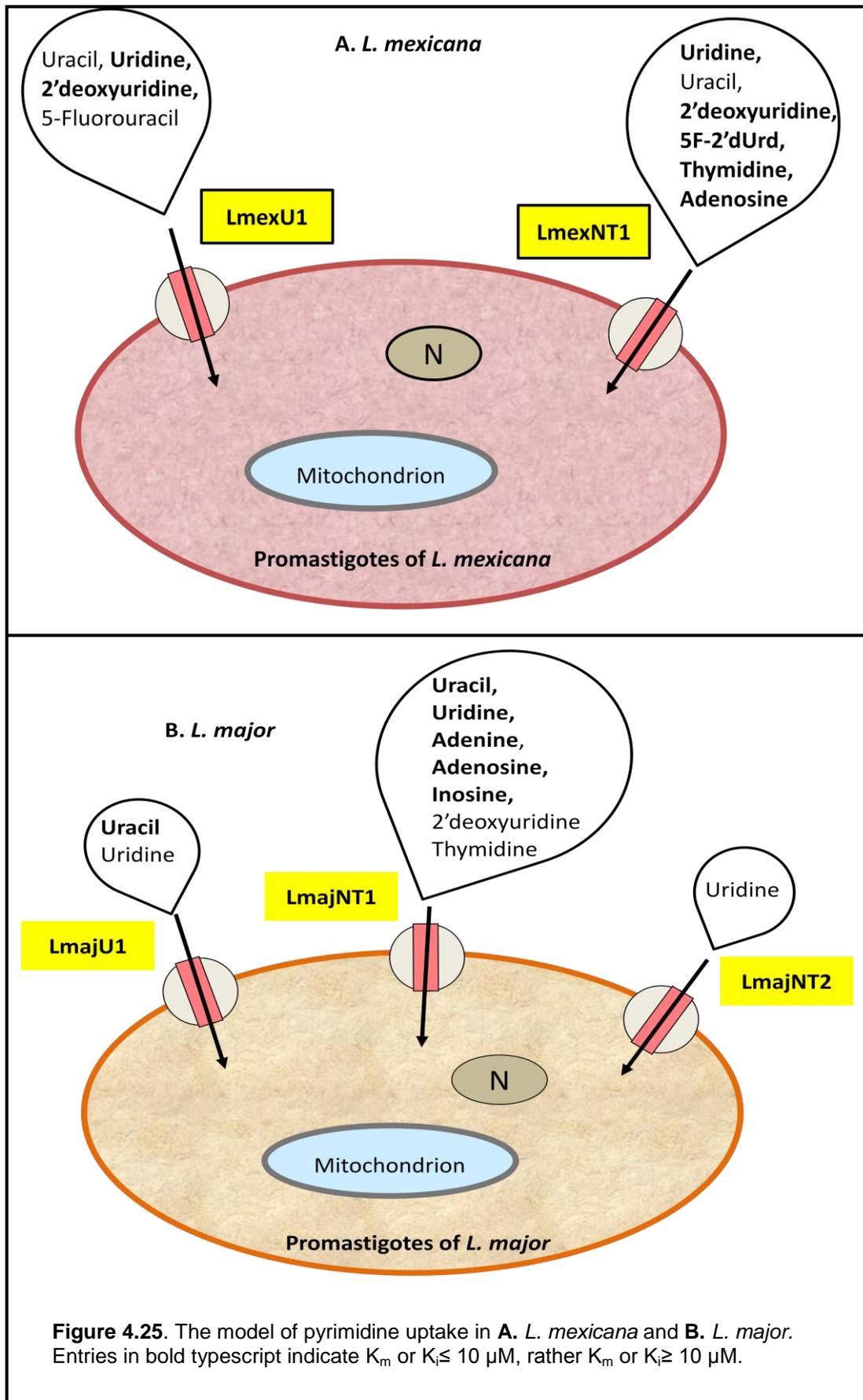
CHAPTER FIVE
Metabolomic investigations of the mechanisms of action and resistance of fluorinated pyrimidines on trypanosomes

5.1. Introduction

African trypanosomes are a complex of single-celled protozoan parasites, as these blood-borne parasites must continually divide to stay ahead of the host immune system, nucleotide metabolism is one obvious drug target, particularly as all protozoan parasites are unable to synthesize the purine ring *de novo* and thus necessarily rely on salvage from the host environment (De Koning *et al.,* 2005). However, no purine-based chemotherapy has emerged for kinetoplastid parasites, in large part because there is so much redundancy in purine transporters and salvage pathways that the inhibition of any one transporter (De Koning *et al.,* 2005) or enzyme (Berg *et al.,* 2010; Luscher *et al.,* 2007) has little or no effect on parasite survival.

The organization of pyrimidine nucleotide metabolism is rather more diverse in protozoan parasites. *Plasmodium* species, for example, are unable to use preformed pyrimidines from the host environment, and rely on biosynthesis alone (De Koning *et al.,* 2005; Van Dyke *et al.,* 1970). Kinetoplastid parasites, including major pathogens such as the *Leishmania* and *Trypanosoma* species, are known to possess both salvage and biosynthesis routes for pyrimidines (De Koning *et al.,* 2005; Hammond & Gutteridge, 1982; Hassan & Coombs, 1986; Papageorgiou *et al.,* 2005) and it has recently become clear that some enzymes of the pyrimidine inter-conversion pathways may be good drug targets in *T. brucei*. One validated target in the pyrimidine pathways is deoxyuridine 5'-triphosphate nucleotidohydrolase (dUTPase), as RNAi knockdown of this enzyme reduces growth rates and causes DNA breaks by allowing a toxic build-up of dUTP in *T. b. brucei* cells (Castillo-Acosta *et al.,* 2008, 2013). Similarly, knockout of dihydrofolate reductase - thymidylate synthase (DHFR-TS) is lethal in *T. b. brucei* unless rescued by very high levels of thymidine *in vitro* (Sienkiewicz *et al.,* 2008). (Arakaki *et al.,* 2008) showed that under conditions of limited pyrimidine salvage RNAi knockdown of dihydroorotate dehydrogenase (DHODH), one of the enzymes in the pyrimidine biosynthesis pathway, caused severe growth defects for bloodstream trypanosomes.

It thus appears, from a combination of genetic and pharmacological evidence, that pyrimidine metabolism in African trypanosomes is replete with drug targets and that a systematic evaluation of pyrimidine salvage mechanisms

is long overdue. The incomplete study about individual pyrimidine metabolites within trypanosome cells, and the poor information about changes that occur in response to pyrimidine analogues in *T. b. brucei* BSF delay efforts to develop a pyrimidine-based chemotherapy, either consisting of inhibitors of the key enzymes of pyrimidine metabolism, or of subversive substrates that would be activated to cytotoxic nucleotides and possibly be incorporated into nucleic acids.

Here, a metabolomic approach was used to assess: (1) whether nucleotide levels or pathways were changed during the process of adaptation to fluoro-pyrimidines; (2) what metabolites are formed from the fluoro-pyrimidine analogues in *T. b. brucei* s427-WT and resistant cells; (3) the mechanisms of action and resistance to these compounds (4) whether these analogues are incorporated into nucleic acids. These metabolomic techniques allowed us to identify the mode of action and metabolites of several trypanocidal pyrimidines. We thus present a first evaluation of pyrimidines as subversive chemotherapeutic agents against these parasites and a much improved model of pyrimidine salvage and metabolism in African trypanosomes (Figure 5.1).
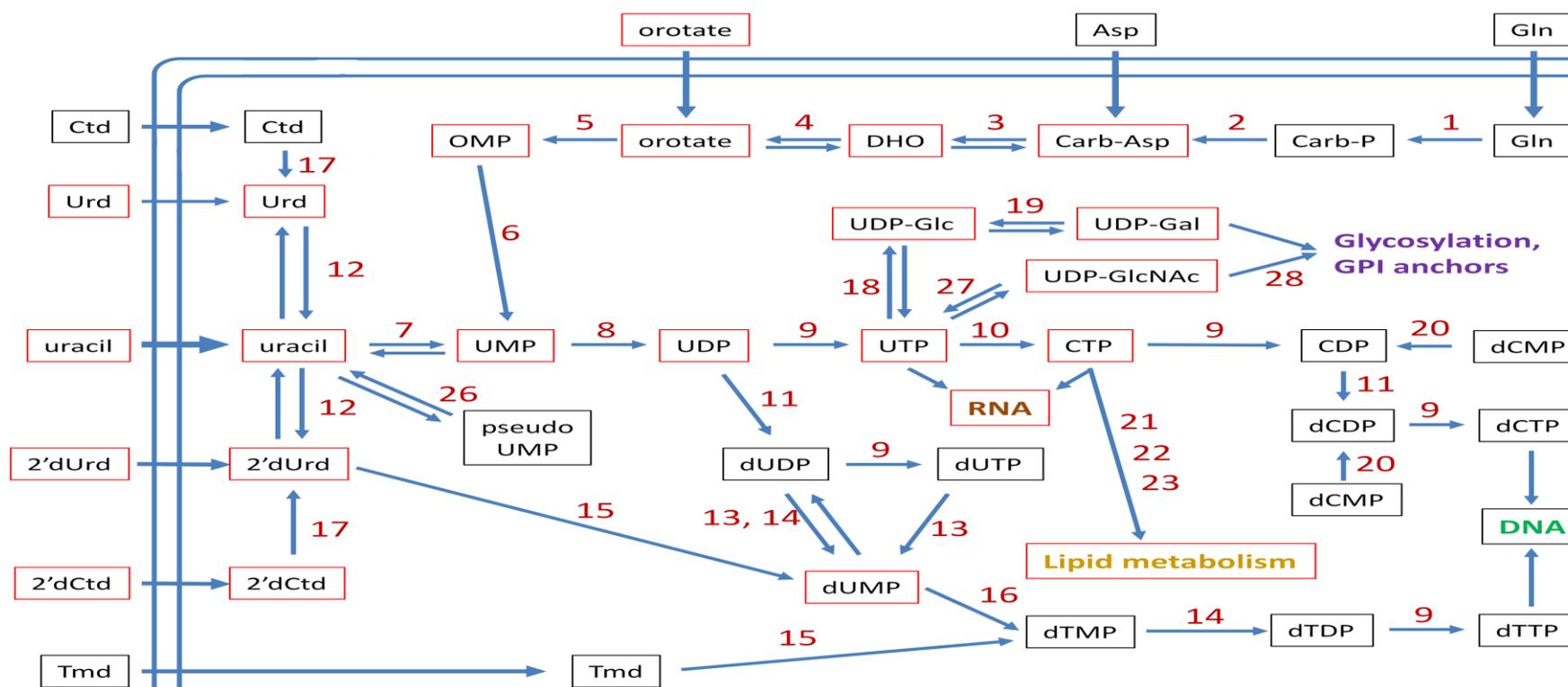
Figure 5.1. Scheme of pyrimidine biosynthesis and metabolism in *T. b. brucei*. The double curved line represents the plasma membrane and arrows across its (potential) transport activities. Red boxes indicate metabolites, of which fluorinated analogues were detected by metabolomic techniques; black boxes indicate metabolites not detected in fluorinated form. Numbers above arrows indicate the following enzymes, listed here with EC numbers. **1**, carbamoyl phosphate synthase (6.3.5.5); **2**, aspartate carbamoyl transferase (2.1.3.2); **3**, dihydroorotase (3.5.2.3); **4**, dihydroorotate dehydrogenase (1.3.3.1); **5**, orotate phosphoribosyltransferase (2.4.2.10); **6**, orotidine 5-phosphate decarboxylase (4.1.1.23); **7**, uracil phosphoribosyltransferase (2.4.2.9); **8**, nucleoside diphosphatase (3.6.1.6). **9**, nucleoside diphosphate kinase (2.7.4.6). **10**, cytidine triphosphate synthase (6.3.4.2); **11**, ribonucleoside-diphosphate reductase (1.17.4.1); **12**, uridine phosphorylase (2.4.2.3); **13**, dUTPase (3.6.1.23); **14**, thymidylate kinase (2.7.4.9); **15**, thymidine kinase (2.7.1.21); **16**, thymidylate synthase (2.1.1.45); **17**, cytidine deaminase (3.5.4.5); **18**, UDP-glucose pyrophosphorylase (2.7.7.9); **19**, UDP-glucose epimerase (5.1.3.2); **20**, adenylate kinase (2.7.4.10); **21**, phosphatidate cytidylyltransferase (2.7.7.41); **22**, ethanolamine-phosphate cytidylyltransferase (2.7.7.14); **23**, choline-phosphate cytidylyltransferase (2.7.7.15); **24**, orotate reductase (1.3.1.14, not present); **25**, dihydroorotate dehydrogenase (1.3.5.2, not present); **26**, pseudouridylate synthase (4.2.1.70); **27**, UTP:N-acetyl-a-D-glucosamine-1-phosphate uridylyltransferase (2.7.7.23); **28**, a-1,6-N-acetylglucosaminyltransferase. Abbreviations: Gln, glutamine; Carb-P carbamoyl phosphate; Asp, aspartate; Carb-Asp, N-carbamoyl-L-aspartate; DHO, dihydroorotate; OMP, orotidine-5-phosphate; Urd, uridine; Tmd, thymidine; 2'dCtd, 2'-deoxycytidine; Glc, glucose; Gal, galactose; GlcNAc, N-acetylglucosamine. Lipid metabolism refers to formation of CDP-diacylglycerol (EC 2.7.7.41), CDP-ethanolamine (EC 2.7.7.14) and CDP-choline (EC 2.7.7.15).

5.2 Metabolomic analysis of fluorinated pyrimidine nucleobases in *T. b. brucei* BSF

5.2.1 5-Fluorouracil

T. b. brucei s427-wild type cells treated with 5-FU metabolized the drug to 5F-UMP, 5F-UDP and 5F-UTP, whereas no 5-fluorouridine or 5-fluoro-2'deoxyuridine were detected. These observations strongly suggest that 5-FU is not a substrate for *T. b. brucei* uridine phosphorylase, but is a substrate for *T. b. brucei* uracil phosphoribosyltransferase (Tbb-UPRT), as well as for nucleoside diphosphatase and nucleoside diphosphate kinase. No fluorinated deoxyuridine nucleotides were detected, making it unlikely that fluorinated pyrimidine nucleotides are a substrate for ribonucleotide reductase. However, a different group was able to detect 5F-dUTP after incubation of *T. b. brucei* with 5-FU (T. Smith, St. Andrews, UK; personal communication) and this may explain our observation that intracellular levels of dUMP were significantly increased in WT and Tbb-5FURes cells treated with 5-FU, compared to their respective untreated control cells. In WT the increase of dUMP was 10.5-fold ($P<0.0001$) and in Tbb-5FURes it was 7.2-fold ($P<0.001$; Figure 5.2).
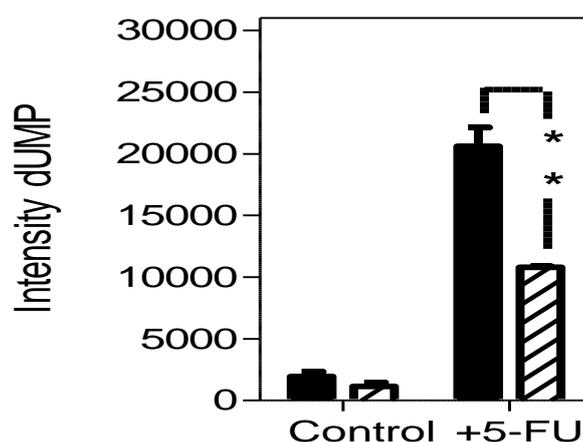
Figure 5.2 Relative levels of dUMP in *T. b. brucei* s427-wild-type (solid bars) and Tbb5-FURes (hatched bars) cells exposed to 100 µM 5-FU for 8 hours. **, $P<0.02$; by unpaired two-tailed Student's T-test comparing intensity of a particular metabolite in WT and resistant lines; n=3.

Interestingly, significant amounts of 5F-UDP-glucose were detected, showing that 5F-UTP is a substrate for UDP-glucose pyrophosphorylase, which couples UTP to glucose-1P. It must be noted that the detection method, based on mass-spectrometry, cannot distinguish between UDP-glucose and UDP-galactose so it is unclear whether 5F-UDP glucose might be a substrate for UDP-Glc 4'-epimerase. Similarly, highly significant amounts of 5F-UDP-N-acetyl-glucosamine were detected which may include the equivalent galactose residues. This indicates that 5F-UTP is a substrate of UTP-N-acetyl-α-D-glucosamine-1-phosphate uridylyltransferase which forms UDP-GlcNAc from UTP and N-acetyl-α-D-glucosamine 1-phosphate (Figure 5.1). UDP-GlcNAc in turn is a substrate of N-acetyl-glucosaminyltransferase, transferring the GlcNAc to protein and glycans. It is thus possible that 5-FU interferes with glycosylation through the production of 5F-UDP hexoses and or hexosamines.

In Tbb-5FURes cells treated with 5-FU the relative amounts of 5-FU, and fluorouridine nucleotides, in the cell were all somewhat lower than in WT cells exposed to the same concentration of 5-FU (Figure 5.3A), consistent with reduced efficiency of 5-FU uptake contributing to some extent to resistance, but dUMP levels were still significant elevated. The largest difference, however, was 6.3-fold and 3.8-fold reduction of 5F-UDP-glucose and of 5F-UDP-GlcNAc in Tbb-5FURes cells relative to WT cells treated with 5-FU ($P<0.05$ and $P<0.01$), respectively (Figure 5.3B), suggesting that sugar nucleotide metabolism contributes significantly to 5-FU mode of action in *T. brucei*, and that changes in this pathway could make major contributions to 5-FU resistance.
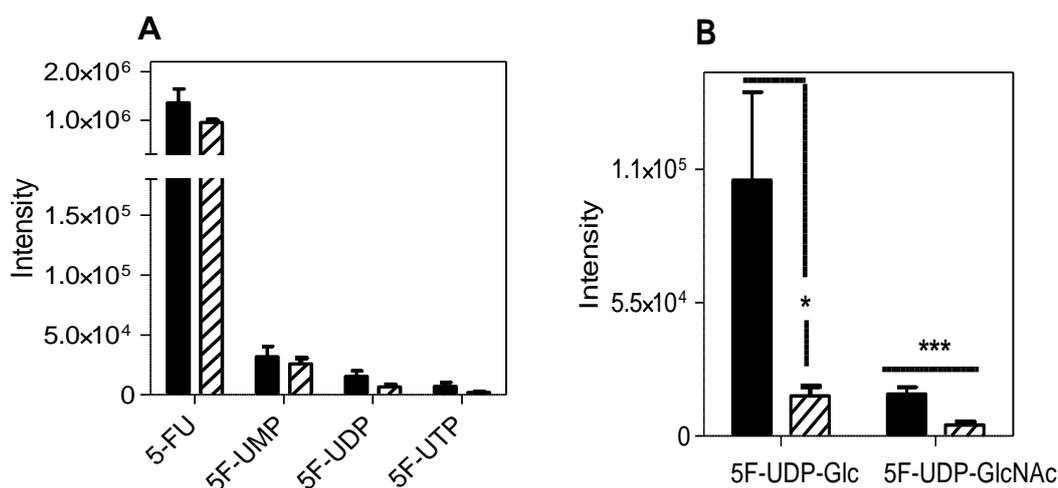
Figure 5.3. Relative levels of **A.** 5-FU and fluorinated nucleotides **B.** fluorinated nucleotide sugars, in *T. b. brucei* WT (solid bars) and Tbb5-FURes (hatched bars) cells exposed to 5-FU. The intensity of the mass spectrometer signal is plotted here for the metabolites observed. *, $P<0.05$; ***, $P<0.01$ by unpaired two-tailed Student's T-test comparing intensity of a particular metabolite in WT and resistant lines.

5.2.2 5-Fluoroorotic acid

Very similar levels of 5-FOA (Figure 5.4) were detected after exposure of s427-WT and Tbb-5FOARes cells to 100 µM of the drug for 8 hours, indicating that uptake was not the main mechanism of resistance, consistent with the non-saturable orotic acid uptake noted in section 3.9 and in Figure 3.22. In both cell types, but particularly in WT, intracellular 5-FU was detected after incubation with 5-FOA (Figure 5.4), this was not a contamination of the chemical as it was not present in fresh medium samples containing drug, and indicates that UPRT can operate to hydrolyse 5F-UMP to 5-FU.
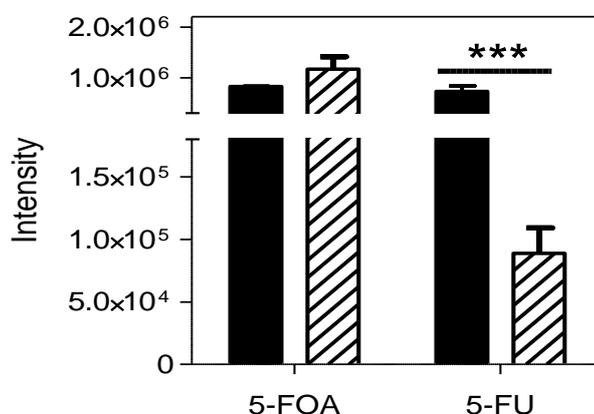
Figure 5.4. Relative levels of 5-FOA, and 5-FU in *T. b. brucei* WT (solid bars) and Tbb-5FOARes (hatched bars) cells exposed to 100 µM of 5-FOA. The intensity of the mass spectrometer signal was plotted here for the metabolites observed. ***, $P<0.01$ by unpaired two-tailed Student's T-test comparing intensity of a particular metabolite in s427-WT and Tbb-5FOARes cells.

Interestingly, orotate levels were also 3.5-fold higher in untreated Tbb-5FOARes cells versus untreated WT cells ($P<0.0001$), indicating an adaptation by either significantly increasing orotate biosynthesis, or a reduction in OPRT activity, or both. The same adaptation of increased baseline orotate concentration was also observed in the 5-FU resistant cells, making it more likely that the orotate increase is the result from increased biosynthesis, as this would 'dilute' the 5F-UMP derived from 5-FU with newly synthesized UMP. 5-FOA was clearly a substrate as well as an inhibitor of OPRT and was converted to fluorinated uridine nucleotides (Figure 5.5A) and 5F-UDP-glucose and 5F-UDP-GlcNAc (Figure 5.5B), reaching levels in WT cells well in excess of those after treatment with 5-FU, consistent with the stronger trypanocidal activity of 5-FOA compared to 5-FU. In Tbb-5FOARes cells, the level of all fluorinated nucleotides was very much reduced with a 50-fold decrease in 5F-UMP, while 5F-UDP and 5F-UTP were below detection limits, resulting in >200-fold reduction in 5F-UDP-glucose.

Another surprise was the detection of fluoro-N-carbamoyl-L-aspartate in both cell types (Fig 5.5B), indicating a partial reversal of the pyrimidine biosynthesis pathway. This may be caused by a build-up of 5-FOA, which seems to inhibit orotate phosphoribosyltransferase (OPRT), leading to an increase in free orotate levels in both s427-WT (3.6-fold; $P<0.01$) and Tbb-5FOARes cells (1.6-fold; $P<0.05$).
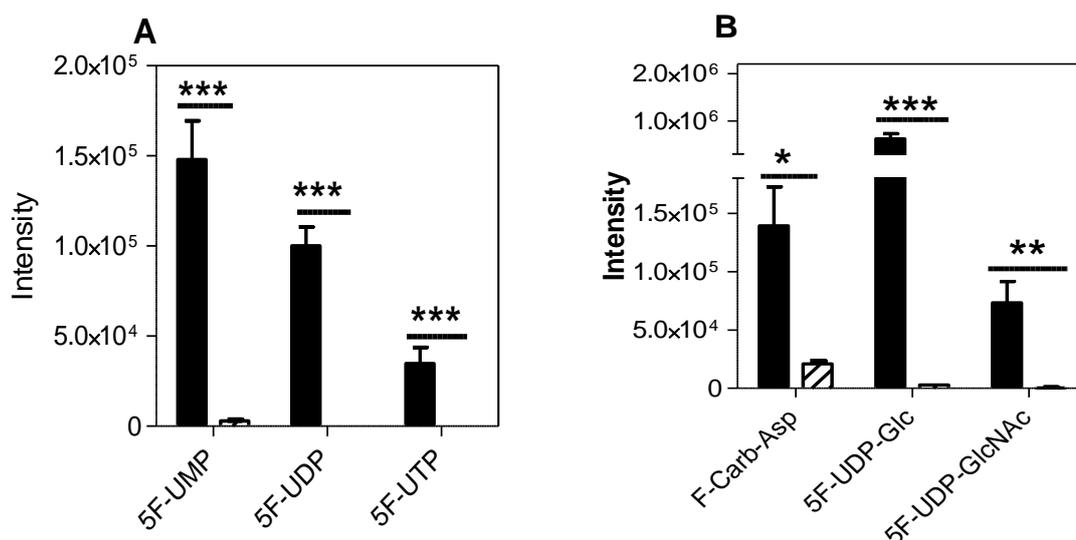
Figure 5.5. Relative levels of **A.** 5-fluoro-nucleotides **B.** F-carb-Asp, 5F-UDP-glu and 5F-UDP-GlcNAc in *T. b. brucei* WT (solid bars) and Tbb-5FOARes (hatched bars) cells exposed to 100 μM of 5-FOA. The intensity of the mass spectrometer signal was plotted here for the metabolites observed. *, $P<0.05$; **, $P<0.02$; ***, $P<0.01$ by unpaired two-tailed Student's T-test comparing intensity of a particular metabolite in s427-WT and Tbb-5FOARes cells.

As with 5-FU-treated cells there was a small but significant (2.5-fold; *P*<0.01) increase in dUMP in 5-FOA-treated WT trypanosomes compared to untreated cells; this effect was not observed in Tbb-5FOARes cells. No fluorinated cytidine or deoxyuridine nucleotides were observed in 5-FOA-treated cells, nor was there any effect of this compound on the levels of thymidine nucleotides. It thus can be concluded that the main adaptation in Tbb-5FOARes cells is by preventing its incorporation into the nucleotide pool, presumably through a change in OPRT, as orotidine-5-phosphate was not detected whereas orotate levels were significantly increased.

5.3 Metabolomic analysis of fluorinated pyrimidine nucleosides in *T. b. brucei*

5.3.1 5-Fluro-2'deoxyuridine

Intracellular levels of 5F-2'dUrd were not different between s427-WT and Tbb-5F2'dURes cells (Figure 5.6), confirming that the resistance mechanism is based on metabolism rather than reduced uptake of the drug.
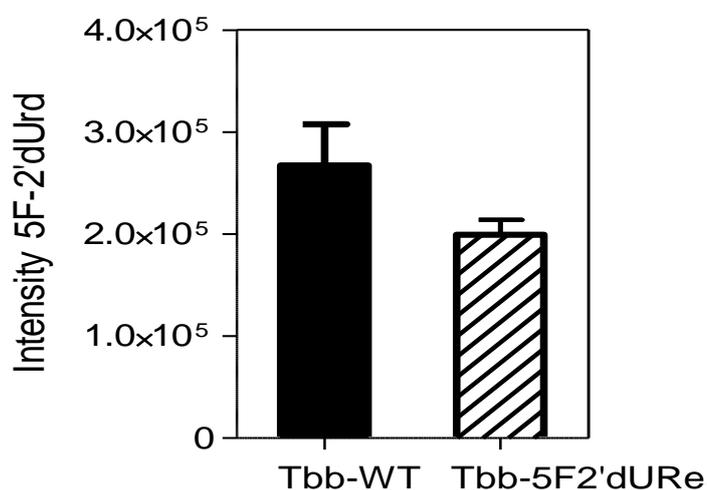
Figure 5.6. Relative levels of 5F-2'dUrd in *T. b. brucei* s427-WT (solid bars) and Tbb-5F-2'dURes (hatched bars) cells exposed to 100 µM of 5F-2'dUrd.

No fluorinated pyrimidine analogues, including ribonucleosides, were detected in WT trypanosomes treated with 5F-2'dUrd, apart from the drug itself (the apparent signal for 5-FU deriving from an in-source fragment of 5F-2'dUrd, as confirmed in the spiked medium). This confirms that 5F-2'dUrd is not a substrate for *T. brucei* uridine phosphorylase, as this would have generated 5-FU and fluorinated ribonucleotides. Interestingly, the automated data analysis did not detect any 5F-dUMP, nor the corresponding di- and tri-phosphonucleotides. However, manual inspection of the raw data revealed low levels of 5F-dUMP in treated cells, confirming that 5F-2'dUrd is a substrate for thymidine kinase. The main difference observed between untreated WT cells and those treated with 5F-2'dUrd was a 36.5-fold increase in dUMP ($P<10^{-5}$; Figure 5.7), highly suggestive of a block in thymidylate synthase (enzyme 16 in Figure 5.1) mediated either by 5F-2'dUrd itself, or by the low levels of 5F-dUMP. Significantly, only a 2.5-fold increase in dUMP was observed in the treated Tbb-5F2'dURes cells relative to untreated wild-type cells (Figure 5.7), clearly showing a link between the dUMP increase and the mechanism of action for this drug. Indeed, dUMP levels were virtually undetectable in untreated Tbb-5F2'dURes cells, indicating a down-regulation of 2'-deoxyuridine nucleotide synthesis as part of the adaptation to 5F-2'dUrd. However, it must be noted that dUMP levels were only two-fold above detection level in untreated WT cells, and it is therefore not possible to estimate the extent of the down regulation.
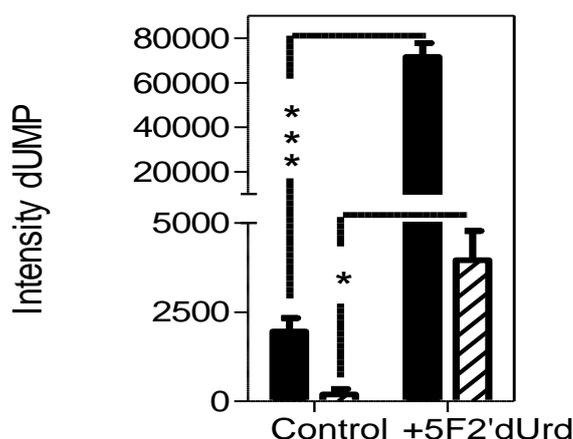
Figure 5.7. Relative levels of dUMP in *T. b. brucei* s427-WT (solid bars) and Tbb-5F-2'dURes (hatched bars) exposed to 100 µM of 5F-2'dUrd for 8 hours. The intensity of the mass spectrometer signal was plotted here for the metabolites observed. *, <0.05; *P****, *P*<0.01 by unpaired two-tailed Student's T-test comparing intensity of a particular metabolite in s427-WT and resistant lines.

However, thymidine nucleotide levels were not significantly different in WT and Tbb-5F2'dURes cells, or after treatment with 5F-2'dUrd (Figure 5.8), presumably through salvage of thymidine, which is present at high concentrations (20 mg/L, i.e. ~83 µM) in standard HMI-9 medium. This confirms (1) that the mode of action is through inhibition of thymidylate synthase rather than thymidylate kinase and (2) that under these conditions the cells succumb to high levels of deoxyuridine nucleotides rather than from lack of thymidine nucleotides.
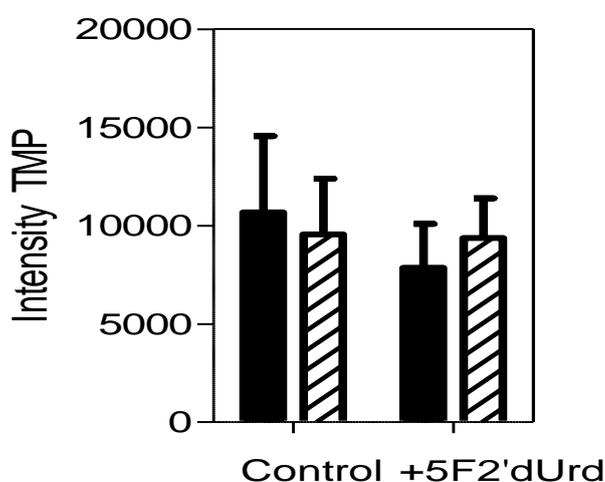
Figure 5.8. Relative levels of TMP in *T. b. brucei* WT (solid bars) and Tbb-5F2'dURes (hatched bars) cells exposed to 100 µM of 5F-2'dUrd. The abundance of TMP, TDP and TTP (not shown) was statistically identical in control and Tbb5FdURes cells, whether 5F-2'dUrd-treated or not.

The emerging model of inhibition of thymidylate synthase predicts that medium thymidine concentrations could greatly impact on the trypanocidal activity of 5F-2'dUrd. Indeed, the presence or absence of thymidine in the extracellular media had a profound effect on sensitivity to 5F-2'dUrd, 5F-2'dCtd and even 5Cl-2'-dUrd, but not to 5-FU, 5-FOA or diminazene aceturate (Table 5.1).

Table 5.1 Average EC$_{50}$ values for fluorinated pyrimidines against *T. b. brucei* BSF of s427-WT and Tbb-5F2'dURes cells in the presence and absence of 100 μM thymidine. Cultures were grown in a minimal version of HMI-9 without pyrimidines using dialyzed fetal bovine serum, to which either 100 μM thymidine or nothing was added. Normal HMI-9 medium and the anti-trypanocidal diminazene were used as controls. The results shown were the average of three independent experiments; error bars were Standard Error of Mean (SEM).

Drug/medium	*T. b. brucei* BSF s427-WT			Tbb-5F2'dURes		
	HMI-9	HMI-9^{+Tmd}	HMI-9^{-Tmd}	HMI-9	HMI-9^{+Tmd}	HMI-9^{-Tmd}
5-FU	35.9 ± 1.5	91.1 ± 8.5	124 ± 8.1	76.1 ± 2.2	15.2 ± 2.0	24.7 ± 2.1
5-FOA	14.1 ± 0.9	33.5 ± 1.3	9.8 ± 0.8	13.3 ± 0.1	7 ± 0.9	7.1 ± 0.2
5F-2'dUrd	5.2 ± 0.16	18.6 ± 3.0	0.77 ± 0.3	4295 ±267	2559 ±280	4.1 ± 0.7
5F-2'dCyd	49.4 ± 3.0	350 ± 27.7	4.5 ± 0.7	>5000	>5000	2.7 ± 0.2
5Cl-2'dUrd	54 ± 1.7	35 ± 3.0	5.4 ± 1.0	22 ± 1.0	20.5 ± 0.5	0.65 ±0.05
diminazene	0.12 ± 0.05	0.13 ± 0.04	0.14 ±0.06	0.12 ±0.07	0.11 ±0.03	0.12 ±0.05

WT trypanosomes in a thymidine-free version of HMI-9 with dialyzed serum were highly sensitive to 5F-2'dUrd (EC$_{50}$ 0.77 ± 0.3 μM); the addition of 100 μM thymidine reduced the sensitivity 24-fold (EC$_{50}$ 18.6 ± 3.0 μM; Figure 5.9A). The same phenomenon was observed even more prominently using Tbb-5F2'dURes cells (>600-fold), and when using 5F-2'dCtd on either cell type (78-fold in WT; Tbb-5F2'dURes cells were insensitive up to 5 mM 5F-2'dCtd; Figure 5.9B), confirming that the two deoxynucleoside analogues have the same mechanism of action, through conversion of 5F-2'dCtd to 5F-2'dUrd.
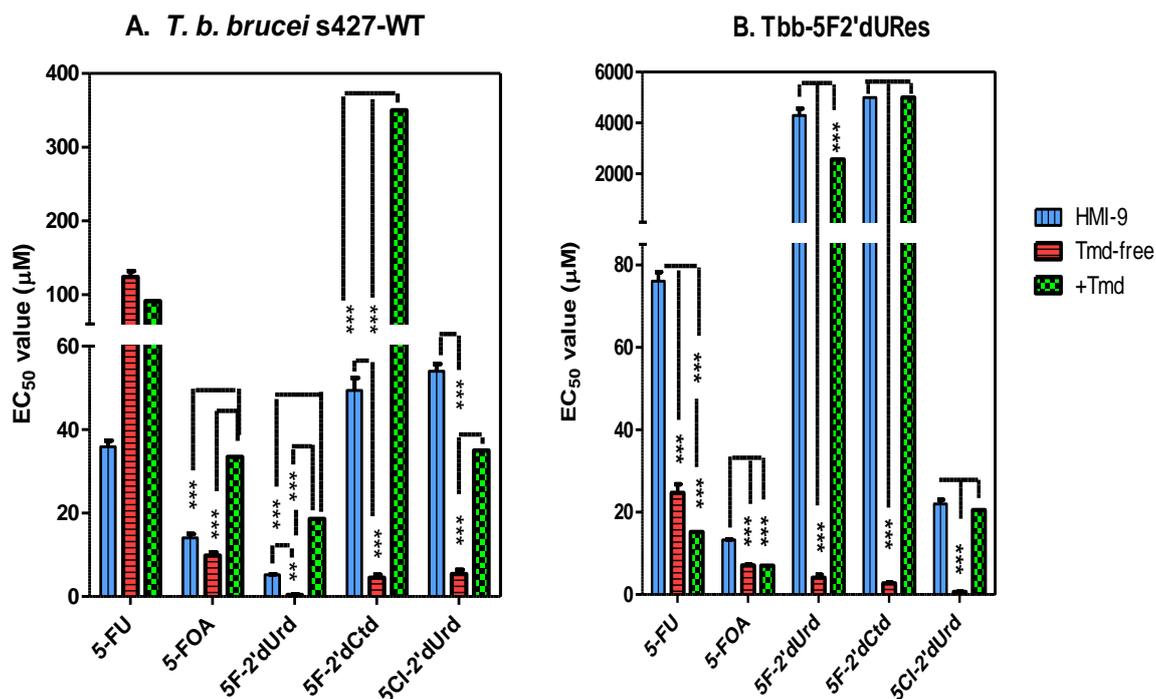
Figure 5.9. Effect of fluorinated pyrimidines on **A.** *T. b. brucei* BSF of WT-s427 and **B.** Tbb5F2'dURes cells in the presence and absence of 100 µM thymidine. Cultures were grown in a minimal version of HMI-9 without pyrimidines using dialyzed fetal bovine serum, to which either 100 µM thymidine or nothing was added. Normal HMI-9 medium on one side and the anti-trypanocidal diminazene on the other side of comparison were used as controls. The results shown were the average of three independent experiments; error bars were SEM. *, P<0.05; **, P<0.02; ***, P<0.01 by unpaired two-tailed Student's T-test**.**

The observation that increased thymidine salvage rescues the effect of 5F-2'dUrd prompted us to next compare thymidine uptake in s427-WT and Tbb-5F2'dURes cells. The study found that uptake of 10 µM [^{3}H]-thymidine over half an hour in Tbb-5F2'dURes was mediated by a medium-high affinity transporter, with significantly different rate of uptake between Tbb-5F2'dURes and s427-WT (*P*= 0.003; Figure 5.10A). We also were able to characterize this activity and found that the K_m = 22 ± 3 µM and the V_{max} = 0.013 ± 0.002 pmol·10^7 cells^{-1}·s^{-1} - a >50-fold increase in thymidine affinity of Tbb-5F2'dURes, and a 6-fold increase in transport efficiency (V_{max}/K_m; Figure 5.10B). It is clear that this adaptation contributes to the 5F-2'dUrd resistance level; as the TbT1-encoding gene has yet to be identified the adaptation could be either the expression of an alternative thymidine transporter, or a mutant form of TbT1.
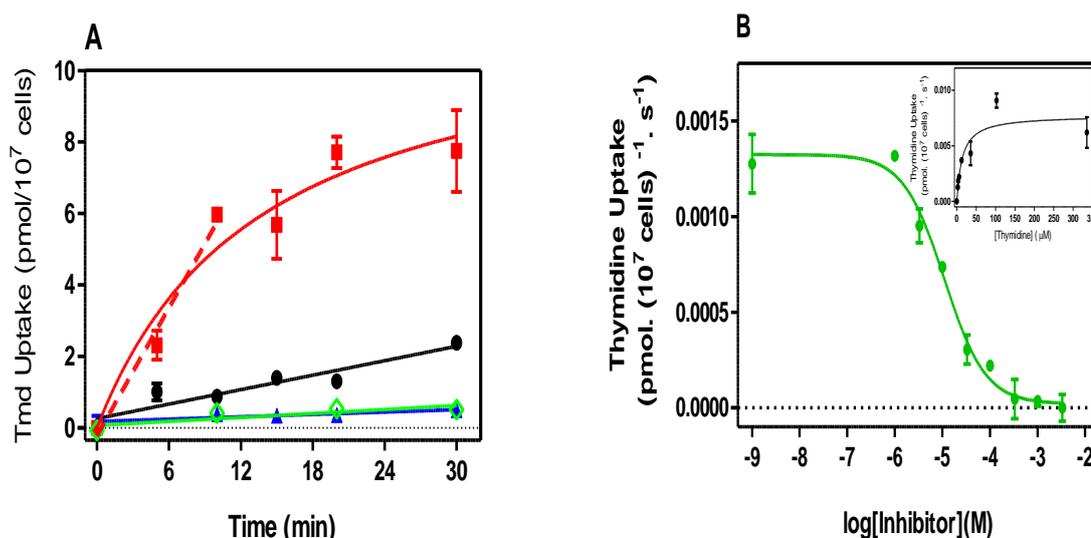
Figure 5.10. Characterization of [3H]-thymidine transport in Tbb-5F2'dURes. **A.** Timecourse of [3H]-thymidine transport in *T. b. brucei* bloodstream forms over 30 minutes. The figure showed transport of 10 µM [3H]-thymidine by Tbb-5F2'dURes (■) and s427-WT (●) was almost totally inhibited in the presence of 10 mM unlabelled thymidine in BSF of Tbb-5F2'dURes (◊) and s427-WT (▲). **B.** Inhibition of 2.5 µM [3H]-thymidine uptake in Tbb-5F2'dURes over 30 minutes by various concentrations of unlabelled thymidine (●). The inset was conversion the data from frame A to Michaelis-Menten saturation plot. The uptakes were terminated by the addition of 1 ml ice-cold 10 mM thymidine in uptake assay buffer and immediate centrifugation through oil. Error bars were SE of triplicate determinations.

5.3.2. 5-Fluoro-2'deoxycytidine

The metabolomic analysis of s427-WT BSF treated with 5F-2'dCtd provided further confirmation that 5F-2'dCtd and 5F-2'dUrd act in a similar way, as the main fluorinated metabolite of 5F-2'dCtd was 5F-2'dUrd. A very small amount of 5F-dUMP was also detected by manual inspection, below the limit of automated detection. As with 5F-2'dUrd treatment there was a massive increase in dUMP levels in the cell (67-fold; $P<10^{-5}$. This was accompanied by a 2.9-fold increase in 2'-deoxyuridine ($P<0.01$). Conversely, there was a small but significant reduction in uridine (41%; $P<0.01$) and UMP (51%; $P<0.01$).

In addition there were significant ($P<0.02$) effects on cytidine nucleotide metabolism. There were significant increases in dCDP (4.6-fold) and dCTP (5.6-fold), as well as an apparent shift in lipid metabolism intermediates. CDP-choline and CDP-ethanolamine were reduced by 42% and 39% respectively, while increases were observed for metabolite peaks putatively identified as dCDP-

choline (2.2-fold) and dCDP-ethanolamine (4.5-fold). There were no significant differences in the cellular levels of the cytidine ribonucleotides CMP, CDP and CTP after incubation with 5F-2'dCtd. These effects were not easily understood as we are not aware of a mechanism for (deoxy)-cytidine utilization in trypanosomes other than through cytidine deaminase. However, the effect on deoxycytidine nucleotide levels may have been through the effects of accumulating dUMP on ribonucleoside reductase (enzyme 11 in Figure 5.1), which can be allosterically regulated by deoxyribonucleotides (Hofer *et al.*, 1998). This notion was greatly supported by the fact that similar effects could be observed after treatment with 5F-2'dUrd, which caused increases in dCMP (2.8-fold; $P<0.001$) and dCDP (3.8-fold; $P<0.001$) as well as in dCDP-choline (2.0-fold; $P<0.01$); while there was no effect on levels of CMP or CDP.

5.3.3. 5-Fluorouridine

This nucleoside analogue had no effect on trypanosome growth when tested in the Alamar blue viability assay. Consistent with this observation, only very low levels of fluorinated metabolites (5-FU, 5-FUMP, 5-FUDP and 5-FUDP-glucose) were observed in WT cells exposed to 100 μM of 5-fluorouridine compared to 5-FU or 5-FOA. No major changes to cellular metabolism were observed.

5.4. Incorporation of fluorinated pyrimidines into nucleic acids

5.4.1 DNA

As part of the investigation of the mechanism of action 5F-2'dUrd on trypanosomes the study isolated and digested DNA from 5F-2'dUrd-treated cells. No 5F-dUMP was detected in the digest in spite of the four natural deoxynucleotides being present at 500 to 5000 fold higher intensity than the detection limit. The study can rule out that significant amount of 5-fluoro-2'deoxyuridine is incorporated into DNA in lieu of thymidine.

5.4.2 RNA

As mentioned above the presence of 5F-UTP raises the possibility of incorporation of fluorinated nucleotides into RNA. Following purification and digestion of RNA from 5-FU treated cells, qualitative LC-MS analysis detected significant amounts of 5F-UMP (~10% of UMP abundance by comparison of LC-MS peak heights), in addition to low levels of 5F-CMP, confirming the incorporation of significant amounts of fluorinated nucleotides into RNA. This data provides evidence that 5F-UTP is a substrate for cytidine triphosphate synthase, as 5F-CTP was not detected in the original extracts of cellular metabolites; however, the purification and digestion of isolated RNA led naturally to a much more concentrated mono-nucleotide pool for HPLC/MS analysis.

5.5. Effect of fluorinated uridines on glycosylation in *T. b. brucei*

To test whether the detection of significant quantities of 5F-UDP-hexoses and hexosamines contribute to trypanocidal action through interference with either protein glycosylation or glycosylphosphatidylinositol (GPI) anchor biosynthesis, protein extracts of BSFs of *T. b. brucei* s427-WT and pyrimidine auxotrophic trypanosomes, incubated for 12 hours in the presence or absence of 100 µM 5-FU or 5F-2'dUrd, were separated by 1D SDS-PAGE and transferred onto Immobilon-P membranes. Two separate blots of the same samples were incubated with *Ricinus communis* lectin, which binds specifically to terminal ß-galactose residues, or with *Erythrina crystalgalli* lectin, which is specific for N-acetyl lactosamine modifications - both are hallmarks of mature N-glucan processing. This experiment was performed on three independent occasions but in no case was a difference in staining pattern or intensity observed between the extracts from treated and untreated trypanosome cultures (Figure 5.11). Furthermore, the intensity and migration position of the variant surface glycoprotein band, as detected by Coomassie staining of gels, was unaltered. In conclusion, no major defects to glycosylation or GPI anchor synthesis took place under the influence of fluorinated pyrimidines. Although it is possible that glycosylation of a relatively rare glycoprotein could have been affected without this being apparent in the blot, it is clear that the bulk of N-glycan and GPI biosynthesis are unaltered.
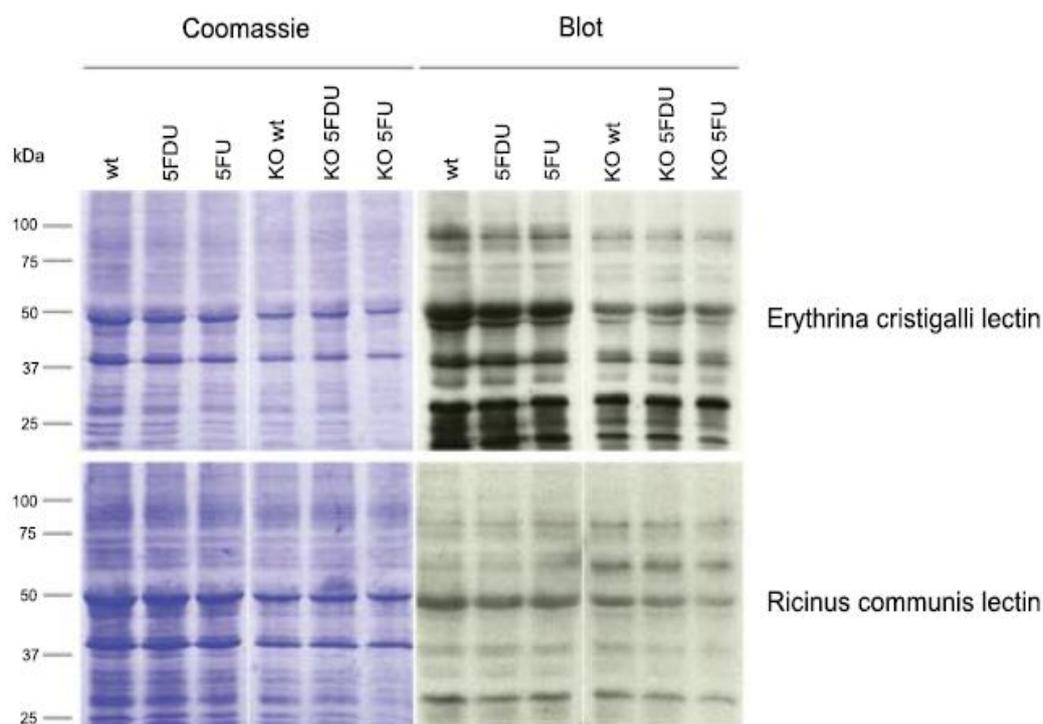
Figure 5.11. Lectin blotting of *T. b. brucei* BSF protein samples after incubation with 5-fluorouracil or 5fluoro-2'deoxyuridine. Cultures of *T. b. brucei* BSF and pyrimidine auxotrophic trypanosomes (KO) were incubated for 12 hours in the presence or absence of 100 μM of either pyrimidine analog, under standard culturing conditions. Protein extracts were separated on 1D polyacrylamide gels (left hand-side, Coomassie Blue stained) and transferred to Immobilon-P membranes to be incubated with either *Erythrina crystalgalli* lectin or *Ricinus Communis* lectin (right hand-side). Lectin binding was visualized by using ECL reagents. The abbreviations: wt = wild-type drug free; 5FDU = WT treated by 5-F2'deoxyuridine; 5-FU = WT treated by 5-FU; KO wt = pyrimidine auxotrophic trypanosomes in free drug medium; KO 5FDU = KO treated by 5-F2'deoxyuridine; KO 5-FU = KO treated by 5-FU. This experiment was carried out in collaboration with Harriet Allison and Mark Field of the University of Cambridge, who performed the lectin blotting from extracts made at the University of Glasgow.

5.6. Genome-wide profiling of trypanosomatid pyrimidine metabolism

The above analyses of pyrimidine metabolism, and of the effects of pyrimidine analogues on this system, resulted in a new overview of the pyrimidine salvage and biosynthesis pathways in *T. b. brucei*. To further validate the presence of the enzymes predicted in the model shown in figure 5.1, the study constructed a library of hidden Markov model (HMM)-based profiles for pyrimidine synthesis and salvage enzymes. Selected parasite proteomes were scanned with this library, *Homo sapiens* and *Mus musculus* served as a reference. The use of the same profiles over different proteomes enabled clustering of the respective species according to their 'pyrimidine metabolic vectors' (Figure 5.12).
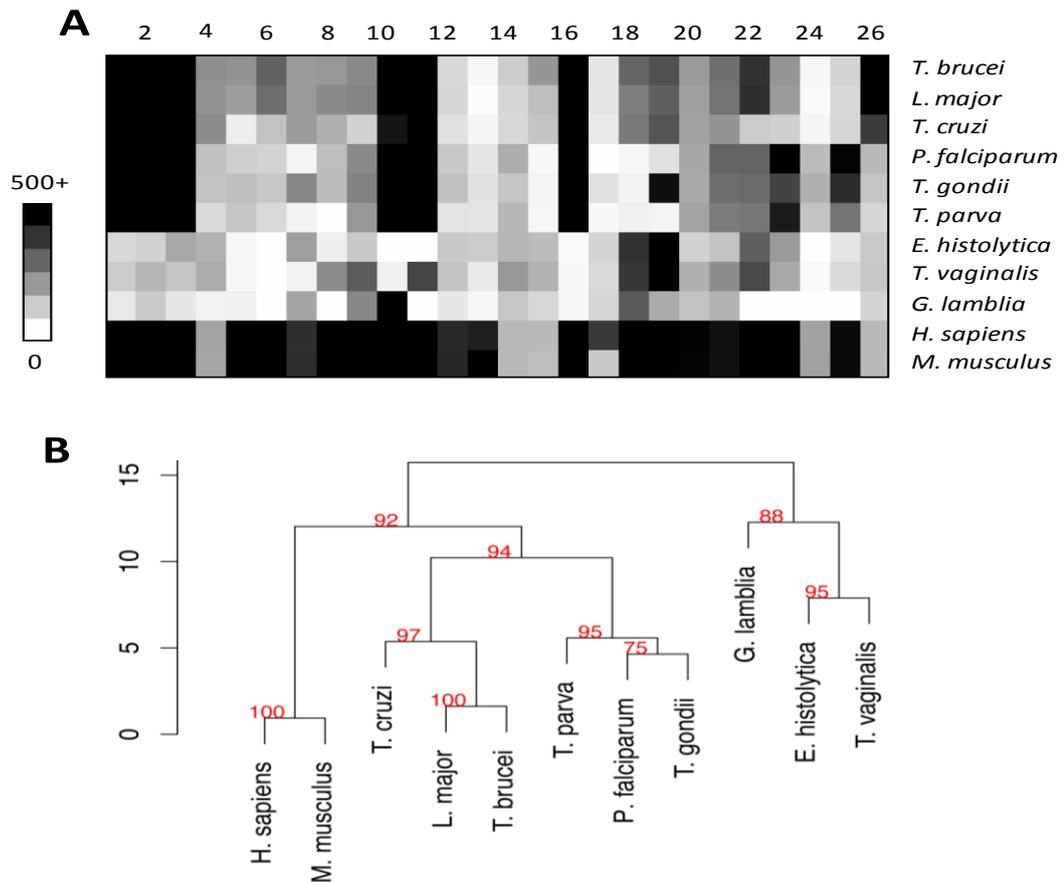
Figure 5.12 Analysis of pyrimidine metabolic enzymes in major protozoan pathogens and two reference mammalian genomes. Profiles specific for the known pyrimidine metabolic enzymes were constructed as described in Methods. The profiles were scanned against selected eukaryote proteomes. **A.** Heat map of the best scores obtained by each proteome against profiles for enzymes of pyrimidine synthesis (1-6), salvage (7-17), sugar (18-19), and lipid metabolism (20-23). Enzyme numbers were the same as in Figure 5.1. **B.** Hierarchical clustering of the 'pyrimidine metabolic vectors' (top) based on Canberra distance (scale bar); the red numbers are 'approximately unbiased' confidence (au), where p = (100-au)/100. This analysis was carried out in collaboration with Pascal Mäser of the Swiss Tropical and Public Health Institute in Basel, who also created this figure.

This analysis clearly separated the pyrimidine auxotrophic *Giardia duodenalis, Entamoeba histolytica,* and *Trichomonas vaginalis* from other protozoa. These parasites lack thymidylate synthase (enzyme number 16; EC 2.1.1.45). Within the pyrimidine prototrophs, the trypanosomatids separated from the apicomplexans mainly due to the presence of thymidine kinase (enzyme number 15; EC 2.7.1.21), UDP-glucose pyrophosphorylase (enzyme number 18; EC 2.7.7.9) and UDP-glucose epimerase (19; EC 5.1.3.2), and the absence of orotate reductase (enzyme 24 not present; EC 1.3.1.14) and dihydroorotate dehydrogenase (enzyme number 25 not present; EC 1.3.5.2). The main distinction between *T. brucei* and its mammalian hosts was the apparent absence of dUTPase (enzyme number 13; EC 3.6.1.23) and dihydroorotate dehydrogenase (enzyme number 4; EC 1.3.5.2), in addition to a relatively low score for uridine phosphorylase (enzyme number 12; EC 2.4.2.3).

The apparent absence of dUTPase, a well-characterized enzyme in *T. b. brucei* (Castillo-Acosta *et al.,* 2008) is explained by the fact that it is highly atypical for a eukaryotic dUTPase: it is dimeric rather than trimeric (possibly unique among eukaryotes (Castillo-Acosta *et al.,* 2008), with a very different 3D structure (Harkiolaki *et al.,* 2004), giving it features different from other eukaryotic dUTPases, including recognition of both dUTP and dUDP as substrates (Bernier-Villamor *et al.,* 2002). These kinetoplastid dUTPases have been classified together with several prokaryotic and bacteriophage dUTPases into an all-α NTP pyrophosphatase superfamily (Moroz *et al.,* 2005). Similarly, trypanosomal uridine phosphorylase has an unusual quaternary structure, although most of its active site layout is conserved (Larson *et al.,* 2010): it is a member of the NP-I family of nucleoside phosphorylases but, unusually, not organized as a stable trimer of dimmers, but rather as a single dimer stabilized by a Ca^{2+} ion. Dihydroorotate dehydrogenase (EC 1.3.5.2) is indeed absent from the *T. b. brucei* genome, its function in the pyrimidine biosynthesis pathway instead being performed by dihydroorotate dehydrogenase (EC 1.3.3.1; Arakaki *et al.,* 2008), which the HMM analysis correctly predicts.

5.7. Discussion

The pyrimidine analogues target rapidly dividing cells and kinetoplastid parasites similarly depend on high growth rates to outpace the host's defenses. Here, we systematically investigate metabolomic effects of pyrimidine antimetabolites and the incorporation of pyrimidine analogues into nucleic acids by trypanosomes. Antiprotozoal pyrimidine therapy would start with cytotoxic pyrimidines efficiently reaching the target cell's interior (De Koning , 2001; Luscher *et al.*, 2007).

5-FU and 5-FOA give rise to the same active metabolites, converging immediately on 5F-UMP (Figure 5.1). As the cells are more sensitive to 5-FOA than to 5-FU, despite a much less efficient uptake, it must be concluded that the 2-step conversion of 5-FOA to 5-UMP (by orotate phosphoribosyltransferase (OPRT) and orotidine monophosphate decarboxylase (OMPDC) is far more efficient than the phosphoribosylation of 5-FU by uracil phosphoribosyltransferase (UPRT). The active sites of OPRT and OMPDC clearly are more tolerant of the 5-position fluorine than UPRT.

As predicted by the current knowledge of pyrimidine pathways in *T. b. brucei* (Figure 5.1) incubation with sub-lethal concentrations of 5-FOA and 5-FU produced essentially the same set of downstream metabolites, although 5-FOA incubation also resulted in detectable levels of fluoro-carbamoylaspartate, indicating the pyrimidine biosynthesis pathway can operate in reverse, at least from orotate. 5-FOA incubation likewise resulted in production of 5-FU by the trypanosomes, thus uracil phosphoribosylation is also reversible. Significant amounts of 5F-UMP, 5F-UDP and 5F-UTP were detected in the metabolome, in addition to 5F-UDP-glucose or -galactose, and 5F-UDP-N-acetylglucosamine and/or 5F-UDP-N-acetylgalactosamine. In contrast, no trace of 5F-2'deoxyuridine nucleotides were detected, indicating that 5F-UDP was not a substrate of *T. b. brucei* ribonucleoside-diphosphate reductase. Yet, incubation with 5-FU did result in an elevation of dUMP levels. The cause of these elevated dUMP levels is not clear but is unlikely to be the result of 5F-dUMP inhibition of thymidylate synthase, as no 5F-dUMP was detected in the metabolomic analysis, nor has any other evidence that fluorinated pyrimidines might be substrates of

ribonucleoside-diphosphate reductase (RNR) come to light in this study. It could be speculated, however, that there is an allosteric effect of a fluorinated nucleotide on RNR, as (Hofer *et al.*, 1998) demonstrated that this key enzyme is allosterically regulated by numerous nucleotides in a complex way. The complete lack of cross-resistance between 5-FU and 5F-2'deoxynucleosides (Table 3.3) seems to definitively show that the increase in dUMP, unlike 5F-2'dUrd, is not the main mechanism of action for the fluorinated nucleobases. These observations suggest therefore (one of) two main mechanisms of action for the fluorinated nucleobases: incorporation as 5-fluoronucleotides into RNA, or an effect of the 5F-UDP-coupled sugars on glycosylation or GPI anchor synthesis. The presence of significant levels of 5F-uridine (and lower levels of 5F-cytidine) nucleotides in digested RNA (but not DNA), coupled with the absence of any observable effect on glycosylation of *T. b. brucei* membrane proteins (>95% Variant Surface Glycoprotein, a GPI-anchored glycoprotein) suggest that the incorporation of fluorinated nucleotides into RNA contributes to 5-FU-induced cell death in trypanosomes but it is highly likely that the trypanocidal activity is multifactorial.

5F-2'dUrd was a substrate for thymidine kinase (5F-dUMP detected), but not for uridine phosphorylase, as no 5-FU or fluorinated uridine ribonucleotides were observed in 5F-2'dUrd-exposed trypanosomes. Nor were 5F-dUDP or 5F-dUTP present in detectable quantities and we conclude that 5F-dUMP was not a substrate for thymidylate kinase. The absence of any incorporation of 5F-deoxynucleotides into DNA supports this conclusion. The notable change in the metabolome of 5F-2'dUrd-treated trypanosomes was a large increase (>35-fold) in dUMP levels, strongly suggesting that its mechanism of action is the inhibition of dihydrofolate reductase-thymidylate synthase. The rescue by excess extracellular thymidine supports this conclusion. The small effects on the levels of 2'deoxycytidine nucleotide levels may indicate allosteric effects on ribonucleoside reductase. Incubation with 5F-2'dCtd caused virtually the same metabolomic changes as with 5F-2'dUrd, consistent with the notion of any 2'deoxycytidine utilization in trypanosome being through deamination to 2'deoxyuridine that were also indicated by the cross-resistance between 5F-2'dUrd and 5F-2'dCtd (Table 3.3). Indeed, 5F-2'deoxyuridine was clearly detected after incubation with the deoxycytidine analogue, as were small

quantities of 5F-dUMP, confirming reports of deoxycytidine incorporation in *T. b. gambiense* (Koenigk, 1976) and of cytidine deaminase activity in several kinetoplastid parasites (Hammond & Gutteridge, 1982) but contrast with evidence from (Hofer *et al.,* 2001) who were unable to detect incorporation of radiolabeled cytosine and cytidine into the *T. b. brucei* nucleotide pool. The likely explanation is the use of submicromolar concentrations of pyrimidines by Hofer for the incorporation studies, which would allow rapid uptake and utilization of uracil but not of cytosine or cytidine.

The metabolomic analysis also supplied further information about a possible uridine phosphorylase. Fluorinated uridine nucleosides are at best poor substrates for this enzyme, as incubation with 5F-2'dUrd resulted in no detectable production of 5-FU or fluorinated ribonucleotides. Incubation with 5F-Urd did produce some of these metabolites, however, showing that this enzyme (EC 2.4.2.3; Tb927.8.4430) is indeed expressed in bloodstream forms as suggested by (Hassan & Coombs, 1988) and favors uridine over 2'-deoxyuridine as shown by (Larson *et al.,* 2010). There is no evidence for a uridine kinase activity in kinetoplastids (Figure 5.12) (Hammond & Gutteridge, 1982).

This study has for the first time established the metabolic space of pyrimidine antimetabolites in kinetoplastid parasites. A surprising number of metabolites were detected, showing that the fluorination on position 5 has limited effect on many enzymes of the pyrimidine pathways. Pyrimidine antimetabolites may be incorporated into RNA, into precursors for lipid biosynthesis and activated sugar metabolism, potentially impacting on VSG glycosylation or GPI anchors - all essential functions to trypanosomes (Donelson, 2003). However, it is equally instructive to observe which into which part of the pyrimidine 'system' the analogues did not penetrate: 5-FU was not a substrate for uridine phosphorylase or ribonucleotide reductase. This is very different from 5-FU metabolism in human cells (Longley *et al.,* 2003), where 5-FU incorporation into deoxynucleotides is mediated by human ribonucleotide reductase, and by uridine phosphorylase and pyrimidine phosphorylase followed by thymidine kinase (forming 5F-2'dUMP) [Note: it is possible that the non-detection of fluorinated deoxyuridine nucleotides after 5-FU exposure is partly due to technical limitations as another group appears to have detected 5F-dUTP as a 5-FU metabolite in trypanosomes (T. Smith, personal communication)]. The

formation of fluorinated deoxynucleotides in human cells leads to their incorporation into DNA and inhibition of thymidylate synthase leading to double strand breaks; 5F-UMP is similarly incorporated into human RNA. It is believed that the inhibition of thymidylate synthase is the main action of 5-FU and its prodrugs on human cells (Ceilley, 2010; Longley *et al.*, 2003), leading to an imbalance between deoxyuridine nucleotides and thymidine nucleotides and the miss-incorporation of the former into DNA. This mechanism is identical to that described here for the trypanocidal action of 5F-2'dUrd and 5F-2'dCtd.

Untargeted metabolomics and HMM profiling were used to map the pyrimidine salvage system, and the passage of pyrimidine antimetabolites through it. This approach proved to be extremely powerful, highlighting even apparently minor metabolites in pathways such as GPI anchor biosynthesis and lipid biosynthesis pathways. In addition, the untargeted metabolomics further highlighted important changes in metabolites that were not directly derived from the active analogue under investigation, such as the accumulation of dUMP after treatment with 5F-2'dUrd, resulting in a much-improved understanding of pyrimidine salvage systems in kinetoplastids, and a first evaluation of its utility in a strategy of antimetabolites for antiprotozoal chemotherapy.

CHAPTER SIX
Metabolomic investigations of the mechanisms of action of fluorinated pyrimidines on *Leishmania*

6.1. Introduction

Most organisms are capable of salvage and biosynthesis of pyrimidine molecules, including kinetoplastid cells. In addition, most of the inter-conversion pyrimidine metabolizing enzymes, and the enzymes of the biosynthesis pathways are shared among the various organisms. The six pyrimidine biosynthesis enzymes in *Leishmania* were detected, as well as identification and characterization of several pyrimidine pathway enzymes have been studied at molecular level (Wilson *et al.,* 2012). Although *Leishmania* cells are pyrimidine prototrophic, several studies have targeted pyrimidine biosynthesis enzymes. Recently, knockout of UMP synthase in *L. donovani* promastigotes led to totally non-viable cells in the absence of pyrimidines *in vitro* conditions, and they were able to grow on low levels of pyrimidines (French *et al.,* 2011).To date, no study has investigated the metabolites and the mode of action of 5-FU (or even any other pyrimidine analogues) in *Leishmania* cells; moreover, the metabolism of individual pyrimidines inside these cells has not been investigated. The incompleteness of this knowledge delays the development of an anti-leishmanial pyrimidine-based chemotherapy. Therefore, the current study used a metabolomic approach to assess: (1) the mechanism of action to 5-fluoro-pyrimidines (2) what metabolites are formed from 5-fluoro-pyrimidines in promastigotes of *Leishmania* spp (3) whether these analogues utilise the same metabolomic pathways in leishmania and trypanosomes. In addition, the considerable differences between *L. mexicana* and *L. major* in terms of 5F-Urd toxicity were investigated here. We selected the active fluorinated pyrimidines (5-FU, 5F-2'dUrd and 5F-Urd), and excluded 5F-2'dCyd as its metabolism in trypanosomes was identical to that of 5F-2'dUrd (chapter 5). We selected the wild type strain of *L. mexicana* sM379 and *L. major* sFriedlin to perform this experiment, and excluded the derived strains resistant to fluorinated pyrimidines from metabolomic assessment as they had lost their natural pyrimidine transporters (Chapter 4).

6.2   Metabolomic   analysis   of   5-fluorouracil   in promastigotes of *Leishmania* spp

Promastigotes of *L. mexicana* and *L. major* incubated with 100 µM of 5-fluorouracil for 8 hours showed a considerable amount of intracellular 5-FU (Figure 6.1A). Neither fresh medium nor intracellular untreated controls showed fluorinated pyrimidines, showing that the identifications were correct. Only low levels of 5F-2'dUrd were detected in *L. major*; however, for *L. mexicana* the level was much lower and below the level at which it could confidently be detected and identified by the automated paradigm used (Figure 6.1B). In contrast, almost identical levels of 5F-dUMP were observed in both *Leishmania* species (Figure 6.1C). The detection limit of 5F-2'dUrd and 5F-dUMP was not a contamination of the drug as added to the cultures, as it was not present in fresh medium samples containing 5-FU. It was notable that promastigotes of both *Leishmania* species produced highly similar levels of the same fluorinated metabolites. Another common aspect between the promastigotes of *Leishmania* was that neither 5-fluorouridine nor fluorinated uridine nucleotides (F-UMP, F-UDP and F-UTP) were observed in extracted cells exposed to the indicated concentration of 5-FU, in complete contrast to the metabolism in *T. brucei*.
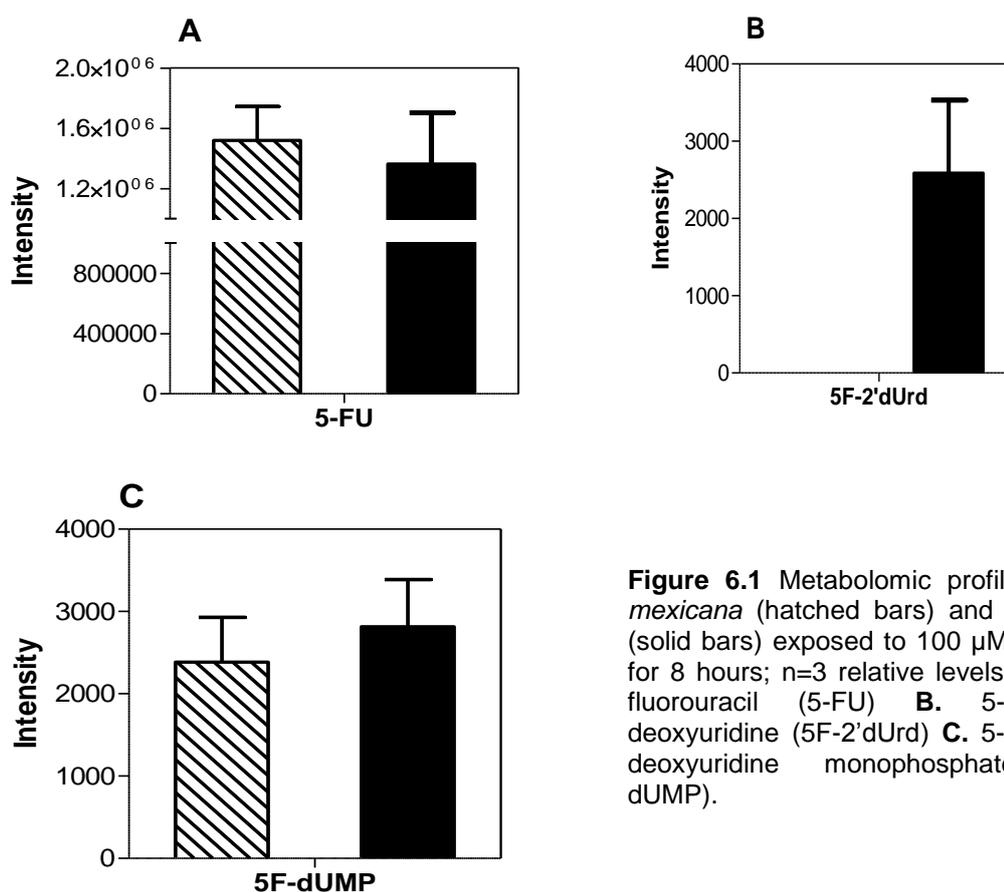
Figure 6.1 Metabolomic profiles of *L. mexicana* (hatched bars) and *L. major* (solid bars) exposed to 100 µM of 5-FU for 8 hours; n=3 relative levels of **A.** 5-fluorouracil (5-FU) **B.** 5-fluoro-2'-deoxyuridine (5F-2'dUrd) **C.** 5-fluoro-2'-deoxyuridine monophosphate (5F-dUMP).

The detection levels of 5F-2'dUrd and 5F-dUMP clarify that leishmania metabolised 5-FU by uridine phosphorylase to 5-F2'dUrd (but not to 5F-uridine), which was subsequently phosphorylated by thymidine kinase to 5F-dUMP, which inhibited thymidylate synthase. Consistent with observations in human cells, 5F-dUMP then inhibited thymidine kinase and/or thymidylate synthase and block deoxythymidine nucleotides biosynthesis. In sharp contrast with 5-FU metabolism in *T. b. brucei*, the drug does not appear to be a substrate for *Leishmania* uracil phosphoribosyl transferase.

Another interesting observation in the pyrimidine pathways of *Leishmania* cells exposed to 5-FU was a change in the level of deoxy-pyrimidine nucleotides. The intracellular levels of dUMP in treated *Leishmania* species were massively increased compared with respective untreated controls, which were very low in comparison, particularly in *L. mexicana* where the level in untreated cells was below automatic detection; therefore, no statistical analysis could be performed (Figure 6.2A). In addition, 5-FU caused a reduction in the intensity of dTMP and dTTP peaks in *L. mexicana* promastigotes (P=0.05 and P=0.03, respectively)

compared with respective untreated control (Figure 6.2B and C). It should be noted that in treated *L. major* cells the reduced level of deoxythymidine nucleotides was not significant, although the reduced dTTP level was observed in two out of three replicates. However, exposure of *L. major* cells to 5-FU showed no significant changes in the level of the nucleoside thymidine compared with untreated controls. The subsequent reduction in 2'deoxy-thymidine nucleotides in *Leishmania* species is thus probably due to the inhibition of thymidine kinase by 5-FU and/or its metabolites. It should be considered that the level of dTMP in *L. mexicana* untreated cells was 3.7-fold higher than in the *L. major* untreated control, whilst the levels of dTTP in the former were 2.2-fold lower than the latter. No traces of dTDP were detected in either treated or untreated promastigotes of *Leishmania* cells.

A

B

C
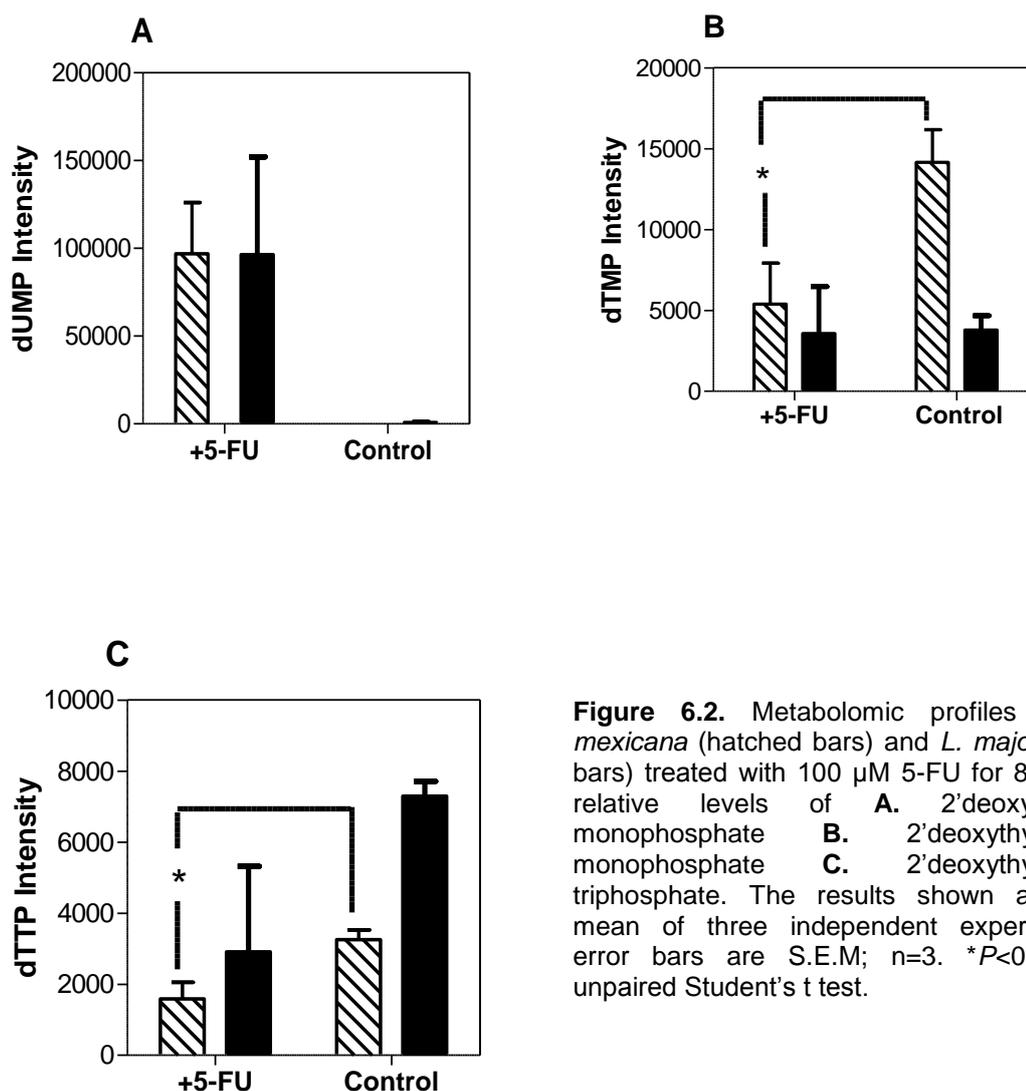
Figure 6.2. Metabolomic profiles of *L. mexicana* (hatched bars) and *L. major* (solid bars) treated with 100 µM 5-FU for 8 hours; relative levels of **A.** 2'deoxyuridine monophosphate **B.** 2'deoxythymidine monophosphate **C.** 2'deoxythymidine triphosphate. The results shown are the mean of three independent experiments; error bars are S.E.M; n=3. *$P<0.05$ by unpaired Student's t test.

Other changes that occurred in both *L. mexicana* and *L. major* treated with 5-FU were an elevation of the levels of deoxynucleosides of uridine (Figure 6.3A; *P*= 0.06 and 0.05, respectively) and adenosine (Figure 6.3B; not significant in both species) compared to untreated controls. We also observed increases in the intensity of 2'deoxycytidine nucleotides (dCMP, dCDP, dCTP) and 2'deoxyadenosine nucleotides (dAMP, dADP) relative to respective untreated controls. It must be noted that the level of 2'deoxycytidine and 2'deoxyadenosine nucleotides were barely detected in leishmania untreated controls; dATP was undetectable in both treated and untreated cells.
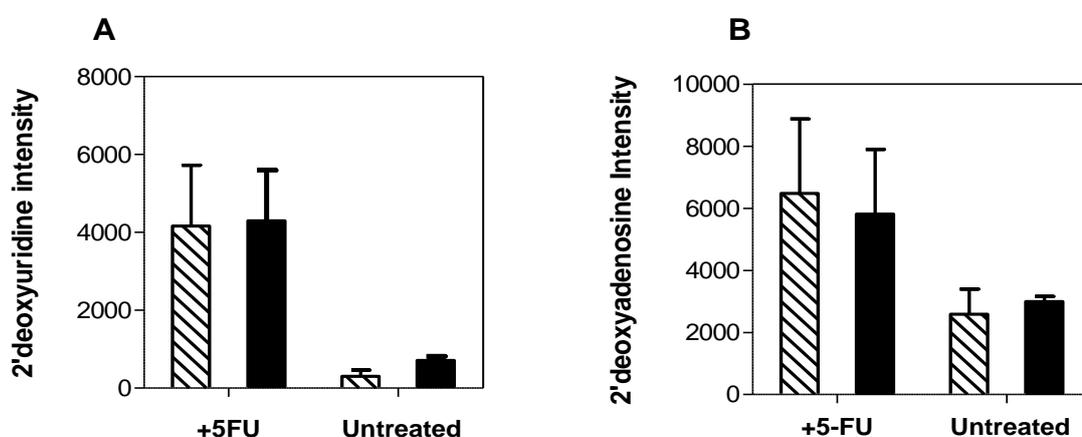
Figure 6.3. Metabolomic profiles of *L. mexicana* (hatched bars) and *L. major* (solid bars) treated with 100 µM 5-FU for 8 hours; n=3; relative levels of **A.** 2'deoxyuridine **B.** 2'deoxyadenosine. The results shown are the mean of three independent experiments; error bars are S.E.M. The differences were insignificant by unpaired Student's t test.

In trypanosomes, 5-FU was incorporated into sugar nucleotides such as UDP-glucose, potentially affecting glycosylation. No direct evidence for a disruption of glycosylation was found in a preliminary investigation but 5-FU resistance coincided with a strongly reduced incorporation into this pathway (Ali *et al.*, 2013a). However, 5-FU showed no effect on the levels of UDP-glucose in *Leishmania* cells, and although the drug increased the intensities of UDP-*N*-acetyl-D-glucosamine, the increase was not statistically significant.

The levels of other natural pyrimidine and purine nucleotides, nucleosides and nucleobases were generally unchanged in promastigotes of *Leishmania* spp treated by 5-FU, relative to their respective untreated controls. However, the intensity of ATP appeared to be higher in treated *L. mexicana* cells than in their control (but insignificant, *P*=0.06). In addition, the levels of cytidine and

thymine in *L. major* were significantly reduced (*P*=0.025 and 0.002, respectively) compared with their untreated counterparts.

The untreated controls of *L. mexicana* and *L. major* commonly displayed the same level of pyrimidine derivatives; however, a few significant differences were observed. For instance, dUMP was clearly detected in *L. major*, even though it was very much below detection limit in *L. mexicana*. The monophosphate nucleotides level (CMP, AMP, and GMP) were significantly higher in *L. mexicana* than in *L. major* (*P* values were 0.028, 0.002, 0.025, respectively), but the intensity of triphosphate nucleotides (UTP, CTP and ATP) were considerably lower in the former than the latter (*P* values were 0.008, 0.042 and 0.004, respectively). Other variations were in the levels of cytidine, thymidine and guanine, which were significantly higher in *L major* than *L. mexicana* (*P*=0.029, *P*=0.023, *P*=0.002, respectively).

6.3. Metabolomic analysis of 5-fluoro-2'deoxyuridine in promastigotes of *Leishmania* spp

Almost the same amount of 5F-2'dUrd was detected in cells of both *Leishmania* species after being exposed to 100 µM of 5F-2'dUrd. In addition, high levels of 5-FU were found after the treatments (Figure 6.4A), with the level of 5-FU in *L. mexicana* slightly higher than in *L. major*; this is most likely the result of conversion of 5F-2'dUrd to 5-FU by uridine phosphorylase. Furthermore, the level of 5F-dUMP in *L. mexicana* was >9-fold higher than in *L. major* (n=3, *P*<0.028, Student's t-test, Figure 6. 4B). The significant difference between the two species of *Leishmania* treated by 5F-2'dUrd, using identical conditions in a parallel experiment, could either be due to a higher activity of thymidine kinase (TK) in *L. mexicana*, or to a higher affinity for 5F-2'dUrd by *L. mexicana*-TK than by *L. major*-TK - both would result in a quick phosphorylation of 5F-2'dUrd in *L. mexicana*. As no 5-fluorouridine was detected in *Leishmania* cells treated by 5F-2'dUrd, we conclude that the drug is converted to 5-FU, in a reversible reaction, and that *Leishmania* uridine phosphorylase specifically generates 2'-deoxyuridine rather than uridine. These findings are consistent with the observations with 5-FU-treated cells (see previous section).
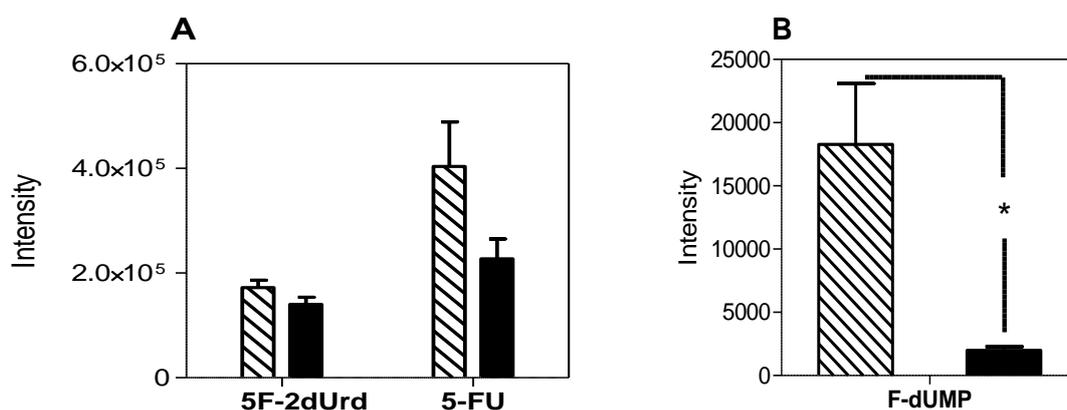
Figure 6.4 Metabolomic profiles of *L. mexicana* (hatched bars) and *L. major* (solid bars) exposed to 100 µM of 5-fluoro-2'deoxyuridine for 8 hours; n=3; relative levels of **A.** 5F-2'dUrd and 5-FU **B.** F-d-UMP in both *Leishmania* species; n=3. *$P< 0.05$ by unpaired Student's t test.

The dUMP levels of *Leishmania* cells were considerably increased after exposure to 5F-2'dUrd (Figure 6.5A), with the drug causing a 67-fold increase in the level of dUMP of *L. major* ($P<0.001$, unpaired Student's t-test), and an even more significant increase in *L. mexicana* cells. In contrast, exposure of *L. mexicana* or *L. major* to 5F-2'dUrd caused a significant reduction in the intensities of dTMP ($P= 0.005$, $P= 0.042$, respectively; Figure 6.5B) and dTTP (Figure 6.5C; in *L. major* $P<0.001$); it should be noted that in *L. mexicana* no statistical analysis can be performed here and onwards as the levels of dTTP for 5F-2'dUrd-treated cells, and of dUMP in control cells, was very much below the detection limit, but the same trends were strongly observed in both *Leishmania* species. The elevations in dUMP and the reductions in deoxythymidine nucleotides were similar to the changes observed in *Leishmania* cells after 5-FU treatment, strongly suggesting that, in *Leishmania*, 5-FU and 5F-2'dUrd have a very similar mode of action.

A

B

C
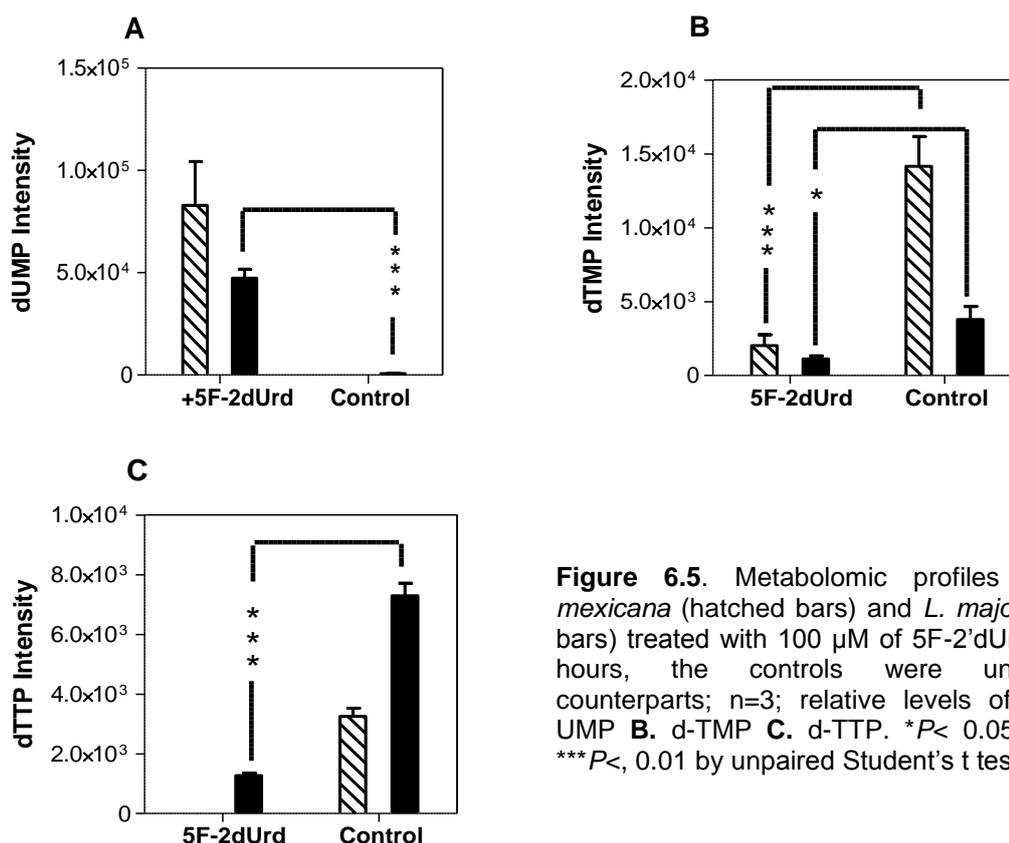
Figure 6.5. Metabolomic profiles of *L. mexicana* (hatched bars) and *L. major* (solid bars) treated with 100 µM of 5F-2'dUrd for 8 hours, the controls were untreated counterparts; n=3; relative levels of **A.** d-UMP **B.** d-TMP **C.** d-TTP. *$P<$ 0.05; 0.02; ***$P<$, 0.01 by unpaired Student's t test.

Other significant changes that occurred in cells treated with 5F-2'dUrd compared to their respective untreated controls were increases in the level of 2'deoxyuridine of both *L. mexicana* and *L. major* (Figure 6.6A; *P*=0.002 and 0.005, respectively), indicating inhibition of thymidine kinase, and an increase in the 2'deoxyadenosine intensity (Figure 6.6B; insignificant in *L. mexicana*, *P*=0.027 in *L. major*). It was further found that 5F-2'dUrd lead to a significant increase in the levels of 2'deoxy-cytidine nucleotides (dCMP, dCDP, dCTP) and 2'deoxyadenosine nucleotides (dAMP, dADP).

A

B
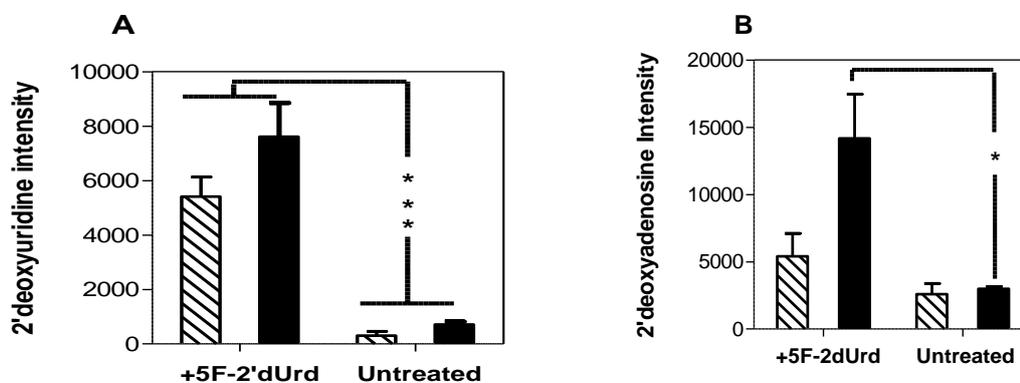
Figure 6.6. Metabolomic profiles of *L. mexicana* (hatched bars) and *L. major* (solid bars) treated with 100 µM 5-F2'dUrd for 8 hours; n=3; relative levels of **A.** 2'deoxyuridine **B.** 2'deoxyadenosine. The results shown are the mean of three independent experiments; error bars are S.E.M. *$P<$ 0.05; ***$P<$, 0.01 by unpaired Student's t test.

Interestingly, even though 5F-2'dUrd and 5F-dUMP were the only fluorinated pyrimidines detected, the treatment led to a significant elevation in the intensities of UDP-*N*-acetyl-D-glucosamine of *L. mexicana* and *L. major* (*P*=0.045, *P*=0.034, respectively; Figure 6.7), possibly through effect/s on nucleotide reductase by build up dUMP, increasing availability of uridine nucleotides and flux through some UTP-dependent pathways. Once again these differences between 5F-2'dUrd-treated and untreated controls were identical to the changes caused by 5-FU, which confirms the common mode of action of the drugs.
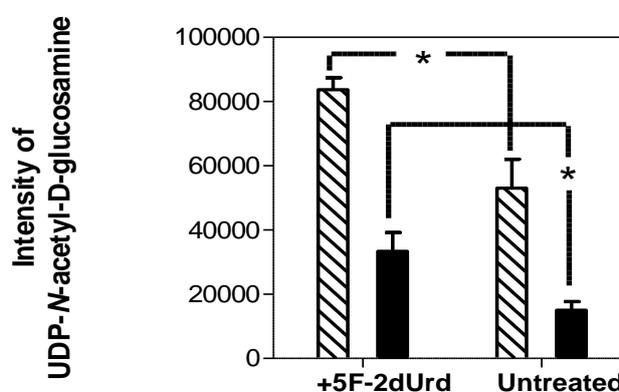
Figure 6.7 Metabolomic profiles of *L. mexicana* (hatched bars) and *L. major* (solid bars) exposed to 100 µM of 5-fluoro-2'deoxyuridine for 8 hours; n=3; relative levels of UDP-N-acetyl-D-glucosamine in both *Leishmania* species. *$P< 0.05$ by unpaired Student's t test.

The rest of the natural pyrimidines and purines were generally not changed in *Leishmania* promastigotes treated by 5F-2'dUrd compared with their respective untreated controls. However, for *L. mexicana* promastigotes, 5F-2'dUrd reduced the level of CMP (*P*=0.049) and increased the level of cytosine (*P*=0.035) compared with untreated control, suggesting either reduced production of CMP or increased CMP catabolism by a nucleoside hydrolase. In *L. major*, the drug significantly elevated the intensity of guanine (*P*=0.002).

6.4. Metabolomic analysis of 5-fluorouridine in promastigotes of *Leishmania* spp

Exposure of *Leishmania* promastigotes to 100 μM of 5-fluorouridine (5F-Urd) for 8 hours produced various levels of 5-FU (Figure 6.8A), 5F-Urd and 5F-2'dUrd (Figure 6.8B), as well as 5F-dUMP (Figure 6.8C), showing that 5-fluorouridine is a substrate of uridine phosphorylase even if it is not a significant product of the enzyme (see above). The most interesting point in this process is the resistance of *L. mexicana* to 5F-Urd (chapter 4): no 5F-2'Urd was detected in *L. mexicana* cells although it was detected at low levels in *L. major*. Notwithstanding the fact that the level of 5F-Urd was ~3-fold higher in *L. major* than in *L. mexicana*, the intensity of 5-FU and 5F-dUMP were considerably higher in *L. mexicana* than in *L. major* (P=0.001 for 5-FU; no detectable intensity of 5F-dUMP in *L. major* to analyse the difference statistically). It thus can be recapitulated that *L. mexicana* and *L. major* both take up 5F-Urd quite well. This observation, along with their inability to convert 5F-2'dUrd to 5F-Urd (see above), again shows that 5-fluorouridine is a very poor substrate for uridine phosphorylase, and is probably not a substrate for thymidine kinase at all, the 2'-hydroxyl group of 5F-Urd preventing this interaction. The small amount of 5F-dUMP detected in 5-fluorouridine treated *L. mexicana* promastigotes seems to be the result of total conversion of the small amount of 5F-2'dUrd by *L. mexicana*-TK, whereas this apparently did not (detectably) happen in *L. major*.

A

B

C
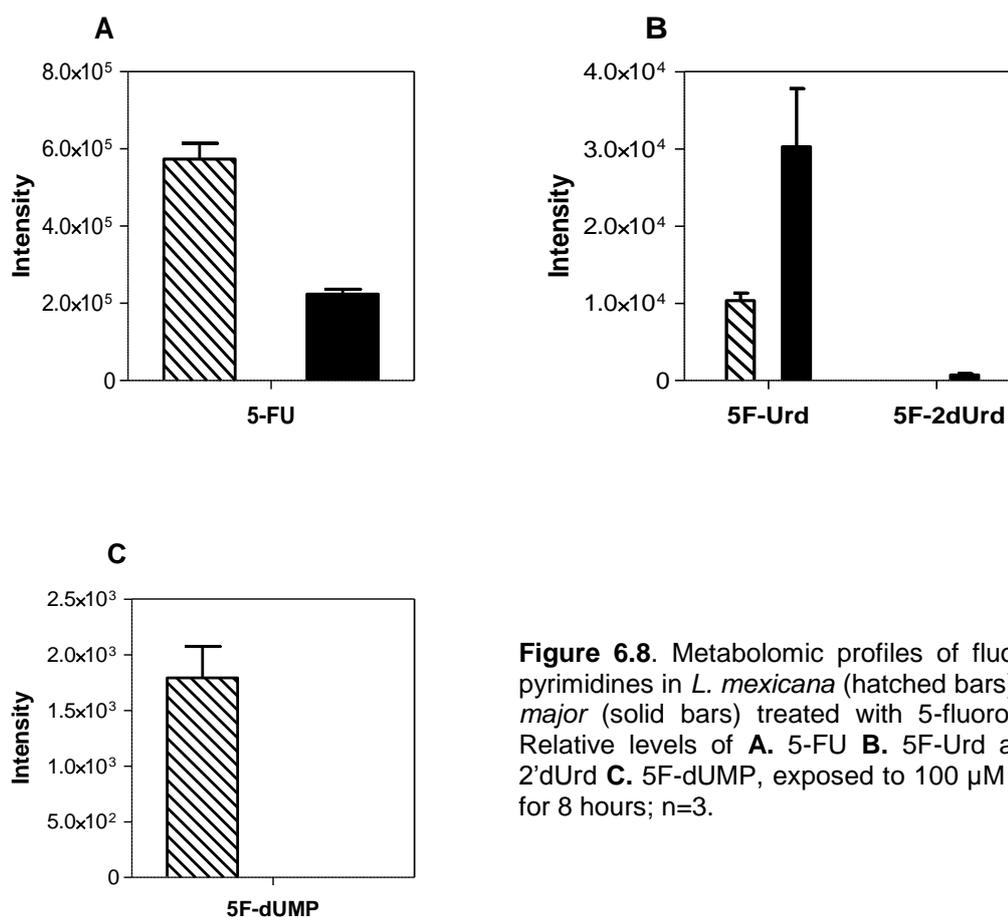
Figure 6.8. Metabolomic profiles of fluorinated pyrimidines in *L. mexicana* (hatched bars) and *L. major* (solid bars) treated with 5-fluorouridine. Relative levels of **A.** 5-FU **B.** 5F-Urd and 5F-2'dUrd **C.** 5F-dUMP, exposed to 100 µM 5F-Urd for 8 hours; n=3.

Promastigotes treated with 5F-Urd led to a significant increase in dUMP levels compared to respective untreated controls in which the dUMP levels were very low. The intensity of dUMP in *L. mexicana* treated cells was 5-fold higher than in *L. major* (Figure 6.9A). It follows that 5F-Urd inhibits thymidylate synthase (TS) in both *Leishmania* species, so that 5F-Urd acts possibly like 5-FU and 5F-2'dUrd. For *L. major* promastigotes, the drug caused a decrease in the level of dTMP as well (P= 0.06, n=3; Figure 6.9B) and a considerable reduction in dTTP intensity (P<0.001; Figure 6.9C). Interestingly, no significant changes were observed in dTMP and dTTP levels of *L. mexicana* cells exposed to 5F-Urd, suggesting that *L. mexicana* is better able to compensate for loss of TS activity, probably by thymidine salvage from the medium and the activity of TK.

Other changes after 5F-Urd exposure were almost identical to the changes caused by 5-FU and 5F-2'dUrd, such as an increase in the level of 2'deoxyuridine in *L. mexicana* and *L. major*. Moreover, it was also found that in both *Leishmania* species 5F-Urd caused a significant increase in the levels of 2'deoxynucleotides of cytidine and adenosine compared with respective untreated controls; these changes were similar to the effects of 5-FU and 5F-2'dUrd on *Leishmania* cells.
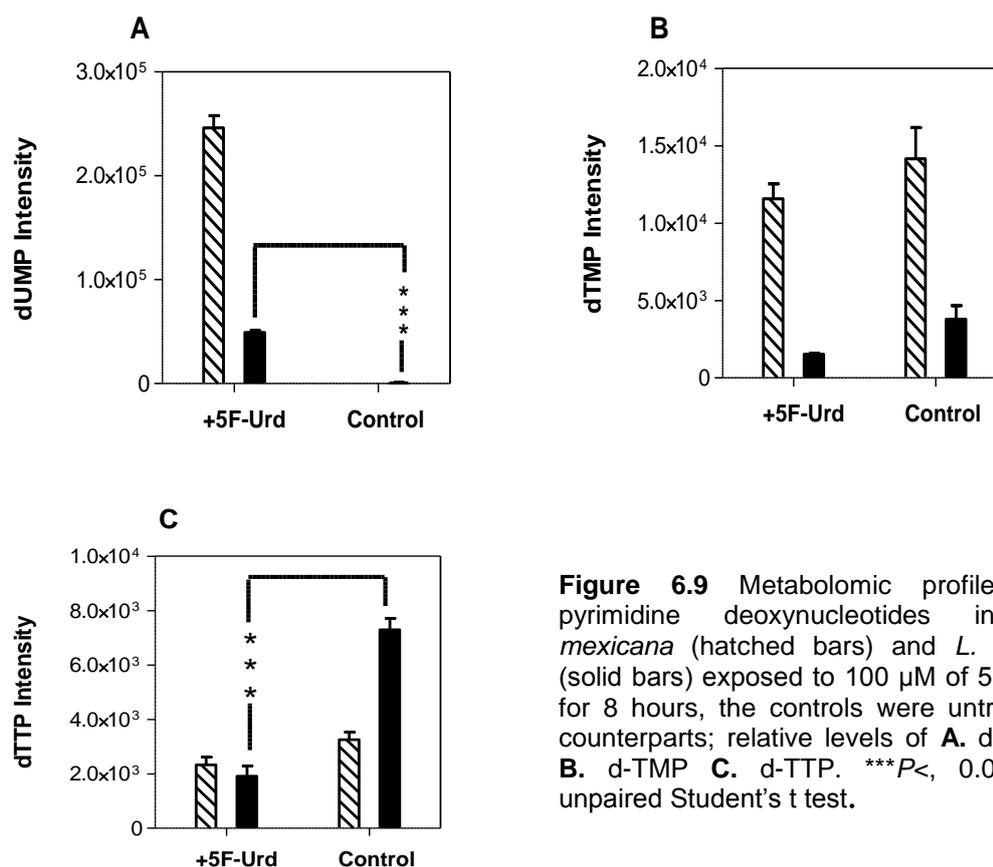
Figure 6.9 Metabolomic profiles of pyrimidine deoxynucleotides in *L. mexicana* (hatched bars) and *L. major* (solid bars) exposed to 100 µM of 5F-Urd for 8 hours, the controls were untreated counterparts; relative levels of **A.** d-UMP **B.** d-TMP **C.** d-TTP. ***$P<$, 0.01 by unpaired Student's t test.

5-Fluorouridine increased the level of 2'-deoxyuridine in *L. mexicana* and *L. major* (P=0.001 and P=0.012, respectively; Figure 6.10A) that was similar to 5-FU and 5F-2'dUrd effect. Exposure of *L. mexicana* to 100 µM of 5F-Urd for 8 hours did not change the level of 2'deoxyadenosine, but did lead to a significant increase of 2'deoxyadenosine in *L. major* promastigotes ($P<0.001$; Figure 6.10B). This observation might be related to the low sensitivity of *L. mexicana* to 5F-Urd as it seems to indicate a difference in regulation of the dinucleotide reductase in the two species. Another notable difference between *L. mexicana* and *L. major* after 5F-Urd treatment was a significant variation in thymidine intensity; while the level of thymidine in *L. mexicana* was significantly elevated (P=0.006) after 5F-Urd exposure, the drug led to a considerably decreased thymidine intensity in *L. major* (P=0.017; Figure 6.10C).

A

B

C
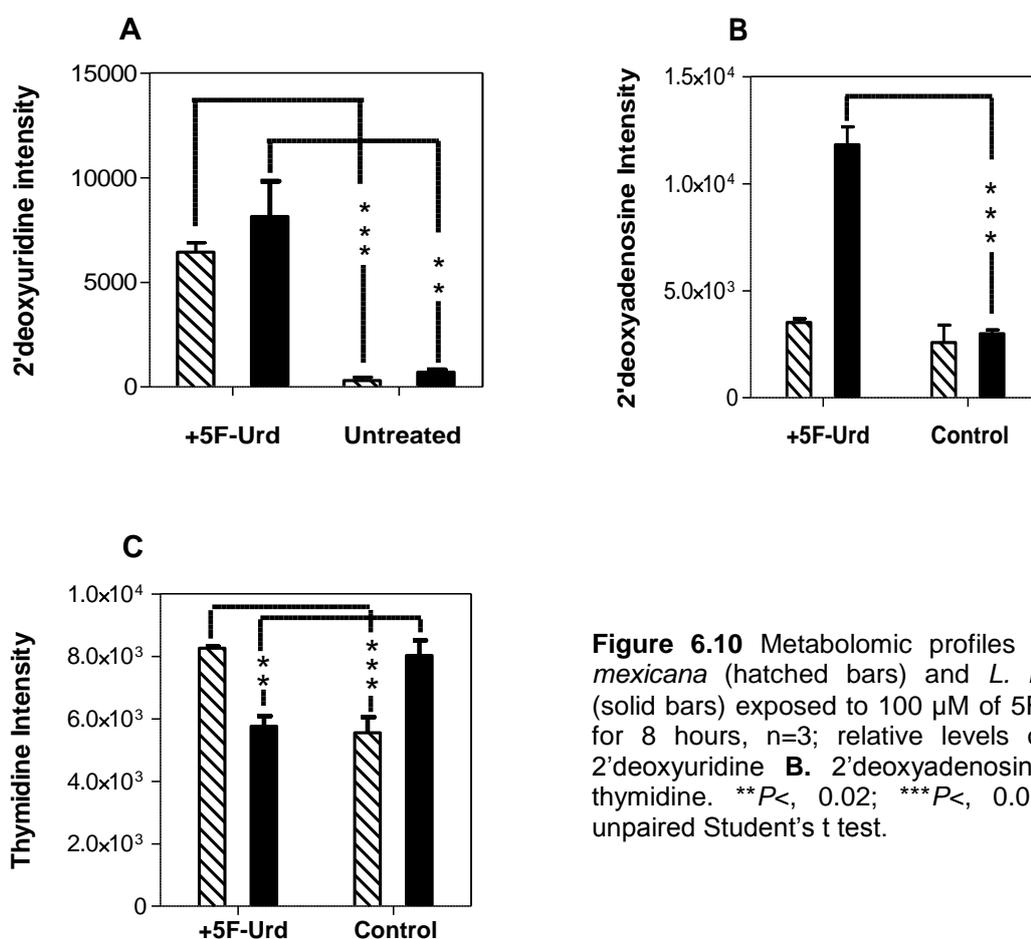
Figure 6.10 Metabolomic profiles of *L. mexicana* (hatched bars) and *L. major* (solid bars) exposed to 100 µM of 5F-Urd for 8 hours, n=3; relative levels of **A.** 2'deoxyuridine **B.** 2'deoxyadenosine **C.** thymidine. **$P<$, 0.02; ***$P<$, 0.01 by unpaired Student's t test.

The other natural pyrimidine and purine metabolites were mostly unchanged in *Leishmania* promastigotes treated by 5F-Urd compared with their relative untreated controls. The only common change in *L. mexicana* and *L. major* species treated by 5F-Urd was a significant increase in the level of uracil (P=0.029, P= 0.044, respectively), this increase was also observed in case of 5F-2'dUrd treatment. This elevation could perhaps be attributed to the inhibition of thymidylate synthase of *Leishmania* spp. Furthermore, there were some other common effects on each species of *Leishmania* by the tested fluorinated pyrimidines. For instance, the level of ATP in *L. mexicana* was elevated by 5-FU, 5F-2'dUrd and 5F-Urd, (P=0.06, 0.09, and 0.025, respectively); all three drugs also increased the level of cytosine intensity (P=0.06, 0.05, and 0.01, respectively); for *L. major*, the drugs led to clear reductions in the level of thymine (P=0.025, 0.01, and 0.003, respectively) and cytidine (P=0.025, 0.017, and 0.1, respectively), and also caused a significant increase in the intensity of guanine (P=0.06, 0.05, and 0.01, respectively).

6.5. Discussion

In order to identify which cytotoxic pyrimidine metabolites would efficiently target *Leishmania*'s pyrimidine pathway enzymes, we attempted to investigate the conversion of most effective pyrimidine analogues into metabolites to form harmful chemicals. The metabolism of fluorinated pyrimidine analogues in *Leishmania* species showed some differences compared to *T. b. brucei*. Although 5-FU and 5F-2'dUrd followed different routes of metabolism in trypanosomes, they follow a similar pathway of metabolism in *Leishmania* cells. The different fluorinated pyrimidines were also differentially metabolised in mammalian cells. For instance, when human L1210 leukaemia cells were exposed separately to 5-FU and 5F-2'dUrd, the drugs showed different metabolic pathways and had different modes of action (Roobol *et al.,* 1984). 5-FU incorporated into the RNA of trypanosomes and into precursors for glycosylation (Ali *et al.,* 2013a), but exposing *Leishmania* cells to effective pyrimidine analogues showed no detectable fluorinated ribonucleotides and we conclude that *Leishmania* uracil phosphoribosyltransferase does not accept 5-FU as a substrate. In fact, the number of detected fluorinated pyrimidine metabolites was very limited after exposing *Leishmania* cells to 100 μM of fluorinated pyrimidine analogues.

However, there were a surprising number of changes detected in natural purine and pyrimidine metabolites, showing that the 5-fluoro- analogues have some (indirect) effect on much of the nucleoside/nucleotide metabolism. *Leishmania* cells, like trypanosomes, are unable to produce 5F-Urd from 5-FU or 5F-2'dUrd, but they can produce very high levels of 5-FU following sub-lethal doses of 5F-Urd. The only fluorinated pyrimidine nucleoside detected after 5-FU treatment was 5F-2'dUrd at a very low level, so that uridine phosphorylase in *Leishmania* seems a reversible enzyme, at least for the 2'dUrd/uracil reaction. Indeed, 5F-2'dUrd and 5F-Urd are efficiently metabolized to 5-FU, which means that these drugs are good substrates for uridine phoshporylase. Notwithstanding the fact that the uracil transporter is >20-fold more sensitive to 5-FU in *L. major* cells than in *L. mexicana* (Chapter 4), both strains showed the same intensity of 5-FU in the metabolomic profile, after exposure to the same concentration of the drug and for an equal incubation period. However, it is not possible to

directly compare the two groups quantitatively without the use of internal controls of known quantity.

The observation that 5-FU is not a substrate for *Leishmania* uracil phosphoribosyltransferase (UPRT), but is for *Leishmania* uridine phosphorylase (UP) indicates changes in the way uracil is bound by these two enzymes, with UPRT more sensitive to 5-position substitutions.

Surprisingly, all of the pyrimidine analogues, 5-FU, 5F-2'dUrd and 5F-Urd, were principally converted to 5F-dUMP, in contrast to the situation in *T. brucei* (Ali *et al.,* 2013a). *Leishmania* cells metabolized 5-fluorouracil and 5-fluorouridine to 5-fluoro-2'deoxyuridine, which was phosphorylated by thymidine kinase to produce 5F-dUMP; no fluorinated uridine nucleotides were detected in the metabolome of the fluorinated pyrimidines-exposed *Leishmania*, nor were 5F-dUDP or 5F-dUTP present in detectable quantities, so it must be concluded that 5F-dUMP is not a substrate for thymidylate kinase. Instead the most important alteration in the metabolome of the fluorinated pyrimidines-treated *Leishmania* species was a large increase in dUMP levels, strongly suggesting that the mechanism of action of these pyrimidine analogues is the inhibition of dihydrofolate reductase-thymidylate synthase (DHFR-TS), blocking the conversion of dUMP to dTMP. This observation is very similar to the effect of 5-FU on human cancer cells (Longley *et al.*, 2003). TS of mammalian cells transfers the methyl group from methylene tetrahydrofolate to carbon in position 5 of dUMP to form dTMP (Santi & McHenry, 1972). In the case of 5F-dUMP, the presence of the fluorine atom at that position prevents the transmethylation and thus stalls the folate cycle; it seems that *Leishmania* thymidylate synthase is unable to break the strong carbon-fluorine bond to allow the methylation to take place. The inhibition of TS thus caused a build-up of dUMP and a concomitant decrease in thymidine nucleotides. The depletion of thymidine nucleotides may be further enhanced by inhibition of thymidylate kinase by 5F-dUMP, a structural analogue of the dTMP substrate, in addition to potential inhibition of thymidine kinase by 5F-2'dUrd.

The combined effect of these enzyme inhibitions is an imbalance between deoxyuridine nucleotides and thymidine nucleotides. It seems that the depletion of deoxythymidine nucleotides activates changes in nucleoside and nucleotide

pools. There were clear increases in the intensity of deoxyuridine and deoxycytidine nucleotides, but these were probably secondary to the dUMP elevation. Furthermore, thymidine deoxynucleotide (dTMP and dTTP) levels were decreased in *Leishmania* promastigotes after exposing to 100 µM of 5-fluoro-pyrimidine analogues (with the exception 5F-Urd on promastigotes of *L. mexicana*). The significant increase in the levels of deoxyuridine might be attributed to the inhibition of thymidine kinase which led to an increase in the free deoxynucleoside levels in fluorinated pyrimidine-treated cells. However, very recently 2-deoxyuridine has been found as a very poor substrate for TK (Castillo-Acosta *et al.,* 2013). Therefore, we suggest that the elevations in 2'deoxy purine and pyrimidine nucleosides and nucleotides in promastigotes of *Leishmania* cells that were exposed to fluorinated pyrimidines could be related to activation of the allosterically regulated enzyme ribonucleoside reductase (RNR). As a result, the enzyme may produce too much dNDP product, which was not being used. Therefore, these are broken down to dNMPs and subsequently to free 2'deoxynucleosides. Particularly, the conversion of dNDPs to dNTPs is highly regulated.

Although *Leishmania* promastigotes showed different mechanisms of resistance to fluorinated pyrimidine analogues, through loss of different transporters (chapter 4), mostly, there were many close similarities between the cellular effects of fluorinated pyrimidine analogues (5-FU, 5F-2'dUrd and 5F-Urd), indicating a common mode of action on *L. mexicana* and *L. major*. The specific difference was the effect of 5F-Urd, particularly in that *L. mexicana* was extremely resistant to the compound, whereas the other species was very sensitive. This cannot be attributed to differences in uridine transport between the species, which, if anything, seems to be higher affinity and more efficient in *L. mexicana* (Tables 4.1 and 4.2). Nor can it be argued that LmexNT1 does not transport substrates with the 5F substitution, as 5F-2'dUrd displayed the exact same affinity as 2'dUrd for this carrier (Table 4.1), and 5F-2'dUrd was highly active against *L. mexicana* promastigotes (Table 4.4). In addition, 5F-uridine was detected in the metabolomic profile of *L. mexicana*, after exposure to this compound, albeit at a lower mass-spectrometric intensity than in *L. major*. However, a notable difference in the metabolomic profile of the two species was that after 5-fluorouridine treatment no 5F-2'dUrd was detectable in *L.*

mexicana, whereas this was clearly present in *L. major*, despite the fact that 5-FU was clearly generated from 5F-Urd in both species, and in comparable amounts. More surprisingly, the level of 5F-dUMP in *L. mexicana* was 9.2-fold higher than in *L. major* (P= 0.028; Figure 6.7C), which can only have been generated from 5F-2'dUrd; this is accompanied by the predicted build-up of dUMP (higher in *L. mexicana*) by inhibition of TS (Figure 6.9A).

It thus follows that, whereas both species generate 5F-2'dUrd from 5F-Urd by the double action of uridine phosphorylase (with 5-FU as intermediate product), this is more rapidly converted by thymidine kinase to 5F-dUMP in *L. mexicana* than in *L. major*, explaining both the absence of the substrate and the higher level of the product in *L. mexicana* promastigotes. The other evidence is that the level of 5F-2'dUrd was below detection limit in *L. mexicana* treated with 5-FU, which shows the rapid conversion of 5F-2'dUrd to 5F-dUMP by promastigotes of this species. However, this still does not appear to explain the insensitivity of *L. mexicana* to 5F-Urd. The key observation for this is that thymidine nucleotide levels in *L. major* are substantially reduced relative to untreated controls, but are not significantly different in *L. mexicana*, in which dTMP levels in any case were much higher than in *L. major* (Figure 6.8B). We conclude that the biosynthesis of thymidine is substantially inhibited in *L. major*, through inhibition of both TS in the *de novo* pathway (by 5F-dUMP) and TK in the salvage pathway (by 5F-2'dUrd), whereas there is no inhibition of TK in *L. mexicana* due to the absence of 5F-2'dUrd, allowing a bypass from the inhibition of TS and a sufficient synthesis of thymidine nucleotides. This interpretation is corroborated by the fact that LmajNT1 has only low affinity for thymidine, allowing at best a poor rate of salvage, whereas LmexNT1 displays a K_m of just 4.2 ± 0.4 μM for thymidine, identical to its affinity for uridine (Table 4.1); the source of the thymidine for salvage is the 10% of FBS in the HOMEM medium. This model also explains why 5F-2'dUrd is active against *L. mexicana*, as this agent generates a sufficiently high concentration of 5F-2'dUrd in the cell to also block TK, despite the efficient conversion to 5F-dUMP. Our overall conclusion is that 5-fluoropyrimidines exert their anti-leishmanial activity through inhibition of both thymidylate synthase and thymidine kinase (Figure 6.11).
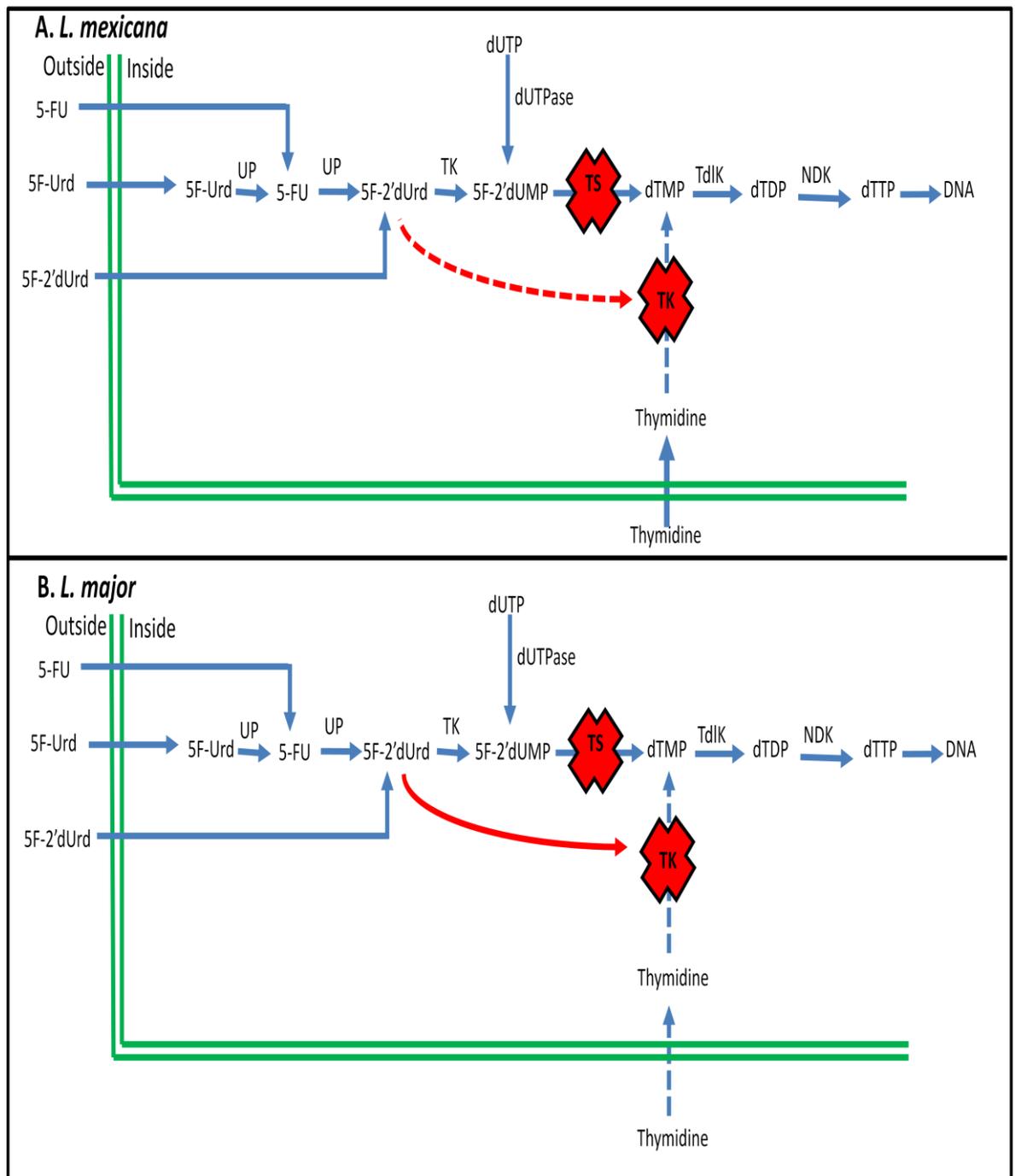
Figure 6.11. The metabolism of fluorinated pyrimidines in promastigotes of **A.** *L. mexicana* and **B.** *L. major*. The double green line refers to cell membrane. The blue arrows refer to pyrimidine salvage or conversion, when thick show high flow and when dotted show poor uptake; the red curved-arrows refer to the block of thymidine kinase by 5F-2'dUrd, the dotted line means low amount and inadequate to block TK when the treatment is with 5F-Urd, although sufficient when the treatment is 5-FU or 5F-2'dUrd. Abbreviations above the blue arrows are referred to: UP = uridine phosphorylase, TK = thymidine kinase, TdlK = thymidylate kinase, TS = thymidylate synthase, NDK = nucleoside diphosphate kinase.

CHAPTER SEVEN

Construction and characterisation of a pyrimidine auxotrophic *Trypanosoma brucei* clone

7.1 Introduction

Trypanosomes possess both the pyrimidine biosynthesis and salvage routes, and that would appear to make pyrimidine metabolism an unattractive drug target. Until the start of this project, it has not been established whether either pyrimidine biosynthesis or salvage is essential in African trypanosomes. Moreover, the salvage and biosynthesis pathways actually share most of the pyrimidine metabolizing enzymes, many of which have now been shown to be essential because (in contrast to purine metabolism) there is little or no redundancy in the pathways. For example, dihydrofolate reductase - thymidylate synthase (DHFR-TS) is essential in trypanosomes and its knockout can only be rescued by high levels of thymidine (Sienkiewicz *et al.*, 2008), and CTP synthetase is essential as *T. b. brucei* are unable to incorporate extracellular cytosine or cytidine in their nucleic acids (Hofer *et al.*, 2001). Furthermore, *T. b. brucei* deoxyuridine 5'-triphosphate nucleotidohydrolase (dUTPase) was recently shown to be essential (Castillo-Acosta *et al.*, 2008, 2013) and it is clear that several other enzymes of the same pathways may equally be good drug targets.

However, it is as yet unclear whether either the uptake of extracellular pyrimidines or the *de novo* biosynthesis of the first pyrimidine nucleotide, UMP, is essential in kinetoplastid parasites. It has been previously shown that in procyclic *T. b. brucei* pyrimidines are mainly taken up through the TbU1 uracil transporter (De Koning & Jarvis, 1998; Gudin *et al.*, 2006) and recently we have completed a study of pyrimidine transport activities in bloodstream form *T. b. brucei* showing the presence of only one high affinity uracil transporter, TbU3, and almost no uptake of other pyrimidines at physiological levels (Ali *et al.*, 2013a). A previous study, by (Arakaki *et al.*, 2008) showed that RNAi disruption of one of the biosynthesis enzymes, dihydroorotate dehydrogenase, led to impaired growth which could be compensated for by pyrimidine uptake. The rescue by extracellular uracil, however, was not observed in the presence of the TbU3 inhibitor 5-fluorouracil (Arakaki *et al.*, 2008). In the present study we simulated complete inhibition of pyrimidine salvage by *in vitro* growth in pyrimidine-free medium and inhibition of *de novo* biosynthesis through the construction of a genetic deletion mutant lacking the final step of the pyrimidine biosynthesis pathway, which in trypanosomes is a fusion of the two

enzymes orotidine monophosphate decarboxylase (*PYR6*, OMPDCase) and orotate phosphoribosyl-transferase (*PYR5*, OPRT) (Gao *et al.,* 1999; Scahill *et al.,* 2008). The *PYR6-5$^{-/-}$* trypanosomes were characterized *in vitro* and *in vivo*. While they were completely non-viable in the absence of pyrimidines *in vitro*, they were able to grow on low levels of pyrimidines, similar as reported for *L. donovani* promastigotes (French *et al.,* 2011). In this chapter we investigated the activity of the TbU3 transporter and expression of uridine-phosphorylase in pyrimidine auxotrophic trypanosomes. We also assessed the sensitivity of *PYR6-5$^{-/-}$* cells to fluorinated pyrimidine analogues, and determined the DNA content of these bloodstream forms. In addition, the study established an infection of *PYR6-5$^{-/-}$* trypanosomes in mice. We exclude *Leishmania* species from this project as (Wilson *et al.,* 2012) have very recently published a paper addressing this issue in *L. donovani*.

7.2.   Generation   and   confirmation   of   pyrimidine auxotrophic *T. b. brucei* s427 mutants

A schematic representation of the generation of a *PYR6-5$^{-/-}$* strain is shown in Figure 7.1A. Plasmids with the positive selection marker hygromycin phosphotransferase (HYG) and the negative selection marker *Herpes simplex* virus thymidine kinase (HSVTK) (generous donation from George Cross, Rockefeller University, New York) were used. Bloodstream forms of *T. b. brucei* s427 (1×10^6 cells ml^{-1}) were transformed with the *loxP*-HYG-HSVTK-*loxP* cassette using an Amaxa Nucleofector. The transformants were grown in selective medium containing 4.5 μg ml^{-1} hygromycin (Sigma) and were cloned using limiting dilution, creating a heterozygote *PYR6-5$^{+/-}$* strain. Viable clones with the desired insert were subjected to increasing drug pressure with 5-fluoroorotic acid (5-FOA) leading to loss of the second *PYR6-5* gene (loss of heterozygosity) at 100 μM (Figure 7.1B). Loss of heterozygosity (LOH) and the generated homozygous *PYR6-5$^{-/-}$* were further confirmed using Southern blot (Figure 7.1C).
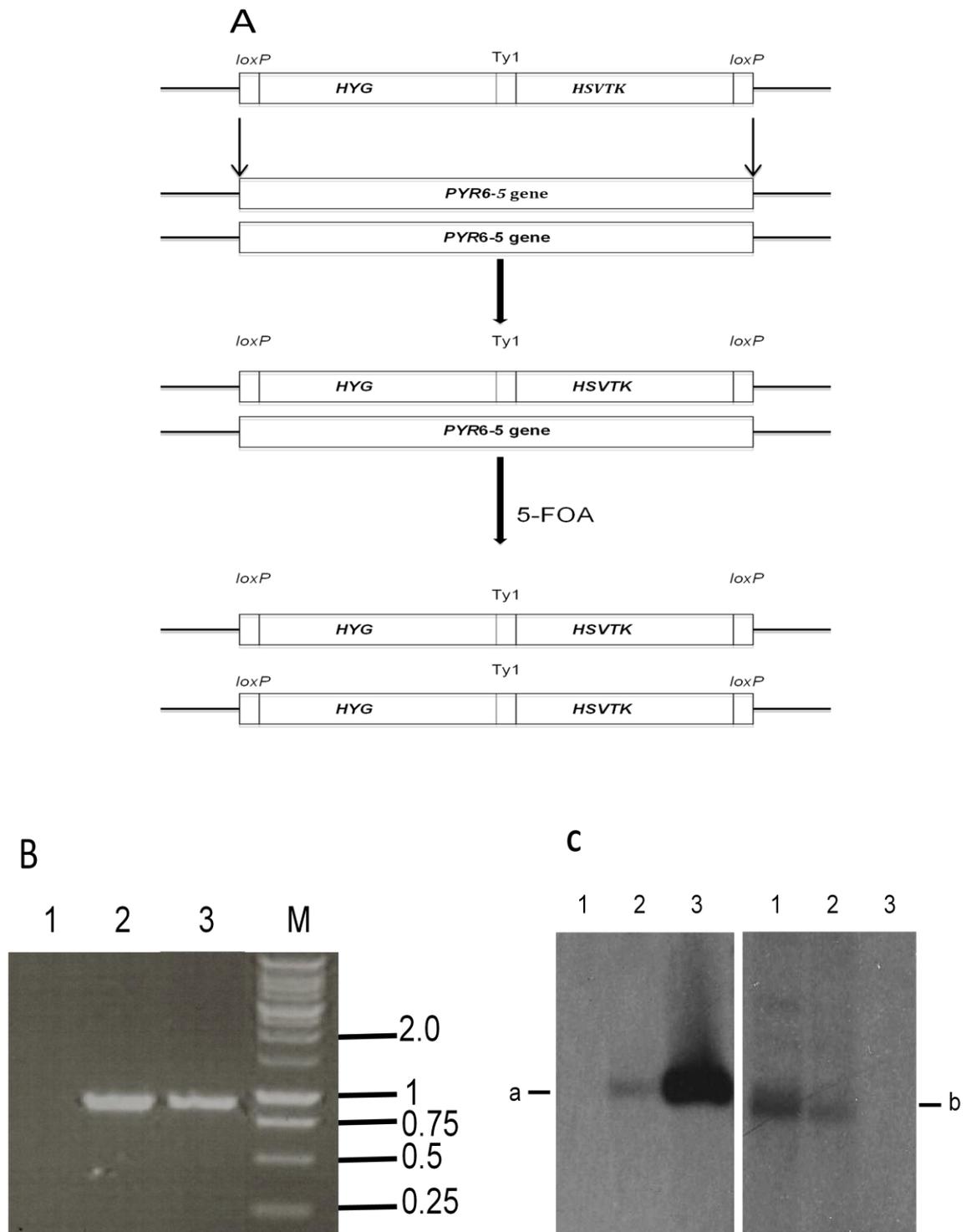
Figure 7.1. Generation of Pyr6-5 Knockouts. **A.** Schematic representation of the generation of Orotidine Monophosphate Decarboxylase (OMPDCase) knockout. The first step is replacement of one PYR6-5 allele with a construct containing both positive selection marker hygromycin phosphotransferase (HYG) and negative marker Herpes simplex virus thymidine kinase (HSVTK) between 34-bp loxP elements. The second step creates the homozygous PYR6-5$^{-/-}$ through drug pressure with 5-fluoroorotic acid, causing loss of heterozygosity. **B.** PCR analysis of the PYR6-5 gene, generating an 870 bp amplicon as described in the Materials and Methods section confirmed the absence of the gene in Pyr6-5$^{-/-}$ (lane 1) and its continued presence in Pyr6-5$^{+/-}$ (lane 2); and lane 3 which is the control with WT s427 DNA. **C.** Southern blot confirming knockout strategy, using probes for the PYR6-5 locus and for the HYG-HSVTK cassette. Lane 1, Pyr6-5$^{-/-}$, lane 2, Pyr6-5$^{+/-}$, Lane 3, WT s427; and 'a' is PYR6-5, band 'b' is HYG-HSVTK.

7.3. Growth of pyrimidine auxotrophs on different pyrimidine sources

Under standard culture conditions there was no clear growth phenotype associated with loss of the *PYR6-5* locus, as growth of the knockout cells in standard HMI-9 was similar to that of WT-s427 trypanosomes in HMI-9[-tmd] supplemented with 10% dialysed FBS (Figure 7.2). *PYR6-5^{-/-}* cells were grown either in standard HMI-9 or in HMI-9[-tmd], which does not contain any pyrimidines but does contain 1 mM hypoxanthine as a purine source (Appendix I) and is supplemented with FBS that was extensively dialysed to remove small molecules such as nucleosides.
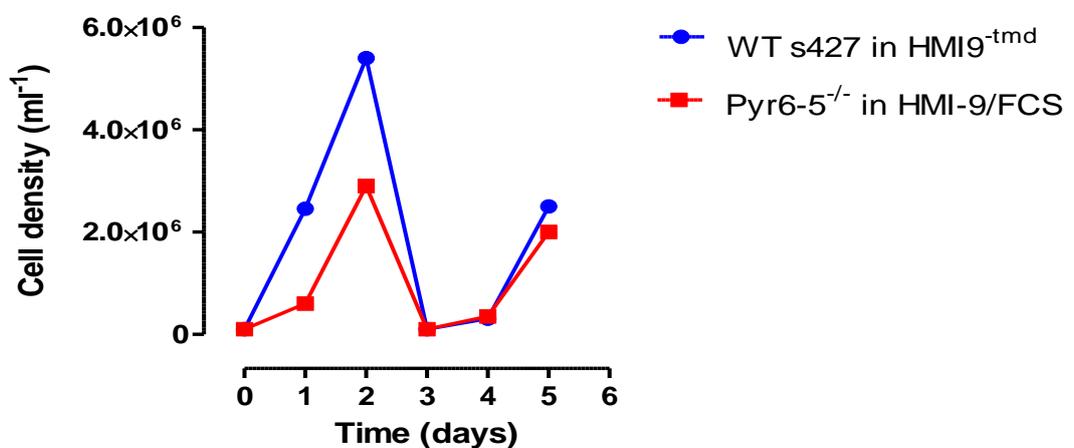
Figure 7.2. Growth of *PYR6-5[/-] T. b. brucei* bloodstream forms in standard HMI-9 and s427-WT in HMI-9[-tmd] supplemented with 10% dialyzed FBS. Seeding density was 1×10^5 cells ml^{-1} and cells were manually counted every 24 hours. On day 3 cells were sub-passaged to relevant fresh medium, again at 1×10^5 cells ml^{-1}.

As expected, *PYR6-5^{-/-}* cells were unable to grow in this semi-defined medium without pyrimidines, and the trypanosome population rapidly declined after 24 hours (Figure 7.3A,B). In contrast, a shift to purine-free conditions only caused growth arrest after approximately 48 hours (Figure 7.3B), consistent with previous observations in procyclic *T. brucei* (De Koning & Diallinas, 2000) and promastigotes of *L. donovani* (Carter *et al.,* 2010). Evidently, any interruption in pyrimidine supply rapidly makes trypanosomes non-viable and we investigated how quickly the damage becomes irreversible (Figure 7.3A), by adding back 100 µM uracil at various times after passage of *PYR6-5^{-/-}* to HMI-9[-tmd]. Cells grew to the same density as in standard HMI-9 when uracil was added immediately after passage (0 hours control) but adding the uracil after as little as 12 hours resulted in irreversible growth arrest and the eventual death of the parasite population. From 24 hours, the addition of uracil was almost redundant, with the cell

population declining as rapidly as in continuously pyrimidine-free conditions (Figure 7.3A).
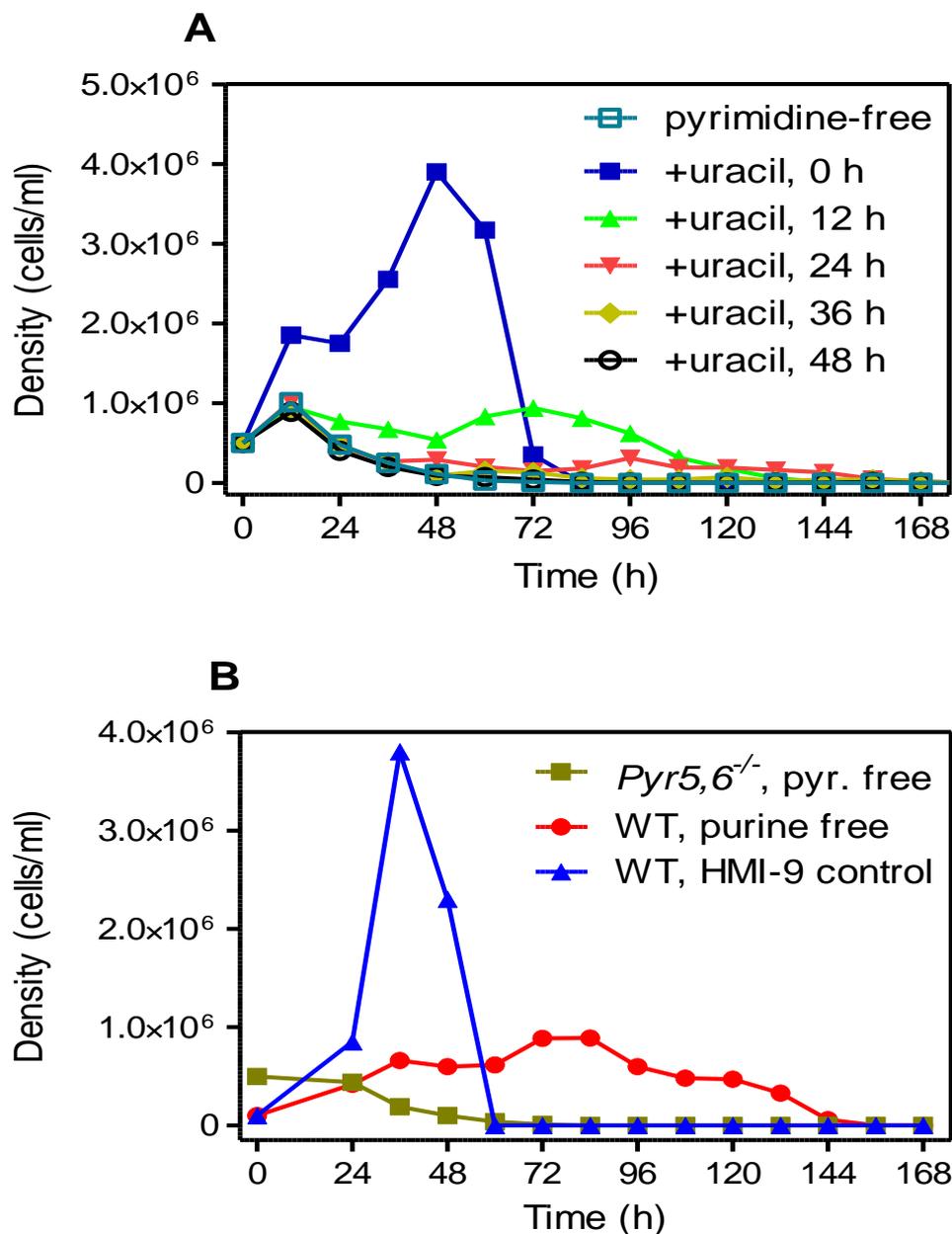
Figure 7.3. Growth of bloodstream form *T. b. brucei* in media with various purine and pyrimidine content. **A.** *Pyr5-6$^{-/-}$* trypanosomes were transferred from HMI-9 to HMI-9^{-tmd} (pyrimidine-free, □) medium to which subsequently uracil was added to a final concentration of 100 µM at the indicated time after seeding the culture. Samples were taken every 12 h and cell densities determined using a haemocytometer. In cultures with conditions that allowed fast growth, the trypanosome population declined after 36 - 48 h due to overgrowth. Cell population in the '0 hours' group declined after 60 h due to over-growth and exhaustion of the medium. **B.** Comparison of purine-free and pyrimidine conditions. WT s427 cells were passaged from mid-log cultures (grown in standard HMI-9 into fresh cultures with the same medium (control, ▲) or the same medium without hypoxanthine and supplemented with dialysed serum (purine free, ●). Pyrimidine-auxotrophic *T. b. brucei* (*PYR6-5$^{-/-}$*) were transferred from standard HMI-9 into HMI-9^{-tmd} (pyrimidine-free, ■) medium. Cell population in the 'WT, HMI-9 control' group declined sharply after 36-48 hours due to over-growth and exhaustion of the media.

We next tested the ability of these cells to grow on 100 µM or 1 mM (Figure 7.4) of each natural pyrimidine nucleoside or nucleobase. At the lower concentration, uracil supported near-normal growth but at 1 mM appeared to have become somewhat growth inhibitory and growth was less pronounced, possibly because the resulting excessive uracil influx could cause an imbalance between pyrimidine nucleotides and 2'deoxyribonucleotides, or between purine and pyrimidine nucleotides. Uridine also supported growth at 100 µM and even better at 1 mM, whereas 2'-deoxyuridine barely had any effect at all at 100 µM. Of the other pyrimidines, only cytidine had any effect on growth, and only at 1 mM.
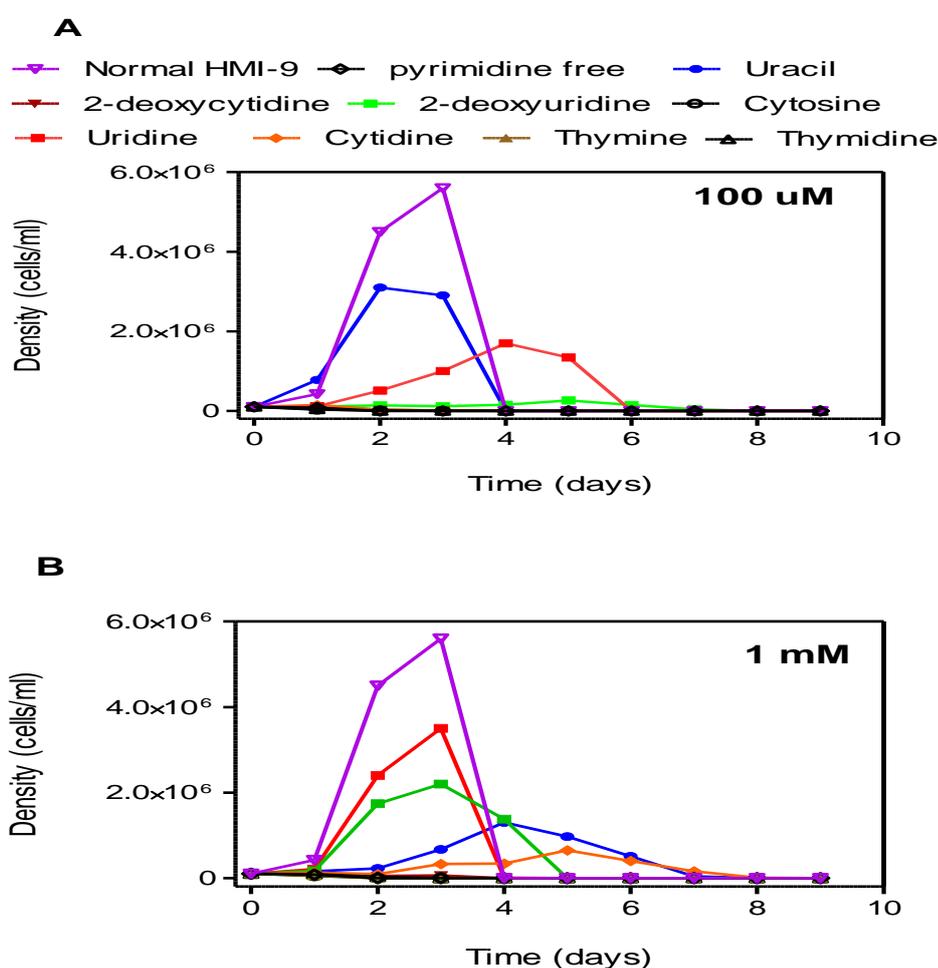
Figure 7.4. Growth of pyrimidine auxotrophic *T. b. brucei* bloodstream forms on various pyrimidine sources. *PYR6-5*^{-/-} cell cultures were seeded at a density of 1×10^5 cells ml^{-1} and cultured at 37 °C/5% CO_2, either in normal HMI-9 or in a simplified pyrimidine version supplemented with dialysed FBS and the indicated pyrimidine source at **(A)** 100 µM or **(B)** 1 mM. Samples were taken every 24 hours and cell densities determined using a haemocytometer, in duplicate. The experiment shown is representative of several similar experiments with essentially identical results. In cultures with conditions that allowed fast growth, the trypanosome population declined after 36 - 48 hours due to overgrowth.

7.4. [^{3}H]-Uracil uptake in pyrimidine auxotrophic *T. brucei*

We determined uracil uptake rates in *Pyr6-5$^{-/-}$* and control s427-WT cells to assess whether uracil uptake capacity in bloodstream form *T. b. brucei* increased in the absence of pyrimidine biosynthesis. WT and *Pyr6-5$^{-/-}$* were grown in standard HMI-9 and uptake of 0.15 μM [^{3}H]-uracil was measured in a timecourse over 120 s. The initial rate of uracil uptake was consistently higher in the *Pyr6-5$^{-/-}$* cells (Figure 7.5A). The rates were 0.0109 ± 0.0001 and 0.0241 ± 0.0014 pmol (10^7 cells)$^{-1}$s^{-1} for WT and *Pyr6-5$^{-/-}$* trypanosomes, respectively (n=3; *P*<0.05, Student's T-test, unpaired). The increased uptake rate could not be attributed to the expression of an additional uracil transporter in the knockout strain not present in the WT cells, as K_m values were identical in both strains (0.31 ± 0.01 and 0.34 ± 0.03 μM, respectively (n=3)) and uracil transport was almost completely insensitive to uridine in both strains (K_i values >3 mM, n=3; Figure 7.5B). Indeed, uptake of 2.5 μM [^{3}H]-uridine was almost undetectable in both strains. However, the V_{max} for uracil transport was significantly increased in *Pyr6-5$^{-/-}$* cells (0.14 ± 0.01 versus 0.087 ± 0.007 pmol (10^7 cells)$^{-1}$s^{-1}, respectively; n=3, *P* = 0.012) (Figure 7.5C), consistent with the increased initial rate seen in the time course, and probably reflecting a higher number of the uracil transporter in the plasma membrane rather than the expression of a different or additional transport protein.

A

B

C
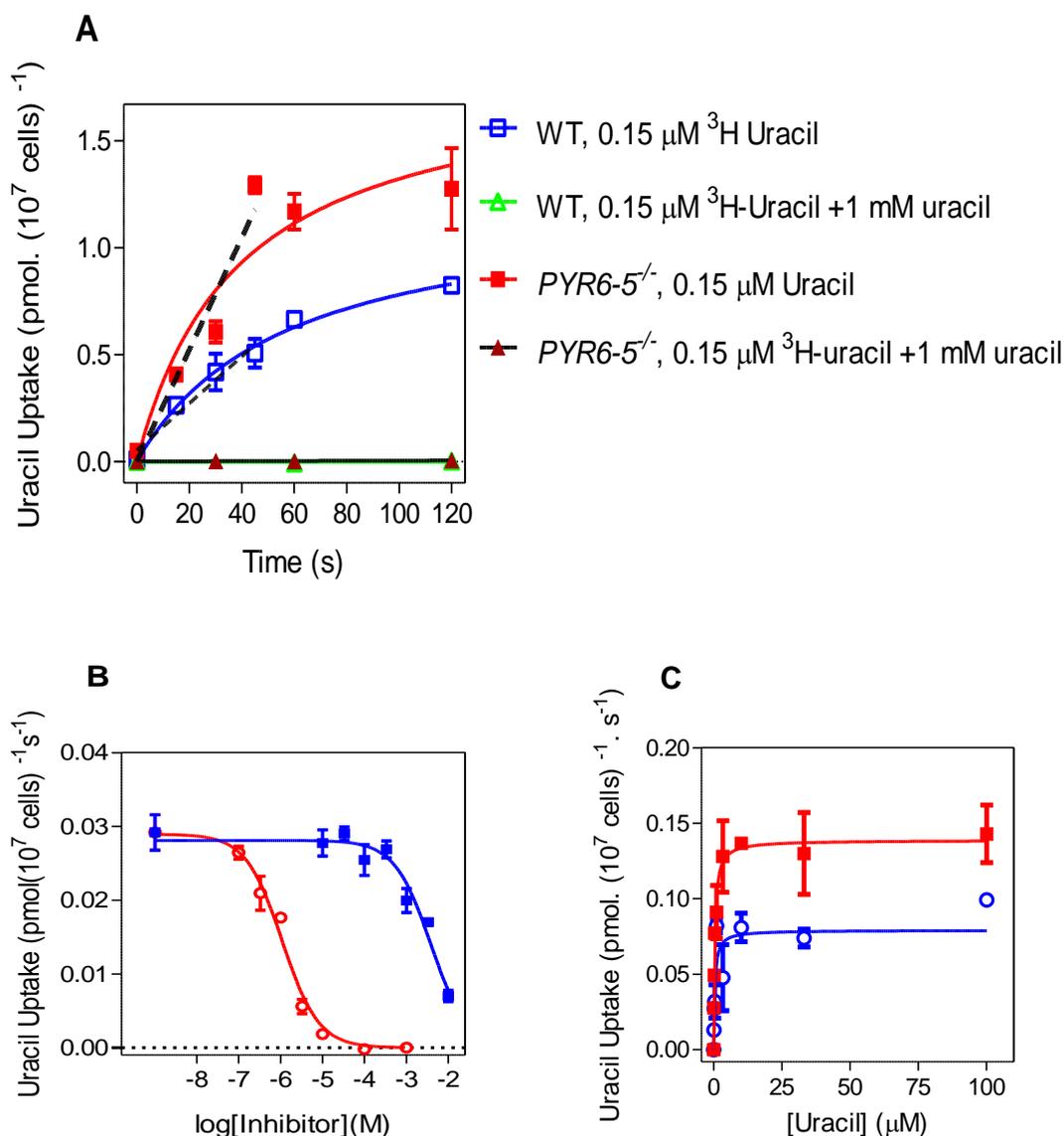
Figure 7.5. Uracil transport by *T. b. brucei* bloodstream forms. **A.** Timecourse of 0.15 µM [^{3}H]-uracil uptake by WT-s427 and by *PYR6-5*$^{-/-}$ cells, in the presence or absence of 1 mM unlabelled uracil, as indicated. Dashed lines represent linear regression over the first 50 s, yielding correlation coefficients of 0.97 and 0.92 for the knockout and WT strains, respectively. In the presence of excess unlabeled uracil uptake was not significantly different from zero (F-test) for both strains. The experiment shown is representative of three identical experiments with highly similar outcomes and shows average and SE of triplicate determinations. In the presence of 1 mM uracil, the lines for WT and *PYR6-5*$^{-/-}$ were superimposed. **B.** Uptake of [^{3}H]-uracil by *PYR6-5*$^{-/-}$ trypanosomes was measured over 30 s in the presence or absence of unlabelled uracil (○) or uridine (■) at the indicated concentrations. The data was plotted to a sigmoid curve with variable slope which in the case of uridine inhibition was set at zero for its minimum. The data are the average and SE of triplicate determinations and the experiment shown is representative of several independent experiments with essentially identical outcomes. **C.** Michaelis-Menten saturation plots for uracil uptake of [^{3}H]-uracil by WT (○) or *PYR6-5*$^{-/-}$ (■) *T. b. brucei* bloodstream forms. The data represents the average and SE of three identical experiments, each performed in triplicate.

7.5. Sensitivity of pyrimidine auxotrophic of *T. b. brucei* to pyrimidine analogues

We tested whether pyrimidine auxotrophs were more sensitive to cytotoxic pyrimidine analogues and found that *Pyr6-5$^{-/-}$* cells are approximately one order of magnitude more sensitive to most analogues, including 5-fluorouracil and 5-fluoro-2'deoxyuridine (Table 7.1). The only exception was 5-fluoroorotic acid, whose action is dependent on OPRTase and OMPDCase, and to which the *Pyr6-5$^{-/-}$* cells were completely impervious up to 5 mM although WT trypanosomes were sensitive to this compound with an EC$_{50}$ of 13.2 ± 1.2 μM. Interestingly, the *Pyr6-5$^{-/-}$* strain was also sensitized to 5-fluorouridine whereas the WT cells were not sensitive to this compound up to the limit tested (5 mM).

Table 7.1. EC$_{50}$ values in μM for some pyrimidine analogues tested on WT-s427 and *PYR6-5$^{-/-}$* bloodstream forms grown in standard HMI-9, using a standard protocol based on the fluorescent indicator dye Alamar Blue. Resistance Factor (RF) is the ratio of the EC$_{50}$ values (μM) for knockout over WT strains. *P* value is based on an unpaired Students t-test.

Pyrimidine analogous	WTs-427 (AVG ± SE)	PYR6-5$^{-/-}$ (AVG ± SE)	RF	*P* value
5-Fluorouracil	35.9 ± 1.5	2.3 ± 0.07	0.06	<0.001
5F-2'deoxyuridine	4.6 ± 0.5	0.77 ± 0.10	0.16	0.002
5F-2'deoxycytidine	43.7 ± 4.4	4.6 ± 0.9	0.105	<0.001
5-Fluorouridine	>5000	472 ± 3	<0.09	<0.001
5-Fluoroorotic acid	13.2 ± 1.2	>5000	>380	<0.001

7.6. Expression of Uridine Phosphorylase in pyrimidine auxotrophs

We observed that cultures of *Pyr6-5*$^{-/-}$ cells appeared to be able to adapt to uridine as a sole pyrimidine source. In order to utilize uridine for the synthesis of pyrimidine nucleotides they need to generate uracil from it, using uridine phosphorylase (UPase) (Larson *et al.,* 2010). We thus inferred that upregulation of UPase could be a possible adaptation to pyrimidine starvation and performed quantitative PCR to assess relative UPase mRNA levels in WT and *Pyr6-5*$^{-/-}$ cells grown in different media. As shown in Figure 7.6, UPase expression was identical in WT cells grown in standard HMI-9 or in HMI-9^{-tmd} supplemented with 100 µM uracil, but was significantly increased after 48 hours growth on HMI-9^{-tmd} supplemented with 1 mM uridine ($P<0.001$). In *Pyr6-5*$^{-/-}$ cells cultured long-term in standard HMI-9 but transferred to HMI-9^{-tmd}/uracil for 48 hours UPase expression levels were higher than for s427-WT under the same conditions ($P<0.001$) and the level was further increased for *Pyr6-5*$^{-/-}$ cells grown 48 hours in HMI-9^{-tmd}/uridine ($P<0.001$). These data appear to indicate that *T. b. brucei* can adjust its UPase expression levels to accommodate growth on uridine as its sole pyrimidine source, whether these cells are pyrimidine auxotrophs or prototrophs. We next investigated whether *Pyr6-5*$^{-/-}$ strains can adapt when long-term cultured (two months) on uridine as sole pyrimidine source. We found that these cells do express significantly higher UPase levels than s427-WT control cells grown in standard HMI-9 or on HMI-9^{-tmd}/uracil ($P<0.01$), but revert quickly to control levels of expression when shifted to HMI-9^{-tmd}/uracil (Figure 7.6).
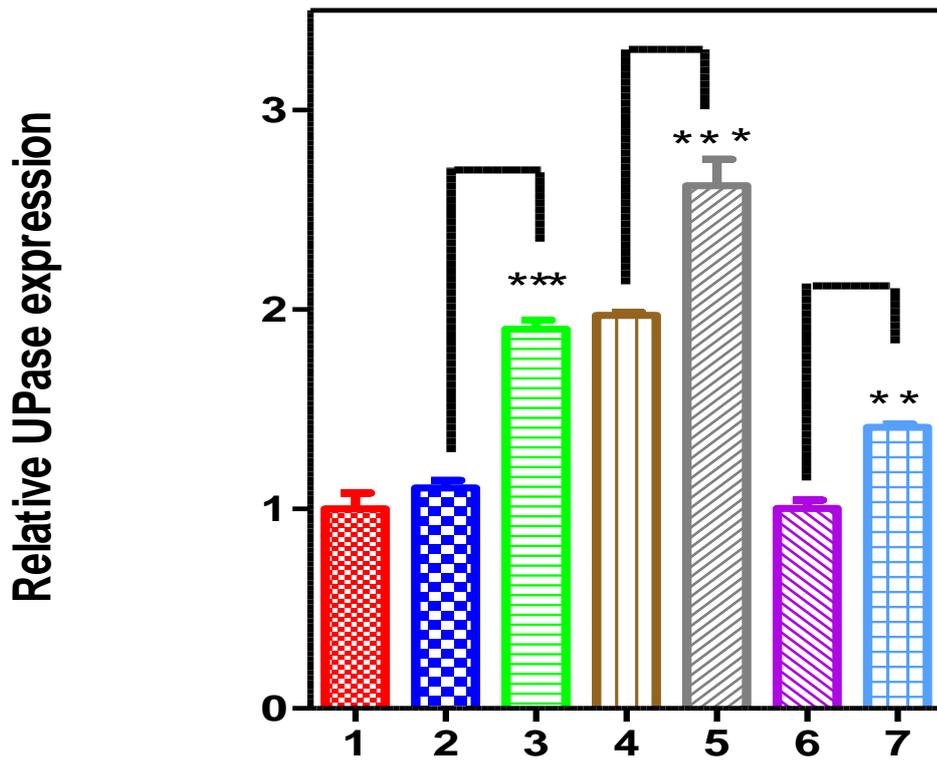
Figure 7.6. Comparative expression of uridine phosphorylase in wild-type and pyrimidine auxotrophic trypanosomes. Expression of uridine phosphorylase (UPase) was assessed by Real Time PCR in WT and *PYR6-5*^{-/-} strains grown under various conditions. The results are presented normalized to the control (group1) and are the average and SE of 8 replicates. **1.** Control: WT grown in HMI-9; **2.** WT grown 48 hours in HMI-9[-tmd] + 100 μM uracil; **3.** WT grown 48 hours in HMI-9[-tmd] + 1 mM uridine; **4.** PYR6-5^{-/-} grown 48 hours in HMI-9[-tmd] + 100 μM uracil; **5.** PYR6-5^{-/-} grown 48 hours in HMI-9[-tmd] + 1 mM uridine; **6.** PYR6-5^{-/-} long-term adapted to growth on uridine, grown 48 hours in HMI-9[-tmd] + 100 μM uracil; **7.** PYR6-5^{-/-} long-term adapted to growth on uridine, grown 48 hours in HMI-9[-tmd] + 1 mM uridine. Data were analysed with a one-way ANOVA with Tukey's correction. Horizontal asterisks indicate significant differences from control; vertical asterisks indicate significant differences between individual bars as indicated. **, $P<0.01$; ***, $P<0.001$.

7.7. The effect of pyrimidine starvation on DNA content and integrity of pyrimidine auxotrophic *T. b. brucei*

Pyrimidine auxotrophs die relatively rapidly in the absence of a salvageable pyrimidine source (uracil>uridine>2'deoxyuridine>cytidine; see figure 7.4), with death of the population progressing soon after 24 hours. To investigate the cause of the rapid cell death we examined DNA content of the *Pyr6-5*^{-/-} cells grown in HMI-9[-tmd] supplemented with 100 μM of various pyrimidines, using flow cytometry with the DNA-binding fluorophore propidium iodide; *Pyr6-5*^{-/-} cells grown in normal HMI-9 served as control. We found that DNA content in control cells presented a classical distribution of most cells in G1 phase (diploid), a small proportion in S-phase undergoing DNA synthesis and finally a percentage of the population in G2 phase (double set of chromosomes) (Figure 7.7). This profile was stable over the 48 hours of the experiment, although the proportion in G2 phase increased somewhat over this period, probably reflecting the mid-log phase of growth of the population at the end of the experiment, compared to early log phase at the start (% in G2 was 4.9 ± 2.8%, 11.6 ± 3.1% and 13.9 ± 1.9% at 24 hours, 36 and 48 hours, respectively; quantified using the ModFit software package). In sharp contrast, there was a rapid increase in cells displaying an incomplete complement of chromosomes in *Pyr6-5*^{-/-} cells grown in HMI-9[-tmd], resulting both in cells with less fluorescence (*i.e.* less DNA) than should be associated with normal G1 phase cells, or cells with a DNA content between G1 and G2 phase (Figure7.7). This clearly indicates that the cells are attempting cell division 'as normal' but are unable to complete chromosome synthesis due to lack of pyrimidine nucleotides, leading to aberrant cells with incomplete and fragmented chromosomes that are ultimately non-viable. This phenomenon progressed rapidly and at 48 hours few live cells could be detected. The cells that could be counted by the flow cytometer almost all contained incomplete and presumably fragmented DNA. Highly similar flow cytometry results were obtained when supplementing HMI-9[-tmd] with cytosine, thymine or thymidine, whereas supplementation with uracil or uridine produced profiles highly similar to the control (growth in standard HMI-9); addition of 2'deoxyuridine, cytidine or 2'deoxycytidine resulted in intermediate levels of DNA damage over 48 hours.
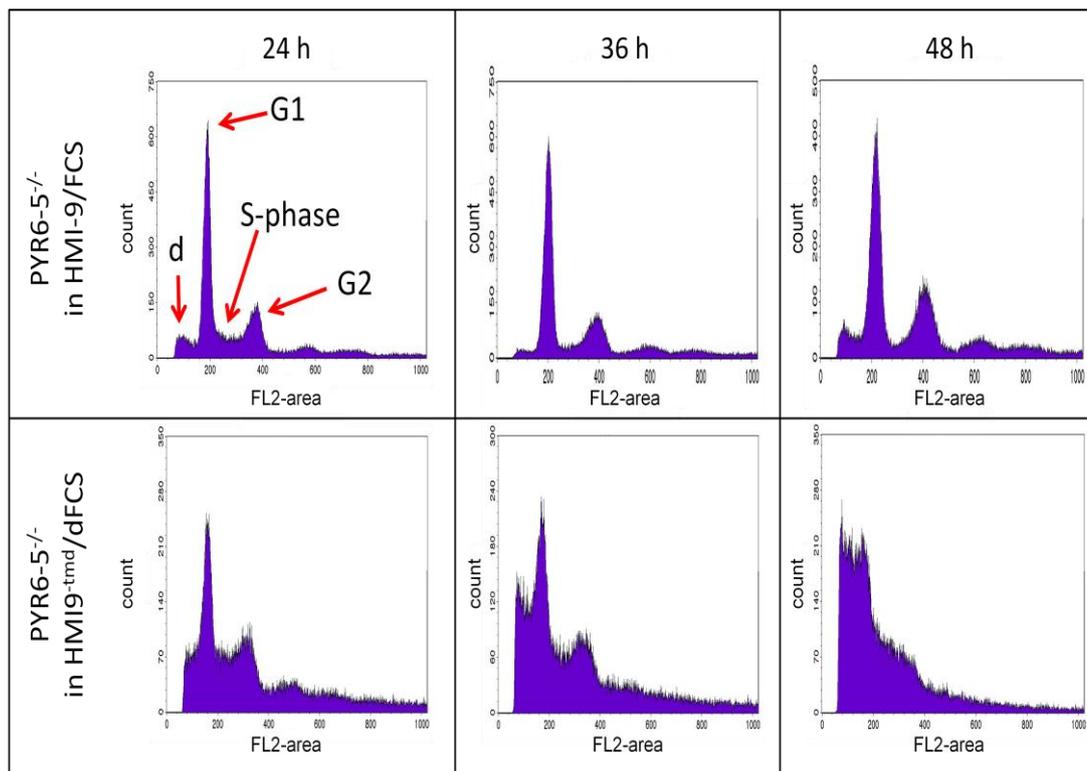
Figure 7.7. Flow cytometry for DNA content in bloodstream form *PYR6-5*^{-/-} cells. Pyrimidine auxotrophic trypanosomes were either incubated in standard HMI-9 or, in parallel, in pyrimidine-free HMI-9[-tmd] for up to 48 hours, stained with propidium iodide and prepared for flow cytometric analysis. Whereas control cultures show a classical distribution of cells in G1, S and G2 phase, as well as a small percentage of cells with less than the normal diploid DNA content (debris, d), cells grown in pyrimidine-free medium showed a much higher percentage of cells with partial DNA content, and this increased dramatically between 24 and 48 hours.

In an effort to quantify the emergence of aberrant cells the flow cytometry profiles were analyzed with the ModFit software package which models the peak area. This was not successful for the 48 hours time points because of the lack of viable cells and too extensive DNA damage, which did not allow reliable estimates of relevant peaks. However, some results for the 24-hours and 36 hours time points are shown in figure 7.8. The use of thymidine as sole pyrimidine source caused a highly significant increase in cells in G2 phase, most likely because of the anticipated imbalance between thymidine nucleotides and deoxycytidine nucleosides, which the cell cannot generate from thymidine. The peak classified as 'DNA debris' increased within 24 hours of pyrimidine-free conditions and this was highly significant ($P<0.01$) after 36 hours; the debris amount was also significantly increased by culturing on thymidine (Figure 7.8). We conclude that any significant interruption of pyrimidine nucleotide availability leads to major defects in DNA synthesis.
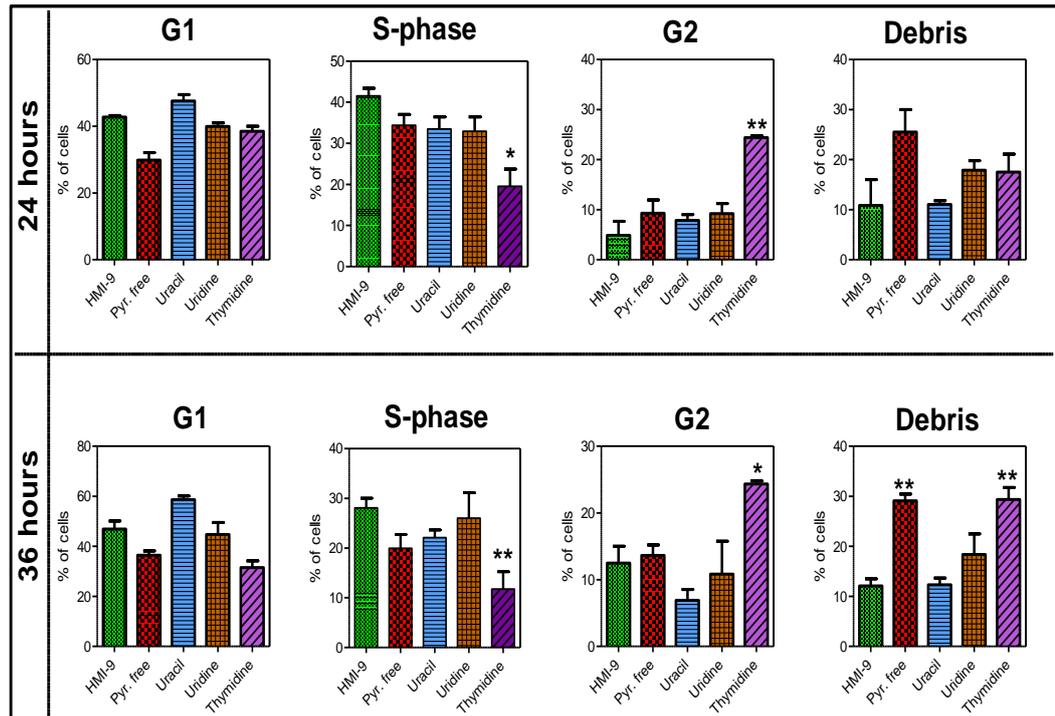
Figure 7.8. Figure 7.8. Quantitative analysis of DNA content in pyrimidine-starved trypanosomes. The peak area of G1, S-phase, G2 and debris of flow cytometric analysis of DNA content (Figure 7.7) was determined using the ModFit software package after 24 or 36 hours of growth under various culturing conditions. Growth was in HMI-9 (considered as a control in each frame) or in HMI-9^{-tmd} with or without the addition of 100 µM of one pyrimidine as indicated. The data are the average of 3 - 6 independent determinations and statistical analysis was performed using one-way ANOVA with Tukey's correction (Prism 5, GraphPad), relative to the HMI-9 control. *, $P<0.05$; **, $P<0.01$.

7.8. Infectivity of pyrimidine auxotrophic *T. b. brucei* in mice

The observation (Figure 7.4) that pyrimidine auxotrophic *Pyr6-5$^{-/-}$* cells grow in standard HMI-9, which contains only thymidine as a pyrimidine source, but cannot grow in thymidine-supplemented medium with dialyzed FBS strongly suggest that (1) *T. b. brucei* cannot use thymidine as its sole pyrimidine source and (2) it is able to salvage sufficient amounts of other pyrimidines from the non-dialyzed serum. It could thus be speculated that pyrimidine auxotrophic trypanosomes should be able to survive *in vivo*. To test this, we infected groups of 6 mice with a high inoculum of 10^5 trypanosomes of s427-WT, *Pyr6-5$^{+/-}$* or *Pyr6-5$^{-/-}$* strains and followed survival and parasitaemia for 15 days. Figure 7.9A shows that WT trypanosomes were the most virulent and killed all mice between 4 and 8 days. The single allele knockout strain *Pyr6-5$^{+/-}$* caused the death of four mice by day 5 but two of the animals survived until day 12. In contrast, all the

animals inoculated with *Pyr6-5$^{-/-}$* survived until day 15, when the experiment was terminated. However, the auxotrophs were able to survive and to multiply in the host, as evidenced by the average parasitaemia, which reached levels of 10^6 cells/ml albeit much more slowly than the other strains (Figure 7.9B). We conclude that *T. brucei* can salvage just enough uracil and/or uridine *in vitro* to maintain an infection.
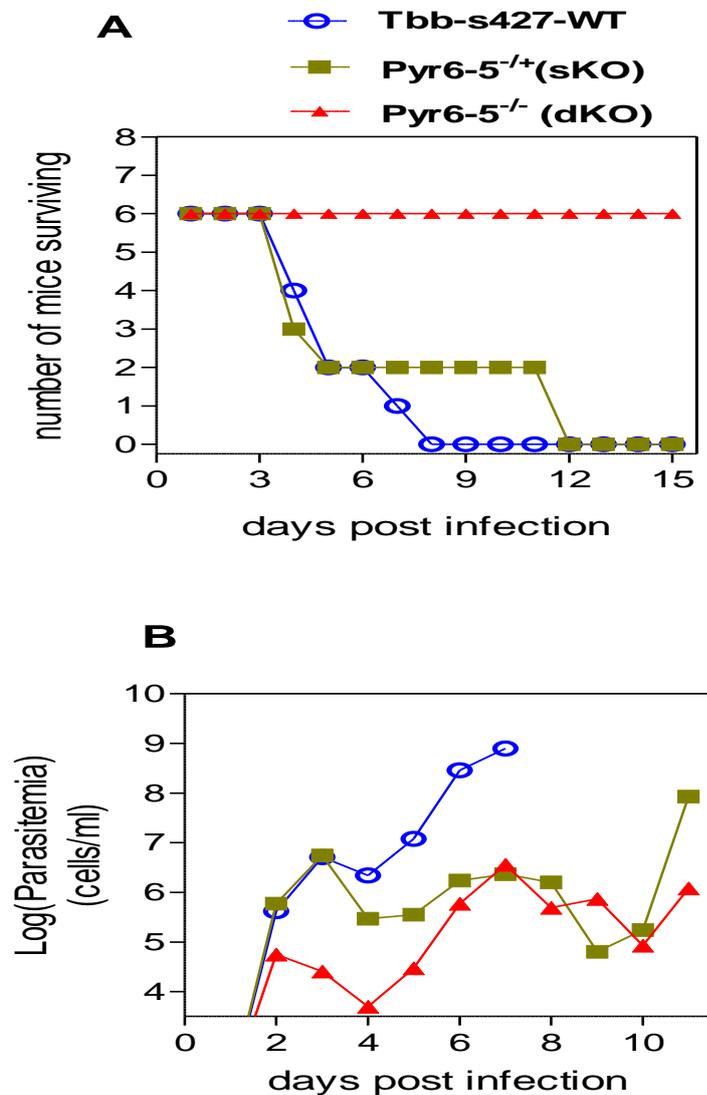
Figure 7.9. Infectivity of pyrimidine auxotrophic *T. b. brucei*. **A.** Survival of mice in groups of 6, each inoculated with 10^5 bloodstream form trypanosomes of various clonal lines. **B.** Parasitaemia of the same mice as depicted for survival in panel A. The average parasitaemia of the surviving mice is shown. Detection was by phase-contrast microscopy and detection limit was 1×10^4; where the infected was sub-patent, a value of 5000 cells ml^{-1} was inserted in order to arrive at a reasonable average. Both panels: ○, WT s427; ■, *PYR6-5$^{+/-}$*; ▲, *PYR6-5$^{-/-}$*.

7.9. Discussion

Kinetoplastid parasites are able to salvage preformed pyrimidine nucleobases and/or nucleosides (Al-Salabi *et al.*, 2007; Bellofatto, 2007; De Koning *et al.*, 2005; Landfear *et al.*, 2004; Papageorgiou *et al.*, 2005) as well as synthesise them *de novo* from glutamine and aspartate (Hammond & Gutteridge, 1982). The two pathways converge at UMP, the end-product of the 6-step biosynthesis pathway as well as the nexus for salvaged cytidine, uridine, 2'deoxyuridine, 2'deoxycytidine and uracil, through the actions of cytidine deaminase, uridine phosphorylase and uracil phosphoribosyltransferase (UPRT). From UMP the cell can then make all pyrimidine ribonucleotides and 2'deoxyribonucleotides that it needs, through non-redundant pathways. Salvaged thymidine can be utilised as thymidine nucleotides but not to produce any other pyrimidine nucleotides (Ali *et al.*, 2013a; Berens *et al.*, 1995; Hassan & Coombs, 1988) and both procyclic and bloodstream form trypanosomes take up thymidine very poorly (Ali *et al.*, 2013a; Gudin *et al.*, 2006). Therefore it is clear that pyrimidine metabolism in protozoa must be replete with good drug targets. Indeed, *T. b. brucei* DHFR-TS, CTP synthetase and dUTPase have all been shown already to be essential enzymes (Castillo-Acosta *et al.*, 2008; Hofer *et al.*, 2001; Sienkiewicz *et al.*, 2008). These enzymes are all in the pathways downstream from UMP and thus shared by the salvage route and the biosynthesis route.

What is less clear is whether either of the two biochemical pathways to obtain UMP in the first place might be essential and thus a potential drug target. In order to therapeutically target the salvage pathway to UMP it would be necessary to inhibit either the uptake of uracil, uridine, 2'deoxyuridine, cytidine and 2'deoxycytidine, or to inhibit UPRT. With regards to the former option it should be noted that cytidine and 2'deoxycytidine are incorporated very poorly into the *T. b. brucei* nucleotide pool (Ali *et al.*, 2013a; Hofer *et al.*, 2001) and it would thus only be necessary to inhibit the carriers for uracil, 2'deoxyuridine and uridine, and we recently reported that all three are mediated by the same transporter, TbU3, in bloodstream forms (Ali *et al.*, 2013a). However, we report here that WT trypanosomes (i.e. pyrimidine prototrophs) grow almost unimpeded in the absence of any pyrimidine source and must conclude that neither pyrimidine transporters nor UPRT are essential functions in bloodstream form *T. b. brucei* - consistent with a recent report that deletion of UPRT in *L.*

donovani promastigotes created a pyrimidine prototrophic parasite with normal *in vitro* growth (Wilson *et al.,* 2012). It can thus be concluded that pyrimidine salvage is not an essential function for trypanosomes.

(Arakaki *et al.,* 2008) previously investigated whether the *de novo* biosynthesis route to UMP was essential to *T. b. brucei in vitro*; they employed RNA-interference (RNAi) to reduce expression of *T. brucei* dihydroorotate dehydrogenase (DHODH). These authors reported that knockdown of this enzyme did not affect growth in standard HMI-9 but greatly reduced growth in pyrimidine-depleted medium using a commercial dialysed serum. Our own observations with a *PYR6-5$^{-/-}$* strain are entirely consistent with Arakaki's report: the growth rate of pyrimidine auxotrophs is at most slightly affected in normal medium with non-dialysed serum. As shown in Appendix I, thymidine (20 mg/L, i.e. ~83 µM) is the only pyrimidine added to that medium but since this nucleoside cannot be converted to uridine and cytidine nucleotides by *T. b. brucei*, it is redundant (Ali *et al.,* 2013a; Gao *et al.,* 1999) and clearly the serum provides sufficient pyrimidines for growth, consistent with the average uracil concentration of 0.17 ± 0.05 µM in human plasma (Bi *et al.,* 2000) and high affinity uptake of pyrimidines, particularly uracil, by *T. brucei* (Ali *et al.,* 2013a; De Koning & Jarvis, 1998). We thus conclude that pyrimidine biosynthesis is not essential for *in vitro* growth, and the fact that even 10% FBS supplies sufficient pyrimidines, seems to indicate that it may not be essential for *in vivo* growth either.

This was tested by infecting mice with s427-WT, *PYR6-5$^{+/-}$* and *PYR6-5$^{-/-}$* trypanosomes. All three strains were able to maintain an infection and although the homozygous knockout strain was clearly less virulent, it unambiguously establishes that inhibition of the *de novo* pyrimidine biosynthesis is not a viable therapeutic strategy against African trypanosomes. These findings are very similar to those reported for promastigote *L. donovani* (French *et al.,* 2011) but, in contrast to the authors of that report, we contend that the fact that disruption of pyrimidine biosynthesis can be compensated for by physiological levels of pyrimidines demonstrates that this pathway is not essential in kinetoplastids, and not a viable drug target. Indeed, the same authors very recently demonstrated that *L. donovani* that lack carbamoyl phosphate synthetase, and are thus pyrimidine auxotrophic, were able to establish a

'robust' infection in mice (Wilson *et al.,* 2012). It is noteworthy, however, that *Leishmania* species are obligated intracellular parasites and that the current report is the first assessment of *in vivo* growth of an extracellular pyrimidine-auxotrophic protozoan. This is relevant as the intracellular and extracellular nucleoside and nucleobase levels are potentially very different, with the intracellular purines and pyrimidines overwhelmingly existing as nucleotides, which cannot be taken up directly by protozoan transporters (De Koning *et al.,* 2005). In addition, a previous report on pyrimidine-auxotrophic *Toxoplasma gondii,* another obligate intracellular protozoan, showed that these parasites were completely avirulent even in immune-compromised mice (Fox & Bzik, 2002) - a phenotype attributed to the lack of free pyrimidines within animal cells which also prevents growth of pyrimidine auxotrophic bacteria (Fields *et al.,* 1986).

Inhibition of the pyrimidine biosynthesis pathway in *T. b. brucei* greatly sensitises the trypanosomes to cytotoxic pyrimidine analogues such as 5-fluorouracil, 5-fluoro-2'deoxyuridine, 5-fluorodeoxycytidine and 5-fluorouridine (Table 7.1). The enhanced effect of 5-fluorouracil was also noted by Arakaki *et al.,* (2008), who attributed it to inhibition of uracil uptake. Whilst this analogue is indeed a competitive inhibitor of uracil transport in *T. brucei,* none of these fluorinated pyrimidines would sufficiently inhibit uracil uptake in bloodstream forms at the EC_{50} values given in Table 7.1, especially not 5F-2'deoxyuridine or 5F-2'deoxycytidine (Ali *et al.,* 2013a). As an alternative explanation, we propose that these fluorinated pyrimidines enter the trypanosomes as prodrugs and subversive substrates for the pyrimidine salvage enzymes, are converted to nucleotides and incorporated into nucleic acids, as indeed is the case in mammalian cells (Longley *et al.,* 2003) and as we have recently shown for 5-fluorouracil in *T. b. brucei* (Ali *et al.,* 2013a). This incorporation is more efficient in the absence of a newly synthesised pool of pyrimidine metabolites that would compete with the halogenated analogues at the level of each enzyme as well as for RNA and/or DNA polymerases.

We thus conclude that an inhibitor of any one of the enzymes of the *de novo* pathway together with either an inhibitor of uracil/uridine uptake, or with a cytotoxic nucleoside analogue, would be a powerful and synergistic combination that would act on trypanosomes through both misincorporation of

false nucleotides, and by causing pyrimidine starvation through inhibition of pyrimidine carriers, and we found that trypanosome populations die much more quickly from a lack of pyrimidines than from a lack of purines (Ali *et al.,* 2013b; De Koning & Diallinas, 2000). It can easily be speculated that kinetoplastid parasites, having evolved without the capacity to synthesise their own purines, must be relatively well-adapted to periods with low purine availability, as demonstrated by the reversibility of purine starvation-induced growth arrest (De Koning & Diallinas, 2000). In contrast, they have not needed to develop a mechanism to cope with a prolonged dearth of pyrimidines, being able to make sufficient amounts themselves, and trypanosomes are therefore unable to recover from even short periods of pyrimidine starvation. We did observe, consistently, increased expression of uridine phosphorylase, and an increase in uracil uptake capacity (both about two-fold), in pyrimidine-starved trypanosomes but this hardly constitutes a major upregulation of the pyrimidine salvage pathway and it is at best uncertain whether this is a regulated, physiological response to low pyrimidine levels. Indeed, the lack of a regulated response to the insufficient level of pyrimidine nucleotides was manifest in the major defects in DNA synthesis after only 24 hours, leading to fragmented and incomplete chromosomes.

In summary, we have shown that neither pyrimidine uptake or *de novo* biosynthesis is essential in African trypanosomes but that a drug combination targeting both systems would be a very powerful and novel therapeutic approach against kinetoplastid parasites.

CHAPTER EIGHT
Genome analyses of *Trypanosoma* and *Leishmania* lines resistant to fluorinated pyrimidines

8.1 Introduction

Pyrimidine analogues showed anti-metabolite activities against *Trypanosoma* and *Leishmania* parasites; therefore, new cell lines that were highly resistant to these analogues were generated as part of the investigation of pyrimidine metabolism as a drug target. The biochemical and metabolomic characterizations showed that the resistance mechanism to fluorinated pyrimidines varied between the indicated kinetoplastids. In recent years, the sequencing of whole genomes has become a possible avenue to investigate drug adaption in microorganisms such as bacteria (Feng *et al.,* 2009; Howden *et al.,* 2008; Lescat *et al.,* 2009; Mwangi *et al.,* 2007), as well as protozoa such as *Plasmodium* species (Hunt *et al.,* 2010; Martinelli *et al.,* 2011). Despite the fact that the chromosome copy number was found to be diverse within different species and strains of *Leishmania* (Rogers *et al.,* 2011), the whole genome of *L. major* resistant to miltefosine drug was generated and this allowed the identification of the resistance factors connected with miltefosine resistance in *Leishmania* (Adriano-Coelho *et al.,* 2012). However, the genome of kinetoplastid parasites that were resistant to fluorinated pyrimidines has thus far not been examined. In order to identify genes potentially associated with resistance to fluorinated pyrimidines in kinetoplastid cells, the entire genomes of resistant strains were sequenced in parallel with their parental wild-type strains. Several alignment services have been used to analyze sequences, such as Illumina/Solexa, AB/SOLiD and Roche/454 (Langmead *et al.,* 2009; Ley *et al.,* 2008; Li *et al.,* 2008). We made Illumina paired-end sequencing libraries that were sequenced on Illumina HiSeq machines as described in Materials and Methods chapter (section 2.6.5), in collaboration with the Wellcome Trust Sanger Institute (Hinxton, UK).

This generated high-quality genome sequences for kinetoplastids resistant to fluorinated pyrimidines, which were used to investigate the genetic variations amongst resistant lines and their background wild-type. For a given resistant line, single nucleotide polymorphisms (SNPs) were identified by comparison with parental wild-type strains *(T. b. brucei* strain 427, *L. mexicana* strain M379 and *L. major* strain Friedlin). Also read depth coverage was used to predict the amplifications or deletions of chromosomal regions, and other copy number variations (CNVs) against the background of each relative strain.

8.2 Genome analysis of *T. b. brucei* resistant to fluorinated pyrimidines

The copy number of chromosomal domains was examined using read depth coverage for each chromosome of the resistant lines (Tbb-5FURes, Tbb-5F2'dURes and Tbb-5FOARes) which were compared with BSF *T. b. brucei* s427 parental wild-type. Any changes could obviously account for the complete loss of a particular metabolite or transport activity. The genome analysis data showed that neither medium scale nor large scale changes in copy number could be observed when the read depth of adapted lines were normalized against the whole genome of *T. b. brucei* strain 427 wild-type (Figure 8.1A&B) - i.e. no significant deletions or duplications were observed in the drug-resistant lines of *T. b. brucei*. These findings suggest that genomes of *T. b. brucei* bloodstream forms are very consistent.
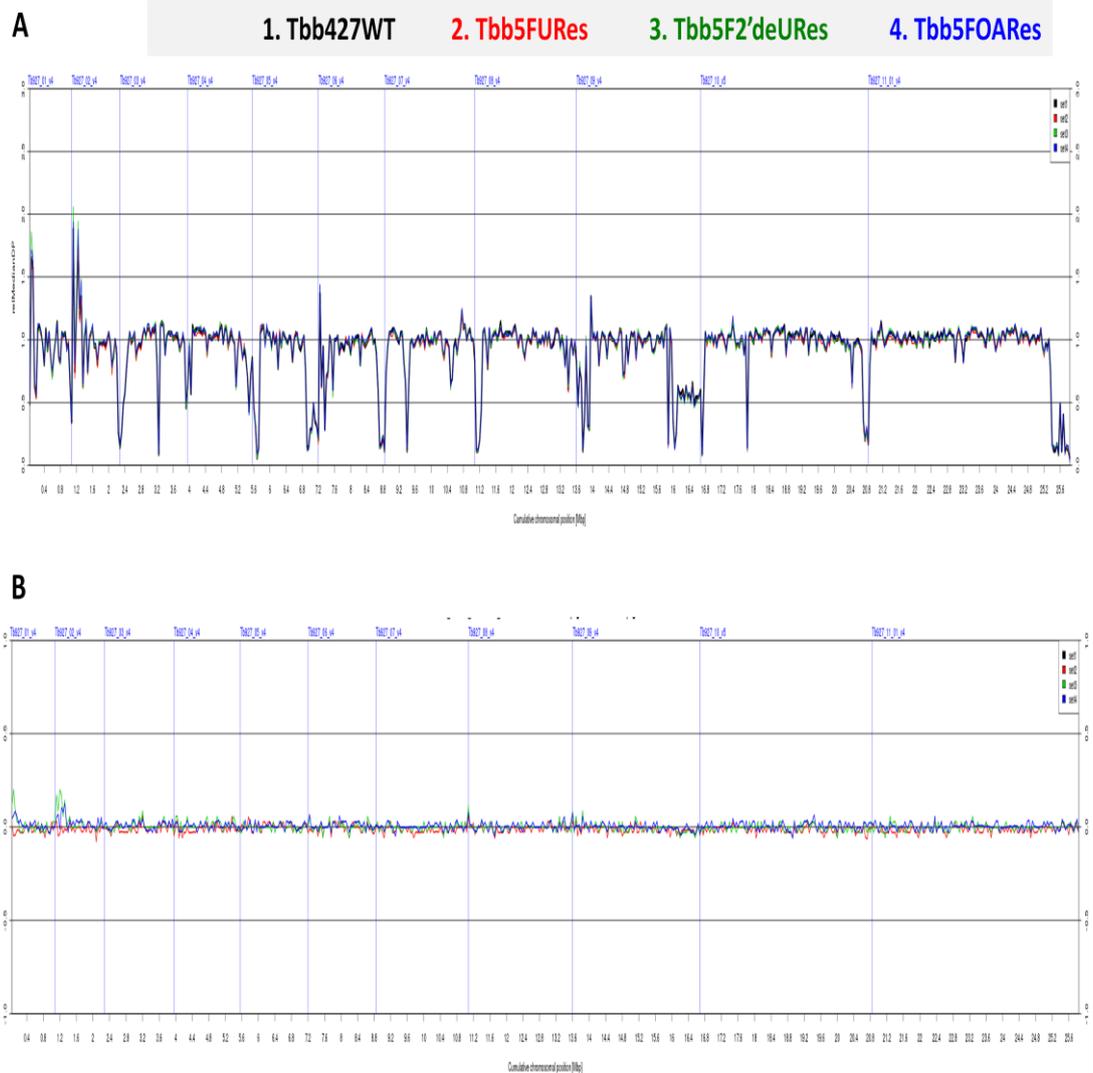
Figure 8.1 Copy number sequencing analysis for all *Trypanosoma* chromosomes of *T. b. brucei* strain 427 wild-type, Tbb-5FURes, Tbb-5F2'dURes and Tbb-5FOARes. The eleven chromosomes have been mapped on a medium and large scale. **A.** The coverage was normalized against the median coverage of the whole genome for a given strain, the graph shows that the DNA sequence of individual strains is identical to parental line. The y-axis represents fold-change of coverage for a particular region of the chromosome compared to the genome-wide median coverage. y-axis: 1.0 is the "neutral" value, 1.5 would be a 50% increase in coverage [e.g. by duplication of one of the homologous chromosomes of a pair, creating a trisomy for the corresponding chromosome], and 0.5 would be a 50% reduction in coverage (loss of one of the two homologous chromosomes of a pair) the coverage of the parental wild-type strain is represented with a thick black line. **B.** Coverage relative to parental strain, essentially shows the difference between a coloured line (red line for Tbb-5FURes, green line for Tbb-5F2'dURes and blue line for Tbb-5FOARes) and the parental black line of Plot A; this makes it easier to spot real changes in coverage in a drug-resistant line compared to the parental line, regardless of uneven coverage in the parental line (caused by varying degrees of repetitiveness or by sequence duplications not represented in the reference genome [e.g. VSG genes in *T. brucei*]; y-axis: 0 is the "neutral" value, 0.5 would be a 50% increase in coverage, and -0.5 would be a 50% reduction in coverage.

8.3 Genome analysis of *L. mexicana* resistant to 5-fluorouracil

When *L. mexicana* cells were adapted to survive and proliferate in 500 μM of 5-FU, four single cells were isolated and cloned from the population and designated intermediate adapted clones 1-4 to 5-FU (Int-Lmex-5FURes). Meanwhile, the rest of the culture was kept to grow under increased drug pressure until it became resistant to very high concentrations of 5-FU (up to 5 mM); these cells were finally cloned out and designated Fin-Lmex-5FURes. We obtained four clones of intermediate strains (Lmex-Int-5FURes) and three clones of final adapted cells (Lmex-Fin-5FURes). [Note: in chapter 4 we only assessed clone Fin2-Lmex-5FURes]. The whole genome of each resistant clone was sequenced and compared with parental wild-type. The genome analysis of *L. mexicana* resistant to 5-fluorouracil (Int-Lmex-5FURes and Fin-Lmex-5FURes) showed different CNVs compared with *L. mexicana* M379-WT. Changes in chromosomes 3, 4, 8, 11, 22, 29, 31, 32 and 34 in drug resistance lines were observed in various clones; all other chromosomes are presumably normal diploid (Table 8.1).

Chromosome 3: the Fin2-Lmex-5FURes strain had lost the start of this chromosome on one of its 2 homologous chromosomes (Figure 8.2; yellow line).
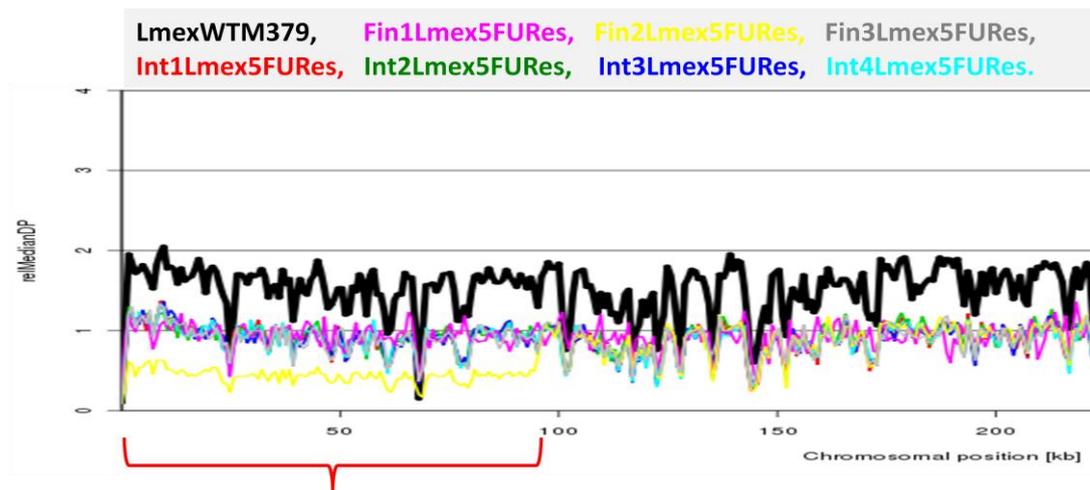
Figure 8.2. The coverage on chromosome 3 normalized against the median coverage of the whole genome for indicated strains; the yellow line referred to Fin2-Lmex-5FURes strain, which lost the start of chromosome 3 on one of its 2 homologous chromosomes. The y-axis represents fold-change of coverage for a particular region of the chromosome compared to the genome-wide median coverage. y-axis: 1.0 is the "neutral" value, 1.5 would be a 50% increase in coverage [e.g. by duplication of one of the homologous chromosomes of a pair, creating a trisomy for the corresponding chromosome], and 0.5 would be a 50% reduction in coverage (loss of one of the two homologous chromosomes of a pair) the coverage of the parental WT strain is represented with a thick black line.

It could be speculated that, as the loss of the start of the polycistron on this chromosome is also likely to impact the transcription of the rest of this polycistron, this CNV could impact on the expression of all genes up to LmxM.03.0680, including eight hypothetical proteins (LmxM.03.0370, LmxM.03.0380, LmxM.03.0400, LmxM.03.0410, LmxM.03.0490, LmxM.03.0550, LmxM.03.0650 and LmxM.03.0660). These open reading frames (ORFs) started from 124,634 to 126,607 and their function was given as "unspecified product"; however, they were predicted to contain more than 4 Trans-Membrane domains (i.e. LmxM.03.0410 contains predicted 12 TM helices; Figure 8.3).
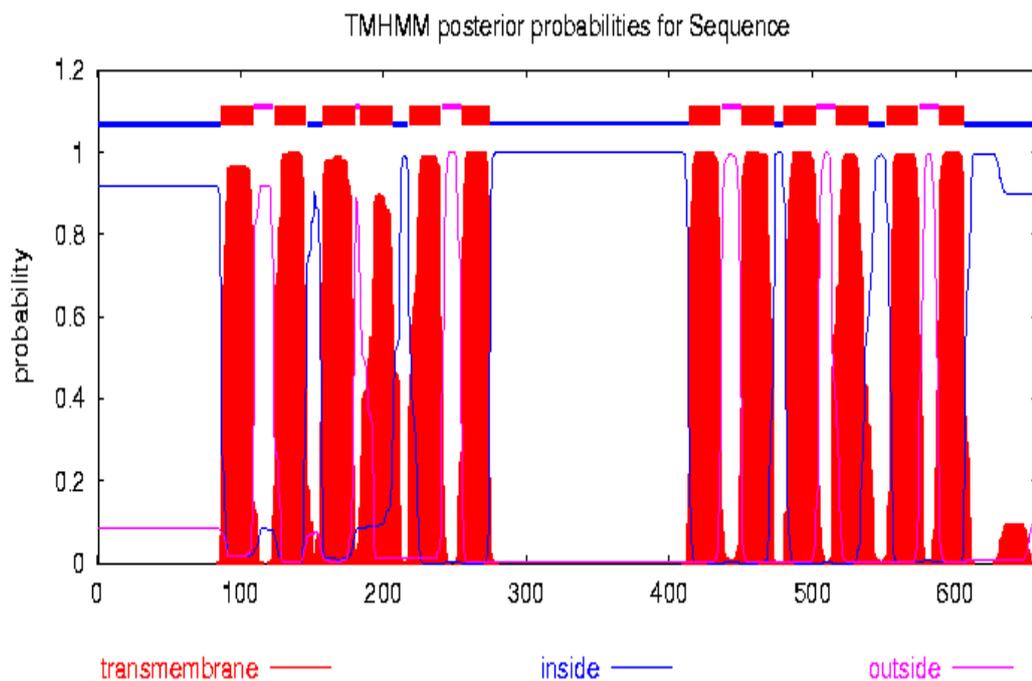
Figure 8.3 The TMHMM Server v. 2.0 predicted 12 transmembrane helices for the protein encoded by gene LmxM.03.0410 located on chromosome 3 of *L. mexicana*.

Furthermore, Fin2-Lmex-5FURes and Fin3-Lmex-5FURes lost heterozygosity over the first 140 kb of chromosome 3, which is a difference from the parental line *L. mexicana* M379-WT and from Fin1-Lmex-5FURes. Only Fin2-Lmex-5FURes showed a deletion of the first 90kb of the chromosome sequence in one of the two chromosomes (Figure 8.4).
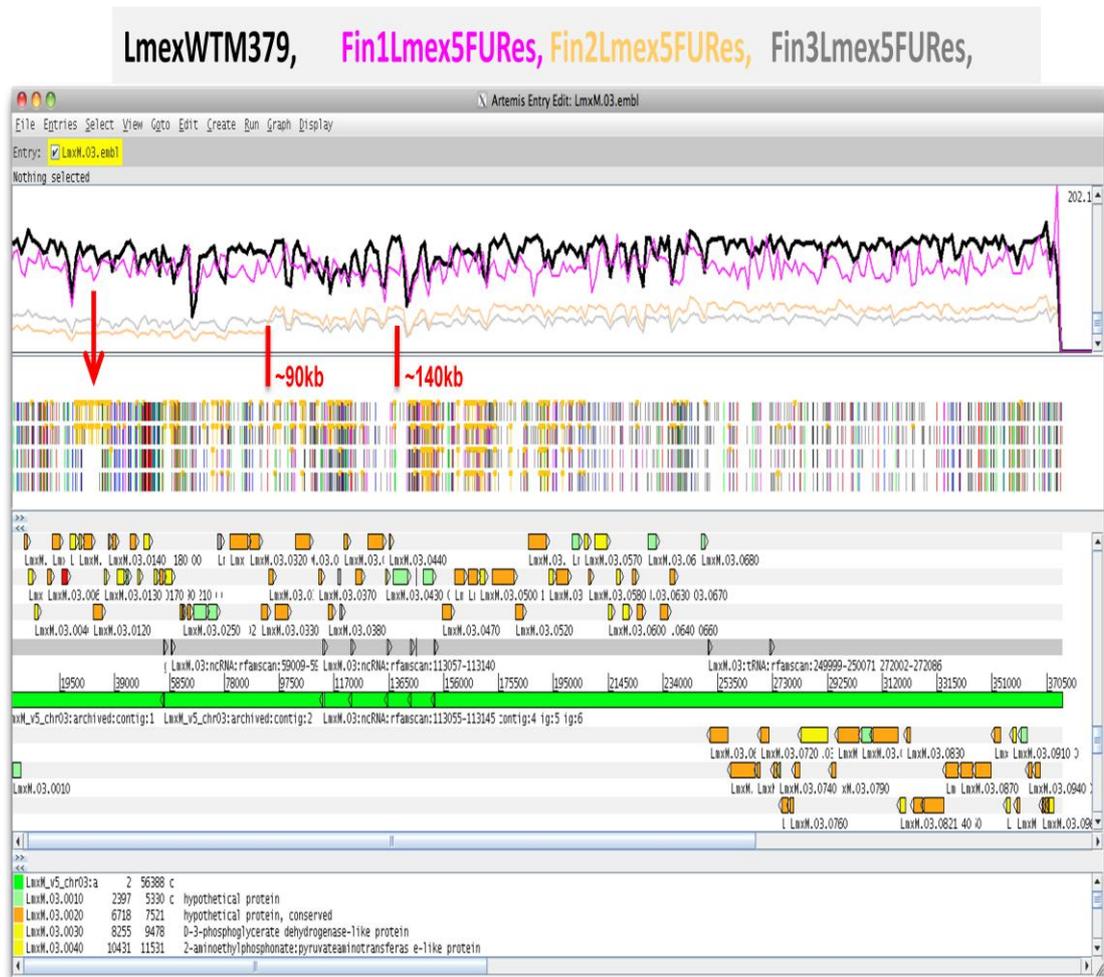
Figure 8.4. Chromosome 3 of *L. mexicana* strains on Artemis entry; 1st row M379-WT, 2nd row Fin1-Lmex-5FURes, 3rd row Fin2-Lmex-5FURes and 4th row Fin3-Lmex-5FURes. The red arrow shows that Fin2 and 3 of Lmex-5FURes lost heterozygosity over first 140 kb, but only the former lost the first 90 kb of sequence in one of the two chromosomes.

Chromosome 4: *L. mexicana* M379-WT and all the three Fin-Lmex-5FURes strains have increased coverage for chromosome 4, whereas the four Int-Lmex-5FURes strains have normal diploid coverage. However, Fin3-Lmex-5FURes has half the copy number for the start of the chromosome 4, and Fin2-Lmex-5FURes has double copy number up to ~35 kb (Figure 8.5A and B). This area includes: LmxM.04.0020 which encodes a pteridine transporter with 12 TM domains, but the coverage was amplification not deletion, so this CNV was unlikely to be linked to a loss of pyrimidine transport phenotype. Also this region contains LmxM.04.0250, which encodes RNA pseudouridylate synthase, the enzyme that catalyses the isomerisation of uridine to pseudouridine. This mechanism may relate to pyrimidine analogous metabolism but not to the pyrimidine uptake.

Figure 8.5 *L. mexicana* strains coverage on chromosome 4; **A.** M379-WT and Final resistant strains have higher coverage than the 4 intermediate drug-resistant lines. The y-axis represents fold-change of coverage for a particular region of chromosome 4 compared to the genome-wide median coverage. y-axis: 1.0 is the "neutral" value, 1.5 would be a 50% increase in coverage and 0.5 would be a 50% reduction in coverage the coverage of the parental WT strain is represented with a black line. **B.** Fin2-Lmex-5FURes has a roughly doubled coverage for the first ~35 kb of chromosome 4. Coverage relative to parental strain (window size = 40 kb), essentially shows the difference between a coloured line and the parental black line of Plot A; y-axis: 0 is the neutral value, 0.5 would be a 50% increase in coverage, and -0.5 would be a 50% reduction in coverage.

Chromosome 8: surprisingly, there was higher coverage in chromosome 8 of *L. mexicana* M379-WT compared to the intermediate and final drug-resistant lines for a patch around position 1,456,000 that carries LmxM.08.0720, an amastin-like gene, which is transmembrane glycoprotein found on cell surface (Figure 8.6). This coverage has no link with the resistance to 5-fluorouracil since it was amplification on the parental wild-type strains.
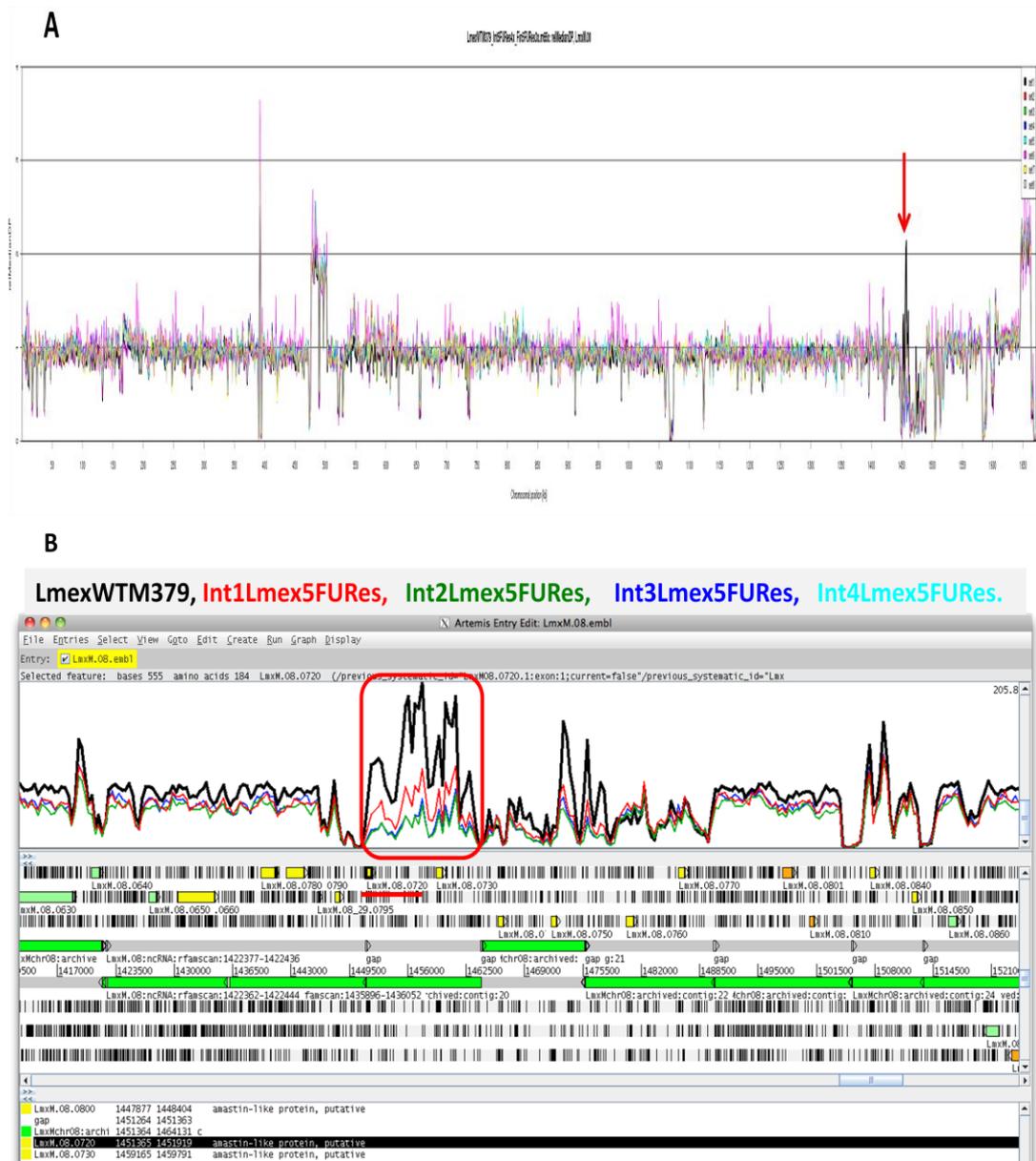
Figure 8.6 Coverage on chromosome 8. **A.** *L. mexicana* M379-WT showed higher coverage around position 1.456 Mbp (red arrow) in contrast to all other resistant strains. The y-axis represents fold-change of coverage for a particular region of chromosome 8 compared to the genome-wide median coverage. y-axis: 1.0 is the "neutral" value, 1.5 would be a 50% increase in coverage and 0.5 would be a 50% reduction in coverage the coverage of the parental WT strain is represented with a black line. **B.** Artemis entry of chromosome 8 shows higher coverage for M379-WT compared with intermediate resistant strains around position 1,456,000 (inside the red box), which carries the amastin-like genes (underlined by a red thick line).

Chromosome 11: In figure 8.7, the normalized row sequence read depth shows that chromosome 11 has higher coverage in all Fin-Lmex-5FURes, particularly in Fin3-Lmex-5FURes, than the four intermediate drug-resistant lines and the parental line. This is of particular interest as chromosome 11 carries many transporter genes including amino acid transporter LmxM.11.0520 with 9 TM domains and a nucleobase transporter (NT4) LmxM.11.0550 with 11 TM domains. Amplification of NT4 in all Fin-Lmex-5FURes might somehow be due to the loss of uracil transport activity, which could cause an imbalance between purine and pyrimidine nucleotides. In *L. major*, the LmajNT4 specifically transports adenine (Ortiz *et al.*, 2009b). The increased coverage of an amino acid transporter allowed us to speculate that the resistant cell lines increased pyrimidine biosynthesis to recover the loss of the uracil transporter, as the first two steps of pyrimidine biosynthesis depend on glutamine and aspartic acid, which are salvaged via amino acid transporters.
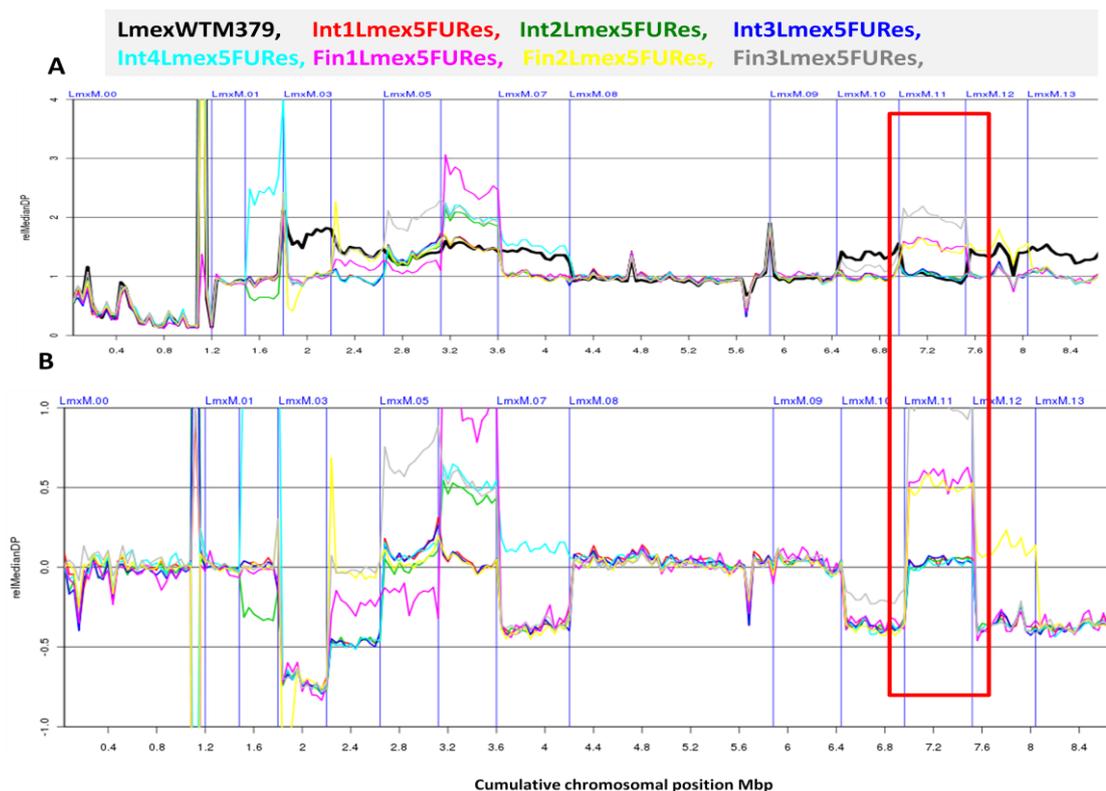
Figure 8.7 Multiple chromosomal CNVs in the drug resistant of *L. mexicana*. **A.** The normalized row sequence coverage of chromosome 11 (red square) on a large scale. The y-axis represents fold-change of coverage for chromosomes 1-13 compared to the genome-wide large coverage, y-axis: 1.0 is the "neutral" value, 1.5 would be a 50% increase in coverage and 0.5 would be a 50% reduction in coverage the coverage of the parental WT strain is represented with a black line. **B.** Coverage relative to parental strain *L. mexicana* M379-WT essentially shows the difference between a coloured line and the parental black line of Plot A; y-axis: 0 is the neutral value, 0.5 would be a 50% increase in coverage, and -0.5 would be a 50% reduction in coverage.

Chromosome 22: Int4-Lmex-5FURes was the only strain that displayed a 50% coverage reduction in a region of chromosome 22 that carries the gene LmxM.22.1290, which encodes a ribonucleoside-diphosphate reductase (Figure 8.8A, B and C). These enzymes are crucial in purine and pyrimidine interconversions, so that the reduced coverage on this gene occurred very early as the changes were only on Int4-Lmex-5FURes. However, the CNV seems not to have been retained by the more highly adapted 'Final' strains.
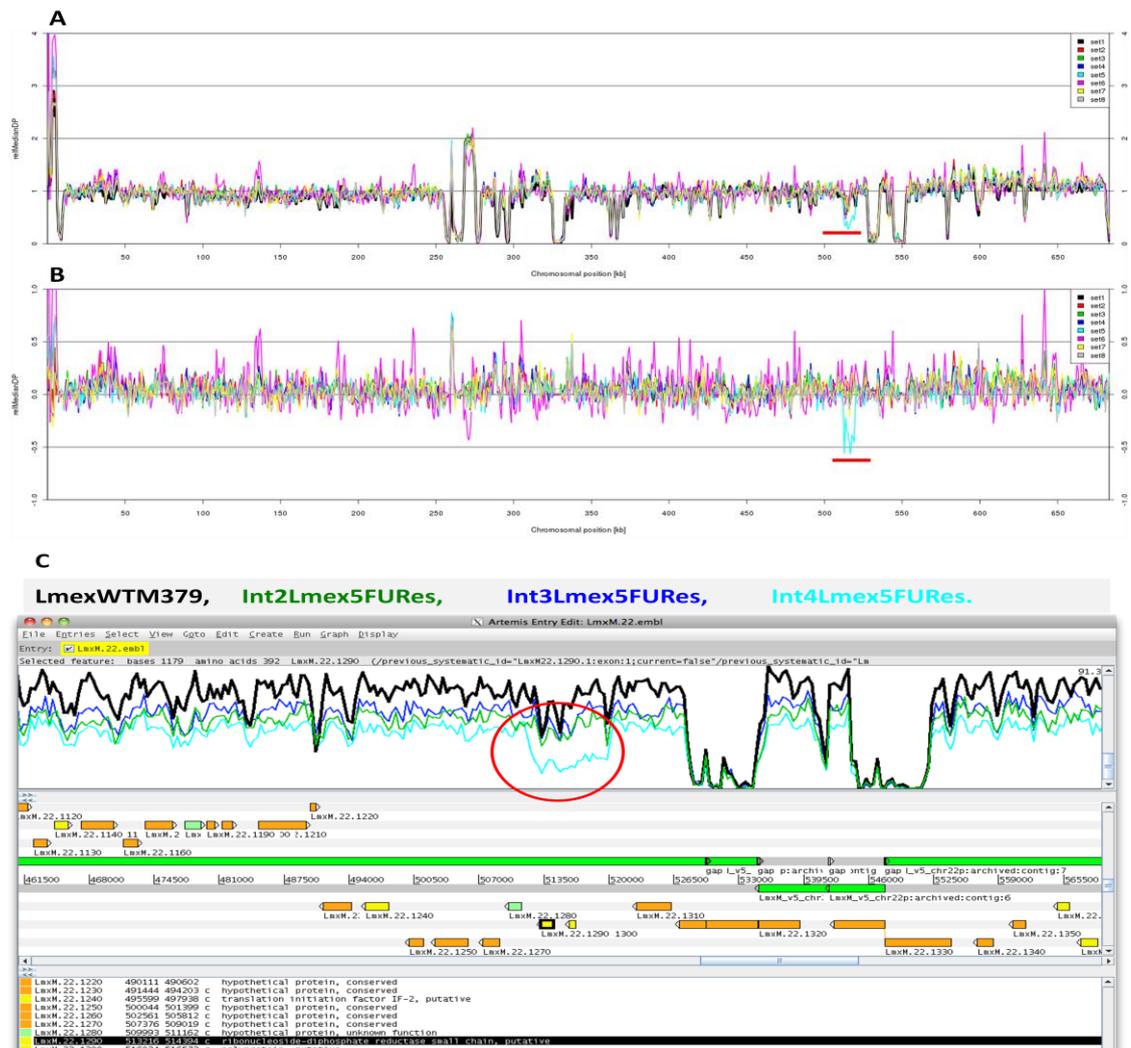
Figure 8.8 *L. mexicana* strains coverage on chromosome 22; Int4-Lmex-5FURes has 50% coverage reduction; the region of chromosome 22 for Int4-Lmex-5FURes is underlined with a red line. **A.** The y-axis represents fold-change of coverage for a particular region of chromosome 22 compared to the genome-wide median coverage. y-axis: 1.0 is the "neutral" value, 1.5 would be a 50% increase in coverage and 0.5 would be a 50% reduction in coverage the coverage of the parental WT strain is represented with a black line. **B.** Int4-Lmex-5FURes has 50% coverage reduction of chromosome 22. Coverage relative to parental strain (window size = 40kb), essentially shows the difference between a coloured line and the parental black line of Plot A; y-axis: 0 is the neutral value, 0.5 would be a 50% increase in coverage, and -0.5 would be a 50% reduction in coverage. **C.** Coverage on chromosome 22 of Int4-Lmex-5FURes; Artemis entry of chromosome 22 shows 50% coverage reduction compared with parental line and other intermediate resistant lines (inside a red circle), which carries the gene LmxM.22.1290 (highlighted gene).

Chromosome 29 has a slight increase in coverage in all Lmex-5FURes cell lines compared to the parental wild type particularly around position 786,000 kbp, which includes gene LmxM.29.2200. As this gene encodes a hypothetical protein without TM domains, we cannot here suggest whether/how this coverage may be associated with the resistance phenotype (Figure 8.9). Instead, the data appears to suggest that a reduced copy number is favourable for chromosome 29, upon exposure to fluoro-pyrimidines, but that this was not possible for the locus containing LmxM.29.2200, perhaps because this is encodes an essential protein.
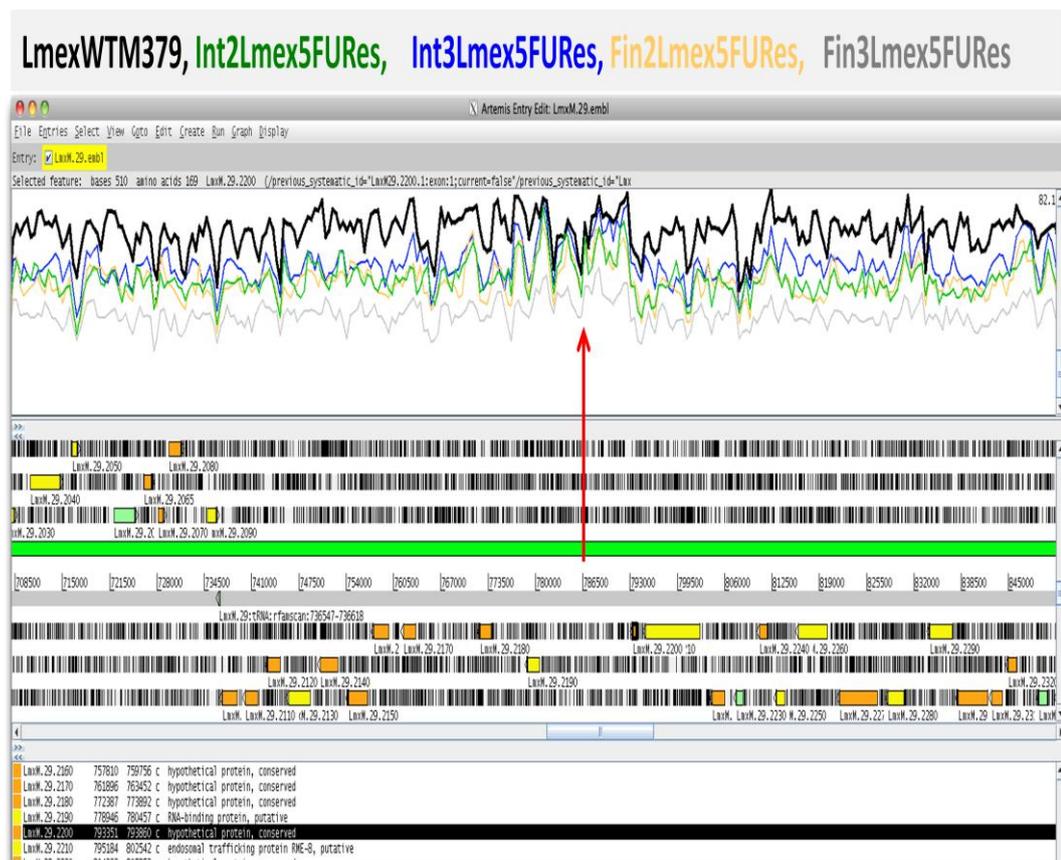
Figure 8.9 All intermediate and final resistant lines of Lmex-5FURes show reduced coverage on chromosome 29 compared with the parental line. However, the Artemis analysis shows a 50% coverage increase at location around 786 kbp (red arrow) compared with parental line, which carries the gene LmxM.29.2200 (highlighted gene).

Chromosome 31: the parental line appears to have a trisomy for a large section of chromosome 31 but none of the drug-resistant lines do (Figure 8.10).
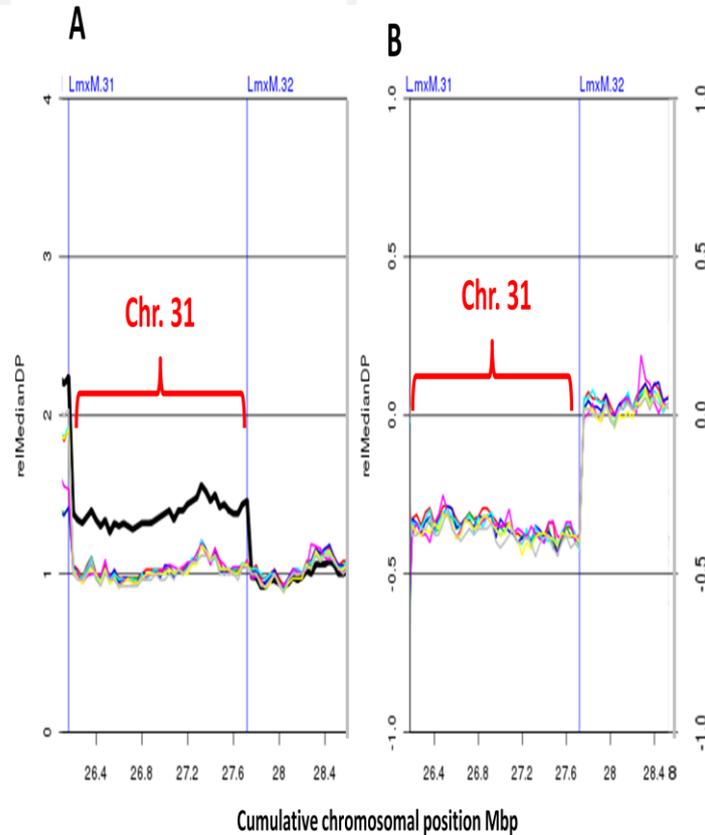
Figure 8.10. Multiple chromosomal CNVs in *L. mexicana* M379-WT and resistant line. **A.** The normalized row sequence coverage of chromosome 31 (marked region) on a large scale. The y-axis represents fold-change of coverage for chromosome 31 compared to the genome-wide large coverage, y-axis: 1.0 is the "neutral" value, 1.5 would be a 50% increase in coverage and 0.5 would be a 50% reduction in coverage the coverage of the parental WT strain is represented with a black line. **B.** Coverage relative to parental strain *L. mexicana* M379-WT essentially shows the difference between a coloured line and the parental black line of Plot A; y-axis: 0 is the neutral value, 0.5 would be a 50% increase in coverage, and -0.5 would be a 50% reduction in coverage.

Chromosome 32: All drug-resistant lines have double coverage in the region ~916,000 - 1,175,000, compared to the parental line, which includes UDP-glc 4'-epimerase (LmxM.32.2300) and UDP-*N*-acetylglucosamine pyrophosphorylase (LmxM.32.2520) this duplication must have happened quite early during drug-adaptation (Figure 8.11). Interestingly, the level of UDP-*N*-acetyl-D-glucosamine was elevated in the metabolomic analyses after treatment with 5F2'dUrd (*P*=0.045 for *L. mexicana* and *P*=0.034 for *L. major*); it was also increased upon incubation with 5F-uracil and 5F-uridine, although this was not statistically significant (see Chapter 4).
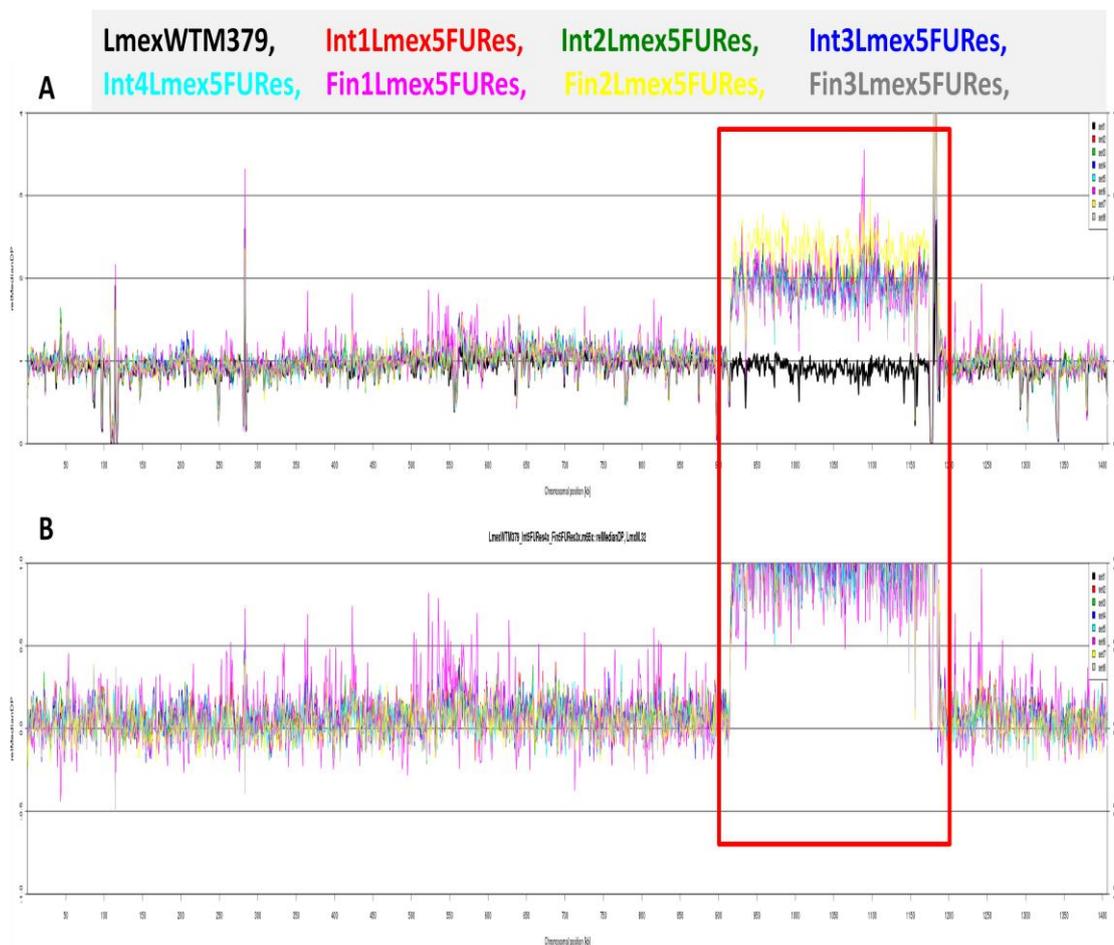
Figure 8.11. Resistant strains of *L. mexicana* have doubled coverage on chromosome 32 (red box). **A.** The y-axis represents fold-change of coverage for chromosome 32 compared to the genome-wide median coverage. y-axis: 1.0 is the "neutral" value, 1.5 would be a 50% increase in coverage and 0.5 would be a 50% reduction in coverage the coverage of the parental WT strain is represented with a black line. **B.** All resistant strains show doubled coverage in region 0.916-1.175 Mbp of chromosome 32. Coverage relative to parental strain, essentially shows the difference between a coloured line and the parental black line of Plot A; y-axis: 0 is the neutral value, 0.5 would be a 50% increase in coverage, and -0.5 would be a 50% reduction in coverage.

Chromosome 34: Int2-Lmex-5FURes showed a 50% increased coverage around positions 1,790,000 - 1,890,000 (Figure 8.12). This region includes LmxM.34.5150, the biopterin transporter with 14 TM domains. As this coverage appeared only on Int2-Lmex-5FURes it is not associated with the high resistant to 5-FU.
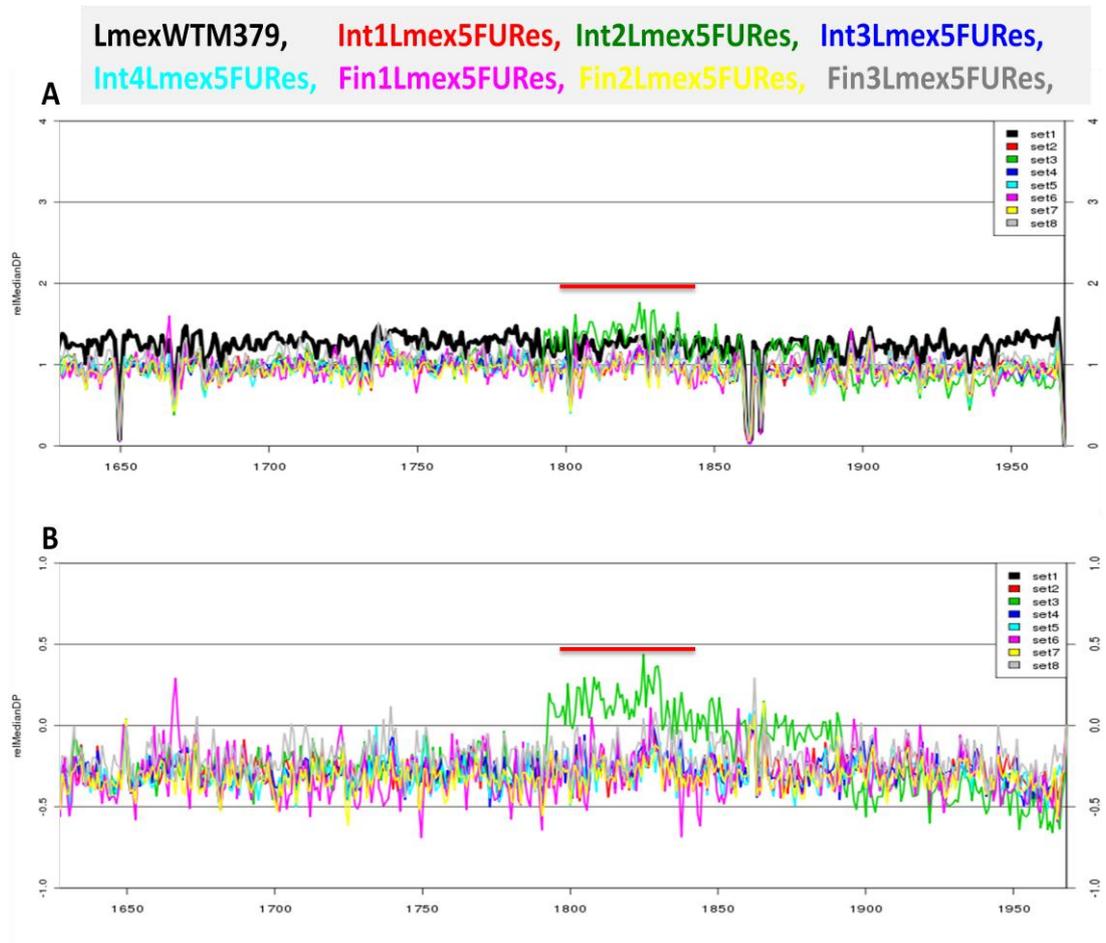
Figure 8.12 Int-Lmex-5-FURes strain has 50% increased coverage around position 1.79-1.89 Mbp (labelled in red). **A.** The y-axis represents fold-change of coverage for chromosome 34 compared to the genome-wide median coverage. y-axis: 1.0 is the "neutral" value, 1.5 would be a 50% increase in coverage and 0.5 would be a 50% reduction in coverage the coverage of the parental WT strain is represented with a black line. **B.** Int-Lmex-5-FURes strain shows 50% coverage in region 1.79-1.89 Mbp of chromosome 34. Coverage relative to parental strain essentially shows the difference between a coloured line and the parental black line of Plot A; y-axis: 0 is the neutral value, 0.5 would be a 50% increase in coverage, and -0.5 would be a 50% reduction in coverage.

Table 8.1: CNVs on *L. mexicana* strains

Gene ID	Gene product and function	TMd	strains	Changes description
Chromosome 3				
LmxM.03.0370	Unspecified product; unknown function	5	Fin2-Lmex-5FURes and Fin3-Lmex-5FURes	Both strains have lost heterozygosity over first 140 kb; only Fin2-Lmex-5FURes lost the first 90 kb of sequence in one of the two chromosomes.
LmxM.03.0380		6		
LmxM.03.0400		6		
LmxM.03.0410		12		
LmxM.03.0490		7		
LmxM.03.0550		5		
LmxM.03.0650		9		
LmxM.03.0660		9		
Chromosome 4				
LmxM.04.0020	Pteridine transporter (truncated) putative. Pteridine is a chemical compound composed of fused pyrimidine and pyrazine rings.	12	Fin1-Lmex-5FURes, Fin2-Lmex-5FURes , Fin3-Lmex-5FURes and M379-WT	Increased coverage (duplication) for chr. 4. Fin3-Lmex-5FURes has half the copy number for the start of chr. 4, Fin2- Lmex-5FURes has double copy number
LmxM.04.0090	Hypothetical protein, conserved; unknown function.	0	Fin1-Lmex-5FURes, Fin2-Lmex-5FURes , Fin3-Lmex-5FURes and M379-WT	Increased coverage (duplication) for chr. 4. Fin3-Lmex-5FURes has half the copy number for the start of chr. 4, Fin2- Lmex-5FURes has double copy number
LmxM.04.0250	RNA pseudouridylate synthase-like protein. Pseudouridine synthases catalyse the isomerisation of uridine to pseudouridine	0	Fin2-Lmex-5FURes and Fin3-Lmex-5FURes	Halved reduction in coverage
LmxM.04.0280	Adenosine monophosphate deaminase catalyzes the hydrolytic deamination of AMP into inosine monophosphate (IMP).	0	Fin2-Lmex-5FURes and Fin3-Lmex-5FURes	Halved reduction in coverage

Table 8.1 continued CNVs on *L. mexicana* strains

Gene ID	Gene product and function	TMd	strains	Changes description
Chromosome 8				
LmxM.08.0720	Amastin-like protein, putative. Amastin surface glycoprotein family contains the eukaryotic surface glycoprotein amastin.	3	*L. mexicana* M379-WT	Higher coverage increase (amplification)
Chromosome 11				
LmxM.11.0520	Amino acid transporter, putative. The best conserved region in this family is located in the second transmembrane segment.	9	Fin1-Lmex-5FURes, Fin2-Lmex-5FURes and Fin3-Lmex-5FURes	High increased coverage (amplification).
LmxM.11.0550	Nucleobase transporter (NT4). These proteins enable the movement of hydrophilic nucleosides and nucleoside analogous across cell membranes.	11	Fin1-Lmex-5FURes, Fin2-Lmex-5FURes and Fin3-Lmex-5FURes	High increased coverage (amplification).
Chromosome 22				
LmxM.22.1290	Ribonucleoside-diphosphate reductase small chain, putative, also known as ribonucleotide reductase (RNR). It catalyzes the formation of deoxyribonucleotides from ribonucleotides. The substrates for RNR are ADP, GDP, CDP and UDP.	0	Int4-Lmex-5FURes	50% reduction in coverage.
Chromosome 29				
LmxM.29.2200	Hypothetical protein, conserved; unknown function	0	All FinLmex-5FURes and Int-Lmex-5FURes strains	Slight reduction in coverage.

Table 8.1 continued CNVs on *L. mexicana* strains

Gene ID	Gene product and function	TMd	strains	Changes description
Chromosome 32				
LmxM.32.2300	UDP-glc 4'-epimerase, putative; activity coenzyme binding. It catalyses the conversion of UDP-galactose to UDP-glucose during galactose metabolism.	0	All FinLmex-5FURes and Int-Lmex-5FURes strains	Doubled increased in converge (amplification).
LmxM.32.2520	UDP-*N*-acetylglucosamine pyrophosphorylase, putative. The enzyme catalyzes the chemical reaction UTP + N-acetyl-alpha-D-glucosamine 1-phosphate $\rightleftharpoons$ diphosphate + UDP-*N*-acetyl-D-glucosamine	0	All FinLmex-5FURes and Int-Lmex-5FURes strains	Doubled increased in converge (amplification).
Chromosome 34				
LmxM.34.5150	Biopterin transporter. Biopterin is a coenzyme, it is an oxidized degradation product of tetrahydrobiopterin	14	Int2-Lmex-5FURes	50% increased in coverage.

8.4 Genome analysis of *L. major* resistant to fluorinated pyrimidines.

Strains of *L. major* promastigotes with high levels of resistance to fluorinated pyrimidine analogues were generated. One such strain was *L. major* resistant to 5-FU (Lmaj-5FURes) and the other strain was resistant to 5F-2'dUrd (Lmaj-5F2'dURes). The extracted DNA from the adapted cell lines was full genome sequenced in parallel parental wild type (*L. major* sFriedlin-WT). The adapted *L. major* clones displayed CNVs on several different chromosomes (2, 6, 12, 14, 18, 20, 31 and 33; see Table 8.2 for an overview).

Chromosome 2: Lmaj-5FURes has apparently lost a section from chromosome 2 around positions 97,000 - 110,000 carrying phosphoglycan galactosyltransferase genes (Figure 8.13A, B and C). It was reported that *L. major* has 8 copies of this gene in different chromosomes (Raymond *et al.,* 2012). Phosphoglycan β-1,3 galactosyltransferase plays a significant role in binding with side chain oligosaccharides (Dobson *et al.,* 2003) and the lack of this activity prevented *L. major* infection of the sand fly vector (Butcher *et al.,* 1996), but its association with pyrimidine antimetabolite resistance is not immediately clear and would require further investigation.

Figure 8.13. The Lmaj-5FURes strain has lost about 13 kbp of chromosome 2 which carries phosphoglycan galactosyltransferase genes. **A.** The y-axis represents fold-change of coverage for chromosome 2 compared to the genome-wide median coverage. y-axis: 1.0 is the "neutral" value, 1.5 would be a 50% increase in coverage and 0.5 would be a 50% reduction in coverage the coverage of the parental WT strain is represented with a black line. **B.** Chromosome 2 region shows the coverage of Lmaj-5FURes. Coverage relative to parental strain essentially shows the difference between a coloured line and the parental black line of Plot A; y-axis: 0 is the neutral value, 0.5 would be a 50% increase in coverage, and -0.5 would be a 50% reduction in coverage. **C.** Lmaj-5FURes shows the coverage on chromosome 2 compared with parental line; Artemis entry of chromosome 2 shows 50% coverage reduction at location around 786 kbp (red mark) compared with the parental line, which carries the gene LmjF.02.0200 (highlighted gene).

Chromosome 6: Lmaj-5F2'dURes has double coverage in a region (around 140,000) carrying ~3 genes: two genes are 60S ribosomal protein L19 (LmjF.06.0410; LmjF.06.0415); one gene is a hypothetical protein (LmjF.06.0412; Figure 8.14 A, B and C). It is not clear how the amplified coverage of this gene on Lmaj-5F2'dURes might influence sensitivity to 5F-2'dUrd, particularly since this gene (LmjF.06.0412) does not have any trans-membrane domains, but may linked to unknown function of metabolomic enzymes.
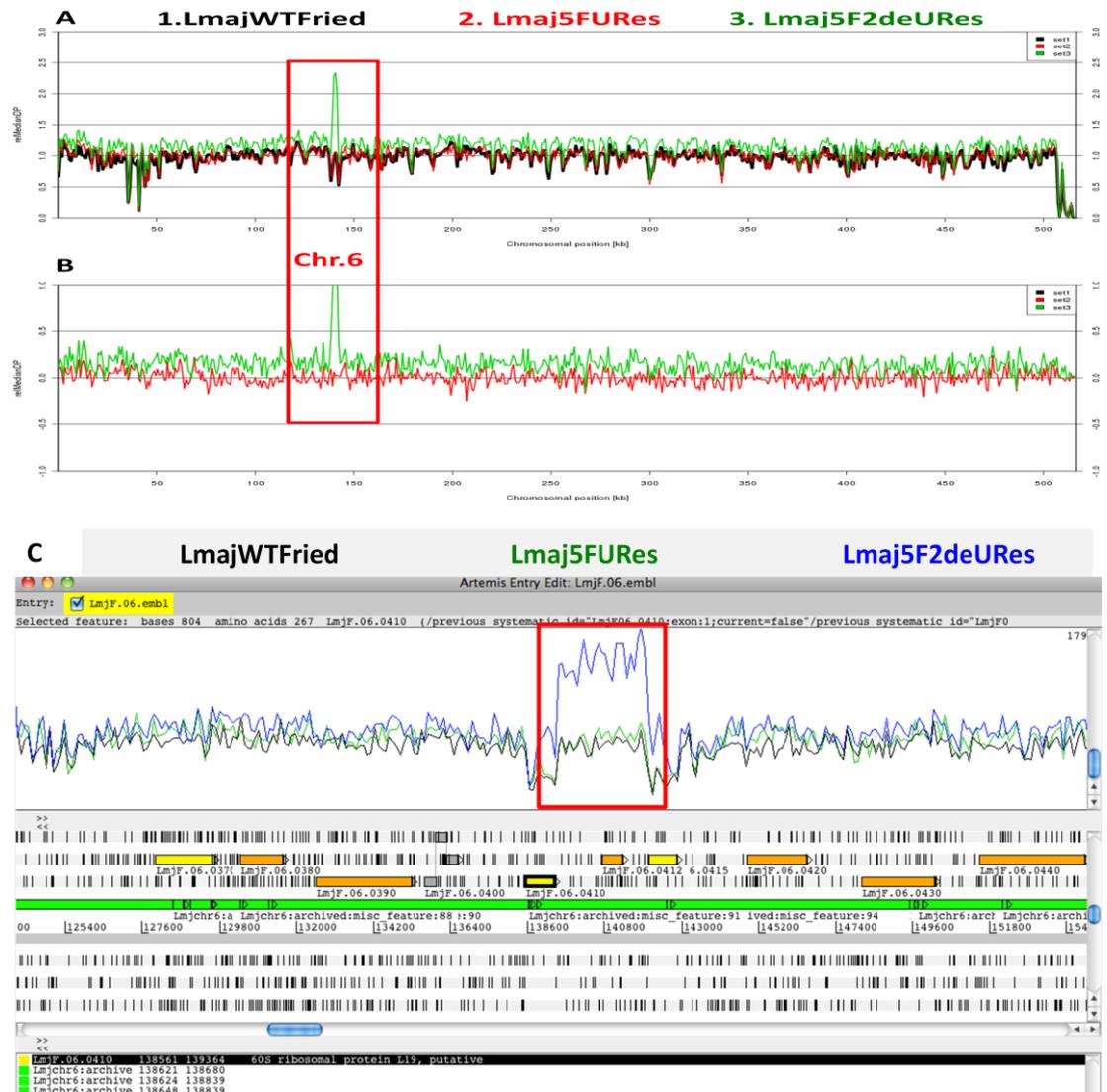
Figure 8.14. The Lmaj-5F2'dURes strain has double coverage for the region around 140 kbp of chromosome 6, which carries about 3 genes. **A.** The y-axis represents fold-change of coverage for chromosome 6 compared to the genome-wide median coverage. y-axis: 1.0 is the "neutral" value, 1.5 would be a 50% increase in coverage and 0.5 would be a 50% reduction in coverage the coverage of the parental WT strain is represented with a black line. **B.** Chromosome 6 shows the coverage of Lmaj-5F2'dURes. Coverage relative to parental strain essentially shows the difference between a coloured line and the parental black line of Plot A; y-axis: 0 is the neutral value, 0.5 would be a 50% increase in coverage, and -0.5 would be a 50% reduction in coverage. **C.** Lmaj-5F2'dURes shows the coverage on chromosome 6 compared with parental line; Artemis entry of chromosome 6 shows double coverage at location around 140 kbp (red box) compared with parental line.

Chromosome 12: in Lamj-5FURes, apparent CNV for surface antigen protein, this coverage is very likely irrelevant to the pyrimidine uptake or metabolism (Figure 8.15).
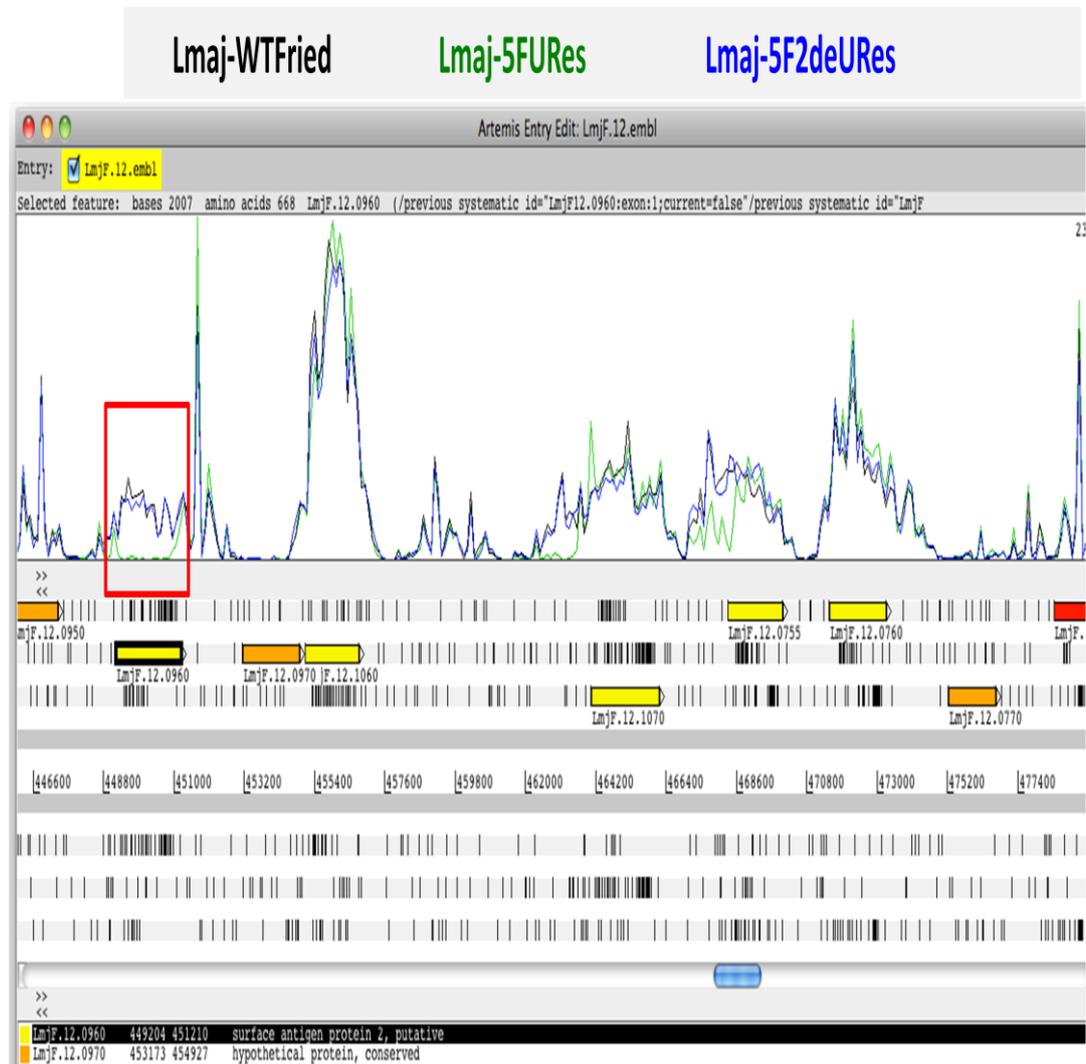
Figure 8.15. Artemis entry of chromosome 12 shows small reduction coverage for Lmaj-5FURes on chromosome 12 (red box) compared with parental line.

Chromosome 14: Lmaj5FURes has 50% reduction in coverage over region 550,000 - 579,000 carrying 9 genes (Figure 8.16), including the gene encoded a pteridine transporter (LmjF.14.1355). This gene has only 3 TM domains; the other eight genes have various functions and are not linked to pyrimidine transporter since they have no TM domains, with exception of delta-4 fatty acid desaturase (LmjF.14.1340) which has 4 TM domains. Interestingly, one of these eight genes that is located in the same region is LmjF.14.1320. The gene encodes serine hydroxymethyl transferase, which may contribute to Lmaj-5FURes resistance to 5-FU, as the enzyme involved in the dTMP cycle.

Figure 8.16. Lmaj-5FURes has 50% reduction in coverage for a region of ~29 kbp of chromosome 14, which carries 9 genes. **A.** The y-axis represents fold-change of coverage for chromosome 14 compared to the genome-wide median coverage. y-axis: 1.0 is the "neutral" value, 1.5 would be a 50% increase in coverage and 0.5 would be a 50% reduction in coverage the coverage of the parental WT strain is represented with a black line. **B.** Chromosome 14 shows 50% reduction in coverage. Coverage relative to parental strain essentially shows the difference between a coloured line and the parental black line of Plot A; y-axis: 0 is the neutral value, 0.5 would be a 50% increase in coverage, and -0.5 would be a 50% reduction in coverage. **C.** Lmaj-5FURes shows 50% reduction in coverage on chromosome 14 compared with parental line; Artemis entry of chromosome 14 shows the 50% reduction in coverage (red mark) compared with parental line.

Chromosome18: Lmaj5FURes has double coverage around position 704,000 carrying one hypothetical gene LmjF.18.1570, which has no TM domains (Figure 8.17A, B and C). As the protein has no known function it is not possible to speculate on any role it may have in Lmaj-5-FURes resistance.

Figure 8.17. Lmaj-5FURes strain has double coverage around position 704 kbp of chromosome 18, which encodes a hypothetical gene. **A.** The y-axis represents fold-change of coverage for chromosome 18 compared to the genome-wide median coverage. y-axis: 1.0 is the "neutral" value, 1.5 would be a 50% increase in coverage and 0.5 would be a 50% reduction in coverage the coverage of the parental WT strain is represented with a black line. **B.** Chromosome 18 shows the coverage of Lmaj-5FURes. Coverage relative to parental strain essentially shows the difference between a coloured line and the parental black line of Plot A; y-axis: 0 is the neutral value, 0.5 would be a 50% increase in coverage, and -0.5 would be a 50% reduction in coverage. **C.** Lmaj-5FURes shows the coverage on chromosome 18 compared with parental line; Artemis entry of chromosome 18 shows doubled coverage at location around 704 kbp (red box) compared with the parental line.

Chromosome 20: Lmaj5FURes has 50% coverage around position 535,000 bp carrying two calpain-like cysteine peptidase genes; neither LmjF.20.1180 nor LmjF.20.1185 has TM domains (Figure 8.18). It was suggested that part of programmed cell death(Gonzalez *et al.*, 2007) in *L. major* has been associated with cysteine proteinases (Arnoult *et al.,* 2002), but this idea was criticized by (Mottram *et al.,* 2004) when they claimed that *L. major* genome has no caspase genes. Here we believe that the calpain-like cysteine peptidase genes (LmjF.20.1180 and LmjF.20.1185) in Lmaj5FURes may in part be involved in *L. major* mechanisms of resistance to 5-FU; however, we could not observe these changes in the other kinetoplastid resistance lines, which is in agreement with (Kaczanowski *et al.,* 2011) findings when they conclude that the mechanisms of PCD in protozoa parasites are due to divergent evolution.

Figure 8.18. Lmaj-5FURes strain has halved coverage around position 535 kbp of chromosome 20. **A.** Chromosome 20 shows 50% coverage. Coverage relative to parental strain essentially shows the difference between a coloured line and the parental black line of Plot A; y-axis: 0 is the neutral value, 0.5 would be a 50% increase in coverage, and -0.5 would be a 50% reduction in coverage. **B.** Lmaj-5FURes shows halved coverage on chromosome 20 compared with parental line; Artemis entry of chromosome 20 (red box) compared with the parental line.

Chromosome 29: Lmaj-5F2'dURes has a 50% increase in coverage around position 770,000 compared to the parental line and Lmaj-5FURes; this locus carries two hypothetical genes, both have no TM domains (Figure 8.19). As before, the absence of any functional information on these genes makes it impossible to evaluate any role in fluoro-pyrimidine resistance.
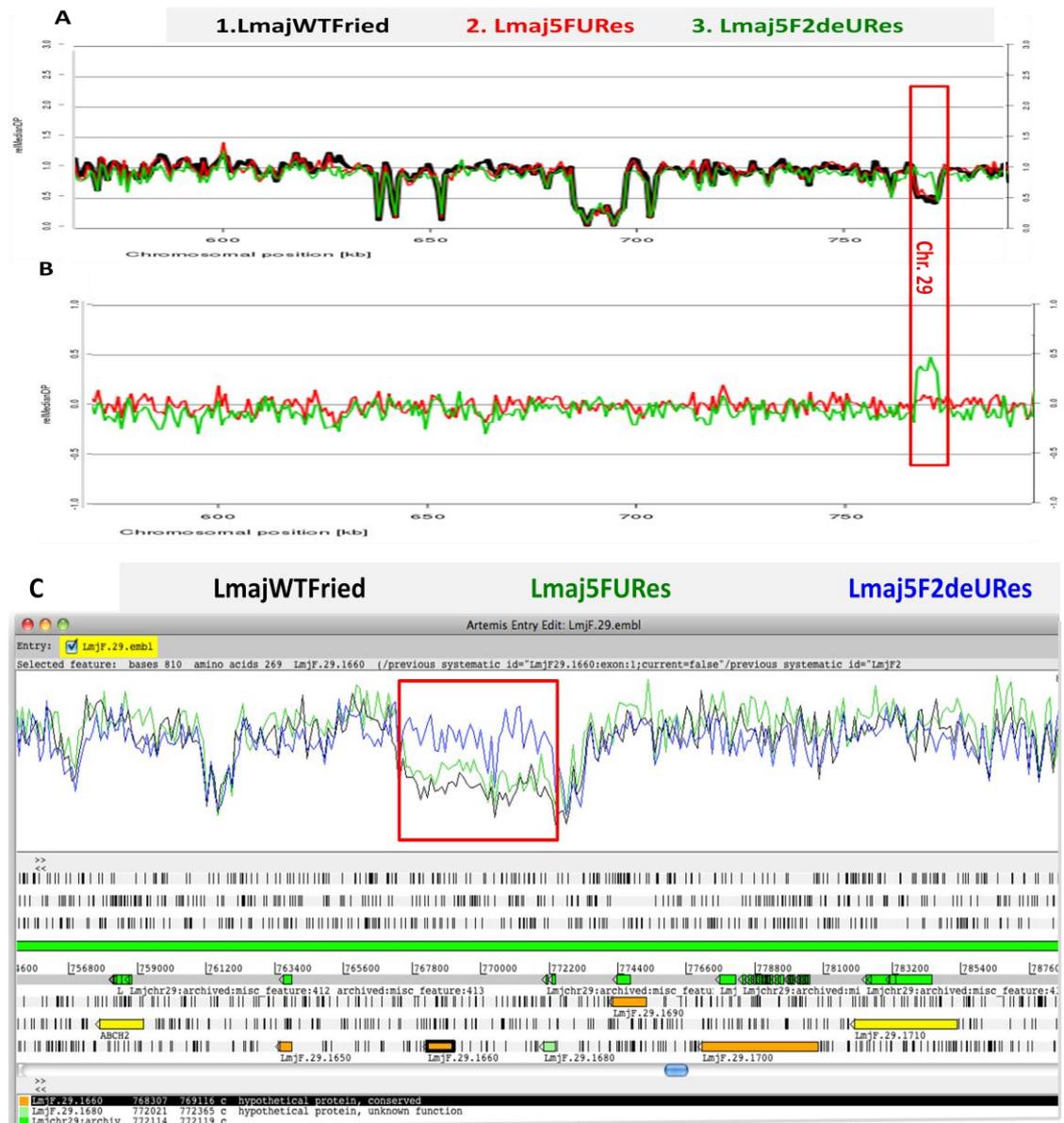
Figure 8.19. The Lmaj-52'dFURes strain has a 50% higher coverage around position 770 kbp of chromosome 29, which carries two hypothetical genes. **A.** The y-axis represents fold-change of coverage for chromosome 29 compared to the genome-wide median coverage. y-axis: 1.0 is the "neutral" value, 1.5 would be a 50% increase in coverage and 0.5 would be a 50% reduction in coverage the coverage of the parental WT strain is represented with a black line. **B.** Chromosome 29 shows the coverage of Lmaj-5F2'dURes. Coverage relative to parental strain essentially shows the difference between a coloured line and the parental black line of Plot A; y-axis: 0 is the neutral value, 0.5 would be a 50% increase in coverage, and -0.5 would be a 50% reduction in coverage. **C.** Lmaj-5F2'dURes shows the coverage on chromosome 29 compared with parental line; Artemis entry of chromosome 29 shows a higher level of coverage for Lmaj5F-2'dUres (red box) compared with the parental line.

Chromosome 31: Both the parental line (*L. major* sFriedlin-WT) and Lmaj-5FURes appear to have 5 copies of chromosome 31 whereas Lmaj-5F2'dURes has 4 copies. Among the potential genes of interest on this chromosome are three hypothetical genes LmjF.31.0030, LmjF.31.0040 and LmjF.31.0300, with 12, 11 and 12 TM domains, respectively. The parental line appears to have lost the first ~78 kb of this chromosome sequence from 3 of its 5 chromosome copies. In addition, Lmaj-5FURes seems to have lost the region 518,000 - 524,000 from two or three of its five chromosome copies, which carries gene LmjF.31.1280 (ABCC5) and borders gene LmjF.31.1290 (ABCC6) with 6 and 10 TM domains, respectively (Figure 8.20).
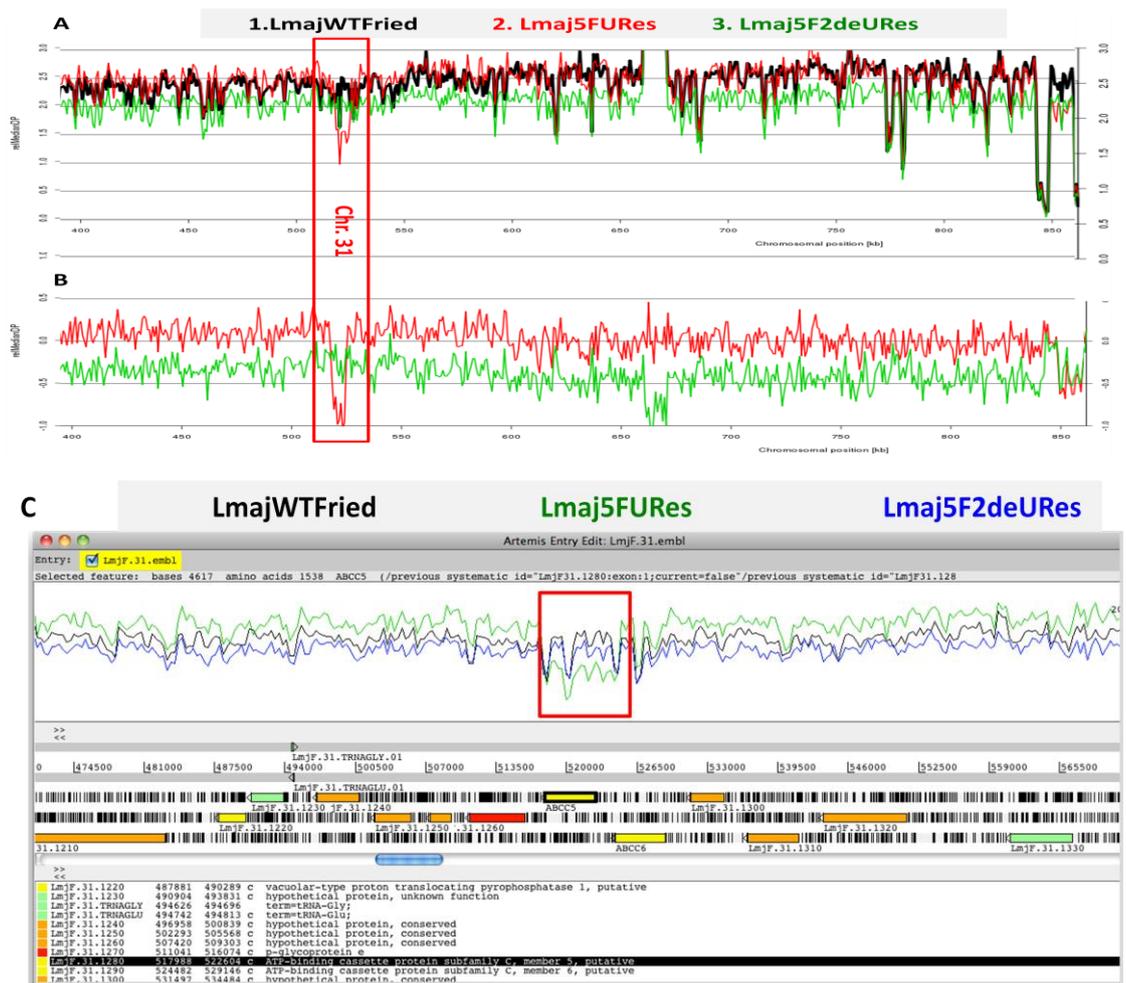
Figure 8.20. Lmaj-5FURes strain has lost ~6 kbp from at least 2 of its 5 copies of chromosome 31. **A.** Chromosome 31 lost region 518-524 kbp. Coverage relative to parental strain essentially shows the difference between a coloured line and the parental black line of Plot A; y-axis: 0 is the neutral value, 0.5 would be a 50% increase in coverage, and -0.5 would be a 50% reduction in coverage. **B.** Lmaj-5FURes shows the lost of chromosome 31. Coverage relative to parental strain essentially shows the difference between a coloured line and the parental black line of Plot A; y-axis: 0 is the neutral value, 0.5 would be a 50% increase in coverage, and -0.5 would be a 50% reduction in coverage **C.** Lmaj-5FURes shows the loss of a section of chromosome 31 compared with parental line; Artemis entry of chromosome 31 (red box) compared with the parental line.

Chromosome 33: Lmaj-5FURes has halved coverage around position 759,000 which affects two genes: peptidase M20/M25/M40 LmjF.33.1610 and LmjF.33.1600, a hypothetical protein without any TM domains (Figure 8.21).

Figure 8.21. Lmaj-5FURes strain has halved coverage around position 759 kbp of chromosome 33. **A.** Chromosome 33 shows halved coverage. Coverage relative to parental strain essentially shows the difference between a coloured line and the parental black line of Plot A; y-axis: 0 is the neutral value, 0.5 would be a 50% increase in coverage, and -0.5 would be a 50% reduction in coverage**. B.** Chromosome 33 shows the coverage of Lmaj-5FURes. Coverage relative to parental strain essentially shows the difference between a coloured line and the parental black line of Plot A; y-axis: 0 is the neutral value, 0.5 would be a 50% increase in coverage, and -0.5 would be a 50% reduction in coverage **C.** Lmaj-5FURes shows halved coverage on chromosome 33 compared with parental line; Artemis entry of chromosome 33 (red mark) compared with parental line.

Table 8.2: CNVs on *L. major* strains

Gene ID	Gene product and function	TMd	strains	Changes description
Chromosome 2				
LmjF.02.0200	Phosphoglycan beta 1,3 galactosyltransferase. Played a significant role in binding with side chain oligosaccharides	1	Lmaj-5FURes	Lost a region around positions 97-110 Kb (deletion)
Chromosome 6				
LmjF.06.0410	60S ribosomal protein L19, putative. Ribosomes are the particles that catalyse mRNA-directed protein synthesis in all organisms.	0	Lmaj-5F2dURes	Increased doubled coverage (amplification)
LmjF.06.0415				
Chromosome 12				
LmjF.12.0960	Surface antigen protein 2, putative. Interacting selectively and non-covalently with any protein or protein complex.	2	Lmaj-5FURes	Reduction coverage (deletion)
LmjF.12.0755				
Chromosome 14				
LmjF.14.1355	Pteridine transporter. Pteridine is a chemical compound composed of fused pyrimidine and pyrazine rings.	3	Lmaj-5FURes	50% reduction in coverage
LmjF.14.1320	Serine hydroxymethyltransferase (SHMT) is a pyridoxal phosphate (PLP). SHMT catalyses the transfer of a hydroxymethyl group from N5, N10-methylene tetrahydrofolate to glycine, resulting in the formation of serine and tetrahydrofolate.	0	Lmaj-5FURes	50% reduction in coverage
LmjF.14.1340	Delta-4 fatty acid desaturase. A fatty acid desaturase is an enzyme that removes two hydrogen atoms from a fatty acid, creating a carbon/carbon double bond, so that it catalyses the insertion of a double bond at the delta position of fatty acids	4	Lmaj-5FURes	50% reduction in coverage
LmjF.14.1360	Inositol-3-phosphate synthase (INO1). Inositol phosphates play an important role in signal transduction.	0	Lmaj-5FURes	50% reduction in coverage
LmjF.14.1370	Tyrosyl-tRNA synthetase, putative. Catalyse the attachment of an amino acid to its cognate transfer RNA molecule in a highly specific two-step reaction.	0	Lmaj-5FURes	50% reduction in coverage (deletion)

Table 8.2 continued: CNVs on *L. major* strains

Gene ID	Gene product and function	TMd	strains	Changes description
LmjF.14.1400	Phosphoglycan beta 1,3 galactosyltransferase, putative (SCGL). No abstract from Pfam or Gene Ontology; no function classes. This gene is not mapped to any metabolic pathway in KEGG. No EC number(s) registered for this gene. No essentiality data collected for this gene and/or its orthologs.	1	Lmaj-5FURes	50% reduction in coverage
LmjF.14.1410	Protein kinase, putative. Protein kinases are a group of enzymes that move a phosphate group onto proteins, in a process called phosphorylation.	0	Lmaj-5FURes	50% reduction in coverage
LmjF.14.1480	Glutathione-S-transferase/glutaredoxin, putative. Glutaredoxin functions as an electron carrier in the glutathione-dependent synthesis of deoxyribonucleotides by the enzyme ribonucleotide reductase.	1	Lmaj-5FURes	50% reduction in coverage
LmjF.14.1490	Synaptojanin (N-terminal domain). It dephosphorylates the D-5 position phosphate from phosphatidylinositol phosphates	1	Lmaj-5FURes	50% reduction in coverage
Chromosome 18				
LmjF.18.1570	Hypothetical protein, conserved.	0	Lmaj-5FURes	Doubled coverage (amplification)
Chromosome 20				
LmjF.20.1180	Calpain-like cysteine peptidase, putative. Members of the calpain family are believed to function in various biological processes.	0	Lmaj-5FURes	Halved reduction in coverage
LmjF.20.1185				

Table 8.2: continued CNVs on *L. major* strains

Gene ID	Gene function	TMd	strains	Changes description
Chromosome 31				
LmjF.31.0030	Hypothetical protein, conserved. Un-specified function	12	Lmaj-5F2dURes	WT and Lmaj-5FURes have 5 copies but Lmaj-5F2dURes has 4 copies
LmjF.31.0040	Hypothetical protein, conserved. Un-specified function	11	Lmaj-5F2dURes	WT and Lmaj-5FURes have 5 copies but Lmaj-5F2dURes has 4 copies
LmjF.31.0300	Hypothetical protein, conserved. Un-specified function	12	Lmaj-5F2dURes	WT and Lmaj-5FURes have 5 copies but Lmaj-5F2dURes has 4 copies
LmjF.31.1280	ATP-binding cassette protein subfamily C, member 5, putative (ABCC5). It is main transmembrane structural unit of ATP-binding cassette transporter.	6	Lmaj-5FURes	Lost the region 518,000-524,000 from 2 of its 5 chromosome copies
LmjF.31.1290	ATP-binding cassette protein subfamily C, member 6, putative (ABCC6). It is main transmembrane structural unit of ATP-binding cassette transporter.	10	Lmaj-5FURes	Its borders have been lost.
Chromosome 33				
LmjF.33.1610	Peptidase M20/M25/M40, putative. It catalysed a reaction involves the release of an N-terminal amino acid, usually neutral or hydrophobic, from a polypeptide.	0	Lmaj-5FURes	Halved reduction in coverage, which effects 2 genes

8.5   Single   nucleotide   polymorphisms   (SNPs)   in kinetoplastid resistant to fluorinated pyrimidines:

As several hundreds of SNPs on each cell line resistant strain were observed they were summarized in tables below. The tables included the SNPs that were high-confidence and led to non-synonymous changes in coding sequences. This omits all low-confidence SNPs that led to non-synonymous changes in coding sequences, SNPs that lead to synonymous changes in coding sequences, and SNPs that lead to changes in UTRs. For *T. b. brucei* bloodstream forms three different resistant strains (Tbb-5FURes, Tbb-5FOARes and Tbb-5F2'dURes) were considered and compared with 427-wild-type. Regarding to *Leishmania* species; for *L. mexicana* there are 4 datasets for the intermediate 5-FU-resistance and 3 datasets for the final 5-FU-resistance; and for *L. major* there is one dataset for 5-FU resistance and one dataset for 5F2'dUrd resistance.

Our data included lists of which genomic position was found to have a high-confidence SNP in each dataset. The collected information about each SNP was: the predicted number of transmembrane domains, the style of mapping sequence reads to the reference, whether SNP is deemed high confidence and the chromosome name and position of the SNPs. Next, for each strain we mention to the genotype of the reference sequence (data from GeneDB), the inferred diploid genotype of the parental strain (wild-type strain) and the inferred diploid genotype of the drug-resistant strain; we also list details regarding the indicated strain, as well as GeneID and description (gene product). For the SNPs information we include: position of open reading frame, the affected triplet in the reference sequence and the changed amino acid between wild-type and resistant line. The information also includes: whether the SNP call has passed the filtering (should always be OK), lists whether the genotypes of the wild-type and the resistant line are different (should always be informative), lists the chromosomal location of SNP (whether it's in the subtelomere "end" or in the chromosome "cores" -not applicable for *Leishmania*), listing quality control indicators that relate to the mapping of the sequence reads to the reference, information on SNPs in protein coding sequences, information on SNPs in 5'UTRs (length of 5'UTR as

defined by George Cross' data or 115 bp as default), information on SNPs in 3'UTRs (length of 3'UTR as defined by George Cross' data or 480bp as default).

In thesis the SNPs were summarized in tables each table has the following columns headings:

Strains = the cell line; GeneID = gene identification; Gene product = the gene description from TriTrypDB; TM = Transmembrane domains; ORF = open reading frame position, GeneDB = the indicated nucleotide is taken from GeneDB; WT = the indicated nucleotide is from the parental wild-type strain of the indicated resistant line; Resis = the indicated nucleotide is from the resistant line; amino acid mutation = the variation between wild type and resistant line (should always be non_syn = non-synonym codon change); codon = the genetic code of the amino acid, the capital letter shows the changed nucleotide in parental WT based on GeneDB code, when it is the same it is located on regular strand and when it is complementary located on reverse strand; Change = the type of change based on the amino acid, these changes were given the following numbers: 0 = No change; 1 = The amino acid changed from negative charge (-) to positive charge (+); 2 = The amino acid changed from positive charge (+) to negative charge (-); 3 = The amino acid changed from negative charge (-) to neutral; 4 = The amino acid changed from positive charge to neutral; 5 = The amino acid changed from neutral to negative charge; 6 = The amino acid changed from neutral to positive charge; 7 = The amino acid changed from negative charge to a different amino acid with negative charge; 8 = The amino acid changed from positive charge to a different amino acid with positive charge; 9 = The amino acid changed from neutral to a different neutral amino acid; 1S = The amino acid changed from stop codon to negative; 2S = The amino acid changed from stop codon to positive; 3S = The amino acid changed from stop codon to neutral; 4S = The amino acid changed from negative to stop codon; 5S = The amino acid changed from positive to stop codon; 6S = The amino acid changed from neutral to stop codon.

We particularly looked for SNPs that have TMDs, and thus may be associated with changes in pyrimidine transport, and for SNPs in genes known to be associated with pyrimidine biosynthesis/metabolism. There was only one SNP that was present in all the *T. b. brucei* fluoro-pyrimidine resistant

lines, on chromosome Tb927_05_v4 position 991523 bp of GeneID Tb927.5.3170 (Table 8.3), which codes for a putative ribose phosphate pyrophosphokinase. However, another SNP occurred only on Tb927.2.3390 of Tbb-5FURes and Tbb-5F2'dURes, this gene encodes hypothetical protein and carries 10 transmembrane domains. The changes on this gene were different in the two strains (Table 8.3). In Table 8.4 we did pairwise blast comparisons to find similar genes that contained SNPs in multiple species (*T. b. brucei, L. mexicana* and *L. major*). The BLAST results show several hundreds of hits in each of the species; therefore, only the closest homologues, with TMDs and/or association with nucleotide metabolism, are listed in the Table. The most interesting finds included some hypothetical proteins from *L. mexicana* and *L. major*, as the only near-identical match is a 5 TMD-protein LmxM.03.0370 in *L. mexicana* and its counterpart LmjF.03.0370 in *L. major*. This gene was mutated in two of the final-adapted *L. mexicana* lines (Fin2-Lmex-5FURes and Fin3-Lmex-5FURes) but in none of the intermediate lines. The *L. major* orthologue was also mutated in Lmaj5FURes, showing that the gene was independently targeted by high concentration of 5-FU in two different species of *Leishmania*.

Table 8.3: Genes that were mutated in multiple *T. b. brucei* fluoro-pyrimidine resistant lines, as compared to WT-s427.

TMd	Tbb-WT	Tbb-5FURes	Tbb-5F2'dURes	Tbb-5FOARes	GeneID	Gene Description	Tbb-5FURes	Tbb-5F2'dURes	Tbb-5FOARes	Type of Change
0	GT	G	G	G	Tb927.5.3170	Ribose-phosphate pyrophosphokinase, putative	nonsyn_Ala/Glu167Ala			0/3
10	T	GT	GT	T	Tb927.2.3390	Hypothetical protein, conserved	nonsyn_Ser131Arg/Ser	nonsyn_Lys650Lys/Asn	No changes	6/0- 0/4

Table 8.4: Pair-wise blast comparisons among kinetoplastids to identify the closest homologues of genes of particular interest, with TM domain(s) or associated with pyrimidine biosynthesis. This table identifies genes that were mutated in more than 1 species after treatment with fluorinated pyrimidines.

L. mexicana versus *L. major*						
GeneID-*L. major*	**GeneID-*L. mexicana***	**Lmaj TMd**	**Lmex TMd**	**Identity %**	**Gene product-*L. major***	**Gene product-*L. mexicana***
LmjF.03.0370	LmxM.03.0370	5	5	79.04	Hypothetical protein, conserved	Hypothetical protein, conserved
LmjF.03.0370	LmxM.03.0380	5	6	27.98	Hypothetical protein, conserved	Hypothetical protein, conserved
LmjF.32.0810	LmxM.08_29.2570	3	0	27.49	Serine/threonine protein kinase, putative.	Serine/threonine-protein kinase, putative.
L. major versus *T. b. brucei*						
GeneID *L. major*	**GeneID *T. b. brucei***	**Lmaj TMd**	**Tbb TMd**	**Identity%**	**Gene product-*L. major***	**Gene product-*T. b. brucei***
LmjF.17.0190	Tb927.4.3860	2	1	34.03	Receptor-type adenylate cyclase, putative	Receptor-type adenylate cyclase GRESAG 4, putative
LmjF.32.0810	Tb11.01.5650	3	3	49.3	Serine/threonine protein kinase, putative	Protein kinase, putative
LmjF.36.0910	Tb11.01.5650	2	3	33.57	Mitogen-activated protein kinase-like protein	Protein kinase, putative
L. mexicana versus *T. b. brucei*						
GeneID *L. mexicana*	**GeneID *T. b. brucei***	**Lmex TMd**	**Tbb TMd**	**Identity%**	**Gene product-*L. mexicana***	**Gene product-*T. b. brucei***
LmxM.28.0890	Tb11.02.5720	0	0	66.31	Ribonucleoside-diphosphate reductase large chain, putative	Ribonucleoside-diphosphate reductase large chain
LmxM.32.2290	Tb11.01.5650	2	3	44.44	Protein kinase, putative	protein kinase, putative
LmxM.30.0700	Tb11.01.6360	2	1	43.6	ATP-dependent zinc metallopeptidase, putative; Clan MA(E), Family M41	Metalloprotease, putative; cell division protein FtsH homologue, putative.
LmxM.30.1270	Tb11.01.8700	10	7	28.39	P-glycoprotein e	ABC transporter, putative

6.5.1 The high-confidence SNPs that lead to non-synonymous changes in coding sequences with ≥5 TM domains (summarized in tables 8.5 – 8.8):

Table 8.5: SNPs with ≥5 TM domains and known function genes, which are divided into groups based on the gene product; the blank gray line separates groups. This table lists the SNPs in identical (Gene ID) and/or highly similar genes (gene product description). NB: in the change column change is listed for both alleles of this gene.

Strains	Gene ID	Gene product	TM	ORF	GeneDB	WT	Resis.	Amino acid mutation	Codon	Change
Tbb-5FURes	Tb11.02.3950	ABC transporter, putative	12	3620	T	T	GT	nonsyn_Asn1207Asn/Thr	aAc	0/9
Tbb-5FURes	Tb11.01.8700		7	1829	A	A	AC	nonsyn_Leu610Leu/Arg	cTt	0/6
Lmex-Int1-5FURes	LmxM.27.0970		14	4151	G	G	AG	nonsyn_Thr1384Met/Thr	aCg	9/0
Lmex-Int3-5FURes	LmxM.11.1290		13	3463	T	T	GT	nonsyn_Phe1155Phe/Val	Ttt	0/9
Lmex-Int4-5FURes	LmxM.33.0990		9	53	G	AG	G	nonsyn_Glu18Ala/Glu	gAg	3/0
Tbb-5F2dURes	Tb927.2.6220	Adenosine transporter 2, putative	10	1036	T	T	GT	nonsyn_Leu346Leu/Val	Ttg	0/9
Tbb-5FOARes	Tb927.2.6150		11	1342	G	A	AG	nonsyn_Thr448Ala/Thr	Gct	9/0
Lmex-Int1-5FURes	LmxM.36.4480	Transmembrane amino acid transporter protein- like protein	11	1309	G	G	GT	nonsyn_Ala437Ala/Ser	Gcc	0/9
Lmex-Int2-5FURes			11	1309	G	G	GT	nonsyn_Ala437Ala/Ser	Gcc	0/9
Lmex-Int3-5FURes			11	1309	G	G	GT	nonsyn_Ala437Ala/Ser	Gcc	0/9
Lmex-Int4-5FURes			11	5089	G	G	GT	nonsyn_Leu/Val1697Leu	Ctg	9/0
Lmex-Fin1-5FURes			11	1309	G	G	GT	nonsyn_Ala437Ala/Ser	Gcc	0/9
Lmex-Fin2-5FURes			11	1309	G	G	GT	nonsyn_Ala437Ala/Ser	Gcc	0/9
Lmex-Fin3-5FURes			11	1309	G	G	GT	nonsyn_Ala437Ala/Ser	Gcc	0/9

Table 8.5 continued SNPs with ≥5 TM domains and known function genes

Strains	Gene ID	Gene product	TM	ORF	GeneDB	WT	Resis.	Amino acid mutation	Codon	Change
Tbb-5FOARes	Tb927.3.4910	Signal peptide peptidase, putative; aspartic peptidase.	8	214	A	AG	G	nonsyn_Ile/Val72Val	Ata	9/0
Tbb-5FOARes			8	689	G	AG	A	nonsyn_Asp/Gly230Asp	gGc	0/5
Lmex-Int1-5FURes	LmxM.30.0350	Amino acid transporter, putative	11	1421	G	G	CG	nonsyn_Thr474Ser/Thr	aCt	9/0
Lmex-Int4-5FURes	LmxM.30.0350		11	628	G	G	CG	nonsyn_His/Tyr210Tyr	Cat	9/0
Lmex-Fin1-5FURes	LmxM.30.0350		11	1421	G	G	CG	nonsyn_Thr474Ser/Thr	aCt	9/0
Lmex-Fin1-5FURes	LmxM.22.0230		10	557	T	T	AT	nonsyn_Asn186Ile/Asn	aAc	9/0
Tbb-5F2dURes	Tb11.02.4520		10	733	T	T	GT	nonsyn_Thr245Pro/Thr	Act	9/0
Lmex-Int2-5FURes	LmxM.27.1580		10	800	A	A	AG	nonsyn_Asn267Asn/Ser	aAc	0/9
Lmex-Int3-5FURes	LmxM.27.1580		10	800	A	A	AG	nonsyn_Asn267Asn/Ser	aAc	0/9
Lmex-Int4-5FURes	LmxM.27.1580		10	1198	A	A	AG	nonsyn_Ile/Val400Ile	Gtc	0/9
Lmex-Int1-5FURes	LmxM.32.3200	Cation transporter, putative	6	934	T	CT	C	nonsyn_Phe/Leu312Leu	Ttc	9/0
Lmex-Int2-5FURes			6	934	T	CT	C	nonsyn_Phe/Leu312Leu	Ttc	9/0
Lmex-Int3-5FURes			6	934	T	CT	C	nonsyn_Phe/Leu312Leu	Ttc	9/0
Lmex-Int4-5FURes			6	686	T	CT	C	nonsyn_Glu229Ala/Glu	gAg	3/0
Lmex-Fin1-5FURes			6	934	T	CT	C	nonsyn_Phe/Leu312Leu	Ttc	9/0
Lmex-Fin2-5FURes			6	934	T	CT	C	nonsyn_Phe/Leu312Leu	Ttc	9/0
Lmex-Fin3-5FURes			6	934	T	CT	C	nonsyn_Phe/Leu312Leu	Ttc	9/0

Table 8.5 continued SNPs with ≥5 TM domains and known function genes

Strains	Gene ID	Gene product	TM	ORF	GeneDB	WT	Resis.	Amino acid mutation	Codon	Change
Lmex-Int4-5FURes	LmxM.34.5150	Biopterin transporter, putative	14	392	T	CT	C	nonsyn_Ala/Glu131Ala	gCg	0/3
Lmex-Fin1-5FURes			14	472	T	CT	C	nonsyn_Phe/Leu158Leu	Ttc	9/0
Tbb-5F2dURes	Tb11.02.3020	Sugar transporter, putative	12	346	C	C	CT	nonsyn_Pro116Pro/Ser	Cca	0/9
Tbb-5F2dURes			12	355	T	T	GT	nonsyn_Leu119Leu/Val	Ttg	0/9
Lmex-Int2-5FURes	LmxM.30.1270	P-glycoprotein e	10	4250	A	AG	A	nonsyn_Leu/Pro1417Leu	cTg	0/9
Lmex-Int2-5FURes			10	4092	C	AC	C	nonsyn_Asp/Glu1364Glu	gaG	7/0
Lmex-Int2-5FURes			10	1702	C	CT	C	nonsyn_Ala/Thr568Ala	Gcc	0/9
Lmex-Int3-5FURes			10	1702	C	CT	C	nonsyn_Ala/Thr568Ala	Gcc	0/9
Lmex-Fin2-5FURes			10	1702	C	CT	C	nonsyn_Ala/Thr568Ala	Gcc	0/9
Lmex-Fin3-5FURes			10	1702	C	CT	C	nonsyn_Ala/Thr568Ala	Gcc	0/9
Lmex-Int1-5FURes	LmxM.23.1510	Vacuolar proton translocating ATPase subunit A, putative	6	1958	A	A	AG	nonsyn_Glu653Glu/Gly	gAg	0/3
Lmex-Int1-5FURes	LmxM.31.0920		6	365	T	CT	C	nonsyn_Ala/Val122Ala	gTg	0/9
Lmex-Fin1-5FURes	LmxM.07.0630	Vacuolar-type Ca2+-ATPase, putative	10	2785	T	T	GT	nonsyn_Cys929Cys/Gly	Tgc	0/9
Tbb-5FOARes	Tb927.3.4220	Zn-finger domain	11	38	T	GT	T	nonsyn_Asn/Thr13Asn	aAt	0/9
Lmex-Int1-5FURes	LmxM.24.2270	Zinc-finger multi-pass transmembrane protein	5	505	A	A	AC	nonsyn_Ser169Ala/Ser	Tcg	9/0

Table 8.6: SNPs in genes of known function with ≥5 TM domains that occurred in only one strain (unique mutations).

Strains	Gene ID	Gene product	TM	ORF	GeneDB	WT	Resis.	Amino acid mutation	Codon	Change
Tbb-5FURes	Tb11.01.8280	CMP-sialic acid transporter, putative	9	281	A	A	AC	nonsyn_Leu94Leu/Arg	cTt	0/6
Tbb-5F2dURes	Tb927.10.13900	UDP-galactose transporter	7	20	A	A	AC	nonsyn_Leu7Leu/Arg	cTt	0/6
Tbb-5F2dURes	Tb11.52.0018	Phospholipid-transporting ATPase, putative	8	3655	A	A	AC	nonsyn_Phe1219Phe/Val	Ttc	0/9
Lmaj-5F2dURes	LmjF.17.0600	P-type ATPase, putative	6	3142	T	T	GT	nonsyn_Thr1048Pro/Thr	Act	9/0
Lmex-Int1-5FURes	LmxM.21.1810	GPI transamidase component GAA1, putative	7	536	A	A	AC	nonsyn_Lys179Lys/Thr	aAg	0/4
Lmex-Int1-5FURes	LmxM.13.1210	Nucleobase transporter	11	493	A	A	AC	nonsyn_Phe165Phe/Val	Ttt	0/9
Lmex-Int2-5FURes	LmxM.18.0040	Transporter, putative; major facilitator superfamily protein (MFS), putative	11	103	A	A	AG	nonsyn_Trp35Arg/Trp	Tgg	6/0
Lmex-Int4-5FURes	LmxM.06.0080	Serine/threonine protein kinase, putative; protein kinase, putative	6	1011	T	T	GT	nonsyn_STOP/Tyr337Tyr	taC	3S/0
Lmex-Fin1-5FURes	LmxM.24.1090	Hypothetical predicted multipass transmembrane protein	10	1402	G	AG	G	nonsyn_Ile/Val468Val	Gtc	9/0
Lmex-Fin2-5FURes	LmxM.23.0830	Na/H antiporter-like protein	12	2248	A	A	AC	nonsyn_Phe750Phe/Val	Ttt	0/9

Table 8.7: SNPs in genes of unknown function with ≥5 TM domains that are found in multiple resistant strains; mutations are divided into groups based on gene ID.

Strains	Gene ID	Gene product	TM	ORF	GeneDB	WT	Resis.	Amino acid mutation	Codon	Change
Tbb-5FOARes	Tb927.3.4110	Hypothetical protein, conserved	14	1176	C	CT	C	nonsyn_Ile/Met392Met	atG	9/0
Tbb-5F2dURes			14	1176	C	CT	C	nonsyn_Ile/Met392Met	atG	9/0
Tbb-5F2dURes	Tb11.18.0010	Hypothetical protein, conserved	7	136	T	CT	T	nonsyn_Pro/Ser46Ser	Tcc	9/0
Tbb-5F2dURes			7	142	A	AG	A	nonsyn_Gly/Ser48Ser	Agt	9/0
Tbb-5F2dURes			7	151	A	AG	A	nonsyn_Gly/Ser51Ser	Agt	9/0
Lmex-Int1-5FURes	LmxM.10.0380	Unspecified product	12	1455	C	CG	C	nonsyn_Ile/Met485Met	atG	9/0
Lmex-Fin2-5FURes			12	1455	C	CG	C	nonsyn_Ile/Met485Met	atG	9/0
Lmex-Fin3-5FURes			12	1455	C	CG	C	nonsyn_Ile/Met485Met	atG	9/0
Lmex-Int1-5FURes	LmxM.17.1440	Hypothetical protein, unknown function	20	479	T	CT	T	nonsyn_Ala/Val160Val	gTc	9/0
Lmex-Int2-5FURes			20	479	T	CT	T	nonsyn_Ala/Val160Val	gTc	9/0
Lmex-Int3-5FURes			20	479	T	CT	T	nonsyn_Ala/Val160Val	gTc	9/0
Lmex-Int4-5FURes			20	1028	T	CT	T	nonsyn_Leu343Leu/Pro	cTg	0/9
Lmex-Fin1-5FURes			20	479	T	CT	T	nonsyn_Ala/Val160Val	gTc	9/0
Lmex-Fin2-5FURes			20	479	T	CT	T	nonsyn_Ala/Val160Val	gTc	9/0
Lmex-Fin3-5FURes			20	479	T	CT	T	nonsyn_Ala/Val160Val	gTc	9/0

Table 8.7 continued SNPs in genes of unknown function with ≥5 TM domains

Strains	Gene ID	Gene product	TM	ORF	GeneDB	WT	Resis.	Amino acid mutation	Codon	Change
Lmex-Int1-5FURes			14	857	C	T	CT	nonsyn_Asp286Asp/Gly	gGc	0/3
Lmex-Int4-5FURes	LmxM.30.0030	hypothetical protein, conserved	14	3745	C	T	CT	nonsyn_Ile/Leu1249Leu	Tta	9/0
Lmex-Fin1-5FURes			14	857	C	T	CT	nonsyn_Asp286Asp/Gly	gGc	0/3
Lmex-Int1-5FURes	LmxM.32.0710	hypothetical protein, conserved	10	730	T	T	CT	nonsyn_Trp244Arg/Trp	Tgg	6/0
Lmex-Fin2-5FURes			10	191	T	CT	C	nonsyn_Ala/Val64Ala	gTt	0/9
Lmex-Int1-5FURes			9	2438	C	AC	C	nonsyn_STOP/Ser813Ser	tCg	3S/0
Lmex-Int2-5FURes			9	2438	C	AC	C	nonsyn_STOP/Ser813Ser	tCg	3S/0
Lmex-Int3-5FURes			9	2438	C	AC	C	nonsyn_STOP/Ser813Ser	tCg	3S/0
Lmex-Int4-5FURes	LmxM.32.1940	hypothetical protein, conserved	9	3028	C	AC	C	nonsyn_His/Asn1010Asn	Cac	9/0
Lmex-Fin1-5FURes			9	2438	C	AC	C	nonsyn_STOP/Ser813Ser	tCg	3S/0
Lmex-Fin2-5FURes			9	2438	C	AC	C	nonsyn_STOP/Ser813Ser	tCg	3S/0
Lmex-Fin3-5FURes			9	2438	C	AC	C	nonsyn_STOP/Ser813Ser	tCg	3S/0
Lmex-Int2-5FURes			5	1457	C	CT	C	nonsyn_Asn/Ser486Ser	aGc	9/0
Lmex-Int2-5FURes			5	892	A	A	AC	nonsyn_Phe298Phe/Val	Ttt	0/9
Lmex-Int2-5FURes	LmxM.30.0800	Hypothetical protein, conserved	5	125	C	CT	C	nonsyn_Glu/Gly42Gly	gGg	3/0
Lmex-Int3-5FURes			5	892	A	A	AC	nonsyn_Phe298Phe/Val	Ttt	0/9
Lmex-Int3-5FURes			5	125	C	CT	C	nonsyn_Glu/Gly42Gly	gGg	3/0

Table 8.7 continued SNPs in genes of unknown function with ≥5 TM domains

Strains	Gene ID	Gene product	TM	ORF	GeneDB	WT	Resis.	Amino acid mutation	Codon	Change
Lmex-Int1-5FURes			5	521	T	T	CT	nonsyn_Glu174Glu/Gly	gAg	0/3
Lmex-Int4-5FURes			5	1343	A	AG	G	nonsyn_Ala/Gly448Ala	gGt	9/0
Lmex-Int4-5FURes	LmxM.34.3190	Hypothetical protein, conserved	5	1334	C	AC	A	nonsyn_Ala/Gly445Gly	gCg	9/0
Lmex-Fin1-5FURes			5	2588	A	AG	G	nonsyn_Leu/Ser863Ser	tTg	9/0
Lmex-Fin1-5FURes			5	2438	C	AC	A	nonsyn_Gly/Val813Val	gGc	9/0
Lmex-Int4-5FURes			9	935	G	CG	G	nonsyn_Gln312Gln/Arg	cAg	0/6
Lmex-Int4-5FURes	LmxM.33.1070	Hypothetical protein, conserved	9	437	T	CT	T	nonsyn_Gln146Leu/Gln	cAg	9/0
Lmex-Int4-5FURes			9	1265	C	AC	C	nonsyn_Cys/Tyr422Cys	tAc	0/9
Lmex-Fin1-5FURes			11	2480	C	AC	A	nonsyn_Ala/Glu827Glu	gCa	5/0
Lmex-Fin1-5FURes			11	3187	A	AG	G	nonsyn_Ala/Thr1063Ala	Aca	0/9
Lmex-Fin1-5FURes	LmxM.24.1451	Hypothetical protein, conserved	11	4384	G	AG	G	nonsyn_Gly/Ser1462Gly	Ggt	9/0
Lmex-Fin1-5FURes			11	5806	G	GT	G	nonsyn_Cys/Gly1936Gly	Ggt	9/0
Lmex-Fin1-5FURes		Hypothetical protein, conserved	9	1562	G	AG	A	nonsyn_His/Arg521His	cGt	0/4
Lmex-Fin3-5FURes	LmxM.26.2590		9	1562	G	AG	A	nonsyn_His/Arg521His	cGt	0/4

Table 8.7 continued SNPs in genes of unknown function with ≥5 TM domains

Strains	Gene ID	Gene product	TM	ORF	GeneDB	WT	Resis.	Amino acid mutation	Codon	Change
Lmex-Fin1-5FURes			12	3030	T	CT	T	nonsyn_Ile/Met1010Ile	atA	0/9
Lmex-Fin1-5FURes			12	3026	C	CG	C	nonsyn_Ala/Gly1009Gly	gGg	9/0
Lmex-Fin1-5FURes	LmxM.30.0300	Hypothetical protein, conserved	12	2531	G	GT	G	nonsyn_Ala/Glu844Ala	gCa	0/3
Lmex-Fin1-5FURes			12	818	C	CT	C	nonsyn_Asn/Ser273Ser	aGc	9/0
Lmex-Fin1-5FURes			12	454	C	CT	C	nonsyn_Gly/Ser152Gly	Ggc	0/9
Lmex-Fin1-5FURes			12	3032	T	CT	T	nonsyn_Asp/Gly1011Asp	gAc	0/5
Lmex-Fin1-5FURes	LmxM.30.0310	Hypothetical protein, conserved	12	1792	C	CT	C	nonsyn_Ile/Val598Val	Gtt	9/0
Lmex-Fin1-5FURes			12	1171	T	CT	T	nonsyn_Gly/Ser391Ser	Agt	9/0
Lmex-Fin2-5FURes	LmxM.03.0370	Hypothetical protein, conserved	5	665	C	C	A	nonsyn_Thr222Asn	aCt	9
Lmex-Fin3-5FURes			5	665	C	C	A	nonsyn_Thr222Asn	aCt	9
Lmex-Fin2-5FURes	LmxM.03.0380	Unspecified product	6	692	C	CT	T	nonsyn_Phe/Ser231Phe	tCc	0/9
Lmex-Fin3-5FURes			6	692	C	CT	T	nonsyn_Phe/Ser231Phe	tCc	0/9

Table 8.8: SNPs with ≥5 TM domains in genes of unknown function; these mutations are unique for the indicated strain only.

Strains	Gene ID	Gene product	TM	ORF	GeneDB	WT	Resis.	Amino acid mutation	Codon	Change
Tbb-5F2'dURes	Tb927.2.3390	Hypothetical protein, conserved	10	1950	T	T	GT	nonsyn_Lys650Lys/Asn	aaA	0/4
	Tb927.2.4470		8	2353	A	A	AC	nonsyn_Leu785Leu/Val	Ttg	0/9
	Tb927.3.3500		8	241	T	T	GT	nonsyn_Phe81Phe/Val	Ttt	0/9
	Tb927.4.320		8	53	A	A	AC	nonsyn_Leu18Leu/Arg	cTt	0/6
	Tb927.8.4360		12	2166	A	A	AC	nonsyn_Asp722Asp/Glu	gaT	0/7
	Tb927.8.6730		6	652	C	CT	C	nonsyn_Ala/Thr218Ala	Gct	9/0
	Tb11.01.6760		6	1639	A	A	AC	nonsyn_Leu547Leu/Val	Ttg	0/9
Tbb-5FOARes	Tb927.3.4200	Hypothetical protein, conserved	4	224	A	AG	A	nonsyn_Met/Thr75Met	aTg	0/9
	Tb927.3.4200		4	205	T	CT	C	nonsyn_Met/Val69Val	Atg	9/0
Lmaj-5FURes	LmjF.03.0370	Hypothetical protein, conserved	5	859	A	A	C	nonsyn_Thr287Pro	Acc	9
	LmjF.32.2310		9	790	A	A	AC	nonsyn_Ser264Ala/Ser	Tcg	9/0
Lmaj-5F2dURes	LmjF.08.0190	Hypothetical protein, conserved	13	2116	G	G	AG	nonsyn_Val706Ile/Val	Gtt	9/0
	LmjF.25.1160		9	1438	T	T	GT	nonsyn_Ser480Arg/Ser	Agc	6/0
	LmjF.26.0520		5	2335	T	T	CT	nonsyn_Lys779Glu/Lys	Aag	2/0
Lmex-Int1-5FURes	LmxM.01.0440	Hypothetical protein, conserved	10	421	C	CT	C	nonsyn_Phe/Leu141Leu	Ctc	9/0
	LmxM.27.1510		5	1376	T	T	GT	nonsyn_Val459Gly/Val	gTg	9/0
Lmex-Int4-5FURes	LmxM.14.0640	Hypothetical protein, conserved	6	904	T	AC	C	nonsyn_Pro/Ser302Pro	Ccg	0/9
	LmxM.14.0730		7	427	C	CT	C	nonsyn_Pro/Ser143Pro	Ccg	0/9
	LmxM.33.1270		13	4196	T	CT	T	nonsyn_Asp/Gly1399Asp	gGc	0/5
	LmxM.34.3320		5	2423	T	CT	T	nonsyn_Ala/Glu808Glu	gCg	5/0
Fin2-Lmex-5FURes	LmxM.34.2810b	Hypothetical protein, conserved	11	530	T	T	CT	nonsyn_Tyr177Cys/Tyr	tAt	9/0
	LmxM.25.0790		6	3503	A	AG	A	nonsyn_Asp/Gly1168Asp	gAc	0/5

6.5.2 The high-confidence SNPs that lead to non-synonymous changes in coding sequences, but with no TM domains (summarized in tables 8.9 and 8.10):

Table 8.9: SNPs that are associated with the pyrimidine biosynthesis and salvage pathways; the gray line divides the groups based on gene function

Strains	Gene ID	ORF	GDB	WT	Resist strain	A.A. mutation	Codon	Type change	Gene product and function
Tbb-5FURes Tbb-5F2'dURes Tbb-5FOARes	Tb927.5.3170	500	G	GT	G	nonsyn_Ala/Glu167Ala	gCa	0/3	Ribose-phosphate diphospho-kinase (RPPK), also known as phosphoribosyl diphosphate synthetase (EC:2.7.6.1), catalyses the transfer of an intact diphosphate (PP) group from ATP to ribose-5-phosphate (R-5-P), which results in the formation of AMP and 5-phospho-D-ribosyl-1-diphosphate (PRPP).
Tbb-5F2dURes	Tb11.02.5720	2042	A	A	AC	nonsyn_Ile681Ile/ Ser	aTt	0/9	Ribonucleotide reductase (RNR) catalyzes the formation of deoxyribonucleotides from ribonucleotides. The substrates for RNR are ADP, GDP, CDP and UDP.
Lmex-Int3-5FURes Lmex-Fin2-5FURes Lmex-Fin3-5FURes	LmxM.28.0890	1918	C	C	AC	nonsyn_Arg640Arg/Ser	Cgc	0/4	
Tbb-5F2dURes	Tb927.10.880	1088	T	T	GT	nonsyn_Leu363Leu/Arg	cTt	0/6	Thymidine kinase, putative, TK catalyses the reaction: deoxythymidine + ATP = deoxythymidine 5'-phosphate + ADP. Thymidine kinases introduce deoxythymidine into the DNA.

Table 8.9 continued SNPs that are associated with the pyrimidine biosynthesis and salvage pathways; the gray line divides the groups based on gene function

Strains	Gene ID	ORF	GDB	WT	Resist strain	A.A. mutation	Codon	Type change	Gene product and function
Lmaj-5F2dURes	LmjF.30.1960	1522	T	T	GT	nonsyn_STOP508STOP/Glu	Tag	0/1S	RNA pseudouridylate synthase-like protein. Members of this family are involved in modifying bases in RNA molecules. They carry out the conversion of uracil bases to pseudouridine
Lmex-Fin1-5FURes	LmxM.16.0550	434	T	T	GT	nonsyn_Gln145Pro/Gln	cAg	9/0	Orotidine 5'-phosphate decarboxylase/ orotate phosphoribosyl transferase, putative (UTPase). It catalyses the last step in the *de novo* biosynthesis of pyrimidines.
Lmex-Fin3-5FURes	LmxM.10.1010	601	T	T	CT	nonsyn_Thr201Ala/Thr	Acc	9/0	Nucleoside phosphorylase-like protein. Members of this family include: Uridine phosphorylase, which catalyses the cleavage of uridine into uracil and ribose-1-phosphate, the products of the reaction are used in the rescue of pyrimidine bases for nucleotide synthesis

Table 8.10: SNPs in genes, without TMDs, involved in nucleotide metabolism, with unique mutation for the indicated strain only.

Strains	Gene ID	ORF	GDB	WT	Resist strain	A.A. mutation	Codon	Type change	Gene function
Tbb-5FURes	Tb927.8.3800	1000	T	T	GT	nonsyn_Ser334Arg/ Ser	Agt	6/0	Nucleoside phosphatase, putative; guanosine diphosphatase, putative. Nucleoside diphosphatase activity as well as guanosine-diphosphatase activity
Tbb-5F2dURes	Tb927.10.5510	1498	T	T	GT	nonsyn_Leu500Leu/ Val	Ttg	0/9	Endonuclease/exonuclease/phosphatase, putative. This is a structural domain found in the large family of proteins including magnesium dependent endonucleases and many phosphatases involved in intracellular signalling
Tbb-5F2dURes	Tb927.10.6090	632	A	A	AC	nonsyn_Leu211Leu/ Arg	cTt	0/6	tRNA pseudouridine synthase A. Pseudouridine synthase activity and RNA binding.
Tbb-5F2dURes	Tb927.10.11100	683	T	T	GT	nonsyn_Glu228Ala/ Glu	gAg	3/0	Deoxyribodipyrimidine photolyase, putative; DNA repair enzymes, putative. They bind to DNA containing pyrimidine dimers. These enzymes catalyse dimer splitting into the constituent monomers.
Lmaj-5F2dURes	LmjF.23.1590	788	C	C	CT	nonsyn_Ser263Leu/ Ser	tCa	9/0	Oxidoreductase-like protein. This group of enzymes utilise NADP or NAD.
Lmex-Fin1-5FURes	LmxM.36.0330	497	T	T	GT	nonsyn_Glu166Ala/ Glu	gAg	3/0	Ribonuclease HII is involved in the degradation of the ribonucleotide moiety on RNA-DNA hybrid molecules carrying out endonucleolytic cleavage to 5'-phospo-monoester.
Lmex-Fin1-5FURes	LmxM.34.4800	281	G	G	AG	nonsyn_Arg94His/ Arg	cGc	4/0	AMP deaminase, putative. It catalyzes the hydrolytic deamination of AMP into IMP.

8.6 Discussion

The generation of genome sequences for trypanosomes and for *Leishmania* species resistant to fluorinated pyrimidines showed numerous changes in each resistant strain. The data showed that the genomes of Tbb-5FURes, Tbb-5FOARes and Tbb-5F2'dURes contained 2561, 2581 and 2605 SNPs, respectively. Out of these SNPs only 697, 135, and 755 SNPs were considered as high-confidence and led to non-synonymous changes in coding sequences, respectively. None of these changes was found in all trypanosomes resistant strains with two exceptions: one occurred on gene Tb927.5.3170, which encodes phosphate pyrophosphokinase. This SNP is probably associated with resistance to fluoro-pyrimidines; the second one occurred on Tb927.2.3390, only on Tbb-5FURes and Tbb-5F2'dURes. Although this gene encodes hypothetical protein and has unknown function, it carries 10 transmembrane domains. The SNPs on this gene were different in the two strains: on Tbb-5FURes the change was from serine at position 131 to arginine or serine, and on Tbb-5F2'dURes was from lysine on position 650 to lysine or asparagine. As both 5-FU and 5F2'dUrd share the same transporter (TbU3) on plasma membrane of bloodstream form of *T. b. brucei*, the SNPs on this gene could be a part of the adaption, particularly as we found a 76 ± 6% reduction of 5-FU uptake by Tbb-5FURes compared with Tbb-WT. None of the chromosomes of trypanosomes resistance strains has shown copy number variations (CNVs), consistent with the general view that *Trypanosoma* species, in contrast, to *Leishmania* species, do not easily undergo CNVs (Bingle *et al.,* 2001;Gaunt *et al.,* 2003).

For the resistant *Leishmania* strains the number of SNPs was also very considerable. The four intermediate strains of *L. mexicana* resistant to 5-FU (Lmex-5FURes-Int -1,2,3,4) showed 849, 868, 618 and 1018 SNPs; out of these SNPs changes the data showed only 204, 197, 138 and 208 SNPs were high-confidence and led to non-synonymous changes in coding sequences, respectively. Similarly numbers of SNPs were observed in the genomes of the three final strains of *L. mexicana* with very high levels of resistance to 5-FU, (Lmex-5FURes-Fin 1,2,3) which showed 1748, 953 and 926 SNPs, respectively. The numbers of SNPs that were high-confidence and led to non-synonymous changes in coding sequences were 447, 210 and 208 SNPs, respectively. SNPs

changes were also observed in the genome of *L. major* with resistance to fluorinated pyrimidines. The number of SNPs in Lmaj-5FURes and Lmaj-5F2'dURes were 212 and 466, but the high-confidence SNPs, which led to non-synonymous changes in coding sequences, were 74 and 116, respectively. Out of thousands of SNPs in all the resistant *Leishmania* strains, there was only one gene independently targeted by 5-FU in both *L. mexicana* and *L. major*, and this was a hypothetical protein identified as LmxM.03.0370 and LmjF.03.0370, respectively. Interestingly, the gene carries a 5 TMD-protein, which might be a candidate gene for 5-FU resistance in *Leishmania* spp.

On the other side, several reductions and elevations have been observed on a whole chromosome or chunk of it on *Leishmania* resistant strains. Therefore, we recommend further investigation on the suspected genes that were known or unknown function and potentially associated with resistance to fluorinated pyrimidines.

CHAPTER NINE

General discussion

Kinetoplastid parasites including: *Trypanosoma brucei brucei, T. b. gambiense, T. b. rhodesiense, T. vivax,* and *T. congolense*, as well as *Leishmania mexicana, L. major, L. donovani, L. braziliensis,* and *L. infantum*, cause a number of medical and veterinary conditions all over the world. As the pathogens have become resistant to most of the drugs currently used, new therapeutic strategies are urgently needed. Since kinetoplastid parasites must continue to divide at a rapid rate, purine and pyrimidine nucleotide metabolism is one obvious drug target. However, no purine-based chemotherapy has successfully emerged against kinetoplastid parasites. The pathway of pyrimidine nucleotide metabolism is rather more diverse in protozoan parasites. Kinetoplastid parasites possess both salvage and biosynthesis routes for pyrimidines (Al-Salabi *et al.,* 2007; De Koning *et al.,* 2005; Papageorgiou *et al.,* 2005) and some enzymes of the pyrimidine inter-conversion pathways may be good drug targets. For instance, bloodstream forms of trypanosomes are unable to incorporate tritium cytosine or cytidine into their nucleotide pool, leaving CTP synthetase as the only route to obtain cytidine nucleotides; inhibition of the enzyme declined the growth in vivo and in vitro (Fijolek *et al.,* 2007; Hofer *et al.,* 2001). Another target in the pyrimidine pathways is RNAi knockdown of dUTPase, the inhibition of which reduces proliferation and leads to DNA damage (Castillo-Acosta *et al.,* 2008, 2013). Furthermore, knockout of DHFR-TS is lethal in *T. b. brucei* (Sienkiewicz *et al.,* 2008). In *L. donovani*, UMP synthase was found to be essential for in vitro growth in the absence of added pyrimidines (French *et al.,* 2011).

Few studies on pyrimidine uptake by kinetoplastid parasites have been performed; procyclic forms of *T. b. brucei* (De Koning & Jarvis, 1998; Gudin *et al.,* 2006) and promastigotes of *L. major* (Papageorgiou *et al.,* 2005) showed high affinity transporters for uracil, identified as TbU1 and LmajU1, respectively. The incomplete information about pyrimidine permease in kinetoplastid and the lack of information about individual pyrimidine metabolism inside the cells hinder efforts to develop a pyrimidine-based chemotherapy, as well as making it difficult to judge the relative importance of salvage and synthesis. Because of that, detailed study of pyrimidine transport and metabolism in kinetoplastid parasites is crucial, and the

identification of pyrimidine analogues against *Trypanosoma* and *Leishmania* species are of great interest.

Characterization of pyrimidine transport activities in bloodstream forms of *T. b. brucei* found that these cells express a high affinity uracil transporter (TbU3) that has a very similar substrate profile compared to TbU1 in procyclic forms. This would usually be indicative of a similar structure for the two transport proteins, but the gene identifications and protein structures are as yet unknown. Of the two, TbU3 has more steric limitations than TbU1 when it comes to binding nucleosides rather than nucleobases – either in the binding site itself or in extracellular access to it, as reflected in its much lower affinity for uridine. Furthermore, the lower affinity for 4-thiouracil by TbU3 is likely to reflect a stronger hydrogen bond at the 4-keto group than was the case for TbU1, as a result of a subtle shift in position or a different amino acid facing this group. However, while procyclic forms expressed TbU1, with high affinity for uracil and uridine, these cells also express a separate uridine transporter, TbU2 (Gudin *et al.*, 2006), giving uridine salvage clearly more importance in this life-cycle stage. Bloodstream forms of *T. b. brucei* expressed only TbU3, which had high affinity and efficiency for uracil, but very low affinity for uridine and 2'-deoxyuridine. In addition, thymidine was taken up by the bloodstream forms, although inefficiently, through a P1-type nucleoside transporter, TbT1. The affinity to thymidine was identical when we assessed the uptake of the nucleoside into trypanosomes grown under in vivo or in vitro conditions. Uptake of uridine, 2'-deoxyuridine, cytidine and 2'-deoxycytidine can all be measured but displays very low affinity and efficiency compared to [^{3}H]-uracil transport, and unlikely to play any significant role in pyrimidine metabolism in vivo.

The evidence showed that the nucleobases and nucleosides of pyrimidines were taken up by *Leishmania* cells via different transporters. We demonstrated that *L. mexicana* expressed at least two pyrimidine transport activities, the first being a pyrimidine nucleobase transporter (LmexU1) responsible for uracil uptake and well inhibited by uridine, but not by thymidine and adenosine. The second was a nucleoside transporter (LmexNT1) sensitive to uridine, thymidine and adenosine, but with low affinity for uracil. For promastigotes of *L. major*, it was demonstrated that these promastigotes also expressed a high affinity uracil transporter (LmajU1)

that was inhibited by uridine (Papageorgiou *et al.,* 2005). However, in this species two distinct nucleoside transport activities were observed: the high affinity uridine transporter (LmajNT1), which was sensitive to uridine, uracil, inosine and adenine; and the low affinity uridine transporter (LmajNT2), which has low affinity to uridine and was insensitive to uracil, inosine and adenine. Both activities are inhibited by 2'-deoxyuridine, thymidine and adenosine. Of importance, the anticancer drug 5-fluorouracil was an excellent substrate for all the kinetoplastid uracil transporters TbU1, TbU3, LmajU1 and LmexU1.

It appears that bloodstream forms of *Trypanosoma brucei* and promastigotes of *Leishmania* are virtually identical with respect to the toxicity of pyrimidine analogues against kinetoplastid parasites. For instance, 5-FU, 5-FOA, 5F-2'dUrd, 5F-2'dCyd and 5F-Urd were much more active against all of the kinetoplastid species than any of the other halogenated pyrimidines tested. However, the effect of 5F-Urd and 5-FOA was an exception. While *L. major* cells were very sensitive to 5F-Urd, *T. b. brucei* and *L. mexicana* cells were resistant to the drug. For *T. b. brucei*, we mostly attributed that to the poor uptake, as well as the low activity of uridine phosphorylase; in *L. mexicana* the promastigotes catalyzed the drug to 5F-2'dUrd and we linked the resistance to the rapid conversion of 5F-2'dUrd to 5F-dUMP that lead to the absence of the metabolite responsible for inhibition of TS. For 5-FOA, it seems that trypanosomes are sensitive to the drug at micromolar level, but *Leishmania* species were resistant to high concentrations. This finding was consistent with French *et al.,* 2011, who found that pyrimidine auxotrophic of *L. donovani* were not able to incorporate orotate into nucleotide pool when the cells exposed to 100 µM orotate as sole pyrimidine source.

Fluorinated pyrimidines such as 5-fluorouracil, 5-fluoroorotic acid, 5-fluoro-2'deoxy- (uridine or cytidine) and 5-chloro-2deoxyuridine displayed anti-trypanosomal activity in the micromolar range. The study induced resistance to 5-FU, 5-FOA and 5F-2'dUrd by in vitro exposure of *T. b. brucei* BSF s427-WT to stepwise increasing concentrations of the compounds. When the trypanosomes became resistance to high concentrations of the drugs the new strains were cloned out, which resulted in the clonal lines Tbb-5FURes, Tbb-5FOARes and Tbb-5F2'dURes with resistance factors 131, 83 and 825,

respectively. Tbb-5FURes cells were cross-resistant to other pyrimidine nucleobase analogues, but not to pyrimidine nucleoside analogues; and vies versa Tbb-5F2'dURes cells were cross-resistant to pyrimidine nucleoside analogues, but not to pyrimidine nucleobase analogues. Interestingly, when the uptake of natural pyrimidines was assessed in resistant *Trypanosoma* clones the results showed that the uptake of natural pyrimidines was not significantly changed. Although the uptake of [³H]-5-fluroruracil and [³H]-orotic acid were reduced by 76% and 68% in the Tbb-5FURes and Tbb-5FOARes cell lines, respectively, we can assume that the reduction in these transport rates is small and most likely only one contributing factor to the very high levels of resistance observed in the resistant lines. The results indicate that the mechanisms of resistance to high levels of pyrimidine analogues in trypanosomes were related to changes in pyrimidine metabolic processes rather than drug transport. Therefore, we assessed the metabolism and mode of action of effective pyrimidine analogues using metabolomic assessments of trypanosomes clonal lines adapted to high concentrations of these pyrimidine analogues, and of the sensitive *Trypanosoma* s427-WT.

Detailed characterization of metabolomic and incorporation of pyrimidine analogues in nucleic acids by trypanosomes was performed. Incubation with 100 µM of 5-FU or 5-FOA led to the same fluorinated metabolites in bloodstream forms of s427-WT and finally converted to 5F-UMP. Considerable amounts of fluorinated-uridine nucleotides were detected in metabolomic extracts, as well as 5F-UDP-glucose or -galactose, and 5F-UDP-N-acetylglucosamine, but no trace of 5-fluoro-2'deoxyuridine nucleotides was observed. These pyrimidine metabolites have also been observed to achieve lower levels in trypanosomes resistant to fluorinated pyrimidine nucleobases, which is consistent with reduced uptake of [³H]-pyrimidine nucleobase transport, the reductions in the level of pyrimidine metabolites in resistant clones (Tbb-5FURes and Tbb-5FOARes) and the reduced rate of [³H]-pyrimidine nucleobase uptake could make major contributions in resistance mechanism to 5-FU and 5-FOA. Furthermore, the intracellular level of dUMP was elevated in trypanosomes of the resistant lines and s427-WT after treatment with 5-FU, which is possibly attributed to an inhibition of thymidylate synthase and/or an allosteric effect of a fluorinated nucleotide on ribonucleoside-diphosphate reductase. Although

fluorinated cytidine nucleotides were not detected in the trypanosomes extract after 5-FU or 5-FOA treatment, significant amounts of 5F-UMP and low levels of 5F-CMP were detected in digested RNA. The reason for the apparently more sensitive detection of fluorinated nucleotides in the digested RNA was attributed to a much more concentrated mono-nucleotide pool for HPLC/MS analysis. However, no fluorinated metabolites were observed in digested DNA after exposing trypanosomes to 5-FU or 5F-2'dUrd, which seems to differentiate the mechanism of action in trypanosomes from the actions in *Homo sapiens* cells; however, we can rule out that very small amounts of fluorinated deoxynucleotides were incorporated into DNA, below the detection level. We also could not observe any effect on glycosylation of *T. b. brucei* membrane proteins. To sum up, the analysis showed that 5-FU and 5-FOA trypanocidal activities are multifactorial, they are incorporated into a large number of metabolites such as precursors for lipid biosynthesis, sugar metabolism and VSG glycosylation or GPI anchors (Donelson, 2003), but likely exert toxicity through incorporation into RNA, and the resistance mechanism was possibly by preventing their incorporation into the nucleotide pool.

Intracellular levels of 5F-2'dUrd were not different between s427-WT and Tbb-5F2'dURes cells, confirming that the resistance mechanism is based on metabolism rather than reduced uptake of the drug. Significant amounts of 2'-deoxyuridine monophosphate were observed in 5F-2'dUrd-exposed trypanosomes, but neither fluorinated uridine ribonucleotides nor fluorinated 2'deoxyuridine nucleotides were detected apart from 5F-dUMP, and the lack of any incorporation of 5F-deoxynucleotides into DNA digests appears to support these findings. This strongly suggests that the mechanism of action of 5F-2'dUrd is the inhibition of dihydrofolate reductase-thymidylate synthase by the drug itself or the low level of 5F-dUMP; this hypothesis was strongly supported when the effect was rescued by excess extracellular thymidine. Particularly, thymidine nucleotide levels were not significantly different in s427-WT and Tbb-5F2'dURes cells after treatment with 5F-2'dUrd. In addition, the affinity and efficiency of thymidine uptake was significantly increased in 5F-2'dURes comparing with s427-WT, which clearly showed that thymidine salvage contributes to 5F-2'dUrd resistance. As the intracellular levels of 5F-2'dUrd were not different between s427-WT and Tbb-5F2'dURes

cells, we conclude that the resistance mechanism is based on metabolism rather than reduced uptake of the drug.

At 100 µM 5F-2'dCtd-exposed trypanosomes displayed almost the same metabolomic alterations as with 5F-2'dUrd. Particularly, the later was clearly detected after trypanosomes were exposed to 5F-2'dCyd; and another strong indication was the cross-resistance between these analogues. Therefore, we can conclude that 5F-2'dUrd and 5F-2'dCtd have an identical mode of action, and are not incorporated into nucleic acids but act as prodrugs by inhibiting thymidylate synthase as 5F-2'dUrd and/or 5F-dUMP.

Compared with 5-FU and 5FOA, there were very low levels of fluorinated metabolites (5F-Urd, 5F-UMP, 5F-UDP and 5F-UDP-glucose) in s427-WT cells exposed to 100 µM of 5-fluorouridine. Trypanosomes were insensitive to the drug and the absence of toxicity may be the result of the non-detectable level of 5F-UTP, as a result of which the drug was not incorporated into RNA.

The study presented an updated model of pyrimidine salvage in bloodstream forms of *T. brucei*, provided by a library of hidden Markov model (HMM)-based profiles for pyrimidine synthesis and salvage enzymes. Selected parasite proteomes were scanned with this library, with *Homo sapiens* and *Mus musculus* serving as references. The analysis clearly separated trypanosomatids from the apicomplexans, mainly because of the presence of TK, UDP-glucose pyrophosphorylase and UDP-glucose epimerase and the absence of orotate reductase and DHOD. The main distinction between *T. brucei* and its mammalian hosts was dUTPase, DHODH and UP. These kinetoplastid dUTPases have been classified together with several prokaryotic and bacteriophage dUTPases into an all-αNTP pyrophosphatase superfamily (Moroz *et al.,* 2005). Similarly, trypanosomal UP has an unusual quaternary structure. DHOD (1.3.5.2) is indeed absent from the *T. b. brucei* genome, its function in the pyrimidine biosynthesis pathway instead being performed by DHOD (1.3.3.1) (Arakaki *et al.,* 2008), which the HMM analysis correctly predicts.

While fluorinated pyrimidines (nucleobases and deoxynucleosides) have different trypanocides effects (Figure 9.1A), in *Leishmania* species, fluoro-pyrimidines have largely the same mechanism of action (Figure 9.1B).

Antifolates like methotrexate and pyrimethamine, which inhibit dihydrofolate reductase (DHFR): the inhibition of thymidine synthesis from dUMP. Although these antifolates and the fluoro-pyrimidine analogues act on different enzymes of the folate cycle, their activities may well be complementary, as in the highly successful, synergistic antimalarial combination Sulfadoxine/pyrimethamine (Fansidar®), where sulfadoxine inhibits folate biosynthesis. The fact that 5F-2'dUrd additionally inhibits both thymidine uptake and thymidine kinase, should potentiate the action of any antifolates against *Leishmania*. The problem with antifolate therapy of *Leishmania* has mostly been the potential for pteridine reductase (PTR1) to reduce dihydrofolate to tetrahydrofolate when DHFR is inhibited, providing a bypass (Bello *et al.,* 1994; Wang *et al.,* 1997), but a joint administration of a DHFR and fluoro-pyrimidine would not be successfully compensated for by upregulation of PTR1. Therefore, the effects of fluorinated pyrimidines as anti-*leishmania*l agents were investigated.

Although *Leishmania* promastigotes showed different mechanisms of resistance to fluorinated pyrimidine analogues, through loss of different transporters, mostly, there were many close similarities between the cellular effects of fluorinated pyrimidine analogues (5-FU, 5F-2'dUrd and 5F-Urd; Figure 9.1B), indicating a common mode of action on *L. mexicana* and *L. major*. The specific difference was the effect of 5F-Urd, particularly in that *L. mexicana* was extremely resistant to the compound, whereas the other species was very sensitive. While both species generate 5F-2'dUrd from 5F-Urd by the double action of uridine phosphorylase (with 5-FU as intermediate product), this is more rapidly converted by thymidine kinase to 5F-dUMP in *L. mexicana* than in *L. major*, explaining both the absence of the substrate and the higher level of the product in *L. mexicana* promastigotes. The other evidence is that the level of 5F-2'dUrd was below detection limit in *L. mexicana* treated with 5-FU, which shows the rapid conversion of 5F-2'dUrd to 5F-dUMP by promastigotes of this species. We also found that thymidine nucleotide levels in *L. major* are substantially reduced relative to untreated controls, but are not significantly different in *L. mexicana*. We conclude that the biosynthesis of thymidine is substantially inhibited in *L. major*, through inhibition of both TS in the de novo pathway by 5F-dUMP and TK in the salvage pathway by 5F-2'dUrd, whereas there is no inhibition of TK in *L.*

mexicana due to the absence of 5F-2'dUrd, allowing a bypass from the inhibition of TS and a sufficient synthesis of thymidine nucleotides. This interpretation is corroborated by the fact that LmajNT1 has only low affinity for thymidine, allowing at best a poor rate of salvage, whereas LmexNT1 displays a Km of 4.2 ± 0.4 µM for thymidine, identical to its affinity for uridine.
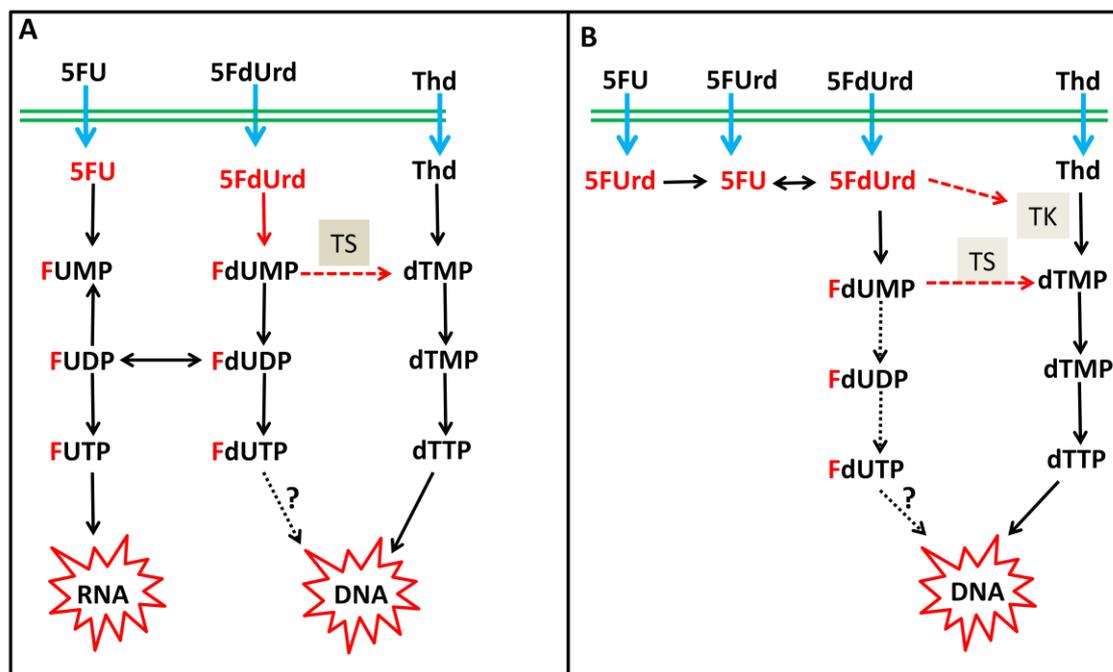
Figure 9.1: The possible mode of action of fluorinated pyrimidines in **A.** *Trypanosoma brucei* and **B**. *Leishmania* spp. Abbreviations: FUMP, FUDP, FUTP: fluorouridine -5'-mono-, di-, and triphosphate, respectively; FdUMP, FdUDP, FdUTP: fluorodeoxyuridine-5'-mono-, di-, and triphosphate, respectively; dUMP: deoxyuridine-5'-monophosphate; dTMP, dTDP, dTTP: deoxythymidine-5'-mono-, di-, and triphosphate, respectively; 5-FU: 5fluorouracil; 5FUrd: 5fluorouridine; 5FdUrd: 5fluoro-2'deoxyuridine; Thd: thymidine; TS: thymidylate synthase; TK thymidine kinase.

To understand in which way effective pyrimidine analogues rely on salvage enzymes or transporters, resistance was induced to 5-FU and 5F-2'dUrd by *in vitro* exposure of *L. mexicana* and *L. major* to stepwise increasing concentrations of the compounds. The lines generated from these cells were Lmex-5FURes and Lmaj-5FURes, which had adapted to 5-FU, and Lmex-5F2'dURes and Lmaj-5F2'dURes which had adapted to 5F-2'dUrd, respectively. Our biochemical assessment showed that the main mechanism of resistance against the anti-leishmanial activity of pyrimidine analogues was the loss of pyrimidine transport/s. *Leishmania* cells become resistant to high concentrations of fluorinated deoxynucleosides faster than to fluorinated nucleobases. Lmex-5FURes and Lmaj-5FURes were unable to take up uracil,

this clearly shows that Leishmania-5FURes cells have lost their uracil transport activity completely (LmexU1 and LmajU1). In addition, *Leishmania* cells adapted to 5-FU were not cross-resistance to fluorinated nucleosides, as evidenced by that the rate of uridine uptake in these strains was identical to their wild-type counterparts. Moreover, in Lmaj-5FURes the rate of uridine uptake exceeded its metabolic usage, resulting in a high initial rate of transport, and a lower secondary rate representing uridine metabolism, which became rate limiting for overall uptake after a few minutes, which could be due to up-regulation of LmajNT1/LmajNT2. Although Lmex-5F2'dURes cells were very resistant to 5-FU, the uracil rate of uptake by Lmex-5F2'dURes was equal to promastigotes of *L. mexicana*-WT, here we suggest that the high level of resistance of Lmex-5F2'dURes to 5-FU is due to changes in 5-FU metabolism, particularly the part of the pyrimidine metabolomic pathway shared by 5-FU and 5F-2'dUrd, i.e. thymidine kinase and thymidylate synthase. Lmaj-5F2'dURes cells are resistant to all fluorinated pyrimidine nucleosides, but are not at all cross-resistant to 5-FU, also the uptake of uridine and uracil was equally reduced in Lmaj-5F2'dURes. This is possibly attributed to the loss of both the LmajU1 and the uracil-insensitive nucleoside transporter (LmajNT2).

In conclusion, the sensitivity and cross-resistance to fluorinated pyrimidines was similar among kinetoplastid cells, but the mechanism of resistance to these analogues is totally different within trypanosomes and *Leishmania* cells. All resistant *Leishmania* promastigotes responded to increased concentrations of pyrimidine analogues by a significant or complete reduction in the transport capacity for natural pyrimidines, that is the cause of their resistance to high concentrations of fluorinated pyrimidines. The apparent ease by which *Leishmania* promastigotes 'loose' a pyrimidine transport activity is possibly related to the fact that they have several, whereas bloodstream trypanosomes express only TbU3. It could be speculated that this reflects the fact that *T. b. brucei* bloodstream forms express only one pyrimidine transporter (TbU3), whereas the *Leishmania* promastigotes express one pyrimidine nucleobase transporter in addition to at least one pyrimidine nucleoside transporter, of which the resistant lines loose only one. While this is an attractive notion, it must be remembered that pyrimidine

salvage is not an essential function for growth of bloodstream trypanosomes (Ali *et al.*, 2013b) and promastigotes of *Leishmania* (French *et al.*, 2011).

The metabolism of fluorinated pyrimidines inside the promastigotes of *L. mexicana* and *L. major* was also investigated using metabolomic analysis. Promastigotes of *Leishmania* converted 5-FU and 5-FUrd to 5-F2'dUrd, which was phosphorylated by TK to produce 5F-dUMP. We also found that 5F-2'dUrd can be converted to 5-FU, the reaction by uridine phosphorylase clearly being reversible. No 5F-dUDP or 5F-dUTP nor 5F-UMP, 5F-UDP and 5F-UTP were detected after *Leishmania* cells exposure to these fluorinated pyrimidines. The analysis produced no evidence for the incorporation of fluorinated pyrimidines into nucleic acids. Consistent with this conclusion we found that 5F-dUMP was most likely not a substrate for thymidylate kinase. The most important effect observed in *Leishmania* species treated with fluorinated pyrimidines was a massive increase in dUMP intensity that was due to the inhibition of TS, which converts dUMP to dTMP. This elevation caused an imbalance between deoxyuridine nucleotides and thymidine nucleotides, as well as a disturbance in the level of purine and pyrimidine derivatives. In addition, we found that accumulation of 5F-2'dUrd inhibited thymidine kinase. In general, we suggest that fluorinated pyrimidines inhibited: thymidylate synthase by accumulation of 5F-dUMP, and thymidine kinase by 5F-2'dUrd.

Although 5-FU and 5F-2'dUrd produced the same fluorinated metabolites and have identical mode of action against promastigotes of *L. mexicana* and *L. major*, the mechanism of resistance to these drugs was very different among *Leishmania* cells. For example, promastigotes of *Leishmania* became resistant to 5F-2'dUrd faster than to 5-FU. The most common observation between kinetoplastid was that trypanosomes and leishmanias resistant to 5F-2'dUrd became highly cross-resistant to 5F-2'dCyd. Alamar blue assay data showed some cross-resistance among pyrimidine nucleobase and nucleoside analogues in *Leishmania* cells. The most interesting data was the investigation of pyrimidine uptake in *Leishmania* resistant cells. The promastigotes of *Leishmania* resistant to 5-FU were completely insensitive to uracil, and resistant strains to 5F-2'dUrd were unable to take up uridine. Further investigations on resistant strains of *Leishmania* cells showed that: Lmex-5FURes and Lmaj-5FURes have lost their uracil transport activities,

LmexU1 and LmajU1, respectively; and Lmex-5F2'dURes and Lmaj-5F2'dURes have lost the nucleoside transporter, LmexNT1 and LmajNT1, respectively. In contrast, the fluoro-pyrimidine-resistant trypanosome lines did not display a significant loss of transport activity.

It has long been established that kinetoplastid parasites biosynthesise pyrimidines and produce UMP, as the end-product of the 6-step biosynthesis pathway, while at the same time salvaging several pyrimidine nucleobases and nucleosides using transporters and different interconversions enzymes such as cytidine deaminase, uridine phosphorylase and uracil phosphoribosyltransferase (Li *et al.,* 2007); this also generally leads to the production of UMP. From UMP the cell can then make all pyrimidine ribonucleotides and 2'deoxyribonucleotides that it requires. Therefore, this study attempted to assess the essentiality of pyrimidine biosynthesis and salvage in *T. b. brucei* bloodstream forms in vitro and in vivo; we exclude *Leishmania* species from this assessment as (Wilson *et al.,* 2012) have addressed this issue in *L. donovani*.

Pyrimidine uptake was not essential for *T. b. brucei* bloodstream forms as growth rates were unchanged in pyrimidine-free medium. The essentiality of the de novo pyrimidine biosynthesis pathway was studied by knocking out the PYR6-5 gene that produces a fusion product of orotate phosphoribosyltransferase (OPRTase; PYR5) and orotidine monophosphate decarboxylase (OMPDCase; PYR6), the two final enzymes of the 6-step pyrimidine biosynthesis pathway. Pyrimidine biosynthesis was essential for growth in the absence of an extracellular pyrimidine source. Flow cytometry showed that pyrimidine starvation caused incomplete DNA content in newly divided cells. The phenotype could be rescued by the addition of uracil, with uridine, 2'deoxyuridine, and cytidine also allowing a diminished growth rate and density; thymidine, thymine, cytosine and 2'-deoxycytidine did not allow growth, even at 1 mM. PYR6-5-/- were more sensitive to a number of cytotoxic pyrimidine analogues. The knockout cells adapted by increasing their rate of uracil uptake and, when growing on uridine, by upregulation of uridine phosphorylase. Survival of PYR6-5-/- trypanosomes in vivo was tested in mice; the infection developed much more slowly than the parental trypanosome line but the pyrimidine auxotrophs were able to establish and maintain a reduced parasitaemia. We conclude that trypanosomes lacking de

novo pyrimidine biosynthesis are highly dependent on an extracellular pyrimidine source, preferring uracil, and display reduced infectivity even though trypanosomes lacking de novo pyrimidine biosynthesis are completely dependent on an extracellular pyrimidine source. As *T. brucei* are able to salvage sufficient pyrimidines from the host environment, the pyrimidine biosynthesis pathway is not a viable drug target, although any interruption of pyrimidine supply was lethal. Neither pyrimidine uptake or de novo biosynthesis is essential in African trypanosomes but a drug combination targeting both systems would be a very powerful approach to novel therapy.

Despite the fact that the genomic data analysis of kinetoplastid resistance to fluorinated pyrimidines showed many changes, in *T. b. brucei* strains resistant to pyrimidine analogues (Tbb-5FURes, Tbb-5FOARes and Tbb-5F2'dURes) there was only one common SNP in all resistance strains, which occurred in gene Tb927.5.3170, which encodes ribose phosphate pyrophosphokinase. However, these resistant strains have not shown any copy number variations. In addition, SNP occurred on Tb927.2.3390, but only on Tbb-5FURes and Tbb-5F2'dURes. This gene encodes hypothetical protein and carries 10 transmembrane domains. Therefore, they could cause a part of the adaption to fluoro-pyrimidines, particularly as we found a 76 ± 6% reduction of 5-FU uptake by Tbb-5FURes compared with *T. b. brucei* wild-type.

Leishmania spp have also shown many SNPs in the resistant cells, but only one common SNP appeared in *L. mexicana* and *L. major* as a result of exposure to a high concentration of 5-FU; this gene encoded an unknown protein with five putative trans-membrane domains. Regarding to copy number variation in resistant *Leishmania* strains, it seems that multiple changes occurred in the entire chromosomes or parts thereof, compared to the wild-type cells. We recommend further investigations to identify the specific changes that led to high resistance to fluorinated pyrimidines, using the SNPs observed in multiple resistant lines as starting points.

The main findings of this thesis are:

- Bloodstream forms of *T. b. brucei* expressed only one pyrimidine transport protein, a high affinity uracil transporter (TbU3), which has high affinity and efficiency for uracil, but very low affinity for uridine and 2'-deoxyuridine. Thymidine is also taken up by the bloodstream

forms, although inefficiently, through a P1-type nucleoside transporter, TbT1 (Chapter 3).

- *L. mexicana* promastigotes expressed at least two pyrimidine transport activities, the first being a pyrimidine nucleobase transporter (LmexU1) responsible for uracil uptake and well inhibited by uridine, but not by thymidine and adenosine. The second was a nucleoside transporter (LmexNT1) sensitive to uridine, thymidine and adenosine, but with low affinity for uracil. *L. major* promastigotes also expressed a high affinity uracil transporter (LmajU1) that was inhibited by uridine. They also expresses two distinct nucleoside transport activities: a high affinity uridine transporter (LmajNT1), which was sensitive to uridine, uracil, inosine and adenine; and a low affinity uridine transporter (LmajNT2), which has low affinity to uridine and was insensitive to uracil, inosine and adenine. Both these activities are inhibited by 2'-deoxyuridine, thymidine and adenosine (Chapter 4).

- *Trypanosoma brucei* bloodstream forms and *Leishmania* promastigotes are more sensitive to fluorinated pyrimidines (5-FU, 5-F2'dUrd and 5-FOA and 5F-Urd) than to other halogenated pyrimidines (Chapters 3 and 4).

- The mechanisms of resistance to high levels of pyrimidine analogues in trypanosomes were mostly related to changes in pyrimidine metabolic processes, possibly by preventing their incorporation into the nucleotide pool. However, the main mechanism of resistance against anti-leishmanial activity of pyrimidine analogues was the loss of pyrimidine transporters (Chapters 3 and 4).

- While bloodstream forms resistant to 5-FU showed only a 76% reduction in 5-FU uptake, resistant strains of *Leishmania* spp completely lost their natural pyrimidine transporters. *Leishmania* cells resistant to 5-FU had lost uracil transport activity (LmexU1 and LmajU1), and cells that were resistant to 5F-2'dUrd had lost uridine transport activity (LmexNT1, LmajNT1 and LmajNT2) (Chapters 3 and 4).

- In *T. b. brucei*, 5-FU and 5-FOA are incorporated into a large number of metabolites such as precursors for lipid biosynthesis, sugar metabolism and VSG glycosylation or GPI anchors, but likely exert their

toxicity, at least in part, through incorporation into RNA as significant amounts of 5F-UMP and low levels of 5F-CMP were detected in digested RNA (Chapter 5).

- 5F-2'dUrd and 5F2d'Cyd have a common a mode of action on trypanosomes, they inhibit dihydrofolate reductase-thymidylate synthase, either as 5F-2'dUrd or the low levels present of the metabolite 5F-dUMP; this hypothesis was proven when the effect of 5F-2'dUrd was rescued by excess extracellular thymidine (Chapter 5).

- Promastigotes of *Leishmania* converted 5-FU and 5-FUrd to 5-F2'dUrd, which was phosphorylated by TK to produce 5F-dUMP. Therefore, we suggest that fluorinated pyrimidines have a common mode of anti-leishmanial action through (a) inhibiting thymidylate synthase by accumulation of 5F-dUMP, and (b) thymidine kinase by 5F-2'dUrd (Chapter 6).

- Trypanosomes that were made pyrimidine auxotrophic by disruption of the OMPDCase gene adapted by increasing their rate of uracil uptake and, when growing on uridine, by upregulation of uridine phosphorylase (Chapter 7).

- Trypanosomes lacking de novo pyrimidine biosynthesis are highly dependent on an extracellular pyrimidine source, preferring uracil, and display reduced infectivity (Chapter 7).

- In all the *T. b. brucei* strains resistant to pyrimidine analogues (Tbb-5FURes, Tbb-5FOARes and Tbb-5F2'dURes) there was only one common SNP, which occurred in gene Tb927.5.3170, which encodes ribose phosphate pyrophosphokinase (Chapter 8).

- A further SNP of interest occurred on Tb927.2.3390, but only on Tbb-5FURes and Tbb-5F2'dURes. This gene encodes for a hypothetical protein and carries 10 transmembrane domains (Chapter 8).

- Only one common SNP appeared in *L. mexicana* and *L. major* as a result of exposure to a high concentration of 5-FU; this gene encoded an unknown protein with five putative trans-membrane domains (Chapter 8).

Appendices

Appendix I: Standard HMI-9 and HMI-9^{-tmd} media. Without adding serum

Compounds	HMI-9 (mg/L)	HMI-9^{-tmd} (mg/L)
CaCl2	165	165
KCl	330	330
KNO3	0.076	0.076
MgSO4	97.67	97.67
NaCl	4500	4500
NaHCO3	3000	3000
NaH2PO4.H2O	125	125
Na2SeO3.5H2O	0.0112	0.0112
Glucose	4500	4500
Phenol Red	15	15
HEPES	5958	5958
β-mercaptoethanol	14.3 M	14.3 M
Bathocuproine disulfonate.Na2	28.225	28.225
Alanine	25	25
Arginine. HCl	84	84
Asparagine	25	25
Aspartic acid	30	30
Cysteine	181.74	181.74
Cystine	91.24	91.24
Glutamic acid	75	75
Glutamine	584	584
Glycine	30	30
Histidine.HCl.H2O	42	42
Isoleucine	105	105
Leucine	105	105
Lysine. HCl	146	146
Methionine	30	30
Phenylalanine	66	66
Proline	40	40
Serine	42	42
Threonine	95	95
Tryptophan	16	16
Tyrosine	104.2	104.2
Valine	94	94
B12	0.013	0.013
Biotin	0.013	0.013
D-Ca pantothenate	4	4
Choline chloride	4	4
Folic Acid	4	4
Inositol	7.2	7.2
Niacinamide	4	4
Pyridoxal. HCl	4	4
Riboflavin	0.4	0.4
Thiamine. HCl	4	4
Pyruvate. Na	220	220
Hypoxanthine	136.1	136.1
Thymidine	**20.176**	**0**

Appendix II: Structures of natural pyrimidines and their analogues
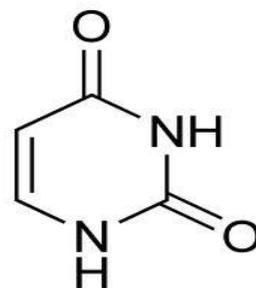
Nucleobases

Uracil
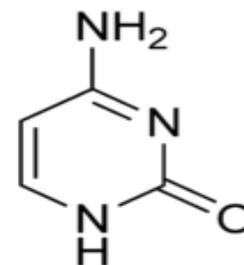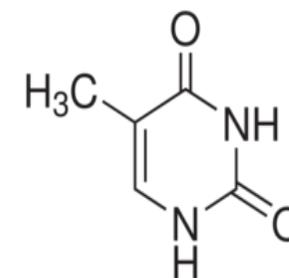
Cytosine

Thymine
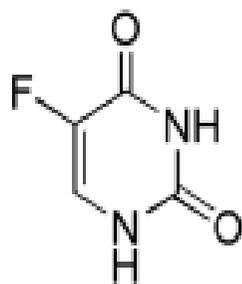
5-Fluorouracil
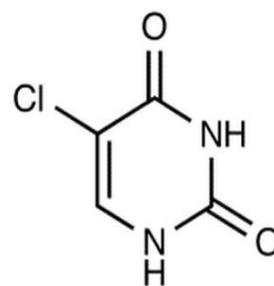
5-Chlorouracil
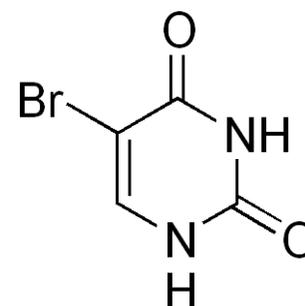
5-Bromouracil
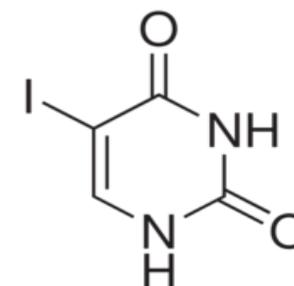
5-Iodouracil

Appendix II: continued structures of natural pyrimidines and their analogues

Nucleobases
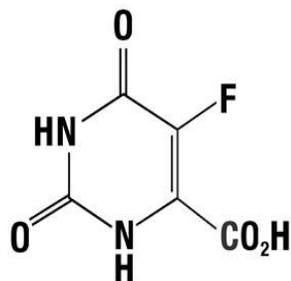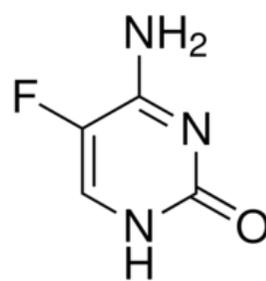
5-Fluoroorotic acid	5-Fluorocytosine	1-methyl uracil	2-Thiouracil
4-Thiouracil	5,6-dihydrouracil	6-Azauracil	6-methyluracil
3-deazauracil	2-mercaptopyrimidine	4 (3H)pyrimidinone	
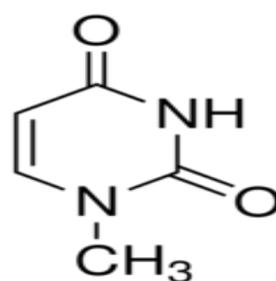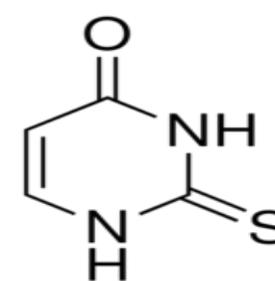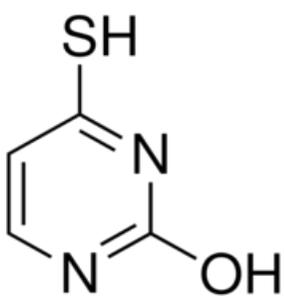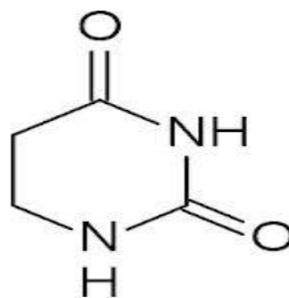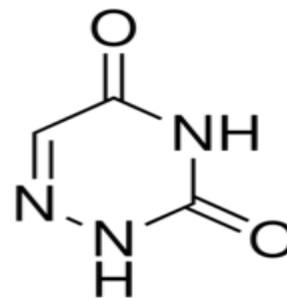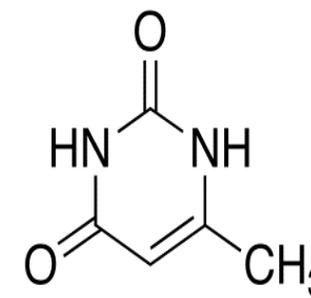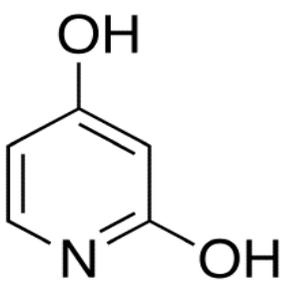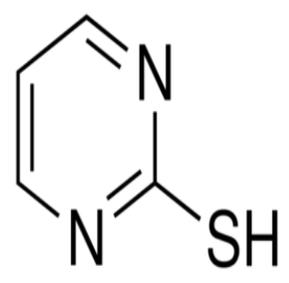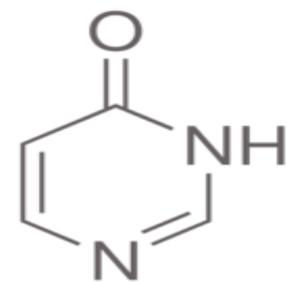
Appendix II: continued structures of natural pyrimidines and their analogues

Nucleosides
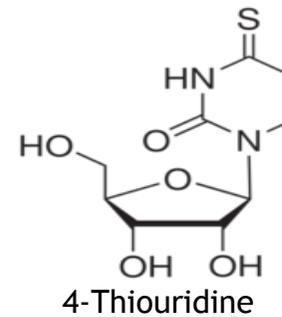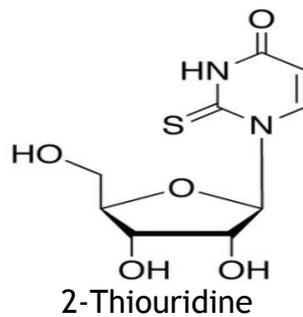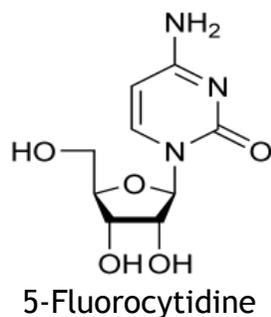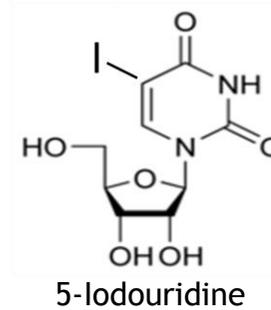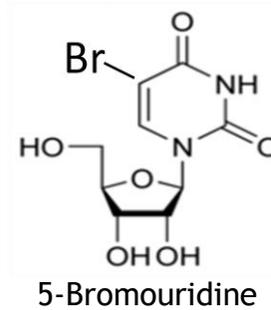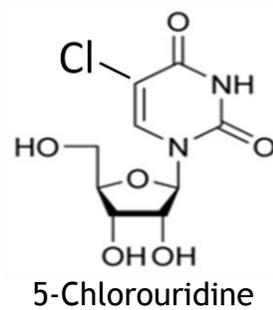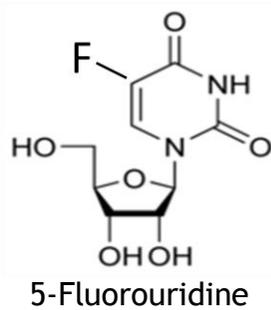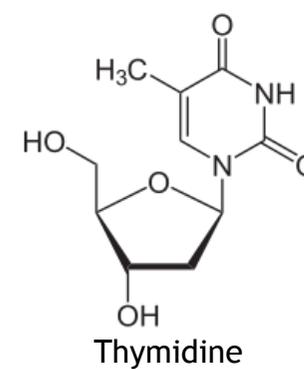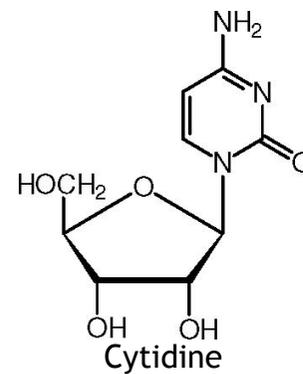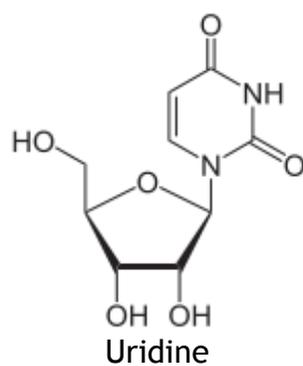
Uridine

Cytidine

Thymidine

5-Fluorouridine

5-Chlorouridine

5-Bromouridine

5-Iodouridine

5-Fluorocytidine

2-Thiouridine

4-Thiouridine

Appendix II: continued structures of natural pyrimidines and their analogues
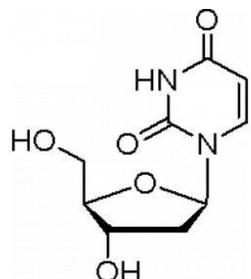
Deoxynucleosides
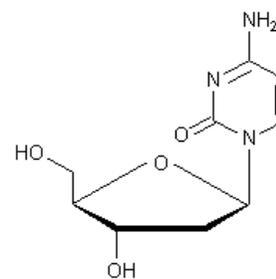
2'-deoxyuridine

2'deoxycytidine
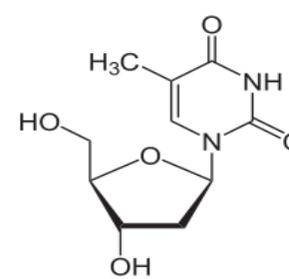
2'deoxythymidine
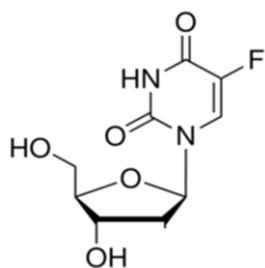
5-Fluoro-2'deoxyuridine
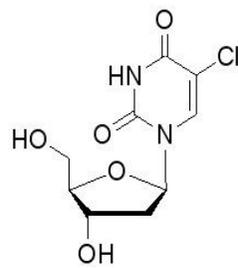
5-Chloro-
2'deoxyuridine
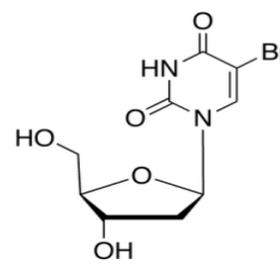
5-Bromo-
2'deoxyuridine
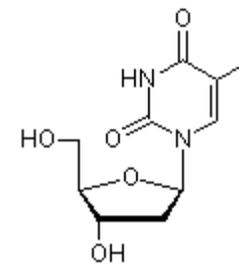
5-Iodo-2'deoxyuridine

Appendix II: continued structures of natural pyrimidines and their analogues

Deoxynucleosides

5-Fluoro-2'deoxycytidine　　2',3'-dideoxyuridine　　2',5'-dideoxyuridine　　5'-deoxyuridine

5'-deoxy-5-fluorouridine　　3'-deoxyuridine　　3'-deoxythymidine
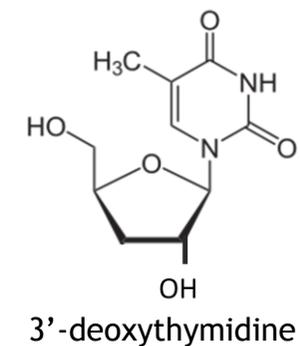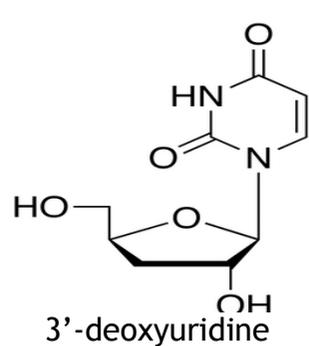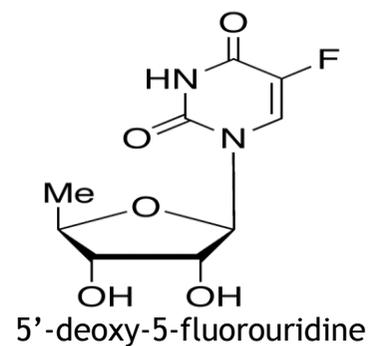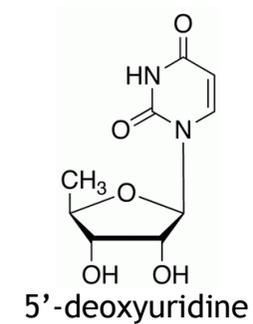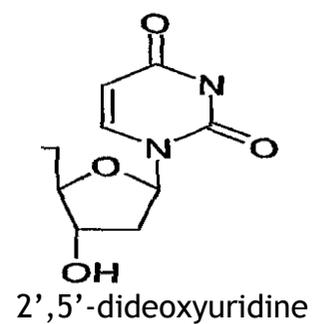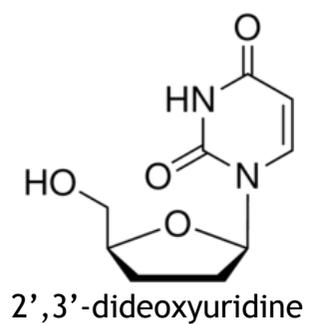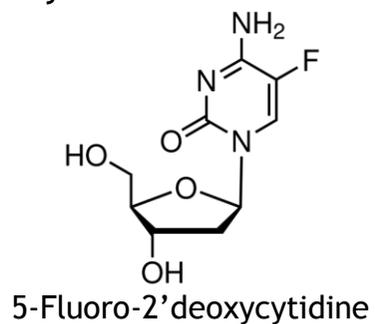
Appendix III: Kinetic characterization of pyrimidine and purine uptakes in kinetoplastid wild-type cells (K_m and V_{max} values).

[^{3}H]-Substrates	*T. b. brucei* bloodstream forms			*L. mexicana* promastigotes			*L. major* promastigotes		
Uracil	K_m (µM)	V_{max} (pmol·10^7 cells^{-1}·s^{-1})	Efficiency	K_m (µM)	V_{max} (pmol·10^7 cells^{-1}·s^{-1})	Efficiency	K_m (µM)	V_{max} (pmol·10^7 cells^{-1}·s^{-1})	Efficiency
1st repeat	0.45	0.26		18.9	0.072				
2nd repeat	0.68	0.18		35.3	0.08				
3rd repeat	1.08	0.17		34.9	0.11				
4th repeat	0.42	0.05							
5th repeat	0.32	0.10							
6th repeat	0.28	0.07							
Mean	**0.54**	**0.14**	**0.25**	**29.7**	**0.088**	**0.0029**	**0.32**	**0.68**	**2.15**
SE	0.11	0.03		4.41	0.01		0.07	0.15	
N	6	6		3	3				
[^{3}H]-Substrates	*T. b. brucei* bloodstream forms			*L. mexicana* promastigotes			*L. major* promastigotes		
Uridine	K_m (µM)	V_{max} (pmol·10^7 cells^{-1}·s^{-1})	Efficiency	K_m (µM)	V_{max} (pmol·10^7 cells^{-1}·s^{-1})	Efficiency	K_m (µM)	V_{max} (pmol·10^7 cells^{-1}·s^{-1})	Efficiency
1st repeat	3397	8.0		8.96	0.79		2.17	0.044	
2nd repeat	10348	17.0		9.10	0.28		2.59	0.026	
3rd repeat	14810	23.1		5.79	0.28		4.6	0.038	
4th repeat				3.88	0.22				
5th repeat				8.01	0.067				
Mean	**9518**	**16**	**0.0016**	**7.2**	**0.33**	**0.046**	**3.12**	**0.036**	**0.011**
SE	2711	4		0.9	0.11		0.61	0.004	
N	3	3		5	5		3	3	
[^{3}H]-Substrates	*T. b. brucei* bloodstream forms			*L. mexicana* promastigotes			*L. major* promastigotes		
Thymidine	K_m (µM)	V_{max} (pmol·10^7 cells^{-1}·s^{-1})	Efficiency	K_m (µM)	V_{max} (pmol·10^7 cells^{-1}·s^{-1})	Efficiency	K_m (µM)	V_{max} (pmol·10^7 cells^{-1}·s^{-1})	Efficiency
1st repeat	1084	0.082		3.69	0.765				
2nd repeat	677.1	0.048		5.21	1.13				
3rd repeat	1959	0.070		3.84	0.66				
Mean	**1240**	**0.067**	**5.42E-05**	**4.24**	**0.85**	**0.20**			
SE	309	0.008		0.39	0.12				
N	3	3		3	3				

Appendix III continued Kinetic characterization of pyrimidine and purine uptakes in kinetoplastid wild-type cells (K_m, V_{max} values).

[³H]-Substrates	*T. b. brucei* bloodstream forms			*L. mexicana* promastigotes			*L. major* promastigotes		
2'deoxyuridine	K_m (μM)	V_{max} (pmol·10^7 cells^{-1}·s^{-1})	Efficiency	K_m (μM)	V_{max} (pmol·10^7 cells^{-1}·s^{-1})	Efficiency	K_m (μM)	V_{max} (pmol·10^7 cells^{-1}·s^{-1})	Efficiency
1st repeat	558	0.26							
2nd repeat	746	0.57							
3rd repeat	1110	3.15							
Mean	**804.7**	**1.32**	**0.0016**						
SE	132.3	0.74							
N	3	3							
[³H]-Substrates	*T. b. brucei* bloodstream forms			*L. mexicana* promastigotes			*L. major* promastigotes		
Uridine + 1mM Uracil	K_m (μM)	V_{max} (pmol·10^7 cells^{-1}·s^{-1})	Efficiency	K_m (μM)	V_{max} (pmol·10^7 cells^{-1}·s^{-1})	Efficiency	K_m (μM)	V_{max} (pmol·10^7 cells^{-1}·s^{-1})	Efficiency
1st repeat				4.12	0.32				
2nd repeat				3.654	0.15				
3rd repeat				4.539	0.477				
Mean				**4.1**	**0.32**	**0.078**			
SE				0.20	0.075				
N				3	3				

Appendix III continued Kinetic characterization of pyrimidine and purine uptakes in kinetoplastid wild-type cells (K_m, V_{max} values).

[^{3}H]-Substrates	*T. b. brucei* bloodstream forms			*L. mexicana* promastigotes			*L. major* promastigotes		
Adenosine	K_m (µM)	V_{max} (pmol·10^7 cells^{-1}·s^{-1})	Efficiency	K_m (µM)	V_{max} (pmol·10^7 cells^{-1}·s^{-1})	Efficiency	K_m (µM)	V_{max} (pmol·10^7 cells^{-1}·s^{-1})	Efficiency
1st repeat				0.80	1.64				
2nd repeat				1.18	0.96				
3rd repeat				0.50	0.79				
Mean				**0.83**	**1.13**	**1.35**			
SE				0.16	0.21				
N				3	3				
[^{3}H]-Substrates	*T. b. brucei* bloodstream forms			*L. mexicana* promastigotes			*L. major* promastigotes		
5-Fluorouracil	K_m (µM)	V_{max} (pmol·10^7 cells^{-1}·s^{-1})	Efficiency	K_m (µM)	V_{max} (pmol·10^7 cells^{-1}·s^{-1})	Efficiency	K_m (µM)	V_{max} (pmol·10^7 cells^{-1}·s^{-1})	Efficiency
1st repeat	2.57	0.24							
2nd repeat	2.55	0.29							
Mean	**2.56**	**0.27**	**0.105**						
SE	0.008	0.015							
N	2	2							
[^{3}H]-Substrates	*T. b. brucei* bloodstream forms			*L. mexicana* promastigotes			*L. major* promastigotes		
Inosine	K_m (µM)	V_{max} (pmol·10^7 cells^{-1}·s^{-1})	Efficiency	K_m (µM)	V_{max} (pmol·10^7 cells^{-1}·s^{-1})	Efficiency	K_m (µM)	V_{max} (pmol·10^7 cells^{-1}·s^{-1})	Efficiency
1st repeat	1.168	0.06092							
2nd repeat	0.532	0.05303							
3rd repeat	0.9837	0.1114							
Mean	**0.89**	**0.075**							
SE	0.15	0.015							
N	3	3							

Appendix IV: Substrate profiles of the pyrimidine transporters (K_i values) in Kinetoplastid wild type cells

Inhibitors/[³H]-substrate		*T. b. brucei* bloodstream forms			*L. mexicana* promastigotes			*L. major* promastigotes		
Uracil		Uracil	Uridine	Thymidine	Uracil	Uridine	Thymidine	Uracil	Uridine	Thymidine
	1st repeat		2.1	>2500		16.52	>2500		3.61	
	2nd repeat		1.38	>2500		33.61	>2500		1.00	
	3rd repeat		1.54	>2500		15.29	>2500		2.78	
	4th repeat					50.97				
	5th repeat					12.20				
Mean			**1.67**	**>2500**		**25.72**	**>2500**		**2.46**	
SE			0.18	0		6.56	0		0.63	
N			3	3		5	3		3	
Inhibitors/[³H]-substrate		*T. b. brucei* bloodstream forms			*L. mexicana* promastigotes			*L. major* promastigotes		
Uridine		Uracil	Uridine	Thymidine	Uracil	Uridine	Thymidine	Uracil	Uridine	Thymidine
	1st repeat	≥10000		178.28	3.52		7.51			
	2nd repeat	≥10000		130.94	0.79		5.29			
	3rd repeat	≥10000		288.67	2.31		5.11			
	4th repeat				1.47					
Mean		**≥10000**		**199.3**	**2.02**		**5.97**	**10.9**		
SE		0		38.2	0.51		0.63	3.2		
N		3		3	4		3			
Inhibitors/[³H]-substrate		*T. b. brucei* bloodstream forms			*L. mexicana* promastigotes			*L. major* promastigotes		
Thymidine		Uracil	Uridine	Thymidine	Uracil	Uridine	Thymidine	Uracil	Uridine	Thymidine
	1st repeat	>10000			>10000	10.17			139.24	
	2nd repeat	>10000			>10000	4.09			81.12	
	3rd repeat	>10000			>10000	15.24				
	4th repeat									
	5th repeat									
Mean		**>10000**			**>10000**	**9.8**		**>200**	**110.18**	
SE		0			0	2.6		0	20.55	
N		3			3	3			2	

Appendix IV: continued Substrate profiles of the pyrimidine transporters (K_i values) in Kinetoplastid wild type cells

Inhibitors/[^{3}H]-substrate		*T. b. brucei* bloodstream forms			*L. mexicana* promastigotes			*L. major* promastigotes		
2'Deoxyuridine		Uracil	Uridine	Thymidine	Uracil	Uridine	Thymidine	Uracil	Uridine	Thymidine
	1st repeat	578.98		367.26	15.24	5.94			9.25	
	2nd repeat	1715.79		169.61	4.73	9.07			4.98	
	3rd repeat	1935.16		422.29	7.83	6.59			23.11	
	4th repeat			322.40						
Mean		**1147**		**320.4**	**9.27**	**7.20**			**12.45**	
SE		343		47	2.55	0.78			4.47	
N		3		4	3	3			3	
Inhibitors/[^{3}H]-substrate		*T. b. brucei* bloodstream forms			*L. mexicana* promastigotes			*L. major* promastigotes		
Cytidine		Uracil	Uridine	Thymidine	Uracil	Uridine	Thymidine	Uracil	Uridine	Thymidine
	1st repeat			>10000		66.61	94.71			
	2nd repeat			>10000		54.23	78.12			
	3rd repeat			>10000		114.80	72.94			
Mean				**>10000**		**78.55**	**81.92**	**>200**		
SE				0		15.09	5.36			
N				3		3	3			
Inhibitors/[^{3}H]-substrate		*T. b. brucei* bloodstream forms			*L. mexicana* promastigotes			*L. major* promastigotes		
Thymine		Uracil	Uridine	Thymidine	Uracil	Uridine	Thymidine	Uracil	Uridine	Thymidine
	1st repeat	>2500		>1000	983.44					
	2nd repeat	>2500		>1000	163.25					
	3rd repeat	>2500		>1000	542.86					
Mean		**>2500**		**>1000**	**563.19**					
SE		0		0	193.5					
N		3		3	3					

Appendix IV: continued Substrate profiles of the pyrimidine transporters (K_i values) in Kinetoplastid wild type cells

Inhibitors/[³H]-substrate		*T. b. brucei* bloodstream forms			*L. mexicana* promastigotes			*L. major* promastigotes		
Cytosine		Uracil	Uridine	Thymidine	Uracil	Uridine	Thymidine	Uracil	Uridine	Thymidine
	1st repeat	>2500			>5000					
	2nd repeat	>2500			>5000					
	3rd repeat	>2500			>5000					
Mean		**>2500**			**>5000**			**>200**		
SE		0			0			0		
N		3			3					
Inhibitors/[³H]-substrate		*T. b. brucei* bloodstream forms			*L. mexicana* promastigotes			*L. major* promastigotes		
5-Fluorouracil		Uracil	Uridine	Thymidine	Uracil	Uridine	Thymidine	Uracil	Uridine	Thymidine
	1st repeat	7.76		>1000	72.14	>5000				
	2nd repeat	5.18		>1000	48.06	>5000				
	3rd repeat	10.68		>1000	48.85	>5000				
Mean		**7.9**		**>1000**	**56.35**	**>5000**		**0.66**		
SE		1.3		0	6.45	0		0.14		
N		3		3	3	3				
Inhibitors/[³H]-substrate		*T. b. brucei* bloodstream forms			*L. mexicana* promastigotes			*L. major* promastigotes		
5Fl-2'dUrd		Uracil	Uridine	Thymidine	Uracil	Uridine	Thymidine	Uracil	Uridine	Thymidine
	1st repeat					6.91				
	2nd repeat					7.25				
	3rd repeat					6.81				
Mean						**7**				
SE						0.11				
N						3				

Appendix IV: continued Substrate profiles of the pyrimidine transporters (K_i values) in Kinetoplastid wild type cells

Inhibitors/[3H]-substrate		*T. b. brucei* bloodstream forms			*L. mexicana* promastigotes			*L. major* promastigotes		
Adenine		Uracil	Uridine	Thymidine	Uracil	Uridine	Thymidine	Uracil	Uridine	Thymidine
	1st repeat				314.70	>1000			10.06	
	2nd repeat				416.00	>1000			3.66	
	3rd repeat				134.73	>1000			1.56	
Mean					**288.48**	**>1000**		**>200**	**5.09**	
SE					67.15	0			2.09	
N					3	3			3	

Appendix IV: continued Substrate profiles of the pyrimidine transporters (K$_i$ values) in Kinetoplastid wild type cells

Inhibitors/[^{3}H]-substrate		*T. b. brucei* bloodstream forms			*L. mexicana* promastigotes			*L. major* promastigotes		
Adenosine		Uracil	Uridine	Thymidine	Uracil	Uridine	Thymidine	Uracil	Uridine	Thymidine
	1st repeat			2.102	2770.36	0.19	0.18		3.02	
	2nd repeat			1.79	946.07	0.58	0.34		1.84	
	3rd repeat			3.006	4817.89	0.40	0.23		0.92	
	4th repeat				6379.60					
Mean				**2.3**	**3728**	**0.39**	**0.25**		**1.93**	
SE				0.3	1026	0.09	0.04		0.49	
N				3	4	3	3		3	
Inhibitors/[^{3}H]-substrate		*T. b. brucei* bloodstream forms			*L. mexicana* promastigotes			*L. major* promastigotes		
Hypoxanthine		Uracil	Uridine	Thymidine	Uracil	Uridine	Thymidine	Uracil	Uridine	Thymidine
	1st repeat	>1000								
	2nd repeat	>1000			>500					
	3rd repeat	>1000			>500					
Mean		**>1000**			**>500**			**>200**		
SE		0			0			0		
N		3			2					
Inhibitors/[^{3}H]-substrate		*T. b. brucei* bloodstream forms			*L. mexicana* promastigotes			*L. major* promastigotes		
Inosine		Uracil	Uridine	Thymidine	Uracil	Uridine	Thymidine	Uracil	Uridine	Thymidine
	1st repeat			0.863		559.55	615.22		0.15	
	2nd repeat			3.28		1364.14	582.35		0.14	
	3rd repeat			0.638		1107.52	722.07		0.13	
Mean				**1.6**		**1010.4**	**639.88**		**0.14**	
SE				0.6		193.74	34.44		0.004	
N				3		3	3		3	

Appendix V: The EC_{50} values of effective pyrimidine analogues on Kinetoplastid strains using Alamar Blue assay

	T. b. brucei bloodstream forms				*L. mexicana* promastigotes			*L. major* promastigotes		
	s427-WT	Tbb5FURes	Tbb5FdURes	Tbb5FOARes	sM379-WT	Lmex5FURes	Lmex5FdURes	sF-WT	Lmaj5FURes	Lmaj5FdURes
5-Fluorouracil										
1st repeat	36.3	3746	80.4	459	9.2	1162	1850	11.2	165	15.8
2nd repeat	33	5905	75	408	10.7	1658	854.8	11	140	12.8
3rd repeat	40	4873	73	446	7.4	1559	1163	7	160	11.3
4th repeat	34.4	5303		458.6	9.9	1119	2500	8.5	129	10.5
5th repeat		4479		589.5			2500	7.3	161	
6th repeat		3933		328.8				8.1	149	
7th repeat								6.7		
Mean ± SE	**35.9±1.5**	**4706±307**	**76.1±2.2**	**448.3±31.6**	**9.3±0.6**	**1374.5± 123**	**1773±301**	**8.5±0.6**	**150±6.2**	**12.6±1.0**
	T. b. brucei bloodstream forms				*L. mexicana* promastigotes			*L. major* promastigotes		
	s427-WT	Tbb5FURes	Tbb5FdURes	Tbb5FOARes	sM379-WT	Lmex5FURes	Lmex5FdURes	sF-WT	Lmaj5FURes	Lmaj5FdURes
5Fluoro-2'deoxyuridine										
1st repeat	4.8	2.7	4512	38	1.4	0.56	> 5000	1.7	6.9	582
2nd repeat	5.2	3.4	3763	28	1.13	1.3	> 5000	1.6	7	248
3rd repeat	5.6	4	4610	33	1.3	1.5	> 5000	1.2	4	314
4th repeat	5.22	3.3		29.2	1.5	2	> 5000	2.2	6.4	
5th repeat		2.4		32.9	1.3	2	>5000	2	6.3	
6th repeat				24.8	1.7			1.4	3.4	
7th repeat					1.5			1.8		
8th repeat					1.3					
9th repeat					1.7					
Mean ± SE	**5.2±0.2**	**3.16±0.25**	**4295±267**	**30.98±1.7**	**1.4±0.06**	**1.47±0.23**	**>5000**	**1.7±0.1**	**6.12 ± 0.48**	**381 ± 83**

Appendix V: continued the IC$_{50}$ values of effective pyrimidine analogues on Kinetoplastid strains using Alamar Blue assay

	T. b. brucei bloodstream forms				*L. mexicana* promastigotes			*L. major* promastigotes		
	s427-WT	Tbb5FURes	Tbb5FdURes	Tbb5FOARes	sM379-WT	Lmex5FURes	Lmex5FdURes	sF-WT	Lmaj5FURes	Lmaj5FdURes
5Fluoro-uridine										
1st repeat	>5000	> 5000	> 5000	> 5000	> 5000	> 5000	> 5000	18.7	103	2044
2nd repeat	>5000	> 5000	> 5000	> 5000	> 5000	> 5000	> 5000	15.3	86	650
3rd repeat	>5000	> 5000	> 5000	> 5000	> 5000	> 5000	> 5000	22	170	1003
4th repeat								14.2		
5th repeat								17.4	81	
6th repeat								17		
7th repeat								22		
Mean ± SE	**>5000**	**>5000**	**>5000**	**>5000**	**>5000**	**>5000**	**>5000**	**18±1.6**	**110 ± 17.7**	**1232 ± 341**
	T. b. brucei bloodstream forms				*L. mexicana* promastigotes			*L. major* promastigotes		
	s427-WT	Tbb5FURes	Tbb5FdURes	Tbb5FOARes	sM379-WT	Lmex5FURes	Lmex5FdURes	sF-WT	Lmaj5FURes	Lmaj5FdURes
5Fluoro-orotic acid										
1st repeat	12.5	94	13.6	1459	> 5000	> 5000	> 5000	> 5000	> 5000	> 5000
2nd repeat	13	96	13.2	1240	> 5000	> 5000	> 5000	> 5000	> 5000	> 5000
3rd repeat	14.2	97	13.3	884.5	> 5000	> 5000	> 5000	> 5000	> 5000	> 5000
4th repeat	16.8	108		1412						
5th repeat		93		1410						
6th repeat				1109						
7th repeat				730						
Mean ± SE	**14.1±0.9**	**97.6±2.4**	**13.3±0.12**	**1177.7±99.**	**>5000**	**>5000**	**>5000**	**>5000**	**>5000**	**>5000**

Appendix V: continued the IC$_{50}$ values of effective pyrimidine analogues on Kinetoplastid strains using Alamar Blue assay

	T. b. brucei bloodstream forms				*L. mexicana* promastigotes			*L. major* promastigotes		
	s427-WT	Tbb5FURes	Tbb5FdURes	Tbb5FOARes	sM379-WT	Lmex5FURes	Lmex5FdURes	sF-WT	Lmaj5FURes	Lmaj5FdURes
5Fluoro-2'deoxycytidine										
1st repeat	46	65	> 5000	124	19.8	22	> 5000	39	13.8	5392
2nd repeat	51	53	> 5000	108	12.6	26	> 5000	41	16	3070
3rd repeat	43.6	46	> 5000	131	21.6	24	> 5000	34	21.2	3148
4th repeat	57		> 5000	102	17.9		> 5000			
5th repeat				166	17					
6th repeat					13.2					
7th repeat					19					
Mean ± SE	**49.4±3.0**	**54.6±4.5**	**>5000**	**126.2±10**	**17.3±1.8**	**24±0.94**	**>5000**	**38±1.6**	**17±1.79**	**3870±621**
	T. b. brucei bloodstream forms				*L. mexicana* promastigotes			*L. major* promastigotes		
	s427-WT	Tbb5FURes	Tbb5FdURes	Tbb5FOARes	sM379-WT	Lmex5FURes	Lmex5FdURes	sF-WT	Lmaj5FURes	Lmaj5FdURes
5-Chloro-2'deoxyuridine										
1st repeat	51	4	21.9	104	> 5000	> 5000	> 5000	> 5000	> 5000	> 5000
2nd repeat	53.8	3.9	20.2	98	> 5000	> 5000	> 5000	> 5000	> 5000	> 5000
3rd repeat	57	3.8	23.7	73	> 5000	> 5000	> 5000	> 5000	> 5000	> 5000
4th repeat		3		76						
5th repeat				106						
Mean ± SE	**54±1.7**	**3.67±0.19**	**21.9±1.0**	**91.4±6.2**	**>5000**	**>5000**	**>5000**	**>5000**	**>5000**	**>5000**

Appendix V: continued the IC$_{50}$ values of effective pyrimidine analogues on Kinetoplastid strains using Alamar Blue assay

	T. b. brucei bloodstream forms				*L. mexicana* promastigotes			*L. major* promastigotes		
	s427-WT	Tbb5FURes	Tbb5FdURes	Tbb5FOARes	sM379-WT	Lmex5FURes	Lmex5FdURes	sF-WT	Lmaj5FURes	Lmaj5FdURes
6-Azauracil										
1st repeat	1000	163	1015	1561	> 5000	> 5000	> 5000	> 5000	> 5000	> 5000
2ndrepeat	875	155	1200	1352	> 5000	> 5000	> 5000	> 5000	> 5000	> 5000
3rd repeat	1000	153	1095	1151	> 5000	> 5000	> 5000	> 5000	> 5000	> 5000
4th repeat				1484						
Mean ± SE	**958±34**	**157±2.49**	**1103±43.7**	**1387±77.7**	**>5000**	**>5000**	**>5000**	**>5000**	**>5000**	**>5000**

Appendix VI: Publications

Rodenko, B, Al-Salabi, MI, Teka, IA, Ho, W, El-Sabbagh, N, **Ali, JAM**, Ibrahim, HMS, Wanner, MJ, Koomen, GJ & de Koning, HP. (2011). Synthesis of Marine-Derived 3-Alkylpyridinium Alkaloids with Potent Antiprotozoal Activity. ACS Med Chem Lett, 2, 901-906.

Ali, JAM, Tagoe, DN, Munday, JC, Donachie, A, Morrison, LJ & de Koning, HP. (2013). Pyrimidine biosynthesis is not an essential function for *Trypanosoma brucei* bloodstream forms. *PLoS One*, 8, e58034.

Ali, JAM, Creek, DJ, Burgess, K, Allison, HC, Field, MC, Maser, P & de Koning, HP. (2013). Pyrimidine salvage in *Trypanosoma brucei* bloodstream forms and the trypanocidal action of halogenated pyrimidines. *Molecular Pharmacology*, 83, 439-453.

Gould, MK, Bachmaier, S, **Ali, JAM**, Alsford, S, Tagoe, DNA, Munday, JC, Schnaufer, AC, Horn, D, Boshart, M & de Koning, HP. (2013). Cyclic AMP effectors in African trypanosomes revealed by genome-scale RNAi library screening for resistance to the phosphodiesterase inhibitor Cpd A. Antimicrob Agents Chemother.

List of References

Abbruzzese, JL, Grunewald, R, Weeks, EA, Gravel, D, Adams, T, Nowak, B, Mineishi, S, Tarassoff, P, Satterlee, W & Raber, MN. (1991). A phase I clinical, plasma, and cellular pharmacology study of gemcitabine. Journal of Clinical Oncology, 9, 491-498.

Abdo, MG, Elamin, WM, Khalil, EA & Mukhtar, MM. (2003). Antimony-resistant *Leishmania donovani* in eastern Sudan: incidence and *in vitro* correlation. East Mediterr Health J, 9, 837-843.

Acimovic, Y & Coe, IR. (2002). Molecular evolution of the equilibrative nucleoside transporter family: identification of novel family members in prokaryotes and eukaryotes. Molecular Biology and Evolution, 19, 2199-2210.

Adriano, CAC, Boisvert, S, Angana, AM, Philippe, PL, Jacques, JC & Marc, MO. (2012). Multiple mutations in heterogeneous miltefosine-resistant *Leishmania major* population as determined by whole genome sequencing. PLoS Negl Trop Dis, 6, e1512.

Aerts, D, Truc, P, Penchenier, L, Claes, Y & Le Ray, D. (1992). A kit for in vitro isolation of trypanosomes in the field: first trial with sleeping sickness patients in the Congo Republic. pp. 394-395.

Afewerk, Y, Clausen, PH, Abebe, G, Tilahun, G & Mehlitz, D. (2000). Multiple-drug resistant *Trypanosoma congolense* populations in village cattle of Metekel district, north-west Ethiopia. Acta Tropica, 76, 231-238.

Aksoy, S, O'Neill, SL, Maudlin, I, Dale, C & Robinson, AS. (2001). Prospects for control of African trypanosomiasis by tsetse vector manipulation. Trends in Parasitology, 17, 29-35.

Aksoy, S. (2003). Control of tsetse flies and trypanosomes using molecular genetics. Veterinary Parasitology, 115, 125-145.

Ali, JAM, Creek, DJ, Burgess, K, Allison, HC, Field, MC, Mäser, P & De Koning, HP. (2013a). Pyrimidine salvage in *Trypanosoma brucei* bloodstream forms and the trypanocidal action of halogenated pyrimidines. Molecular Pharmacology, 83, 439-453.

Ali, JAM, Tagoe, DN, Munday, JC, Donachie, A, Morrison, LJ & De Koning, HP. (2013b). Pyrimidine biosynthesis is not an essential function for *Trypanosoma brucei* bloodstream forms. PLoS One, 8, e58034.

Allsopp, R. (2001). Options for vector control against trypanosomiasis in Africa. Trends in Parasitology, 17, 15-19.

Al-Salabi, MI & De Koning, HP. (2005). Purine nucleobase transport in amastigotes of *Leishmania mexicana*: involvement in allopurinol uptake. Antimicrob Agents Chemother, 49, 3682-3689.

Al-Salabi, MI, Wallace, LJM & De Koning, HP. (2003). A *Leishmania major* nucleobase transporter responsible for allopurinol uptake is a functional homolog of the *Trypanosoma brucei* H2 Transporter. Molecular Pharmacology, 63, 814-820.

Al-Salabi, MI, Wallace, LJM, Lüscher, A, Mäser, P, Candlish, D, Rodenko, B, Gould, MK, Jabeen, I, Ajith, SN & De Koning, HP. (2007). Molecular interactions

underlying the unusually high adenosine affinity of a novel *Trypanosoma brucei* nucleoside transporter. Molecular Pharmacology, 71, 921-929.

Alsford, S, Eckert, S, Baker, N, Glover, L, Sanchez-Flores, A, Leung, KF, Turner, DJ, Field, MC, Berriman, M & Horn, D. (2012). High-throughput decoding of antitrypanosomal drug efficacy and resistance. Nature, 482, 232-236.

Arakaki, TL, Buckner, FS, Gillespie, JR, Malmquist, NA, Phillips, MA, Kalyuzhniy, O, Luft, JR, DeTitta, GT, Verlinde, CLMJ, Van Voorhis, WC, Hol, WGJ & Merritt, EA. (2008). Characterization of *Trypanosoma brucei* dihydroorotate dehydrogenase as a possible drug target; structural, kinetic and RNAi studies. Molecular Microbiology, 68, 37-50.

Arias, JR, Monteiro, PS & Zicker, F. (1996). The re-emergence of visceral leishmaniasis in Brazil. Emerg Infect Dis, 2, 145-146.

Arlin, ZA, Feldman, E, Kempin, S, Ahmed, T, Mittelman, A, Savona, S, Ascensao, J, Baskind, P, Sullivan, P & Fuhr, HG. (1988). Amsacrine with high-dose cytarabine is highly effective therapy for refractory and relapsed acute lymphoblastic leukaemia in adults. Blood, 72, 433-435.

Arnoult, D, Akarid, K, Grodet, A, Petit, PX, Estaquier, J & Ameisen, JC. (2002). On the evolution of programmed cell death: apoptosis of the unicellular eukaryote *Leishmania major* involves cysteine proteinase activation and mitochondrion permeabilization. Cell Death and Differentiation, 9.

Aronow, B, Kaur, K, McCartan, K & Ullman, B. (1987). Two high affinity nucleoside transporters in *Leishmania donovani*. Molecular and Biochemical Parasitology, 22, 29-37.

Aymerich, I, Duflot, S, Fernández-Veledo, S, Guillèn-Gómez, E, Huber-Ruano, I, Casado, FJ & Pastor-Anglada, M. (2005). The concentrative nucleoside transporter family (SLC28): new roles beyond salvage? Biochem Soc Trans, 33, 216-219.

Bacchi, CJ, Nathan, HC, Hutner, SH, McCann, PP & Sjoerdsma, A. (1980). Polyamine metabolism: a potential therapeutic target in trypanosomes. Science (New York, N Y), 210, 332-334.

Baker, N, Alsford, S & Horn, D. (2011). Genome-wide RNAi screens in African trypanosomes identify the nifurtimox activator NTR and the eflornithine transporter AAT6. Molecular and Biochemical Parasitology, 176, 55-57.

Baker, N, de Koning, HP, Maser, P & Horn, D. (2013). Drug resistance in African trypanosomiasis: the melarsoprol and pentamidine story. Trends in Parasitology, 29, 110-118.

Baker, N, Glover, L, Munday, JC, Aguinaga, AD, Barrett, MP, De Koning, HP & Horn, D. (2012). Aquaglyceroporin 2 controls susceptibility to melarsoprol and pentamidine in African trypanosomes. Proc Natl Acad Sci U S A, 109, 10996-11001.

Balana-Fouce, R., Reguera, R. M, J. C. Cubría & D. Ordóñez. (1998). The Pharmacology of Leishmaniasis. General Pharmacology: The Vascular System, 30, 435-443.

Balasegaram, M, Harris, S, Checchi, F, Ghorashian, S, Hamel, C & Karunakara, U. (2006). Melarsoprol versus eflornithine for treating late-stage Gambian trypanosomiasis in the Republic of the Congo. Bulletin of the World Health Organization, 84, 783-791.

Baldwin, J, Michnoff, CH, Malmquist, NA, White, J, Roth, MG, Rathod, PK & Phillips, MA. (2005). High-throughput Screening for Potent and Selective Inhibitors of *Plasmodium falciparum* dihydroorotate dehydrogenase. Journal of Biological Chemistry, 280, 21847-21853.

Baldwin, SA, Mackey, JR, Cass, CE & Young, JD. (1999). Nucleoside transporters: molecular biology and implications for therapeutic development. Molecular Medicine Today, 5, 216-224.

Barrett, MP & Fairlamb, AH. (1999). The biochemical basis of arsenical diamidine cross resistance in African trypanosomes. Parasitology Today, 15, 136-140.

Barrett, MP & Gilbert, IH. (2006). Targeting of toxic compounds to the trypanosome's interior. In Advances in Parasitology. ed. Baker,J.R. pp. 125-183. Academic Press.

Barrett, MP, Boykin, DW, Brun, R & Tidwell, RR. (2007). Human African trypanosomiasis: pharmacological re-engagement with a neglected disease. Br J Pharmacol, 152, 1155-1171.

Barrett, MP, Burchmore, RJ, Stich, A, Lazzari, JO, Frasch, AC, Cazzulo, JJ & Krishna, S. (2003). The trypanosomiases. Lancet, 362, 1469-1480.

Barrett, MP, Zhang, ZQ, Denise, H, Giroud, C & Baltz, T. (1995). A diamidine-resistant *Trypanosoma equiperdum* clone contains a P2 purine transporter with reduced substrate affinity. 134. Mol Biochem Parasitol, 73, 223-229.

Basselin, M, Denise, H, Coombs, GH & Barrett, MP. (2002). Resistance to pentamidine in *Leishmania mexicana* involves exclusion of the drug from the mitochondrion. Antimicrob Agents Chemother, 46, 3731-3738.

Bastin, P, Stephan, A, Raper, J, Saint-Remy, JM, Opperdoes, FR & Courtoy, PJ. (1996). An Mr 145000 low-density lipoprotein (LDL)-binding protein is conserved throughout the Kinetoplastida order. Molecular and Biochemical Parasitology, 76, 43-56.

Bates, PA & Rogers, ME. (2004). New Insights into the Developmental Biology and Transmission Mechanisms of *Leishmania*. pp. 601-609.

Bello, AR, Nare, B, Freedman, D, Hardy, L & Beverley, SM. (1994). PTR1: a reductase mediating salvage of oxidized pteridines and methotrexate resistance in the protozoan parasite *Leishmania major*. Proc Natl Acad Sci U S A, 91, 11442-11446.

Bellofatto, V, Fairlamb, AH, Henderson, GB & Cross, GA. (1987). Biochemical changes associated with alpha-difluoromethylornithine uptake and resistance in *Trypanosoma brucei*. Molecular and Biochemical Parasitology, 25, 227-238.

Bellofatto, V. (2007). Pyrimidine transport activities in trypanosomes. Trends Parasitol, 23, 187-189.

Berens, RL, Krug, EC & Marr, JJ. (1995). Purine and pyrimidine metabolism. In Biochemistry and Molecular biology of parasites. ed. Marr,J.J. & Muller,M. pp. 89-117. Academic Press: London.

Berg, M, Kohl, L, Van der Veken, P, Joossens, J, Al-Salabi, MI, Castagna, V, Giannese, F, Cos, P, Versees, W, Steyaert, J, Grellier, P, Haemers, A, Degano, M, Maes, L, De Koning, HP & Augustyns, K. (2010). Evaluation of nucleoside hydrolase inhibitors for treatment of African trypanosomiasis. Antimicrob Agents Chemother, 54, 1900-1908.

Berman, JD, Gallalee, JV & Best, JM. (1987). Sodium stibogluconate (Pentostam) inhibition of glucose catabolism via the glycolytic pathway, and fatty acid beta-oxidation in *Leishmania mexicana* amastigotes. Biochemical Pharmacology, 36, 197-201.

Berman, JD, Waddell, D & Hanson, BD. (1985). Biochemical mechanisms of the antileishmanial activity of sodium stibogluconate. Antimicrob Agents Chemother, 27, 916-920.

Bernhard, SC, Nerima, B, Maser, P & Brun, R. (2007). Melarsoprol- and pentamidine-resistant *Trypanosoma brucei rhodesiense* populations and their cross-resistance. International Journal for Parasitology, 37, 1443-1448.

Bernier-Villamor, V, Camacho, A, Hidalgo-Zarco, F, Perez, J, Ruiz-Perez, LM & Gonzalez-Pacanowska, D. (2002). Characterization of deoxyuridine 5'-triphosphate nucleotidohydrolase from *Trypanosoma cruzi*. FEBS Lett, 526, 147-150.

Berriman, M, Ghedin, E, Hertz-Fowler, C, Blandin, Gl, Renauld, H, Bartholomeu, *et al.,* (2005). The Genome of the African Trypanosome *Trypanosoma brucei*. Science, 309, 416-422.

Bhamrah, HS & Juneja, K. (2001). An Introduction to Protozoa. Anmol Publication PVT LTD: New Delhi.

Bi, D, Anderson, LW, Shapiro, J, Shapiro, A, Grem, JL & Takimoto, CH. (2000). Measurement of plasma uracil using gas chromatographyGÇômass spectrometry in normal individuals and in patients receiving inhibitors of dihydropyrimidine dehydrogenase. Journal of Chromatography B: Biomedical Sciences and Applications, 738, 249-258.

Bingle, LEH, Eastlake, JL, Bailey, M & Gibson, WC. (2001). A novel GFP approach for the analysis of genetic exchange in trypanosomes allowing the in situ detection of mating events. Microbiology, 147, 3231-3240.

Bisser, S, N'Siesi, FX, Lejon, V, Preux, PM, Van Nieuwenhove, S, Miaka Mia Bilenge, C & Buscher, P. (2007). Equivalence trial of melarsoprol and nifurtimox monotherapy and combination therapy for the treatment of second-stage *Trypanosoma brucei gambiense* sleeping sickness. Journal of Infectious Diseases, 195, 322-329.

Bitonti, AJ, Bacchi, CJ, McCann, PP & Sjoerdsma, A. (1986). Uptake of alpha-difluoromethyl-ornithine by *Trypanosoma brucei brucei*. Biochemical Pharmacology, 35, 351-354.

Blum, J, Nkunku, S & Burri, C. (2001). Clinical description of encephalopathic syndromes and risk factors for their occurrence and outcome during melarsoprol treatment of human African trypanosomiasis. Tropical Medicine & International Health, 6, 390-400.

Boitz, JM, Strasser, R, Hartman, CU, Jardim, A & Ullman, B. (2012a). Adenine aminohydrolase from *Leishmania donovani*: a unique enzyme in parasite purine metabolism. Journal of Biological Chemistry.

Boitz, JM, Ullman, B, Jardim, A & Carter, NS. (2012b). Purine salvage in *Leishmania*: complex or simple by design? pp. 345-352.

Borst, P & Ouellette, M. (1995). New mechanisms of drug resistance in parasitic protozoa. Annu Rev Microbiol, 49, 427-460.

Borst, P. (2002). Antigenic variation and allelic exclusion. Cell, 109, 5-8.

Bray, PG, Barrett, MP, Ward, SA & De Koning, HP. (2003). Pentamidine uptake and resistance in pathogenic protozoa: past, present and future. Trends Parasitol, 19, 232-239.

Brun, R, Blum, J, Chappuis, F & Burri, C. (2010). Human African trypanosomiasis. Lancet, 375, 148-159.

Brun, R, Schumacher, R, Schmid, C, Kunz, C & Burri, C. (2001). The phenomenon of treatment failures in Human African Trypanosomiasis. Tropical Medicine & International Health, 6, 906-914.

Burchmore, RJ, Wallace, LJ, Candlish, D, Al-Salabi, MI, Beal, PR, Barrett, MP, Baldwin, SA & De Koning, HP. (2003). Cloning, heterologous expression, and in situ characterization of the first high affinity nucleobase transporter from a protozoan. J Biol Chem, 278, 23502-23507.

Burri, C, Baltz, T, Giroud, C, Doua, F, Welker, HA & Brun, K. (1993). Pharmacokinetic Properties of the trypanocidal drug melarsoprol. Chemotherapy, 39, 225-234.

Burri, C, Nkunku, S, Merolle, A, Smith, T, Blum, J & Brun, R. (2000). Efficacy of new, concise schedule for melarsoprol in treatment of sleeping sickness caused by *Trypanosoma brucei gambiense*: a randomised trial. The Lancet, 355, 1419-1425.

Burri, C, Stich, A & Brun, R. (2004). Current chemotherapy of human African trypanosomiasis. In The Trypanosomiases. ed. Maudlin,I., Holmes,P. & Miles,M.A. pp. 403-419. CABI Publishing: Wallingford, UK.

Burris, HA, Moore, MJ, Andersen, J, Green, MR, Rothenberg, ML, Modiano, MR, Cripps, MC, Portenoy, RK, Storniolo, AM, Tarassoff, P, Nelson, R, Dorr, FA, Stephens, CD & Von Hoff, DD. (1997). Improvements in survival and clinical benefit with gemcitabine as first-line therapy for patients with advanced pancreas cancer: a randomized trial. Journal of Clinical Oncology, 15, 2403-2413.

Butcher, BA, Turco, SJ, Hilty, BA, Pimenta, PF, Panunzio, M & Sacks, DL. (1996). Deficiency in beta 1,3-galactosyltransferase of a *Leishmania major*

lipophosphoglycan mutant adversely influences the leishmania-sand fly interaction. Journal of Biological Chemistry, 271, 20573-20579.

Carrey, EA. (1995). Key enzymes in the biosynthesis of purines and pyrimidines: their regulation by allosteric effectors and by phosphorylation. Biochem Soc Trans, 23, 899-902.

Carter, N, Yates, P, Arendt, C, Boitz, J & Ullman, B. (2008). Purine and pyrimidine metabolism in *Leishmania*. In Drug Targets in Kinetoplastid Parasites. ed. Majumder,H. pp. 141-154. Springer New York.

Carter, NS & Fairlamb, AH. (1993). Arsenical-resistant trypanosomes lack an unusual adenosine transporter. Nature, 361, 173-176.

Carter, NS, Berger, BJ & Fairlamb, AH. (1995). Uptake of diamidine drugs by the P2 nucleoside transporter in melarsen-sensitive and -resistant *Trypanosoma brucei brucei*. Journal of Biological Chemistry, 270, 28153-28157.

Carter, NS, Drew, ME, Sanchez, M, Vasudevan, G, Landfear, SM & Ullman, B. (2000). Cloning of a novel inosine-guanosine transporter gene from *Leishmania donovani* by functional rescue of a transport-deficient mutant. Journal of Biological Chemistry, 275, 20935-20941.

Carter, NS, Rager, N & Ullman, B. (2003). Purine and pyrimidine transport and metabolism. In Molecular and Medical Parasitology. ed. Marr,J.J., Nilsen Timothy, Komuniecki & Richard,W. pp. 197-223. Elsevier Science: London.

Carter, NS, Yates, PA, Gessford, SK, Galagan, SR, Landfear, SM & Ullman, B. (2010). Adaptive responses to purine starvation in *Leishmania donovani*. Molecular Microbiology, 78, 92-107.

Cass, CE, Young, JD & Baldwin, SA. (1998). Recent advances in the molecular biology of nucleoside transporters of mammalian cells. Biochem Cell Biol, 76, 761-770.

Cassera, MB, Zhang, Y, Hazleton, KZ & Schramm, VL. (2011). Purine and pyrimidine pathways as targets in *Plasmodium falciparum*. Curr Top Med Chem, 11, 2103-2115.

Castillo, E, Dea-Ayuela, MA, BolAs-Fernandez, F, Rangel, M & Gonzalez-Rosende, ME. (2010). The kinetoplastid chemotherapy revisited: current drugs, recent advances and future perspectives. Curr Med Chem, 17, 4027-4051.

Castillo-Acosta, VcM, Aguilar-Pereyra, F, Garc+¡a-Caballero, D, Vidal, AE, Ruiz-P+®rez, LM & Gonz+ílez-Pacanowska, D. (2013). Pyrimidine requirements in deoxyuridine triphosphate nucleotidohydrolase deficient Trypanosoma brucei mutants. Molecular and Biochemical Parasitology, 187, 9-13.

Castillo-Acosta, VcM, Estevez, AM, Vidal, AE, Ruiz-Perez, LM & Gonzalez-Pacanowska, D. (2008). Depletion of dimeric all-alpha dUTPase induces DNA strand breaks and impairs cell cycle progression in *Trypanosoma brucei*. The International Journal of Biochemistry & amp; Cell Biology, 40, 2901-2913.

Castro, JA, deMecca, MaM & Bartel, LC. (2006). Toxic side effects of drugs used to treat Chagas' Disease (American Trypanosomiasis). Human & Experimental Toxicology, 25, 471-479.

Cattand, P, Jannin, J & Lucas, P. (2001). Sleeping sickness surveillance: an essential step towards elimination. Tropical Medicine & International Health, 6, 348-361.

Ceilley, RI. (2010). Mechanisms of action of topical 5-fluorouracil: Review and implications for the treatment of dermatological disorders. J Dermatolog Treat, 23, 83-89.

Cerecetto, H & Gonzalez, M. (2002). Chemotherapy of Chagas' disease: status and new developments. Curr Top Med Chem, 2, 1187-1213.

CFSPH. (2009). African Animal Trypanosomiasis. Nagana, Tsetse Disease, Tsetse Fly Disease. ed. The Center for Food Security and Public Health Jowa State University.

Chalabi, KA & Gutteridge, WE. (1977). Catabolism of deoxy-thymidylate in some trypanosomatids. Parasitology, 74, 299-312.

Chappuis, F, Loutan, L, Simarro, P, Lejon, V & Buscher, P. (2005). Options for field diagnosis of human African trypanosomiasis. Clinical Microbiology Reviews, 18, 133-146.

Checchi, F, Piola, P, Ayikoru, H, Thomas, F, Legros, D & Priotto, G. (2007). Nifurtimox plus eflornithine for late-stage sleeping sickness in Uganda: A case series. PLoS Negl Trop Dis, 1, e64.

Chiurillo, MA, Sachdeva, M, Dole, VS, Yepes, Y, Miliani, E, Vazquez, L, Rojas, A, Crisante, G, Guevara, P, Anez, N, Madhubala, R & Ramirez, JL. (2001). Detection of *Leishmania* causing visceral leishmaniasis in the Old and New Worlds by a polymerase chain reaction assay based on telomeric sequences. The American Journal of Tropical Medicine and Hygiene, 65, 573-582.

Choudhury, K, Zander, D, Kube, M, Reinhardt, R & Clos, J. (2008). Identification of a *Leishmania infantum* gene mediating resistance to miltefosine and SbIII. International Journal for Parasitology, 38, 1411-1423.

Chunge, CN, Gacmra, G, Muigai, R, Wasunna, K, Rashid, JR, Chulay, JD, Anabwani, G, Oster, CN & Bryceson, ADM. (1985). Visceral leishmaniasis unresponsive to antimonial drugs III. Successful treatment using a combination of sodium stibogluconate plus allopurinol. Transactions of the Royal Society of Tropical Medicine and Hygiene, 79, 715-718.

Coppens, I & Courtoy, PJ. (2000). The adaptive mechanisms of Trypanosoma *brucei* for sterol homeostasis in its different life-cycle environments. Annu Rev Microbiol, 54, 129-156.

Courtin, F, Jamonneau, V, Duvallet, G, Camara, M, Kaba, D & Solano, P. (2008). One century of "sleeping sickness" in West Africa. Bull Soc Pathol Exot, 101, 287-289.

Creek, DJ, Anderson, J, McConville, MJ & Barrett, MP. (2012a). Metabolomic analysis of trypanosomatid protozoa. Molecular and Biochemical Parasitology, 181, 73-84.

Creek, DJ, Jankevics, A, Breitling, R, Watson, DG, Barrett, MP & Burgess, KE. (2011). Toward global metabolomics analysis with hydrophilic interaction

liquid chromatography-mass spectrometry: improved metabolite identification by retention time prediction. Anal Chem, 83, 8703-8710.

Creek, DJ, Jankevics, A, Burgess, KE, Breitling, R & Barrett, MP. (2012b). IDEOM: an Excel interface for analysis of LC-MS-based metabolomics data. Bioinformatics, 28, 1048-1049.

Croft, SL, Barrett, MP & Urbina, JA. (2005). Chemotherapy of trypanosomiases and leishmaniasis. Trends Parasitol, 21, 508-512.

Croft, SL, Sundar, S & Fairlamb, AH. (2006). Drug resistance in leishmaniasis. Clinical Microbiology Reviews, 19, 111-126.

Cruz, I, Nieto, J, Moreno, J, Canavate, C, Desjeux, P & Alvar, J. (2006). Leishmania/HIV co-infections in the second decade. Indian J Med Res, 123, 357-388.

Dal, BD, Buccioni, M, Lambertucci, C, Marucci, G, Volpini, R & Cristall, G. (2011). The importance of alkynyl chain presence for the activity of adenine nucleosides/nucleotides on purinergic receptors. Curr Med Chem.

Das, VN, Ranjan, A, Sinha, AN, Verma, N, Lal, CS, Gupta, AK, Siddiqui, NA & Kar, SK. (2001). A randomized clinical trial of low dosage combination of pentamidine and allopurinol in the treatment of antimony unresponsive cases of visceral leishmaniasis. J Assoc Physicians India, 49, 609-613.

Davidson, RN, den Boer, M & Ritmeijer, K. (2009). Paromomycin. Transactions of the Royal Society of Tropical Medicine and Hygiene, 103, 653-660.

Davies, C, Kaye, P, Croft, S & Sundar, S. (2003). Leishmaniasis: new approaches to disease control. BMJ (Clinical research ed), 326, 377-382.

De Alencar, JE & Neves, J. (1982). Leishmania visceral (Calazar). In Doencas Infecciosas e Parasitarias. ed. Veronesi,R. p. 724. Editora Guanabara Koogan SA: Rio de Janeiro.

De Koning, H & Diallinas, G. (2000). Nucleobase transporters (review). Mol Membr Biol, 17, 75-94.

De Koning, HP & Jarvis, SM. (1997a). Hypoxanthine uptake through a purine-selective nucleobase transporter in *Trypanosoma brucei brucei* procyclic cells is driven by protonmotive force. Eur J Biochem, 247, 1102-1110.

De Koning, HP & Jarvis, SM. (1997b). Purine nucleobase transport in bloodstream forms of *Trypanosoma brucei brucei* is mediated by two novel transporters. Molecular and Biochemical Parasitology, 89, 245-258.

De Koning, HP & Jarvis, SM. (1998). A highly selective, high-affinity transporter for uracil in *Trypanosoma brucei brucei*: evidence for proton-dependent transport. Biochem Cell Biol, 76, 853-858.

De Koning, HP & Jarvis, SM. (1999). Adenosine Transporters in Bloodstream Forms of *Trypanosoma brucei brucei*: Substrate Recognition Motifs and Affinity for Trypanocidal Drugs. Molecular Pharmacology, 56, 1162-1170.

De Koning, HP, Al-Salabi, MI, Cohen, AM, Coombs, GH & Wastling, JM. (2003). Identification and characterisation of high affinity nucleoside and nucleobase transporters in *Toxoplasma gondii*. International Journal for Parasitology, 33, 821-831.

De Koning, HP, Anderson, LF, Stewart, M, Burchmore, RJ, Wallace, LJ & Barrett, MP. (2004). The trypanocide diminazene aceturate is accumulated predominantly through the TbAT1 purine transporter: additional insights on diamidine resistance in African trypanosomes. Antimicrob Agents Chemother, 48, 1515-1519.

De Koning, HP, Bridges, DJ & Burchmore, RJ. (2005). Purine and pyrimidine transport in pathogenic protozoa: from biology to therapy. FEMS Microbiol Rev, 29, 987-1020.

De Koning, HP. (2001). Uptake of pentamidine in *Trypanosoma brucei brucei* is Mediated by Three Distinct Transporters: Implications for Cross-Resistance with Arsenicals. Molecular Pharmacology, 59, 586-592.

De Koning, HP. (2008). Ever-increasing complexities of diamidine and arsenical cross resistance in African trypanosomes. Trends Parasitol, 24, 345-349.

De Lima Barros, MnB, Schubach, A, Francesconi-do-Valle, AnC, Gutierrez-Galhardo, MC, Schubach, TMP, *et al.,* (2005). Positive Montenegro skin test among patients with sporotrichosis in Rio De Janeiro. Acta Tropica, 93, 41-47.

De Oliveira, CI, Bafica, A, Oliveira, F, Favali, CBF, Correa, T, Freitas, LAR, Nascimento, E, Costa, JM & Barral, A. (2003). Clinical utility of polymerase chain reaction-based detection of *Leishmania* in the diagnosis of American cutaneous leishmaniasis. Clinical Infectious Diseases, 37, e149-e153.

De Raadt, P. (1985). Congenital trypanosomiasis and leishmaniasis. Arch Fr Pediatr, 42 Suppl 2, 925-927.

Deborggraeve, S, Koffi, M, Jamonneau, V, Bonsu, FA, Queyson, R, Simarro, PP, Herdewijn, P & Buscher, P. (2008). Molecular analysis of archived blood slides reveals an atypical human *Trypanosoma* infection. Diagnostic Microbiology and Infectious Disease, 61, 428-433.

Debroise, A, Debroise-Ballereau, C, Satge, P & Rey, M. (1968). African trypanosomiasis in young children. Arch Fr Pediatr, 25, 703-720.

Delespaux, V & De Koning, HP. (2007). Drugs and drug resistance in African trypanosomiasis. Drug Resistance Updates, 10, 30-50.

Demicheli, C, Frezard, Frederic, Lecouvey, M & Garnier-Suillerot, A. (2002). Antimony(V) complex formation with adenine nucleosides in aqueous solution. Biochimica et Biophysica Acta (BBA) - General Subjects, 1570, 192-198.

Denise, H & Barrett, MP. (2001). Uptake and mode of action of drugs used against sleeping sickness. Biochem Pharmacol, 61, 1-5.

Denton, H, McGregor, JC & Coombs, GH. (2004). Reduction of anti-leishmanial pentavalent antimonial drugs by a parasite-specific thiol-dependent reductase, TDR1. Biochem J, 381, 405-412.

Desjeux, P & Alvar, J. (2003). Leishmania/HIV co-infections: epidemiology in Europe. Annals of Tropical Medicine and Parasitology, 97 Suppl 1, 3-15.

Desjeux, P & UNAIDS. (1998). *Leishmania* and HIV in Gridlock. In World Health Organization and United Nations Programme on HIV/AIDS, WHO/CTD/LEISH/98.9 Add . ed. Beales,P.F. pp. 5-14. WHO.

Desjeux, P. (1996). Leishmaniasis: Public health aspects and control. Clinics in Dermatology, 14, 417-423.

Desjeux, P. (2004). Leishmaniasis: current situation and new perspectives. Comparative Immunology, Microbiology and Infectious Diseases, 27, 305-318.

Dobson, DE, Mengeling, BJ, Cilmi, S, Hickerson, S, Turco, SJ & Beverley, SM. (2003). Identification of genes encoding arabinosyltransferases (SCA) mediating developmental modifications of lipophosphoglycan required for sand fly transmission of *Leishmania major*. Journal of Biological Chemistry, 278, 28840-28848.

Docampo, R. (1990). Sensitivity of parasites to free radical damage by antiparasitic drugs. Chemico-Biological Interactions, 73, 1-27.

Donelson, JE, Hill, KL & El-Sayed, NMA. (1998). Multiple mechanisms of immune evasion by African trypanosomes. Molecular and Biochemical Parasitology, 91, 51-66.

Donelson, JE. (2003). Antigenic variation and the African trypanosome genome. Acta Tropica, 85, 391-404.

Drain, J, Bishop, JR & Hajduk, SL. (2001). Haptoglobin-related protein mediates trypanosome lytic factor binding to trypanosomes. Journal of Biological Chemistry, 276, 30254-30260.

Eddy, SR. (2009). A new generation of homology search tools based on probabilistic inference. Genome informatics International Conference on Genome Informatics, 23, 205-211.

Eholie, SP, Aoussi, FE, Ouattara, IS, Bissagnene, E & Anglaret, X. (2012). HIV treatment and care in resource-constrained environments: challenges for the next decade. J Int AIDS Soc, 15, 17334.

El Rayah, IE, Kaminsky, R, Schmid, C & El Malik, KH. (1999). Drug resistance in Sudanese *Trypanosoma evansi*. Veterinary Parasitology, 80, 281-287.

Enanga, B, Ariyanayagam, MR, Stewart, ML & Barrett, MP. (2003). Activity of megazol, a trypanocidal nitroimidazole, is associated with DNA damage. Antimicrob Agents Chemother, 47, 3368-3370.

Erwin, BG & Pegg, AE. (1982). Uptake of alpha-difluoromethylornithine by mouse fibroblasts. Biochemical Pharmacology, 31, 2820-2823.

Fairlamb, AH & Bowman, IBR. (1980). Uptake of the trypanocidal drug suramin by bloodstream forms of *Trypanosoma brucei* and its effect on respiration and growth rate *in vivo*. Molecular and Biochemical Parasitology, 1, 315-333.

Fairlamb, AH, Henderson, GB & Cerami, A. (1989). Trypanothione is the primary target for arsenical drugs against African trypanosomes. Proceedings of the National Academy of Sciences, 86, 2607-2611.

Fairlamb, AH, Henderson, GB, Bacchi, CJ & Cerami, A. (1987). *In vivo* effects of difluoromethylornithine on trypanothione and polyamine levels in bloodstream forms of *Trypanosoma brucei*. Molecular and Biochemical Parasitology, 24, 185-191.

Farber, S, Diamond, LK, Mercer, RD, Sylvester, RF & Wolff, JA. (1948). Temporary remissions in acute leukemia in children produced by folic acid antagonist, 4-aminopteroyl-glutamic acid (Aminopterin). N Engl J Med, 238, 787-793.

Fath, MJ & Kolter, R. (1993). ABC transporters: bacterial exporters. Microbiological Reviews, 57, 995-1017.

Feliciano, PcR, Cordeiro, AT, Costa-Filho, AJ & Nonato, MC. (2006). Cloning, expression, purification, and characterization of *Leishmania major* dihydroorotate dehydrogenase. Protein Expression and Purification, 48, 98-103.

Feng, J, Lupien, A, Gingras, H, Wasserscheid, J, Dewar, K, Legare, D & Ouellette, M. (2009). Genome sequencing of linezolid-resistant *Streptococcus pneumoniae* mutants reveals novel mechanisms of resistance. Genome Res, 19, 1214-1223.

Fernandez, MM, Malchiodi, EL & Algranati, ID. (2011). Differential effects of paromomycin on ribosomes of *Leishmania mexicana* and mammalian cells. Antimicrob Agents Chemother, 55, 86-93.

Fields, PI, Swanson, RV, Haidaris, CG & Heffron, F. (1986). Mutants of *Salmonella typhimurium* that cannot survive within the macrophage are avirulent. Proc Natl Acad Sci U S A, 83, 5189-5193.

Fijolek, A, Hofer, A & Thelander, L. (2007). Expression, purification, characterization, and *in vivo* targeting of trypanosome CTP synthetase for treatment of African sleeping sickness. Journal of Biological Chemistry, 282, 11858-11865.

Flynn, IW & Bowman, IBR. (1974). The action of trypanocidal arsenical drugs on *Trypanosoma brucei* and *Trypanosoma rhodesiense*. Comparative Biochemistry and Physiology Part B: Comparative Biochemistry, 48, 261-273.

Ford, WCL & Bowman, IBR. (1973). Metabolism of proline by the culture midgut form of *Trypanosoma rhodesiense*. p. 257.

Fox, BA & Bzik, DJ. (2002). De novo pyrimidine biosynthesis is required for virulence of *Toxoplasma gondii*. Nature, 415, 926-929.

French, JB, Yates, PA, Soysa, DR, Boitz, JM, Carter, NS, Chang, B, Ullman, B & Ealick, SE. (2011). The *Leishmania donovani* UMP synthase is essential for promastigote viability and has an unusual tetrameric structure that exhibits substrate-controlled oligomerization. Journal of Biological Chemistry, 286, 20930-20941.

Frezard, F, Martins, PS, Barbosa, MC, Pimenta, AM, Ferreira, WA, de Melo, JE, Mangrum, JB & Demicheli, C. (2008). New insights into the chemical structure and composition of the pentavalent antimonial drugs, meglumine antimonate and sodium stibogluconate. J Inorg Biochem, 102, 656-665.

Friedheim, EAH. (1949). Mel B in the treatment of human trypanosomiasis. The American Journal of Tropical Medicine and Hygiene, s1-29, 173-180.

Gale, EF & Taylor, ES. (1947). The assimilation of amino-acids by bacteria: 2. the action of tyrocidin and some detergent substances in releasing amino-acids from the internal environment of *Streptococcus faecalis*. Microbiology, 1, 77-84.

Gallego, C, Estevez, AM, Farez, E, Ruiz-Perez, LM & Gonzalez-Pacanowska, D. (2005). Overexpression of AP endonuclease protects *Leishmania major* cells against methotrexate induced DNA fragmentation and hydrogen peroxide. Molecular and Biochemical Parasitology, 141, 191-197.

Galmarini, CM, Jordheim, L & Dumontet, C. (2003). Pyrimidine nucleoside analogs in cancer treatment. Expert Rev Anticancer Ther, 3, 717-728.

Gao, G, Nara, T, Nakajima-Shimada, J & Aoki, T. (1999). Novel organization and sequences of five genes encoding all six enzymes for de novo pyrimidine biosynthesis in *Trypanosoma cruzi*. J Mol Biol, 285, 149-161.

Garcia, L. (2007). Diagnostic Medical Parasitology. ASM Press.

Garofalo, Joan, Bacchhi, CJ, McLaughlin, SD, Mockenhaupt, Dian, Trueba, Gene & Hutner, SH. (1982). Ornithine Decarboxylase in *Trypanosoma brucei brucei*: Evidence for selective toxicity of difluoromethylornithine1. Journal of Eukaryotic Microbiology, 29, 389-394.

Garrett, CE, Coderre, JA, Meek, TD, Garvey, EP, Claman, DM, Beverley, SM & Santi, DV. (1984). A bifunctional thymidylate synthetase-dihydrofolate reductase in protozoa. Molecular and Biochemical Parasitology, 11, 257-265.

Gaunt, MW, Yeo, M, Frame, IA, Stothard, JR, Carrasco, HJ, Taylor, MC, Mena, SS, Veazey, P, Miles, GAJ, Acosta, N, de Arias, AR & Miles, MA. (2003). Mechanism of genetic exchange in American trypanosomes. Nature, 421, 936-939.

Geiser, F, Luscher, A, De Koning, HP, Seebeck, T & Maser, P. (2005). Molecular Pharmacology of Adenosine Transport in *Trypanosoma brucei*: P1/P2 Revisited. Molecular Pharmacology, 68, 589-595.

Gero, AM & O'Sullivan, WJ. (1985). Human spleen dihydroorotate dehydrogenase: Properties and partial purification. Biochemical Medicine, 34, 70-82.

Ghosh, M & Mukherjee, T. (2000). Stage-specific development of a novel adenosine transporter in *Leishmania donovani* amastigotes. Molecular and Biochemical Parasitology, 108, 93-99.

Gomes-Cardoso, L, Echevarria, A, Aguiar-Alves, F, Jansen, AM & Leon, LL. (1999). Amidine derivatives are highly effective against *Trypanosoma evansi* trypomastigotes. Microbios, 100, 181-187.

Gonzalez, IJ, Desponds, C, Schaff, C, Mottram, JC & Fasel, N. (2007). *Leishmania major* metacaspase can replace yeast metacaspase in programmed cell death and has arginine-specific cysteine peptidase activity. International Journal for Parasitology, 37, 161-172.

Gossage, SM, Rogers, ME & Bates, PA. (2003). Two separate growth phases during the development of *Leishmania* in sand flies: implications for understanding the life cycle. International Journal for Parasitology, 33, 1027-1034.

Gould, MK, Vu, XL, Seebeck, T & De Koning, HP. (2008). Propidium iodide-based methods for monitoring drug action in the kinetoplastidae: comparison with the Alamar Blue assay. Anal Biochem, 382, 87-93.

Gournas, C, Papageorgiou, I & Diallinas, G. (2008). The nucleobase-ascorbate transporter (NAT) family: genomics, evolution, structure-function relationships and physiological role. Mol BioSyst, 4, 404-416.

Gradoni, L, Gramiccia, M, Leger, N, Pesson, B, Madulo-Leblond, G, Killick-Kendrick, R, Killick-Kendrick, M & Walton, BC. (1991). Isoenzyme characterization of *Leishmania* from man, dog and sandflies in the Maltese islands. Transactions of the Royal Society of Tropical Medicine and Hygiene, 85, 217-219.

Gray, J, Owen, R & Giacomini, K. (2004). The concentrative nucleoside transporter family, SLC28. Pflugers Archiv European Journal of Physiology, 447, 728-734.

Greene, S, Watanabe, K, Braatz-Trulson, J & Lou, L. (1995). Inhibition of dihydroorotate dehydrogenase by the immunosuppressive agent leflunomide. Biochemical Pharmacology, 50, 861-867.

Grevelink, SA & Lerner, EA. (1996). Leishmaniasis. Journal of the American Academy of Dermatology, 34, 257-272.

Grivicich, I, Mans, DRA, Peters, GJ & Schwartsmann, G. (2001). Irinotecan and oxaliplatin: an overview of the novel chemotherapeutic options for the treatment of advanced colorectal cancer. Brazilian Journal of Medical and Biological Research, 34, 1087-1103.

Grootenhuis, JG, Dwinger, RH, Dolan, RB, Moloo, SK & Murray, M. (1990). Susceptibility of African buffalo and Boran cattle to *Trypanosoma congolense* transmitted by *Glossina morsitans centralis*. Veterinary Parasitology, 35, 219-231.

Gudin, S, Quashie, NB, Candlish, D, Al-Salabi, MI, Jarvis, SM, Ranford-Cartwright, LC & De Koning, HP. (2006). *Trypanosoma brucei*: A survey of pyrimidine transport activities. Experimental Parasitology, 114, 118-125.

Gutteridge, WE & Coombs, GH. (1977). Biochemistry of Parasitic Protozoa. MacMillan Press: London.

Gutteridge, WE & Trigg, PI. (1970). Incorporation of radioactive precursors into DNA and RNA of *Plasmodium knowlesi* in vitro. J Protozool, 17, 89-96.

Gutteridge, WE. (1985). Existing chemotherapy and its limitations. British Medical Bulletin, 41, 162-168.

Hadighi, R, Mohebali, M, Boucher, P, Hajjaran, H, Khamesipour, A & Ouellette, M. (2006). Unresponsiveness to Glucantime treatment in Iranian cutaneous leishmaniasis due to drug-resistant *Leishmania* tropica parasites. PLoS Med, 3, e162.

Hager, KM & Hajduk, SL. (1997). Mechanism of resistance of African trypanosomes to cytotoxic human HDL. Nature, 385, 823-826.

Hammarton, T. (2003). The cell cycle of parasitic protozoa: potential for chemotherapeutic exploitation. Progress in Cell Cycle Research, 5, 91-101.

Hammond, DJ & Gutteridge, WE. (1982). UMP synthesis in the kinetoplastida. Biochimica et Biophysica Acta (BBA) - General Subjects, 718, 1-10.

Hammond, DJ & Gutteridge, WE. (1984). Purine and pyrimidine metabolism in the trypanosomatidae. Molecular and Biochemical Parasitology, 13, 243-261.

Hanau, S, Rippa, M, Bertelli, M, Dallocchio, F & Barrett, MP. (1996). 6-Phosphogluconate dehydrogenase from *Trypanosoma brucei*. Kinetic analysis and inhibition by trypanocidal drugs. Eur J Biochem, 240, 592-599.

Handman, E & Bullen, DVR. (2002). Interaction of *Leishmania* with the host macrophage. Trends in Parasitology, 18, 332-334.

Hansen, BD, Perez-Arbelo, J, Walkony, JF & Hendricks, LD. (1982). The specificity of purine base and nucleoside uptake in promastigotes of *Leishmania braziliensis panamensis*. Parasitology, 85 (Pt 2), 271-282.

Harkiolaki, M, Dodson, EJ, Bernier-Villamor, V, Turkenburg, JP, Gonzalez-Pacanowska, D & Wilson, KS. (2004). The crystal structure of *Trypanosoma cruzi* dUTPase reveals a novel dUTP/dUDP binding fold. Structure, 12, 41-53.

Harms, G & Feldmeier, H. (2005). The impact of HIV infection on tropical diseases. Infectious Disease Clinics of North America, 19, 121-135.

Hashimoto, M, Morales, J, Fukai, Y, Suzuki, S, Takamiya, S, Tsubouchi, A, Inoue, S, Inoue, M, Kita, K, Harada, S, Tanaka, A, Aoki, T & Nara, T. (2012). Critical importance of the de novo pyrimidine biosynthesis pathway for *Trypanosoma cruzi* growth in the mammalian host cell cytoplasm. Biochemical and Biophysical Research Communications, 417, 1002-1006.

Hassan, HF & Coombs, GH. (1986). A comparative study of the purine- and pyrimidine-metabolising enzymes of a range of trypanosomatids. Comp Biochem Physiol B, 84, 219-223.

Hassan, HF & Coombs, GH. (1988). Purine and pyrimidine metabolism in parasitic protozoa. FEMS Microbiology Letters, 54, 47-83.

Heidelberger, C, Chaudhuri, NK, Danneberg, P, Mooren, D, Griesbach, L, Duschinsky, R, Schnitzer, RJ, Pleven, E & Scheiner, J. (1957). Fluorinated pyrimidines, a new class of tumour-inhibitory compounds. Nature, 179, 663-666.

Heidelberger, C, Griesbach, L, Cruz, O, Schnitzer, RJ & Grunberg, E. (1958). Fluorinated pyrimidines. VI. Effects of 5-fluorouridine and 5-fluoro-2'-deoxyuridine on transplanted tumors. Proc Soc Exp Biol Med, 97, 470-475.

Heidelberger, C. (1967). Cancer chemotherapy with purine and pyrimidine Analogues. Annu Rev Pharmacol, 7, 101-124.

Heikkila, T, Ramsey, C, Davies, M, Galtier, C, Stead, AM, Johnson, AP, Fishwick, CW, Boa, AN & McConkey, GA. (2007). Design and synthesis of potent inhibitors of the malaria parasite dihydroorotate dehydrogenase. J Med Chem, 50, 186-191.

Henriques, C, Sanchez, MA, Tryon, R & Landfear, SM. (2003). Molecular and functional characterization of the first nucleobase transporter gene from African trypanosomes. Molecular and Biochemical Parasitology, 130, 101-110.

Herbert, WJ & Lumsden, WH. (1976). *Trypanosoma brucei*: a rapid "matching" method for estimating the host's parasitemia. Exp Parasitol, 40, 427-431.

Herwaldt, BL. (1999). Leishmaniasis. The Lancet, 354, 1191-1199.

Hirumi, H & Hirumi, K. (1989). Continuous cultivation of *Trypanosoma brucei* blood stream forms in a medium containing a low concentration of serum protein without feeder cell layers. J Parasitol, 75, 985-989.

Hofer, A, Ekanem, JT & Thelander, L. (1998). Allosteric regulation of *Trypanosoma brucei* ribonucleotide reductase studied *in vitro* and *in vivo*. Journal of Biological Chemistry, 273, 34098-34104.

Hofer, A, Steverding, D, Chabes, A, Brun, R & Thelander, L. (2001). *Trypanosoma brucei* CTP synthetase: a target for the treatment of African sleeping sickness. Proc Natl Acad Sci U S A, 98, 6412-6416.

Hoffmann, HH, Kunz, A, Simon, VA, Palese, P & Shaw, ML. (2011). Broad-spectrum antiviral that interferes with de novo pyrimidine biosynthesis. Proc Natl Acad Sci U S A, 108, 5777-5782.

Howden, BP, Stinear, TP, Allen, DL, Johnson, PD, Ward, PB & Davies, JK. (2008). Genomic analysis reveals a point mutation in the two-component sensor gene graS that leads to intermediate vancomycin resistance in clinical *Staphylococcus aureus*. Antimicrob Agents Chemother, 52, 3755-3762.

Hunt, P, Martinelli, A, Modrzynska, K, Borges, S, Creasey, A, Rodrigues, L, et al., (2010). Experimental evolution, genetic analysis and genome re-sequencing reveal the mutation conferring artemisinin resistance in an isogenic lineage of malaria parasites. BMC Genomics, 11, 499.

Hunter, CA, Murray, M, Jennings, F, Adams, JH & Kennedy, PGE. (1992). Subcurative chemotherapy and fatal post-treatment reactive encephalopathies in African trypanosomiasis. The Lancet, 339, 956-958.

Hyde, RJ, Cass, CE, Young, JD & Baldwin, SA. (2001). The ENT family of eukaryote nucleoside and nucleobase transporters: recent advances in the investigation of structure/function relationships and the identification of novel isoforms. Mol Membr Biol, 18, 53-63.

Ibrahim, HM, Al-Salabi, MI, El, SN, Quashie, NB, Alkhaldi, AA, Escale, R, Smith, TK, Vial, HJ & De Koning, HP. (2011). Symmetrical choline-derived dications display strong anti-kinetoplastid activity. J Antimicrob Chemother, 66, 111-125.

Ingraham, HA, Dickey, L & Goulian, M. (1986). DNA fragmentation and cytotoxicity from increased cellular deoxyuridylate. Biochemistry, 25, 3225-3230.

Ivanetich, KM & Santi, DV. (1990). Bifunctional thymidylate synthase-dihydrofolate reductase in protozoa. The FASEB Journal, 4, 1591-1597.

Ivens, AC, Peacock, CS, Worthey, EA, Murphy, L, Aggarwal, G, Berriman, M, *et al.,* (2005). The Genome of the Kinetoplastid Parasite, *Leishmania major.* Science, 309, 436-442.

Jaffe, JJ. (1961). The effect of 6-Azauracil upon *Trypanosoma equiperdum.* Biochemical Pharmacology, 8, 216-223.

Jannin, J & Cattand, P. (2004). Treatment and control of human African trypanosomiasis. Current Opinion in Infectious Diseases, 17.

Jean-Moreno, V, Rojas, R, Goyeneche, D, Coombs, GH & Walker, J. (2006). *Leishmania donovani*: Differential activities of classical topoisomerase inhibitors and antileishmanials against parasite and host cells at the level of DNA topoisomerase I and in cytotoxicity assays. Experimental Parasitology, 112, 21-30.

Jeganathan, S, Sanderson, L, Dogruel, M, Rodgers, J, Croft, S & Thomas, SA. (2011). The distribution of nifurtimox across the healthy and trypanosome-infected murine blood-brain and blood-berebrospinal fluid barriers. Journal of Pharmacology and Experimental Therapeutics, 336, 506-515.

Jennings, FW. (1991). Chemotherapy of CNS-trypanosomiasis: the combined use of the arsenicals and nitro-compounds. Trop Med Parasitol, 42, 139-142.

Jennings, FW. (1995). Suramin treatment of experimental *Trypanosoma brucei* infection of the central nervous system. p. 677.

Jha, SN, Singh, NK & Jha, TK. (1991). Changing response to diamidine compounds in cases of kala-azar unresponsive to antimonial. J Assoc Physicians India, 39, 314-316.

Jhingran, A, Chatterjee, M & Madhubala, R. (2008). Leishmaniasis: Epidemiological Trends. *Leishmania* After the Genome . ed. Myler,P. & Fasel,N. pp. 01-14. Caister Academic Press.

Jhingran, A, Chawla, B, Saxena, S, Barrett, MP & Madhubala, R. (2009). Paromomycin: uptake and resistance in *Leishmania donovani.* Mol Biochem Parasitol, 164, 111-117.

Jones, ME. (1980). Pyrimidine nucleotide biosynthesis in animals: genes, enzymes, and regulation of UMP biosynthesis. Annu Rev Biochem, 49, 253-279.

Jordan, AM. (1993). Tsetse-flies (Glossinidae). In Medical insects and arachnids. ed. Lane,R.P. & Crosskey,R.W. pp. 333-388. Chapman and Hall: London.

Joshi, PP, Shegokar, VR, Powar, RM, Herder, S, Katti, R, Salkar, HR, Dani, VS, Bhargava, A, Jannin, J & Truc, P. (2005). Human trypanosomiasis caused by *Trypanosoma evansi* in India: the first case report. Am J Trop Med Hyg, 73, 491-495.

Kaczanowski, S, Sajid, M & Reece, S. (2011). Evolution of apoptosis-like programmed cell death in unicellular protozoan parasites. Parasites & Vectors, 4, 44.

Kalu, AU. (1995). Prevalence of trypanosomiasis among Trypanotolerant cattle at the lower Benue River area of Nigeria. Preventive Veterinary Medicine, 24, 97-103.

Kamhawi, S. (2006). Phlebotomine sand flies and *Leishmania* parasites: friends or foes? Trends in Parasitology, 22, 439-445.

Katakura, K, Fujise, H, Takeda, K, Kaneko, O, Torii, M, Suzuki, M, Chang, KP & Hashiguchi, Y. (2004). Overexpression of LaMDR2, a novel multidrug resistance ATP-binding cassette transporter, causes 5-fluorouracil resistance in Leishmania amazonensis. FEBS Letters, 561, 207-212.

Kaur, K, Coons, T, Emmett, K & Ullman, B. (1988). Methotrexate-resistant *Leishmania donovani* genetically deficient in the folate-methotrexate transporter. Journal of Biological Chemistry, 263, 7020-7028.

Kaye, SB. (1994). Gemcitabine: current status of phase I and II trials. Journal of Clinical Oncology, 12, 1527-1531.

Khabnadideh, S, Pez, D, Musso, A, Brun, R, Perez, LMR, Gonzalez-Pacanowska, D & Gilbert, IH. (2005). Design, synthesis and evaluation of 2,4-diaminoquinazolines as inhibitors of trypanosomal and leishmanial dihydrofolate reductase. Bioorganic & Medicinal Chemistry, 13, 2637-2649.

Kidder, GW. (1984). Characteristics of cytidine aminohydrolase activity in *Trypanosoma cruzi* and *Crithidia fasciculata*. J Protozool, 31, 298-300.

Kim, P, EricM, F, Martin, O, Mark, C, Mark, CE, Ian, M & Susan, CW. (2005). Sleeping sickness in Uganda: a thin line between two fatal diseases. BMJ, 331.

Koenigk, E. (1976). Comparative aspects of nucleotide biosynthesis in parasitic protozoa.In Biochemistery of Parasites and Host-Parasite Rlationships. ed. Van den Bossche,H. pp. 51-58. North Holand, Amsterdam.

Kramer, R. (1994). Secretion of amino acids by bacteria: Physiology and mechanism. FEMS Microbiology Reviews, 13, 75-93.

Kristjanson, PM, Swallow, BM, Rowlands, GJ, Kruska, RL & de Leeuw, PN. (1999). Measuring the costs of African animal trypanosomosis, the potential benefits of control and returns to research. Agricultural Systems, 59, 79-98.

Lachaud, L, Bourgeois, N, Plourde, M, Leprohon, P, Bastien, P & Ouellette, M. (2009). Parasite susceptibility to amphotericin B in failures of treatment for visceral leishmaniasis in patients coinfected with HIV type 1 and *Leishmania infantum*. Clinical Infectious Diseases, 48, e16-e22.

Laguna, F. (2003). Treatment of leishmaniasis in HIV-positive patients. Ann Trop Med Parasitol, 97 Suppl 1, 135-142.

Lainson, R & Shaw, JJ. (1987). Evolution, classification and geographical distribution. In The Leishmaniases in Biology and Medicine. ed. Peters,W. & Killick-Kendrick,R. pp. 1-120. Academic Press: London.

Landfear, SM, Ullman, B, Carter, NS & Sanchez, MA. (2004). Nucleoside and Nucleobase transporters in parasitic protozoa. Eukaryotic Cell, 3, 245-254.

Lane, R. (1993). Sandflies (Phlebotominae). In Medical Insects and Arachnids. ed. Lane,R.P. & Crosskey,R.W. pp. 78-119. Chapman and Hall: London.

Langmead, B, Trapnell, C, Pop, M & Salzberg, S. (2009). Ultrafast and memory-efficient alignment of short DNA sequences to the human genome. Genome Biology, 10, R25.

Lanham, SM. (1968). Separation of trypanosomes from the blood of infected rats and mice by anion-exchangers. Nature, 218, 1273-1274.

Larson, ET, Mudeppa, DG, Gillespie, JR, Mueller, N, Napuli, AJ, Arif, *et al.,* (2010). the crystal structure and activity of a putative trypanosomal nucleoside phosphorylase reveal it to be a homodimeric uridine phosphorylase. Journal of Molecular Biology, 396, 1244-1259.

Lee, G, Dallas, S, Hong, M & Bendayan, R. (2001). Drug transporters in the central nervous system: brain barriers and brain parenchyma considerations. Pharmacological Reviews, 53, 569-596.

Legros, D, Evans, S, Maiso, F, Enyaru, JCK & Mbulamberi, D. (1999). Risk factors for treatment failure after melarsoprol for *Trypanosoma brucei gambiense* trypanosomiasis in Uganda. Transactions of the Royal Society of Tropical Medicine and Hygiene, 93, 439-442.

Legros, D, Ollivier, Gl, Gastellu-Etchegorry, M, Paquet, C, Burri, C, Jannin, J & Buscher, P. (2002). Treatment of human African trypanosomiasis-present situation and needs for research and development. The Lancet Infectious Diseases, 2, 437-440.

Lejon, V, Kwete, J & Buscher, P. (2003). Short communication: Towards saliva-based screening for sleeping sickness? Tropical Medicine & International Health, 8, 585-588.

Lescat, M, Calteau, A, Hoede, C, Barbe, V, Touchon, M, Rocha, E, Tenaillon, O, Medigue, C, Johnson, JR & Denamur, E. (2009). A module located at a chromosomal integration hot spot is responsible for the multidrug resistance of a reference strain from *Escherichia coli* clonal group A. Antimicrob Agents Chemother, 53, 2283-2288.

Levine, RL, Hoogenraad, NJ & Kretchmer, N. (1974). A Review: Biological and clinical aspects of pyrimidine metabolism. Pediatr Res, 8, 724-734.

Ley, TJ, Mardis, ER, Ding, L, Fulton, B, McLellan, MD, Chen, *et al.,* (2008). DNA sequencing of a cytogenetically normal acute myeloid leukaemia genome. Nature, 456, 66-72.

Li, H, Handsaker, B, Wysoker, A, Fennell, T, Ruan, J, Homer, N, Marth, G, Abecasis, G, Durbin, R & Genome Project Data Processing Subgroup. (2009). The

sequence alignment/map format and SAMtools. Bioinformatics, 25, 2078-2079.

Li, H, Ruan, J & Durbin, R. (2008). Mapping short DNA sequencing reads and calling variants using mapping quality scores. Genome Res, 18, 1851-1858.

Li, J, Huang, S, Chen, J, Yang, Z, Fei, X, Zheng, M, Ji, C, Xie, Y & Mao, Y. (2007). Identification and characterization of human uracil phosphoribosyltransferase (UPRTase). J Hum Genet, 52, 415-422.

Lillico, S, Field, MC, Blundell, P, Coombs, GH & Mottram, JC. (2003). Essential roles for GPI-anchored proteins in African trypanosomes revealed using mutants deficient in GPI8. Molecular Biology of the Cell, 14, 1182-1194.

Lindner, AK & Priotto, G. (2010). The unknown risk of vertical Transmission in sleeping sickness - Literature Review. PLoS Negl Trop Dis, 4, e783.

Lineweaver, H & Burk, D. (1934). The Determination of enzyme dissociation constants. J Am Chem Soc, 56, 658-666.

Liu, S, Neidhardt, EA, Grossman, TH, Ocain, T & Clardy, J. (2000). Structures of human dihydroorotate dehydrogenase in complex with antiproliferative agents. Structure, 8, 25-33.

Lolli, ML, Giorgis, M, Tosco, P, Foti, A, Fruttero, R & Gasco, A. (2012). New inhibitors of dihydroorotate dehydrogenase (DHODH) based on the 4-hydroxy-1,2,5-oxadiazol-3-yl (hydroxyfurazanyl) scaffold. European Journal of Medicinal Chemistry, 49, 102-109.

Longley, DB, Harkin, DP & Johnston, PG. (2003). 5-Fluorouracil: mechanisms of action and clinical strategies. Nat Rev Cancer, 3, 330-338.

Looker, DL, Berens, RL & Marr, JJ. (1983). Purine metabolism in *Leishmania donovani* amastigotes and promastigotes. Mol Biochem Parasitol, 9, 15-28.

Lorenz, P, Owen, JS & Hassall, DG. (1995). Human serum resistant *Trypanosoma brucei rhodesiense* accumulates similar amounts of fluorescently-labelled trypanolytic human HDL3 particles as human serum sensitive *T.b. brucei*. Molecular and Biochemical Parasitology, 74, 113-118.

Lugli, EB, Pouliot, M, Portela, MdPM, Loomis, MR & Raper, J. (2004). Characterization of primate trypanosome lytic factors. Molecular and Biochemical Parasitology, 138, 9-20.

Lumsden, WH, Kimber, CD, Evans, DA & Doig, SJ. (1979). *Trypanosoma brucei*: Miniature anion-exchange centrifugation technique for detection of low parasitaemias: Adaptation for field use. Transactions of the Royal Society of Tropical Medicine and Hygiene, 73, 312-317.

Luscher, A, Onal, P, Schweingruber, A & Maser, P. (2007). Adenosine kinase of *Trypanosoma brucei* and its role in susceptibility to adenosine antimetabolites. Antimicrob Agents Chemother.

Lux, H, Heise, N, Klenner, T, Hart, D & Opperdoes, FR. (2000). Ether-lipid (alkyl-phospholipid) metabolism and the mechanism of action of ether-lipid analogues in *Leishmania*. Molecular and Biochemical Parasitology, 111, 1-14.

Lynen, L & Van Damme, W. (1992). Local application of diminazene aceturate: an effective treatment for cutaneous leishmaniasis? Ann Soc Belg Med Trop, 72, 13-19.

Maarouf, M, de Kouchkovsky, Y, Brown, S, Petit, PX & Robert-Gero, M. (1997a). *In vivo* interference of paromomycin with mitochondrial activity of *Leishmania*. Experimental Cell Research, 232, 339-348.

Maarouf, M, Lawrence, F, Brown, S & Robert-Gero, M. (1997b). Biochemical alterations in paromomycin-treated *Leishmania donovani*; promastigotes. Parasitology Research, 83, 198-202.

Maarouf, M, Lawrence, F, Croft, SL & Robert-Gero, M. (1995). Ribosomes of *Leishmania* are a target for the aminoglycosides. Parasitology Research, 81, 421-425.

Major, PP, Egan, EM, Beardsley, GP, Minden, MD & Kufe, DW. (1981). Lethality of human myeloblasts correlates with the incorporation of arabinofuranosylcytosine into DNA. Proceedings of the National Academy of Sciences, 78, 3235-3239.

Major, PP, Egan, EM, Herrick, DJ & Kufe, DW. (1982). Effect of ara-C incorporation on deoxyribonucleic acid synthesis in cells. Biochemical Pharmacology, 31, 2937-2940.

Maltezou, HC. (2010). Drug resistance in visceral leishmaniasis. J Biomed Biotechnol, 2010, 617521.

Malvy, D & Chappuis, F. (2011). Sleeping sickness. Clinical Microbiology and Infection, 17, 986-995.

Mandell, GL, Bennett, JE & Dolin, R. (2005). Mandell, Douglas and Bennett's principles and practice of infectious diseases. Elsevier Churchill Livingstone: Philadelphia.

Markell, E, John, D & Krotoski, W. (1999). Markell and Voge's Medical Parasitology.

Marsden, PD. (1975). Mucocutaneous leishmanisis-a review of clinical aspects. Rev Soc Bras Med Trop, 9, 309-326.

Martin, KL & Smith, TK. (2006). Phosphatidylinositol synthesis is essential in bloodstream form *Trypanosoma brucei*. Biochem J, 396, 287-295.

Martinelli, A, Henriques, G, Cravo, P & Hunt, P. (2011). Whole genome re-sequencing identifies a mutation in an ABC transporter (mdr2) in a *Plasmodium chabaudi* clone with altered susceptibility to antifolate drugs. International Journal for Parasitology, 41, 165-171.

Maser, P, Sutterlin, C, Kralli, A & Kaminsky, R. (1999). A nucleoside transporter from *Trypanosoma brucei* involved in drug resistance. Science, 285, 242-244.

Matlashewski, G. (2001). *Leishmania* infection and virulence. Medical Microbiology and Immunology, 190, 37-42.

Matovu, E, Enyaru, JCK, Legros, D, Schmid, C, Seebeck, T & Kaminsky, R. (2001). Melarsoprol refractory *T. b. gambiense* from Omugo, north-western Uganda. Tropical Medicine & International Health, 6, 407-411.

Matovu, E, Stewart, ML, Geiser, F, Brun, R, Maser, P, Wallace, LJ, Burchmore, RJ, Enyaru, JC, Barrett, MP, Kaminsky, R, Seebeck, T & De Koning, HP. (2003). Mechanisms of arsenical and diamidine uptake and resistance in *Trypanosoma brucei*. Eukaryot Cell, 2, 1003-1008.

Matthews, KR, Ellis, JR & Paterou, A. (2004). Molecular regulation of the life cycle of African trypanosomes. Trends in Parasitology, 20, 40-47.

Matthews, KR. (1999). Developments in the differentiation of *Trypanosoma brucei*. Parasitology Today, 15, 76-80.

Matthews, KR. (2005). The developmental cell biology of *Trypanosoma brucei*. Journal of Cell Science, 118, 283-290.

Mavrova, AT, Vuchev, D, Anichina, K & Vassilev, N. (2010). Synthesis, antitrichinnellosis and antiprotozoal activity of some novel thieno[2,3-d]pyrimidin-4(3H)-ones containing benzimidazole ring. European Journal of Medicinal Chemistry, 45, 5856-5861.

Maya, JD, Cassels, BK, Iturriaga-Vasquez, P, Ferreira, J, Faundez, M, Galanti, N, Ferreira, A & Morello, A. (2007). Mode of action of natural and synthetic drugs against *Trypanosoma cruzi* and their interaction with the mammalian host. Comparative Biochemistry and Physiology - Part A: Molecular & Integrative Physiology, 146, 601-620.

Mbongo, N, Loiseau, PM, Billion, MA & Robert-Gero, M. (1998). Mechanism of amphotericin B aesistance in *Leishmania donovani* promastigotes. Antimicrob Agents Chemother, 42, 352-357.

McCann, KA, Williams, DW & McKee, EE. (2012). Metabolism of deoxypyrimidines and deoxypyrimidine antiviral analogs in isolated brain mitochondria. Journal of Neurochemistry, 122, 126-137.

McCulloch, R. (2004). Antigenic variation in African trypanosomes: monitoring progress. Trends in Parasitology, 20, 117-121.

McLean, JE, Neidhardt, EA, Grossman, TH & Hedstrom, L. (2001). Multiple inhibitor analysis of the brequinar and leflunomide binding sites on human dihydroorotate dehydrogenase. Biochemistry, 40, 2194-2200.

Mehlert, A, Wormald, MR & Ferguson, MA. (2012). Modeling of the N-glycosylated transferrin receptor suggests how transferrin binding can occur within the surface coat of *Trypanosoma brucei*. PLoS Pathog, 8, e1002618.

Mehta, A & Shaha, C. (2004). Apoptotic death in *Leishmania donovani* promastigotes in response to respiratory chain inhibition. Journal of Biological Chemistry, 279, 11798-11813.

Melaku, Y, Collin, SM, Keus, K, Gatluak, F, Ritmeijer, K & Davidson, RN. (2007). Treatment of Kala-Azar in Southern Sudan using a 17-day regimen of sodium stibogluconate combined with paromomycin: A retrospective comparison with

30-day sodium stibogluconate monotherapy. The American Journal of Tropical Medicine and Hygiene, 77, 89-94.

Mercer, L, Bowling, T, Perales, J, Freeman, J, Nguyen, T, Bacchi, C, Yarlett, N, Don, R, Jacobs, R & Nare, B. (2011). 2,4-Diaminopyrimidines as potent inhibitors of *Trypanosoma brucei* and identification of molecular targets by a chemical proteomics approach. PLoS Negl Trop Dis, 5, e956.

Meyer, LM, Miller, FR, Rowen, MJ, Bock, G & Rutzky, J. (1950). Treatment of acute leukemia with amethopterin (4-amino, 10-methyl pteroyl glutamic acid). Acta Haematologica, 4, 157-167.

Mikus, J & Steverding, D. (2000). A simple colorimetric method to screen drug cytotoxicity against *Leishmania* using the dye Alamar Blue. Parasitol Int, 48, 265-269.

Ministério, dS & Saúde, S. (2005). Brazilian Consensus on Chagas disease. Rev Soc Bras Med Tropy, 38, 7-29.

Minodier, P & Parola, P. (2007). Cutaneous leishmaniasis treatment. Travel Med Infect Dis, 5, 150-158.

Mitchell, P. (1949). The osmotic barrier in bacteria. In The nature of the bacterial surface. ed. Miles,A.A. & Pine,N.W. pp. 55-75. Blackwell: Oxford, UK.

Molyneux, D. (2007). Control of Human Parasitic Diseases. Elseiver Books: Oxford.

Momeni, AZ, Reiszadae, MR & Aminjavaheri, M. (2002). Treatment of cutaneous leishmaniasis with a combination of allopurinol and low-dose meglumine antimoniate. International Journal of Dermatology, 41, 441-443.

Moore, A & Richer, M. (2001). Re-emergence of epidemic sleeping sickness in southern Sudan. Tropical Medicine & International Health, 6, 342-347.

Moreno, T, Pous, J, Subirana, JA & Campos, JL. (2010). Coiled-coil conformation of a pentamidine-DNA complex. Acta Crystallogr D Biol Crystallogr, 66, 251-257.

Moroz, OV, Murzin, AG, Makarova, KS, Koonin, EV, Wilson, KS & Galperin, MY. (2005). Dimeric dUTPases, HisE, and MazG belong to a new superfamily of all-alpha NTP pyrophosphohydrolases with potential "house-cleaning" functions. J Mol Biol, 347, 243-255.

Mottram, JC, Coombs, GH & Alexander, J. (2004). Cysteine peptidases as virulence factors of *Leishmania*. Current Opinion in Microbiology, 7, 375-381.

Mukherjee, A, Padmanabhan, PK, Sahani, MH, Barrett, MP & Madhubala, R. (2006). Roles for mitochondria in pentamidine susceptibility and resistance in *Leishmania donovani*. Mol Biochem Parasitol, 145, 1-10.

Mukherjee, T, Roy, K & Bhaduri, A. (1990). Acivicin: A highly active potential chemotherapeutic agent against visceral Leishmaniasis. Biochemical and Biophysical Research Communications, 170, 426-432.

Murray, HW, Berman, JD, Davies, CR & Saravia, NG. (2005). Advances in leishmaniasis. Lancet, 366, 1561-1577.

Murta, SMF, Gazzinelli, RT, Brener, Z & Romanha, AJ. (1998). Molecular characterization of susceptible and naturally resistant strains of *Trypanosoma cruzi* to benznidazole and nifurtimox. Molecular and Biochemical Parasitology, 93, 203-214.

Mutomba, MC, To, WY, Hyun, WC & Wang, CC. (1997). Inhibition of proteasome activity blocks cell cycle progression at specific phase boundaries in African trypanosomes. Mol Biochem Parasitol, 90, 491-504.

Mutugi, MW, Boid, R & Luckins, AG. (1994). Experimental induction of suramin-resistance in cloned and uncloned stocks of *Trypanosoma evansi* using immune-suppressed and immune-competent mice. Trop Med Parasitol, 45, 232-236.

Mwangi, MM, Wu, SW, Zhou, Y, Sieradzki, K, de, LH, Richardson, P, Bruce, D, Rubin, E, Myers, E, Siggia, ED & Tomasz, A. (2007). Tracking the *in vivo* evolution of multidrug resistance in *Staphylococcus aureus* by whole-genome sequencing. Proc Natl Acad Sci U S A, 104, 9451-9456.

Nakajima-Shimada, J, Hirota, Y & Aoki, T. (1996). Inhibition of *Trypanosoma cruzi* growth in mammalian cells by purine and pyrimidine analogs. Antimicrob Agents Chemother, 40, 2455-2458.

Nara, T, Kamei, Y, Tsubouchi, A, Annoura, T, Hirota, K, Iizumi, K, Dohmoto, Y, Ono, T & Aoki, T. (2005). Inhibitory action of marine algae extracts on the *Trypanosoma cruzi* dihydroorotate dehydrogenase activity and on the protozoan growth in mammalian cells. Parasitology International, 54, 59-64.

Navin, TR, Arana, BA, Arana, FE, Berman, JD & Chajon, JF. (1992). Placebo-controlled clinical trial of sodium stibogluconate (pentostam) versus ketoconazole for treating cutaneous leishmaniasis in Guatemala. Journal of Infectious Diseases, 165, 528-534.

Nikolskaia, OV, de, AL, Kim, YV, Lonsdale-Eccles, JD, Fukuma, T, Scharfstein, J & Grab, DJ. (2006). Blood-brain barrier traversal by African trypanosomes requires calcium signaling induced by parasite cysteine protease. J Clin Invest, 116, 2739-2747.

Nyeko, JHP, Ole-Moiyoi, OK, Majiwa, PAO, Otieno, LH & Ociba, PM. (1990). Characterization of trypanosome isolates from cattle in Uganda using species-specific DNA probes reveals predominance of mixed infections. International Journal of Tropical Insect Science, 11, 271-280.

Olliaro, P, Lazdins, J & Guhl, F. (2002). Developments in the treatment of leishmaniasis and trypanosomiasis. Expert Opin Emerg Drugs, 7, 61-67.

Ortiz, D, Sanchez, MA, Koch, HP, Larsson, HP & Landfear, SM. (2009b). An acid-activated nucleobase transporter from *Leishmania major*. Journal of Biological Chemistry, 284, 16164-16169.

Ortiz, D, Sanchez, MA, Pierce, S, Herrmann, T, Kimblin, N, Archie Bouwer, HG & Landfear, SM. (2007). Molecular genetic analysis of purine nucleobase transport in *Leishmania major*. Molecular Microbiology, 64, 1228-1243.

Ortiz, D, Sanchez, MA, Quecke, P & Landfear, SM. (2009a). Two novel nucleobase/pentamidine transporters from *Trypanosoma brucei*. Molecular and Biochemical Parasitology, 163, 67-76.

Overath, P, Czichos, J & Haas, C. (1986). The effect of citrate/cis-aconitate on oxidative metabolism during transformation of *Trypanosoma brucei*. European Journal of Biochemistry, 160, 175-182.

Padron-Nieves, M, Diaz, E, Machuca, C, Romero, A & Sucre, AP. (2009). Glibenclamide modulates glucantime activity and disposition in *Leishmania major*. Experimental Parasitology, 121, 331-337.

Paila, YD, Saha, B & Chattopadhyay, A. (2010). Amphotericin B inhibits entry of *Leishmania donovani* into primary macrophages. Biochemical and Biophysical Research Communications, 399, 429-433.

Pal, A, Hall, BS & Field, MC. (2002). Evidence for a non-LDL-mediated entry route for the trypanocidal drug suramin in *Trypanosoma brucei*. Molecular and Biochemical Parasitology, 122, 217-221.

Pandey, BD, Pandey, K, Kaneko, O, Yanagi, T & Hirayama, K. (2009). Short report: Relapse of visceral leishmaniasis after miltefosine treatment in a nepalese patient. American Journal of Tropical Medicine and Hygiene, 80, 580-582.

Papageorgiou, IG, Yakob, L, Al Salabi, MI, Diallinas, G, Soteriadou, KP & De Koning, HP. (2005). Identification of the first pyrimidine nucleobase transporter in *Leishmania*: similarities with the *Trypanosoma brucei* U1 transporter and antileishmanial activity of uracil analogues. Parasitology, 130, 275-283.

Paulsen, IT, Brown, MH & Skurray, RA. (1996a). Proton-dependent multidrug efflux systems. Microbiological Reviews, 60, 575-608.

Paulsen, IT, Brown, MH, Littlejohn, TG, Mitchell, BA & Skurray, RA. (1996b). Multidrug resistance proteins QacA and QacB from *Staphylococcus aureus*: membrane topology and identification of residues involved in substrate specificity. Proceedings of the National Academy of Sciences, 93, 3630-3635.

Pays, E, Vanhamme, L & Perez-Morga, D. (2004). Antigenic variation in *Trypanosoma brucei*: facts, challenges and mysteries. Current Opinion in Microbiology, 7, 369-374.

Pepin, J, Milord, F, Mpia, B, Meurice, F, Ethier, L, DeGroof, D & Bruneel, H. (1989). An open clinical trial of nifurtimox for arseno-resistant *Trypanosoma brucei gambiense* sleeping sickness in central Zaire. Transactions of the Royal Society of Tropical Medicine and Hygiene, 83, 514-517.

Perez-Morga, D, Vanhollebeke, B, Paturiaux-Hanocq, F, Nolan, DP, Lins, *et al.*, (2005). Apolipoprotein L-I promotes trypanosome lysis by forming pores in lysosomal membranes. Science, 309, 469-472.

Perez-Victoria, FJ, Sanchez-Canete, MaP, Seifert, K, Croft, SL, Sundar, S, Castanys, S & Gamarro, F. (2006). Mechanisms of experimental resistance of *Leishmania* to miltefosine: Implications for clinical use. Drug Resistance Updates, 9, 26-39.

Peters GJ & Jansen G (1996). Resistance to antimetabolites. In: Schilsky RL, Milano GA & Ratain MJ (Editors), Principles of Antineoplastic Drug Development and Pharmacology. Marcel Dekker, Inc., New York.

Pez, D, Leal, I, Zuccotto, F, Boussard, C, Brun, R, Croft, SL, Yardley, V, Ruiz Perez, LM, Gonzalez Pacanowska, D & Gilbert, IH. (2003). 2,4-Diaminopyrimidines as inhibitors of leishmanial and trypanosomal dihydrofolate reductase. Bioorganic & Medicinal Chemistry, 11, 4693-4711.

Phillips, MA, Coffino, P & Wang, CC. (1988). *Trypanosoma brucei* ornithine decarboxylase: enzyme purification, characterization, and expression in *Escherichia coli*. J Biol Chem, 263, 17933-17941.

Phillips, MA, Gujjar, R, Malmquist, NA, White, J, El, MF, Baldwin, J & Rathod, PK. (2008). Triazolopyrimidine-based dihydroorotate dehydrogenase inhibitors with potent and selective activity against the malaria parasite *Plasmodium falciparum*. J Med Chem, 51, 3649-3653.

Piscopo, TV & Mallia, AC. (2006). Leishmaniasis. Postgraduate Medical Journal, 82, 649-657.

Priotto, G, Fogg, C, Balasegaram, M, Erphas, O, Louga, A, Checchi, F, Ghabri, S & Piola, P. (2006). Three Drug Combinations for late-Stage *Trypanosoma brucei gambiense* sleeping sickness: A randomized clinical trial in Uganda. PLOS Clin Trial, 1, e39.

Rassi, A, Jr., Rassi, A & Marin-Neto, JA. (2010). Chagas' disease. Lancet, 375, 1388-1402.

Rathod, PK, Khatri, A, Hubbert, T & Milhous, WK. (1989). Selective activity of 5-fluoroorotic acid against *Plasmodium falciparum in vitro*. Antimicrob Agents Chemother, 33, 1090-1094.

Raymond, Fdr, Boisvert, S, Roy, Gt, Ritt, JF, Legare, D, Isnard, A, Stanke, M, Olivier, M, Tremblay, MJ, Papadopoulou, B, Ouellette, M & Corbeil, J. (2012). Genome sequencing of the lizard parasite *Leishmania tarentolae* reveals loss of genes associated to the intracellular stage of human pathogenic species. Nucleic Acids Research, 40, 1131-1147.

Raz, B, Iten, M, Grether-Buhler, Y, Kaminsky, R & Brun, R. (1997). The Alamar Blue assay to determine drug sensitivity of African trypanosomes (*T.b. rhodesiense* and *T.b. gambiense*) *in vitro*. Acta Trop, 68, 139-147.

Reid, RS, Kruska, RL, Wilson, GJ & Perry, BD. (1995). The impacts of controlling the tsetse fly on land use and the environment. In Spatial and Temporal Dynamics of African Farming Systems. ed. Lynam,J.S., Carter,S. & Reid,R.S. Maputo.

Rifkin, MR. (1978). Identification of the trypanocidal factor in normal human serum: high density lipoprotein. Proceedings of the National Academy of Sciences, 75, 3450-3454.

Rifkin, MR. (1991). Role of phospholipids in the cytotoxic action of high density lipoprotein on trypanosomes. Journal of Lipid Research, 32, 639-647.

Rittig, MG & Bogdan, C. (2000). Leishmania-cell interaction: Complexities and alternative views. Parasitology Today, 16, 292-297.

Rittig, MG, Burmester, GR & Krause, A. (1998). Coiling phagocytosis: when the zipper jams, the cup is deformed. Trends in Microbiology, 6, 384-388.

Roditi, I & Liniger, M. (2002). Dressed for success: the surface coats of insect-borne protozoan parasites. Trends in Microbiology, 10, 128-134.

Rogers, DJ & Randolph, SE. (1986). Distribution and abundance of tsetse flies (*Glossina* spp.). Journal of Animal Ecology, 55, 1007-1025.

Rogers, M, Chance, M & Bates, P. (2002). The role of promastigote secretory gel in the origin and transmission of the infective stage of *Leishmania mexicana* by the sandfly *Lutzomyia longipalpis*. Parasitology, 124, 495-507.

Rogers, MB, Hilley, JD, Dickens, NJ, Wilkes, J, Bates, PA, Depledge, *et al.*, (2011). Chromosome and gene copy number variation allow major structural change between species and strains of *Leishmania*. Genome Research, 21, 2129-2142.

Rojas, R, Valderrama, L, Valderrama, M, Varona, MX, Ouellette, M & Saravia, NG. (2006). Resistance to antimony and treatment failure in human *Leishmania* (*Viannia*) infection. Journal of Infectious Diseases, 193, 1375-1383.

Roobol, C, De Dobbeleer, GB & Bernheim, JL. (1984). 5-fluorouracil and 5-fluoro-2'-deoxyuridine follow different metabolic pathways in the induction of cell lethality in L1210 leukaemia. Br J Cancer, 49, 739-744.

Rosowsky, A, Papoulis, AT & Queener, SF. (1997). 2,4-Diaminothieno[2,3-d]pyrimidine lipophilic antifolates as inhibitors of pneumocystis carinii and *Toxoplasma gondii* dihydrofolate reductase. J Med Chem, 40, 3694-3699.

Ruiz van Haperen, VWT, Veerman, G, Vermorken, JB & Peters, GJ. (1993). 2',2'-Difluoro-deoxycytidine (gemcitabine) incorporation into RNA and DNA of tumour cell lines. Biochemical Pharmacology, 46, 762-766.

Saier, J. (2000b). Families of transmembrane transporters selective for amino acids and their derivatives. Microbiology, 146, 1775-1795.

Saier, MH. (2000a). A functional-phylogenetic classification system for transmembrane solute transporters. Microbiology and Molecular Biology Reviews, 64, 354-411.

Sanchez, MA, Drutman, S, van Ampting, M, Matthews, K, Landfear, SM, Sanchez, MA, Drutman, S, van Ampting, M, Matthews, K & Landfear, SM. (2004). A novel purine nucleoside transporter whose expression is up-regulated in the short stumpy form of the *Trypanosoma brucei* life cycle. Molecular and Biochemical Parasitology, 136, 265-272.

Sanchez, MA, Tryon, R, Green, J, Boor, I & Landfear, SM. (2002). Six related nucleoside/nucleobase transporters from *Trypanosoma brucei* exhibit distinct biochemical functions. Journal of Biological Chemistry, 277, 21499-21504.

Sanchez, MA, Ullman, B, Landfear, SM & Carter, NS. (1999). Cloning and functional expression of a gene encoding a P1 type nucleoside transporter from *Trypanosoma brucei*. Journal of Biological Chemistry, 274, 30244-30249.

Santi, DV & McHenry, CS. (1972). 5-Fluoro-2'-deoxyuridylate: covalent complex with thymidylate synthetase. Proc Natl Acad Sci U S A, 69, 1855-1857.

Saunders, EC, DE Souza, DP, Naderer, Thom, Sernee, MF, Ralton, JE, Doyle, MA, Macrae, JI, Chambers, JL, Heng, Joan, Nahid, Amsh, Likic, VA & Mcconville, MJ. (2010). Central carbon metabolism of Leishmania parasites. Parasitology, 137, 1303-1313.

Scahill, MD, Pastar, I & Cross, GA. (2008). CRE recombinase-based positive-negative selection systems for genetic manipulation in *Trypanosoma brucei*. Mol Biochem Parasitol, 157, 73-82.

Scheltema, RA, Jankevics, A, Jansen, RC, Swertz, MA & Breitling, R. (2011). PeakML/mzMatch: A File Format, Java Library, R Library, and Tool-Chain for Mass Spectrometry Data Analysis. Anal Chem, 83, 2786-2793.

Schlein, Y, Jacobson, RL & Shlomai, J. (1991). Chitinase secreted by *Leishmania* functions in the sandfly vector. Proceedings of the Royal Society of London Series B: Biological Sciences, 245, 121-126.

Schlosser, M & Michel, D. (1996). About the "physiological size" of fluorine substituents: Comparison of sensorially active compounds with fluorine and methyl substituted analogues. Tetrahedron, 52, 99-108.

Schonian, G, Nasereddin, A, Dinse, N, Schweynoch, C, Schallig, HD, Presber, W & Jaffe, CL. (2003). PCR diagnosis and characterization of *Leishmania* in local and imported clinical samples. Diagn Microbiol Infect Dis, 47, 349-358.

Schonian, G, Schnur, L, el, FM, Oskam, L, Kolesnikov, AA, Sokolowska-Kohler, W & Presber, W. (2001). Genetic heterogeneity in the species *Leishmania* tropica revealed by different PCR-based methods. Trans R Soc Trop Med Hyg, 95, 217-224.

Schumann Burkard, G, Jutzi, P & Roditi, I. (2011). Genome-wide RNAi screens in bloodstream form trypanosomes identify drug transporters. Molecular and Biochemical Parasitology, 175, 91-94.

Scott, AG, Tait, A & Turner, CM. (1997). *Trypanosoma brucei*: Lack of cross-resistance to melarsoprolin vitroby cymelarsan-resistant parasites. Experimental Parasitology, 86, 181-190.

Scott, DA, Coombs, GH & Sanderson, BE. (1987). Folate utilisation by *Leishmania* species and the identification of intracellular derivatives and folate-metabolising enzymes. Molecular and Biochemical Parasitology, 23, 139-149.

Seifert, K, Perez-Victoria, FJ, Stettler, M, Sanchez-Canete, MaP, Castanys, S, Gamarro, F & Croft, SL. (2007). Inactivation of the miltefosine transporter, LdMT, causes miltefosine resistance that is conferred to the amastigote stage of *Leishmania donovani* and persists in vivo. International Journal of Antimicrobial Agents, 30, 229-235.

Senkovich, O, Bhatia, V, Garg, N & Chattopadhyay, D. (2005). Lipophilic antifolate trimetrexate is a potent inhibitor of *Trypanosoma cruzi*: prospect for chemotherapy of Chagas' disease. Antimicrob Agents Chemother, 49, 3234-3238.

Service, M. (1996). Medical Entomology. Chapman and Hall: London.

Seymour, KK, Lyons, SD, Phillips, L, Rieckmann, KH & Christopherson, RI. (1994). Cytotoxic effects of inhibitors of de novo pyrimidine biosynthesis upon *Plasmodium falciparum*. Biochemistry, 33, 5268-5274.

Shaked-Mishan, P, Ulrich, N, Ephros, M & Zilberstein, D. (2001). Novel Intracellular SbV reducing activity correlates with antimony susceptibility in *Leishmania donovani*. Journal of Biological Chemistry, 276, 3971-3976.

Shi, W, Schramm, VL & Almo, SC. (1999). Nucleoside hydrolase from *Leishmania major*. Journal of Biological Chemistry, 274, 21114-21120.

Shreffler, WG, Burns, JM, Jr., Badaro, R, Ghalib, HW, Button, LL, McMaster, WR & Reed, SG. (1993). Antibody responses of visceral leishmaniasis patients to gp63, a major surface glycoprotein of *Leishmania* species. J Infect Dis, 167, 426-430.

Sienkiewicz, N, Jaroslawski, S, Wyllie, S & Fairlamb, AH. (2008). Chemical and genetic validation of dihydrofolate reductase-thymidylate synthase as a drug target in African trypanosomes. Molecular Microbiology, 69, 520-533.

Simarro, PP, Diarra, A, Ruiz Postigo, JA, Franco, JR & Jannin, JG. (2011). The human African trypanosomiasis control and surveillance programme of the world health organization 2000-2009: The Way Forward. PLoS Negl Trop Dis, 5, e1007.

Simarro, PP, Franco, J, Diarra, A, Postigo, JAR & Jannin, J. (2012). Update on field use of the available drugs for the chemotherapy of human African trypanosomiasis. Parasitology, 139, 842-846.

Singh, N. (2006). Drug resistance mechanisms in clinical isolates of *Leishmania donovani*. Indian J Med Res, 123, 411-422.

Singh, S & Sivakumar, R. (2003). Recent advances in the diagnosis of leishmaniasis. J Postgrad Med, 49, 55-60.

Sirawaraporn, W, Sertsrivanich, R, Booth, RG, Hansch, C, Neal, RA & Santi, DV. (1988). Selective inhibition of *Leishmania* dihydrofolate reductase and *Leishmania* growth by 5-benzyl-2,4-diaminopyrimidines. Molecular and Biochemical Parasitology, 31, 79-85.

Sokolova, AY, Wyllie, S, Patterson, S, Oza, SL, Read, KD & Fairlamb, AH. (2010). Cross-resistance to nitro drugs and implications for treatment of human African trypanosomiasis. Antimicrob Agents Chemother, 54, 2893-2900.

Soto, J, Arana, BA, Toledo, J, Rizzo, N, Vega, JC, Diaz, A, Luz, M, Gutierrez, P, Arboleda, M, Berman, JD, Junge, K, Engel, J & Sindermann, H. (2004). Miltefosine for New World cutaneous leishmaniasis. Clinical Infectious Diseases, 38, 1266-1272.

Srivastav, NC, Shakya, N, Mak, M, Agrawal, B, Tyrrell, DL & Kumar, R. (2010). Antiviral Activity of Various 1-(2'-deoxy-beta-d-lyxofuranosyl), 1-(2'-Fluoro-beta-d-xylofuranosyl), 1-(3'-Fluoro-beta-d-arabinofuranosyl), and 2'-Fluoro-2',3'-didehydro-2',3'-dideoxyribose pyrimidine nucleoside analogues against duck hepatitis B virus (DHBV) and human hepatitis B virus (HBV) Replication. J Med Chem, 53, 7156-7166.

Stanghellini, A & Josenando, T. (2001). The situation of sleeping sickness in Angola: a calamity. Tropical Medicine & International Health, 6, 330-334.

Sternberg, JM. (1998). Immunobiology of African trypanosomiasis. Chem Immunol, 70, 186-199.

Sternberg, N, Hamilton, D & Hoess, R. (1981). Bacteriophage P1 site-specific recombination: II. Recombination between loxP and the bacterial chromosome. Journal of Molecular Biology, 150, 487-507.

Steverding, D. (2008). The history of African trypanosomiasis. Parasites & Vectors, 1, 3.

Stewart, ML, Boussard, C, Brun, R, Gilbert, IH & Barrett, MP. (2005). Interaction of monobenzamidine-linked trypanocides with the *Trypanosoma brucei* P2 aminopurine transporter. Antimicrob Agents Chemother, 49, 5169-5171.

Strosselli, S, Spadari, S, Walker, RT, Basnak, I & Focher, F. (1998). Trichomonas vaginalis thymidine kinase: purification, characterization and search for inhibitors. Biochem J, 334, 15-22.

Sudhandiran, G & Shaha, C. (2003). Antimonial-induced increase in intracellular Ca2+ through non-selective cation channels in the host and the parasite is responsible for apoptosis of intracellular *Leishmania donovani* amastigotes. Journal of Biological Chemistry, 278, 25120-25132.

Sundar, S & Chakravarty, J. (2010). Antimony toxicity. Int J Environ Res Public Health, 7, 4267-4277.

Sundar, S, Chakravarty, J, Rai, VK, Agrawal, N, Singh, SP, Chauhan, V & Murray, HW. (2007). Amphotericin B treatment for Indian visceral leishmaniasis: Response to 15 daily versus alternate-day infusions. Clinical Infectious Diseases, 45, 556-561.

Sundar, S, Gupta, LB, Makharia, MK, Singh, MK, Voss, A, Rosenkaimer, F, Engel, J & Murray, HW. (1999). Oral treatment of visceral leishmaniasis with miltefosine. pp. 589-597.

Sundar, S, Jha, TK, Thakur, CP, Engel, J, Sindermann, H, Fischer, C, Junge, K, Bryceson, A & Berman, J. (2002). Oral miltefosine for Indian visceral leishmaniasis. N Engl J Med, 347, 1739-1746.

Sundar, S, More, DK, Singh, MK, Singh, VP, Sharma, S, Makharia, A, Kumar, PCK & Murray, HW. (2000). Failure of pentavalent antimony in visceral leishmaniasis in India: Report from the center of the Indian Epidemic. Clinical Infectious Diseases, 31, 1104-1107.

Sundar, S. (2001). Drug resistance in Indian visceral leishmaniasis. Tropical Medicine & International Health, 6, 849-854.

Suzuki, R & Shimodaira, H. (2006). Pvclust: an R package for assessing the uncertainty in hierarchical clustering. Bioinformatics, 22, 1540-1542.

Tautenhahn, R, Bottcher, C & Neumann, S. (2008). Highly sensitive feature detection for high resolution LC/MS. BMC Bioinformatics, 9, 504.

Thakur, CP, Kanyok, TP, Pandey, AK, Sinha, GP, Messick, C & Olliaro, P. (2000). Treatment of visceral leishmaniasis with injectable paromomycin (aminosidine). An open-label randomized phase-II clinical study. Transactions of the Royal Society of Tropical Medicine and Hygiene, 94, 432-433.

Thompson, JD, Gibson, T & Higgins, DG. (2002). Multiple sequence alignment using ClustalW and ClustalX. In Current Protocols in Bioinformatics. John Wiley & Sons, Inc..

TKindt, R, Jankevics, A, Scheltema, R, Zheng, L, Watson, D, Dujardin, JC, Breitling, R, Coombs, G & Decuypere, S. (2010). Towards an unbiased metabolic profiling of protozoan parasites: optimisation of a *Leishmania* sampling protocol for HILIC-orbitrap analysis. Anal Bioanal Chem, 398, 2059-2069.

Truc, P, Jamonneau, V, N'Guessan, P, N'Dri, L, Diallo, PB & Cuny, G. (1998). *Trypanosoma brucei* ssp. and T. congolense: mixed human infection in Cote d'Ivoire. Transactions of the Royal Society of Tropical Medicine and Hygiene, 92, 537-538.

Tsuhako, MH, Alves, MJM, Colli, W, Filardi, LS, Brener, Z & Augusto, O. (1991). Comparative studies of nifurtimox uptake and metabolism by drug-resistant and susceptible strains of *Trypanosoma cruzi*. Comparative Biochemistry and Physiology Part C: Comparative Pharmacology, 99, 317-321.

Umemoto, T, Kobayashi, Y, Suzuki, M, Sanada, Y & Yamamoto, T. (2009). Cloning and pharmacological characterization of a novel gene encoding human nucleoside transporter 1 (hNT1) from a human breast cancer cDNA library. Life Sciences, 84, 45-51.

Van Den Abbeele, J, Claes, Y, Van Bockstaele, D, Le Ray, D & Coosemans, M. (1999). *Trypanosoma brucei* spp. development in the tsetse fly: characterization of the post-mesocyclic stages in the foregut and proboscis. Parasitology, 118, 469-478.

Van Dyke, K, Tremblay, GC, Lantz, CH & Szustkiewicz, C. (1970). The Source of purines and pyrimidines in *Plasmodium berghei*. The American Journal of Tropical Medicine and Hygiene, 19, 202-208.

Vanhamme, L, Paturiaux-Hanocq, F, Poelvoorde, P, Nolan, DP, Lins, L, Van Den Abbeele, J, Pays, A, Tebabi, P, Van Xong, H, Jacquet, A, Moguilevsky, N, Dieu, M, Kane, JP, De Baetselier, P, Brasseur, R & Pays, E. (2003). Apolipoprotein L-I is the trypanosome lytic factor of human serum. Nature, 422.

Vansterkenburg, ELM, Coppens, I, Wilting, J, Bos, OJM, Fischer, MJE, Janssen, LHM & Opperdoes, FR. (1993). The uptake of the trypanocidal drug suramin in combination with low-density lipoproteins by *Trypanosoma brucei* and its possible mode of action. Acta Tropica, 54, 237-250.

Vasudevan, G, Carter, NS, Drew, ME, Beverley, SM, Sanchez, MA, Seyfang, A, Ullman, B & Landfear, SM. (1998). Cloning of *Leishmania* nucleoside transporter genes by rescue of a transport-deficient mutant. Proc Natl Acad Sci U S A, 95, 9873-9878.

Vickerman, K. (1971). Morphological and physiological considerations of extracellular blood protozoa. In Ecology and physiology of parasites. ed. Fallis,A.M. pp. 58-91. University of Trononto: Trononto.

Vickerman, K. (1985). Developmental cycles and biology of pathogenic trypanosomes. British Medical Bulletin, 41, 105-114.

Vincent, IM, Creek, D, Watson, DG, Kamleh, MA, Woods, DJ, Wong, PE, Burchmore, RJ & Barrett, MP. (2010). A molecular mechanism for eflornithine resistance in African trypanosomes. PLoS Pathog, 6, e1001204.

Vreysen, MJB, Saleh, KM, Ali, MY, Abdulla, AM, Zhu, ZR, Juma, KG, Dyck, VA, Msangi, AR, Mkonyi, PA & Feldmann, HU. (2000). *Glossina austeni* (Diptera: Glossinidae) eradicated on the Island of Unguja, Zanzibar, using the sterile insect technique. Journal of Economic Entomology, 93, 123-135.

Wallace, LJM, Candlish, D & De Koning, HP. (2002). Different substrate recognition motifs of human and trypanosome nucleobase transporters. Journal of Biological Chemistry, 277, 26149-26156.

Wang, CC & Cheng, HW. (1984). Salvage of pyrimidine nucleosides by *Trichomonas vaginalis*. Molecular and Biochemical Parasitology, 10, 171-184.

Wang, CC. (1995). Molecular mechanisms and therapeutic approaches to the treatment of African trypanosomiasis. Annu Rev Pharmacol Toxicol, 35, 93-127.

Wang, J, Leblanc, E, Chang, CF, Papadopoulou, B, Bray, T, Whiteley, JM, Lin, SX & Ouellette, M. (1997). Pterin and folate reduction by the Leishmania tarentolae H locus short-chain dehydrogenase/reductase PTR1. Arch Biochem Biophys, 342, 197-202.

Ward, CP, Wong, PE, Burchmore, RJ, De Koning, HP & Barrett, MP. (2011). Trypanocidal furamidine analogues: influence of pyridine nitrogens on trypanocidal activity, transport kinetics, and resistance patterns. Antimicrob Agents Chemother, 55, 2352-2361.

Wasan, KM, Morton, RE, Rosenblum, MG & Lopez-Berestein, G. (1994). Decreased toxicity of liposomal amphotericin B due to association of amphotericin B with high-density lipoproteins: role of lipid transfer protein. J Pharm Sci, 83, 1006-1010.

WHO. (1998). Expert Committee on Control and surveillance of African trypanosomiasis. ed. WHO. pp. 1-36. Geneva: World Health Organization.

WHO. (2000). The leishmaniasis and leishmania HIV co-infection.

WHO. (2006). Fact Sheet. ed. WHO World Health Organization.

WHO. (2010). Control of Leishmaniasis. Geneva: WHO export committee.

WHO. (2012). Human African trypanosomiasis (Sleeping sickness). World Health Organization.

Wilkinson, SR, Bot, C, Kelly, JM & Hall, BS. (2011). Trypanocidal activity of nitroaromatic prodrugs: current treatments and future perspectives. Curr Top Med Chem, 11, 2072-2084.

Wilson, WD, Tanious, FA, Mathis, A, Tevis, D, Hall, JE & Boykin, DW. (2008). Antiparasitic compounds that target DNA. Biochimie, 90, 999-1014.

Wilson, ZN, Gilroy, CA, Boitz, JM, Ullman, B & Yates, PA. (2012). Genetic dissection of pyrimidine biosynthesis and salvage in *Leishmania donovani*. Journal of Biological Chemistry, 287, 12759-12770.

Wimmer, E, Mueller, S, Tumpey, TM & Taubenberger, JK. (2009). Synthetic viruses: a new opportunity to understand and prevent viral disease. Nat Biotech, 27, 1163-1172.

Woo, PTK. (1971). Evaluation of the haematocrit centrifuge and other techniques for the field diagnosis of human trypanosomiasis and filariasis. Verlag fur Recht und Gesellschaft.

Wyllie, S, Cunningham, ML & Fairlamb, AH. (2004). Dual action of antimonial drugs on thiol redox metabolism in the human pathogen *Leishmania donovani*. Journal of Biological Chemistry, 279, 39925-39932.

Wyllie, S, Vickers, TJ & Fairlamb, AH. (2008). Roles of trypanothione S-transferase and tryparedoxin peroxidase in resistance to antimonials. Antimicrob Agents Chemother, 52, 1359-1365.

Yamamoto, S, Inoue, K, Murata, T, Kamigaso, S, Yasujima, T, Maeda, Jy, Yoshida, Y, Ohta, Ky & Yuasa, H. (2010). Identification and functional characterization of the first nucleobase transporter in mammals: Implication in the species difference in the intestinal absorption mechanism of nucleobases and their analogs between higher primates and other mammals. Journal of Biological Chemistry, 285, 6522-6531.

Yao, SYM, Ng, AML, Cass, CE, Baldwin, SA & Young, JD. (2011). Nucleobase transport by human Equilibrative Nucleoside Transporter 1 (hENT1). Journal of Biological Chemistry, 286, 32552-32562.

Yao, SYM, Ng, AML, Vickers, MF, Sundaram, M, Cass, CE, Baldwin, SA & Young, JD. (2002). Functional and molecular characterization of nucleobase transport by recombinant human and rat Equilibrative Nucleoside Transporters 1 and 2: Chemeric constructs reveal a role for the ENT2 helix 5-6 region in nucleobase translocation. Journal of Biological Chemistry, 277, 24938-24948.

Yarlett, N & Bacchi, CJ. (1988). Effect of dl-alpha-difluoromethylornithine on methionine cycle intermediates in *Trypanosoma brucei brucei*. Molecular and Biochemical Parasitology, 27, 1-10.

Youn J H, H W Nam, D J Kim and W Y Choi (1990) Effects of pyrimidine salvage inhibitors on uracil incorporation of Toxoplasma gondii. Korean J Parasitol. 1990 Jun;28(2):79-84.

Zhang, T, Creek, DJ, Barrett, MP, Blackburn, G & Watson, DG. (2012). Evaluation of coupling reversed phase, aqueous normal phase, and hydrophilic interaction

liquid chromatography with Orbitrap mass spectrometry for metabolomic studies of human urine. Anal Chem, 84, 1994-2001.

Zijlstra, EE & El-Hassan, AM. (2001). Leishmaniasis in Sudan. Visceral leishmaniasis. Trans R Soc Trop Med Hyg, 95 Suppl 1, S27-S58.

Zillmann, U, Konstantinov, SM, Berger, MR & Braun, R. (1996). Improved performance of the anion-exchange centrifugation technique for studies with human infective African trypanosomes. Acta Tropica, 62, 183-187.

Zuccotto, F, Brun, R, Pacanowska, DG, Ruiz Perez, LM & Gilbert, IH. (1999). The structure-based design and synthesis of selective inhibitors of *Trypanosoma cruzi* dihydrofolate reductase. Bioorganic & Medicinal Chemistry Letters, 9, 1463-1468.